College of Instrumentation & Electrical Engineering, Jilin University

Academic Practice "Six in One" Training Project

English Proceedings

2017 (First Half)

CONTENTS

Research on Sparse Representation and Reconstruction of Nuclear Magnetic Resonance Signal Based on Wavelet Transform

Tang Xuewei; Peng Bo; Wang Zhaoyang

(College of Instrument Science and Electrical Engineering, Jilin University changchun130000)

***Abstract*—The NMR signal is very weak and susceptible to noise. To analyze the NMR signal, it is necessary to perform noise reduction on the first signal. In this paper, the wavelet transform method is used to sparse the NMR signal and reconstruct it by the appropriate method. The wavelet transform concentrates the energy of the signal on a few coefficients, and the energy of the noise is scattered throughout the wavelet domain. The wavelet coefficients of the signal will be greater than the noise. Based on this, the transform coefficients are cut, threshold processing and other methods to denoise. Finally, the wavelet coefficients of the threshold processing are used to reconstruct the original signal to obtain the estimated value of the original signal.**

***Key words*—Sparse representation Wavelet transform Coif3 wavelet basis Threshold Restructure**

I.PREFACE

THE NMR signal is very weak and susceptible to noise. To analyze the NMR signal, it is necessary to perform noise reduction on the first signal. In this paper, the wavelet transform method is used to sparse the NMR signal and reconstruct it by using the appropriate method.

The Ramall frequency of the magnetic resonance signal is related to the geomagnetic field, and the Ramol frequency of the MRS signal is proportional to the geomagnetic field. Therefore, the frequency of the MRS signal is different in different places. It is in the range of 1.3 kHz to 3.7 kHz The In addition, the MRS signal is very weak, the signal within the frequency range will be subject to power frequency harmonics, spike noise, random noise and other complex non-stationary noise interference [1], so the appropriate filtering algorithm for nuclear magnetic resonance It is very important to extract the noise signal and eliminate the noise signal. It will affect the accuracy of the follow-up characteristic parameters, and then the inversion interpretation results are credible.

The wavelet transform concentrates the energy of the signal on a few coefficients, and the energy of the noise is scattered throughout the wavelet domain. The wavelet coefficients of the signal will be greater than the noise. Based on this, the transform coefficients are cut, threshold processing and other methods to denoise. Finally, the wavelet coefficients of the threshold processing are used to reconstruct the original signal to obtain the estimated value of the original signal. Wavelet transform has the following advantages: (1) wavelet decomposition can cover the entire frequency domain (provides a mathematically complete description); (2) wavelet transform by selecting the appropriate filter, can greatly reduce or remove the proposed (3) wavelet transform with "zoom" feature, available in the low frequency band with high frequency resolution and low temporal resolution (wide analysis window) available in the high frequency band with low frequency resolution and high time resolution (5) multi-resolution features: edge, spikes, breakpoints and other methods, so it can be a good description of the signal of the non-resolution (wavelet); (4) wavelet transform to achieve a fast algorithm (Mallat wavelet decomposition algorithm) Smooth performance; (6) selection flexibility: the wavelet transform can be flexible choice base, bottom, can also be based on signal characteristics and denoising requirements to select multi-band wavelet, wavelet packet, translation invariant wavelet; (7) wavelet transform One of the biggest advantages is that the function system is very rich, there can be a variety of options, different wavelet coefficients generated by the wavelet will have different effects.

II.RSEARCH STATUS OF MAGNETIC RESONANCE SIGNAL DENOISING AT HOME AND ABROAD

In the early 1980s, the nuclear magnetic resonance method was successfully studied by the Soviet Union, and the first generation of nuclear magnetic resonance layer was developed. In 2006, the United States carried out nuclear magnetic resonance water exploration technology research work, for the first time proposed adaptive noise cancellation (Adaptive Noise Cancellation, ANC) thinking to achieve noise filtering. Through the adaptive algorithm to adjust the weight coefficient to track the statistical characteristics of learning noise, to extract the signal from the noise. In 1984, the geophysicist Morlet of France, when analyzing the local properties of seismic waves, first introduced the concept of wavelet to decompose the signal. In the late 1980s and early 1990s, Meyer, Grossman, Coifman and Daubechies et al. Established a theoretical framework for wavelet analysis[2]. Wavelet transform because of its good time-frequency characteristics, its emergence completely changed the monopoly of Fourier transform[3].

WANG Xi-wu, et al. (School of Computer Science and Technology, Nanjing University of Aeronautics and Astronautics, Beijing 100083, China) Based on the wavelet transform technique, the wavelet transform characteristics of effective signals and noise are analyzed[4]. SUN Ling-chuan (School of Computer Science and Technology, Nanjing University of Aeronautics and Astronautics, Beijing 100083, China) Wavelet denoising is introduced in detail. Wavelet threshold denoising is used to simulate the signal by MATLAB tool. The wavelet denoising method is used to denoise the nuclear magnetic resonance echo signal collected in the field[5]

III.THEORETICALl BASIS OF SPARSE RCEONSTRUCTION ALGORITHM

A.Sparse representation of NMR signals

Scheme 1: Sparse Representation of Discrete Fourier Spaces

In the case of one dimension, set the discrete signal $N[n]\epsilon C^N$, Its discrete Fourier transform is:

$$[k]=\sum_{n=0}^{N-1}x(n)e^{-2\pi ikn/N}\ X=<x,e_k>,k=(0,1,...,N-1)\in Z_N \quad (1)$$

among them $\{e_k[n]=e^{2\pi ikn/N}\}$ is on a set of orthogonal bases of C^N. Discrete Fourier transform can be expressed as:

$$x[n]=\frac{1}{N}\sum_{k=0}^{N-1}X[k]e^{2\pi ikn/N},X[k]\in C^N \quad (2)$$

From Fourier inverse formula 2, the signal can be accurately reconstructed in the frequency domain space Z^N.In order to meet the need for compression, the signal $x[n]$ on the orthogonal basis $\{e_k\}$ the better the number of measurements, so that the maximum compression of the data at the same time, but also to ensure the accuracy of signal reconstruction.

Scenario 2: Sparse representation of wavelet space

Assuming that the vector space of the square integrable of the one-dimensional discrete signal f(x) is $L^2(R)$ there is an approximate subspace $V_i(i)$, and they are nested with each other, the scale function $\phi(t)$, $\phi(t)$ Is the standard orthogonal basis of V_0, which can be obtained by stretching and transforming the standard orthogonal basis of subspace V_i $\{\phi_{ik}(t)=2^{i/2}\phi(2^i t-k)\}_{t\in z}$, $V_0\subset V_1$ then the scale function Satisfied:

$$\phi(t)=\sqrt{2}\sum_k c_k\phi(2t-k) \quad (3)$$

Where the function is a function of the c_k, but for the function $f(t)\in L^2(R)$, the mapping index on V_i can be understood as the approximation of the function i scale, and the remaining details are mapped in the wavelet subspace W_i, among them $V_{i+1}=W_i\oplus V_1$. as the same ,a single wavelet function $\psi(t)$ can be

obtained by stretching and translating the standard orthogonal basis in W_i,and ψf （t）$=\sqrt{2}\sum_k d_k \psi$ （2t-k）, Where d_k is the expansion function and the （t）ϵL^2（R） is expanded:

$$f(t)=\sum_{k\in Z} a_{i,k}\Phi_{i,k}(t+\sum_{i\geq 1}\sum_{k\in Z} b_{i,k}\psi_{i,k}(t) \quad (4)$$

After join the separable multi-resolution analysis:$V_i^{(2)}=V_i^{(1)}\oplus V_i^{(2)}$,
Among them ,the dimensional scale parameters:

$$\phi_{i,k,l}(t,s)=\phi_{i,k}(t)\phi_{i,t}(s) \qquad i,k,l\epsilon Z \qquad (5)$$

Wavelet can be decomposed into three directions of wavelet high frequency detail (horizontal, vertical, diagonal), which is expressed as orthogonal wavelet basis. The biorthogonal wavelet is chosen, which has symmetry, and there is no redundant information between the wavelet coefficients on each scale.

The Fourier transform can not correlate the time domain signal and the frequency domain signal organically by comparing the two schemes of the sparse representation of the NMR signal, and the complex mechanism and operation limit its application. Compared with the Fourier transform, the wavelet basis function has the advantages of good multiresolution characteristic, optimal approximation to point singularity, and time domain localization. Wavelet transform can make better use of the singularity of the signal in the signal, through the translation transformation and telescopic transformation of the signal optimal expression, often use two-dimensional wavelet transform as a sparse base to thin MR images, so here the use of wavelet transform.

B.Reconstruction method

From wavelet Transform Mallat Tower Algorithm .We can Find Wavelet Decomposition Algorithm:

$$①C_k^0=f_k \quad ②C_k^j=\sum_{n=-\infty}^{+\infty} C_n^{j-1} h_{n-2k} \quad ③d_k^j=\sum_{n=-\infty}^{+\infty} c_n^{j-1} g_{n-2k}$$

，k=0,l,2,3,4…,N-1

f_k is the original image signal sampling sequence, N is the number of sampling points, h(n) and g(n) are the impulse responses of a pair of mirror filters H and G, j is the different scale of decomposition, and when different wavelet is selected, Choosing different coefficients h(n) and g(n) to achieve.Multi-resolution analysis is the use of two sets of filter coefficients $h_n g_n$ the signal f(t) is divided into smooth signal and fine signal, h_n for the low-pass filter, through the filter to get a smooth low-frequency signal, g_n for band-pass filter Device, through the filter can be obtained in the fine part of the signal that high-frequency components. Assuming that the frequency of the data in the system is f_s, the smoothing signal gets the signal frequency[$0\sim f_s/4$]through the filter coefficient hn, and the fine signal passes through the filter g_n to obtain the signal frequency [$f_s/4\sim f_s/2$] , And further smoothing the signal through the low-pass and band-pass filter, you can get a scale of 2 smooth signal and fine signal. This decomposition process can be carried out indefinitely. The reconstructed reduction of the original signal can be achieved by using the smoothing signal of the lowest layer and each fine signal.

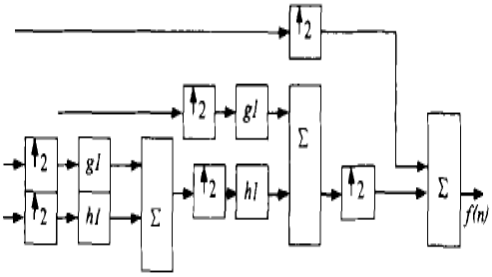

Fig.1 Schematic diagram of signal reconstruction

After the Malalt tower decomposition, the reconstruction algorithm can be used to reconstruct the signal, the signal reconstruction algorithm is as follows:

$$C_k^j=\sum_{n=-\infty}^{+\infty} C_n^{j-1} h_{n-2k}+\sum_{m=-\infty}^{+\infty} C_n^{j+1} g_{n-2k} \qquad (6)$$

IV.WAVEET BASE SELECTION

Find the appropriate wavelet base for signal sparse representation. It should be considered: (1) orthogonality, strict norms of orthogonal characteristics is conducive to the precise decomposition of wavelet decomposition coefficient.

(2) Tightness and attenuation, tightness and attenuation are important properties of wavelet, the narrower the narrower or the faster the attenuation, the better the localized characteristics of the wavelet (3) symmetry, symmetry of the signal When the topology is reconstructed, the distortion of the signal is small, which is beneficial to obtain high quality reconstruction signal. (4) Regularity, the higher the regularity for most orthogonal wavelet bases means higher vanishing moments. On the other hand, the regularity characterizes the smoothness of the wavelet, the regularity is related to the size of the support set, the greater the support, the better the regularity. The regularity of the wavelet basis is very important to minimize the quantization error, so the larger the regularity, the better the wavelet basis.

At here,the wavelet transform is carried out by comparing the signal of the signal with the signal -to-noise ratio and the peak error of the original signal to select the optimal wavelet basis.

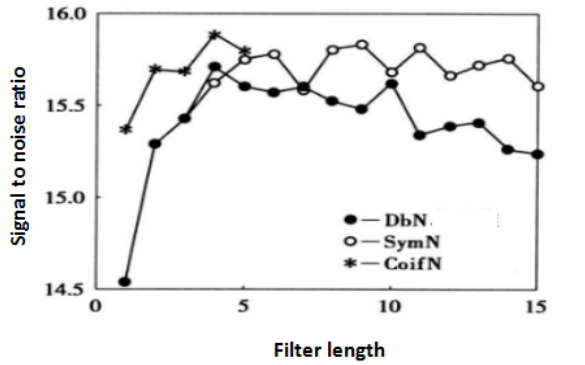

Fig.2 Different filters are used for Bumps

It can be seen from Figure 2, the test signal in the case of the same denier length, consider the different wavelet family, compared to the signal to noise ratio can be seen, are basically CoifN wavelet family is better.

And the measured MRS data signal to noise ratio is also around -16dB, so the final decision to select Coif3 wavelet base.

V TYPICAL SIGNAL DECOMPOSITION RECONSTRUCTION PROCESS

The algorithm is decomposed and reconstructed by amplitude modulation signal with frequency interference. AM signal frequency is 100Hz, plus the frequency interference.

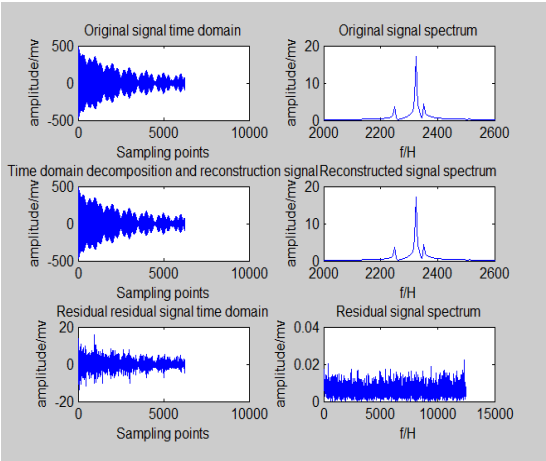

Fig.3 Signal time-frequency graph

It can be seen that the time domain residual signal value is less than 5mV, and the order of the original signal is several hundred millivolts, the amplitude of the frequency domain residual signal is less than 0.01mV, so it can be determined that the process of signal decomposition and reconstruction of the algorithm is correct .

VI.SPARSE DECOMPOSITION OF SIMULATED NMR SIGNALS

The expression of the nuclear magnetic resonance (MRS) signal is:

$$E(t) = E_0 \exp(-t/T_2^*)\cos(\omega_0 t + \theta) \quad (7)$$

The Lamaer frequency of changchun area is about 2325Hz, frequency of harmonic frequency is set to 2250Hz and 2350Hz[7], and then add random noise, constitute the noise-containing nuclear magnetic resonance signal. Useful signal frequency 2325Hz, the sampling rate of up to 25000Hz, points up to 6250 points, run the program after the discovery of too many points, so that the number of atoms in the atomic library too much, too many cycles, resulting in the program running for too long, Signal [8]So use the sub-processing signal to solve this problem.

The specific approach is to select the appropriate length and number of segments, according to the data points, divided into the entire number of paragraphs, each section of the data length is too long will make

the program run slowly, too short will lose some of the characteristics of the signal. This is divided into 250, each 25 points, the results shown in Figure 4.

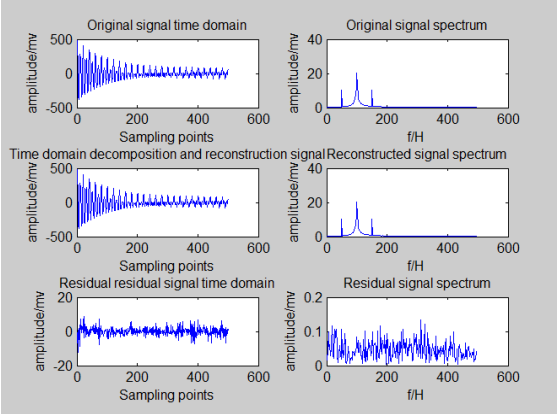

Fig.4 Signal time-frequency domain graph

From the time domain diagram can be seen, the decomposition of the reconstructed signal with the original signal is basically the same, the maximum residual residual amplitude has been controlled within 20 millivolts, from the frequency domain map reconstruction The frequency of the signal and the energy distribution are the same as the original signal, and the energy at the frequency of the residual signal is below 0.005 mV, so we can think that the decomposition and reconstruction of this method achieves the requirement.

VII.RECONSTRUCTION OFSIMULATED NUCLEAR MAGNETIC RESONANCE SIGNALS

The de-noising of the signal needs to analyze the decomposed atoms, distinguish which atoms represent the components of the useful signal, which atoms represent the components of the noise signal, and then remove the atoms that belong to the noise signal to achieve the purpose of denoising.

A.Window function filter denoising effect

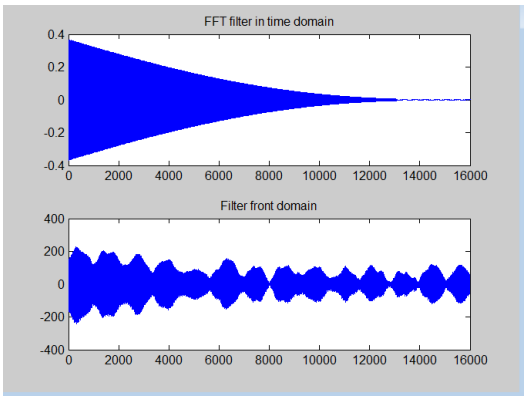

Fig.5 FFT denoising effect

Figure 5 is the using of window function signal denoising process, before the decomposition of the signal, we discussed, the Fourier transform can not be time domain signal and frequency domain signal organically linked, while the complex mechanism and computing limit Its application. From the above chart, from the time domain point of view, we can find a large part of the noise has been eliminated, the useful signal can be basically displayed, for the frequency domain, the frequency harmonic frequency of 2250Hz interference were all filtered , The frequency of 2350Hz frequency harmonic energy values reduced a lot, but we found that the useful signal 2325Hz frequency of energy also decreased, so this method is not the best.

B.Wavelet sparse reconstructed denoising

The value of the reconstructed scale parameter is related to the number of data points, the number of data points is small, the parameter value is small, and the maximum value is also reduced. The scale parameter of denoising and reconstructing is related to the distribution of signal energy. The greater the parameters, the more concentrated the signal energy, in other words, the more energy on the spectrum is at a certain frequency, rather than being distributed over a range, so we have to increase the number of data points for each segment, When the number of points is large, the signal decomposition can be completed. We reduce the sampling rate of the signal = 12500 and the number of sampling points = 3125.

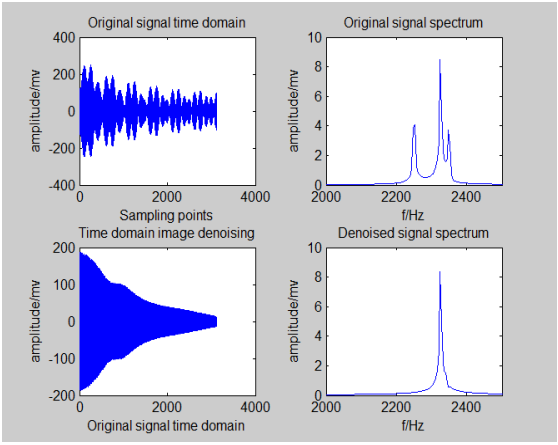

Fig.6 Wavelet sparse denoising reconstruction

Figure 6 is the result of the actual operation of the program after the map, from the time domain diagram, basically all of the noise are filtered out, and the effective signal components have a good reservation, making the time domain of the denoising effect is very good , From the frequency domain map point of view, obviously found that power frequency harmonics have been filtered out of the clean, while random noise is also filtered, so the final use of this method to reconstruct the denoising.

VIII.RESEARCH ON NOISE FILTERING OF MEARSURED SIGNAL

In order to ensure the practicability of de-noising algorithm, the noise of the measured MRS signal is filtered to verify the effectiveness of the algorithm.

The measured data of this study has a group of 102.text, including 16 single-point data, select any one of the single point of data for processing. The sampling rate of the measured signal = 128000Hz, the sampling rate is too high, the load on the algorithm is too large, thus reducing the sampling rate, the sampling rate reduced to the original 1/5, the program needs to run about 30 minutes, too long, 12800Hz, take = 3125 points for denoising. Figure 7 is the result of the processing of 102.text data.

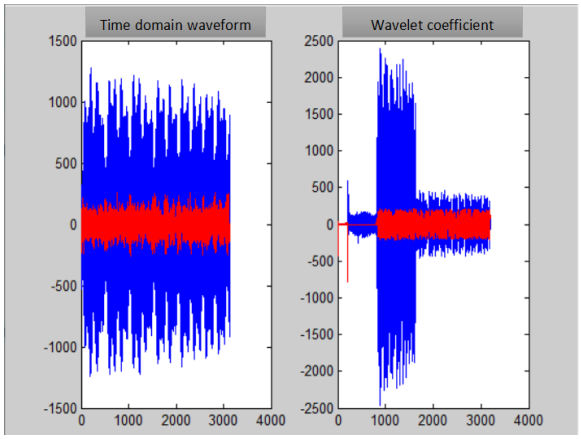

Fig.7 Measured data 102 signal time-frequency graph

From the time domain, the algorithm is very useful to extract the noise from the useful sinagal out.From the frequency domain to see the noise before, the signal contains a lot of frequency points of noise interference, especially power frequency harmonics = 2350Hz interference Very large, and useful signal energy is very small, but after the algorithm to deny the other noise has been removed, the interference of the largest power frequency harmonics are also very good to remove the useful signal = 2325Hz at the signal was very good .And the energy value is not lost, but the effective signal is lost.

FFT analysis of the measured signal, the frequency of 2325Hz near the point as a valid signal, the other as a noise signal, calculate the signal to noise ratio.

Table1 Signal to noise ratio（dB）

Data group	Group 1 data 102
Signal to noise ratio before denoising	-16.0935
Signal to noise ratio before denoising	2.1051
Increased signal to noise ratio	18.1986

It can be seen from Table 1 that the signal-to-noise ratio of the group is less, but it also achieves 18.0dB, which satisfies the requirement of 5-15dB SNR.

IX.CONCLUSION

MRS signal in the initial amplitude, the average relaxation time and other parameters to characterize the water content of the information, and often detect the data there is a lot of noise interference, affecting

the extraction of water information, sparse reconstruction algorithm to decompose the signal denoising, In the case of ensuring that the effective signal is not lost, a higher signal to noise ratio is obtained. This method has a very important significance.

Based on the extensive literature review, this paper proposes a sparse reconstruction algorithm denoising. The MRS signal is processed by means of constructing complete atomic library, segmentation processing and FFT spectrum analysis. The validity of the method is verified by the simulation and the measured data. By comparing with the window function filtering algorithm, Which further validates the superiority of denoising performance of sparse reconstruction algorithm.

References

[1] Hernnann F J. Curvelet-domain matched filtering [C]. Expanded Abstracts of Annual International SEG Meeting, 2008.

[2] I.Daubechies.Ten Lectures on Wavelets.Journal of Approximation Theory,1994,78(3):460-461.

[3] Liu X W, Nian J B, Liu H.Generalized S-transform based seismic Attenuation analysis[C]. Progress in Geophysics, 2006,29(1):20-24.

[4] WANG Xi-wu, DONG Guang-bo, XIE Gui-hai.Research on Denoising Method of Nuclear Magnetic Resonance FID Signals Based on Wavelet Transform [J]. Nuclear Electronics and Detection Technology, 2008,2 (28): 365-370.

[5] Shen Lingchuan.Study on Denoising of Nuclear Logging Signal Based on EMD and Wavelet Transform [D]. Northeast Petroleum University, 2014.

[6] WANG Xiao-chu.Wavelet Analysis and Application [M]. Chongqing: Chongqing University Press, 2006: 58-70.

[7] LI Xin-bin, MA Yang, QIU Jian-kun, ZHANG Shu-qing. Signal Feature Extraction Based on Compressed Sensing Weak Matching Tracking Algorithm, China Mechanical Engineering, 2014,25 (24) 3314: 3320

[8] Application of fast independent analysis method based on matching tracking in blind source separation of bearing composite fault, Journal of Beijing University of Technology, 2014,40 (6)

Design of the Magnetically-coupled Resonant Wireless Transmission System

Li Penghui; Zhang Yuan; Yang Tao

(College of Instrumentation and Electrical Engineering ,Jilin University, Changchun 130026, China)

***Abstract*—Based on the Magnetic-coupled resonant theory, we designd a medium-power wireless transmission system. The system uses high/very high frequency sinusoidal signal generator to generate the desiered sinusoidal signal. The signal goes through the push-pull wideband linear power amplifier, after the pre-amplifier. Then the amplified-signal is transferred by the four coils magnetic-coupled structure to the load receiving terminal. Finally we achieve the wireless power transmission using the rectifier bridge made of schottky diode and the DC-DC adjustable manostat module as the high frequency signal conditioning circuit. The system is power-supplied by the DC 50 voltage.**

***Keywords*— Magnetic coupling resonnance push-pull power amplifier wireless power transmit**

I. INTRODUCTION

WITH the development of society, new inventions based on power technology is widely used in life and industrial production. Traditional point-to-point metal wire transmission and battery power, etc have more and more disadvantages, since wear and aging of the equipment greatly reduce the reliability and safety of transmission lines[1]. Some special occasions such as underwater, medical and other urgently need to be wireless[2], wireless transmission technology came into being. Compared with electromagnetic induction[3,4], electromagnetic radiation[3], strong magnetic coupling resonant wireless power transmission technology can guarantee the distance, power and efficiency at the same time with little effect on the non-resonant object, which gradually become the most development potential of wireless energy transmission technology[1].

Since 2006, the Marin Soljacic team of the MIT has proposed the technology and has been experimentally verified[2]. Some universities and institutions at home and abroad have carried out corresponding research[3,4,5], but mainly on the transmission efficiency analysis and low power Of the experimental verification, the power of the above research and application of relatively small. In this paper, a set of wireless charging system is designed based on the analysis of the principle of strong magnetic coupling resonance, and the results are analyzed and summarized for further reference.

II. THE BASIC THEROY

A. Magnetic Coupling Resonance

Fig.1 is a schematic diagram of the experimental principle, including the transmitter circuit source coil, transmit coil, receiver coil, load circuit. When it works, the source coil generates the high frequency magnetic field as the excitation source, and the transmitting coil and the receiving coil generate magnetic coupling resonance to deliver the energy from the source to the load circuit. Among them, the source coil, the transmitting, the receiving and the load coil have the same natural frequency.

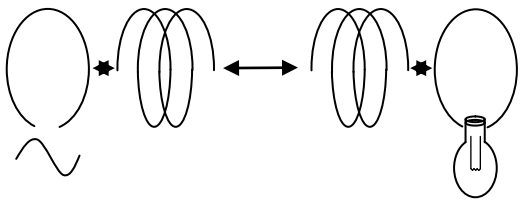

Fig.1 Schematic of the wireless energy transfer system based on strongly coupled magnetic resonances

In the practical application of the wireless power transmission system, the loss is inevitable. It mainly includes the coil's own resistance and radiation loss[6,7], where the radiation loss can be converted into radiation resistance called loss resistance as well, as shown in the coupling system model in Fig.2.

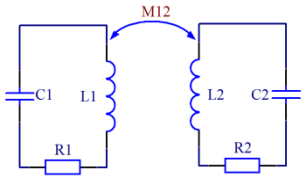

Fig.2 Loss transmitter and reveiver model of wireless power transfer

The system coupling equation is given by formula(1).

$$\begin{cases} \frac{da_1}{dt} = -(j\omega_1 + \Gamma_1)a_1 + j\kappa a_2 \\ \frac{da_1}{dt} = -(j\omega_2 + \Gamma_2)a_2 + j\kappa a_1 \end{cases} \quad (1)$$

here a is the oscillation modulus of oscillator in the coupling system, ω refers to natural angular frequency, Γ is the inherent loss coefficient from their own ohmic loss, radiation loss and so on, 1 and 2 respectively represent the transmittor and the receiver, κ means the coupling coefficient between the transmitor and receiver.

Known initial conditions $a_1(0) = 1$ and $a_2(0) = 0$, after taking Laplace transformation of the formula(1), and then take Inverse transformation of Laplace, we get formula(2).

$$\begin{cases} a_1(t) = \exp - (j\omega + \Gamma_1)t \times \cos(\kappa t) \\ a_2(t) = j\exp - (j\omega + \Gamma_2)t \times \sin(\kappa t) \end{cases} \quad (2)$$

When the system resonants, then $\omega_1 = \omega_2 = \omega$, $\Gamma_1 = \Gamma_2 = \Gamma$, and the total energy of the launcher and recevier of the magnetically-coupled resonant wireless transmission system is

$$W(t) = |a_1(t)|^2 + |a_2(t)|^2 = \exp(-2\Gamma t) \quad (3)$$

The energy of the Resonator is decided by the inherent loss coefficient[3,6] Γ and coupling coefficient κ according to formula(3).

Suppose $\gamma = \frac{\kappa}{\sqrt{\Gamma_1\Gamma_2}} = \frac{\kappa}{\Gamma_0}$, to characterize the energy transfer in a magnetically coupled resonant radio transmission system. As shown in Fig.3, the black curve indicates the total energy of the transmitting and receiving resonator when the power transmission system resonates. When γ<0.5, the system energy quickly decay to zero, which means the rate of energy decaying is faster than it transmits and so there is no stable energy transmission channel between transmitor and receiver. When γ>1000, the transmission rate of the energy is faster than it decays. According to the simulation results we can see that γ is more conducive to the transmission of energy.

The coupling coefficient of the resonant system can be calculated by equation (4). Then the coupling coefficient increases while the coil spacing reducing when the coil radius is constant.

$$\kappa = \frac{1}{\left[1+2^{3/2}\left(d/(R_1R_2)\right)^2\right]^{3/2}} \quad (4)$$

The inherent loss coefficient of the system is determined by formula(5), so we choose high quality factor wire to reduce the coefficient.

$$\Gamma = \frac{\omega}{2Q} \quad (5)$$

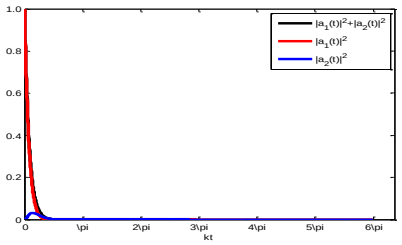

（a） γ =0.5

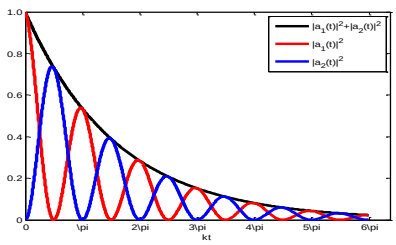

（b） γ =10

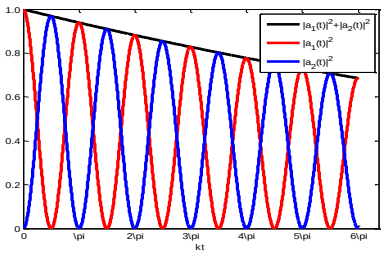

（c） γ =100

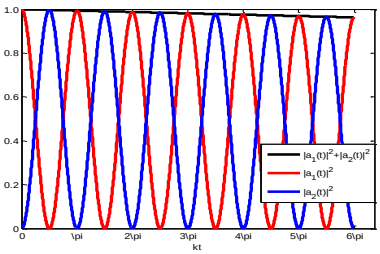

（d） γ =1000

Fig.3 Energy exchange when loss oscillators working under different coupling constant

B. Impedance Matching

The impedance matching problem is considered between the power amplification and the source coil, the load coil and the rectified regulator module, since it relates to the power and efficiency of the transmitted energy.

Suppose $Z_S = R_S + jX_S$ as the power supply impedence, $Z_L = R_L + jX_L$ as the load impedence, then the current is $I = U_S/\sqrt{(R_S + R_L)^2 + (X_S + X_L)^2}$, when both the load resistance and the impedence are independently changeable. Then the power supplied for the load is $P_L = I^2R_L = R_L{U_S}^2/[(R_S + R_L)^2 + (X_S + X_L)^2]$, we can get the maximum[7] when $X_L = -X_S$ and $\frac{dP_L}{dR_L} = 0$, then$R_L = R_S$, that is $Z_L = {Z_S}^*$.

III. SYSTEM OVERALL DESIGN

The overall design of the scheme consists of signal generating module, high frequency power amplification module, resonant coupling module, rectification regulator module, power source module and load. First of all, the signal generator circuit generates the high-frequency sinusoidal signal, the output voltage amplitude of which is adjustable, then the signal is amplified by the high-frequency power amplifier circuit energy-supplied by the power source. The energy is coupled to the receiving coil which is in the resonant state, from the transmission coil in the resonant state as well, and is rectified by the rectified voltage regulator circuit to supply the DC stabilized voltage to the load. The overall block diagram of the system is shown in Fig.4.

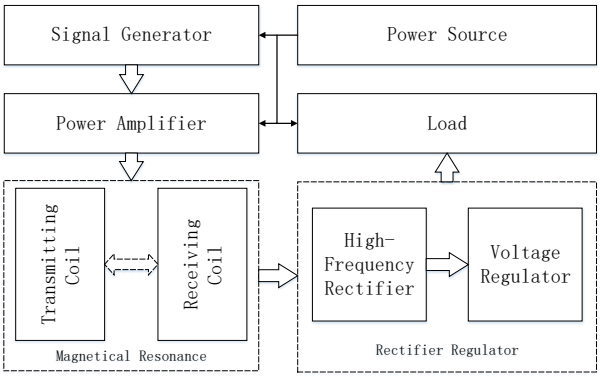

Fig.4 The block diagram of the system

IV. MAIN MOUDLES DESIGN

High-frequency signal source can usually be achieved in two ways, one is the inverter circuit, the other is the signal generated by the signal generated by the signal amplification. Forward-type inverter circuit, due to the excitation voltage waveform contains more efficient harmonics and can not be eliminated by resonance, usually in the form of heat dissipation in the loop, the efficiency is low. The full-bridge inverter efficiency is higher than the forward-type inverter, but the control is complicated and the cost is high. Half-bridge inverter due to the drive chip switching frequency, can not achieve a high inverter frequency. Therefore, this paper will signal and power amplification combined as a high-frequency signal source.

A. Signal Generator Circuit

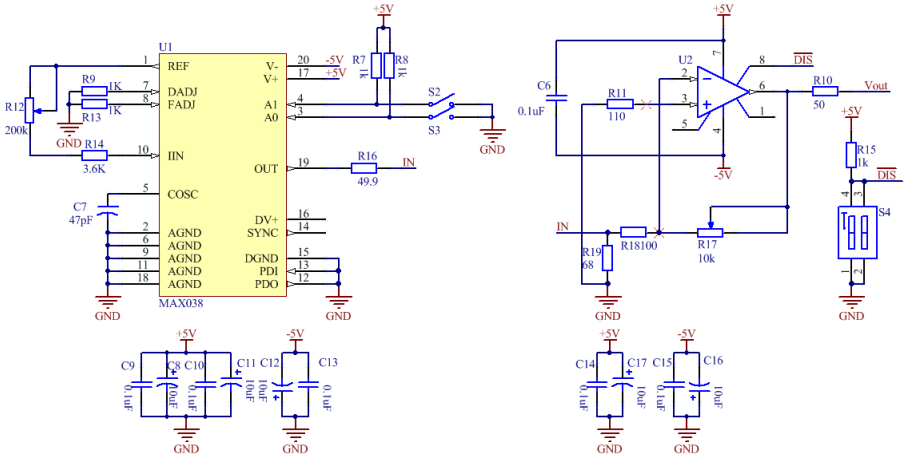

Fig.5 Sinusoidal signal generator circuit

We choose MAX038 to provide the 1MHz sinusoidal signal for our wireless power transmission system. The chip can provides 0.1Hz~20MHz signal, with frequency-adjustable. Its sine wave distortion is

less than 0.75 percent. The non-linearity of the chip is low to 2 percent, when the duty cycle is changed. It has the low impedance constant pressure output. The output resistance is 0.1Ω, with the short circuit protection circuit as well.

The input current can be changed by adjusting the sliding rheostat R12 as shown in Fig.5. According to the formula(6), we know the frequency of the ouput signal is proportional to IIN when C7 is fixed. And we can get 1MHz sinusoidal wave. Then we should add the operational amplifier circuit based on OPA690 to amplifier the small signal.

$$F_o(\mathrm{MHz}) = \mathrm{IIN}(\mu\mathrm{A})/C_7(\mathrm{pF}) \qquad (6)$$

The processed high-frequency sinusoidal signal is amplified by a power amplifier circuit as a larger power high-frequency signal source for the wireless power transmission system. According to the impedance matching theory, the module output impedance is designed to be 50 ohms.

B. Power Amplifier Ciucuit

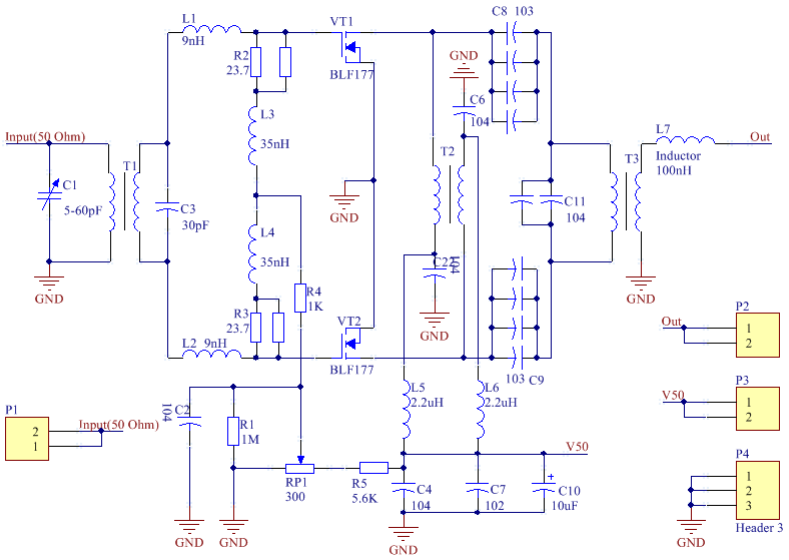

Fig.6 The diagram of power amplifier circuit

This section is used to amplify the high-frequency sine wave signal with a smaller amplitude generated by the signal generating circuit by using a power amplifier. Because ordinary power amplifiers can not meet the requirements to drive 60W load, so we use the high/very-high frequency power MOSFET BLF177 as the basic electronic component.

The linear wide band amplifier circuit is shown in Fig.6. The circuit is a kind of AB-Class amplifier. It is powered by the 50V DC-power supply. And the quiescent current of each MOSFET is 0.5A. According to the impedance matching theory, the module output impedance is designed to be 50 ohms.

C. Magnetic Coupling Resonance Coils

The system uses four-coil transmission structure: source coil, transmit coil, receive coil, load coil. The source coil adopts the series resonance mode, and the load coil adopts the parallel resonance mode.

Series resonant mode supply voltage must be constant, the total resistance of the circuit is minimum, the energy transmission efficiency is high, the power source supplies only the resistive components.The local voltage of the capacitor or inductance can be higher than the power supply voltage. While the parallel resonant mode voltage under certain conditions, the total resistance is infinitely large when resonance state, with a strong load capacity. Tuning is relatively stable and easy to control, and can get rid of the voltage oscillation of the series line tuning process.

The inductor value[8,9] of the close coil made up of enamelled copper wire in the design can be calculated by the formula(7).

$$L = N^2 R\mu_0\left[\ln\left(\frac{8R}{a}\right) - 1.75\right] \qquad (7)$$

Where N is the number of the wire coils, $\mu_0 = 4\pi \times 10^{-7}\mathrm{H/m}$ is the vacuum permeability, R is the coil radius(m), and a is the coil wire radius(m).

Tab.1 The paraments of the coupling coils

Coil Diameter/cm	Wire Diameter/mm	Coil Turns
30	2	12
L/uH	C/pF	Natural Frequency/kHz
64.4	390	1004

D. Rectifier Regulator Circuit

In the wireless power transmission system, the power can be transmitted through the sinusoidal AC voltage coupling between coupling coils, and thus we get the high frequency sinusoidal AC signal from the coupling load coil. The center frequency of the design is around 1MHz. It's also ok for us, if we directly light the incandescent using the received signal or provide energy for the load that needs electrothermal conversion, but in most cases we need a DC voltage. So we need the rectifier filter[10] to deal with the signal received first.

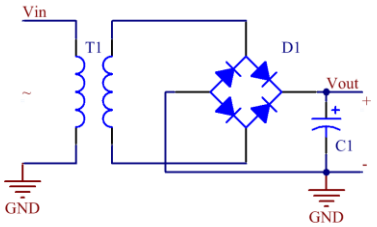

Fig.7 High frequency rectifier bridge circuit

In addition, the DC energy signal may change with the change of the coil pitch, the fluctuation of the transmission voltage and the drift of the operating frequency of the system. Therefore, the DC / DC module is needed to regulate the signal before the load.

Due to the large required transmission power, many modules can not statisfy the system requirement, such as LM2596 module designed for less than 15W andXL4005 module usually working under 50W. So the high power DC-DC adjustable buck regulator module which can no more than 300W is used. The range of the input voltage is DC 3.5V~30V, and the output voltage is DC0.8V~29V. The maximum current is up to 10A while the efficiency of the transmission is up to 90 percent.

The signal can be used as the DC power supply to load, since the ripple of it is small and it is much more stable than before, after the regulator.

V. ANALYSIS OF RESULTS

Multi-experiment measured data are shown in Fig.8 and Fig.9.

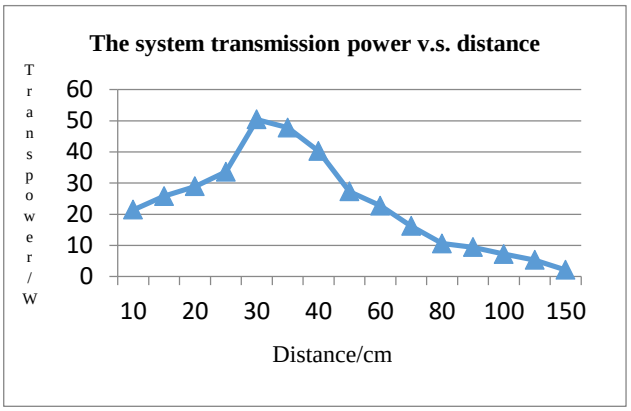

Fig. 8 The transmitting power of the system with the change of the distance of two coils

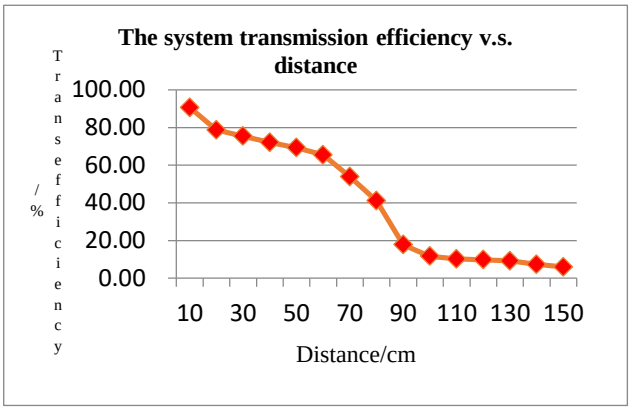

Fig.9 The transmitting effiency of the wireless power transmitting system with the distance of the two coils

It can be seen from Fig.8 that the transmission power increases first and then decreases with the increase of the distance between the two coils, and there is an extreme value during 30cm~35cm. It shows that the power transmission has the best match point with the distance when the system parameters fixed, we can make appropriate adjustments to ensure a better performance during the experiment. According to Fig.9, the system power transmission efficiency gradually reduced while the coil spacing increases and sharply reduced to below 5% at 90cm, which is different from the curve of the transmission power. So the actual application should be based on the requirements of the power and efficiency trade-off to ensure the overall performance of the transmission system.

VI. CONCLUSION AND DEVELOPMENT

After testing, the system basically achieved the design indicators: The 60W DC-bulb 60cm away can

be light by the system,which can suply stable voltage for the load to charge, while the transmission efficiency can be 30%. But there are still some details need to be improved. First of all, system has not yet achieved frequency tracking, so the efficiency still can be improved with a fixed distance. Besides, the system is still large for many occasions, so we need to further reduce the size of the system when it is applied actually. Then the impact of the obstacle remains to be tested and adjusted for optimization.

References

[1] X.M.Fan, X.Y.Mo, X. Zhang. Research Status and Application of Magnetic Coupling Resonant Wireless Power Transmission[J]. Journal of Electrotechnical Technology, 2013,12:75~99.

[2] Andre Kurs, Aristeidis Karalis, Robert Moffatt, J.D. Joannopoulos, Peter Fisher, Marin Soljacic. Wireless Power Transfer via Strongly Coupled Magnetic Resonances[J]. Research Articles, Vol 317, 2007.7.6:83~86.

[3] W.D.Ding. High power electromagnetic resonant wireless power transmission[D]. University of electronic science and technology, 2015.

[4] G.D.Wang, L.L.Yuan,Y.J.Wang. Study on Four - coil Model of Magnetic Coupled Resonant Wireless Power Transmission System[J] Journal of Power, 2105.1,13(1):101~106.

[5] C.D.Li, S.D.Huang, Z.Q.Li, Y.huang. Power and Efficiency Analysis of Magnetic Coupled Resonant Wireless Power Transmission[J]. Power electronic technology, 2014,3:28~31.

[6] Q.Wang, H.Li, D.X.Chen. Analysis and Design of Magnetic Coupling Resonant Wireless Power Transmission System[J]. Power Technology, 2012,11:1741~1750.

[7] M.Yu. Research on a Magnetic Coupled Resonant Wireless Power Transmission System[D]. Anhui University of Science and Technology, 2015.

[8] Keisuke Kusaka, Jun-ichi Itoh. Experimental verfication of rectifiers with SiC or GaN for wireless power transfer using a magnetic resonance coupling[J]. IEEE PEDS 2011, Singapore, 5-8 December 2011:1094~1099.

[9] David S.Ricketts, Matthew Chabalko, Andrew Hillenius. Tri-Loop impedance and frequency matching with High-Q resonators in wireless power transfer[J]. IEEE Antennas And Wireless Propagation Letters, Vol.13, 2014:341~344.

[10] H.G.Kang. Electronic technology foundation(Analog part)[M]. High education press. 2002.

Noise Acquisition System of 1/f noise

ZhongHao Fu; HeMing You; XiYao Wang
(College of materials Science and Engineering, Jilin University, Changchun 130022,China)

***Abstract*—The low frequency noise of electronic devices is usually related to semiconductor surface defects and internal conditions, where 1/f noise has become the standard for reliability evaluation for electronic devices. In this paper, a low frequency electrical noise acquisition system with low noise preamplifier and high precision ADC conversion, using FPGA as logic control chip, is proposed by analyzing the characteristics of 1/f noise itself and the anti - jamming design idea of amplifier. After a actual test of the system, it is found that the system can realize the requirement of low noise amplifier at the frequency of 1Hz-10KHz and the minimum amplitude of 1mV. At about 10Hz, the system has the equivalent input noise of 2.12nV/√Hz, with noise density of about 33nV or so.**

***Key words*—1/F Electronic noise Low frequency Acquisition System**

I. INTRODUCTION

1/F noise is the electronic device itself to bring low-frequency electrical noise[1], to some extent, is to evaluate its internal status and design process reliability evaluation of one of the important criteria [2].

Agilent 2010 The latest product, the E4725A 1/f noise test system, offers industry-leading extremely low system noise and high-precision test results to maximize system sensitivity, allowing the system to be as low as -177dBV ?Hz system noise, and the lowest measurable to 1E-25A ?Hz noise superior performance [3]. Jinan Lennon Electronics 1/f noise test system 9812D, can be in the 1Hz-10MHZ frequency range without attenuation measurement of semiconductor devices low frequency noise characteristics[4], including 1/f noise and RTS noise. It is also possible to use different low-noise amplifiers for different device types to ensure maximum test accuracy for different devices and test conditions.

The low frequency electrical noise collection system designed in this paper includes low noise preamplifier circuit, ADC acquisition circuit and communication part with the host computer. Which pre-amplifier circuit and active filter circuit as a hardware acquisition circuit, itself requires a very low noise floor[5], that is, the need to design a low noise amplifier (Low Noise Amplifier, referred to as LIA), for receiving and amplification Voltage amplitude of the weak input signal; In addition, because the collected signal frequency concentrated in the 1Hz-1kHz between, so the ADC circuit selection of low sampling rate Sigma-Delta precision ADC1251[6], the sampling rate is controlled at 1k, its built-in anti-Stack filter can greatly simplify the circuit design. The main controller part of the use of FPGA, mainly for timing control and communication.

II. DISINEG OF LOW NOISE PREAMPLIFIE

A. LT1028 Equivalent noise model

Due to the need to amplify very weak signals, the preamplifier circuit needs to have low noise, low DC drift characteristics, so the use of low noise high-precision amplifier LT1028 to enlarge, LT1028 LINEAR company produced low noise amplifier, is currently very common on the market Of the amplifier, the noise frequency characteristics and voltage noise density shown in Figure 2.1.

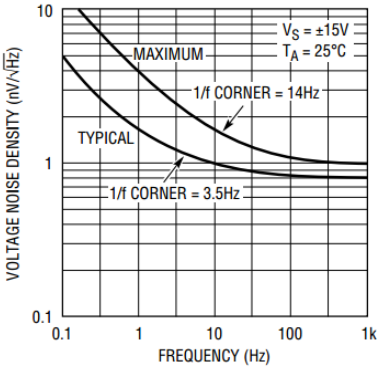

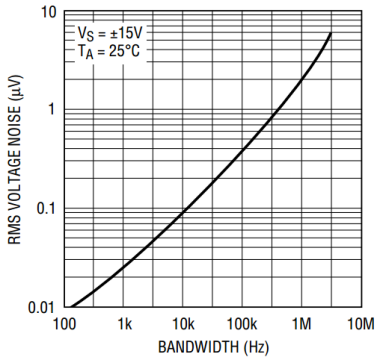

Fig 2.1. Voltage noise density and RMS of LT1028

By referring to the chip data, the corresponding relationship between the voltage noise density and the noise power spectral density of the LT1028 can be obtained as shown in Table 2.1.

TABLE 2.1. NOISE DENSITY AND RMS OF LT1028

Freq (Hz)	Em	RMS(v)
0.1	-	1.5nV/√Hz
1	-	1.6nV/√Hz
10	-	1.0nV/√Hz
100	40nV	0.86nV/√Hz
1k	80nV	0.82nV/√Hz
10k	0.19uV	0.86nV/√Hz

As can be seen from the above table, LT1028 in the 10Hz-1kHz frequency range of voltage noise as low as 1nV / √Hz, the frequency can be 0.1Hz-10Hz, due to 1 / f noise, the voltage noise to 1nV / √Hz or more , Still has excellent noise characteristics.

B. Instrumentation Amplifier

In order to further improve the performance of preamplifier, the use of instrument amplification structure[7], the design circuit shown in Figure 2.2,

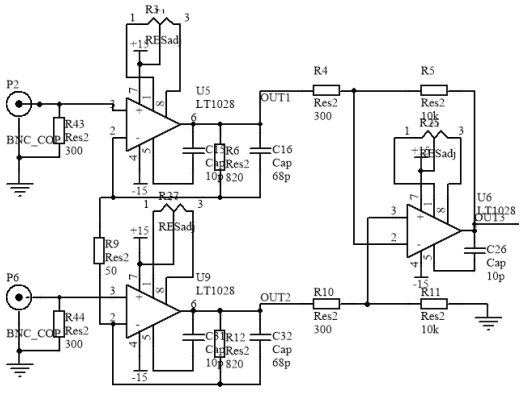

Fig 2.2. Instrumentation amplifier structure

$R_5 = R_{11} = 10k\Omega$, $R_4 = R_{10} = 300\Omega$,

$R_6 = R_{12} = 820\Omega$, $R_9 = 5k\Omega$, Calculate the available circuit gain:

$$Av = -(\frac{R5}{R4}) * \left(1 + 2\frac{R6}{R9}\right) = -20\text{dB} \quad (2.1)$$

C. Circuit performance

--First, SNIR test.While loading a 500Hz, 1mV sinusoidal signal ,we observe and store the test data using the Agilent DSO-X 3024A 500MHz oscilloscope.

Through the instrumentation amplifier amplification 20dB, the final output signal shown in Figure 2.3 (AC coupling).

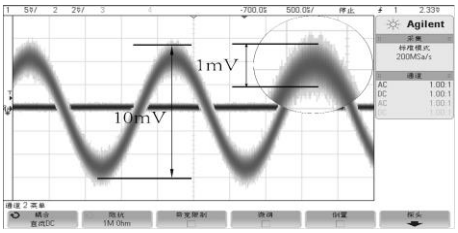

Fig 2.3. Amplified signal output image

It is estimated that when the noise signal is superimposed on the input signal, the output SNIR is:

$$SNIR = 10\log\frac{(\frac{P_S out}{P_S in})}{(\frac{P_N out}{P_N in}/)} = 60\text{dB} \quad (3.5)$$

This result meets the overall design requirements for low noise preamplifier circuits.

--Second, in-band flatness test. In the former test based on the multi-frequency test, the input signal amplitude is fixed at 1mV, gain 20dB, using (Agilent-500Mhz) oscilloscope to observe and store the test data, the output amplitude and frequency relationship shown in Figure 2.4.

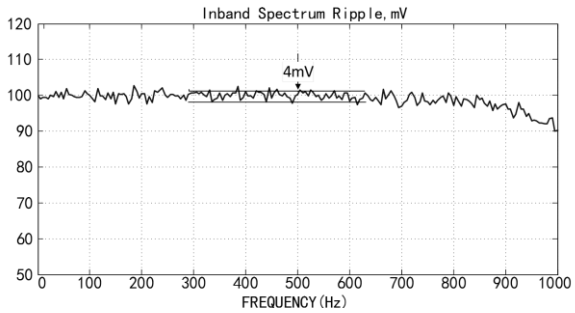

Fig 2.4. In-band flatness curve

As can be seen from the above figure, the maximum fluctuation in the range of 0.1 Hz to 1 kHz is -0.34 dB.

III. ADC CONVERSION AND TIMING LOGIC

A. Characteristics of ADS1251

ADS1251 is a high-precision, delta-sigma ADC converter from Texas Instruments, powered by a single 5V supply with data rates up to 20kHz and still has 19 significant resolutions. The main advantages of the ADS1251 are:

1, with high precision 24-bit lossless data code,

2, the main clock up to 8MHZ, the data transfer rate can reach 20 kHz, and there are still 19 effective resolution,

3, the noise as low as 1.5x10-6,

4, with internal anti-aliasing filter,

5, can use the external reference voltage 0.5V-5V,

6, with program-controlled power-down mode and synchronization mode.

Figure 3.1 shows the interface connection between the ADS1251 and the FPGA.

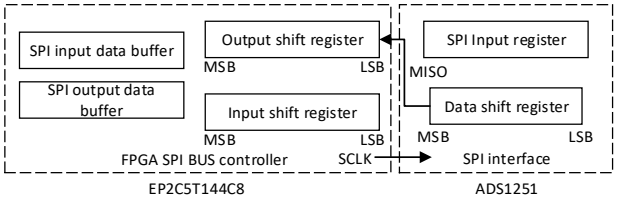

Fig 3.1. Interface diagram between ADS1251 and FPGA

ADS1251 for the SPI serial interface, reducing the complexity of its control, FPGA only through the CLK, SCLK and Dout three serial lines can be achieved as follows:

1, controllable power-up and power-down mode,

2, PFGA and ADS1251 achieve synchronization,

3, to control the sampling rate of data updates, the sampling rate provided by the FPGA master clock CLK control.

The timing diagram for the ADS1251 is shown in Figure 3.2.

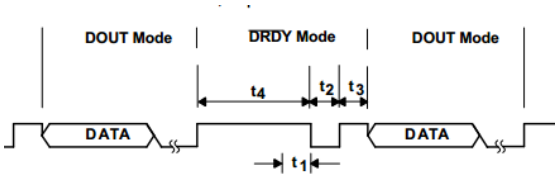

Fig 3.2. Timing diagram of ADS1251

Each ADS1251 conversion cycle requires a total of 384 main clocks (184CLK), including two modes: / DRDY mode and DOUT mode, where / DRDY mode occupies 36CLK for data conversion, DOUT mode using the remaining 348CLK for data transmission.

In the / DRDY mode, the data preparation cycle (t4) takes 24CLK, then the ADS1251 pulls the DOUT line low by 6CLK (t2) and pulls up 6CLK (t3). The FPGA detects the status of the DOUT line Is ready and read.

The ADS1251 state transition diagram for the FPGA is shown in Figure 3.3.

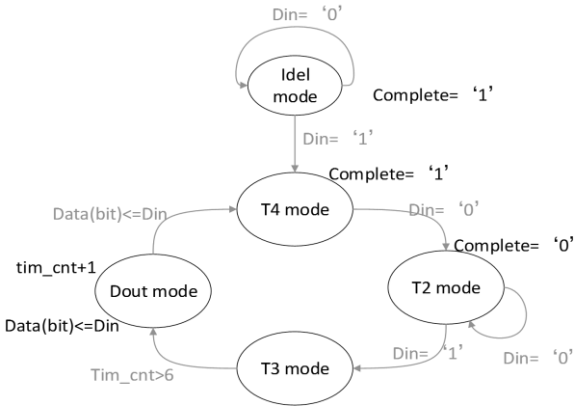

Fig 3.3. State transition of ADS1251

B. FPGA internal timing design

FPGA internal logic control mainly includes ADS1251 driver, FIFO buffer interface and serial communication program. FIFO interface and serial communication are called third-party IP core, to achieve the purpose of fast and reliable design, this article describes the FIFO interface design and use, because the serial communication is relatively simple, do not do this.

FIFO (First In First Out) has a synchronous FIFO and asynchronous FIFO of the points, which asynchronous FIFO read and write using mutually asynchronous clock, the main advantage is that it can achieve two different clock systems between real-time data transmission, usually in the read clock The rising edge of the time to read the data, write the clock when the rising edge of the write data.

FPGA provides a FIFO core, which can be customized by the user FIFO width, depth, status flag and memory type, etc. Figure 3.4 for the FIFO data transfer mechanism

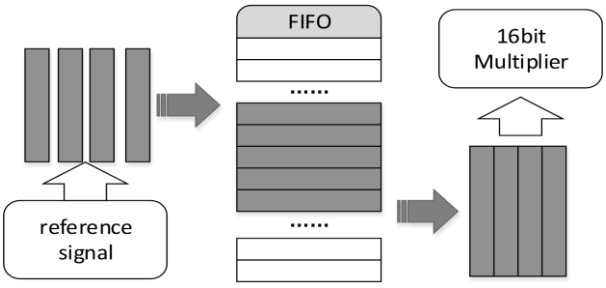

Fig 3.4. FIFO transfer mechanism

As can be seen from the above figure, the FIFO module mainly in the sine and cosine reference signal

module and the multiplier module between the data buffer role, the cosine signal generation module to store data faster, and the multiplier module to read the data slower. It is therefore necessary to determine the FIFO status according to the 'fill full' flag and the 'read empty' flag and to control the write and readout separately according to the fifo_rd_req (fifo_wr_req) signal. Figure 3.5 shows the multi-cycle sinusoidal signal read by the sub-FIFO buffer module.

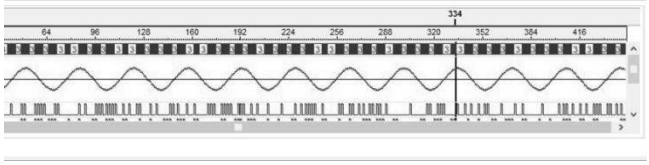

Fig 3.5. FIFO signal buffering data

C. Host computer in Labview

The use of serial communication between the FPGA and the host computer for data transmission, the PC platform LabVIEW has been integrated into a complete serial module, that users can easily build based on the VISA node function of the serial data acquisition module, with convenient, high merit.

After the completion of the serial port configuration, through the serial port data collected through the data type conversion and other processing directly into the waveform chart function, you can complete the current signal waveform real-time display function. With the LabVIEW file processing functions, you can also record the data saved, generate txt and other formats of data files. The complete completion of the function of the complete PC LabVIEW program and interactive interface shown in Figure 3.6-3.7.

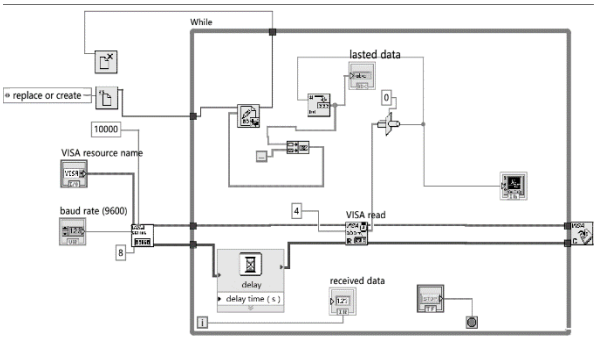

Fig 3.6. LabVIEW program

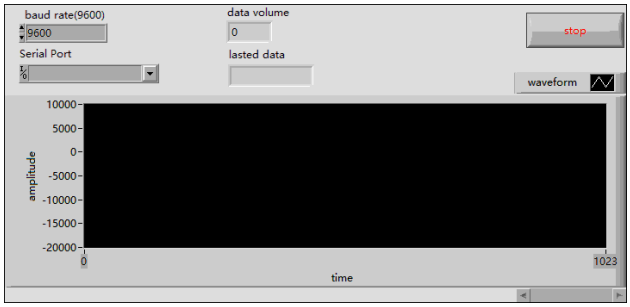

Fig 3.7. LabVIEW interface

IV. DATA ANALYSIS

We input the ground, use Labview host computer to observe and save the final output, and the data into MATLAB for frequency analysis, get the noise characteristic curve shown in Figure4.1-4.2.

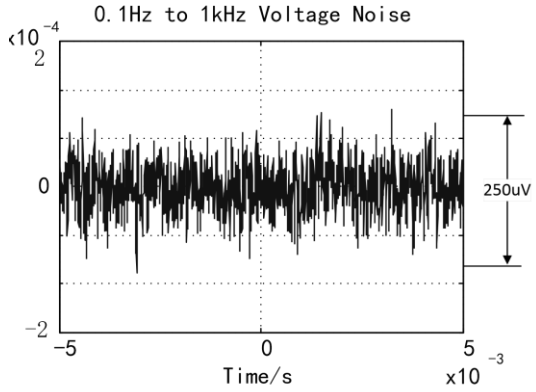

Fig 4.1. White noise with zero input

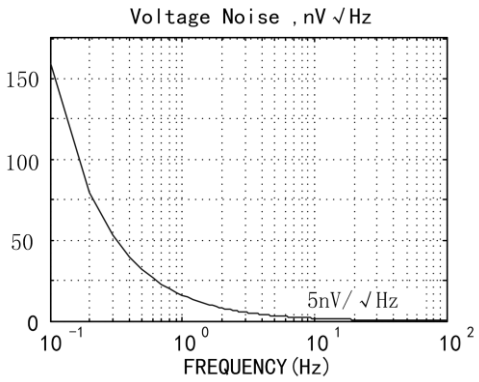

Fig 4.2. Spectrum Analysis with zero input

According to Figure 4.2, the equivalent input noise of the critical frequency point can be obtained as shown in Table 4.1:

TABLE 4.1. RMS OF THE ACQUISITION SYSTEM

Frequency(Hz)	RMS(v)
1	15.5nV/√Hz
10	2.12nV/√Hz
100	300pV/√Hz

Calculate the low frequency voltage noise density

$$\begin{cases} V_{n,rms}(F_L,F_H)=V_{nw}\sqrt{F_C \ln[\frac{F_C}{F_L}]+(F_H-F_C)} \\ F_L=1\text{Hz}, F_H=100\text{Hz}, V_{nw}=3\text{nV}/\sqrt{\text{Hz}}, F_C=10\text{Hz} \end{cases} \quad (3.6)$$

$$V_{n,rms}=33.14\text{nV} \quad (3.7)$$

V. CONCLUSION

The article analyzes the need to pay attention to the 1 / f noise collection system.

And introduces the instrumentation amplifier system in detail, and further improves the circuit performance of the LT1028 weak signal on the basis of high precision op amp. The resulting 1 / f noise acquisition system has good noise characteristics. At the frequency of 10Hz, the acquisition system measured the equivalent input noise to 2.12nV / √Hz, the voltage noise density of 33.14nV.

Reference

[1] Design and Simulation of Low Noise Amplifier for Detecting 1 / f Electrical Noise [J]. Li Yifan, Guo Shutu, Gao Fengli. Modern Electronics Technology. 2015 (04)

[2] The relationship between resistance change rate and noise in instrumentation amplifier [J]. Sun Xun, Sun Lende. The practice and understanding of mathematics 2014 (07)

[3] The Design of the Weak Signal Amplification Circuit of the Nafu Level [J] .Analysis of the East, Liu Jie, Bao Dezhou, Liu Pingan. Electronic Testing. 2012 (08)

[4] Journal of Spring University 2012 (06)

[5] Application of instrumentation amplifier in laser heterodyne glass thickness measurement system [J]. Lan Yu, Lu Qinglin. Foreign Electronic Measurement Technology. 2012 (03)

[6] Fractal Analysis 1 / f Noise Performance [J] .Chen Xiaojuan, Tang Longyou, Sui Jisheng, Wu Jie. Journal of Henan University of Science and Technology (Natural Science Edition). 2012 (01)

[7] Instrumentation amplifier circuit design [J]. CUI Li-ping. Modern electronic technology

The intelligent parkassist system of multi sensors based on the Raspberry pie

Yingqi Bi; Ziwei Chai; Jiawei Hou

(The College of Instrumentation and Electrical Engineering, Jilin University, Changchun 130022,China)

***Abstract*—With the development of society and the progress of science and technology,cars have gradually entered the thousands of households, But it is a difficult thing for the novice to enter garage.Considering the strong function of raspberry pie and its structure,using a variety of sensor fusion technology,through the algorithm to develop the best reversing program.Raspberry pie comes with audio output interface,so considering the external audio device to remind and guide the driver reversing.**

***Key words*—reversing raspberry pie sensor fusion**

I. INTRODUCTION

RASPBERRY PI,is a card sized computer system that is designed for students in computer programming education,it can achieve a powerful function through loading the Linux and the corresponding corresponding application program, raspberry pie also has the advantages of small size and low price advantage.At present, a large number of domestic and foreign reversing system is composed of a camera and a display.When the system is working, the screen will display two scale lines,and they can not change, at reversing car, the driver can not determine how many degrees of the wheel that do not touch the wall after the car, they can not determine how to reverse to arrive at the correct position,and now the prices of the reversing system on the market are more expensive.

The research and development of the new functional of raspberry pie, intelligent parking assist system of multi-sensor fusion based on raspberry pie .That is designed to achieve the intelligent reversing,the reversing will be more convenient and more secure.And that provides more convenient conditions for new drivers,making their skills can correct for reversing in the absence of skilled driving and providing a very good training conditions for them.In addition,the intelligent reversing auxiliary system has low cost and good social value and economic value.

II. OVERALL DESIGN SCHEME

Based on powerful function of raspberry pie and its structure,designing the intelligent parking assist system of multi-sensor fusion based on Raspberry pie.Raspberry pie comes with audio output interface,so the use of external audio equipment,in order to remind the driver how to reverse .We use multi sensor fusion technology, through the analysis of the algorithm to develop the best driver parking plan.The main application of sensor system is that collects the required data,with raspberry pie as control core,through the corresponding algorithm to make the driver parking scheme,tell the driver how to operate through the language.So that even if the driver closed his eyes can successfully reverse the storage[1].

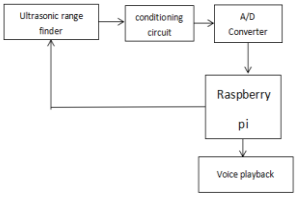

Fig.1 The overall structure of the system

III. HARDWARE DESIGN

The data acquisition module uses the ultrasonic range finder US-100 to collect the data, and uses the sensor to get the distance between the vehicle and the vehicle[2].

US-100 ultrasonic ranging module can achieve 2cm-4.5m non-contact ranging function,it has a wide input voltage range with 2.4-5.5V,the static power consumption is less than 2mA, the location results are

corrected by the temperature sensor,at the same time with GPIO, serial port and other means of communication, with the watchdog, stable and reliable.The ultrasonic ranging module has two ways of triggering ,this design uses the level trigger.

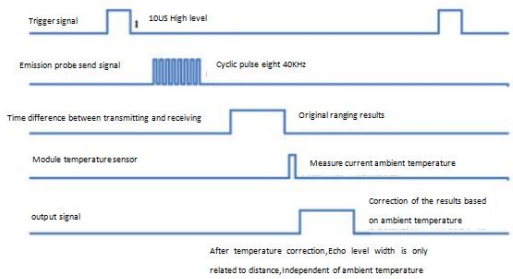

Fig.2 US-100Timing diagram

The working principle of ranging module is:to give the Trig pin of a sensor 10us high leve.The sensor sends a signal after receiving the trigger signal.Then the signal is reflected back when it comes into contact with an object.Received by sensor.Finally, the Echo pin outputs a high level.High level duration t.S= (340m/s*t) 340m/s was calculated by the sound velocity of /2.

The angular distance is calculated by measuring the distance information measured by the ultrasonic distance measuring module,receive the angle.

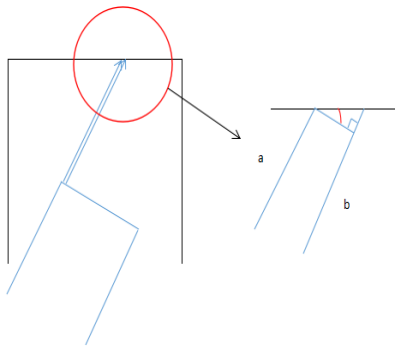

Fig.3 Principle of angle measurement

The distance between the wall is measured by the ultrasonic range finder.That is a and b.By judging the size of a and b.Use a large distance to subtract a small distance.And the distance between the two ultrasonic rangefinder is fixed to C (set b greater than a).While the reversing angle θ=arctan（（b-a）/c）.

By the key control the operation of the system.And because the reverse direction is different,So through different buttons to choose the right or left back reversing.After collecting the data in the system,by the raspberry pie to judge.Determine the location of the vehicle in the garage,and the voice prompts the driver.Voice broadcast using sound to put out,real time alerts to drivers[3].

IV. SOFTWARE DESIGN

This system uses raspberry pie as control center,to achieve the acquisition of data processing and voice prompt output.Raspberry pie is based on a micro computer motherboard ARM,SD card for memory hard disk.There are two USB interfaces and a network port around the card board,keyboard, mouse and cable.TV output interface and HDMI HD video output interface with video analog signal.All of the above components are integrated on a board that is slightly larger than a credit card,with all the basic functions of PC,system for Linux system.

Fig.4 Raspberry pie

When the driver is reversing,manual reversing switch,Raspberry pie starts to work.Reversing is divided into left and right back.Different direction reversing control right raspberry pie ultrasonic ranging module different measurement.The programming flow chart is as follows.

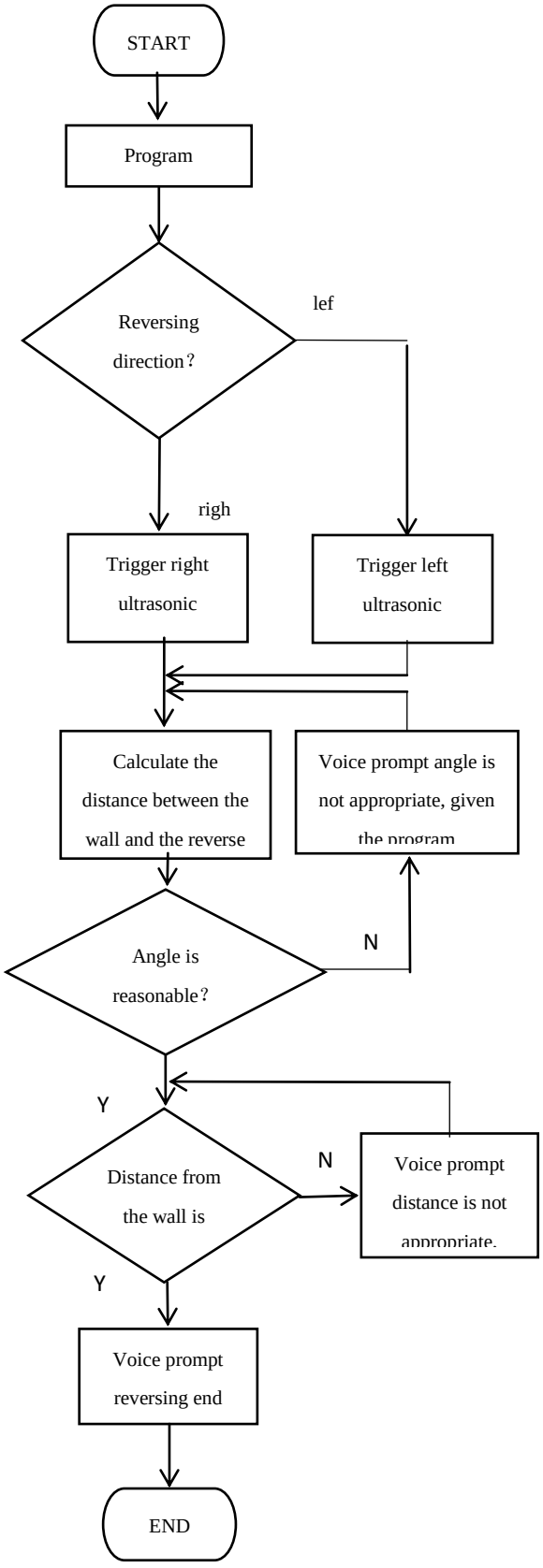

Fig.5 Software flow chart

V. TEST AND ANALYSIS

According to the above hardware and software design,sub module debugging,testing distance and angle measurement can be carried out correctly.The results of each module are running normally[4].

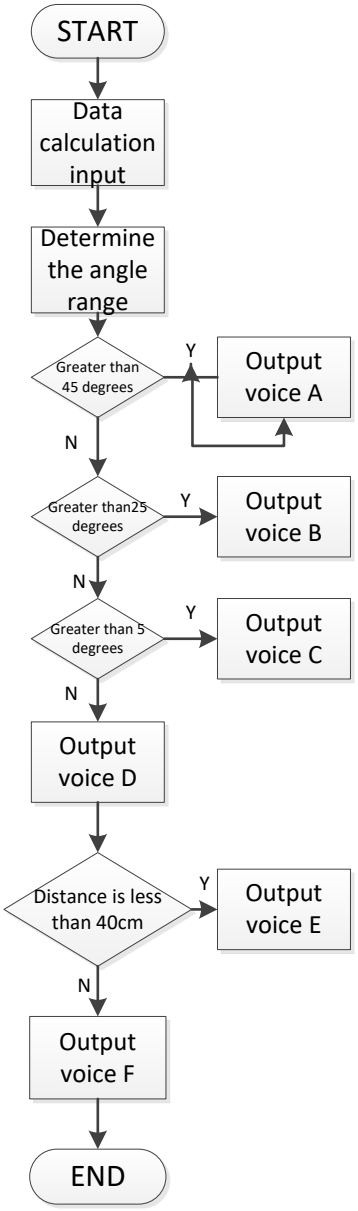

Fig.6 flow chart

Final test,using tools to simulate garage and vehicle,artificial simulation reversing environment,test the different reverse angles, test results is good,system running normally.When the reverse angle is greater than 45 degrees,voice prompts too large reversing angle reversing;In the reverse angle of 45 degrees -25 degrees between the tips is to keep the steering wheel does not move,please continue to reverse;When the reversing angle is less than 25 degrees and greater than 5 degrees, please slow down the steering wheel;When the angle is less than 5 degrees, the reasonable angle,can continue to reverse.In the distance, when the distance from the car and the rear wall is less than 40 cm issued a security warning[5].

VI. CONCLUSION

In this paper based on raspberry pi multi-sensor fusion intelligent parking assist system,By using the structure of raspberry pie has powerful function and small size itself,the accurate measurement of the distance and the temperature compensation of the US-100 ranging module,the distance and angle of the distance from the wall are obtained accurately,and the voice output function of pi,voice prompts for drivers,so that the driver can be simple, convenient and safe backing.Besides， Raspberry pie is very powerful,you can also add other features on this basis,very practical[6].

References

[1] Wensheng Li.To explore the development of embedded Linux teaching based on raspberry pie [M].Electronic technology and software engineering,2014.

[2] Ping Zhang.Principle and application of ultrasonic sensor[M].Examination weekly,2011（62）.

[3] Longqi Li,Meifa Fang,Xiaoteng Tang.Raspberry pie development platform of the real-time monitoring system[W].Minjiang University Journal,2014.

[4] M Richardson, S Wallace. Getting Started with Raspberry Pi[J]，2012.

[5] E Upton, and G Halfacree. Meet the Raspberry Pi[J]，2012.

[6] E Upton, and G Halfacree. Raspberry Pi user guide[C]，2014.

Design of New Type Indoor Air Purifier System Based on MSP430

ZHU Yunan; REN Xiaochuang; LIU Guohong

(College of Instrument Science and electrical engineering,Jilin University,Changchun 130021)

***Abstract*—Now the air pollution problem is increasingly serious, people are increasingly concerned about the quality of indoor air, the market is also a wide variety of air purifiers, air purifier function, technology, user experience is also different, but overall, the use of purification Single material, the purification effect is not good enough, and the purification efficiency is low, not efficient enough. Most importantly, it is important to control CO_2 concentrations for small indoor spaces where people live, and existing products do not control CO_2 and ignore the adverse effects of high CO_2 concentrations on the human body. Therefore, for these problems, Report and the analysis of market demand, integrated existing resources and conditions, we have designed a design for the living environment of air quality testing and purification devices, the use of MSP430 as a controller, the system can display real-time data on the LCD screen, through Serial communication, the host computer shows the results of purification. In addition to these basic functions, we have added the CO_2 module to monitor and control the CO_2 concentration. At the same time, the design of the use of composite composite materials to build a filter system, making a variety of pollution can be purified, the purification capacity of more than 50% of a single structure of the purifier to enhance,the design of the use of vertical double fan cycle system, making the filter efficiency increased 30% more than the centrifugal fan structure.**

***Key words*—PM2.5 CO_2 MSP430 HEPA purifyI.**

I INTRODUCTION

WITH the increasing living standard, the indoor environment has been paid more and more attention. Indoor air quality inspection device has been applied to home, office and other fields. When design the circuit, whether the developer or the user, will pay more attention to the purification process after the detection of air quality[1]. The indoor environment is closely related to human health, and the indoor air detection and purification device can effectively improve the indoor air quality[2]. Indoor air detection purification refers to the detection of indoor air pollutants, when the pollutants beyond a certain range, the purifier work, from the air to separate or remove one or more air pollutants.Indoor air purifier equipment sub-industrial, military and civilian three, of which China's earliest from the late 1960s began to use civil air purifier[3]. Indoor air purification involves both interior and interior spaces of manned spacecraft, submarines, aircraft and various types of vehicles[4]. Several current purification technologies include adsorption filtration technology, nano-materials photocatalytic technology, low temperature plasma technology, ozone technology, biological purification technology and membrane separation technology[5]. The adsorption filtration technology because of the high efficiency of removal, enrichment and strong, suitable for almost all of the odor of harmful gas treatment[6], and thus is more commonly used methods to remove harmful gases. It is also the method used in this research.In recent years has developed a variety of new activated carbon adsorbent, the current research focused on the application of activated carbon adsorption and adsorption performance improvement[7]. Among them, ACF due to adsorption capacity, adsorption speed and other superior performance, much attention. Japan is the first one who use ACF for organic waste gas treatment technology, since then the study has been obtain people's attention. China's research on activated carbon adsorption has also made great progress.In the future, indoor air quality inspection and purification system must move towards high precision, multi-functional, integrated and systematic development[8].

Through the analysis of the current situation of air quality detection and purification system, we know

that the relevant domestic research practice has been more systematic, but there is still a gap with foreign countries[9]. The main drawback of domestic research is that the purification effect is not particularly good, the portability and accuracy are also lacking, and do not have the function of CO_2 detection.However, the CO_2 concentration is relatively high, and long-term high CO_2 concentration in the environment will cause dizziness, nausea and other hazards (as shown in Table 1).

Table1

CO_2 risk list

CO_2 concentration（ppm）	350~700	700~1000	1000~2000	2000~5000	>5000
Harm to the human body	none	Slightly discomfort	Dizzy, sleepy	Headache,rapid heartbeat, nausea	Permanent brain damage, and even death

In view of these problems, based on the research report and the analysis of the market demand, based on the existing resources and conditions, we have formulated and designed a device for the detection and purification of air quality in the living environment. Considering the large population in the interior space, The CO_2 module was added to monitor and control the CO_2 concentration. At the same time, the design of the composite composite material to build the filter system, making the purification effect is greatly improved, the design uses a vertical double fan circulation system, making the filter efficiency increased by 30% or more.

II. System Overall Design

The system mainly includes acquisition module, control module, power module, purification module, and display monitoring module. The overall structure of the system shown in Figure 1.

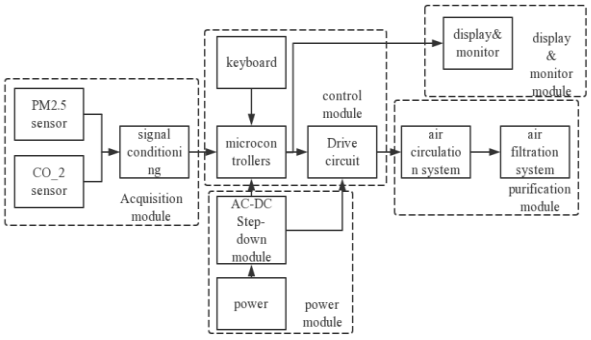

Fig.1 The overall structure of the system

The system through the PM2.5 sensor, CO_2 sensor to collect information, processed by the microprocessor, through the MSP430 serial port to send data to the host computer,And show real-time data on the display.Press the key to set the threshold, when the data below the set upper limit, The controller controls the purifier to work until the data reaches the lower threshold and the purifier stops working.

For the system function and the actual situation considerations, the system technical indicators parameters as shown in Table 2：

Table2

Technical Parameters list

technical indicators	Work atmosphere	PM2.5 measuring range and accuracy	CO_2 measuring range and accuracy	purification capacity
index	-10℃~30℃	0~999μm/m^3（±5%）	0~2000ppm（±50ppm）	30m^3/h

III. System Hardware Design

A. Acquisition Module Design

As shown in Figure 2, the acquisition module consists of CO_2 sensor, PM2.5 sensor, signal conditioning circuit. The main task is to collect the data, sent to the main controller.

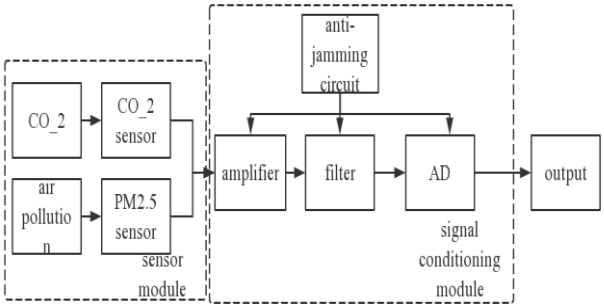

Fig.2 acquisition module structure

1. The PM2.5 Sensor

The PM2.5 sensor using DSL-01 laser dust sensor,using light scattering principle, the laser particles in the scattered light generated by the photoelectric receiver into electrical signals, and then through a specific algorithm to calculate the PM2.5 mass concentration.The sensor is a digital output type,small size,accurate detection and consistency, to ensure the accuracy of PM2.5 detection and system stability.

2. The CO_2 Sensor

The CO_2 sensor uses MH-Z14A CO_2 sensor, which uses non-dispersive infrared principle to detect CO_2 in the air, with good selectivity and anaerobic dependence, long life, built-in temperature compensation. Provide a variety of output mode, lower prices and better performance, in full compliance with the system design needs.

B.Control Module Design

The control module mainly comprises a keyboard control module and an MCU module.Mainly processing and analyzing data.

1. The MCU Module

MCU uses MSP430F449 microcontrollers, it has low price, fast, anti-interference and low power consumption advantages, as a 16-bit processing chip, fully capable of performance requirements of the system, while low power for the system is also very important, so choose MSP430 as the main controller.

2. The Keyboard Control Module

Keyboard control using eight independent mechanical buttons connect with MCU.It is used for PM2.5 concentration upper limit setting, lower limit setting, CO_2 concentration threshold setting,and controlling the start and stop of the purifier.

C. Purification Module Design

The purification module is mainly composed of the filter system and the circulatory system, the module receives the command issued by the control module to provide pollution purification, clean air function, the purification system structure is shown in Figure 3, the air through the circulatory system into the purifier cavity, followed by Through the electrostatic filter and coarse filter composed of the primary filter, activated carbon filter, high efficiency HEPA filter, to purify the air.

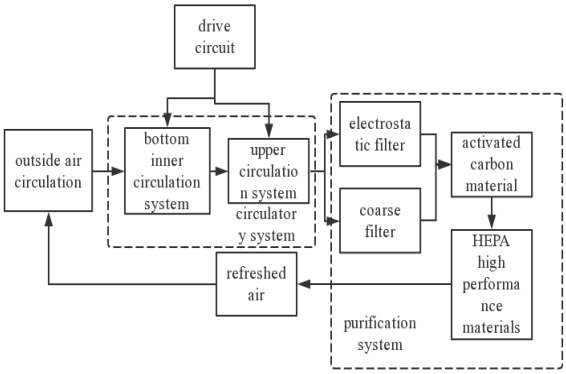

Fig.3 purification system structure

The purification system is shown in Figure 4, the air in the role of the circulatory system, was pumped into the purifier cavity, through the composite material purification filter, the vertical double-layer fan sent out, and indoor air exchange, the formation of the cycle. To achieve the role of air purification.

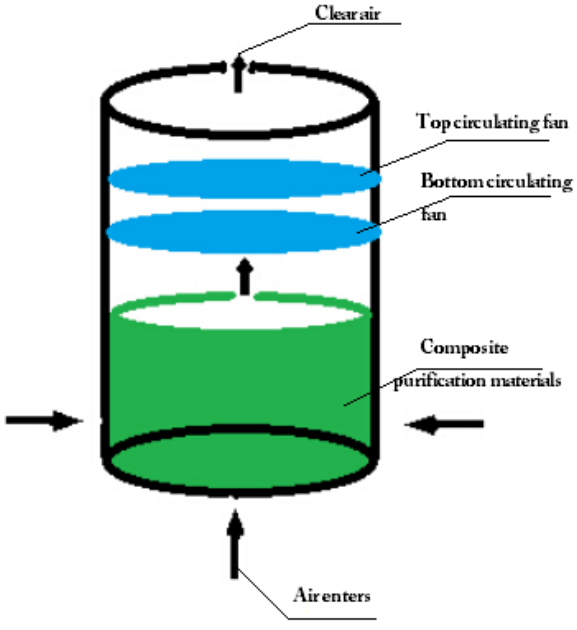

Fig.4 purification system diagram

The traditional filtration system technology with a single structure shows a weak purification effect[10]

(as shown in Table 3).

Table3

Traditional filter consequent

Purification Technology Contaminants	Suspended particles Dust, pollen, cigarette smoke, soot and other diameter: 0.01—100 μm	Harmful gas Formaldehyde, benzene, ammonia and so on diameter: 0.0001—0.001μm	Microorganism bacterial diameter: 0.2—10 μm	Microorganism virus diameter: 0.01—0.3 μm
Filter Adsorption	effective	invalid	invalid	invalid
	Partially effective	Efficient	Partially effective	invalid
Washed with water	effective	Partially effective	invalid	invalid
Static electricity	effective	Not obvious	Partially effective	invalid
Negative ions	effective	Not obvious	Partially effective	invalid
Photocatalytic	Not obvious	effective	effective	effective
Plasma	Not obvious	effective	effective	effective
Ultraviolet	invalid	invalid	Efficient	Efficient

We designed the filter system using composite adsorption filtration technology shown in Figure 5.

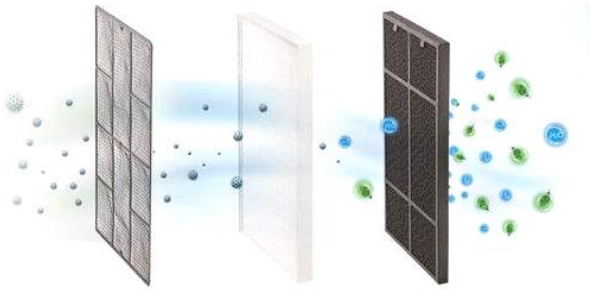

Fig.5 Filter system material diagram

It combines the initial filter &HEPA high efficiency filter&high quality activated carbon structure, combined with the advantages of a variety of materials (Table 4), into the lungs particles, respirable particulate matter, and irritating chemical gases are harmful to the human body of the air pollution source has a strong purification effect, for more than 0.3 micron particles purification rate of ≥ 99.97%, so that purification purity has increased by 50% or more than single-layer HEPA material.

Table4

Filter system material functions

structure	Early filter	HEPA filter	High quality activated carbon
Purify contaminants	Dust, fines, hair and so on	pollen and so on	Formaldehyde and so on

We designed the circulatory system for the vertical double fan circulation system, so that the indoor air faster and more efficient through the purifier cycle,as shown in Fig. 6 (red), the theoretical circulation air volume is more than 30% higher than that of the traditional structure under the 300 Pa wind resistance (HEPA200Pa plus other losses 100Pa). Improve the air circulation speed, to prevent the CO_2 concentration is too high on the human body harm.

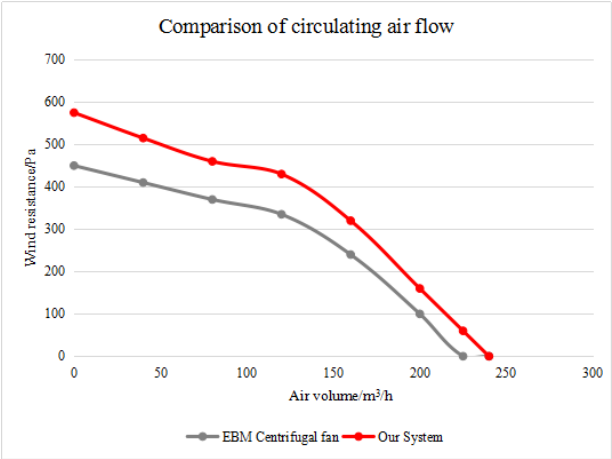

Fig.6 comparison of wind turbine air volume

D. Display Donitoring Module

Display module using Nokia5110 display screen, displaying CO_2 concentration value, CO_2 threshold, PM2.5 upper limit, PM2.5 lower limit, the current PM2.5 concentration value and so on. Monitoring module through the serial port to receive pollution concentration value, sent to the host computer, real-time data monitoring and data logging.

E. Power Supply Module

The power supply module is divided into 220V AC and AC-DC modules. The purification system uses 24V DC power supply,and the controller uses 5V DC power supply.

IV. System Software Design

A. Overall Program Design

Dust sensor detection data and sent to the MSP430, MSP430 comparing it with the threshold, if the concentration exceeded, will make the relay pull, and then drive the purifier to work.If the concentration reaches the standard, it will continue to be tested. When the purification system is working, the MCU will control relay disconnected when the concentration is reduced to meet the requirements,and the purge is

completed. The overall software flow chart of the system is shown in the Fig 7.

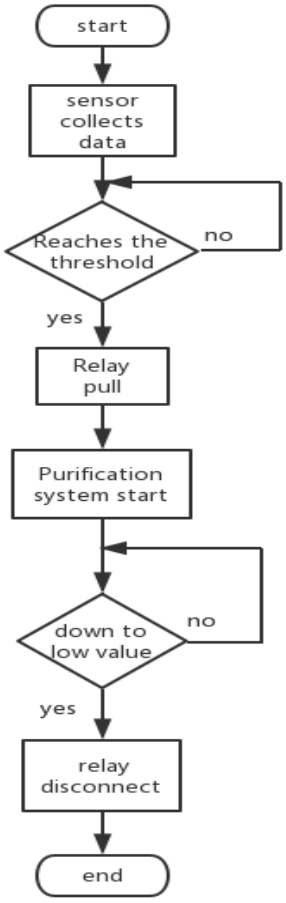

Fig.7 The software flow chart of the system

B. Data Acquisition Program Design

The CO_2 data is analog and converted to digital using the 12-bit AD in the MSP430,and then sent to the MCU for processing.The PM2.5 data is digital, through the program to read out the value, and sent to the MSP430 for processing. The data acquisition program flow chart is shown in the Figure 8.

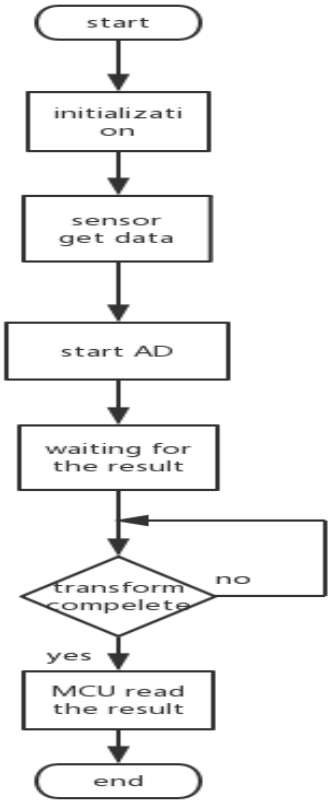

Fig.8 Data acquisition program flow chart

C.Host Computer Monitoring System Program Design

Using MATLAB to write the program, the host computer through the serial port to receive pollution concentration data, and after the numerical conversion real-time display it in the monitoring interface.

V. TEST AND ANALYSIS

A. Air Detection Purification Test

After connect the system line, turn on the 24V DC power supply, simulate the change of the concentration control signal of the PM2.5 through a lighted cigarette, simulate the CO_2 concentration change through the CO_2 cylinder, test the working condition of the system and the measuring range. As the time increases, the value of the bin is increasing on the display, and the CO_2 value continues to increase. When the upper limit is increased, the purifier starts to work and the purifier stops working until the value drops below the preset limit. When PM2.5, CO_2 concentration reaches the upper limit, the warning light is on, the concentration drops to the lower limit when the warning light goes out. After several tests, the system works well. Can achieve the desired target, CO_2, PM2.5 measurement range shown in Fig.9&Fig.10.

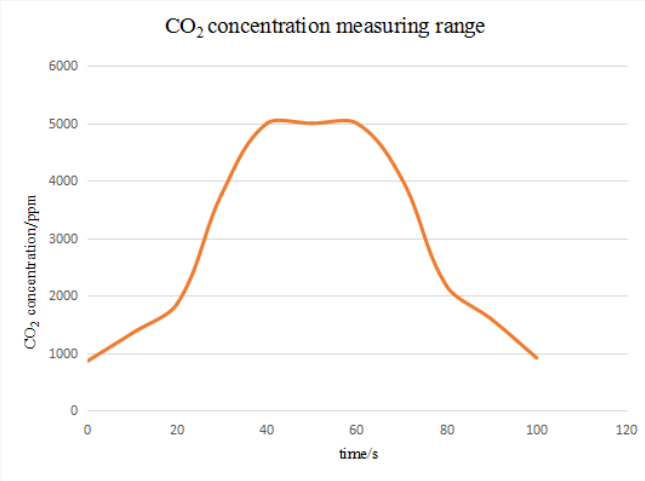

Fig.9 CO_2 concentration measuring range test chart

It can be seen from Fig. 9 that the CO_2 concentration is in the range of 0 to 5000 ppm.

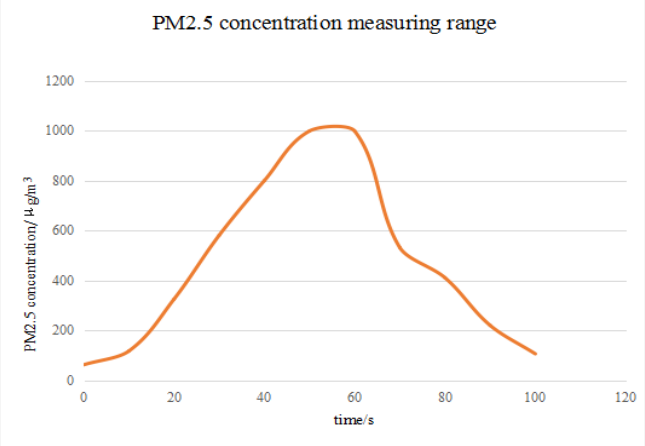

Fig.10 PM2.5 concentration measuring range test chart

It can be seen from Fig. 10 that the PM2.5 concentration is in the range of 0 to 1000 μg/m^3.

After that, the performance of the system is tested according to the technical specifications. In the same environment, and TSI8530 standard instruments for comparison, the detection accuracy of PM2.5 test, the test time is 100 minutes. The test results are shown in Figure 11.

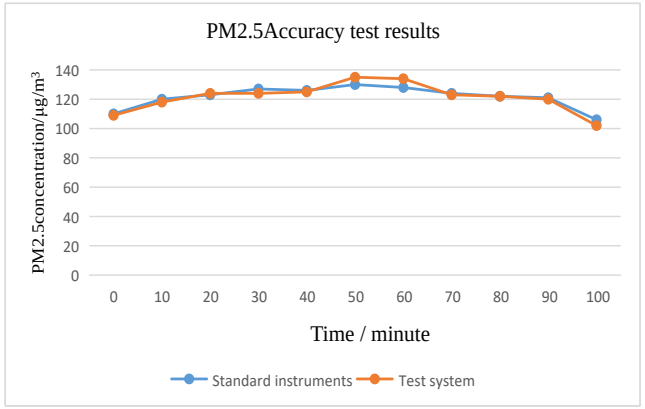

Fig.11 PM2.5 accuracy test test chart

It can be seen from the figure, with the standard instrument control, PM2.5 detection error <5%.

In the same environment, with the HT2000 standard instrument for comparison, the accuracy of CO_2 testing, testing time is 100 minutes. The test results are shown in Figure 12.

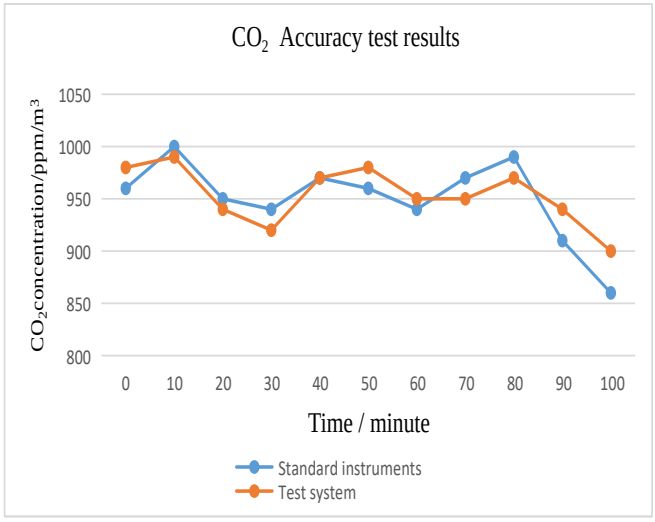

Fig.12 CO2 accuracy test test chart

It can be seen from the figure, compared with the standard instrument, CO_2 error <50ppm.

In the 40m^3 indoor space, the system purification capacity of the test, the test results shown in Figure 13.

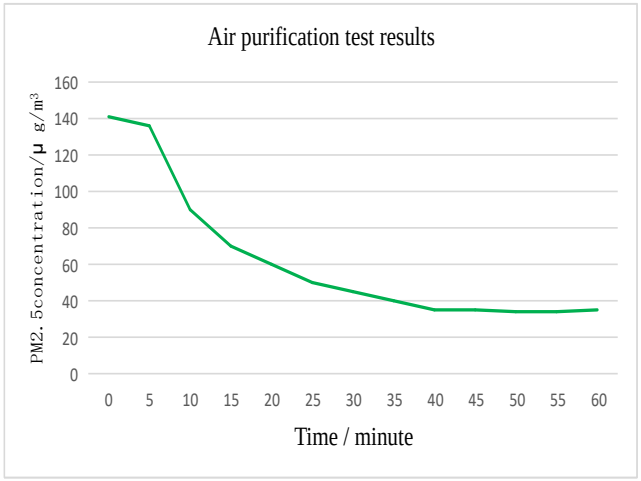

Fig.13 System performance test chart

It can be seen from the figure, the system within 40 minutes to reduce the concentration of pollution to a normal level, the system purification capacity of more than 40m^3/h, meet and exceed the technical requirements.

Overall, the system PM2.5 detection range 0-999μg/m^3, the error is less than 5%, while the CO_2 detection range of 0-5000ppm, the error is less than 50ppm. System purification capacity greater than 40m^3/h. The results are shown in Table 5.

Table5

Test results list

technical indicators	Work atmosphere	PM2.5 measuring range and accuracy	CO_2 measuring range and accuracy	purification capacity
index	-10℃~40℃	0~999μm/m^3 (±5%)	0~2000ppm （±50ppm）	40m^3/h

We tested the purification purity of the system and purified the interior space in the same environment. As shown in Figure 14, compared with the general purification structure of the single-layer HEPA structure, the lowest concentration of pollution could be reduced to below 20, while the single-layer HEPA structure The pollution concentration of the lowest to about 30, we can see that the purification purity than HEPA single-layer structure increased by 50% or more.

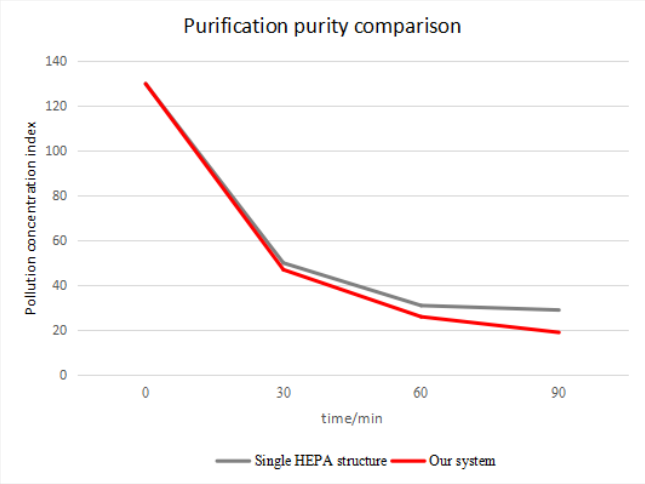

Fig.14 Comparison of purification purity chart

We tested the system purification efficiency,which is in the indoor space of the same starting concentration and purified in the same environment. As shown in Fig.15,the pollution concentration index is reduced to 40 in 40 minutes in comparison with the EBM general structure purifier, which took 63 minutes, It can be seen that the purification efficiency has increased by 30% or more than the traditional structure.

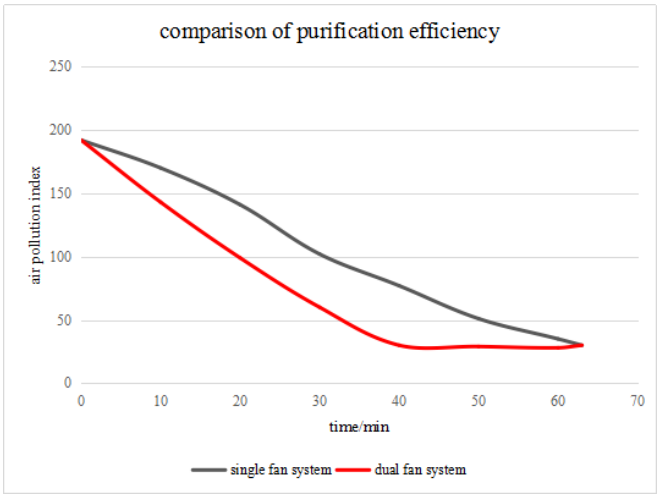

Fig.15 Comparison of purification efficiency chart

B. Host Computer System Test

The host computer receives the data transmitted by the MCU through the serial port, realizes the real-time monitoring function.After several tests, the host computer can clearly and intuitively display the real-time value of PM2.5 concentration and the change situation, the system works well and stable.

VI. CONCLUSION

This essay presents a design scheme of indoor air quality detector, which is controlled by MSP430. The concentration of PM2.5 is collected by the CO_2 sensor and the PM2.5 concentration is collected by the serial communication and AD technology. The PM2.5 concentration is compared with the set value Judgment, through the relay of the strong weak conversion, to achieve the automatic control of the purification system, through the 5110 display, the PM2.5, CO_2 concentration state value, set the threshold displayed, the keyboard can operate on the set value, and the value Through the serial port sent to the host computer interface, to achieve real-time monitoring and data logging. Innovative combination of the actual need to add a CO_2 module, and a variety of composite materials combined into a filter system, making a variety of pollution can be purified, purified purity than a single HEPA structural purifier has more than 50% enhancement, design Using a vertical double fan cycle system, making the efficiency of filtering has increased by 30% or more than the EBM single centrifugal fan structure.

References

[1] Cheng Yuanyuan, Guo Ting, Geng Chunmei, Yu Haiying, Wang Fangyuan, Xu Haiya. New Status of Indoor Air Pollution and Pollution Control Technology [J]. Environmental Science and Technology, 2013, (S2): 229-231 + 235.

[2] Ma Chao.State and development trend of indoor air pollution purification technology [J]. Environmental Engineering, 2011, (S1): 168-170.

[3] Xiao Feng, Mei Bo, Wei Li-hong, Li Zhan-chen, Kang Xiao-ou, Yang Shuo.Study on Application Effect of Indoor Air Purification Technology [J]. Journal of Safety and Environment, 2015, (06): 202-206.

[4] Sheng Fangfang, Qiu Limin, Yu Chuan, Zhang Lin, Song Jia, Yan Renyuan. Indoor air purification technology and product overview [J]. Journal of Refrigeration, 2014, (05): 14-18 +37.

[5] Yu Xiao-ping, Liu Li-ying, Li Wen-jie.Effects of CO_2 Concentration on the Minimum Fresh Air Volume Standard in Indoor and Outdoor [J]. HVAC, 2015, (05): 21-26.

[6] Xu Kai-yun, Chen Li-ping, Gong Yan-feng, Zhou Bin.Numerical Simulation of Influencing Factors of PM Particles (PM2.5) [J]. HVAC, 2016, (09): 120-123 + 20.

[7] Yao Jia, Zhang Zi-jia, Zhu Li.Design of Intelligent Indoor Air Purification System [J]. Electronic Devices, 2015, (01): 203-208.

[8] Xie Hui, Zhao Shen, Cao Guoqing. Control Standard and Comparison of PM2.5 at Home and Abroad [J]. Building Science, 2014, (06): 37-43.

[9] Wang Guo-ping, Nie Hui-fen, Wan Zhi-qiang,

[10] Wang Hui.The development of small indoor air purifier based on Atmega16 single chip microcomputer [J]. Manufacturing Automation, 2012, (16): 128-130.

[11] Wu Ning, Shang Baoli, Cai Zhuoen.Study and Design of Indoor Air Detection and Purification System Based on Single Chip Microcomputer [J]. Automation and Instrumentation, 2015, (02): 105-106.

The Design of Intelligent Residential Security System

Mingyang Sun; Libin Wang; Zhengan Nie
（*Jilin university instrument science and engineering institute,Changchun,130026*）

***Abstract*—The system will comprise fingerprint identification, video transmission and other technology applied in the housing security system research, in the establishment of the related module and program writing, on the basis of establishing the complete intelligent security system of the house. The whole residential intelligent security systems in security based on infrared pyroelectric devices, video fingerprint identification device, transmission device, and air conditioning system based on temperature control stepping motor devices, smoke alarm device. The whole system interlocking, the function is all ready. System after relevant debugging, meet the relevant requirements, and can be further extended related functions.**

***Keywords*—MCU Video transmission Control stepping motor Fingerprint recognition technology Pyroelectric infrared device**

0 PREFACE

RESIDENTIAL intelligent security system is the use of door window detector, the human body movement detector, gas detector and smoke detectors such as the new components, with a perfect control, communication and alarm system able to living in the life easy to produce risk warning, the integrated system of the warning role[1].

As people living standard rise, people more and more attention to housing security, so residential intelligent security system also arises at the historic moment, with the development of technology, to further improve system availability, residential intelligent security system will eventually get social recognition[2].

1 EXPERIMENT CONTENT

1.1Smoke Alarm Device

This design by sensor and single chip microcomputer as core components of smoke alarm design, in combination with other devices can be realized sound and light alarm, automatic exhaust ventilation and fire extinguishing, and other functions.Microcontroller STC89C52 chosen as the control device, in the design of sensor selection of MQ - 2 type semiconductor gas sensitive element smoke sensor for detecting smoke.Smoke alarm is mainly composed of smoke signal acquisition and preamplifier circuit, analog-to-digital conversion circuit, single-chip microcomputer control circuit, display circuit, sound and light alarm circuit and safety protection circuit, reasonable design, simple and easy to understand, the price is low, make SCM are fully applied in the smoke alarm system control, has a certain practical value.

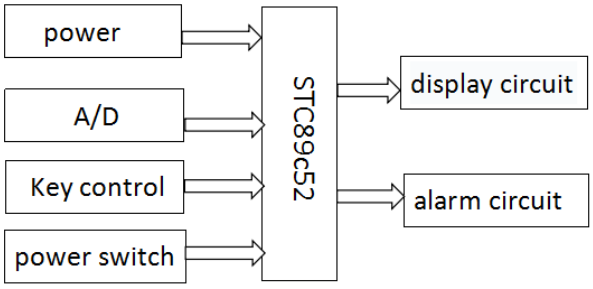

Figure 1 circuit diagram of the total

1.2Temperature control stepper motor drives

This device through collecting DS18B02 digital temperature sensor temperature to control the step motor rotation.Based on 51 single chip DS18B20 as the core temperature automatic control system, temperature detection, temperature display function, and can according to the preset program control operation functions, including: building SCM smallest system, including the reset circuit, power supply circuit, clocking circuit, to join the display module, using DS18B20 temperature data collection, implement different temperature control of the stepper motor speed.

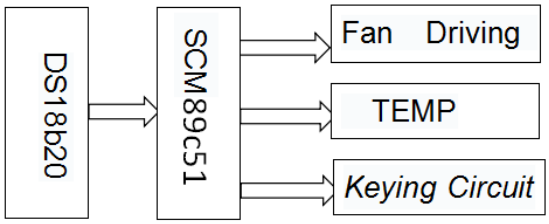

Figure 2 system design structure diagram

1.3 video real-time transmission function

Camera video transmission system used in embedded door, form the monitoring device, formed in the door video sampling end of video image acquisition. Implementation of video transmission in the barrier-free space simulation.

System is mainly divided into two parts, video sampling end and receiving end, video sampling requirements acquisition device installed in a fixed position, complete the video acquisition, image compression, digital transmission ways in the form of PZP complete the wireless image transmission. The receiver in the use of screen as the main body, with wireless data receiving device to complete video accept, decompression, preservation and display of work. The whole system run time video camera area can be received signal real-time transmission to the receiver.

Orthogonal frequency division multiplexing (OFDM) is the basic thought of multiple parallel low speed data stream and mutual orthogonal modulation in the corresponding number of subcarrier on transmission. Due to the subcarrier orthogonal each other, so when the receiver demodulation there is no interference between each subcarrier. So the choice of a transmitter and a receiver TS832 adopt orthogonal frequency division multiplexing technology and RC832.Because of the 5.8 GHz wireless broadband access system can provide telephone, video, high speed data access; Risk investment is small, low startup costs, the initial user environments; Easy expansion, enlarge the coverage area, meet the needs of users rapidly increasing; Simple, reliable, reduce maintenance costs; Packing and unpacking, it is easy to move, to guarantee the *investment* without precipitation; With flexible interface capabilities, in order to adapt to and different network connection, etc. So we chose to use 5.8 GHz frequency band transmitter and receiver devices.

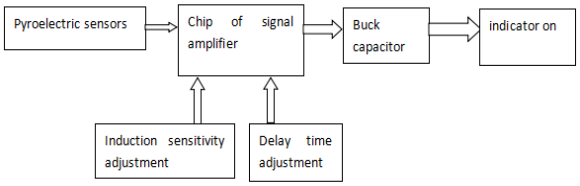

Figure 3 Pyroelectric infrared device unit block diagram

1.4 The Fingerprint Identification Device

Make a STC89C52 SCM as the core controller.Through SCM serial communication to send commands to control the fingerprint identification module for the work of storing and matching fingerprints.The concrete principle of work is as follows：

(1)The Process of Fingerprints Logging In

When fingerprints log in ,the instructions are sent by STC89C52 SCM.Through optical sensors for each fingerprint entry twice，then dispose the two input images to compound a template stored in the module.

(2)The Process of Fingerprint Matching

Through the fingerprint sensor to entry and process the fingerprint image that needs to be verified，then match and compare with the fingerprint template in the module（Matching a specified template in the module is called the fingerprint matching method, named 1:1;Matching multiple templates is called the fingerprint searching method, named 1: N）,and the module gives matching results (pass or fail).The results transmit to SCM through the serial port,At the same time the SCM react accordingly to control the Liquid crystal to display ，the relay to close or the Indicator light to be turned on，and control the switch of pyroelectric infrared alarm device through the relay.

The fingerprint identification device specific component unit block diagram as shown in figure 4:

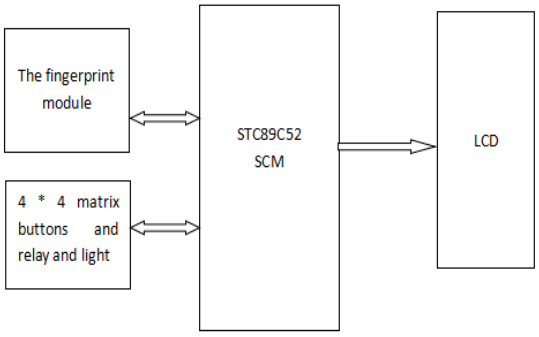

Figure 4 The fingerprint identification device unit diagram

2 EXPERIMENTAL PROCESS

2.1Smoke alarm

The most basic part of the alarm system should include: the signal acquisition module conversion circuit, single-chip microcomputer control circuit, characters display circuit, sound and light alarm circuit and safety protection circuit and other parts.

Alarm using delay works, smoke detector alarm STC89C52 single-chip microcomputer as control core, selects the MQ - 2 semiconductor gas sensor to collect smoke smoke concentration information, cooperate with peripheral circuit constitute a smoke From the design requirements for the analysis of the design shall include the following structure: smoke detection part, STC89C52 single-chip microcomputer control part, alarm, four most AD collection.

The processor with 51 series microcontroller STC89C52.The whole system is the system software work under control.Set on the monitoring of smoke detection probe to detect the smoke into electrical signals, sends out the analog signals, to the AD sampling circuit.Within the single chip microcomputer, the query and recognition judgment of real-time signal smoke alarm state control.And drive buzzer alarm indicator light alarm[3].

2.2Temperature control of stepping motor drive

Fan based on single chip microcomputer temperature controller adopts DS18B20 sensors, to detect the temperature of the converted into digital signals, the microcontroller to analyze the input digital signal processing, when the temperature is higher than the threshold value, the fan is spinning at full speed;When the temperature is lower than the lower limit, fan stalling;Between when the temperature in the upper limit and lower limit value, the fan speed according to the setting of an intermediate value.

```
{
                temp=get_temp();
                EA=1;
                dis_buf[1]=temp/100;
                dis_buf[2]=temp/10%10;
                dis_buf[3]=temp%10;
                xsd=2;
                if(temp<limt[0])
  {grade=0;}                              else
if(temp<limt[1])          {grade=1;}
      else if(temp<limt[2])          {grade=2;}
                          else if(temp>=limt[2])
    {grade=3;}

                dis_buf[0]=grade;
                if(grade==0)   dis_buf[0]=10;
            }
        }
        if(grade>0)
            motor_ffw(G_value[grade]);
        if(k) key_do(k);
        }
```

2.3 video real-time transmission function

The following functions:

(1) The client part. Will get the video and audio/video capture device audio signal to MPEG4 code encoder, the encoder output data is encrypted, transmitted to the user units of 5.8 GHz wireless transmission system;

(2) The wireless transmission part of the wireless network signal transmission application is 5.8 GHz wireless bridge equipment, it is a kind of simple use, plug and play type wireless Ethernet communication equipment, it can be dispersed within a few kilometers between adjacent buildings provide people with good and high performance wireless network service. Wireless Bridges for point to multi-point wireless connection;

(3) Part of the VLAN switches VLAN switches may, according to Mr SU and bsus VLAN label, will be the same information output to the specified port of virtual group. VLAN switches can isolate the flow of data between different computing unit, which helps to establish a separate between source and destination of the transfer, which does not exist in the network data flow has multiple purposes, made on the same network, can provide service for multiple units of the user at the same time at the same time, to make better use of the network bandwidth. Virtual LAN also can simplify the management of the network.

Monitoring host used in video monitoring system. Monitoring host can be used as a digital audio monitoring server, include the MPEG audio compression and transmission software, such as MPEG video decompression software, realizes the control channel multiplexing. Our video transmission

device is based on this principle, within the residential space in accessibility to monitor real-time transmission of the picture.

2.4 pyroelectric detectors

Pyroelectric sensors are sensitive to temperature sensors. The human body has about the constant temperature of 37 ℃. So have a wavelength of about lO mu m infrared. Pyroelectric infrared sensor is about 10 microns of ir detecting human work. Pyroelectric infrared sensor is a polarization of hot crystal or referred to as a "ferroelectric". When the infrared radiation to have thin section of polarization of the electric iron on the surface, cause the chip temperature. Reduce its polarization. Surface charge less.This is equivalent to release part of the charge, it is called a pyroelectric infrared sensor. If the load resistance and ferroelectric thin slices are linked together, the load resistance and produce an electrical signal output. Output signal depends on the size of the chip temperature the speed of change, to reflect the infrared light intensity of the incident. Thus, pyroelectric infrared sensor voltage response rate is proportional to the incident rate of infrared light.When a constant infrared irradiation on the pyroelectric infrared sensor, the sensor without electrical signal output, and only the ferroelectric in change process have electrical signal output. So, there must be alternating infrared irradiation, cause the temperature of the sensor, can cause the pyroelectric alternating signal and output. We use this feature to make it to principle as alarm detection device[4].

2.5 The Fingerprint Identification Device

2.5.1 Specific Hardware System Architecture Design

Fingerprint identification module needs high recognition rate, fast processing speed, and high accuracy，So we define to use FM - 70 optical fingerprint collection device.Liquid crystal display module LCD12864 can display 4 * 8 Chinese characters, and the interface is clear, so we choose LCD12864.The SCM need quick calculation and control, as well as a large storage space, so we choose STC89C52.The independent DC power supply uses a USB line to 5 v power supply, and the keys USE 4 x4 independent type.

(1)STC89C52 core processor

P0, P1, P2, P3, a total of 4 * 8 = 32 pins.These pins are mainly used as I/O input and output to control some external devices, such as LED lights, switches, etc.The P3 port has special uses, it can be used for serial transmission and interrupt and timer, this design mainly uses the P3 port.

(2)The clock circuit

Clock circuit is the heart of the single chip microcomputer and the source of power, controls the work of the SCM.The SCM sends signals to other components to drive the operation of the SCM through clock signals.

(3) FM - 70 fingerprint identification module

For the selection of fingerprint identification module of this system, the FM - 70 fingerprint identification module is chosen.This series of optical fingerprint module are based on high-speed DSP processor as the core, combined with optical fingerprint sensor with independent intellectual property rights,without the upper computer participating in the management, it has fingerprint inputting, image processing, fingerprints searching and templates storing and other functions. There are a total of 6 external pins of FM - 70 ,the function of each pin shown in the following table1:

TABLE 1 THE FUNCTION OF THE PINS

Pin Number	Name	Type	Functional Description
1	Vtouch	In	Input of the touching induction power supply
2	Sout	Out	Output of the Induction signal
3	Vin	In	positive input of the module power supply
4	TD	Out	Serial data output, TTL logic level
5	RD	In	Serial data input, TTL logic level
6	GND	-	Signal ground, connected with the internal power supply ground

(4)The relay and LED module

LED is connected to the P3.6 pin by a PNP transistor, and SCM reset pin is high level, If we use NPN transistor, after the SCM's reset it'll be on state, and LED will light up,so we need to chose PNP transistor.When P3.6 pin is at high level, transistor doesn't breakover, LED lamp doesn't light up; When P3.6 pin is at low level, transistor breakover, LED lamp lights up.

(5)LCD12864 Liquid crystal display module

We choose the type LCD12864 as the liquid crystal display module, it is a complete module, only need to send instructions to the module to complete the corresponding work. LCD12864 module contains font library and processor, has its own set of instruction system, according to the instruction system in the

manual, in accordance with the provisions of the instruction format to send instructions to the module ,to complete the corresponding functions.

2.5.2 The implementation of software system

(1) The program design of fingerprint identification module

As a fingerprint identification module, FM - 70's inside has completed, we only need to appropriate orders to the module to realize the control of the module, and then realize some corresponding functions.Different function needs different instructions to implement, and each instruction has a prescribed format.

The tasks that need to be completed by Fingerprint identification module are : access to fingerprint images, to generate templates of fingerprint characteristic, and storage of fingerprint templates and the fingerprint characteristic matching work. According to the instructions of the module system,the SCM sends instructions' information to the module, and control the module to complete the corresponding work.

The flow diagram of fingerprint entry process is shown as figure5:

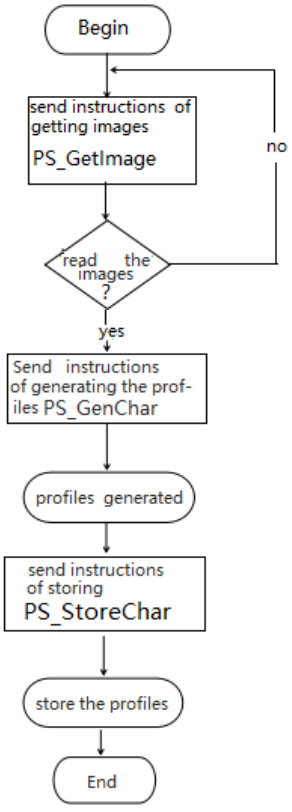

Figure 5 fingerprint entry process flow chart

Fingerprint entry process is for the registration of new users, when there are new users need to register , get the user's fingerprint image at the head of fingerprint first, then generate the template of fingerprint characteristic, then store the template, and the new user's registration is completed.

The main instructions in the process of fingerprint entry :

①Input image PS_GetImage：Scan the detected finger, and form the image, it'll be used in later steps.

②Generate characteristics PS_GenChar:make the original fingerprint image we've got to generate the file of fingerprint features.

③Store template PS_StoreChar:Make the generated files of fingerprint features stored in the flash, they won't lost when power supply drop.

According to format of the three instructions,design corresponding subroutine in the SCM's program, and try to call them,so that we can finish the above functions.

The flow diagram of Fingerprint identification process is shown as figure 6:

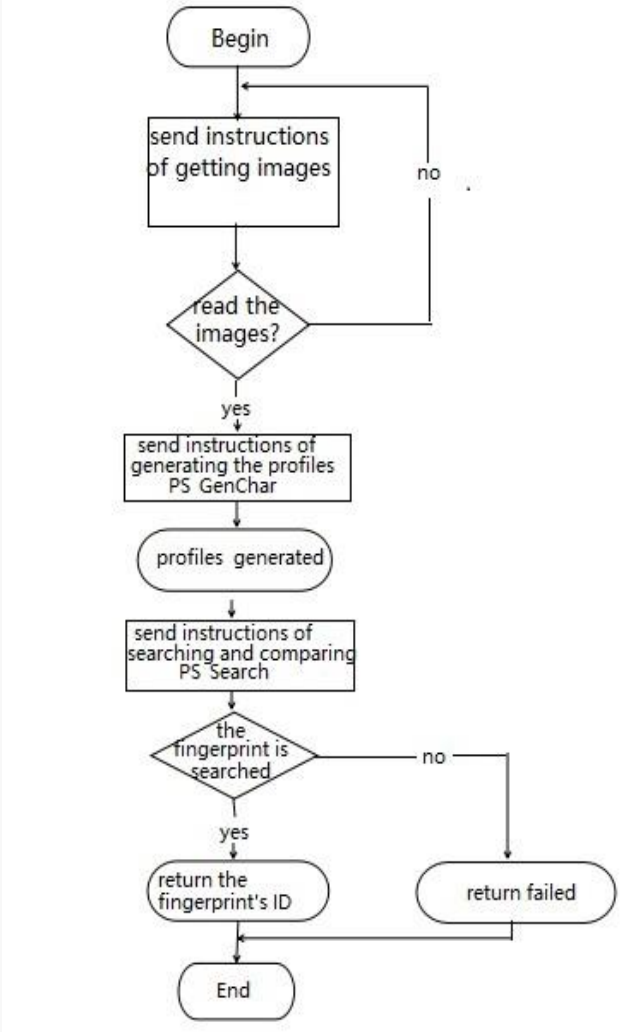

Figure 6 fingerprint identification process flow chart

Fingerprint identification process is similar to the

fingerprint entry process,they both need to get the fingerprint images first, then generate feature templates according to the images.After get the fingerprint feature templates in the fingerprint identification process, contrast with the repository of fingerprint templates, if it succeeds, it'll returns the ID of corresponding fingerprint template; If it fails, it'll return failure.

Fingerprint search PS_Search: Based on the files of fingerprints' characteristics in charbuffer to search the entire fingerprint, and returns the result.

Using the instructions' system given by FM - 70 fingerprint identification module, to design the programs of the fingerprint identification module's part , through such a fingerprint inputting and identifying process, it can realize the function of user's fingerprint inputting and identifying, then use the SCM to control the locks and the communication with the upper computer, etc.

(2) SCM Programming

Using STC89C52 SCM, its main programs mainly complete the task of communication between upper computer and lower computer , SCM and module, the first thing to set the baud rate to 9600 BPS (and correspond with the module), and then according to the format of instructions of the module package to send commands. Use Keil4 software version , and use c language to write the main program. SCM sends commands to the fingerprint identification module,and get a result of identification,then according to the result to control displaying module, relay module and electronic lock module.

SCM's initialization consists of baud rate setting, time setting and interrupt Setting, as shown below:

```
void UART_Init()
{
   SCON= 0x50;
   PCON=0x00;
   TMOD= 0x21;
   TH1= 0xFD;
   TR1= 1;
   EA=1;
}
```

After the completion of SCM's initialization, according to the buttons to trigger the subroutine. For example,click buttons to select the administrator mode, by calling the administrator subroutine ,then select to call other subroutines according to the situation of the later buttons' selection;click buttons to select fingerprint entry, call the fingerprinted subroutine, then call the subroutine of profile generating, call the subroutine of fingerprints storing next , such a whole series of process of fingerprint entry is completed.If click buttons to select fingerprint identification,call fingerprinted subroutine first,then call the subroutine of profile generating, finally call the fingerprinting subroutine, return the result of comparison, complete the function of fingerprint identification.If click buttons to select the function to delete, call the subroutine of deletion, and return the result of deletion.

3 THE RESULTS

Smoke sensor needs to be under heating condition, the higher the temperature, the faster the reaction, the faster response time and recovery time. To improve the response and to guarantee the accuracy of the sensor, stable work, need continued to smoke sensor supply heating voltage of 5 v. Smoke alarm can work in a wide temperature range, the smoke concentration can be display with LED digital tube display. When the concentration of the smoke concentration reaches set, issued a report to alarm.

Through on-site calibration and test, analysis of smoke concentration signal of experimental data, calculate the alarm display smoke concentration and the error between the actual concentration of 2.55% LEL, specified within the scope of error of plus or minus 5% LEL, meet the requirement of testing, and has achieved expected effect of the design of the conclusion.

Stepper motor drives, based on 51 single chip microcomputer intelligent fan, can display the indoor temperature, can according to indoor temperature automatically adjust fan speed control and buttons, the use of four digital tube display of fan model, and its temperature display. Through the temperature sensor to measure temperature, rotation speed control of step motor.

Pyroelectric infrared detection device, a switch can be adjusted by infrared detection reaction time, time to adjust the range of 0 s - 18 s, switch 2 can adjust sensitivity, highest can adjust to 8 m, and the parts work normally.

Video transmission module: when the infrared detection device sensing signal, video device can begin to work.

Fingerprint identification device: this device can realize the basic function such as fingerprint entry, storage, identification, and can enter the password into the "administrator mode" to realize add, delete the fingerprint samples, emergency unlock, change passwords, and other functions, at the same time through the relay to control the switch of pyroelectric infrared alarm device, when in a normal way through the fingerprint identification, pyroelectric infrared alarm device disconnect.

4 CONCLUSION

We can design the building safety device can accurately detect the change of indoor and outdoor environment, and according to the change automatically adjusting device status, ensure the safety, suitable for the actual installation, and for further development, and related functions of further expansion of laying a good foundation, to provide the correct ideas.

This study will be a variety of detection feature set at a suit, the fingerprint identification technology, infrared measuring human body electric heat release device, video data transmission device fuses in together, and indoor temperature sensor, humidity sensor measuring environmental parameters, and speed control air conditioning, smoke alarm device control water valve. This study can be realized on the height of the housing security guarantee, break through the traditional, the new technology is applied to daily life.

References

[1] Present situation and the trend of development of the foreign family security analysis in 2013 Gui-xiang Chen - the security of the People's Republic of China

[2] In the next decade American family security system users will rise 10% the 2014-02-26 network security knowledge

[3] Wang yong-ming zhang, jun-jian hu, etc. The time point ion smoke fire detector hysteresis "[J]. Journal of fire science, 2012

[4] The pyroelectric sensor principle and application - "sensor world 2010-07

Design of Anti-overspeed and Anti-overload System for Simulated Car

Zhang Hong; Chen Ming; Ye Qing

(College of instrumentation &Electrical Engineering, Jilin University,Changchun 130000,China)

***Abstract*—The problem of road safety is related to everybody's life. According to the survey, the overspeed and overload of the car is the main factor which causes traffic accidents,and it's necessary to design a device of prevention and restrain to get the problem solved.Our research is aimed at testing the speed and weight signal of the car effctively.then we can decide then we can decide whether it'soverspeed or overload.Finally,the signal will be send to the display module to show.When it's overspeed or overload,the system began to sound and light alarm.The car will be forced to get the speed down to the set value,and cut down the power to prevent the car from starting while the car overloaded.**

Apart from this,the bluetooth module can send the information to the monitoring device and form the traffic record list that is convenient for the police to consult.The experiment showed the design takes the overspeed and overload into considerition, wihch can truly meet the need of real-time control.

***Key words*--Overspeed protection ;Anti overloading ;Bluetooth ;real-time control**

I. INTRODUCTION

IN recent years, with the improvement of people's living standards, travel mode is also imperative to change, go out to ride or driving cars are welcomed by more and more people.But in recent years, many major traffic accidents began to attract people's attention, so the road traffic safety problem has become an urgent problem to be solved. After investigation, it was found that the overspeeding and overloading of automobiles was a major factor in the induction of traffic accidents. Therefore, it was necessary to design a preventive and restraint system to solve this problem effectively.

Now the market-related products only consider a certain aspect, and can not really meet the smart demand of "real-time". Based on the above considerations, the purpose of this study is to effectively detect the current vehicle's loading and speed information,make sound and light alarm, immediately force the car to slow down to the specified value, and cut off the power when the vehicle can not start.At the same time,we can send information to the monitoring device,so that it is effectively received within a certain distance.

II. SYSTEM DESIGN

This project designs a vehicle anti-overspeed anti-overload device to detect the current load and speed information of the vehicle, judge whether the vehicle is overloaded and overspeed, and finally send it to the display module for display. At the same time, the vehicle's current information is modulated and transmitted to the monitoring device through the Bluetooth module and form the driving records table, to prevent the drivers from deliberately concealing the information. Project research mainly consists of anti-speeding module, anti-overload module and Bluetooth transceiver module.

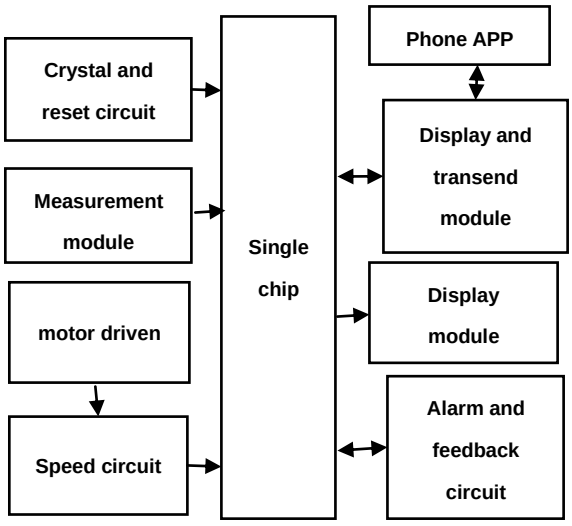

Fig 1 System Block Diagram

III . CONCEPTUAL DESIGN AND DEMONSTRATION

According to the requirements, the following plan is determined: On the basis of the existing simulation car, the photodetector, the load sensor and the Bluetooth module are installed to realize the real-time measurement of the speed, load and running status of the car and transmit the measurement data to the single chip to process, and then according to the various data measured by the single chip achieves the intelligent control of the electric car, the measured data is displayed in the LCD and sent through the Bluetooth module to the phone app. This program can realize the real-time monitoring of the movement state of the car, and can realize the automatic control,which is flexible and relable;it can also meet the requirements of the system.

A. Motor Driven

The car uses a DC motor. The signal power output from the microcontroller is very weak, even in the absence of other external load it can not drive the motor, so in the actual circuit we joined the motor driver chip to improve the input motor signal power, which can control the motor rotation as needed. DC motors are commonly driven by PWM mode. We can use the microcontroller to adjust the PWM pulse and high and low level to drive and control the DC motor.

PWM wave works is: the use of PWM motor speed control, the actual is to keep the motor armature on the pulse voltage frequency unchanged, adjust the pulse width. The motor is an inertia link, its armature current and speed can not mutated .A very high frequency of the PWM is added to the motor, the effect is equivalent to the application of a constant voltage DC[1].

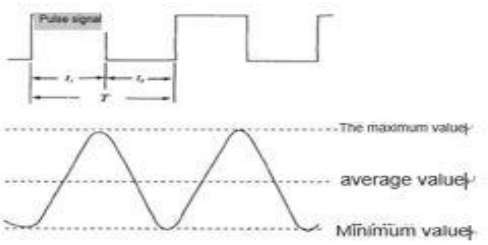

Fig 2 Voltage "duty cycle" and the average voltage

$$Vd = Vmax*D \quad (1)$$

In the formula,Vd is the average speed of the motor;Vmax is the the maximum speed when the motor is fully energized;D=t1/T.

By the formula (1) we can see that when we change the duty cycle forD = t1 / T, you can get a different motor average speed, so as to achieve the purpose of changing speed. Strictly speaking, the average velocity n is not strictly linear with the duty cycle D, and in general applications it can be seen as a linear relationship [2]. By changing the DC motor armature voltage "duty cycle" to change the size of the average voltage, thus controlling the motor speed. Therefore, PWM is also known as "switch drive".

B. Speed Circuit

The photoelectric sensor is a sensor using a photovoltaic element as a detection element. It first converts the measured change into a change in the optical signal, and then further converts the optical signal into an electrical signal by means of the photoelectric element[3].

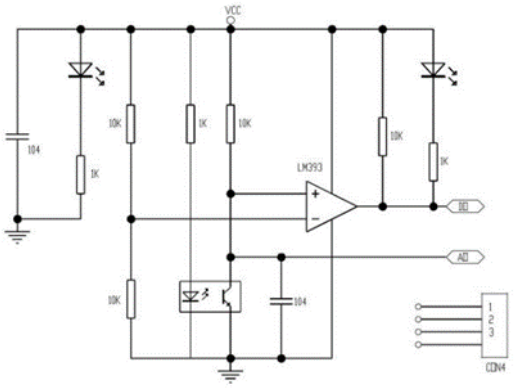

Fig 3 Speed sensor circuit diagram

The photoelectric detection method has the advantages of high precision, fast response and non-contact, and can measure the parameters, the structure of the sensor is simple and the form is flexible and diverse; and because the sensor principle of the photoelectric sensor is based on the light sensor,it has the advantage of anti-interference ability,fast response, high precision measurement. Therefore, the design choice to use photoelectric sensor measurement.

The photoelectric encoder is composed of an infrared transmitting receiving device and a code disc. When the infrared light from the transmitter to the black stripes, it will be intermittently reflected on the

receiver, the receiver input will be connected with the wheel speed proportional to the relationship between the optical pulse signal, and then the output of the receiver forms an electrical signal with a certain frequency. And then use the microprocessor to calculate the electrical pulse, you can get the speed of movement of the car[4].

$$v = \frac{\pi D}{n * t} N \quad (2)$$

In formula (2), N is the number of positive and negative transitions in the actual measurement, n is the number of black and white stripes on the code, D is the outer diameter of the drive wheel, and t is the time.

C. Weighing Circuit

The HX711 is a 24-bit A / D converter chip designed for high-precision load cells. Compared with other chips of the same type, the chip integrates the peripheral circuits needed by other similar chips including voltage stabilization power supply, on-chip clock oscillator, etc[5]. It has the advantages of high integration, fast response and strong anti-interference. Reducing the overall cost of electronic scales, improve the performance and reliability of the machine. The chip and the back-end MCU chip's interface and programming is very simple, all the control signal is driven by the pin,there is no need to register the chip registers. The power supply provided in the chip can directly supply power to the external sensor and chip A/ D converter, the system board don't need additional analog power supply. The clock oscillator in the chip does not require any external devices. The power-on auto-reset feature simplifies the initialization process.

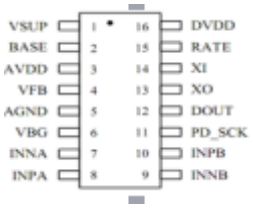

Fig 4 HX711 pin package

D. Display and Alarm Circuit

According to the requirements, the design needs to real-time display car speed, load, and speed and load limit value, so we select the LCD monitor. LCD1602 can display 32 characters, and Nokia5110 can display 15 Chinese characters, 30 characters. And Nokia5110 is cheaper and more cost-effective than the LCD1602. Nokia5110's interface is simple, it only need four I / O lines to be driven, and it's fast, working voltage is 3.3V, the normal display current is 200uA below with power-down mode,and it is easy to carry.

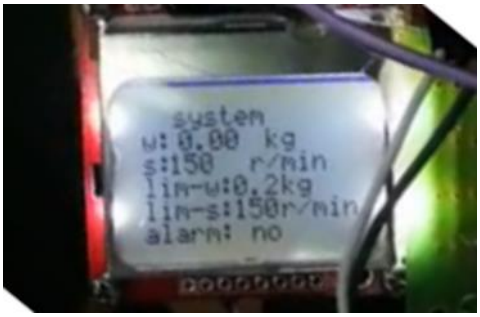

Fig 5 LCD 5110 display

Alarm circuit uses the sound and light alarm, when the car overspeed,the alarm indicator lights and the buzzer alarms.

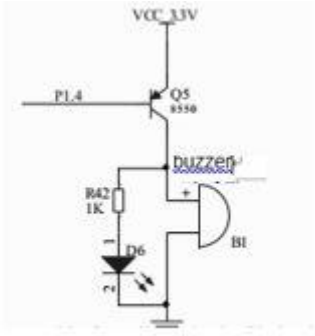

Fig 6 Alarm circuit

E. Bluetooth Module and Mobile APP Design

ATK-HC05 is a high-performance master-slave Bluetooth serial module that can be paired with a variety of Bluetooth-enabled computers, Bluetooth consoles, mobile phones, PDAs, PSP and other intelligent terminals, the module supports a very wide baud rate range: 4800 ~ 1382400, and the module is compatible with 5V or 3.3V microcontroller system, you can easily connect it with your product. The application is very flexible and convenient[6].

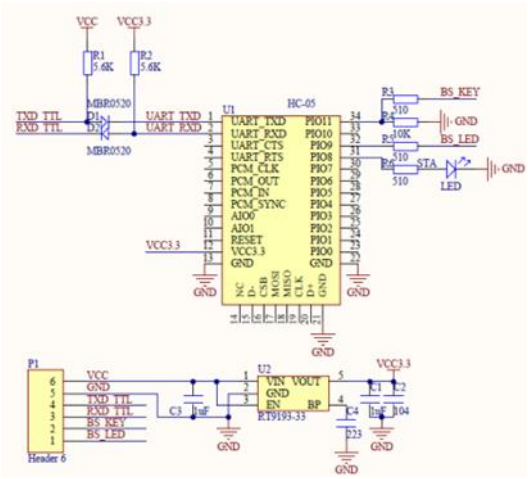

Fig 7 ATK-HC05 Schematic

IV EXPERIMENTAL RESULTS

After continuous improvement of debugging, the design of the final completion of the project is expected to meet the requirements. Through the button to control the car speed to simulate the operation of the car, the use of photoelectric sensors and HX711 load cell measured car current speed and load values, and displayed on the LCD 5110. At the same time, the car real-time status was sent to the phone app through the Bluetooth, and formed traffic records, through the phone we can set the car's load limit and speed limit, when the current state of the car was over the speed limit, the sound and light alarms, car automatically slow down to safety speed; when the car overloaded, the system alarm and forced braking of the car.

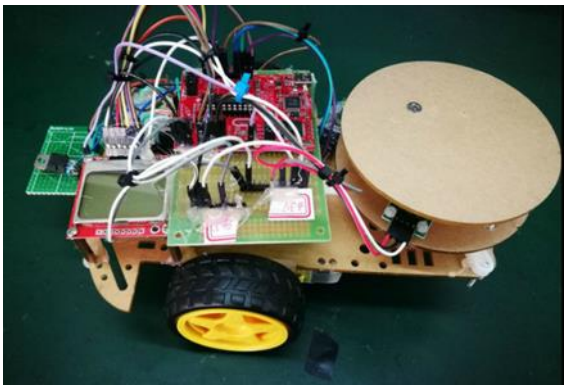

Fig 8 Physical display

Fig 9 Mobile app interface

V. CONCLUDING

This article designed an anti-overload and anti-overspeed system which can monitor the running status of the car in real time and alarm and automatic control when it's overspeed and overload. The design is convenient and practical, easy to promote, there is great practical significance.

Under Zhang Huazhu teacher's careful guidance and strict requirements the design has been completed under the title requirements, from the project selection, program demonstration to the specific design and debugging, we always feel the mentor's careful guidance and selfless care, we benefit a lot,there,we express deep gratitude to Mr.Zhang!

References

[1] Xu Nanyan, Hao Jifei, Xing Qingqing. PWM control method research [J]. Industrial and mining automation, 2005, (04): 22-25.

[2] Xian Kaiyi, Li Xianxiang.Design of DC Motor Control System Based on PWM Control [J]. Journal of Foshan University (Natural Science Edition), 2000, (03): 16-19.

[3] GAO Yan, GUO Hong-ying.Application of Photoelectric Sensors in Motor Tachometer [J]. Chinese Journal of Digital Technology and Applications, 2013, (08): 63 + 65.

[4] Li Juye, Ji Luli. Design of photoelectric tachometer [J]. Journal of Hainan University (Natural Science Edition),

2012, (01): 66-70.

[5] Liu Meijuan, Zhang Qi, Mu Yuanwei.Design of high precision electronic scale based on HX711 [J]. Information and Communication, 2017, (01): 142-144.

[6] Bai Yunfei, Wang Ping, Sun Pan. Bluetooth communication module design and implementation [J]. Digital Communications World, 2006, (09): 72-7

The Fast Non-contact Size Measuring Instrument

MA Li-Dong; LI Zhe; LIU Yuan

(College of Instrumentation &Electrical Engineering,Jilin University,Changchun 130022,China)

***Abstract*—The project uses the laser ranging principle, aiming at the requirement of modern measurement, this paper designs a non-contact instrument for rapid measurement of size.Using laser sensors measure the distance between the object and instrument information.Through the microprocessor for processing and analysis, the size of the analyte displayed on the LCD screen.Via bluetooth remote communication, real-time display data on mobile phones, remote real-time observation of the analyte in a sample size.The instrument can meet the requirements of current social non-contact measurement, the practicality is strong, rapid measurement, low cost, has certain market prospects.**

Key words—Laser ranging Non-contact Bluetooth communication

I.INTRODUCTION

WITH the development of science and technology, measurement instruments is in constant progress, people often tend to use more convenient, fast, high precision measuring instruments.At present, most of the size of the existing measuring instruments are contact of vernier caliper, micrometer, etc give priority to, although the instrument accuracy is higher, but it can't direct contact measurement in some cases (such as transfigure object under test changes, or cause corrosion,etc.) and can't satisfy people's requirements.And now in the market of portable laser measuring instrument is rare, most of the laser length measuring instrument volume and complex internal composition.Therefore,design a portable, non-contact measuring instrument is great significance [1].The traditional laser length measuring instrument is more complicated and larger power consumption.The instrument according to the traditional advantages and disadvantages of the two kinds of measuring apparatus to optimize design, using the laser ranging principle and using untreated analysis processing, via bluetooth communication implement long-range observation data.The equipment has simple structure, low power consumption, low cost, practical [2].

II. THE OVERALL SCHEME DESIGN

The fast non-contact size measuring instrument mainly includes the control module, measuring module, bluetooth communication module, liquid crystal display module, power supply module.The overall designs diagram of instrument as shown in figure 1 [3].

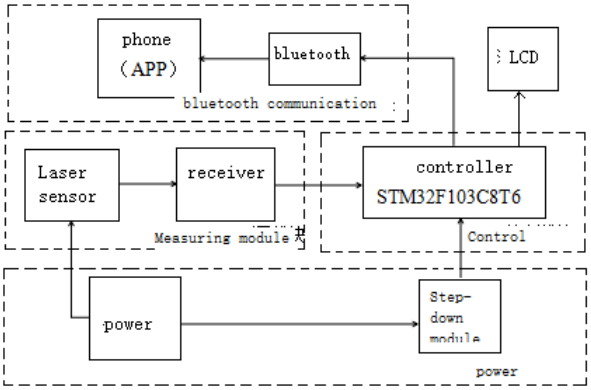

Fig.1 The overall structure of the instrument

Instrument with a laser distance sensor collects information and by the receiver, after dealing with the controller in the size of the analyte displayed on the LCD panel and send data to the mobile phone via bluetooth remote observation data [4].

III. THE HARDWARE DESIGN

A. Control Module

Control module is the core of the whole instrument, instrument control center [5] of each module.The controller is based on STM32F103C8T6 micro-controller. The controller uses the ARM Cortex-M3kernel, ARM Cortex-M3 processor is a 32 bit processor industry leading, it not only has excellent computing capacity, quick response capability and

excellent stability, but also meet the actual environment of low power consumption, the demand for high performance, has been widely used in the high real-time scene. Has the characteristics of high performance, low cost, low power consumption [6].Compared with the traditional 51 singlechip, it is the working frequency of up to 72 MHZ, storage space is bigger, faster, and themicrocontroller program is modular, abundant peripheral interface, the interface is simple, the processor itself comes with many functions, save development cost, high cost performance. Therefore, using the microcontroller as the instrument control chip [7].

B. Measuring Module

Measuring module mainly is the use of laser sensor, monochrome laser has good nature and direction, is widely used in fields ranging [8]. By using the principle of Laser Ranging: the measurement module two opposite to each other, the distance between the fixed (30cm), and then the measurement module and the measured distance to calculate the measured object the size.

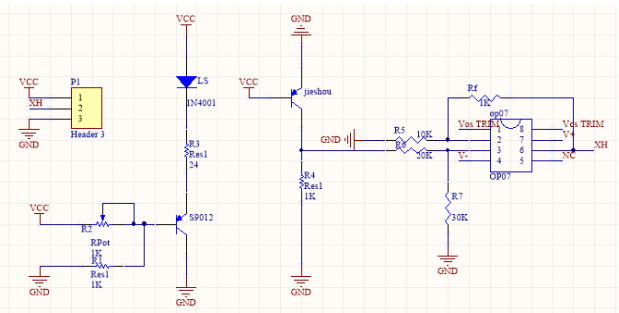

Fig.2 Measuring module circuit diagram

After electrify, transmission laser pulse by analyte laser sensor alignment.Measured after reflection by the laser scattering in all directions, part of the scattered light to return to the receiver to detect extremely weak light signal, and converting it into corresponding electrical signals.Due to the electrical signal range is larger, of transformation of STM32 receiving signal range is limited, so increased the voltage conversion circuit, ensure electrical signals can be STM32 receives and analyzes processing [9].

C. The Bluetooth Communication Module

Instrumentation and mobile phone via bluetooth, the realization of remote observation data.Bluetooth choose Hc-05, Hc-05 is a master-slave a body can be set to the bluetooth chip, has the function of traditional bluetooth module interface has a serial port, spi interface, usb interface, can be up to 10 m Hc05 tested in indoor communication distance within [10].

D. The Liquid Crystal Display Module

The instrument adopts two kinds of observation modes, one is through the realization of Bluetooth remote procedure; another is to install the LCD screen in the instrument. Because it only needs the display size information of the measured object, so it has no special requirements on the LCD screen, the instrument using LCD1602 character LCD, micro power consumption, small size, suitable for in this instrument.

E. The Power Supply Module

The instrument measurement module to use 5 V dc power supply, while the STM32 need 3.3 V power supply, therefore, the instrument overall introduction of step-down power is supplied by 5 V dc power supply module for the STM32 power supply.

IV. The Software Design

The instrument adopts the STM32F103C8T6 microcontroller for data processing, using C language for software development and design, the software has advantages of good readability and portability of higher. Using the JAVA language for mobile APP design, has the advantages of simple, reliable, multithreading. In the process of instrument software design using modular design is a relatively independent module for reducing complexity, make the program design, debugging and maintenance, etc. The operation is simple. Instrument software flow chart is shown in figure 3.

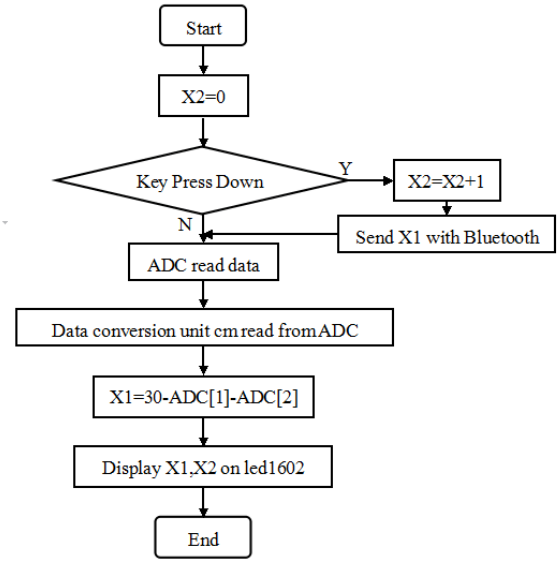

Fig.3 The software flow chart

In terms of measurement software STM32 chip with built-in ADC for real-time measurement, but to be able to send the measurement data to the phone through the button, to avoid the waste of information storage space. And can record number has been sent data onLED1602, zero power, can achieve the function of the counting.

A. Mobile Phone APP Design

Through the phone APP to connect with the STM32 bluetooth module, receiving data and data processing [11].APP interface and data processing interface as shown in figure 4 and figure 5 [12].Through the mobile phone bluetooth module, the receiving measurement data collected from the STM32 end and data processing, finally displayed on the APP interface [13].

Fig.4 APP interface

Fig.5 Data processing interface

V. TEST AND ANALYSIS

Instrument as a whole by the framework and three pieces of PCB (the main part of the instrument and two measurement module).

A. Measuring module testn

Measuring instrument module to be tested individually, get the output signal measurement module under different distances through the test, the fitting formula for data processing and analysis provide the basis for the [14]. after the actual test, the fitting curve shown in Figure 6 measurement module.

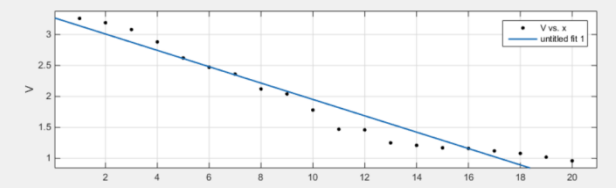

Fig.6 The fitting curve

The fitting curve of the corresponding calculation formula is:

$$F(x) = -0.1321x + 3.272 \quad (1)$$

B. Overall Test

Instrument as a whole is supported by frame, various modules are connected, the instrument assembly after the completion of the connected power supply.Will fast non-contact size measuring instrument of analyte laser sensor alignment began measuring, the display screen shows the size of the measured data;The bluetooth to send data at the same time, display size

data on mobile phones.

TABLE I

MEASUREMENT DATA TABLE

On the left side of the laser		On the left side of the laser		measurement size (cm)	actual size (cm)
Distance (cm)	V	Distance (cm)	V		
18	1.08	3	3.08	9.87	8.98
16	1.16	6	2.47	8.74	8.03
6	2.45	9	2.04	15.39	14.97

Fitting data due to the error of measuring distance itself, the timeliness principle error, and reading error and so on, the analyte measured size and actual size error.Analyte and the same in two different distance apart of the laser measurement size is error.The distance between two laser sensors at constant distance measuring different size of measured object, because of the different size error of the result also to have certain change [15].

Instruments in the practical measurement due to the approximate processing data processing, and the influence of the instrument itself, the actual measurement results have a certain error [16].

VI. CONCLUSION

This paper proposes a fast non-contact size measuring instrument design, Uses the STM32F103C8T6 as main control chip, using laser ranging principle of measuring the size of the measured object information, and the results show that the instrument itself of liquid crystal screen, or send to a phone via bluetooth communication for display. This design has realized the non-contact measurement and easy to carry, the purpose of make up the deficiency of existing measurements; The instrument is small in size, low power consumption, is practical.

References

[1] Chuang Wang,Based on the STM32 series ARM Gortex - M3 micro-controller micro thermal printer firmware development[D].ShanDong university,2015,04.

[2] Hua-feng Ding. Based on CPLD is the design and implementation of high precision laser length measuring instrument.Nanjing university of science and technology.2009, 12.

[3] You-fa Wei.Research and design LED lighting controller based on the Android [D]. Overseas Chinese university. 2015.6.

[4] Gerd Nunitor.Stm32 Mcrocontroller,STM icroelectronics.Reduced instruction set computing[M].Flu Press,2012.

[5] Li-Gong Zhou.The ARM embedded system based tutorial (second edition) [M]. Beijing: Beijing university of aeronautics and astronautics press, 2008.

[6] Shyh-Ming Jong.A Design of Automatic Speed Adjustable System for Five.Phase Hybrid step Moter Driver[C].

[7] Shurui Fan.ARM processor and C language development application (first edition) [M]. Beijing: Beijing university of aeronautics and astronautics press, 2008.

[8] Peter Van Der Linden.ExpeIrt C Programming D eep C Secrrts[M].

[9] Er wen (Kip R.I rvine) assembly language programming (6th edition) [M]. Beijing: tsinghua university press, 2011.

[10] Tie Qiu. ARM embedded system structure and programming [M]. Beijing: tsinghua university press, 2009.

[11] Yu-kun Wu. Based on the Android mobile learning platform design [J]. Computer CD software and applications, 2013, (1).

[12] Sorin. GoogleAndroid development guide [M]. 2nd Ed. Beijing: people's posts and telecommunications publishing house, 2009.

[13] Yongsong Wang. Android platform development journey [M]. Beijing: mechanical engineering press, 2010.

[14] Jiliang Song. Practical computer drawing program design and examples [M]. Harbin: Harbin industrial university press, 1996.

[15] AutoCAD Development System Programmer'S Reference,AutoDesk,Inc.

[16] Chaoyong Guo. AutoCAD customization and development [M]. Beijing: people's posts and telecommunications publishing house, 1998.

The Flame Temperature Measurement System Based on Principle of Colorimetric Temperature Measurement

Chen Xiaojin; Zhao Pengfei; Li Jinqi
(The College of Instrumentation and Electrical Engineering, Jilin University, Changchun 130012, China)

***Abstract*—This project designed a flame temperature measurement system based on the principle of colorimetric temperature measurement. Based on the digital image processing technology, optical and radiological knowledge, a calculation model of two-color temperature measurement is established. A CMOS camera was used to capture the alcohol lamp flame and get the temperature field from the flame image. The system used MATLAB to program and achieved the control of the camera for alcohol lamp flame image acquisition, flame image preprocessing, temperature field calculation and display, and other functions. The temperature field is obtained by the colorimetric algorithm, and outputs pseudo-color maps and isotherms.**

***Keywords*—Colorimetric Method Temperature Measurement Flame Image CMOS Digital Image Processing**

I. INTRODUCTION

IN recent years, with the continuous development of computer technology, domestic and foreign researchers are increasingly turning their attention to the visual combustion monitoring system, that is, digital image processing technology is used in combustion flame treatment. The main approach is through the intake of burning flame image, use optical theory, radiation theory and computer image processing technology, to calculate the entire temperature field and achieve non-contact flame temperature field measurement.

The traditional non-contact temperature measurement is generally based on the CCD colorimetric temperature measurement method. With the CMOS (complementary metal oxide semiconductor) technology matures, CMOS imaging devices' imaging quality is improved. It has the advantages of a lower power requirements, greater dynamic range, better sensitivity and higher system integration [1]. So this article selected CMOS webcam for flame image acquisition.

According to the ratio of two coinstantaneous measured adjacent wavelength radiation, colorimetric temperature measurement can determine the temperature, so that the influence factors of optical path of the two bands are the same. The influence of bad environment can be eliminate, such as lens contamination, device characteristics drift and other time-varying factors, they can cancel each other, that's why the measurement process can be repeated and extended, which it's unique to apply to the measurement of the combustion flame. This project based on the principle of colorimetric temperature measurement, used two-color temperature measurement method, obtained the RGB values of flame image that taken by CMOS webcam, to measure the temperature.

The system was designed to improve the operability of flame temperature detection. It used the alcohol lamp flame as the measurement object, and used MATLAB as a compiler to build a colorimetric flame temperature measurement system, based on digital image processing technology, optical and radiological knowledge. This paper introduced its principle and structure. The system is simple to construct, with no complex hardware erection, the software interface is relatively simple and easy to operate, the entire system is easy to implement.

II. THEORY FOUNDATION

Radiant Energy of Radiation Burning Flame:

$$M(T)=\int_{-\infty}^{+\infty} M_{\lambda}(T)\mathrm{d}\lambda \tag{1}$$

$M_T(\lambda)$ is the flame monochromatic radiant energy, according to the law of radiation, can be expressed by the Planck radiation formula as follows:

$$M_T(\lambda)=\frac{\xi(\lambda,T)C_1}{\lambda^5(e^{\frac{C_2}{\lambda T}}-1)} \tag{2}$$

In the above formula, λ is the wavelength of radiated electromagnetic wave (m); $\xi(\lambda,T)$ is the spectral emissivity of the radiator; T is the temperature (K); C_1=3.7411844×10^{-16}（W·m^2）; C_2=1.438833×10^{-2}（m·K）.

When the wavelength of the combustion flame is in the range of 380 to 780 nm and the temperature is below 3000 K, the Planck's radiation law can be replaced by the Wien radiation law. So there is

$$M_T(\lambda)=\frac{\xi(\lambda,T)C_1}{\lambda^5 e^{\frac{C_2}{\lambda T}}} \tag{3}$$

So the radiant energy of the burning flame can be expressed as [2]:

$$M(T)=\int_{-\infty}^{+\infty}\frac{\xi(\lambda,T)C_1}{\lambda^5 e^{\frac{C_2}{\lambda T}}}d\lambda \tag{4}$$

If both monochromatic radiant energy $M_T(\lambda_1)$ and $M_T(\lambda_2)$ at the same point are measured under two different wavelengths λ_1 and λ_2, the temperature of that point can be obtained by the ratio of $M_T(\lambda_1)$ and $M_T(\lambda_2)$:

$$T=\frac{C_2(\frac{1}{\lambda_2}-\frac{1}{\lambda_1})}{\ln\frac{M_T(\lambda_1)}{M_T(\lambda_2)}-\ln\frac{\xi(\lambda_1,\ T)}{\xi(\lambda_2,\ T)}-5\ln(\frac{\lambda_2}{\lambda_1})+K} \tag{5}$$

With the assumption of flame gray radiant property

$$\frac{\partial(\lambda,\ T)}{\partial\lambda}=0 \tag{6}$$

There is $\xi(\lambda_1,\ T)=\xi(\lambda_2,\ T)$; K is the standardized coefficient constant.

So we can get the colorimetric temperature measurement formula:

$$T=\frac{C_2(\frac{1}{\lambda_2}-\frac{1}{\lambda_1})}{\ln\frac{M_T(\lambda_1)}{M_T(\lambda_2)}-5\ln(\frac{\lambda_2}{\lambda_1})+K} \tag{7}$$

III. K VALUE CALIBRATION

The K value of the temperature measurement method calibration process is [3]: collect multiple temperature optical images, select one group (R/G, T) value substitute into equation (8), and one K value can be obtained. Then we use that K value to calibrate the equation, and substitute the R/G values of other pictures into the equation, and the colorimetric temperature of the corresponding picture can be obtained [4]:

$$T=\frac{C_2(\frac{1}{\lambda_2}-\frac{1}{\lambda_1})}{\ln\frac{M_T(\lambda_1)}{M_T(\lambda_2)}-5\ln(\frac{\lambda_2}{\lambda_1})+K} \tag{8}$$

IV. THE COMPOSITION AND FUNCTION OF SYSTEM

This system could intuitive response to alcohol lamp flame image, at the same time, using computer analysis to obtain the flame temperature field. The system mainly included image acquisition part (CMOS camera), computer and image processing software (see figure 1).

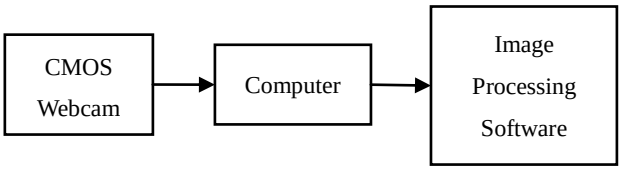

Fig.1 System block diagram

A. CMOS Webcam

CMOS webcam is a camera with CMOS image sensor. In some products that use CMOS as photosensitive device, they can achieve the same effect as CCD webcams by the use of image light source automatic gain enhancement technology, automatic brightness, white balance control technology, color saturation, contrast, edge enhancement and gamma correction and other advanced image control technology. This system used Microsoft's LifeCam

Studio Webcam.

B. System Software Implementation

The system used MATLAB as a compiler, the realization of the main functions included control webcam for alcohol lamp flame image acquisition, flame image preprocessing, temperature field calculation and display. The software flow chart was shown in Fig.2. The software system could also achieve real-time monitoring of the flame, save the screenshot, save the image after processing and other functions.

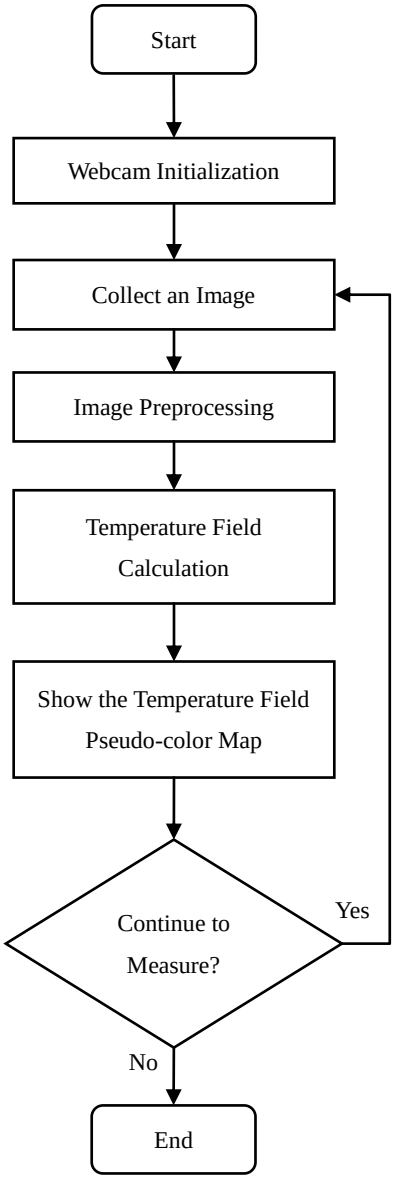

Fig.2 Software flow chart

C. Flame image processing

For different application requirements, there are different image processing methods. The temperature measurement system is mainly to obtain the combustion flame temperature field distribution, in order to improve the visual function, if necessary, would carry out some enhancements and optimization based on the intention.

The flame image processing included image preprocessing and display of the temperature field pseudo-color map. Image preprocessing included color image grayscale, median filter processing, grayscale transformation stretching, binarization processing and etc. The purpose of this series of processing is to effectively separate the part of flame image, thus facilitating the realization of subsequent temperature algorithms. The collected flame image and the post-processing image are shown in Fig.3 and Fig.4.

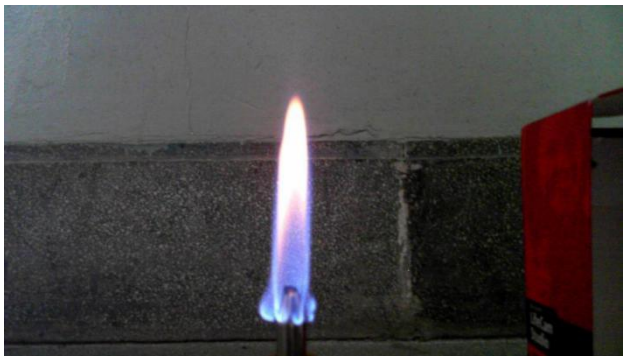

Fig.3 The original image before processing

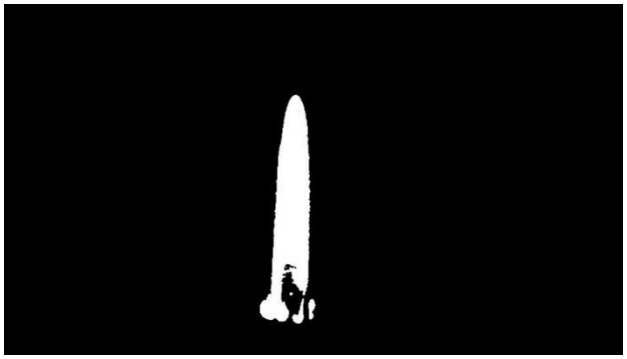

Fig.4 Post-processing image

D. Temperature Field Calculation and Display

Before calculating the flame temperature, it is necessary to obtain the red and green components of each pixel in the flame image. The red and green components of the image are shown in Fig.5 and Fig.6. The system used the R and G values of each pixel in the image ,with the K value obtained by calibration, and substitutes them into the colorimetric temperature measurement equation to obtain the colorimetric temperature of each pixel.

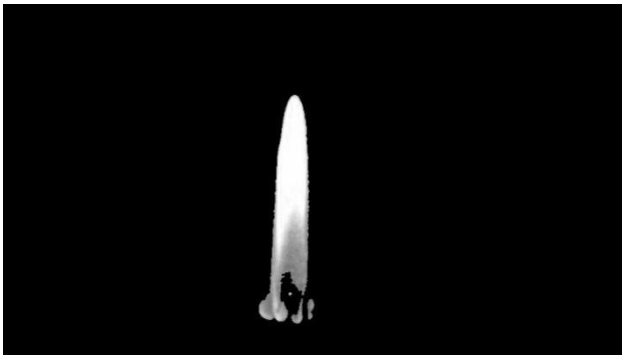

Fig.5 Red component image

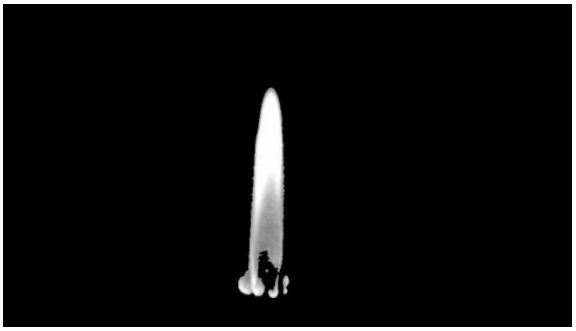

Fig.6 Green component image

After calculating the colorimetric temperature, in order to better realize the visual display of the alcohol lamp flame temperature field and enhance the visual effect, the system used the pseudo color map and the isotherm diagram to reflect the distribution of the temperature field.

Pseudo-color map is not really directly get the target color image[6], the image of each pixel value represents an index value, through some algorithm after the CLUT color table to find the three primary colors RGB value, and then synthesized to obtain color visual effects. In fact, it embodies a mapping of ideas, this approach is called pseudo-color processing, the view is called pseudo-color map. The main method of pseudo-color enhancement is grayscale - color transformation. According to the principle of color analysis, the target gray scale image is divided into several small segments according to certain standard, and the corresponding three primary colors RGB values are obtained by the algorithm, and then a pseudo-color map of the target is displayed by combining.

After the temperature algorithm was calculated, the calculation results of the temperature field are displayed by the pseudo color map and the isotherm diagram, as shown in Fig.7.

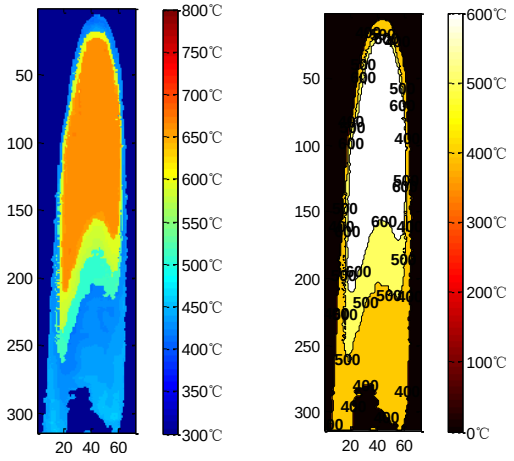

Fig.7 Pseudo color chart (left) and isotherm diagram (right)

V. Software Test

We chose the alcohol lamp and K-type thermocouple thermometer to test the entire system, the test device structure shown in Fig.8.

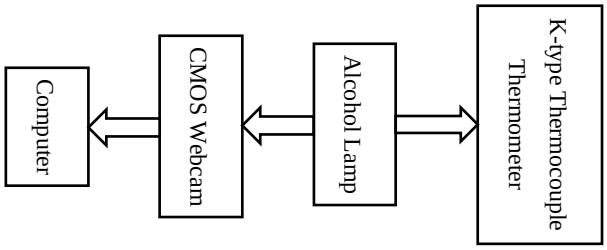

Fig.8 Test device structure chart

A. Testing Process

a. The acquisition of the flame image: open the software, ignite the alcohol lamp flame, and determine the location of the CMOS webcam and flame. Through the software real-time monitoring interface to observe the flame shape, shooting flame images and save. At the same time record the thermocouple thermometer measured value.

b. Select the desired flame image, after a series of pretreatment, obtain the flame part of the image, and the calculation of the temperature field, showing the corresponding temperature field pseudo-color map and isotherm.

B. Test Directions

a. In order to make the measurement process more intuitive clear, the area other than the alcohol lamp flame is treated as zero at the time of calculation.

b. The K value of the test process is 4.8614.

C. Test Results and Analysis

TABLE I

SYSTEM TEST RESULTS

	K-Type Thermocouple Thermometer/ ℃	Colorimetric Temperature Measurement System /℃	Relative Error/ ℃	Absolute Error/%
1	639.0	633.72	-5.28	-0.83
2	630.1	644.56	14.46	2.29
3	655.1	650.90	-4.20	-0.64
4	633.2	619.31	-13.89	-2.19
5	624.2	617.12	-7.08	-1.13
6	637.5	638.64	1.14	0.18
7	624.7	648.57	23.87	3.82
8	627.2	635.03	7.83	1.25

From the system test results, we could know that the temperature of the alcohol lamp flame measured by the colorimetric temperature measurement system was different from that measured by the K-type thermocouple thermometer.

VI. CONCLUSION

The realization of the system improved the operability of flame temperature detection. The system used the flame image as the basis for obtaining the temperature field, and used the two-color temperature method to measure the temperature field of the combustion flame. Software tests showed that, the area other than the alcohol lamp flame was treated as zero to make the observation more intuitive and clear. The temperature of the detected point was within the normal range, the purpose of temperature measurement was achieved. System structure was simple, no complicated hardware set up, the software interface was relatively simple and easy to operate, the entire system was easy to achieve. This system not only could detect the temperature of the alcohol lamp flame object, but also could calculate its R, G, B value, for other detection and judgment of the flame image provides the basis.

References

[1] Mou Xiangyang, Jiang Haiying, Li Baozhu, etc. Study on portable CMOS radiation temperature measurement system [J]. Electronic Measurement Technology, 2010, 33(3):102-105.

[2] Dan Danhua, Zhao Chunhe, Wang Weiyan. Study on Radiation Temperature Measurement System Based on Virtual Instrument Technology [J]. Instrument Technique and Sensor, 2007(3):41-42.

[3] Zhang Hua. Study on real-time temperature detection of image colorimetric method [J]. Journal of Mechanical Engineering, 1998, 34(2):1-7.

[4] Quan Huiyun. Numerical Analysis and Application [M]. Wuhan: Wuhan University Press, 2007:28-32.

[5] Qian Yangyi, Chen Jianbin, Wu Zongzhi, etc. In the palm lab to explore the alcohol lamp flame temperature - draw different conclusions [J]. Chemical Education, 2003(1):39-41.

[6] Sheng Xiaobei, Xi Tao, Zeng Zhibin. Study on Two-color Measurement System for Finding Temperature Field from Flame Image [J]. Journal of Automotive Safety and Energy Conservation, 2014, 5(1):83-90.

[7] Zeng Zhibin. Design of two-color temperature measurement system based on flame image temperature field [D]. Wuhan: Huazhong University of Science and Technology, 2013.

[8] Xiao Xiaojuan, Bu Leping, Li Qixiu. Study on fire detection based on image processing [J]. Journal of Naval University of Engineering, 2007, 19(3):6-11.

[9] Zhang Honglin. Digital image pattern recognition technology and engineering practice [M]. Beijing: People's Posts and Telecommunications Press, 2003.

[10] Yang Fei. Fast temperature field measurement and combustion diagnosis based on computer image processing technology [D]. Hangzhou: Zhejiang University, 2001.

Design of the Exhaust gas condensate collecto

He Chen; Bingli Wang; Jun Ma; Huaide Kong
(jilin university instrument science and engineering institute,changchun,130021)

***Abstract*—Respiratory diseases are harmful to people's health and life as a common and frequently occurring disease, how to collect samples to reflect the changes before and after the treatment of airway inflammation accurately is always a difficult problem in the process of diagnosis and treatment of respiratodiseases .Exhaled breath condensate detection has become a new method for monitoring respiratorsy disease. As a completely non-invasive detection t echnology, it has the advantages of reliability, safety and simplicity in understanding airway inflammation，also it can collect exhaled breath condensate continuously.This topic designs through the gas path part, th e refrigeration part and the monolithic integrated circuit ，by improving the experiment we can make the EBC collector to become commercialized.so that it can provide convenience for patients with respiratory diseases.**

***keywords*—respiratory disease EBC exhalation gas condensate collector independent researchI.**

INTRODUCTION

RESPIRATORY disease as a harm to people's health and life of common diseases and frequently-occurring disease, how to collect specimens to accurately reflect the state of airway inflammation and changes before and after treatment, has been the diagnosis and treatment of respiratory diseases in the process of the problem. At present, the method used to detect airway secretions of inflammatory respiratory disease specimen collection methods are mainly sputum collection, and bronchoalveolar lavage fluid collection. Among them, the sputum collection includes ordinary sputum specimens and induced sputum specimens. [1]As we all know, in many cases, the limitations of the specific circumstances of the patient, the general sputum specimens difficult to meet the requirements of clinical testing, for example, some patients with symptoms of less sputum or no sputum; some critically ill patients or infants and young children unable or not Expectoration, so that the sputum specimens can not truly reflect the situation of the next airway. Induction of sputum technology, although noninvasive examination, but the inhalation of hypertonic saline itself is an inflammatory stimulus, the bronchial stimulating effect,even if the use of 2-receptor agonists in advance, the patient may still occur in the process of respiratory tract There is an increase in the disease. In addition, induced sputum surgery is disabled in children and in patients with severe asthma. Bronchoscopic alveolar lavage fluid (BALF) is the most able to respond to changes in airway airway inflammation, but because of an invasive examination, poor patient acceptance, especially for mild, recurrent disease (such as asthma) patients . It is difficult to repeat the above check. (EBC) is a new method of detecting airway inflammation in recent years. It is a noninvasive method for evaluating airway inflammation and oxidative stress. It is a simple method for the detection of airway inflammation and oxidative stress. Easy repeatability and other advantages, more and more extensive attention at home and abroad and research. In view of these problems, based on the research report and the analysis of the market demand, combined with the existing resources and conditions, we prepared to study the design of exhaled condensate collector.

II. SYSTEM OVERALL DESIGN

The EBC collector developed by this experiment is realized by the following methods: the air part of the device, the cooling part and the single chip system are composed of three parts:

(1) air part: by the changeable air nozzle, suction check valve, saliva residual night collection of containers, resistance to saliva casing.

(2) cooling part: EBC collection is through the low temperature so that the patient's breath of water vapor

liquefaction, the invention of the exhaled gas liquefaction device to achieve the cooling part of the device. This part of the refrigeration chamber and its outer layer of the cold layer, insulation layer, semiconductor cooling film[2], heat sink components.

(3) single-chip system: by the conditioning circuit, analog-digital conversion, microprocessor, clock circuit, keyboard, drive circuit and display. The system through the DS18b20 sensor to collect temperature information, processed by the microprocessor, send data, while the display on the display real-time data, press the button to adjust the set temperature, when the data below the set lower limit,The controller controls the cooling system to operate until the data reaches the upper threshold and stops working.

III. SYSTEM HARDWARE DESIGN

3.1 System acquisition module

3.1.1 Selection of sensors

DS18B20 temperature sensor, DS18B20 is a commonly used temperature sensor, with a small size, low hardware overhead, anti-interference ability, high precision. We need the temperature range of -30 ℃ - +40 ℃, its available range in this Interval[3].

3.1.2 Sensor working principle

The oscillation frequency of the low temperature coefficient crystal is very little affected by the temperature, and the pulse signal for generating the fixed frequency is supplied to the counter 1. The high temperature coefficient of the crystal with the temperature changes its oscillation rate changes significantly, the resulting signal as the counter 2 pulse input. The counter 1 subtracts the pulse signal generated by the low temperature coefficient crystal. When the preset value of the counter 1 is reduced to 0, the value of the temperature register is incremented and the preset of the counter 1 is reloaded and the counter 1 is restarted The pulse signal generated by the low temperature coefficient crystal is counted and circulated until the counter 2 counts up to 0 to stop the accumulation of the temperature register value. The value in the temperature register is the measured temperature. The slope accumulator is used to compensate and correct the non-linearity in the temperature measurement process, and its output is used to correct the preset value of the counter 1.

3.1.3 Temperature collection

The corresponding sensor to detect the temperature signal, and these non-electrical parameters into the corresponding electrical signal; and then through the signal conditioning circuit to the microcontroller to collect and store and send to the data transmission module, in order to achieve the transmission of information.

3.1.4 Acquisition system block diagram

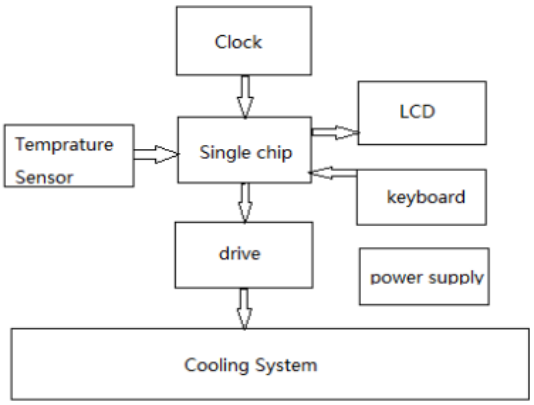

Fig. 1 block diagram of the acquisition system

3.2 Control module design

The control module mainly comprises a keyboard control module, a driving control module and an MCU.

3.2.1MCU The module

MCU use AT89 - C51 microcontroller,It has low price, fast speed, anti-interference, and low power consumption, as a eight processing chip, completely can be competent the performance requirements of the system, at the same time, low power consumption for the purposes of this system is also very important, so choose the AT89 - C51 as the main controller.

3.2.2 The keyboard control module

Keyboard control USES four independent mechanical keys and MCU to connect main switch button control, real-time temperature and set temperature and temperature regulation.

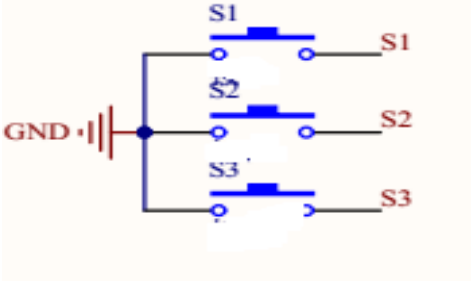

Fig.2 button control circuit diagram

3.2.3 Drive control module

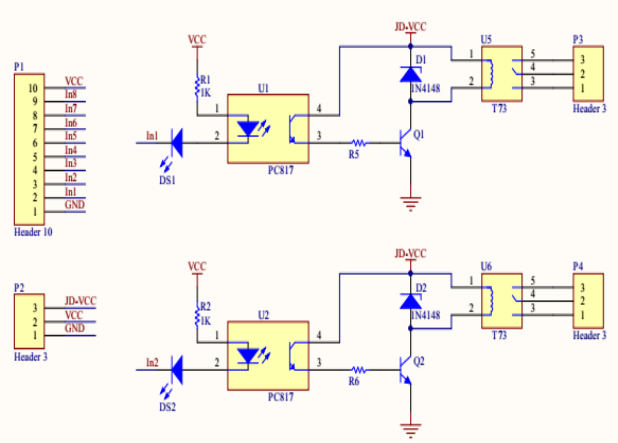

fig.3 drive module circuit diagram

3.3 Display module

Use JM12864M LCD display, branch of jilin university, real-time temperature and set temperature. JM12864M is the most commonly used in the MCU application design of display devices, it belongs to the character LCD module, is specially used to display Chinese characters, letters, Numbers, symbols, such as the dot matrix LCD module

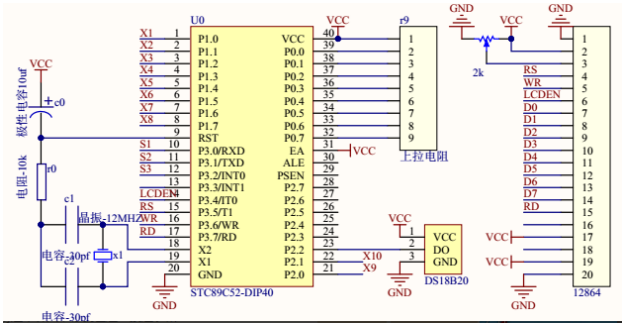

Fig.4 shows the module circuit diagram

IV. THE MECHANICAL PARTS OF THE SYSTEM DESIGN

4.1 Cold cavity

Cold cavity parts with aluminum piece design, aluminum using square, facilitate refrigeration piece of paste, aluminum piece middle hollow out, can make a tube inserted into, used to gather breath condensate, the cold chamber to ensure good air tightness, should make its internal can achieve the desired temperature, also to ensure the breath there would be no other pollutants into[4].

4.2 Air inlet structure design

4.2.1 Design requirements:

(1). Good sealing.

(2). When patients exhale, air inlet are connected to the refrigerating container, isolation with the outside world. Breath gas condensate into the refrigeration system.

(3). When patients inhale, containers of air inlet is connected with the outside world, and the refrigerating plant quarantine. The gas into the container, for patients with inhalation.

4.2.2 Design method

The production prOcess is simple and convenient to use in and out of the air and the resistance effect of salivary ZhiGuanXing resistance saliva air inlet. The design is the main advantage of ptfe products, production of simple, convenient, practical, can be used supine position[5].

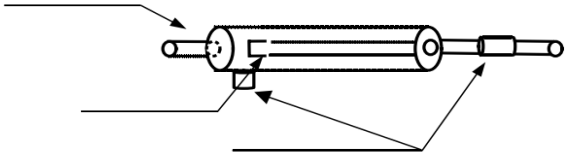

Fig.5 air inlet design

V.SYSTEM SOFTWARE PART DESIGN

5.1 the overall program design

The system overall software flow chart is shown in figure 6.

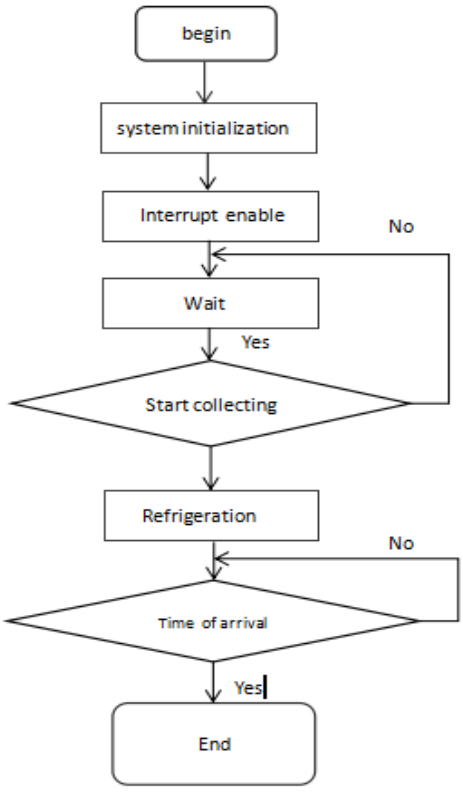

Fig.6 The software flow chart of the system

5.2 System programming

Analog signal to go through internal microcontroller A / D converter then the data can be processing or display,And digital signals have to go through the internal counter after counting the data processing, so these have to rely on software to achieve,Here we use the interruption of the software design.After entering the system first through the initialization function of the microcontroller ports, AD and timers accordingly initialized.After entering the EBC collection of measurement menu, the first control of the semiconductor device on the collection device to cool,When the preset temperature is reached, the operator is instructed to start the measurement,At this point the microcontroller AD interrupt is turned on,And the temperature measured in the cold cavity in real time displayed on the LCD screen,The AD interrupt is stopped when the set temperature is reached.The system enters the key waiting state,Can exit the system.

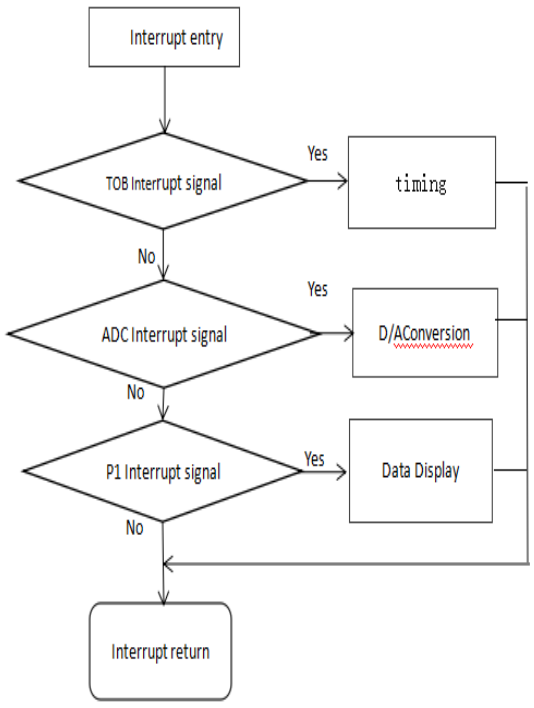

Fig.7 interrupt flow chart

VI.TESTING AND ANALYSIS

6.1 System overall physical map

Fig.8 System overall physical map

Figure LCD real-time display temperature and set the temperature, plastic pipe connected to the air inlet and cold chamber test tube, blowing or breathing to collect condensate. Internal use of water cooling way.

6.2 Temperature and collection device testing

At room temperature of 32 ℃, the coolant is water, the cold chamber temperature test. Table 1 shows

Table 1 cold chamber real-time temperature and the time required to reach the temperature

Cool-ing temp-era-tu re /℃	30	20	15	10	5	0	-5	-10
Time/ m	2	5	9	14	18	26	33	45

From the experimental data available: when the cold chamber temperature dropped to more than five degrees, the cooling rate is relatively fast, when to five degrees below, the cooling rate began to slow down. The reason may be that the insulation measures are not perfect, or the cooling system is not fully functional[6].

Condensate collection is carried out at a cooling temperature of minus five degrees and minus ten degrees，The experimenter is a team member, Table 2:

Table 2 Collect the liquid volume in different cases

Experi-mental temper-ature /℃	Inspiratory way	duration /m	Collect the volume of liquid /ml
-5	Mouth sucks	10	2.54
-5	Nasal suction	10	1.43
-10	Mouth sucks	10	2.63
-10	Nasal suction	10	1.74
-10	Mouth sucks	15	3.01
-10	Nasal suction	15	2.25

From the above data available, the lower the temperature, the more condensate collected, the wayto absorb the liquid also have an impact, the mouth of the way to collect more liquid. The longer the duration, the more liquid is collected.

6.3 Temperature control system test

The temperature control system can control the temperature inside the cold chamber and can show the temperature in the cold chamber. After testing the mercury thermometer in the cold cavity of the test, compared with the temperature on the display, both temperature, the temperature error is less than ± 1 ℃. [7]Temperature control system can also control the temperature inside the cold cavity, the error is ± 1 ℃. Meet design requirements

VII. CONCLUSION.

Respiratory disease is a common disease and morbidity that endangers people's health. In the process of clinical diagnosis often based on the patient's clinical symptoms and pulmonary function to determine the severity of the disease and treatment. But the clinical symptoms and lung function may not be able to timely and accurately reflect the lung disease and physiological changes, it limits the diagnosis of the disease and the timeliness of treatment.[8] Exhaled gas condensate detection is a new measure of respiratory disease in the past few years. It is also a noninvasive method for evaluating airway inflammation and oxidative stress. It is simple, easy and reproducible. It is suitable for the condition Severe patients and children, including infants. For the monitoring of lung disease progression and treatment effect provides a new way. This design is very good to complete the design of the condenser, with good practicality.

References

[1] Xiaohong Li,Development of new exhaled condensate collector and its application in clinical practice [D]. Doctoral Dissertation of Jilin University, 2008.

[2] JianzhengHu.Discussion on semiconductor chiller. Household appliances .2001,8: 40-42. [Ni Meiqin, Chen Xinghua, Zhuang Bin ru. Concerned about the semiconductor refrigeration research [J] Refrigeration and air conditioning .2001.

[3] Jun Wang , Zhenbao Ling. Sensor principle and detection technology [M]. Changchun: Jilin University Press, 2003.

[4] YudongLi ,Maode Li , WeijiangLi . Optimization Design of Two-stage Semiconductor Refrigeration Performance [J]. Journal of Applied Energy Technology, 2006,5 (101) 62-66.

[5] Jinjing Wang ,Zijun Liu , Zhicui Zhang ,Jiaping Zhao , Xianhong Wu , Jiahe Wang, Exhalation of the exhalation device and disinfection of exhaled breath [J]. Chinese Medical Device Information. 2004 (04)

[6] Yang Ou, Sheng Jin,Shaobin Liu .Application of Exhaled Air Condensate Technology [J]. Fujian Medical Journal. 2006 (03)

[7] JimeiXu .Study on the Simple Method of Collecting Exhaust Gas Condensate [J]. Chinese Journal of Nursing. 2004 (11)

[8] Hua Qiao , Guangfa Wang ,Cuimin Ding . Design and clinical application of expulsion gas condensate collector [J]. Journal of Clinical Internal Medicine, 2005,22 (9): 625-626

Single document keyword automatic extraction system based on big data

Wu Guanliang; Wei Jinhe; Dang Wenjie; Wang Yongzhi

(School of Instrument Science and electrical engineering, Jilin University, Changchun 130000,China)

***Abstract*—The rapid growth of the information age has brought convenience to the people, but also brought difficulties. In order to deal with massive information quickly, an automatic keyword extraction system based on large data is designed. In the Linux system to build a large data Hadoop platform. Keywords automatic extraction system on this platform to design integrated word segmentation system, word frequency statistics and weight calculation technology. Verified by experiment, the system meets the extracted keywords recall and precision can be used, and the extraction time is very short, it is feasible.**

***Key words*—Hadoop platform word frequency count participle weight**

1. INTRODUCTION

WITH the development of the network, a variety of information to millions of orders of magnitude per day growth rate doubled. If people want to find their own care in a lot of information, the difficulties also followed. Therefore, we must come up with an effective way to help us to efficiently and accurately identify and distinguish these large amounts of information and find what we really need. Which is a great challenge for the current computer natural language processing technology. And in the document automatic clustering, document retrieval, document automatic summary and other fields need high-quality keywords as a starting point for the entire system to support the system, so automatically extract the text keywords is very important. With the gradual development of keyword automatic extraction technology, on the one hand, the function of full-text indexing is more and more difficult to meet the actual needs of users[1]; on the other hand, many document information services, such as automatic summary, document classification and clustering, text Analysis, subject retrieval and so on are the keywords automatically extract the results have a strong dependence, and keywords in the document to characterize the document important information and core content, to facilitate the reader to quickly understand the abstract information and quickly retrieve the specific documents , For the news reading, advertising recommendations, historical and cultural studies, text processing, machine translation, input method vocabulary selection and a series of industries and research have a vital role, so to fundamentally improve the quality of information services only better Solve keyword extraction problem.

At present, the main trend of automatic extraction of key words is based on linguistic keyword extraction and automatic extraction based on statistical keywords. Automatic keyword extraction based on statistics is the use of statistical methods to calculate the frequency of independent vocabulary in the document to get the key words. Linguistic based keyword extraction is the use of natural language processing techniques, such as lexical analysis, syntax analysis, semantic analysis, chapter analysis and other methods[2]. But the lexical analysis needs to solve the problem of unregistered words and vocabulary maintenance. Syntax analysis and semantic analysis are not high in accuracy, affect word recognition, and the chapter analysis is strict to the format and difficult to solve the general problem. The effect of the method is not ideal. The advantage of statistical method is that the statistics have been developed, and the statistical results can be easily obtained by analyzing the statistical indexes in the academic papers[3]. According to these statistical indicators, the candidate keywords can be analyzed synthetically.

For the Chinese language has no obvious boundaries such as the characteristics of the word, resulting in the automatic extraction of Chinese keywords more difficult to achieve, if not consider the Chinese word segmentation process, the English keyword automatic

extraction method can be used directly. On the basis of the research on the automatic extraction of keywords in foreign countries, the domestic scholars have carried on the thorough research and the development to the keyword automatic extraction, have put forward many representative algorithms and models. Du Yuncheng (2011) proposed the keyword automatic extraction based on the word extraction frequency[4], improved the TF / IDF algorithm according to the word position and text length, calculated the amount of information under the same word frequency, calculated the weight of the word using feature weighting, selected the weight of the word as a key word. Xie Jin (2011) proposed the Chinese keyword extraction method based on the word span[5]. Sun Xingdong (2014) proposed a method to obtain microblogging keywords based on clustering[6].

Based on the above, this paper designs a single document automatic extraction system based on Hadoop platform and using the programming language oriented to the program (Java language), comprehensively applying document processing, word segmentation, word frequency statistics and weight calculation to improve the information service quality.

2. Big Data Platform Hdaoop

The era of big data, the so-called big data, "big", said the data is not only "more". Cannot use the data to the number of TB or the number of PB .For large data, you can use four words to express: large, diverse, real-time, uncertain. That is, the amount of data is huge, the variety of data types, data changes quickly, the data of true and false doubts. According to the above characteristics, so the birth of such a platform: Hadoop. It has the following characteristics: the ability to store large amounts of data, quickly deal with large amounts of data, from a large number of data for analysis.

Hadoop platform has high reliability, high scalability, high fault tolerance and high efficiency and many other advantages, and it is open source free, very suitable for scientific research, so this paper select Hadoop platform to build large data storage system. HDFS which is mainly used to store massive amounts of data, it is divided into several files of the same size of the file block, and then these files are stored in different nodes. Map / Reduce is mainly responsible for the calculation of massive data.

Hadoop implements a distributed file system (Hadoop Distributed File System), referred to as HDFS. HDFS is characterized by high fault tolerance and is designed to be deployed on low-cost hardware; and it provides high throughput to access the application's data for those with large data sets Set of applications. HDFS relaxed the requirements of POSIX and can stream the data in the file system as a stream.

Hadoop is widely used in large data processing applications thanks to its inherent advantages in data extraction, deformation and loading (ETL). Hadoop's distributed architecture places the large data processing engine as close as possible to storage, as opposed to batch operations such as ETLs, since batch results like this can go directly to storage. Hadoop's MapReduce feature enables the fragmentation of a single task and the fragmentation task (Map) to multiple nodes, and then in a single data set to load (Reduce) to the data warehouse[7].

3. Technology Of The Keywords Automatic Extraction

Keyword extraction, also known as keyword indexing[8], is a technique that identifies meaningful and representative vocabulary, and refers to the extraction of a number of important vocabularies that can cover the original theme or generalize the original text. In this paper, an automatic word extraction method based on word frequency is used. After the word segmentation and word removal, the statistical word frequency and position information are obtained. Finally, according to the influence factors such as word frequency, occurrence position and word segmentation order, The weight of the article, extracted by the weight of the key words.

3.1 Chinese Word Segmentation Technology

Chinese word segmentation, as the name implies refers to the Chinese sentence for word segmentation[9], where the computer is a processing tool. For example, the English sentence is usually separated by spaces to separate the word, then we use the separator is to use the separator to cut a Chinese

word, because the Chinese sentence in addition to the punctuation mark there is no other separators, and punctuation It is only a separate, not a word. Chinese information processing is a direction in natural language processing, and Chinese word segmentation is the first step in Chinese information processing, but also the most basic and most critical link.

Chinese word segmentation is a basic work in the process of Chinese text processing, the advantages and disadvantages of word segmentation directly affect the machine's understanding of Chinese sentences. At present, there are many methods of Chinese word segmentation, although the names are different, word segmentation effect is different, but according to its basic principles can be classified as dictionary segmentation, statistical analysis, semantic grammar rules segmentation and artificial intelligence law four Class[10].

3.1.1 Chinese Lexical Analysis System ICTCLAS

Chinese lexical analysis is the basis and key of Chinese information processing. In this paper, the Chinese lexical analysis system ICTCLAS is used to preprocess the text. In order to facilitate the extraction of the lexical features, position analysis and word segmentation are carried out at the same time. ICTCLAS (Institute of Computing Technology, Chinese Lexical Analysis System), developed by the Institute of Computing Technology, Chinese Academy of Sciences, the main function covers the Chinese word segmentation, part of the annotation, named entity recognition, new word recognition, while supporting the user dictionary[11]. Upgraded to ICTCLAS3.0.

ICTCLAS advantage is mainly reflected in the following four aspects:

(1)Comprehensive performance is optimal

ICTCLAS has applied the perfect PDAT large-scale knowledge base management technology , in the high speed and high precision has made a major breakthrough between the management of millions of dictionary knowledge base, single machine can query 1 million entries per second, while the memory Consuming less than 1.5 times the size of the knowledge base. Based on this technology, ICTCLAS3.0 word rate of stand-alone 996KB / s, segmentation accuracy of 98.45%, API does not exceed 200KB, a variety of dictionary data compression less than 3M, is the world's best Chinese lexical analyzer.

(2)A unified theoretical framework for language computing

ICTCLAS uses the Hierarchical Hidden Markov Model to unify all aspects of Chinese lexical analysis into a complete theoretical framework , to obtain the best overall effect, and related theoretical research published in the top international Meetings and magazines, both in theory and practice have confirmed the advanced nature of the model.

(3)All-round support for application development in a variety of environments

ICTCLAS all prepared by C / C ++, support Linux, Free BSD and Windows series operating system, support C / C ++ / C # / Delphi / Java and other mainstream development language[12].

(4) Need to change, tailored

All functional modules can be disassembled assembly, the user can according to their own needs, tailored self-help for their own word segmentation system.

3.1.2 Insert The User Dictionary

For specific areas of the article, such as the medical field, the power field, the geological field, which must contain some of the proper nouns used in this field. These proper nouns may be divided into several words in the word segmentation system, such as "renewable energy" is divided into "can", "regeneration" and "energy" three parts, which is expressed in the original word far. To solve this problem, this article allows the insertion of user dictionaries. User dictionaries should include as many relevant terms as possible in the relevant field. When the word is compared with the dictionary, the proper noun will not be divided.

3.1.3 Remove the Stop Word

The term "stop" refers to those functional words that do not reflect the subject, such as "yes", "that is"," so ","and so on", although they appear in the article a high number of times, but they cannot reflect the subject of the document, The extraction of the keyword causes interference, so it is necessary to filter it out[13]. It is well understood that the stop word is defined as all the functional words and punctuation, and the definition of the deactivation of the vocabularies and for word segmentation based on these tables is well understood. What is the purpose of the

lexical filtering? In the Chinese language, the ability to identify the text is often the text of the words. And some of the text in the text, for the identification of the text of the category and did not contribute. If these words are not meaningful meaning of the text as a text feature words, will bring a lot of errors, which directly reduce the efficiency of text classification and accuracy. Such as "very" "already" and so on, they appear in the text of the number will often be high, will affect the accuracy of keyword extraction. Therefore, in the extraction of text feature words, we first consider the elimination of these text classification is useless for the use of the word, in the text preprocessing stage can avoid the interference of the extraction results, so that the extraction results more accurate.

3.2 Word Frequency Statistics

In the process of keyword extraction, the key is determined by calculating the weight of the keyword candidate. Firstly, analyze the frequency of the word, the relative frequency of the word, anti-literature frequency factor, location, part of speech, the value of the word itself and the word length and other information[14]. At the same time, introduce some certain statistical methods, such as mutual information, TFIDF, maximum entropy, etc. To weight the words, and finally sort the words according to the weight of the words, the output weight of the larger words, that is, the extraction of keywords.

To this end, this paper uses two methods to count the frequency of words: Chinese Academy of Chinese lexical analysis system ICTCLAS and Word Count. And analyzes the advantages and disadvantages of the two methods.

ICTCLAS has been mentioned above and is not mentioned here. After the text preprocessing, continue to call the system's word frequency statistics module to count the number of words appear in the text (word frequency), and the word frequency marked in the back of each word. This method has high speed, accurate advantages, in actual use can save a lot of time, the statistical results are more accurate. The shortcomings of the word frequency statistics are directly used for the system itself, the keyword extraction module, cannot be extracted for the next step to bring difficulties.

Word Count is the use of Hadoop platform map-reduce prepared by a program to count the text word frequency. In the experiment, this statistical method is running slowly, and the accuracy of statistical results compared to the Chinese Academy of Sciences ICTCLAS poor, so in actual use, the accuracy requirements are not very high circumstances can use the method. The advantage is that the statistical results can be extracted, and used for other modules of the system analysis and calculation.

4. Keyword Extraction Algorithm TFLD

4.1 Feature Term

For a single text, there are many features that can reflect the importance of the word to the text. In addition to the commonly used word frequency TF, the characteristic position of the word appears, the word length, the part of speech, and the word distance order. Have a certain value[15]. After extracting the words and phrases of the text after the word segmentation and deactivation words, in order to extract the keywords of the text, the following three feature items are selected to calculate the weight value of each word.

(1) Word Frequency tf: is one of the most commonly used parameters in the extraction of words, is the simplest measure of the word. In this paper, the word frequency is calculated by the nonlinear function:

$$tf_i = \frac{f_i}{1+f_i} \quad (1)$$

Where f_i is the number of occurrences of each word in the text. The advantages of nonlinear processing are as follows: 1) The frequency characteristic of the word frequency increases with the number of occurrences, and the frequency of the word converges to 1, indicating that the number of occurrences is more. 2) When the number of occurrences of a word is relatively high, then the word frequency characteristic value does not change greatly with the number of occurrences of the word, so that the probability of the word as a keyword does not occur with the number of occurrences Continuous increase and a substantial increase, more in line with the language of reality.

(2)Location Area: the study found that a word or phrase appears in the text of the position to determine its value has an important role in different locations have a relatively different importance. The words that

appear in the title and the abstract are more likely to be keywords than appear in the text, and the words appearing in the first or the end of the text reflect the subject of the article more than the words that appear in the other parts. So you can use the following formula to calculate the position feature:

$$area_i = (X_1 \times 5 + X_2 \times 3 + X_3 \times 2)/L \quad (2)$$

Where X_1 is the number of occurrences in the title or digest, X_2 is the number of occurrences in the first sentence, X_3 is the number of occurrences in the end sentence, and L is the total number of words.

In order to distinguish the importance of reflecting the subject of the article, here we assign different weights to the number of words X appearing in different positions.

(3)Word Segmentation Order dis: the word extraction process is always extracted a lot of words are not keywords, these words appear because they have a real keyword and similar features: high frequency, appear in important places and many more. After a statistical study found[14], the first occurrence of a word from the beginning of the distance of the article on the extraction of keywords is also very meaningful. So this article also uses this factor as a feature to reflect the weight of the word in the article. In this paper, we use a linear function: $v_i = a \times i + b$ to represent the order of word segmentation. Where is the order in which the words appear in the text, and a, b is the adjustable constant factor. And then by the following formula to calculate the weight of the nonlinear function:

$$dis_i = v_i / lnv_i \quad (3)$$

4.2 Weight Calculation

After the above analysis and quantization of each feature, the above-mentioned feature is added to the following weight calculation formula by linear weighting:

$$W_i = tf_i \times A + area_i \times B + dis_i \times C \quad (4)$$

Where W_i is the weight value of the word i in the text, and A, B, and C are the proportional coefficients, which are used to show the proportion of each feature in the weight formula. After linguistic research, word frequency is the most important in each feature, so A assigns 1.5; position occupies second, B assigns 1.0; sub-distance order again, C assigns 0.8. Finally, the weights of each word are calculated by this formula, and the candidate keywords are obtained in descending order, and the keywords can be extracted from the candidate keyword set according to the weight.

5. Analysis

In order to test the usability of the system, a number of articles on the power system downloaded from China are selected. When extracting keywords, insert the power system user dictionary, word segmentation results than the user dictionary is more accurate.

5.1 Evaluation Criteria

The evaluation method of the keyword automatic extraction system is to match the extracted keywords with the keywords given in the article and the article. In this paper, two evaluation criteria to determine the performance of the extraction system, respectively, the precision and recall rate. Where the precision rate P = automatically extract the correct number of keywords / automatically extract the number of keywords, it can reflect the accuracy of the system; recall rate R = automatic extraction of the correct number of keywords / knowledge and articles given the key The number of words, it can reflect the integrity of the system.

5.2 Evaluation Results

By analyzing the experimental results, compared with the keywords given in the article and knowledge, calculate the precision and recall rate. Calculated analysis, check the rate of distribution in the 70-85% between the detection rate distribution between 65-75%. After several tests, it is found that the system extraction result is stable and reliable, which can meet the actual demand, and the extraction time is short and the extraction efficiency is higher.

6. Concluding Remarks

In this study, the Hadoop platform was built under the Linux system, and a keyword automatic extraction system was designed under the platform. The system uses the Chinese language lexical analysis system ICTCLAS and the user dictionary to pre-word the article, and in the word segmentation result by inserting the deactivation of the vocabulary to remove the words, so that the word is more accurate; on this basis, select the word frequency TF , The position and

the fractional distance order are the main factors to measure the weight of the keyword, and the nonlinear function is constructed for each feature item, which makes it more in line with the law of natural language. In the test, through several tests, constantly adjust the weight of the formula in the proportion coefficient, improve the system performance. In the actual use, but also to get a better effect.

References

[1] Gao Yan. Key words automatic indexing method overview [J]. Electronic World .2012, (6): 118-120.

[2] Zheng Jiaheng, Lu Jiaoli. Key words extraction method research [J]. Computer Engineering, 2005,18 (9): 194-196.

[3] Pan Limin, Wu Junhua, Lin Meng, et al. Chinese keyword extraction method based on fusion multi-feature [J]. Information Network Security, 2014, (8): 40-44.

[4] Du Yuncheng, Zhou Wei, Han Yanhua, Lu Xueqiang. Automatic extraction of keywords based on word frequency [J]. Journal of Beijing Information Technology University (Natural Science Edition), 2011 (6): 35-38.

[5] Xie Jin Word-based Chinese text keyword extraction and its application in text categorization [D]. Zhejiang University of Technology, 2011.

[6] Sun Xingdong,Li Aiping,Li Shudong. Research and implementation of a method of extracting microblogging keywords based on clustering [J]. Information Network Security, 2014, (12): 27-31.

[7] http://www.hadoop.org last accessed by 2017.1.20

[8] Cohen J D. Highlights :Language and Domain-independent Automatic Indexing Terms for Abstracting[J].Journal of the American Society for Information Science,1995,46(3):162-174.

[9] Feng Guohe,Zheng Wei.A Summary of Domestic Chinese Word Segmentation Technology [J]. Library and Information Work .2011,55 (2): 41-45.

[10] Huang Changning,Zhao Shuang.Review of Chinese word segmentation in the past ten years [J]. Chinese Journal of information science, 2007 (3): 8-19.

[11] Multilingual Entity Task Conference(MET). http://www.itl.nist.gov/iaui/894.02/related_projects/tipster/met.htm.

[12] Zheng Jiaheng, Lu Jiaoli.Research on Keyword Extraction Method [J]. Computer Engineering, 2005, 18 (9): 194-196.

[13] Sun Yufang, Chen Xiaoli, Xiong Zhongyang. Effects of information gain-based feature word weight adjustment algorithm [J]. Computer Engineering and Applications, 2007,43 (35): 159-161.

[14] He Xingui, Peng Puyang.Chinese words of the keyword automatic extraction and fuzzy classification [J] .Chinese Journal of Information, 1999, 13 (1): 9 -15.

[15] Guan Ruixia, Lu Bei.TFLD a Chinese text keyword automatic extraction method [J]. Electrical and Mechanical Engineering, 2010.

A system for monitoring snoring based on piezoelectric thin film sensors

Wei Dexin; An Yuting; Wang Chengmu

(College of Instrument Science and electrical Engineering, Jilin University,Changchun 130026,China)

***Abstract*—Snoring is a common sleep phenomeno which is easily ignored. Actually it is theperformance of breathing weaken and a sign of health problems.People who snore areassociated with significant apnea or hypopnea phenomenon,for most people,occasional transient respiratory obstruction is very common,but if the obstruction orhypopnea is very frequent and the respiratory obstruction is in serious condition,thenthis will become a disease we called Sleep Apnea Hypopnea Syndrome(SAHS). The contents of this paper is to design a snore monitoring system based on piezoelectric film sensor which can real time monitoring of snoring phenomenon at night,can record and display the snoring phenomenon,and can automatically identify and alarm prompt.**

***Key words*—Snore Apnea PVDF Monitor**

I. INTRODUCTION

IN recent years, the incidence of chronic respiratory diseases, cardiovascular disease increased year by year which caught the attention of society.Therefore, non-invasive respiratory and pulse monitoring technology has been rapid development,and in early detection and diagnosis of chronic diseases have been widely used. such as sleep apnea syndrome, chronic obstructive pulmonary disease.In daily life,we need to achieve the purpose of real-time monitoring and prevention as little as possible on many occasions,so we need to design a detection device with more convenient to carry, low power consumption and easy to operate[1,2]. The purpose of this project is to design a wearable instrument which detect the breathing of body with the PVDF piezoelectric film sensor. On the basis of dynamic monitoring techniques for human physiological parameters to achieve higher accuracy of the test results.This kind of body-based dynamic breathing monitoring system can meet the needs of the free activities of the detectors by wirelessly transmitting the relevant signals.More importantly,the detection system can monitor, collect and process the human body in real time physiological parameters, and detection of breathing.To a certain extent,it can discover and prevent some chronic respiratory diseases.

II. RESEARCH STATUS AT HOME AND ABROAD

There are several main types of equipment currently used to observe the state of breathing during sleep: (1) Electrocardiogram (ECG): W. Einthoven [3] et al. first used this method to Observe breathe. He attached the electrocardiogram to the chest, through the electrode to detect the pressure changes in the blood flow to the blood pressure, heart rate and respiratory status recorded. Through the instrument can be indirectly observed the state of breathing, but can not monitor the strength of breathing and other information, which can not determine the severity of the patient blocked or low ventilation. （ 2 ） Transthoracic impedance plethysmography signal (IP): the device through the electrode to conduct a small current, when people breathe ， the chest resistance and the current conduction path will change ， in order to observe breathing state. Through the respiratory process changes in chest impedance to detect the respiratory state. The disadvantage of this method is that the impedance of the human body is affected by many other factors, such as body movement, sleeping position changes, so the data is often inaccurate and contains a lot of noise[4].(3) Photoplethysmography signal (PPG):I observes blood pressure by measuring the periodic vibration of arterial pulse.Frey [5]and Hartert [6]et al.use PPG to observe the breathing cycle by studying the relationship between PPG signal and

respiration. The method also does not directly observe the respiratory signal and It is difficult to measure the intensity of respiration and the exact duration.(4)Air guide microphone: This method is greatly affected by the surrounding environment, the distance between the microphone and the respiratory system is also difficult to guarantee,which will affect the signal acquisition. Such as Alshaer et al.use a directional air guide microphone to record the acoustic signals of snoring when sleeping, and detect snoring by analyzing the acoustic signals.(5) Polysomnography (PSG): The current PSG is the "gold standard" in the diagnosis of SAHS. The patient underwent a variety of sensors to be monitored and monitored throughout the monitoring room, including blood oxygen saturation(Sao2), thoracic and abdominal breathing exercise ,electroencephalogram (EEG), electrocardiogram (ECG), electromyography(EMG), Electroretinogram (EOG), nasal airflow, snoring index and body position. And according to the collection of different sensor data, to facilitate the doctor to conduct a comprehensive, comprehensive diagnosis. So now almost all doctors adopted, and as the authority of the industry diagnostic means. Of course, through the fiber nasopharyngeal laryngoscopy, imaging (CRM, CT and MRI), esophageal pressure detection and other diagnostic methods.

III. DESIGN PRINCIPLE AND THE DESIGN OF SYSTEM

A. Piezoelectric Sensor Principle

Some dielectric materials in the direction of the external force due to the role of external deformation, the internal polarization will occur, while there will be positive and negative charge appears in its two opposite surfaces[8]. When the external force disappears, it will return to the non-charged state, saying that this phenomenon is positive piezoelectric effect[9]. On the contrary, when the electric field is applied in the direction of polarization, these dielectric materials are deformed, and the deformation disappears as the electric field is removed. Our phenomenon is called the inverse piezoelectric effect[7]. As shown in Figures 1 and 2.

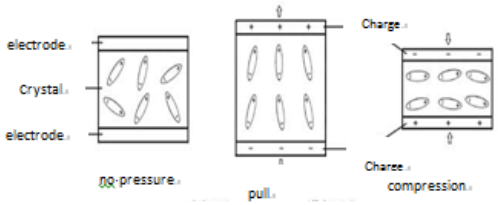

Fig. 1. Positive piezoelectric effect

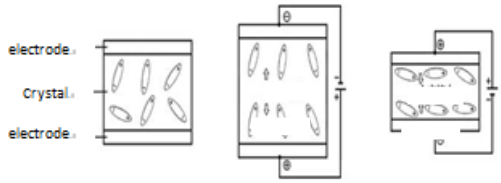

Fig. 2. Negative piezoelectric effect

Piezoelectric sensor is a class of sensors，based on the dielectric material annoying piezoelectric effect developed.Piezoelectric materials are roughly classified into piezoelectric crystals, piezoelectric ceramics and piezoelectric polymers. In this design, PVDF piezoelectric film sensor is a new type of polymer element based on PVDF as the main material and piezoelectric effect. The PVDF film material has good resistance to chemical corrosion, high temperature resistance, oxidation resistance, weather resistance, radiation resistance [10]. It consists of four parts: metal electrode, lamination, lead and shielding. The structure is shown in Figure 3.

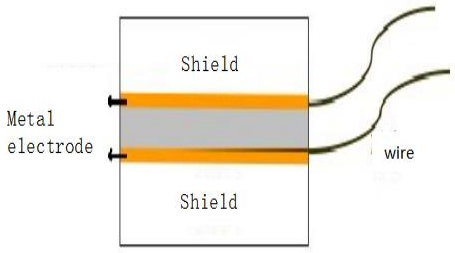

Fig.3. piezoelectric film sensor structure

When the crystal force is deformed, the internal electrode is generated, and the opposite sign is generated on both surfaces. When the external force is removed, the crystal is restored to the uncharged state; when the external force direction changes, the polarity of the charge. The amount of charge produced by the force of the crystal is proportional to the magnitude of the external force.

$$P = \mathrm{d}\sigma \tag{1}$$

Among them, P is the crystal of the rate, the unit is C/m2, D is the piezoelectric constant, the unit is C/N,

σ is the stress, the unit is N/m2.

B. Charge Amplifier Principle

As can be seen from the above, the PVDF piezoelectric thin film sensor output signal for the amount of charge, it need to match the front of the circuit connected with it to output a complete signal. PVDF piezoelectric film has a high internal resistance, the need for pre-circuit circuit in the first stage of the amplifier output signal can be converted into low-impedance output signal, while the weak charge signal into a voltage signal [11]. Therefore, in the design of the front circuit,we use the charge amplification circuit as the first stage amplifier circuit. The charge amplification circuit is a high gain amplifier with deep negative feedback. The basic circuit is shown in Figure 4.

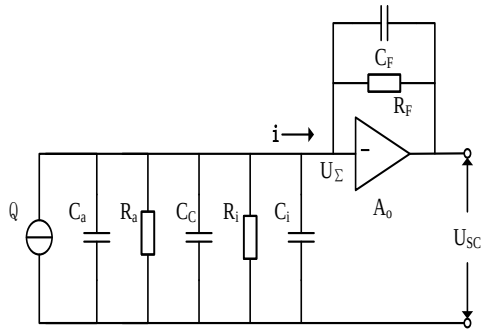

Fig.4. Equivalent circuit of charge amplifier

In the figure, the Ca is the sensor capacitance; Ra is the sensor insulation resistance including the connecting wire; Cc is the connecting wire to ground capacitance; Ri is the preamplifier input resistance; Ci is the preamplifier input capacitance. When the open-loop gain AO of the amplifier is large enough and the input impedance is high, the amplifier input is almost no shunt and the operating current flows only into the CF and RF in the feedback loop. We can see i expression:

$$i=(U_\Sigma-U_{SC})\left(j\omega C_F+\frac{1}{R_F}\right)=\left[U_\Sigma-(-A_0U_\Sigma)\right]\left(j\omega C_F+\frac{1}{R_F}\right)$$
$$=U_\Sigma\left[j\omega(A_0+1)C_F+(A_0+1)\frac{1}{R_F}\right] \quad (2)$$

And then by the "Miller effect" can be obtained node UΣ and voltage output USC:

$$U_\Sigma=\frac{j\omega q}{\left[\frac{1}{R_F}+(A_0+1)\frac{1}{R_F}\right]+j\omega\left[C_F+C_C+(A_0+1)C_F\right]} \quad (3)$$

$$U_{SC}=-A_0U_\Sigma=\frac{-j\omega qA_0}{\left[\frac{1}{R_F}+(A_0+1)\frac{1}{R_F}\right]+j\omega\left[C_F+C_C+(A_0+1)C_F\right]} \quad (4)$$

From (4), if the cable capacitance Cc is omitted, the output voltage USC only depends on the input charge q and the feedback loop parameters CF and RF, and the capacity of the capacitor CF should be selected in the range of 100pF to 104pF.

C. Overall Design

System signal acquisition is mainly based on PVDF piezoelectric film sensor to achieve, the sensor through the elastic fabric and the human body to get in contact with the signal,and then deal with it by the circuit board on the hardware circuit.

Circuit board have the signal conditioning circuit, MSP430 minimum system circuit and the Bluetooth module, the entire circuit board voltage supply by the 3.7V Keng battery pack;The collected data channel to enlarge the conditioning, A / D conversion, the data obtained by the single-chip software filtering, numerical conversion, and then through the Bluetooth and computer wireless communication, the corresponding data will be in the computer through the LabVIEW software once again.And finally in the form of a graphical display and determine whether the snoring and apnea. The overall design of the system is shown in Figure 5.

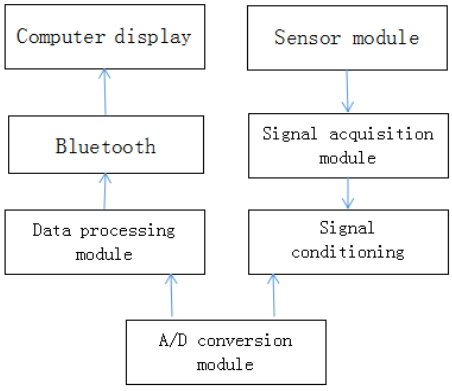

Fig .5. System overall design diagram

The signal conditioning circuit comprises a first stage charge amplification circuit, a second stage voltage amplification circuit, a low pass filter circuit and a voltage lifting circuit; the single chip data processing module mainly performs control A/D conversion, numerical conversion and performing Bluetooth communication; PC development is mainly based on LabVIEW serial data reception, software

filtering, man-machine interface design, signal waveform display and judgment processing.

IV. MODULE MODULE DESIGN

A.Signal Acquisition Module Design

Signal acquisition module mainly by the PVDF piezoelectric film sensor, insulation elastic fabric composition, physical as shown in Figure 6.

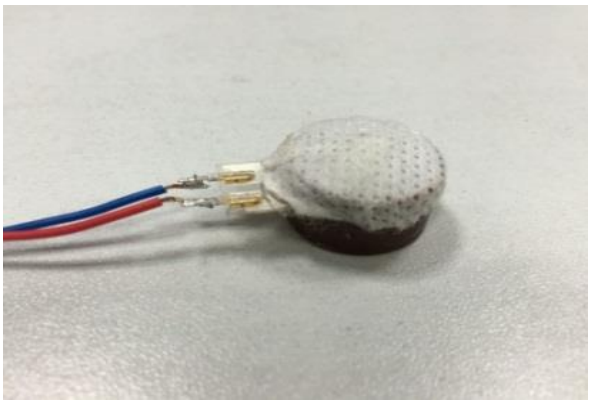

Fig.6.physical Sensor

PVDF Piezoelectric Thin Film Sensor is the most important part of this module and is the main sensing part of signal acquisition. The sensor is placed in the elastic fabric inside, and one side completely fit in the arch structure, the other side with the human body directly touch; from the piezoelectric film on both sides of the electrode leads to two lines access belt, wristbands on the other side of the circuit board, The piezoelectric signal is generated and enters the signal conditioning circuit.

B. Signal Conditioning Module Design

The piezoelectric signal output from the signal acquisition module needs to undergo charge conversion, amplification ,uplift,and other conditioning to form the ideal analog signal[12] .The signal conditioning module includes a charge amplifying circuit, a voltage amplifying circuit, a low-pass filter circuit and a voltage uplift circuit.

1.Charge amplifier circuit

As can be seen from the second chapter,Due to the piezoelectric effect, PVDF piezoelectric film will produce the amount of charge, the amount of charge will be converted to the amount of voltage for further signal conditioning, analog-to-digital conversion,so the charge amplifier should be used as the first stage of the signal conditioning circuit.The main function of charge amplifier circuit as the first stage circuit of signal conditioning circuit:（1）The charge amplifying circuit converts the weak electric signal which is difficult to measure and regulate, into a voltage signal and amplifies it;（2）The selected charge amplifier circuit is matched with the die electrical characteristics of the PVDF piezoelectric film sensor, and the high impedance input is converted into a low impedance output ;The output impedance of the PVDF piezoelectric thin film sensor is about 1013Ω，therefore, the core of the selected charge amplifier circuit should be a voltage control current type field effect tube integrated amplifier which is high input impedance and controlled by low noise voltage.This topic designs using CA3140 amplifier produced by the Intersil, with the advantages of piezoelectric PMOS transistor technology and high voltage electric double grant transistor, When it is working properly,the input impedance of the normal work of about 1.57T, the working voltage is 4V~36V (either single or dual power supply).The design of the basic circuit diagram of the charge amplifier circuit is shown in figure 7.

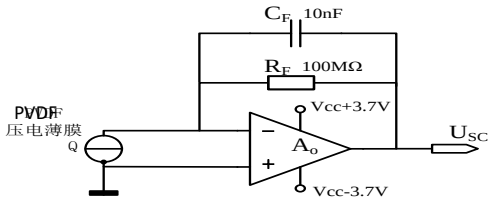

Fig.7 The charge amplification circuit diagram

In the figure, the charge amplifier circuit output voltage USC is ：

$$U_{SC} = -\frac{Q}{C_F} \qquad (5)$$

On the one hand, the introduction of RF in the circuit provides DC feedback for the integral capacitor CF; on the other hand, RF make the charge amplifier circuit has the function of negative feedback and improve the stability of the system.In addition, the selection of CF will also affect the signal amplification effect, if the CF is too small, it will make the whole system noise increases, the distortion of the signal, thereby affecting the signal acquisition; if CF is too large, then the amplification effect is not obvious, so that the effective signal submerged in the noise, will put forward higher requirements on filtering and amplifying circuit. Capacitance CF capacity should be selected within the range of 100~104pF.The capacity of the CF capacitor

should be selected in the range of 100~104pF. After the actual test of the CF with many times, CF selects the 10nf capacitor, and the R3 selects the 100MΩ resistance to be possible to achieve the electric charge amplification ideal effect very well, in order to reduce the difficulty of the subsequent conditioning circuit.

2. Voltage amplifier circuit

The amount of voltage obtained by the conversion of the upper level charge amplifier circuit has been enlarged,, but in the charge amplifier circuit, we pay more attention to the charge signal into a voltage signal of the low noise and stability, so determining the two indexes of RF and CF is used to prevent signal distortion, stable output. Therefore, it is necessary to place a voltage amplifier circuit in the second stage of the preamplifier circuit in order to enlarge the voltage signal to the desired amplitude. The basic circuit diagram of the voltage amplification circuit is shown in figure 8.

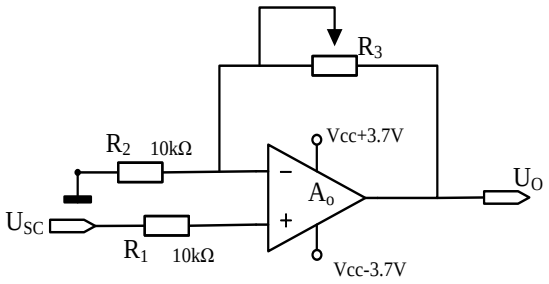

Fig.8. The voltage amplification circuit diagram

The USC of figure is the output of the charge amplifier circuit, which is the input voltage of the circuit, UO is the output voltage, the two have the following relations:

$$\frac{U_O - U_{SC}}{R_3} = \frac{U_{SC} - 0}{R_2} \tag{6}$$

$$U_O = \left(1 + \frac{R_3}{R_2}\right) U_{SC} \tag{7}$$

Set $K = \frac{R_3}{R_2}$, after a number of tests can be seen in the above amplifier circuit work, the K value of 15~45 amplification effect is best.when the circuit works, operating characteristics of the amplifier itself will be affected by the change of the supply voltage, so when the supply voltage is not absolute stable value, effective value of amplifier will also appear some differences, need by adjusting the K value to achieve the best effect of amplification, the circuit in Figure 3.3 using R3 adjustable potentiometer to replace fixed resistance, in order to improve the signal conditioning system flexibility and operability.

3. Low pass filter circuit

In the acquisition of breathing and pulse signals at the same time, will be disturbed by other noise, such as thermal noise of the human body, Other electric appliance frequency noise the noise will affect the accuracy of signal detection and the precision of signal waveform. Because of the high frequency of these noise relative to the respiratory signal and pulse signal, the two order active low-pass filter is used to filter the noise interference in the analog signal. This topic design using the active low-pass filter circuit, the active filter circuit load without affecting the filtering characteristics, and the active filter circuit consists of RC network and integrated operational amplifier, therefore, in the case of a suitable DC power supply, the circuit can be used, and can also be enlarged. In low voltage , low current and low power signal processing, the active low-pass filter circuit can meet the requirements, as shown in Figure 9.

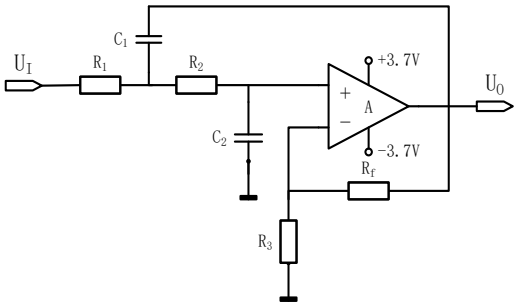

Fig.9. Two order active low-pass filter circuit diagram

For the low-pass filter shown above, the cutoff frequency is:

$$f_0 = \frac{1}{2\pi}\sqrt{\frac{1}{R_1 R_2 C_1 C}} \tag{8}$$

If you simplify the parameters, so that R1=R2=R, C1=C2=C, you can get the cut-off frequency :

$$f_0 = \frac{1}{2\pi RC} \tag{9}$$

The voltage gain is:

$$A_0 = A_{VF} = 1 + \frac{(A_{VF} - 1)R_1}{R_1},\ A_{VF} = \frac{R_1 + R_f}{R_1} \tag{10}$$

The selected capacitor C1=C2=C=0.1μF, resistance

R1=R2=R=18kΩ, so the cut-off frequency of 88.46Hz, in line with the circuit parameters and system requirements, for the MCU and PC software filter to reduce the difficulty.Two order low-pass filter circuit structure is simple and the input impedance is high, the output impedance is low, in the circuit parameters set reasonable, can meet the requirements of the system precision and achieve the desired filtering effect [13].

4. Voltage uplift circuit

According to the test, the amplitude of the respiratory signal and the pulse signal by the PVDF piezoelectric film sensor to collect income the existence of negative and the negative voltage signal is needed acquisition and processing, but the MSP430 can only recognize and deal with positive voltage ,therefore,by the voltage rise circuit ,the negative voltage of the respiratory and pulse signal voltage will be uplift into positive,, as shown in figure10.

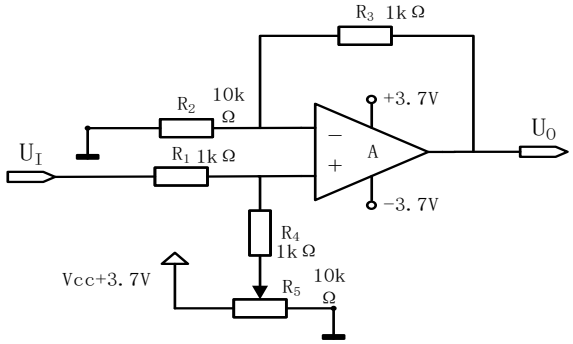

Fig.10. Voltage uplift circuit diagram

C. MCU Data Processing Module Design

1. MSP430 minimum system design

MSP430 Series MCU is a mixed signal processor (Mixed Signal Processor) with the16 bit ultra low power consumption and the reduced instruction set (RISC) which began to be promoted by TIIn the United States in 1996.This topic is using the MSP430F149 model of the microcontroller, the minimum system design diagram as shown in figure 11.

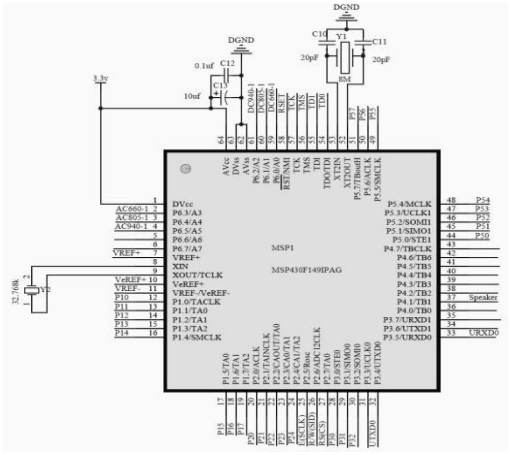

Fig.11.MSP430F149 microcontroller minimum system

MSP430F149 Type MCU has 48 I/O ports, 96 LCD drive, the ultra low power MCU based on the flash or ROM can provide 8MIPS and realize two 12 bit D/A conversion of the road; It realizes the memory serial expansion of the hardware I2C serial bus interface. At the same time, in order to improve the data transmission speed, the DMA module is adopted.It operates from 1.8V - 3.6V, with a 60KB flash and a variety of high performance simulationand intelligent digital peripherals [14]. It has the advantages of strong processing ability, high operation speed, low power consumption, rich in the resources of the chip, etc., and can meet the relevant design requirements of the project.

2.A/D conversion design

PVDF piezoelectric film sensor measures the breath and pulse signal (physical), and convertes into electrical signals, the electrical signal is converted into digital quantity by analog to digital conversion, so that the analog can be processed and controlled by the MSP430 .A/D conversion program design as shown in figure 12.

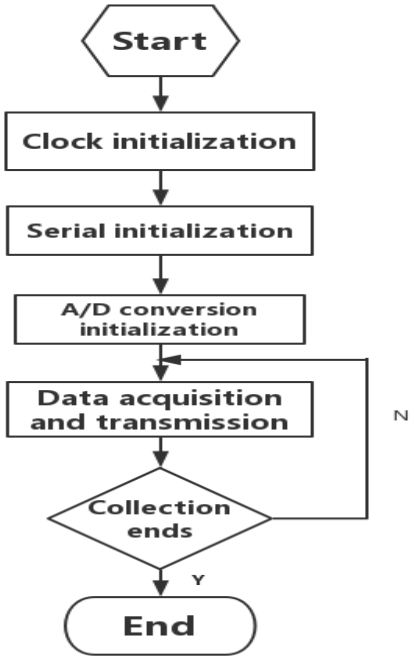

Fig.12. A/D conversion design flow chart

First, define the delay subroutine and serial data function;then the MSP430 MCU initialization, including ADC12module initialization, it uses the sequence channels switch in turn and automatically trigger mode,conversion sampling timer for the first time ,the rising edge of the SHI signal will triggeres,, then immediately starts after the last time.open the internal reference voltage generator, set the internal reference voltage of 2.5V, open the ADC12 kernel, the rising edge of the trigger conversion, the same direction signal input, single channel multiple conversion mode;Clock initialization, set the SMCLK=8M, using an external crystal 8M; serial initialization, sending register is set to the same clock polarity , selection SCLK (8MHZ), no trigger detection, receive register settings: (default) without frame error, check the correct, not allowed to interrupt and IO port initialization.After the initialization, A/D converter for analog signal rising edge trigger, trigger A/D sampler start sampling, sampling the analog to digital conversion from analog digital converter, converted after data conversion to an array of bytes stored in the memory chip address, then the first address is accessd by the processor , the data in the form of a byte string began to send computer.When the flag bit of the register (UTXIFG0) is 1, completion of sending a byte, experiments show that at this point should reset the flag bit IFG2t and prepare to send the next byte.So the cycle, the respiratory signal is continuously acquisition, conversion, processing and transmission to the next node, in order to achieve the real-time detection and display.

D. Bluetooth Module Design

In the actual design, in order to achieve the effect of convenient wear and minimize the impact on the normal activities of the human body's own, in the choice of signal transmission mode should avoid using solid lines, so using the wireless transmission mode for data transmission between the PC and wearable parts. In this paper, the design uses wireless Bluetooth transmission technology as a support for real-time data transmission.Bluetooth is a wireless personal area network (Wireless PAN), is a kind of short-range communications support equipment (general 10m) radio technology, it makes electronic devices with communication ports in the small scope canwireless communication. Bluetooth uses the radio interface of the universal frequency 2.45GHZ, IEEE802.15 protocol.This topic in the design of bluetooth module uses the silent state to work for data transmissionk; Baud rate is set to 9600; No parity bit; Computer parts of bluetooth serial port and single-chip microcomputer the bluetooth serial port set up primarily from one mode [15]. The design structure of the Bluetooth module is shown in figure 13.

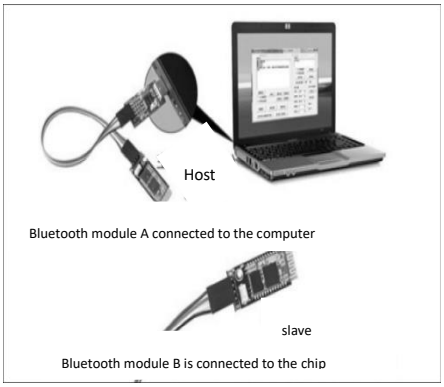

Fig.13. The Bluetooth module structure diagram

V. PC SOFTWARE DEVELOPMENT

LabVIEW (Laboratory Virtual Instrument Engineering Workbench) is a program development environment developed by the National Instruments (NI) company, similar to the BASIC and C language development environment, but LabVIEW is clearly

different from other. other computer language generation code is almost always in the language of the text, and LabVIEW in the form of a block diagram and the use of graphical source code programming [16]. LabVIEW software is not only an excellent platform for virtual instrument development, but also a powerful tool for engineering to design and development [17].In this design, the main work of using LabVIEW includes reading the data from the Bluetooth, performing the type conversion, software filtering, real-time display of the waveform and judging the calculation.

A. Read The Serial Data Program

The respiratory data processed by the MSP430 microcontroller is sent to the computer via a pair of Bluetooth serial ports, and the serial data is read directly by software.So you need to design the relevant LabVIEW module to read it out for subsequent data processing. The block diagram of the read module is shown in Figure 14.

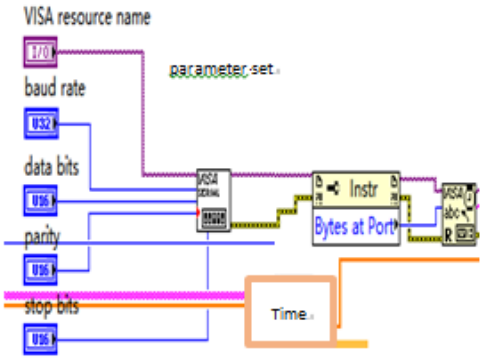

Fig.14. LabVIEW file read block diagram

B. Data Type Conversion Procedures

The respiratory data received by the Bluetooth serial port is a continuous string of data, no separation mark, so the computer can not be converted into a two-dimensional waveform chart in the form of display.It is necessary to design the LabVIEW program to restore these string data to separate the limited string.In addition, LabVIEW filter module can not directly deal with string data, so also need to convert a single string into a single double real number. that is, string to array conversion.The data type conversion block diagram is shown in Figure 15.

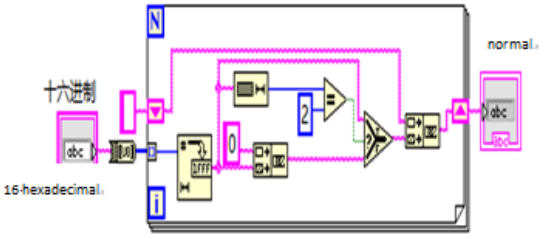

Fig.15. LabVIEW data type conversion program

C. Low-pass Filter Procedures

As mentioned earlier, the human body's breathing is less than 10Hz low-frequency signal, so should use a low-pass filter to filter the body thermal noise and other electrical power frequency noise.In the field of digital image processing and the frequency domain applications, low-pass filtering can be smooth processing of image processing.There are many kinds of low-pass filters, the Butterworth filter and Chebyshev filter is most common.This topic is designed using the Butterworth low-pass filter module, the main program block diagram shown in Figure16.

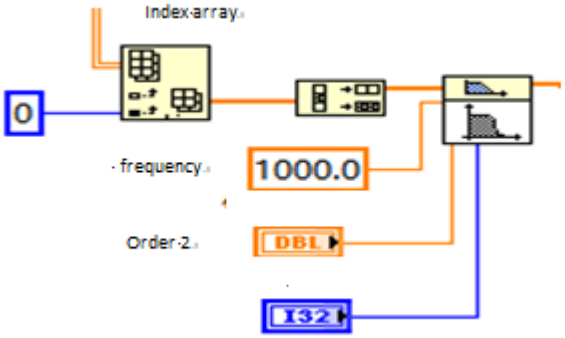

Fig.16. LabVIEW low pass filter block diagram

D. Judgment Procedure

The received data need to use the conditional structure to determine whether the normal breathing, set the normal breathing frequency and amplitude, beyond or fail to show that breathing is not normal, when more than 3 times per minute more than 10s time each time Will alarm, so as not to cause harm to human life. The block diagram of the judgment block is shown in Figure 17.

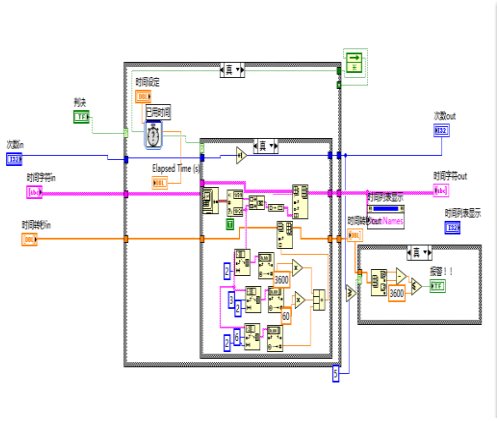

Fig.17. Judgment block diagram

E. While Loop Program

During the operation of the entire LabVIEW program, the host computer system needs to cooperate with the microcontroller module and the hardware system to operate continuously, so that the relevant TXT file in the breathing data constantly, immediately be extracted, converted, calculated and displayed.For this purpose, the overall program in the run-time of the structure should be automatic loop structure, which requires the use of LabVIEW while loop module to achieve this effect, the main program block diagram shown in Figure18.

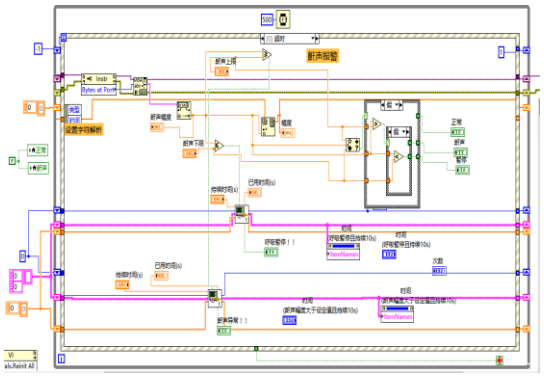

Fig.18. A while loop general program block

The block diagram also adds an event structure in the while loop to handle multiple events. Wait for the event to breathe normally and perform a corresponding conditional branch to handle the event. The event structure consists of one or more subroutine block diagrams or event branches, and when the structure is processed, only one subroutine block diagram or branch is executed. Wait for event notification, the structure can be timed out.

F. Interface Display

In the interface can be based on different groups such as children, the elderly and other settings of different snoring amplitude, through the procedure to determine whether it is normal breathing, whether snoring and apnea. If the breathing is normal, the indicator light shows green . if there is abnormal breathing, ther light is red and alarm, to remind people to pay attention, so as not to endanger life and health. The interaction interface is shown in Figure 19.

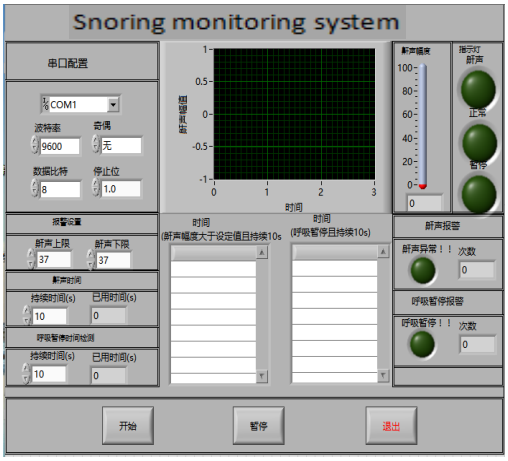

Fig.19. interaction interface

VI. EXPERIMENTAL TEST

System test is an important step in the design and must be do. Whether The entire system of software and communication parts to achieve the desired operational results, whether the system indicators to achieve the desired requirements, need to be tested to determine. This chapter tests the main functional modules of the system.

A. Signal Conditioning Circuit Test

Use the oscilloscope to measure the original signal output by the sensor and get the waveform shown on the left side of Figure 20. And then measure the signal after the conditioning circuit processing, as shown in Figure20 on the right side . Through the comparison of the two figures to determine the signal conditioning circuit is working properly.

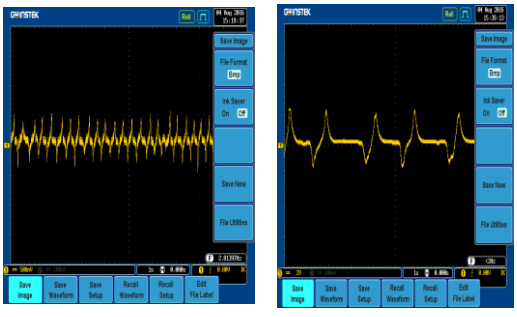

Fig.20. Signal comparison between the original signal (left) and the processed (right)

From the above test results, the hardware circuit part

of the breathing was effectively amplified and extracted.And through the low-pass filter circuit processing, you can clearly distinguish the waveform of the respiratory signal.But after the conditioning output of the waveform is still with the body's thermal noise signal and other DC interference signal, so it need to further software filtering, so that the detection of breathing can be more intuitive to be observed.Tested by the signal conditioning circuit shows that the output of the waveform is still with the body after the thermal noise signal and other DC interference signal, the need for LabVIEW low-pass filter program to test.

B. LabVIEW low Pass Filter Test

Run the LabVIEW program to observe the signal waveform after low pass filtering. The waveforms before and after filtering are shown in Figure 21.

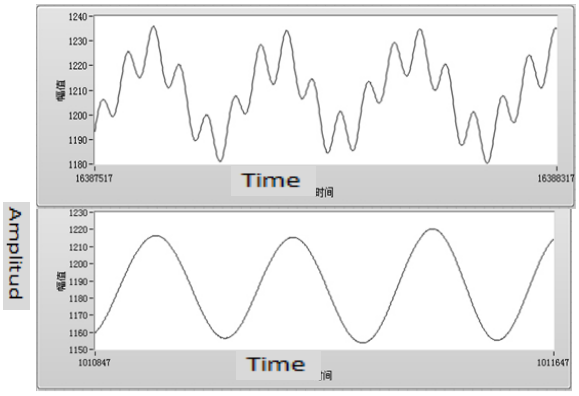

Fig.21. the Comparison of breathing signals before and after (lower)

From the above test results,the high frequency interference signal of the respiratory signal through the LabVIEW low-pass filter processing, the interference signal can be effectively filtered.Respiration signal can be better displayed and improve the quality of testing.it achieves the requirements of this subject design.

C. Functional Tests

The functional test mainly tests whether the overall monitoring system can complete the acquisition, transmission and display of the breathing data in real time and give the correct physiological parameter value.

(1)The tester wears a good breath measurement experiment device, and the computer is connected to the Bluetooth master and slave device in place.Then open the monitoring system switching power supply, then the Bluetooth device light should be fast flashing state.Then observe the connection of the computer and monitor the Bluetooth module light flashing law, to be from the fast flash to a flash once a time, on behalf of the successful pairing.

(2)Open the serial debugging assistant, receive the serial port is set to COM1, the baud rate is 9600bps, 8 bit data bit, 1 stop bit, the computer directly receives the data.

(3) data sent by the Bluetooth serial port one by one to the computer.The read module of the LabVIEW design reads it and then displays the waveform in real time and stores it.The computer interface has the function of waveform display, waveform filtering, waveform storage, and physiological parameter calculation.When the breathing is abnormal, it will alarm.

VII SUMMARY

The design of this topic is mainly based on PVDF piezoelectric film sensor. Through the LabVIEW software development, and using the Bluetooth transmission technology to achieve real-time detection of human breathing. We Completed the design process, including hardware design, software design, modeling structure design and communication design.In general, the system device can achieve real-time acquisition of breathing signals, and can be displayed through the interface in a straightforward and clear manner, while also a simple feedback to achieve the desired detection results.In the process of completing the design of this issue, it is not smooth sailing, encountered difficulties and temporarily difficult to answer the question.we consult the literature, ask the teacher or hands-on practice, etc. one by one to solution.

References

[1] Meng Jun-ren、Ding Xin. Development and application of PVDF piezoelectric sensors which can be embedded in clothing. Industry with the imitation fabrics[J]，2010.2

[2] Wu Dan,Xu Xiaowen,wang lei, et al. Dynamic sleep apnea wearable monitoring system design [J].Journal of sensing technology,2010,23(3):322-325.

[3] Goldshtein,E.,Tarasiuk,A.,Zigel,Y.,"Automatic detection of obstrutive sleep apnea using speech signals, "Biomedical Engineering, IEEE Transactions

on,vo1.58,no.5, pp.1373,1382,May 2011

[4] Zeng Xianglong， Gao Xuemei.Department of Oral Medicine, Obstructive Sleep Apnea-hypopnea Syndrome [J] Journal of Peking University (Medical Sciences), 2009, 01

[5] L R Rabiner, A tulorial on Hidden Markov Models and selected applications in speechrecognition, Proc.of the IEEE, 1989,77(2):257 一 285

[6] Fang Zheng,Guoliang Zhang, Zhanjiang Song, Comparison of different implementations of MFCC,Journal of computer science and technology, 2001,16(6): 582589

[7] Hu Yuan,Gong Guobin,Cao Dongsheng,et al.Laminated piezoelectric magnetostrictive/epoxy resin composite material of the magnetoelectric effect and its frequency response characteristics[J].Journal of composite materials,2007,24(4):29-33.

[8] Ling Zhengbao，Qi Xiaohiu，Xin Yi.PVDF-based breathing signal detection belt research [J]. Piezoelectric and acousto-optic, 2014, 36 (1): 72-75.

[9] Y.Y.Chiu, W.Y.Lin,H.Y.Wang. Development of a piezoelectri polyvinylidenefluoride (PVDF) polymer-based sensor patch for simultaneous heartbeat and respiration monitoring [J]. Sens Actuat A-Phy, 2013, 189:328-334.

[10] Wu Jinwu Jiang Zhe. Based on PVDF piezoelectric sensor structure vibration displacement volume [J]. Journal of vibration engineering, 2007,20 (1) : 73-78.

[11] Fan ChunLing Li Zhiquan. The design of a new type of charge amplifier and study [J]. Journal of sensing technology, 2000, 13 (4): 297-302.

[12] Cheng Defu, Wang Jun, Ling Zhenbao, Wang Yanzhang, principle and application of sensor [M], Beijing: China machine press, 2007,12.

[13] Kang Huaguang, Chen Daqin, Zhang Lin, electronics (simulation) [M], Beijing: higher education press, 2006,01.

[14] Shen Jianhua, colourful, Xiao start, etc. MSP430 series 16 ultra-low power consumption single-chip microcomputer principle and application [M]. Tsinghua university press, 2004.

[15] Li wei, Wu Xiaoming. Based on bluetooth technology embedded multiple physiological parameters monitoring [J]. Microcomputer information, 2006(01Z):29-31.

[16] Zheng Duiyuan, proficient in programming LabVIEW virtual instruments [M], Beijing: Tsinghua University Press, 2012,5.

[17] Li Xin，Qi Jingyao.Development and Application of Virtual Instrument for Water Quality Monitoring Based on LabVIEW [J]. Water Supply and Drainage .2002,28 (10)

Remote Control Communication Intelligent Socket Based On Internet of Things

Yibing Yu; Jikang Kong; Yue Yu

(College of Instrumentation and Electrical Engineering, Jilin University, Changchun 130000 China)

***Abstract*—Smart home is one of the main applications for Internet of things, it has realized the home of intelligent and information technology. Smart socket is an important part of the smart home, the current smart socket on the market only has the power supply remote control function, also can't meet the requirements of intelligent home system, so we need to add new features to improve the traditional smart socket. We designed the smart socket mainly using AT89C51 microcontroller, SIM900A, MQ-2, HC06 and the other modules. The application of GSM technology, Bluetooth technology and the other control methods, not only achieves the use of mobile phone APP on the socket for remote control purposes, but also have two functions of detection Smoke automatic alarm and remote adjustment LED lighting, such a smart socket is more practical and universal, it is in line with the smart socket market prospects.**

***Keywords*—Mobile phone APP Smoke alarm Lighting adjustment**

I.PREFACE

ELECTRONIC information technology, the increasing control technology and the gradual acceleration of social information, promote people's lives, work and communication relations to become increasingly close. Information society change people's habits and working methods, but also poses a challenge to our traditional house. People's requirements for the home are no longer just a simple material space, but more concerned about a highly safe, comfortable, beautiful and convenient living environment. Advanced communication facilities, complete and efficient information terminals, automatic, intelligent home appliances, networked resource management and shopping are more suitable for modern life rhythm.

The most convenient and practical is the smart socket. Although the current smart socket has a certain development, and the market began to appear corresponding products, but the overall development point of view, is still in the initial stage, especially the uniform standards and the lack of authoritative products seriously affected the development. With the improvement of technology, economic, people's material living standards, the requirements of the home environment is also getting higher and higher, the growing needs of today's society makes the socket intelligent has become a trend. Therefore, we designed a SMS smart socket and Bluetooth smart socket, to achieve high intelligence of remote communications, to facilitate people's daily life.

II. INTRODUCTION

2.1. Research background and significance

With the economic development and technological progress, our life is also going to a high-quality, high-level situation step by step. Therefore, the living environment, especially the residential environment requirements is gradually improved for people. People not only concerned about the residential area, the degree of decoration, but put forward higher requirements for the residential intelligent, security. As a result, smart home came into being.

The smart home with technical support for the Internet has been put forward in the early 1980s, and today, smart home has been recognized and widely accepted. Intelligent home control, especially the realization of remote control, will greatly improve people's quality of life, provide people with a more comfortable and convenient life experience. Smart socket is smart because it is small, easy to use, cheap and widely used, this article focuses on SMS smart socket and Bluetooth smart socket.

The current smart socket on the market is mainly

WiFi control, but the scope of use of WiFi is very limited, it is difficult to achieve a wide range of coverage, but a large number of people use the text for remote, as the most basic mobile phone features, If you can use SMS to control the smart socket, then it can expand the control of the socket control distance, may increase the number of people, and greatly improve the ease of use and convenience. Bluetooth is mainly has practicality and convenience, such as using Bluetooth on the dimming of the lamp is very convenient and simple[1].

III. System Overall Design

3.1. The basic working principle of the smart socket

In this paper, the SMS smart socket and Bluetooth smart socket, can be used to send SMS or send instructions using Bluetooth to achieve control, thus controlling the opening and closing of household appliances. They are used to adjust the power supply regulator, the main chip of a pin control relay module, the relay module and the relay in the intelligent socket are connected, as long as the microcontroller pin control the level of high and low, the socket will switch[2].

SMS smart socket with breaking function, and when the indoor smoke concentration reaches the system default value, the intelligent socket can automatically power off, so that the plug in the above household appliances power, reduce losses. Under normal circumstances, the same can be used to remotely break the message, so that people's lives more convenient.

Bluetooth smart socket in the control distance is much smaller than the SMS smart socket, but it has a great advantage in the regulation. First, the Bluetooth smart socket can control the switch within a certain distance of the smart socket, and can be inserted in the socket on the light dimming, so that the light to keep in the human eye to adapt to the brightness, convenient people's lives, more humane.

3.2. The overall design of the system

SMS smart socket control system block diagram is shown in Figure 1. It is composed of MCU control module, power supply module, smoke sensor module, relay module, GSM module and controllable socket.

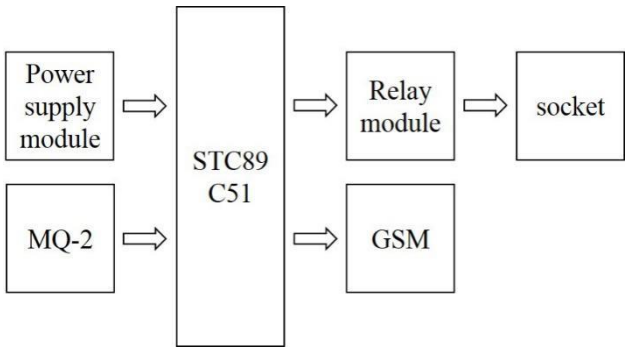

Figure 1.the Schematic diagram of SMS smart socket

Bluetooth smart socket control system block diagram is shown in Figure 2. It is composed of the MCU control module, power supply module, Bluetooth module, relay module, zoom module, controllable socket.

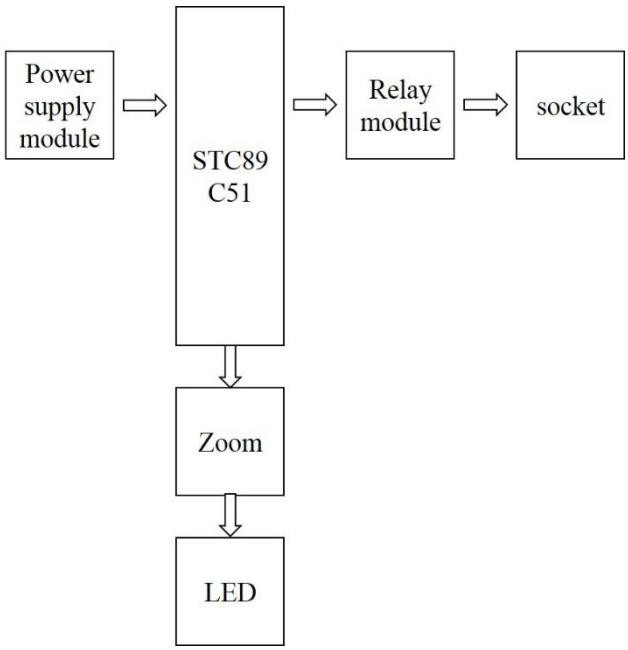

Figure 2.the Schematic diagram of Bluetooth smart socket

3.2.1 SMS GSM smart socket

The smoke sensor is in real time to monitor the smoke content in the indoor air environment, when the smoke content exceeds the expected value at a certain time, the smoke sensor will send the high level signal to the single chip computer, the MCU receives and recognizes the signal, passes the control relay Household electricity to break off, then it will prevent the occurrence of fire. At the same time another pin send the signal to the GSM main module, GSM module send text messages to the user's mobile terminal to alarm.

Users can send SMS instructions through the mobile phone APP, the instructions by the GSM module will be transmitted to the microcontroller, the

microcontroller read the state of the instructions, understand the user needs, and achieve the outlet break. Using the control relay to switch household electricity, will achieve long-range intelligent control and facilitate people's lives.

3.2.2. Bluetooth smart socket

Mobile phone APP and Bluetooth module match, the user access to the Bluetooth Android client to send control instructions, the instructions transmitted to the Bluetooth module, the microcontroller on the state of the instruction will understand the user needs, and Using the control relay to connect the socket or adjust the lighting of the lamps directly.

3.3. System hardware design

For the SMS smart socket and Bluetooth smart socket, the master chip selects 51 single-chip, 51 single-chip is the most basic single-chip, it is starting quickly, full-featured, enough to achieve the function in this article. The adjustable power supply using of LM317 and transformers will power to the microcontroller and other modules, using the mobile phone APP to send commands to the Bluetooth module or GSM module, it will make the microcontroller pin level changes and then control the relay module connected with it. We will make the open or close contact of relay module contact with the contact of the relay in the smart socket, so as to achieve the control of the smart socket. Smoke sensors for SMS-type sockets are made of MQ-2 smoke sensors, which have a high sensitivity to the smoke concentration in the air[3].

3.4. System software design

3.4.1. SCM software programming

The design used in this article is the microcontroller STC89C51RC, in order to make the preparation of the program more clear and simple, we will use C language programming, use Keil software to compile, use stcisp software to download and burn program.

SCM programming include following things. GSM module controls socket off by sending text messages and receiving text messages[4], Bluetooth controls the smart socket, the procedures of smoke detection and Bluetooth dimming.

3.4.2. Mobile APP development

First, we download Android mobile phone APP development software, such as eclipse software and Android Tool, then install the java language and other development environment to make java programming.

The main need of the java programming is to achieve the function of receiving and sending text messages, as well as the development of Bluetooth APP. It includes XML interface design programming, button jump function programming, text input and text display programming. At the same time, we need a Bluetooth search matching function, we need input and receive data programming, as well as the requirements of the broadcast statement.

IV. System Test

4.1. Hardware debugging

First, we make the hardware circuit in the breadboard lap, and test the data, everything is normal. Then we complete the actual circuit with a board full of hole, and do the actual test. But we found that the relay voltage and current have a certain demand, although the microcontroller pin is rated as 5V, but the actual current is too small, can’t meet the needs of opening and closing relays, so after several tests and adjustments, we choose to use the method of the current amplification by transistor to solve the problem of opening and closing relays[5].

At the same time, through a number of investigation and modification, we solve a series of problems such as, the instability of the ground, the size of the resistance is not appropriate, and ultimately to achieve normal work, that is, under the control of the socket, it can be off, smoke sensor work normally, Bluetooth connect stably, GSM signal is normal.

4.2. Software debugging

In the software design, the first general process is to sort out the process, and then debug sub-module, debug the part module of the program before feasible and then integrated together, the preparation of the main program will go on.

First, we need to write SMS smart socket program. In the process of programming, we need to use the AT command to set and change the GSM module, so it has a greater difficulty. After several changes and debugging, we prepare the required procedures successfully, it can make the GSM module sending text messages when the smoke is greater than the set value, while the socket will power off automatically. On the other hand, it will achieve the received SMS

commands of GSM module, control socket disconnect.

Second, we need to write a Bluetooth control program. Through the preparation of the program, we achieve the function of Bluetooth controlling socket, after several tests, we found that the voltage is not enough when we make dimming lights, we need for a magnification equipment. By looking for information, we chose to add L298N module in front of the lamp to enlarge, it can meet the needs of the voltage.

After repeated debugging and improvement, the system has been able to achieve the desired results.

4.3. Data testing

Bluetooth smart socket physical map is shown in Figure 3, intelligent socket power to the LED light, we can adjust the brightness of the lamp. The main method is to adjust the power supply voltage of the lamp, the brightness of the lamp is divided into five levels, each level of the supply voltage are different, making the brightness of the lamp different, table 1 records the different brightness levels in different supply voltage.

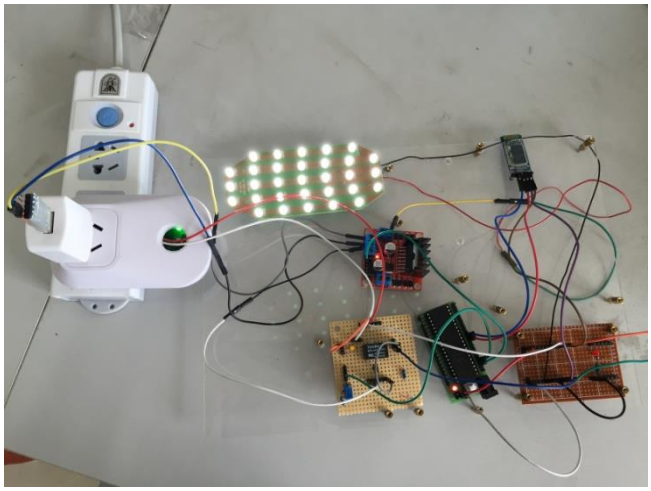

Figure 3.Physical map of Bluetooth smart socket

Table 1.the relationship between Lamp brightness and voltage

Brightness level	1	2	3	4	5
voltage (V)	0.721	1.301	1.861	2.412	2.997

V. CONCLUSION

We have proposed the program to achieve long-range intelligent communication by the socket controlled of the SMS and Bluetooth technology, which mainly uses GSM module and Bluetooth module to achieve communication functions, uses relay to achieve on-off function. In addition, the travel of the sensor and actuator network can enter the home environment by deploying the smart outlet along with other sensor nodes. The basic functions of the remote communication smart socket has been fully tested and basically achieved. Experimental results show that our proposed smart socket successfully achieved the basic functions of remote control of various types of home appliances, at the same time it has the function of the smoke alarm and brightness adjusting, it has a certain degree of innovation and practicality. It provides a faster, more flexible way to build and deploy a home automation network, so that people's daily lives become more convenient, it has good application value.

References

[1] Yuesheng Xiang, Ruixia Gao, Yangbo Wu, etc. Design and Implementation of Intelligent Socket Based on Single Chip Microcomputer [J]. Industrial Control Computer, 2012, 25(9):129-131.

[2] Jiabao Zheng, Yanling Guo, Hanyu Tang, etc. Design of Intelligent Socket Based on Remote Control of Mobile Phone [J]. Science and Technology Innovation and Application, 2015(17):56-56.

[3] Wei Nie, Xiaoqing Li. Design of intelligent fire alarm system [J]. Information and Communication, 2012(2):92.

[4] Zhongwang Li. Designed Scheme of Intelligent Fire Alarm System [J]. Security Technology, 2008(2):48-49.

[5] Huaguang Kang. Electronic technology foundation (analog part) sixth edition [M]. Beijing: Higher Education Press, 2013.12.

The Research of Delivery system based on O2O

Wei-Yiming; Gao-Zhiyuan; Wang-Haiyang

(College of Instrumentation and Electrical Engineering Jilin University, Changchun 130012)

***Abstract*—This paper introduces the establishment of the three party client delivery system,Implementation of user registration, user login, user ordering, business update food businesses to confirm the order, delivery room.System uses JavaWeb technology, the main use of JSP+SERVLET is to complete the system function, the data stored in the database, and through the WebView will be embedded into the mobile client.Finally it can complete the whole system of order, delivery, delivery process, solve the problem of ordering and delivery efficiency, provide a reference for the implementation of delivery system using specific technology.**

***Key words*—O2O Ordering Delivery system**

I. INTRODUCTION

WITH the accelerated pace of urban life,many office workers don't have time to eat. So the takeaway became their first choice now.Chinese takeaway market is broad for different people whether it is Chinese food or foreign food. At lunch time, we can see the delivery in the office[7].In fact, takeout has become many consumers, especially young workers accustomed to the way of eating.

Takeaway system is the businesses and users connected with the ordering platform through the Internet.Users through online ordering, business orders, the under line of business service, users receive to complete the transaction process of ordering.Because of the convenience of ordering, takeout system has been widely used since the rise of the takeaway O2O this model[3]. However, the current delivery system due to its only focus on businesses and users to establish their clients, while ignoring the delivery plays an important role in the object in the delivery process, it is difficult to effectively improve the delivery efficiency.It is difficult to use the network will order information between the three transfer and save used of traditional print orders.The efficiency by using telephone is low.

Later, with the development of the mobile Internet, take away the industry has been rapid development. 2009, ele.me was established, until 2011, the whole industry is in the embryonic stage. 2011, the year of the outbreak of the mobile Internet, take away the industry began to enter the growth period. In 2013, hungry and began to crazy expansion. At the same time, the meituan was established , to the new year, Baidu takeaway to join, so that the whole market competition is more intense. In 2015, began to take out the industry subsidy war, the push is also increasingly fierce battle. After 2015, the takeaway industry has entered a mature stage[6].

Now,the popular takeaway system is mainly ele.me, Meituan takeaway and Baidu takeaway. And the three delivery systems are different.The ele.me’s client structure is simple and clear, and the depth of the sub module is kept in the 2 floor.Scheduled breakfast and other popular features consisting of takeaway on the home page, highlighting the takeaway features, user-friendly.Compared to the ele.me, the meituan takeaway layout is more abundant,Supermarket purchase and fruit and other popular procurement on the home page for the wider population. Baidu takeaway layout is similar to the meituan takeaway. Home features more, business classification, intelligent recommendation to eat what as a characteristic function as a Tab, is easy to use[4].

Compared to the above delivery system, the author puts forward a kind of effective management can delivery plan and order information. That is to establish businesses, delivery member user three party client, as well as for the preservation of the QR code to store the information of orders.

II. TAKEAWAY SYSTEM DESCRIPTION

A. Take out system

Delivery system using the cash on delivery (COD) transaction model.In order to link the entire ordering smoothly, users need to register to get permission ordering. Users are free to choose the required goods, and fill out the types of goods, the number of ordering information, and address, the name of the personal information to confirm the order. Businesses to confirm the order after the user orders, then the production and delivery in accordance with the address, user identification and payment.

B. Functional Processes

The functional flow chart is shown in Figure 1

(1)Ordering by ordering client orders. Orders issued, the specific ordering information to the backend server.

(2)The backend server sends the information to the restaurant client after receiving the order information. The restaurant will confirm the information and delivery information to the backend server.

(3)The background server generates QRcode for the received information and the information is sent to the client.

(4)The sending client sends the information to the backend server for ordering client querying. After the meal sending information for ordering the client to confirm in the same way .

(5)The user through the client to confirm the meal ordering information. Then feedback to the backend server . End of the transaction, and sending the end of the information to the restaurant client.

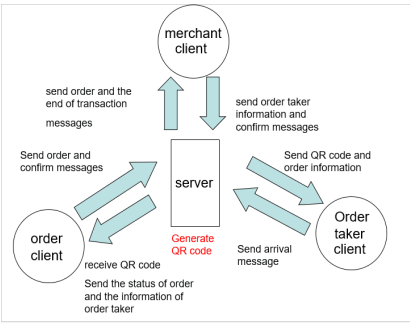

Figure. 1 flow chart of system function

C. Demand analysis of takeaway system

Online meal ordering work includes three clients user login (Registration), and each client to browse, order, order processing and other aspects. Therefore, the system should be able to link to the takeaway ordering provides basic technical support or service.

（1）User management. For the user to provide registration and login function, and its proper authority and function management.

（2）Release commodity information. Including stores, merchandise information and notifications, etc..

（3）Selection of goods. Users browse web information to select dishes.

（4）Order information management. Single user, business confirmation order processing and delivery orders and delivery.

III. ORDERING SYSTEM DESIGN

A. Restaurant client design

As shown in Figure 2, The function of client business is divided into five modules: user management module, menu management module, ordering management module, message board module and room management module.

Each module has different functions.(1)User management module should have user registration, user login and function of user information modification,used to determine the different account information for each restaurant .(2)Meal management module corresponds to the increase in food items, delete items, update the meal, check the food and other functions. To provide information to the food ordering. (3) Ordering management module has the fuctions of order confirmation, adding the delivery staffs ,order query,, saving the two-dimensional code .(4)Message board module corresponds to view the message, reply message function. The reply to the order can improve the business service.(5)Meal delivery service management module has function of hirinf staff and firing staff. To maintain the relationship between the client and the room .

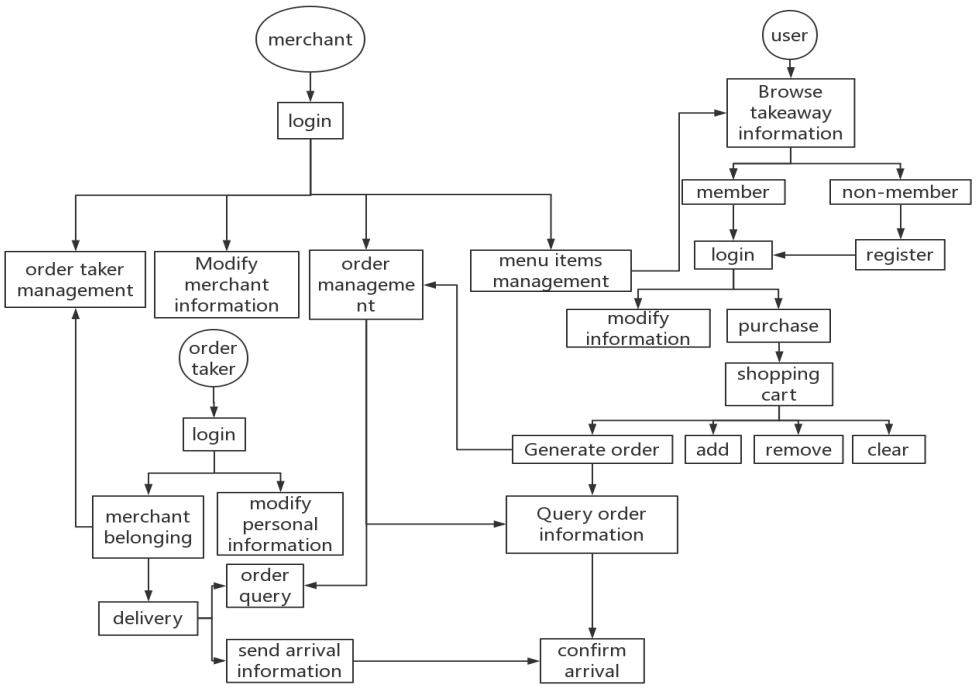

Figure 2 business client function block diagram

B. Ordering client design

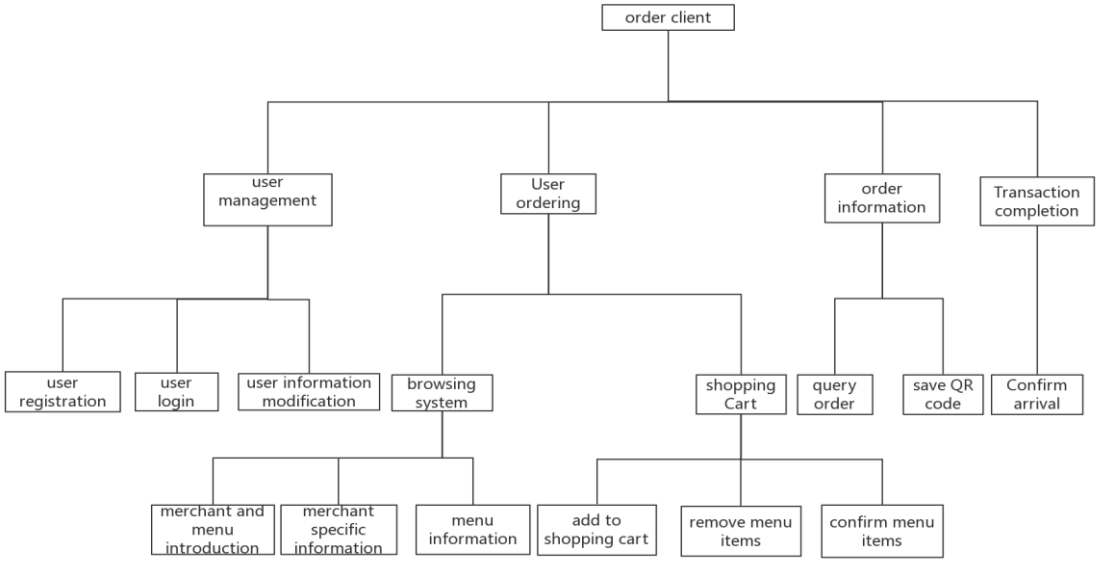

Figure 3 ordering client function diagram

As shown in Figure 3, ordering the function of client is divided into four modules: user management module, user ordering module, ordering information module , Transaction completion module. Each module has different functions.

(1)user management module should have user registration, user login and the function of user information modification. Used to identify different accounts for each user.

(2)The user ordering module should have browsing system and shopping cart, browse system has the introduction of merchants and dishes, specific information of business ,evaluating, function of food information , the shopping cart is added to the shopping cart, good food, empty the shopping cart, confirm the food function. To complete the ordering main link.

(3)the order information module corresponds to a query order, the function of saving the two-dimensional code, which can be preserved as a reservation voucher .

(4)The completion of the transaction module has the

function of evaluating and confirming the meal . Complete the delivery process, and feedback to the businesses, provide food and delivery service evaluation.

C. Room client design

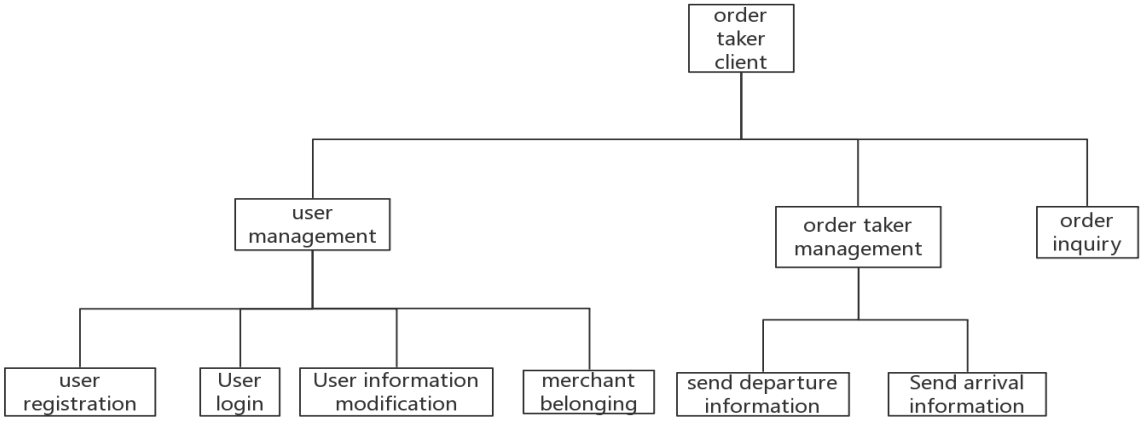

Figure 4 room client function diagram

Figure 4 the client function room is divided into three modules: user management module, room management module and order query module.

Each module has different functions.

(1)User management module should have the functions of user registration, user login, user information changes and businesses belonging to. To confirm the orders'different account information.

(2)Delivering management module should have sending message, sending the meal to the information and other functions. To improve the efficiency of the delivery.

(3)Order inquiry modules have the function of inquiring order content,used to inquire address for the delivery staff in the delivery stage.

D.Core technology

Using J2EE architecture, using JavaWeb technology, Building the website and the backstage server, and then embedded into the mobile web client through WebView, using MySQL database to store, processing the data needed to design, the final completion of the entire delivery system.

Restaurant client and background through the JSP+Servlet to achieve the entire function. Tomcat server is used as the server of the whole system, generating dynamic Web content using Servlet(read request, request access to the database, send data). When the server receives a Servlet request for a new thread, let the Servlet object Service object called HTTP to check the type of request on this thread (get, post), and the service method according to the request type calls doGet, doPost method, complete the interactive operation[3].

Mobile client also through the JSP+Servlet technology into the Tomcat container . Then in the Android client (sending APP and ordering APP) Webview page which embedded, and a reference to WebView is obtained in Activity[3]. When the client is started, the corresponding web server load and then complete the ordering of the registration, login, view order etc[4]..

Data exchange between the database and the client is mainly carried out by JDBC. Establish a database for the operation of the Servlet and then write to the MySQL database to operate on the Servlet database. Merchants, ordering, delivery of the generated entity can be invoked by the database operation to change the corresponding data stored in Servlet in the actual process[5].

QRCode uses open source technology. introducing of the name "core" and QRcode_swetake.jar package in the project delivery system[2]. By calling the two jar packets generated two-dimensional code method, the need to generate the data needed to generate two-dimensional code image in Servlet. In the JSP needs to display the two-dimensional code, the IO image flow generated by the two-dimensional code display.

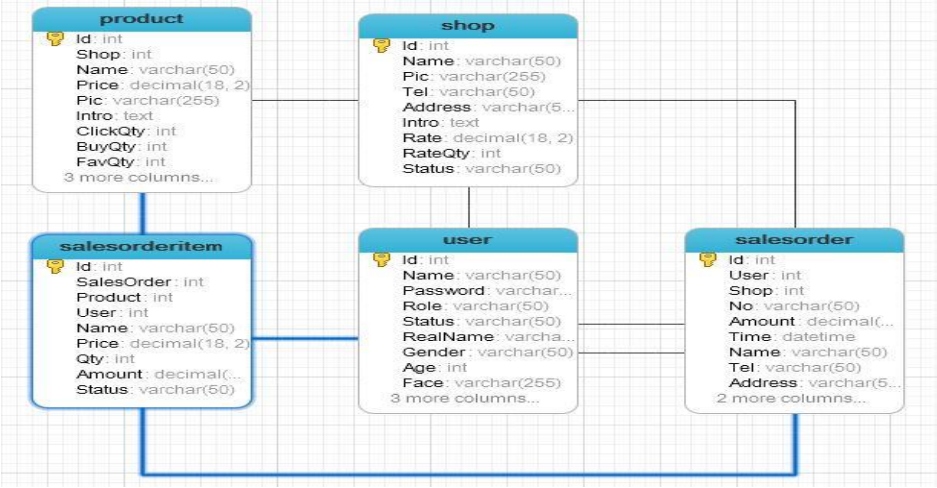

Figure 5 data structure

E.System business process

The business process of the system is shown in figure 6.

The user can browse the food product information provided by the business, The user can modify the information and order the meal to join the shopping cart through the registration. After the operation of the shopping cart to confirm the formation of orders sent to the merchant.

At the same time businesses to send the order information to staff room.(business by logging can be achieved on the staff room, message board, food and order management.)

Delivery login information delivery order. After the meal to send delivery information. Meal to confirm. End user evaluation.

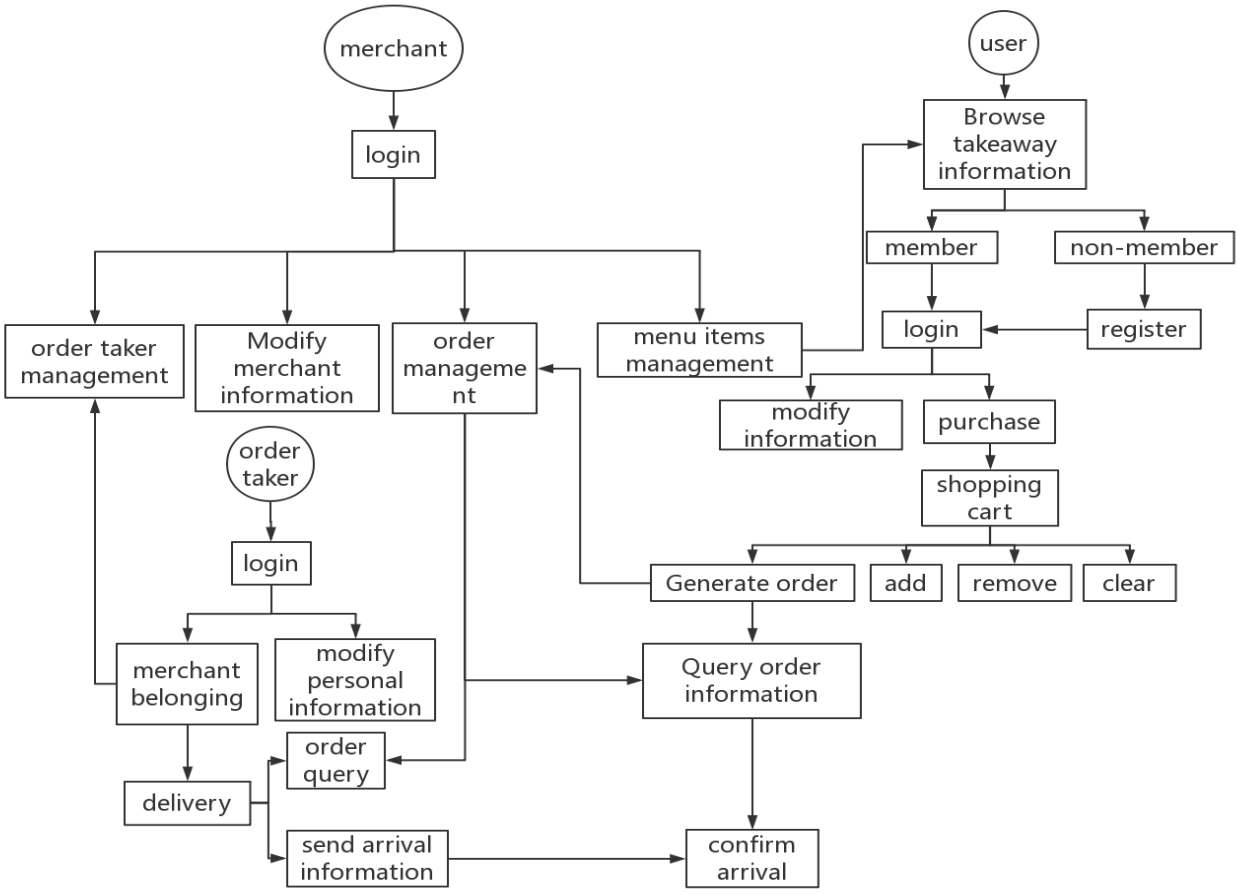

Figure. 6 system business flow chart

V. FUNCTION INTERFACE

Figure 7 shows the website and business system, you can add business information in the system to achieve the management of the business.

Figure 7 Business management interface

As shown in Figure 8, businesses can be in the food management interface to modify the food information, but also in the restaurant management and other interface to add, send meals.

Figure 8 Food management interface

As shown in Figure 9,10, the user logs in to the mobile phone APP, enters the merchant to place the order, adds the desired food item to the shopping cart, completes the order flow.

Figure 9 Choose a business interface

Figure 10 Shopping cart interface

As shown in Figure 11, the merchant logs in to the client, confirms the user order and assigns the meal attendant.

Figure 11 Confirm the order interface

As shown in Figure 12,13, the meal attendant logs in to the meal App to confirm the order and send the message to the post. Once the order has been confirmed, the order is confirmed, the transaction is completed, and the order information is generated. The two-dimensional code is used as the transaction certificate to complete the transaction.

Figure12 Sender client interface

Figure 13 Shopping cart interface

V. SUMMARY

Unlike today's takeaway website and client,the delivery system is based on the three parties , defines the relationship and responsibility between the restaurant, ordering, delivery staff better. The responsibility of the staff began to establish after the start of delivery delivery and the confirm of the ordering , and the restaurant staffs always hire the delivery staffs .And the account of the delivery staffs is beneficial to the restaurant to manage the delivery staffs better .And after the delivery staffs'leaving from a restaurant ,they also can be bound with other

restaurants. Different delivery man get different delivery feedback, so that you can improve the efficiency of delivery.

Unlike today's takeaway website and client, in order to solve the dispute documents after ordering, the two-dimensional code will be provided as a voucher .The two-dimensional code information includes: ordering content, single time, single user, restaurant information, orders, delivery staff information and so on.

In order to save the time of the delivery staff in the downstairs to send messages and phone calls and solve the problem due to poor telephone signals, resulting in the problem that customs can not receive the phone call,Can sent ‘he meal has arrived, please take meal’,news to the specified ordering in the client by a key in the delivery man client.Wait for the reservation confirmation. This will save the delivery man’s time for waiting the customers ,in order to maximize the use of the time, to concentrate on delivery.

VI. CONCLUSIONS

In this paper, the realization of the delivery system are described , combined with the ordering process ,the function demand analysis of the platform, designs the overall architecture of the system and the specific function, analysis of business processes,Perfect delivery system optimization reflected in what? Introduced in the function or the core technology,it should have a clear description, to provide a certain reference for the use of specific technologies and to achieve the delivery system

References

[1] Xu F,Deng N,Wang HE,Zhao BY. Design and implementation of online meal ordering system based on MOSS. "Computer CD-ROM software and Applications",2013(6).

[2] Hu Gui Z.Study on the application of O2O model in Chinese catering enterprises[J].China Business and Trade，2013(7).

[3] Yang YunJ.Design and implementation of Android[M]. China Machine Press，2013:5-65.

[4] R & D Center.Detailed JSP application development (Second Edition)[M].BeiJing :Publishing House of Electronics Industry，2004.

[5] Zhang X, Yang San C. JSP and JDBC detailed applications[M].China Railway Press, 2010.11.

[6] Zhu DingZ,Zhang Hai,The core of insider My SQL[M].Publishing House of Electronics Industry.2009.11：35-50.

[7] Zhang XinM.Proficient in JSP-Web development technology and typical application[M]. Beijing:Posts and Telecommunications Press ,2007：2-1.

[8] CherLee.ele.me and meituan takeaway & Baidu takeaway food analysis report[EB/OL]. http://www.chinaz.com/manage/2015/1105/466594.shtml

GSM-based intelligent design watering

Tong.Leng; Xujian.Qin; Xinglin.Yang
（*Jilin university, College of Instrument Science and Electrical Engineering,changchun,130021*）

***Abstract*—This project mainly through the YL-69 hygrometer for soil moisture measurement, and then by the ADC0832 the humidity information into the 51 single-chip, and then through the nrf24l01 wireless transmission of different data transmission between the summary, and the use of GSM to achieve information transmission and control , The last mobile device on the APP program will extract the information into a table, so that users can intuitively see their own flower environment, and also has a mobile phone can control the way watering function.**

***Keywords*—Wireless transmission GSM APP**

I. INTRODUCTION

NOWADAYS natural vegetation is less and less, potted flowers planted up, intelligent watering machine also produced. Intelligent watering machine is the use of certain electronic equipment to detect and control the soil moisture[1]. At present, the market of intelligent watering machine is generally automatic timing water or humidity detection automatic watering device, while computer-controlled large-scale irrigation system has also been produced. The project uses 51 single-chip programming, GSM communication technology, NRF24L01 wireless transceiver technology and mobile phone APP programming to achieve mobile phone intelligent watering design.

II. SYSTEM DESIGN

A. System Structure

This project mainly through a single point of measurement of soil moisture, through the wireless transmission of different data transmission between the measurement points, and the use of GSM to achieve the transmission and control of information, the final APP program on the mobile information extraction into a table, so that users can Intuitive to see the environment of flowers. In addition, the system also has a mobile phone to control the watering function. The main contents of the project include four parts:

Single point data collection; information transmission between different measuring points; GSM-based information transmission and control; APP-based mobile phone control software. The overall technical roadmap is shown in Figure 1.

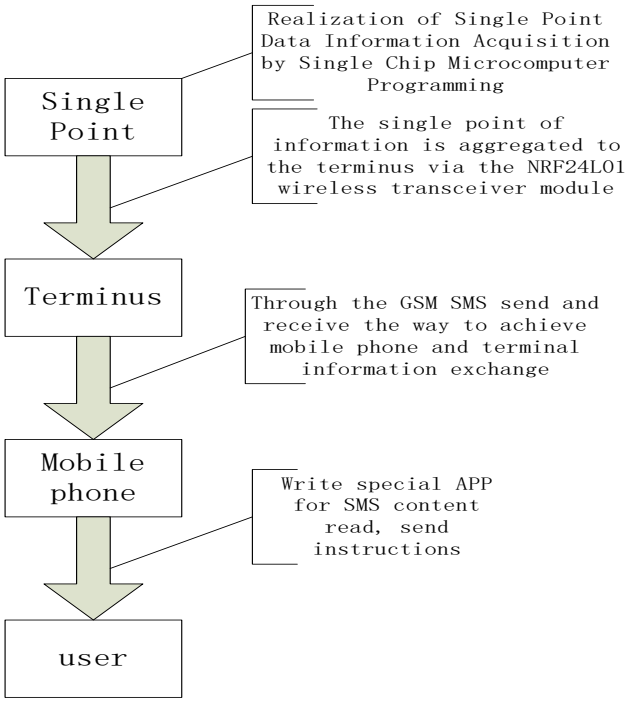

Fig. 1. The overall technology roadmap

B. Device Selection

(1) Humidity sensor: YL-69 is a simple soil moisture sensor, the principle of the humidity-sensitive capacitor, when the humidity changes in the environment, will make the humidity-sensitive capacitor in the environment of the medium changes, resulting in the capacitance of the humidity capacitance The value changes, and the value of the capacitance is proportional to the humidity value. As the humidity sensor has a high sensitivity, fast response, low hysteresis characteristics, so the humidity capacitance is easy to miniaturization and integration. In this system, soil moisture data collection is done by YL-69[2].

(2) A / D conversion: ADC0832 circuit connection

is simple, only three lines and single-chip connection, you can complete the AD conversion. In addition, it has a cost-effective, low energy consumption characteristics, suitable for use in small smart devices. ADC0832 is 8-bit resolution, the highest resolution can reach 256, to meet the design requirements of this project.

(3) Relay selection: the device in the design process requires a relay to control the work of the solenoid valve. Since the operating voltage is about 5V, and the cost is relatively low, so select the model for the song SRS-05VDC-SL model of the relay.

(4) Wireless transmission module selection: In a variety of wireless transmission mode, NRF24L01 low power consumption, in the -6 dBm power transmission, the operating current is only 9 mA; reception, the working current is only 12.3 mA, a variety of low-power work Mode (power down mode and idle mode) make energy saving design more convenient. Therefore, through the NRF24L01 to establish wireless transmission.

(5) GSM module selection: GSM network is improving today, TC35i application is more extensive, easy integration, system development costs are low, the development time is short. Therefore, the system uses TC35i to achieve SMS communication function.

C． System Hardware Structure

From the system structure and device structure we can see that the system components are more, including mobile phone APP, SMS transceiver module, terminal 51 MCU, wireless transceiver module, single point 51 single chip, the specific structure and connection relationship shown in Figure 2.

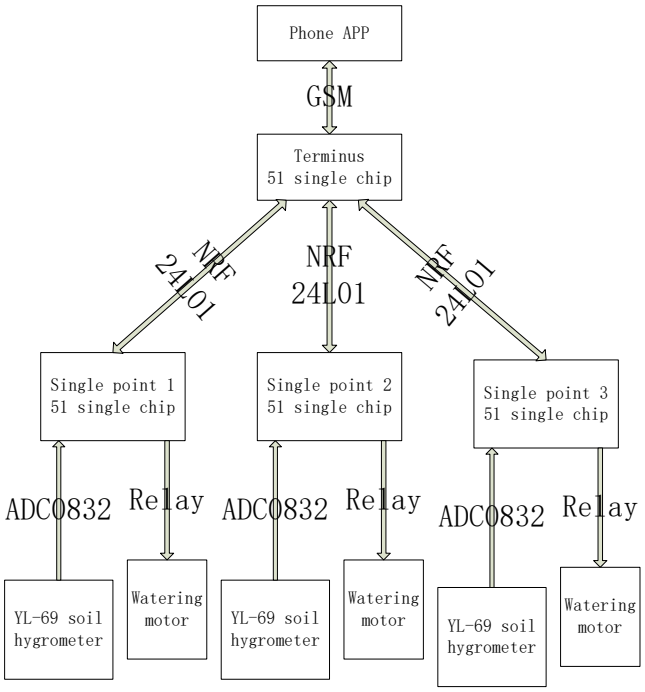

Fig. 2. System Hardware Structure

III. SINGLE POINT DATA COLLECTION

Single point microcontrollers have the following features:

(1) Watering device to achieve watering action mode is divided into two categories: by monitoring the pottery soil moisture, when the humidity is lower than the preset value, you can achieve automatic watering; set the time to automatically watering. Different working modes are controlled to achieve different soil moisture control.

(2) The system can send commands to the user to produce a corresponding response, the corresponding function switch.

A． Single point circuit workflow

Through the soil moisture by the YL-69 hygrometer collection, and then through the ADC0832 analog-to-digital conversion of the humidity information into the microcontroller, and then with the current set of operating mode comparison, through the relay control watering motor work.

B． Watering motor control circuit

The control circuit of the watering motor is shown in Fig. 3, when the Q2PNP type three-level tube b-level low potential, the transistor turns on, and the control circuit of the watering motor is controlled by the output of the single- Relay control K1 single pole double throw switch to the right deviation, motor M

pump power, D2 LED lights up, the pump began to work.

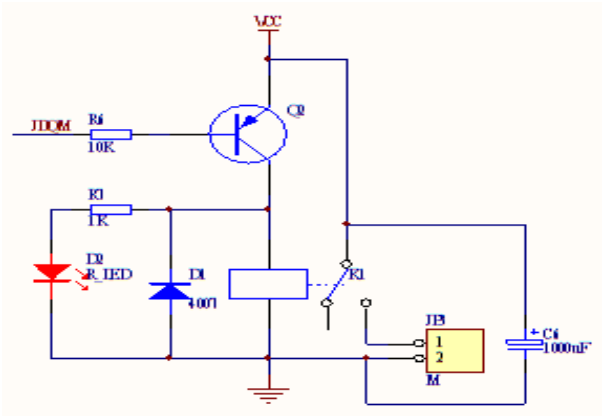

Fig. 3. Watering motor control circuit

IV. Information Transmission and Control Based on GSM

A. GSM module selection

At present, GSM is a mobile communication system is more mature, perfect, the most widely used system.

(1) The use of GSM for information transmission coverage is wide. GSM cellular digital mobile communication system in China has been all over the country, covering more than 98% of the city and the vast rural areas.

(2) GSM module TC35i has a good application prospects. With the rapid spread of global mobile communication systems and communication networks and the increasing competition. New technology and new business development and application is very important.If the TC35i module and single-chip combination, you can achieve long-distance data transmission on the microcontroller, which in the practical application is very useful.

(3) TC35i use is relatively simple. TC35i circuit design is very simple, only need a small amount of line connection can be used. TC35i system software design to C language programming based on a simple AT command can be achieved by SMS send and receive.

Therefore, the terminal between the mobile phone and the transmission of information between the final choice of GSM module[3].

B. GSM module workflow

GSM module will be the main station information through the form of text messages sent to the user, while the user sent the information to the terminal. GSM SMS service SMS transmission using signaling channel, do not have to dial the connection, the information to be sent with the destination address sent to the SMS service center, the SMS service center storage and then sent to the sink[4].

C. GSM module design

TC35i module and PC after the success of the test, the TC35i module and 51 single-chip connection, through the preparation of the PC program instructions into a microcontroller can identify the instructions, and then the software debugging to achieve SMS send and receive function.Therefore, through the use of RS232 interface And PC connection, and then through the serial port debugging software can be achieved TC35i module short message launch operation[5].

V. Wireless Transceiver

A. The choice of wireless transceiver module

The system uses wireless transceiver for the following considerations:

(1) The system is the object of multi-potting, the need for information after the convergence with the mobile phone to establish contact, so set the main station for a single point of information summary;

(2) There is a certain interval between the points, or even distributed in different rooms, after the establishment of the terminus and single point through the cable transmission of information exchange is not convenient.

(3) Family farming flowers have a certain distance, but not too far, if the use of wireless modules for information summary, NRF24L01 transmission distance can reach tens of meters to hundreds of meters, if the increase in power amplifier chip, up to a thousand meters ,[6] Can cover the whole family.

B. Single point wireless information transmission

Since the collection of soil moisture information is periodic, it is necessary to set a clock. And information exchange between the single point and the terminus,

there is no single point and single point of information exchange between, so the clock set in the terminal 51 single-chip, which is more conducive to system synchronization.

As shown in Figure 4, the NRF24L01 at a single point should be in the accept mode and ready to accept the command sent by the terminal. A single point should be different for the different instructions of the terminus:

When the station clock full cycle, the station will be issued to the single point of instruction, single point of receipt, switch to send mode, and to the main station to send the current humidity information, send back to the receiving mode, waiting for the next station command.

When the station receives the GSM mode switch command, it will switch to the single point of sending mode instructions, a single point after receiving the instructions to change the working mode of the watering device, and then continue to wait for the next station command.

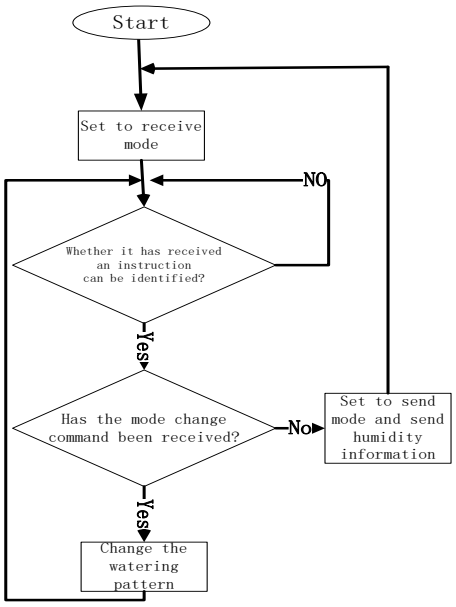

Fig.4. Single point NRF24L01 working flow chart

C．Terminal station wireless information transmission

The station's wireless information transmission workflow is more complex than the single point, because each single point only communicates with the main station, but the terminal station wants to communicate with multiple points and communicate with the GSM module. Terminal station wireless information transmission mode shown in Figure 5. The station needs to set a clock, the clock as the whole system clock.

First of all, to judge whether or not to receive text messages, if the instruction from the GSM module to change the mode mode, directly to the three single-point send mode change instructions, each single point to read their own corresponding single point mode information, Make the appropriate mode transformation, and then continue to determine whether to receive text messages.

If the SMS command is not received, the clock is judged. If the clock is not full, return to the previous step, continue to SMS command to judge. If the clock is full, the master station switches to the transmit mode, sends the command to the single point 1, the command single point 1 switches to the sending state and sends the soil humidity information to the main station. At the same time, the master station switches to the receiving mode and waits to accept the single point 1 Of the soil moisture information, after receiving, to switch to the sending state, followed by the single point 2, single point 3 the same operation. After all the single point of humidity information collection is completed, then return to determine whether to accept the SMS command, start the next cycle.

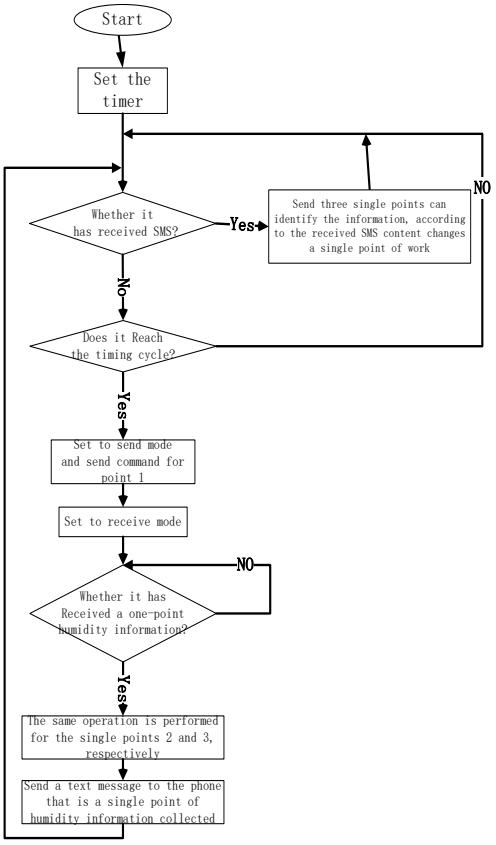

Fig.5. Terminator NRF24L01 working flow chart

VI. APP

A. Interface introduction and function

(1)The main interface introduced

The right side of the main interface for the three pots of flowers show the humidity of the dial, the humidity information for the last received data. And is equipped with three buttons on the left side, respectively, for controlling the working pattern of the three pots of flowers[7]. The main interface is shown in Figure 6.

(2)Real-time update of the main interface humidity information

After receiving the message, then refresh the humidity dashboard operation[8].

(3) Exit the application prompt

If you do not want the program to run in the background, you do not want the application to receive any humidity data, click "OK", otherwise click "Cancel", if you want to let the program run in the background[9], the exit prompt interface is shown in Figure 7.

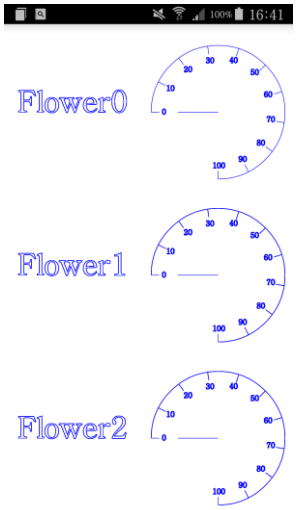

Fig.6. Main interface

Fig.7. Exit the interface

(4) Watering machine working mode selection

Select the working mode interface with a radio list with the dialog box to control, the user can click on the list of different work methods, then the application can send control commands SMS to the terminal (no need to use the phone comes with SMS application), to achieve the mode of switching The blue dot on the right side of the list can remember the mode before switching. Mode switch interface shown in Figure 8, watering machine mode, including automatic and periodic watering.

User clicks will appear by Process Dialog provided "is switching" prompt, as shown in Figure 9. This means that the application is sending text messages to the terminal.

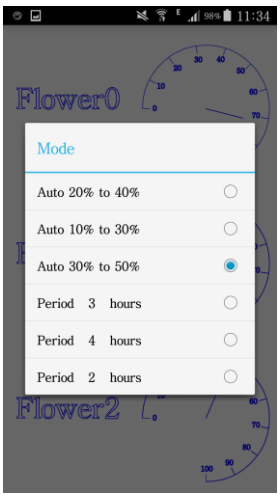

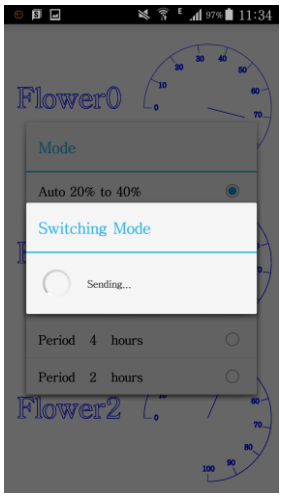

Fig.8. Mode switch interface Fig.9. Send the process interface

After the message is sent, there are two cases, namely, success or failure. After sending, the status of the sending status reminder provided by the "bread bar" is displayed at the bottom of the screen. If successful, as shown in Figure 8, the application will remember the state after the switch, the user can not repeat the same item; if the signal, arrears and other reasons to send failure, as shown in Figure 9, the application will not memory mode switch , The user can click again to try to send again. This ensures that the current mode of operation on the phone is synchronized with the actual working mode of the watering device at home[10].

(5) Humidity information summary line chart

The interface shows the flower soil moisture values at each time node as a line graph[11], as shown in Figure 10.

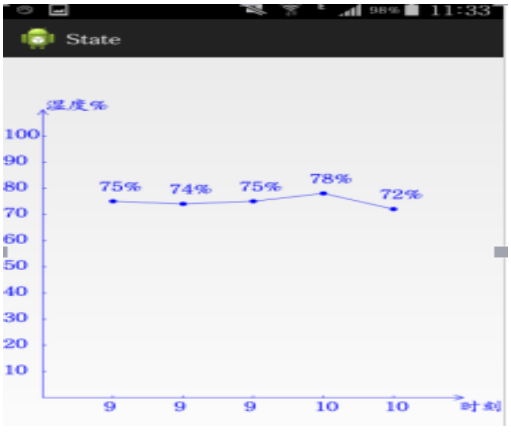

Fig.10. Humidity line chart

VII. CONCLUSION

The entire system can perform the following functions:

(1)Single point watering system can complete the soil moisture collection, and can be based on the current model to complete the corresponding watering function.

(2)NRF24L01 module can achieve multi-machine half-duplex communication, that is, the terminal can be regularly obtained for each single point of humidity information, and can adjust the single point of the work mode.

(3)Mobile phone can be through the APP to monitor the flow of soil moisture information and change the mode of operation of the watering device.

References

[1] Zhang Zhaopeng. Based on AT89S52 the design of home intelligent watering device. Electronic design project .2013,5: 39.

[2] Yuexue Jun, Liu Yongxin, Hong Tiansheng, Yevgeny king, full sun, Chenzhu Liang-based automatic irrigation control system design and test soil moisture farm machinery reported .2015 S2:.. 241.

[3] Jiang Jie,,Song Honglong. Smoke sensor alarm system based on GSM SMS. Measurement and control technology .2014,1: 1.

[4] LIN Tian-cheng, LINTIAN-cheng. Remote home control system based on GSM [J]. Equipment Manufacturing Technology, 2010 (5): 75-76.

[5] ZHU Dan. Family anti-theft alarm system based on GSM SMS module [J]. Journal of Shaoxing University, 2010, 30 (10): 69-72.

[6] Li Shihong. Based on nRF2401 multi-point wireless temperature and humidity alarm system design [J]. Journal of Wenzhou Vocational College of Science and Technology, 2015 (2): 53-57.

[7] Guo.Lin. The first line of code. Beijing: People's Posts and Telecommunications Press, 2013.

[8] Sun Xiehua. Java programming tutorial. Beijing: Tsinghua University Press, 2008

[9] Sun Tao. Java language programming practice tutorial. Beijing: Tsinghua University Press, 2012.

[10] Taoyang. APP Android platform design and implementation [J] Computer Programming Skills & Maintenance, 2014 (9) based on: 23-27.

[11] Wang Yongsong. Andrews mobile phone APP development routines of information processing [J]. Computer Programming Skills and Maintenance, 2014 (20): 57-62.

Information Collection and Display System in the Study

Zhang Rongguang; Gao Hui; Tu Zhitian; Wang Shilong
（Jilin university instrument science and engineering institute, Changchun, 130021）

***Abstract*—In order to monitor the population and temperature of classroom, a system based on Wi-Fi has been designed to count the number of people. The system consists of three parts. Information collecting part, information transmission part and analysis part. Information collecting part comprises a number of statistics to determine the situation of classroom. Information transmission part transmitted the collected information to control center. The analysis part analyses collected information and use the website to display the information of each classroom. Students can easily log on site through computers and mobile phones to know the information of each study room.**

***Keywords* — Self-study room, Campus network, Indoor number of people**

I. INTRODUCTION

THE system enables students to quickly and accurately grasp the information of each classroom, thereby saving time and improving learning efficiency. At the same time, the system has broad application prospects. At this stage, domestic and foreign statistical techniques of counting people is a face detection based on the number of statistical techniques [1]. This kind of technology has a great influence on the statistical speed and the statistical error is large. In addition, the application of infrared induction for statistics the number of students is universal. This technique is simple and sensitive. Similar techniques are used in this design. And some related improvement has been made. In data transmission, Zig-Bee [2] can be used. However, this technology is limited by transmission distance. Owe to use of campus network in this design, realize data transmission on Wi-Fi. In terms of data display, build own website, do data analysis and display. Users can quickly get the information of study room by logging on site.

II. OVERALL DESIGN SCHEME

The whole system can be divided into three parts. The first part is mainly to gain the information of the study room, including the number of people, the temperature, and the use of self-study room. The second part is to transfer the measured data to the server. The third part is to build a website, displaying the data. The overall hardware structure is shown in Figure 1. The overall software structure is shown in figure 2.

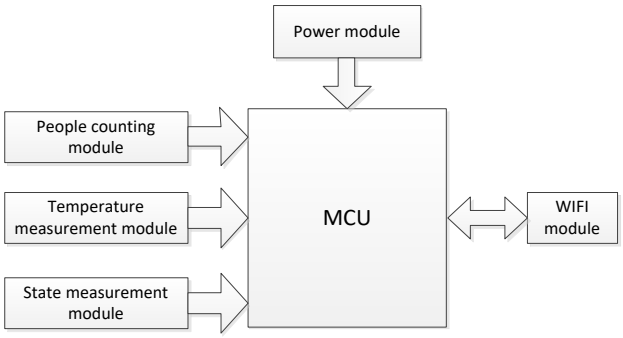

Fig.1 Overall hardware structure

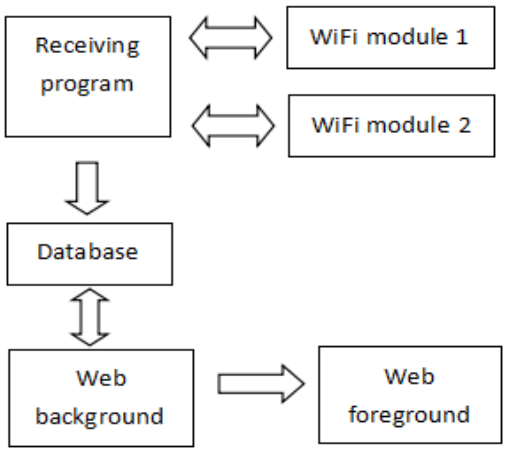

Fig.2 Overall software structure

III .HARDWARE DESIGN

A. Statistics Module

In the statistics of the number, infrared photoelectric switch is used. The infrared emitter is composed of transmitter and receiver. Its working principle is that in this system, two groups of infrared photoelectric switches are introduced. Detect the human body through two sets of photoelectric switch order and time to judge people in and out of the direction. Use programming to achieve the number of statistics. The statistical algorithm is shown in figure 3.

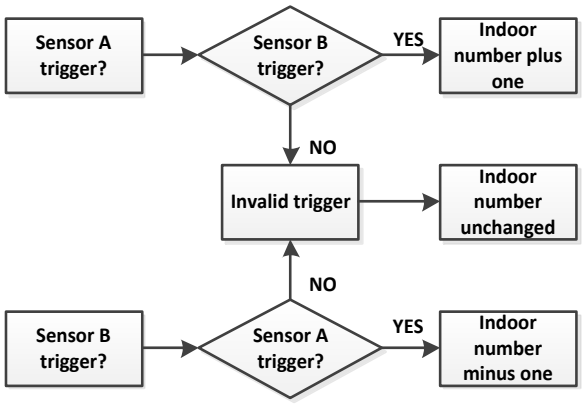

Fig.3 Statistical flow chart

B. Temperature Collection Part

Digital output integrated temperature sensor has been applied to measure temperature. Its inner low temperature coefficient oscillator can produce accurate and stable frequency signal f_0. While the high temperature coefficient oscillator measured temperature into frequency signal f_0. When the counter is open, DS18B20 counts f_0, but the opening time of the counter is determined by the high temperature coefficient oscillator.

C. Data Transmission Module

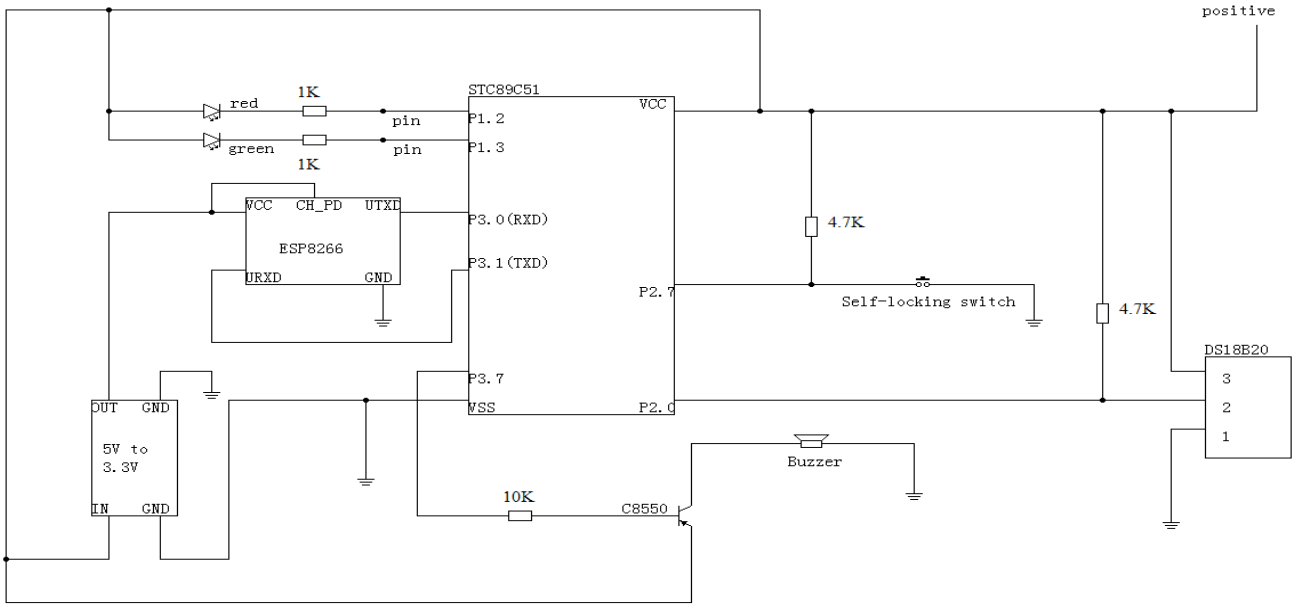

Fig.4 Circuit diagram

In the transmission of data, the ESP8266 serial port WIFI wireless module is used. ESP8266 wireless Wi-Fi module currently sold on the market has 8 pins. VCC and GND are respectively connected to the positive and the ground of the 3.3V power supply when in use. UTXD and URXD for its serial transmit and receive pins. Finally, the CH_PD pin is connected to the VCC. The remaining three pins can be suspended. At the same time, a series of initialization is needed for ESP8266. Connect it to the USB TTL module, and connect to the computer's USB port. Through the computer serial debugging assistant a series of AT instructions can be sent to the ESP8266 set. The AT+CWMODE=1 command is used to set the operating mode to 1, which is the STA model, as the client model. The next instruction is AT+CWJAP= "JLU.PC","". Its role is to let the Wi-Fi module connected to the campus network. The first parameter is the name of the network that needs to be connected. The second is password. As long as the connection, the

Wi-Fi module can remember this connection. Then it can be connected to the microcontroller automatically. Finally, the Wi-Fi module transfers the data to the server and also needs to be connected to the corresponding host according to the IP address. The host need to be connected according to the IP address. The Instruction is AT+CIPSTART= "TCP", "202.198.156.55", 8080. The first parameter is connected by TCP. The second parameter is the IP address of the host to be connected. The third parameter is the port of the host that needs to be connected. After successfully connecting to the host, Data Transmission Module can send information. The actual hardware circuit is shown in figure 4.

IV. SOFTWARE DESIGN

A. Data Transmission

A local area network (LAN) is a network made up of multiple computers or mobile devices. Under normal circumstances, the two LAN is not visible to each other, that is, between different LAN they cannot visit each other.

On the campus network, each classroom can connect to wireless Wi-Fi. But such a network is just a LAN. If the server is built in such an environment, then other teaching facilities in the building will not be able to access the server. So the server needs to have a public IP. But the server is not fully built in outer net. Because on one hand, the speed of access to the Internet is very slow. It is difficult to achieve real-time updates of data. On the other hand, campus network equipment to access the Internet through client authentication, and each account can only log in once. Performance is very weak and unable to run the client, it will not be able to access the Internet. This system makes use of the characteristics of the campus network. Use public IP to build server in campus network. Therefore, any device connected to the campus network does not need to log in to access this server to realize real time data transmission.

B. Data Transmission

When the Wi-Fi module transfers data to the computer through the campus network, the computer side needs a program to receive the data sent by the Wi-Fi module and save it. This program is designed using the Java language, Eclipse as development tools, which is based on TCP/IP protocol. The machine is bound connection port, waiting for the Wi-Fi module. When a device is connected in this device to open a separate thread for processing, TCP is used for data transmission, according to the data transmitted in real time to update the database, every time the real-time data alone to save time, as a historical record. The block diagram of the receiving program is shown in figure 5.

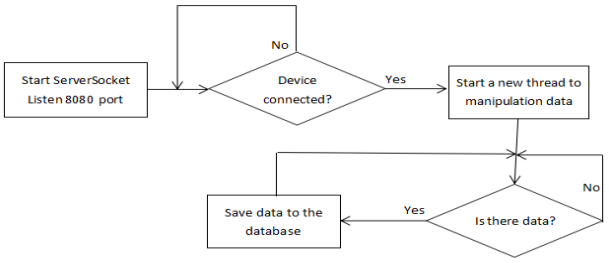

Fig.5 Receiver block diagram

C. Web Server Building

The display of system data takes use of the web. The advantages compared to the Windows desktop client is that students can be accessed by computer or mobile phone to use the campus network in the classroom, view data, and more practical.

In the design of the Web server, hiring third-party server is not chosen and we choose to build our own, mainly because the data is real-time changes. These real-time data are not easily transferred to the third party server in real time. The system is based on the use of Java language web site development background, using Tomcat as a Web server, which is a free open source small server.

D. Web Programming

Web program uses My Eclipse tools for development, including two parts: foreground and background. The main function of the foreground is to provide users with a query page, which you can query to the real-time temperature, people in classroom, and the information of classroom. Ensure the real-time data, by using Ajax refresh every 0.1s. Page is programmed using Html, CSS, and JavaScript language. Background is developed mainly by the use of Java Web. The foreground visits a servlet, which is responsible for reading data from the database to the foreground. The Web program logic block diagram is shown in Figure 6, the query page is shown in figure 7.

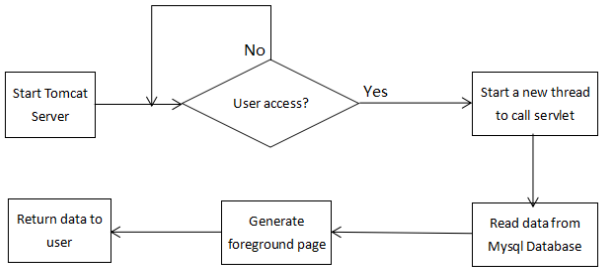

Fig.6 Web program block diagram

Fig.7 Client interface

E. Database Design

This project is based on MySQL database. Two tables are designed in the database: current data table and history data table. Current data table keeps the current number of each classroom in real time, and the client program receive the data sent by the Wi-Fi module real-time and update this table. The history data table is used to save the historical data, and the data of the classrooms in the current data table is saved to the history data table once every other time (this time can be set dynamically) as a history record, which is prepared for system maintenance and data analysis. The details of the two tables are as follows.

Table 1 Real-time data table

Field	Description
id	primary key id
name	classroom name
num	number of people
temperature	temperature
state	statement
flag	flag bit

Table 2 Historical data table

Field	Description
id	primary key id
name	classroom name
num	number of people
temperature	temperature
state	statement
time	measurement time

V .DATA RECORDING AND ANALYSIS

A. People Counting System Stability Test

The capacity of 150 people in the classroom 101 as the experimental object, install the information collection system designed in this paper at the only import and export channel in the classroom to conduct experiment. The experiment time starts from 18:30 to 22:00. Because the fundamental purpose of the system is to enable students to quickly find a suitable study room. The main factors affecting is the number of people, and the temperature acquisition module and classroom state control button structure is simple but high stability. So here only the number of modules to be tested. In the course of the experiment through manual and system, record the flow of indoor staff room. The data recorded in the experiment include the number of actual classrooms, the number of people displayed by the system, and the number of people. The test data results are shown in Figure 8.

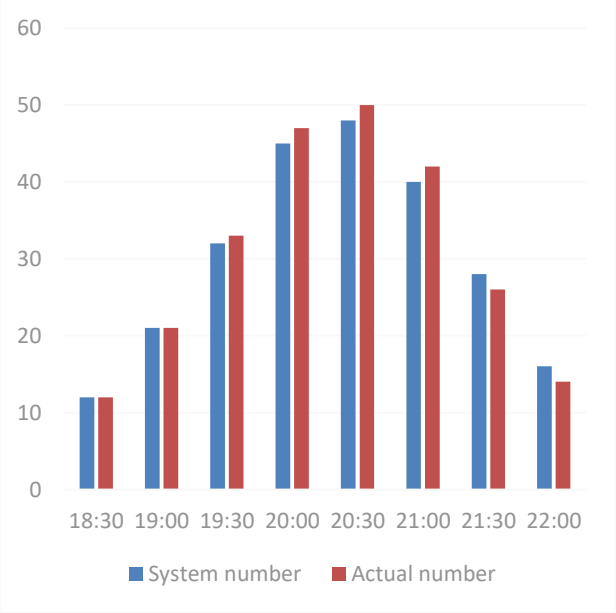

Fig.8 Test data

B. People Counting System Stability Test

The relative error of the number of artificial and systematic statistics is calculated from the data in Figure 5. The results are shown in Table 3. From the calculation data we can see that the system in nearly three and a half hours of the experimental process is stable and the relative error is small. The measurement results are in good agreement with the actual data. The possible cause of the error is the arm swing to block the photoelectric switch.

Table 3 Relative error chart

Artificial statistical data	System statistics	Relative error
13	12	7.7%
22	21	4.5%
33	32	3.1%
47	45	4.3%
50	48	4.0%
42	40	4.8%
26	28	7.7%
15	16	6.7%

VI. CONCLUSION

The system will collect the information through the web display, so that students can quickly and easily query the information of each study room to choose the appropriate study room. At the same time, through the data statistics of school administration department can understand the use of the classroom, which is conducive to the rational allocation of classroom educational resources and improve the utilization rate. By comparing the data of artificial and systematic statistics, we can see that the system has good stability and high statistical precision.

References

[1] Qian Heqing, Chen Gang, Shen Ruimin. People Counting System Based on Face Detection [J].Computer Engineering, 2012, 38(13):188-191.

[2] Jin Zhongchao, Su Benyue, JingWei,Jiang, Yu-e. Design and Implementation of Self - Study room People Number Intelligent Query System Based on Zigbee [J].Journal of Guizhou University (Natural Sciences), 2014, 31(6):85-88.

[3] Xie Yajun, Li Jianrong, Wang Huifang. Appl ication of ZigBee Wireless Communication Technology on AMR System[J].Journal of electric power, 2009, 24(5)：435-436.

[4] Cheng Defu, Wang Jun, Ling Zhenbao, Wang Yanzhang. Sensor principle and application [M]. Beijing: Mechanical Industry Press, 2007.

Energy consumption GDP per capita model prediction BP neural network

E.Y.Fan; S.Ma; Y.J.Huang

（College of Instrument science and electrical engineering , Jilin University,Changchun 130026,China)

***Abstract*—This paper introduces the energy consumption and GDP per capita in recent decades; And on this basis, using the neural network algorithm and genetic algorithm to establish the mathematical model of the relationship between energy consumption and GDP per capita, reveal the United States into the deep reasons behind "zero growth" energy consumption and energy consumption and GDP per capita between a series of important laws; By using the model to the United States made accurately predict future long-term energy movements, the model can predict, validation, to 2020, 2025, 2030 American energy consumption; The mathematical model was implemented using c # language computing, simulation, visual display, etc.**

***Key words*—Energy consumption GDP per capita Model prediction BP neural network**

I. INTRODUCTION

AS an important energy material elements, closely related with the development of economy and society. From the mid 80s on developed countries since industrialization, Britain, Germany, Italy, the United States, Japan and other countries per capita energy consumption has showed zero growth or even negative growth. As a representative of early industrialization, change the trend of energy consumption in developed countries, the future of the global energy consumption has a reference. And the United States as a pivotal role in the global economy in typical developed countries, the development process can be representative[1-3].

According to the quantitative prediction of the selected prediction approaches can be divided into different departments forecast method, energy consumption intensity method, elastic coefficient method, the input-output method, the total energy of mathematical simulation method of several main methods, the common defects of these methods is the lack of demand for energy and the quantitative relationship between economic development scale to grasp, only using the mathematical simulation to predict the future or deduction of analogy, lack of scientific and accurate results of large deviation. This study uses quantitative analysis to construct the mathematical model of energy consumption prediction, the United States is a mathematical model of energy consumption and people are based on GDP, is used to predict the long-term U.S. energy consumption. The number of The model will solve the qualitative prediction with strong subjectivity, lack of rigorous and scientific issues, in order to perfect Wang Anjian and a number of researchers have invented the "S" shape physical model, improve the long-term energy consumption prediction accuracy[4-5].

II.ANALYSIS OF THE RELATIONSHIP BETWEEN ENERGY CONSUMPTION AND PER CAPITA GDP

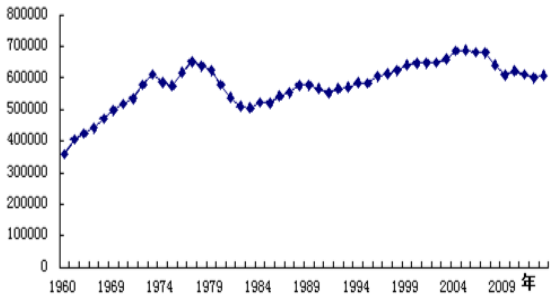

Fig.1 Oil consumption curve

The picture shows the United States from 1960 to 2013 the energy consumption of oil by 1973 this year the trend of.1960 for 13 years, all kinds of oil consumption are showing a growth rate of.1973 fast the first oil crisis happened in America, after the U.S. oil consumption declined. Volatility in oil prices the first oil crisis caused by the extremely unstable and supply the U.S. economy has been hit hard,.1981 years to 2005, energy consumption trend rebound. But from

2005 to 2013, due to the implementation of the "oil independence" strategy, the domestic oil consumption continued to decline.2012 Drop to 6 billion 767 million barrels, consumption less than 6 billion 796 million barrels in 1997. In the past 50 years, U.S. oil consumption from 3 billion 586 million barrels to 1960 in 2005 rose to 7593 of the total 111.74%. million barrels, up by a figure also shows that the United States at different times, the oil consumption growth rate and growth percentage is different. Generally speaking, the last century before 80s, oil consumption growth was significantly faster in 80s.

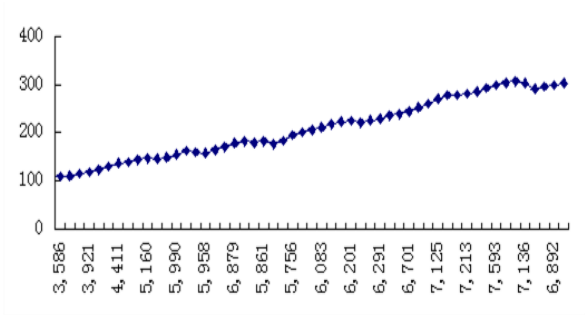

Fig.2 The energy consumption and GDP per capita diagram

The United States energy consumption characterizes the scientific index of national energy consumption to a certain extent. To eliminate the oil consumption of population expansion or atrophy factors, and Research on the dynamic comparative analysis of per capita GDP will be more profoundly reveals the economic development and oil consumption. The relationship of figure three correlation analysis results show that two cases showed obvious linear relationship. The linear relationship showed good growth, in the process of economic development, with the growth of GDP per capita, oil consumption will take a larger proportion of the increase, is a basic rule that exists in reality.

III.MATHEMATICAL MODEL

A.BP neural network

Artificial neural network can be fitted with any complicated nonlinear relationship, does not need the mathematical modeling of complex.BP neural network input output model mapping a large number of learning and memory, and without prior explanation of the mathematical equations describing the mapping relation of the.BP network is a multilayer feedforward neural network, its name is derived from the in network training the training algorithm, adjustment of network weights are the backpropagation neural network model, according to statistics, about 80% of the BP network or its variants.

BP neural network based nonlinear function fitting algorithm can be divided into BP neural network, BP neural network training and BP neural network prediction three steps.

MATLAB software includes MATLAB neural network toolbox. It is based on the artificial neural network theory, using MATLAB language constructs involved in the theoretical formula calculation, matrix operations and equations for most subroutine designing and training of neural network.

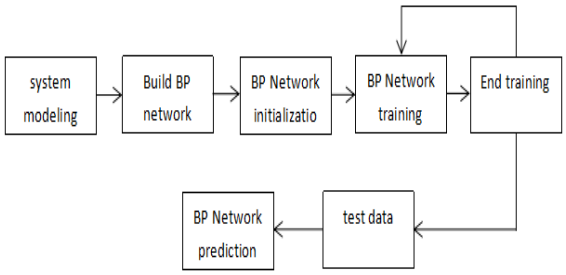

Fig.3 The BP neural network algorithm flow chart

The model for the prediction and relationship between energy consumption and per capita GDP, per capita GDP as independent variables in the prediction of energy consumption must first predict the per capita GDP. And basically the same method to establish BP neural network model and energy consumption of GDP per capita.

BP neural network is trained using the training data to train the BP neural network. A total of 50 sets of data, selection of 50 sets of data from (1960 - 2009) as training data to train the network, 3 sets of data (2010 - 2012) as test data to test network prediction ability.

Based on neural network algorithm, using Matlab to achieve the initial energy consumption data fitting and prediction (graphics)

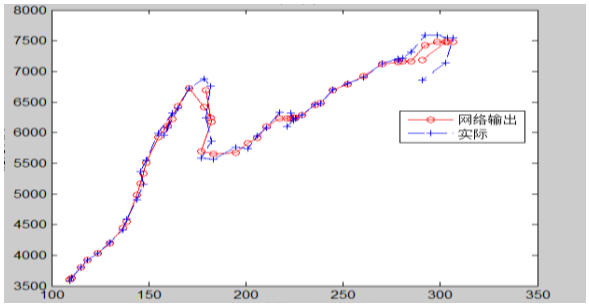

Fig.4 Neural network algorithm of data fitting and forecast figure

B.genetic algorithm

Genetic algorithm is a bionic algorithm, namely the evolution of life simulation algorithm. It is starting from an initial population, repeated execution of selection, crossover and mutation process, the evolution of population more and more close to a target. If the population regarded as a set of points, super space selection, hybridization and mutation process that is a transform between sets of points in super space, make the population changing through the exchange of information. The genetic algorithm through the simulation of Darwin "survival of the fittest, the principle of survival of the fittest" good incentive structure, at the same time looking for a better structure.

The genetic algorithm to solve the problem, first in search of initial population randomly generated space, calculate the objective function of the individual, then optimize the appropriate fitness value, through mutation, crossover operation to produce the next generation, the maximum number of iterations is reached 500, output the best individual, and then terminate the algorithm

Genetic algorithm is used to optimize the neural network to fit and predict the energy consumption data

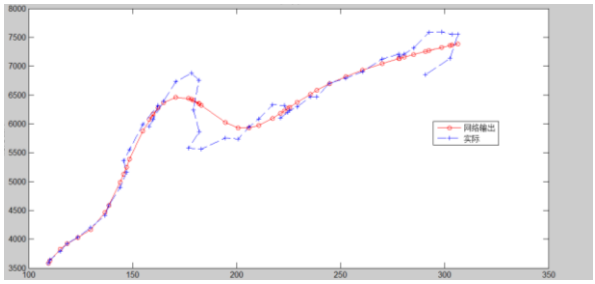

Fig.5 Genetic algorithm fitting curve

The model is used to predict the energy consumption from 2015 to 2030:

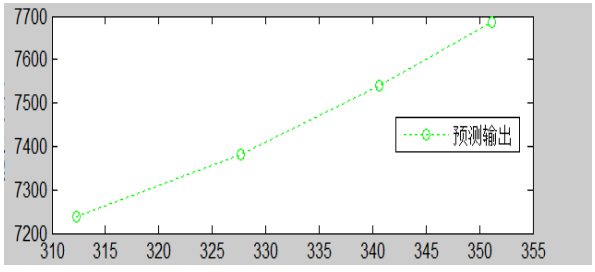

Fig.6 The genetic algorithm to predict trend chart

By querying the relevant information, learning c# language knowledge, and know how to use the WinForm visual programming interface and backstage programming. To import and export data, EXCAL image data processing, the final call, complete the visual program.

IV.WINFORM VISUAL PROGRAMMING

```
using System;
using System.Collections.Generic;
using System.ComponentModel;
using System.Data;
using System.Drawing;
using System.Linq;
using System.Text;
using System.Threading.Tasks;
using System.Windows.Forms;
using System.Data.OleDb;
using System.IO;
using System.Drawing.Drawing2D;

namespace WindowsFormsApplication14
{
    public partial class Form1 : Form
    {
        public Form1()
        {
            InitializeComponent();
        }

        private void Form1_Load(object sender,
EventArgs e)
        {

        }
        private void button2_Click(object sender,
EventArgs e)
        {
            {
                OpenFileDialog fd = new
OpenFileDialog();
                fd.Filter = "表格|*.xls";
                string strPath;
                if (fd.ShowDialog() ==
DialogResult.OK)
                {
                    try
                    {
                        strPath = fd.FileName;
                        string strCon =
```

```
"provider=microsoft.jet.oledb.4.0;data source=" +
strPath + ";extended properties='Excel
8.0;HDR=YES;IMEX=1'";
                    OleDbConnection
Con = new OleDbConnection(strCon);
                    string strSql = "select
* from[Sheet1$]";
                    OleDbCommand Cmd
= new OleDbCommand(strSql, Con);
                    OleDbDataAdapter da
= new OleDbDataAdapter(Cmd);
                    DataSet ds = new
DataSet();
                    da.Fill(ds, "biaoge1");

dataGridView1.DataSource = ds.Tables[0];
                }
                catch (Exception ex)
                {

MessageBox.Show(ex.Message);
                }
            }
        }
    }

    private void button1_Click(object sender,
EventArgs e)
    {
        DataTable dt = new DataTable();
        dt.Columns.Add("GDP平均值(百美
元)");
        dt.Columns.Add("能耗平均值(百万
桶)");
        dataGridView2.DataSource = dt;
        DataRow dr = dt.NewRow();
        dr[0] = "209.1968";
        dr[1] = "6129.895";
        dt.Rows.Add(dr);
    }

    private void button3_Click(object sender,
EventArgs e)
    {
        FileStream fs = new
FileStream(@"f:\dc.txt", FileMode.OpenOrCreate,
FileAccess.Write);
        StreamWriter m_streamWriter = new
StreamWriter(fs);
        m_streamWriter.BaseStream.Seek(0,
SeekOrigin.End);
        for (int i = 1; i <
dataGridView2.Rows.Count; i++)
        {

m_streamWriter.WriteLine("209.1968    6129.895");
        }
        m_streamWriter.Flush();
        m_streamWriter.Close();
        fs.Close();
```

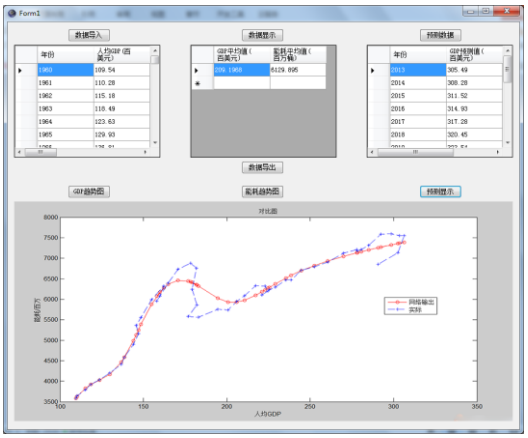

Fig.7 The software operation interface

V.CONCLUSION

Through the BP neural network algorithm and genetic algorithm to complete the relationship between GDP and energy consumption prediction and trend model construction, can be achieved with the software, the trend and the actual trend, the completion of the medium and long term prediction

Reference

[1] A.J.Wang,Energy demand forecasting based on "S" shape model[P].Beijing City,2011.02.21.

[2] W.J.Yu,Analysis of the zero growth of per capita energy consumption in developed countries[A].industry Watch.

[3] W.J.Yu,When China's energy consumption zero growth[J].Earth Journal,2010.10(5).

[4] A.J.Wang,Mineral resources demand theory and model prediction[J].Earth Journal,2010.4(2).

[5] A.J.Wang,World resources pattern and Prospect[J].Earth Journal 2010,pp,621-627.

The research and design of lead acid battery charger

Yu Qiang; Han Xing; Lan Fa

（College of Instrumentation and Electrical Engineering Jilin University, Changchun 130012）

***Abstract*—This paper presents a design of 12V lead-acid battery charger, which is based on the positive and negative pulse charging theory. This charger is based on the switching power supply technology, and the MSP430 single chip microcomputer with ultra low power is used to realize the control, the overall design scheme is given. And we have given the design of main power transformation structure, the design of control circuit, the design of charging and discharging circuit introduction. We have divided the entire charging process into precharging, fast pulse charging, complement charging and trickle charging in 4 stages. Experiments show that it can realize nondestructive quick charge for 12V lead-acid battery, and the charging information of the current, voltage and temperature can be displayed in real time through the LCD screen. In addition, the circuit contains over-voltage, over-current, short circuit protection.**

***Key words*—Lead-acid batteries Positive and negative pulse charging PFC correction Flyback topology**

I.INTRODUCTION

LEAD acid battery is widely used in electric vehicles, battery cars, electric toys and other fields because of its mature technology, reliable safety and high reuse rate[1,2]. At present, the design of lead-acid battery charger is also endless. With the continuous expansion of the application field, the demand for lead-acid battery charging is also getting higher and higher. The new charging method is proposed to improve the charging speed, reduce the damage to the charger and battery, and prolong the service life.

A scheme of a fast charger for 12V lead-acid battery is presented in this paper. A positive and negative pulse fast charge method is adopted in this scheme. It combines the hardware and software, for it's based on the switching power supply technology, with MSP430 single chip microcomputer as the main controller. By the discharge depolarization, we improve the battery charging speed and reduce loss and damage to the battery charging. This design can also display the charging process of the current, voltage, temperature and other charging information in real time. Therefore, it has great practical value.

II.CHARGING THEORY

The main purpose of battery charging is to restore the battery capacity as soon as possible. To achieve this goal, we hope to achieve a larger charging rate. But large charging rate is bound to cause the overcharge, produce gas analysis, which is damage to the battery life. The use of a small charge rate can prevent overcharge reactions, and the impact to the battery life is small. But it can not meet the requirements of fast charging[3]. Therefore, advanced charging technology should deal with this contradiction.

Polarization reaction will happen in the process of lead-acid battery charging. The polarization can prevent battery charging, and increase the battery outgassing rate and temperature, which will affect the charging speed and the service life of the battery. At present, the main solution to the problem of polarization is intermittent charging during the charging, or using negative pulses for discharge[4]. So this design adopts the positive and negative pulse charging method. In the process of positive pulse charging, the negative pulse is added to remove the polarization of the battery, so as to improve the capacity of the battery to accept the current, and restore the capacity as soon as possible to reduce the damage to the battery.

III.CHARGING PROCESS

The charging method used in the charging device

described in this paper divides the whole charging process into four stages: precharge, pulse fast charging, make up charging and trickle charge.

A.Precharging

When the charger just starts to work, in order to protect the battery pack and charger from the strong current shock damage, we started charging with stabilize and small current to rise the battery voltage. When the batteryccept the high current charge, we then use high cur voltage is up to the threshold which can arent for fast charging.

B.Pulse Fast Charging

In the process of pulse fast charging, the charger work in positive and negative pulse charging process. The average width of positive pulse is 900 ms and the average width of negative pulse is about 20 ms. In the process of positive and negative pulse charging alternately, there are 40 milliseconds apart. The amplitude of negative pulse is about 1.5 times of positive pulse. This process takes about 85% of the battery charge. During the charging process, the battery voltage rises rapidly. And when the voltage rises to the secondary voltage threshold, it is transferred to the complement charging stage.

C.Complement Charging

After the pulse fast charging procedure is terminated, the battery is not necessarily fully charged. In order to ensure that the battery charge 100% of the electricity, we need to complement charging the battery. This stage is charged with constant voltage charging，which can make the battery capacity further recovery. At this time the charging current gradually decreases, when the current drops to a certain threshold, the charging mode is transferred to the trickle charge stage.

D.Trickle Charging

This stage is mainly used to supplement the energy consumed by the battery self-discharge. As long as the battery connected to the charger and the charger connected to the power supply, the charger will continue to add the battery charge, so that the battery is always in a fully charged state. This also indicates that the charging process has ended.

IV.Design of Overall Structure of Charger

Considering the design of positive and negative pulse fast charging method, we combine the current research situation of the charger[5]，this paper presents the charger structure as shown in Figure 1.

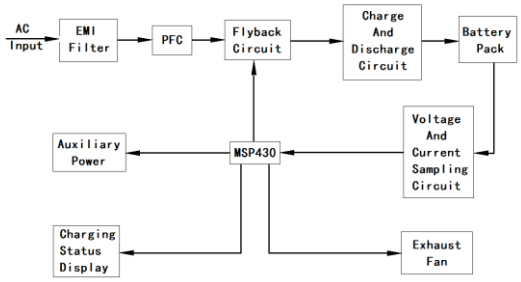

Fig.1 The overall structure of the charger

This design uses the overall structure of the AC/DC-DC/DC. The charger connected to 220V AC mains first, and then through the EMI filter and PFC correcting circuit, finally capturing the circuit module. The main circuit adopts flyback isolation topology. The output of the flyback circuit is connected with the charging and discharging circuit after filtering, finally through the wires connect battery charging. The charger is controlled by MSP430 MCU as the center of the unit. The main function of MCU is: first, adjust the feedback microcontroller output signal to achieve the control of the output of the flyback circuit; second, the microcontroller output two control signals, respectively, used to control the charging circuit and discharge circuit; third, the microcontroller receives voltage, current, temperature detection signal; fourth, MCU control LCD displaying, fan operation, and the connection button. In addition, the MCU also participate in the implementation circuit of over voltage, over current, short circuit protection and meter, etc.

V.Main Circuit Design

A. PFC Circuit Design

This part uses the boost active PFC correction circuit. The control chip is UC3854. By setting up the peripheral circuit of the UC3854 chip, we can control the on-off of the switch in the boost circuit, so that the waveform of the input current changes with the change of the voltage waveform. The voltage and current phases are basically the same, which greatly improving the power factor, and reduce the pollution to the power grid[6].

B.Flyback Circuit Design

DC/DC transform is the key part of the whole

charger. Usually the charger is directly connected to the power grid. Considering the design of security, we will choose to use isolated topology. The charger is designed for 12V lead-acid batteries. Considering the full voltage of general 12V lead-acid battery may be more than 14V, and the factor of MOS tube's voltage drop，we set the maximum output of the main circuit to 16V. The designed output power is 120W. According to these design goals, the flyback circuit is a quite good choice here. The flyback circuit has the advantages of few components, simple structure, small size, high modulation amplitude of the output voltage by the duty cycle and low cost. If we design the power under 200W, we often adopt flyback circuit[7]. Therefore, this design uses flyback topology, which mainly includes the transformation of the main circuit, drive circuit, feedback circuit, detection circuit, as shown in Figure 2.

The main circuit of the converter is the high frequency transformer, and the design of the high frequency transformer determines the merits of the flyback circuit[8]. The flyback circuit design has a frequency of 100kHz. High-frequency transformer using EI40 magnetic core, the original edge number of turns is 29 turn 2 strands and rao, attached to the edge number of turns is 4 turns 16 and rao. This design adopts the sandwich winding, which is used to reduce the leakage inductance, and help to improve the EMC characteristics. Considering the stability of the circuit, we choose the design of DCM (discontinuous mode). In the actual work, with the increase of the load current output, from discontinuous to CCM (continuous mode). MOS tube is IRFPE50, whose withstand voltage is 800V. The circuit of the output will pass through a schottky diode rectifier, and then through Π type filter circuit.

The control chip used in the drive circuit is UC3842, which is an ideal current mode pulse width modulator. We adopt the method of 2 feet ground here. 1 foot feedback voltage signal, 3 feet by current signal. The resistance R6 provide UC3842 starting voltage, as shown in Figure 2. In normal operation, a special winding from the high frequency transformer is used to supply power to the chip. The rectification with D3 is for forward, the rectification with D4 is for flyback. Both the two windings work at the same time to the chip power supply. In the actual work, light load case mainly use the forward winding, overloading situation mainly use the flyback winding [9].

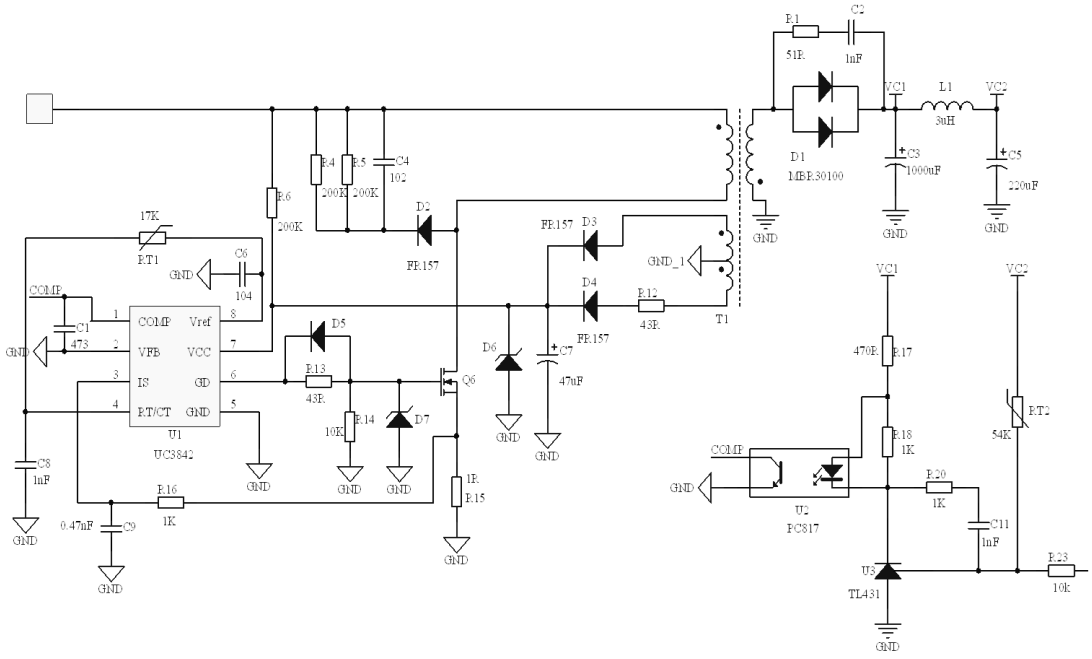

Fig.2 Part of the flyback circuit

The feedback circuit adopts a voltage stabilizing structure of linear optocoupler PC817 and TL431, which limits the maximum output voltage to 16V, thus forming a voltage limiting ring. Normally, the feedback loop does not work, because the charge output is always below 16V, which is controlled by the feedback loop of the microcontroller. The output of the single chip computer through DAC0832, converted to

analog signals, and then after two stage operational amplifier, converted into a positive voltage signal, through the optocoupler PC817 feedback to the UC3842, to achieve the control of the flyback circuit output.

The detection circuit mainly includes voltage detection circuit, current detection circuit and temperature sampling circuit. Through the 12-bit precision AD comies with MSP430 mcrocontroller, we detect the analog signal into a digital signal.

C.Charging And Discharging Circuit Design

Charge and discharge circuit is actually a combination of two circuits, including the charging circuit and discharge circuit, as shown in Figure 3. Transistors and resistors constitute the driving circuit. Q1 and Q3 respectively for the charging circuit and discharge circuit of the MOS tube. Normally, the Q1 is turned on, the positive pulse is charged, and then the Q1 is turned off. After a period of rest, the Q3 is turned on and the battery is discharged through a resistance R3. In this way, positive pulse charging and negative pulse discharge are realized. During this period the positive pulse occupies 90% of the cycle. Negative pulse time is very short, which mainly give the battery a very small discharge time gap.

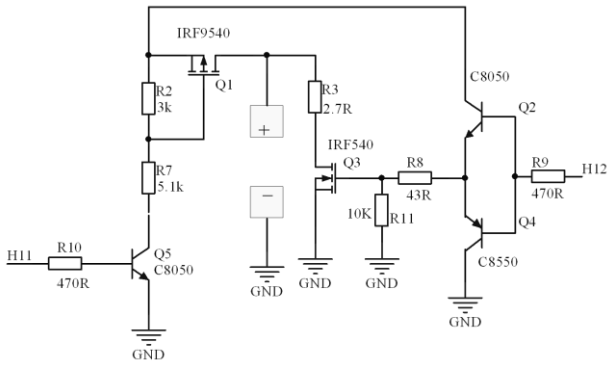

Fig.3 Charge and discharge circuit

VI.SOFTWARE PART DESIGN

The software is mainly to control the whole process of the design of the program, as well as the protection of the circuit, LCD display and other functions. We use MSP430 microcontroller as the control center. The MCU need to control the conversion of 4 stages in the process of charging. This requires real-time detection of voltage, current and temperature signal, and judge the battery status, then adjust the feedback and output control charge and discharge circuit. Finally, we have detected voltage, current and other information in real time on the LCD displaying software, as shown in Figure 4.

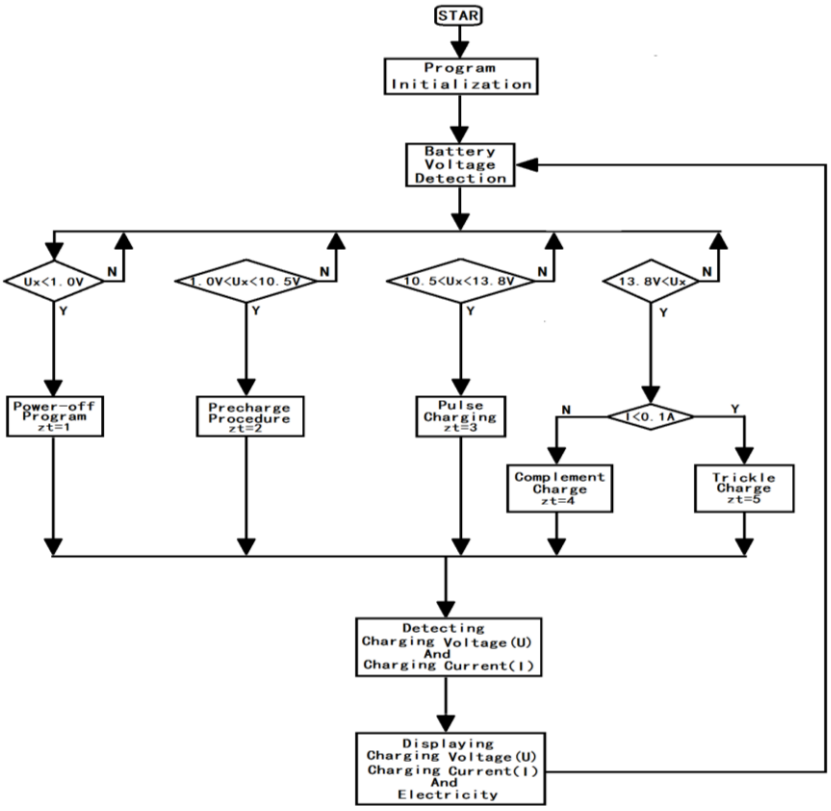

Fig.4 Software flow chart

Once the microcontroller is powered on, it will be initialized, including initializing the LCD screen information, checking whether the battery is connected, and whether the polarity is connected correctly. Only after the charging conditions are reached, will it enter the charging process.

Throughout the charging process, the MCU will continue to test the battery voltage and current information, judge the battery status, and adjust the charging current and voltage in real time. The LCD screen will displays test information. When the circuit occurs short circuit, overvoltage and other abnormal circumstances, the software will immediately respond to emergency procedures, cut off the circuit output to ensure that the circuit is safe. At the same time the LCD panel will display fault indicator. If you want to make the system back to normal work, we need to disconnect the power supply, and then restart. When the temperature reaches 65 degrees, the fan will start to heat up until the last battery is full of electricity. At the same time, the LCD screen will display that the charging is completed. When the module occurs short circuit, overvoltage and other abnormal circumstances, the software will immediately respond to emergency procedures, cut off the circuit output to ensure that the circuit is safe. The LCD screen displays a fault indication. If we want to make the system work properly, you need to power off and then reboot. When the temperature reaches 65℃, the battery charging mode will be in the trickle charge state.

Table 1 The power factor varies with the output power

power（W）	≤20	20-50	50-80	80-100	100-120
The power factor	0.93-0.94	0.94-0.97	0.97-0.98	0.98-0.986	0.986-0.99

Table 2 Variation of voltage, current and ripple under different loads

The output voltage（V）	12.8	12.6	12.4	12.2	12.0	11.9
The output current（A）	0.25	1.0	2.8	5.05	7.8	9.1
Ripple voltage（mV）	8	20	50	90	160	250

VII.RESULT

After the actual test, the results are shown in Table 1. After PFC correction, the input current of the circuit can follow the change of the input voltage, the circuit has a high power factor, not less than 0.93. The waveform of the switching tube is consistent with the theoretical analysis, and the voltage spike is smaller in the switching off period, which shows that the leakage inductance of the transformer is small, the parameters of the RCD absorption loop are reasonable and the power conversion loss is small. Table 2 shows the measured values of voltage, current and ripple under different loads. We can see that with the increase of the output power, the ripple is also increasing. When the output power is higher than 100W, the ripple has exceeded 200mV, which has a great impact on the battery charge. So the actual charging output power is lower than the design value. The efficiency of the whole device is about 80%. On the whole, the whole charger can be very good to complete the 12V lead-acid battery charging.

VIII.CONCLUSION

The design of lead-acid battery charger presented in this article is based on positive and negative pulse charging theory, which is different from the traditional constant voltage charging or three-stage charging, etc. It divides the whole charging process into 4 stages. By adding the negative pulse of the discharge during the positive pulse charging, it removes the polarization of the battery. This can effectively improve the capacity of the battery to accept the current, speed up the charging speed and improve the battery capacity, and finally realize the lead-acid battery charging requirements. On the basis of the basic functions of charging and circuit protection, we also use the LCD screen to display the voltage, current, power and other

information, as well as fault indication information. The whole system also includes EMI filter, PFC correction and other improved performance of the module, which have small size, high reliability. They comply with the general specification.

In summary, the lead-acid battery charger has a very strong application value and broad market prospects.

References

[1] Liu Chao.Study on the fast charging system of HEV vehicle mounted lead-acid battery [D]. Harbin: Harbin Institute of Technology, 2007

[2] Harwood R C, Manoranjan V S, Edwards D B. Lead-Acid Battery Model Under Discharge With a Fast Splitting Method[J]. Energy Conversion IEEE Transactions on, 2011, 26(4):1109-1117.

[3] Deveau J, White C, Swan L G. Lead-acid battery response to various formation levels – Part A: Recommended formation levels for off-grid solar and conventional applications[J]. Sustainable Energy Technologies & Assessments, 2015, 11:1-10.

[4] Song Yun Qing.Design of intelligent high power fast pulse charger [D]. Nanjing: Southeast University, 2008

[5] Dong Yun Hong,Zhao Zhong Min. Design of a high power charging power supply [J]. aviation computing technology, 2001,31 (1):52-54

[6] Yang Ting，Jing Zhan Rong，Gao Tian.Research and design of intelligent and fast charger for electric vehicle [J]. modern electric power, 2010,10.

[7] Wang Meng Meng, Liu Bin, Wang Dan.Computer measurement and control [J].2013,21[8].

[8] Zhao Jiao MIn.Design and application of switching power supply [M]. Shanghai: Shanghai science and Technology Press, 1995.9.

[9] Gao Zhi Jun.Design of intelligent charger for automatic voltage identification [D]. Suzhou: Soochow University, 2015

Intelligent wireless fast charging station based on solar energy

HU Xin-lei; YU Meng-meng; LUO Yan

(College of Instrumentation &Electrical Engineering, Jilin University, Changchun 130012,China)

***Abstract*—At present, with the increasing number of portable mobile devices, a variety of different specifications of the data line intertwined, bringing great inconvenience to people's lives. In view of this problem, this paper put forward that the green solar energy technology and the current research on wireless power transmission technology should be combined, and according to the Qi wireless charging standard and electromagnetic induction--wireless energy transmission principle, set up the intelligent wireless charging system based on solar energy. The system has many advantages, such as green environmental protection, saving power resource, high degree of modularization, and so on.**

***Key words*— Solar energy Qi standard Wireless charging Full bridge inverter STM32**

INTRODUCTION

SINCE the discovery of electro-magnetic induction law in 1840, people began to study the wireless transmission technology [1]. The communication technology based on mobile phones and network has leaped from the wired transmission to the wireless transmission, but the wireless transmission of energy has been developing very slowly. In addition, with the increasingly depleting of non-renewable fossil energy, the world is constantly studying toward the direction of new energy research and development. As a new energy, in the development and use, solar energy will not produce waste residue, waste gas and waste water, and there is no noise pollution. It will not affect the ecological balance, either [2]. So the research on the combination of solar energy and wireless transmission technology is particularly important.

Intelligent wireless fast charging station based on solar energy uses solar green energy to improve the efficiency of power transmission and conversion. It will be able to achieve multi-terminal fast charging function through the independent design of the wireless transmission and reception unit, which is used to build a green, convenient and fast charging system. This system has a wide range of applications, which can be not only placed in the station, airport and other public occasions for mobile phones and other low-power mobile device charging, but also as one of the sources of home power and charging for the small power equipment in field research and experimental. It has good prospects for development.

I. THE DESIGN PRINCIPLES OF SOLAR WIRELESS

1.1 Wireless charging principle

At present, there are three main principles of wireless transmission: electromagnetic induction, magnetic coupling resonant and electromagnetic wave. According to the first coil electromagnetic induction principle, electromagnetic induction type wireless transmission of energy transmission level mainly used in close and small power energy transmission; Magnetic coupling resonant wireless transmission is through the primary coil resonance phenomenon occurs for energy transmission, higher requirements of first grade coil parameters [3]. Qi standard is the world's first to promote the standardization of wireless charging technology, the wireless charging alliance (WPC) launched the "wireless charging standards", adopted the most mainstream technology of electromagnetic induction type, has two big features convenience and versatility [4]. In addition, the electromagnetic induction type wireless charging technology has passed security and market validation, after the production cost is lower than the two technologies, therefore this article is based on electromagnetic induction type wireless transmission technology to the design and manufacture of intelligent solar wireless fast charging stations.

A typical electromagnetic induction type wireless energy transmission block diagram is shown in figure 1.

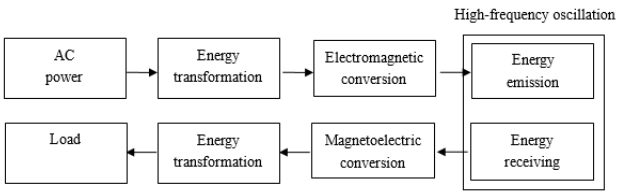

Fig.1 Electromagnetic induction wireless energy transfer diagram

Electromagnetic induction type intelligent solar wireless quick charging system is mainly composed of various parts, such as energy sources, energy emission and receiving, energy management and user interaction. The DC of the input transmitting unit is invertered by the inverter circuit, the alternating voltage generated by the inverter circuit is input to the primary coil of the separate transformer, the secondary coil is for coupling, Thereby generating an induced electromotive force in the secondary coil, the user can through the buttons to adjust the transmission power size. The overall system block diagram is shown in figure 2.

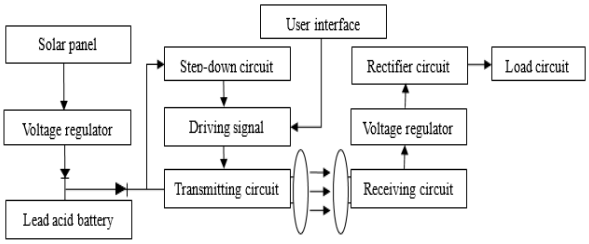

Fig.2 System block diagram

II. SYSTEM MODULES DESIGN AND PRODUCTION

2.1 The power source management unit

The DC voltage output from the solar panel contains a large fluctuating component, it must be set to 12V regulator circuit output firstly for lead-acid battery charging. When the regulator circuit output voltage is higher than the voltage of Lead-acid battery, after the regulator, the solar panel output voltage directly supply the power to the transmitter circuit .When regulating circuit output voltage is lower than the lead-acid battery voltage, transmission circuit power automatic switch to the lead-acid battery, and it will not affect the normal power supply system. This part of the circuit as shown in figure 3.

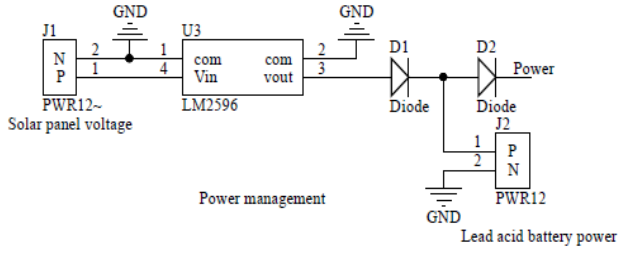

Fig.3 Power management circuit

LM2596 - ADJ is Texas instruments (TI) in the production of 3A output current step-down switch mode integrated regulator chip, it contains a fixed frequency oscillator (150 KHZ) and reference voltage stabilizer (1.23 V), and has perfect protection circuit, current limiting and thermal shut off the circuit, etc. By an external sliding rheostat, the output voltage can achieve the function which is adjustable continuously. The system will adjust output voltage to slightly higher than that of lead-acid battery voltage of 12.7 V, the purpose is to compensate the reverse diode D1 pressure drop. When the LM2596 output voltage is lower than the lead-acid battery voltage, the power supply through the D2 automatically switch to lead-acid batteries to achieve uninterrupted power supply system.

2.2 Transmission circuit unit

The transmitting circuit needs to convert the 12V DC voltage outputted by the solar panel to the positive and negative alternating voltage, which is applied to the two segments of the transmitting coil to generate the alternating electromagnetic field in the coil to couple the induced electromotive force in the receiving coil. The transmitter coil uses the Qi standard A11 transmitter coil, and the structure and size as shown in figure 4 and are shown in table 1.

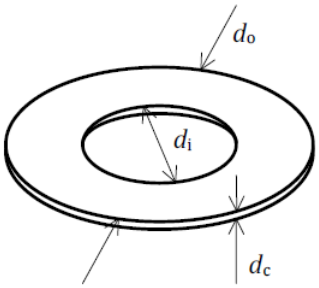

Fig.4 Structure of transmitting coil

Table 1

Dimensions of transmitting coil

parameter	Name	Value
Inner Coil Diameter	do	44mm
Outer Coil Diameter	di	20.5mm
Coil Thickness	dc	2.1mm
the winding number of Each layer	N	10 laps

Through the measured, the coil inductance is 10.07μH, the capacitance in parallel with the coil is 0.1μF. From the formula$\omega = \frac{1}{2\pi\sqrt{LC}}$resonance frequency f = 158.6 KHz. When the drive signal frequency and the coil resonant frequency is the same, then the transmission power is maximum.

2.2.1 Ac/dc conversion circuit

AC-DC conversion circuit will be converted to ±12 V alternating voltage by using full-bridge inverter 12V DC voltage, the full-bridge circuit as shown in Figure5.

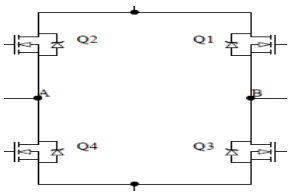

Fig.5 Full bridge circuit schematic

The whole bridge circuit is composed of four MOS power tube, including a group of Q1 and Q4 bridge (K1), controlled by the signal PWMA, Q2 and Q3 (K2), another group of bridge are controlled by signal PWMB.K1 and K2 two bridge time-sharing conduction, to A and B respectively put forward voltage and negative voltage on both ends, when two bridge are disconnected, the sender to stop working. Two bridge cannot at the same time conduction, so A and B must be the control signals of the opposite polarity. PWMA PWMB and AB, the voltage is shown in figure 6.

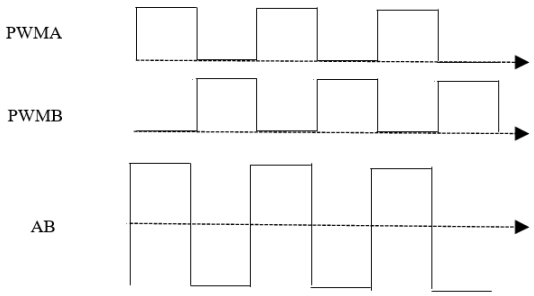

Fig.6 Driving signal timing diagram

2.2.2 Drive circuit

IR2103 is produced by IR company with dead zone time control of the half bridge driver chip, which is independent high-end and low-end control channel, compatible with 3.3 V, 5 V and 15 V logic level, can also be composed of two full bridge drive. A typical half bridge driver circuit diagram as shown in figure 7.

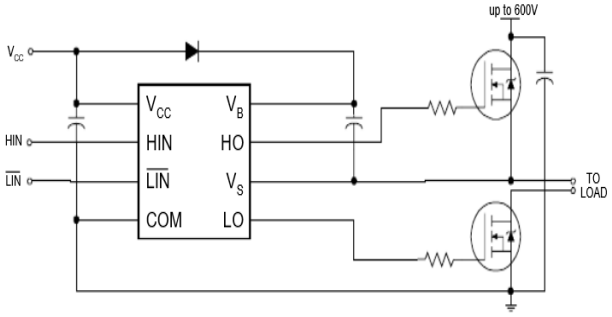

Fig.7Driving circuit schematic

IF HIN input high level, HO output high level relative to Vs. If LIN input low level, LO output low level relative to the COM. The capacitance between Vb and Vs plays a role of bootstrap, it provides high-end drive power Vb: high-end driver output side Vs is high frequency oscillation, when the tube on the turn-on voltage of the high pressure, the current tube conduction is ground level, Vs for electricity at ordinary times, the Vcc diode to recharge to close to Vcc voltage bootstrap capacitance. Vcc supply power to Vb at the same time. When Vs is high, the diode is turned off and the bootstrap capacitor discharges power to Vb.

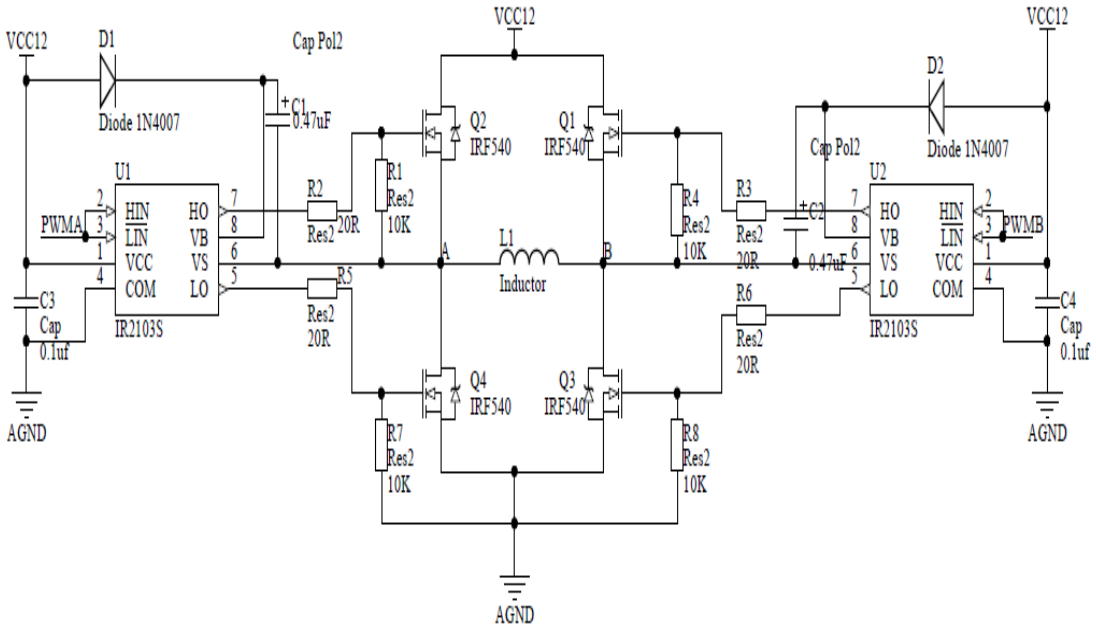

Fig.8The transmitting circuit diagram

This paper carry out the AC-DC transformation which adopt two pieces of IR2103 bridge driving circuit, circuit as shown in figure 8

Full-bridge circuit chip using IRF540N channel MOS tube, and the resistance is only 55mΩ, the drain current can reach 22A, the small heat can effectively improve the energy transmission efficiency.

2.3 Drive signal generation unit

Compared with the use of analog devices to build drive signal generation circuit, digital circuit is more convenient, with simple control, accurate, easy maintenance and so on. The system master control chip are adopts STM32C8T6 embedded 32-bit microprocessor chips produced by ST company. There are many different kinds and abundant resources of the product family greatly simplifies the design of this system.STM32C8T6 controller peripheral circuit as shown in figure 9:

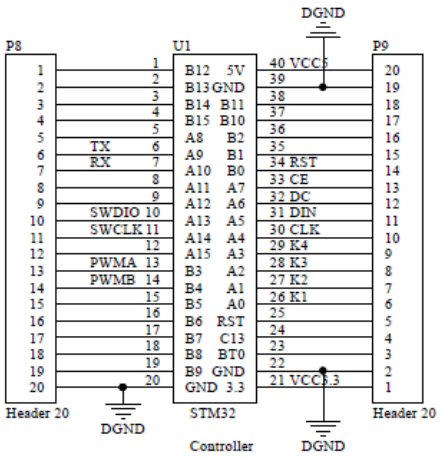

Fig.9 Controller peripheral circuit

STM32C8T6 encapsulation can have up to 36 normal IO for user to use which adopts LQFP48 tube feet. The CPU frequency up to 72 MHZ, The chip has 64 KB of Flash and 20 KB RAM, it does not need external expanding memory. The chip has three 16 –bit common timer and a 16-bit senior timer, each regular timer has four independent input/output channels, for inputting capture and comparing the output.. The senior timer with dead zone time control and emergency stop six channel PWM output channel, are specialized in motor control. This system uses the microprocessor senior timer 1, two complementary PWM output, 20 us of dead zone time.

PWM square wave signal is continuously adjustable in the frequency range of 50 KHZ to 250 KHZ, and 2 KHZ of step frequency, 1% of accuracy; Continuous adjustable duty ratio range, 1% of step-by-step, 1% of the accuracy.

2.4 User interface

The user interface is mainly used for system information display and adjust the system transmit power. The user interface circuit is shown in Figure 10.

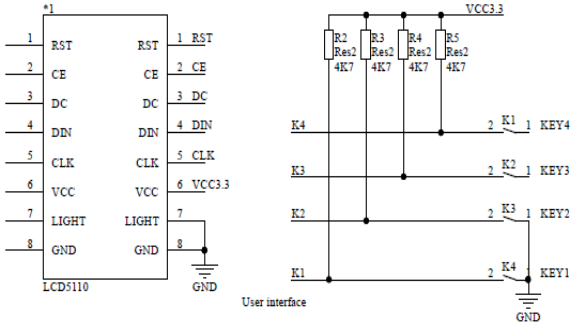

Fig.10 User interface circuit

The System displays use LCD5110 display, which uses the serial interface to communicate with the main processor. The number of interface signal lines is greatly reduced, the transmission rate is up to 4Mbps, and the display data can be written at full speed without waiting time. LCD5110 can display four lines of Chinese characters to display the system current drive signal frequency and duty cycle. The transmit power of the system is adjusted by four independent keys, plus pull-up resistors connected to the four common IO of the processor. The System transmission power is adjusted by four independent keys, add pull-up resistors connected to the processor. IO operates in interrupt mode for real-time response to user operations and changes in system transmit power.

2.5 Receive rectifier regulator unit

The coupling electromotive force coupled in the secondary coil is an alternating electromotive force similar to that of the sinusoidal and needs to be rectified, filtered and regulated for load. The circuit is shown in Fig. 11.

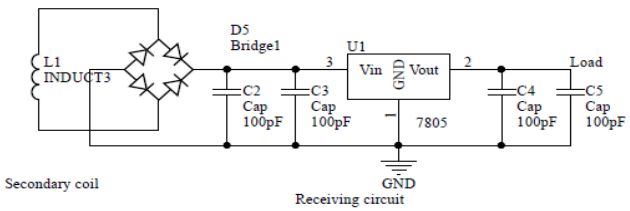

Fig.11Receiving circuit

The receiving coil adopts the A11 receiving coil

specification conforming to the Qi standard, directly connected to the AC end of the rectifier bridge, C2, C3, C4, C5 for the filter capacitor, LM7805 for the 5V output linear regulator, the maximum current can reach 800mA. In order to reduce the size of the entire receiving circuit, all devices are used patch package to carry easily.

III. TEST RESULT

The following tests are in the lead-acid battery-powered and laboratory conditions, the system sample is shown in Figure 12.

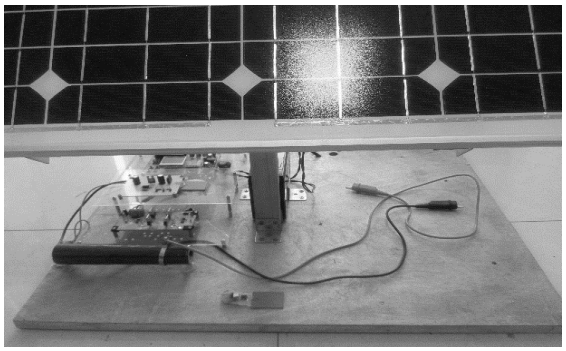

Fig.12 Principle prototype

3.1 Mobile phone charge test

Under this test, the phone model is lenovoA378t and the battery capacity is 2000mAh, the remaining power of 15%. Transmitting the power to XXX, the center of the receiving coil coincides with the center of transmitting coil, and record the time battery charge to 20% at the same time.

Table 2

Relationship between charging distance and charging time

Phone mode	Charging distance	Charging interval
LenovoA378t	5mm	10min
LenovoA378t	10mm	25min
LenovoA378t	15mm	58min
LenovoA378t	20mm	>60min
LenovoA378t	25mm	--

3.2 The load test

Under this test, the transmit power is set to XXX, and the center of the receiving coil coincides with the center of the transmitting coil at a distance of 5 mm. The load is 50Ω100W sliding rheostat, change the sliding rheostat resistance, record the load current and load voltage relationship.

Table 3

Relationship between load current and load voltage

Load current/mA	Load voltage/V	Received power/W	Efficiency
100	5.0	6.0	8%
120	5.0	7.2	8%
160	5.0	9.6	8%
220	5.0	9.1	11%

After the above test, the system can basically achieve the function of phone charging. To a certain extent, it can solve the problem which is not compatible for wired charging interface and inconvenient to carry.

IV. CONCLUSION

This paper expounds a kind of intelligent solar wireless quick charging system which can achieve the function of small power mobile charging. After further research and improvement, the problem can be solved which is not compatible for wired charging interface and inconvenient to carry. The system hardware and software adopts modular design, easy to debug and expand. It is advantageous for the transformation and upgrading of equipment. The current problem is that the charging efficiency is not high and the transmission distance is not far enough. This problem can be selected from the device and parameters, software optimization, increase the transmission power to be further resolved.

References

[1] Su Qing, Jing Shi-kai, Wu Xiao-qi, Chen Guang-ren, Tian Ruo-song, Hou Mi-lan ,30 Scientific Technologies Leading the Future[J]. Future and development , 2008, (08):44-48.

[2] Fang Chuang-lin, Yang Yu-mei. The Call of Green Solar Energy Era [J]. Encyclopedia Knowledge, 1997, (02):25-26.

[3] Cheng Shi-jie, Chen Xiao-liang, Wang Jun-hua, Wen Jin-yu, Li Jing-hua. Key Technology of Wireless Transmission and Its Application [J]. Journal of Electrotechnical Society, 2015, (19):68-84.

[4] Zhang Bao-qun, Li Xiang-long. Research and Practical Analysis of Non - contact Charging of Electric Vehicle [J], Electronic measurement technology, 2012, (03):1-6.

New Bus Service System Based on Visual Recognition

Lu Zhongqiang; Liu Yuntao; Liu Yingnan
(College of Instrument Science and Electrical Engineering, Jilin University, Changchun 130022, China)

***Abstract*—In this paper, the face detection and tracking technology is applied to the study of population statistics and bus service system. Firstly, the training process and the method of human face classifier are studied, and the Haar feature based on extended class is improved, Face detection is more accurate, higher recognition. The method of Adaboost training face classifier has been studied deeply and improved and used. Using the Hue information to establish the face area to hold the block diagram, and use the CamShift algorithm to track the face area, according to the location of the face to determine whether the passengers on the train, the face detection and tracking technology used in bus passenger statistics. GPS positioning and navigation technology into the bus service system, to complete the service system for the auxiliary role.**

***Key words*—Face detection Dynamic object tracking GPS**

I.INTRODUCTION

FOR the existing public transport service system is not perfect, bus passenger volume statistical methods behind the statistical algorithm is too low accuracy, detection of false inspection more false. In view of the above phenomenon, this paper applies the face detection and tracking technology to the bus passenger volume statistics, and applies the GPS technology to the bus location, and designs a more advanced and perfect bus service system. After studying and comparing some existing face training methods, this paper adopts the Adaboost algorithm, which is more advanced and perfect, to carry out face training, and apply the algorithm to the passenger face detection. For the face tracking method, this paper uses the camshift algorithm, which can be used for multi-target tracking. ACCORDING to the location of the face in the camera to determine whether the passengers on the train, and to count the amount of passengers.

II.TEST METHODS AND EXPERIMENTAL PROGRAMS

The system first calls the camera information and initializes the image information. Then we use the Viola-Jones algorithm to extract the Haar-like feature of the target image. Then we use the method of strong classifier and weak classifier to detect the face region and use the Hue information to establish the face region.[13] Face color chart. The camshift algorithm is used to track the face region. In the extracted camera image on the left side of the interface delineates a boundary, in the face area over the boundary when the passengers have been on the train, and automatically count the number.[6]

The haar feature is related only to the sum of the values of the pixels in a rectangular region whose characteristic value is the sum of the pixel values of the corresponding image of the white region minus the sum of the pixel values of the corresponding image of the black region.[1]For the Haar-like feature Viola is used in 12 different face pixel features.[5]

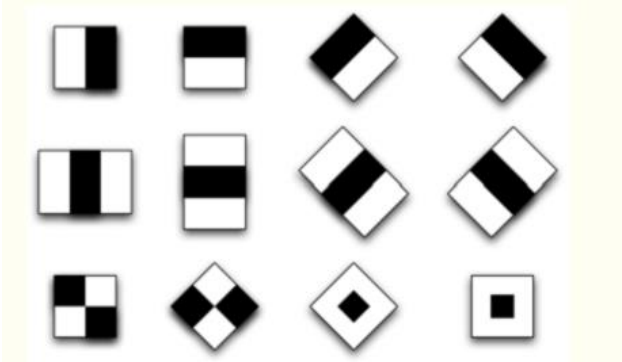

Fig. 1 Haar-like face pixel feature

In this paper, the feature is improved, the Haar-like feature is reduced to eight, and the feature is redesigned to improve the detection efficiency and detection accuracy.

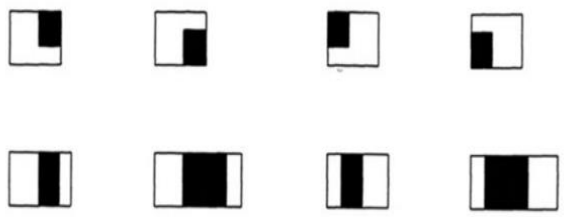

Fig. 2 Modified Haar-like feature

According to the Haar-like eigenvalue, the face region is detected, and the face region is framed by Hue information. The face region is framed and the target area is tracked by CamShift algorithm[2].

The full name of the CamShift algorithm is "Continuously Adaptive Mean-SHIFT", which is a continuous adaptive MeanShift algorithm. The basic idea is to make the MeanShift operation on all the image frames of the video sequence and use the result of the previous frame (ie, the center position of the search window and the window size) as the initial value of the search window of the next frame MeanShift algorithm.[7] The Simply point of view, meanShift is for the single picture to find the optimal iteration results, and camShift is for the video sequence to deal with, and the sequence of each frame call meanShift to find the optimal iterative results.[9] It is because camShift for a video sequence to deal with, so as to ensure that it can continue to adjust the size of the window, so that when the size of the target changes, the algorithm can adaptively adjust the target area to continue tracking.[11]

The meanshift algorithm is a nonparametric method of density function gradient estimation, and the extreme value of the probability distribution is found by iterative optimization to locate the target.

III. FACE DETECTION AND TRACKING DETAILS

A. Detecion algorithm detailed

As shown in the figure below, the middle of the figure shows that the color of the eye area is deeper than the color of the cheek area, and the last one indicates that the sides of the human nose are deeper than the color of the human nose, and other rectangular features can be used to represent other areas of the face.

The Adaboost classifier used by Voial is a strong classifier that concatenates multiple weak classifiers

The mathematical structure of the weak classifier is as follows:

$$h(x, f, p, \theta) = \begin{cases} 1 & pf(x) < p\theta \\ 0 & others \end{cases} \quad (1)$$

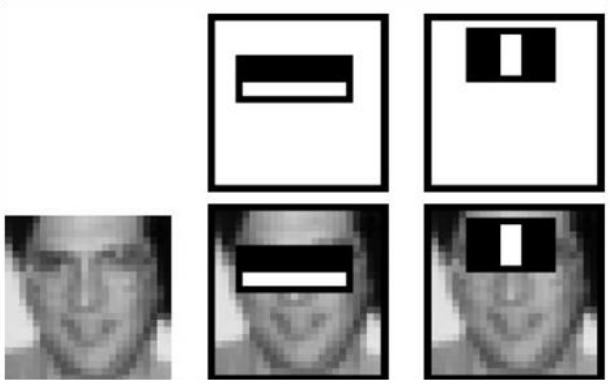

Fig. 3 Haar-like detecting example

A weak classifier consists of the sub-window image x, a feature f, the p and the threshold indicating the unequal direction. [13]The role of P is to control the direction of inequality, making the inequality are <number, more convenient.

As can be seen from the mathematical structure, when the eigenvalue is less than the threshold, the weak classifier output is 1, that is, the face is greater than the threshold, the determination of non-human face. It can be seen that the key to training the optimal weak classifier is to find the appropriate threshold so that the classifier has the lowest interpretation error for all samples.

The principle of cascading strong classifier is to arrange several strong classifiers from simple to complex, hoping to be trained so that each strong classifier has a higher detection rate, and the error rate can be reduced, such as almost 99% Face can pass, but 50% of non-human face can also be passed, so if there are 20 strong classifier cascade, then their total recognition rate of 0.99 ^ 20=81%, the error acceptance rate is only 0.5 ^ 20=0.0001 % [3].

B. Tracking algorithm details

Camshift uses the color histogram model of the target to convert the image to a color probability distribution map, initializes the size and position of a search window, and adapts the position and size of the search window adaptively from the results obtained from the previous frame to locate the current image The center of the target. As mentioned above, camshift is a meanshift operation for all image frames of a

video sequence.

The meanshift algorithm is a nonparametric method of density function gradient estimation, and the extreme value of the probability distribution is found by iterative optimization to locate the target[14].

The algorithm is:

(1) Select the search box W in the color probability distribution

(2) Calculate the zero order distance

$$M_{\infty} = \sum_{x}\sum_{y} I(x,y) \tag{2}$$

Calculate the first order:

$$M_{10} = \sum_{x}\sum_{y} xI(x,y) \tag{3}$$

$$M_{01} = \sum_{x}\sum_{y} yI(x,y) \tag{4}$$

Calculate the center of the search box：

$$x_c = M_{10} / M_{\infty} \tag{5}$$

$$y_c = M_{01} / M_{00} \tag{6}$$

(3) Adjust the size of the search box:

Length of 1.2s, width is

$$s = \sqrt{M_{\infty} / 256} \tag{7}$$

(4) If the moving distance is greater than the preset fixed threshold, repeat 2) 3) 4) until the distance between the center of the search window and the center of mass is less than the preset fixed threshold, or the number of cycles Reach a maximum value, stop the calculation[10].

C．Analysis of experimental results

Set the cline at the left border of the video image and set ‘cline’ at the left of the image at 1/3 of the image. When the center of the face rectangle is the center of the camshift search box, move past the border from right to left count. And each cross over the boundaries of the cumulative face, thus achieving the purpose of counting statistics.

IV．Analysis of experimental results

In order to detect the performance of the system, this paper first detects the single face, and then multi-face detection, and finally ensure the detection, tracking and counting the integrity of the overall system and stability. The pixel scale of the sequence image is 'YUY2_1280x720"YUY2_160x120' 'YUY2_176x144' 'YUY2_320x240', respectively. Experiments show that the pixel selection for the 'YUY2_1280x720' when the detection accuracy of the highest, but the speed is slow, can not meet the requirements of the pixel selection for 'YUY2_160x120' when the operation efficiency is high, but the accuracy is low. After weighing the detection efficiency and detection accuracy of the two, the selected pixel scale for the 'YUY2_320x240'. Experimental platform for the Dell notebook computer, processor i5-73337U, 1.80GHz CPU, 4G memory. The system to meet the bus to detect whether the passenger on the reliability and real-time. In order to system aesthetics and intuition, the experiment uses GUI interface design.

The following figure shows the results of some experimental tests.

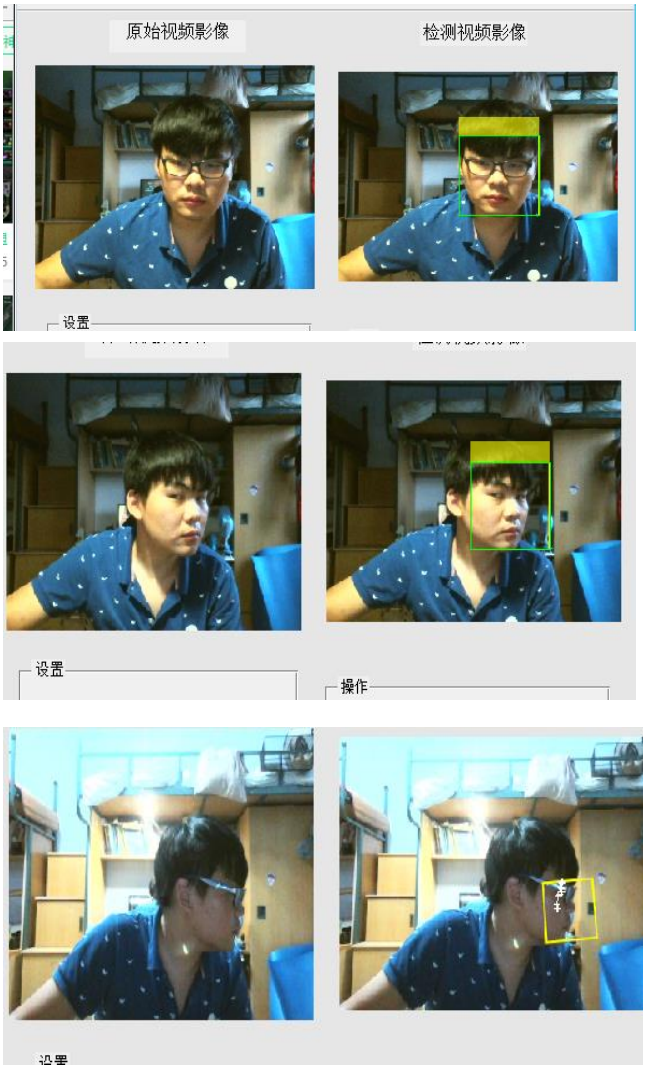

Fig. 4 Single face detection

Table.1 Single face detection test results

The total number of people	the number of the correct detection	the number of missing number	the number of false detection	The speed of processing
202	196	6	4	32~38
	Accuracy rate	False detection rate	false detection rate	
	97%	3%	2%	

Experiments show that the detection accuracy is high, the detection tracking speed to meet real-time. But in the side of the face detection has some defects, when the face deflection angle greater than 90 degrees, the higher the rate of missed.

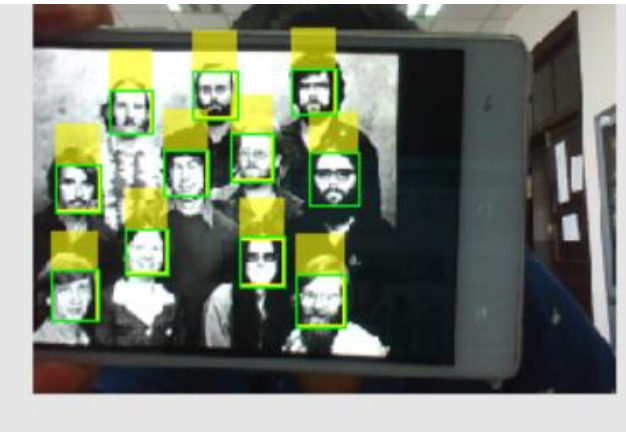

Fig. 5 Multi-face detection

Table.2 Multi-face detection test results

The total number of people	the number of the correct detection	the number of missing number	the number of false detection	The speed of processing
378	366	12	14	32~38
	Accuracy rate	False detection rate	false detection rate	
	96.8%	3.2%	3.7%	

V. ANALYSIS OF EXPERIMENTAL RESULTS

In recent years, with the development of China's industrialization, air pollution is serious, and a large number of private cars emerge not only increase the air pollution, but also lead to traffic congestion. At present, the bus has become a better choice for people, how to improve the bus service system without delay, this paper from the bus passenger statistics from the perspective of the design of face detection, identification based on the new public transport service system to help the bus company rationalization, Intelligent distribution of the various sections of the bus trips. This paper is based on the more modern and intelligent face detection, and the statistical method of tracking and counting design is accurate and intelligent. The characteristics of face pixels in the system dynamic image are measured and tracked by the monitoring camera of the bus. The passenger's face is recorded and the passengers are recorded. According to the GPS positioning module in the bus service system, the traffic conditions of each section The information is uploaded in real time to provide the basis for better service to passengers.

References

[1] Prashanth Kumar G., Shashidhara M .. Real Time Detection and Tracking of Human Face using Skin Color Segmentation and Region Properties [J]. International Journal of Image, Graphics and Signal Processing (IJIGSP), 2014, :.

[2] Juan A. Bot í a, Hedda Schmidtke, Tatsuo Nakashima, Mohammed R. Al-Mulla, Juan Carlos Augusto, Asier Aztiria, Matthew Ball, Victor Callaghan, Diane J. Cook, James Dooley, John O'Donoghue, Simon Egerton, Pablo A. Haya, Miguel J. Hornos, Eduardo Morales, Juan Carlos Orozco, Otniel Portillo-Rodr í guez, Alejandro Rodriguez-Gonz á lez, Oscar Sandoval, Paolo Tripicchio, Minjuan Wang, Victor Zamudio, Hector Vargas, Esperanza Medina , Daniel Martinez, Edson Olmedo, Gerson Beristain. Human-Robot Interface using Face

Detection and Recognition, for the Service Robot, "Donaxi" [J] Ambient Intelligence and Smart Environments, 2012, 13:

[3] Qingshan Liu, Jing Yang, Jiankang Deng, Kaihua Zhang. Robust facial landmark tracking via cascade regression [J]. Pattern Recognition, 2016,.

[4] Ghulam Ali, Muhammad Amjad Iqbal, Tae-Sun Choi. Boosted NNE collections for multicultural facial expression recognition [J]. Pattern Recognition, 2016,

[5] HAN Le, HE Ye-qiu, GAO Wen-hua.Experiment Design of Face Detection Based on Matlab [J]. Computer Knowledge and Technology, 2016, (22): 165-166 + 184.

[6] Li Changfeng. Face detection based on AdaBoost algorithm [D]. Lanzhou University of Technology, 2014.

[7] Yi Hu Huang, Ji Xiang Ma, Xiao Dong Han, Ning Hu, Xi Mei Jia. Design of Human Tracking Algorithm Based on Improved Camshift [J]. Key Engineering Materials, 2013, 2445 (561):

[8] Zhiyu Zhou, Dichong Wu, Xiaolong Peng, Zefei Zhu, Kaikai Luo. Object Tracking Based on Camshift with Multi-feature Fusion [J]. Journal of Software, 2014,9 (1) :.

[9] Quan Tang, Shu Guang Dai, Jie Yang. Object Tracking Algorithm Based on Camshift Combining Background Subtraction with Three Frame Difference [J]. Applied Mechanics and Materials, 2013,2594 (373):

[10] Shwu Huey Yen, Jui Chen Chien, Hsiao Tsung Lin. An Improved CAMSHIFT Tracking Algorithm Applying on Surveillance Videos [J]. Advanced Materials Research, 2013, 2455 (717):

[11] Pan Jie. Multi-angle face detection and tracking in video sequence [D]. Shanghai Jiaotong University, 2010.

[12] Liu Xinyong, Cai Fengli, Wang Zhiyang.Study on Face Detection and Location Algorithm Based on MATLAB [J]. Journal of Tonghua Teachers College, 2015, (12): 11-13.

[13] Cao Yonghui. Face Detection and Tracking in Video Sequences [D]. University of Electronic Science and Technology of China, 2008.

[14] Research on Face Detection and Recognition Method Based on Fast-AdaBoost Algorithm [D]. Taiyuan University of Technology, 2014.

Design and implementation of personnel positioning system based on ZigBee wireless sensor network

Ximing Zhang; Danlin Xu; Yujia Chen

（*College of Instrumentation and Electrical Engineering, Jilin University,Changchun 130012,China* ）

***Abstract*—Aiming at the problem of low accuracy of the existing wireless sensor network positioning system.In the system, the three side location algorithm based on the calibration model is used to realize the positioning of the personnel. Through the research of ZigBee wireless communication technology， analysis of radio propagation path loss model, combining RSSI(Received Signal Strength Indication) ranging model by experiment test, and introducing the Gaussian filter model and the self correction model to correct the range values. On the basis of the three side measurement method which combined with the idea of centroid localization, using the estimation position of the centroid of the three circle intersection as the blind node. By testing, the positioning error of the system is less than 10%, which reduces the blind node position error caused by the environment effectively and improves the positioning accuracy.**

***keywords*—three side ranging centroid localization algorithm; Gaussian filter; self correction model ; ZigBee**

0 INTRODUCTION

WIRELESS sensor network is a kind of distributed sensor network which consists of three parts: node, gateway and software and can achieve a wide range, low cost, flexible laying of real-time data acquisition [1]. At present, most of the WSN are only limited to the collection of scalar data such as light intensity, temperature, humidity and pressure [2]. In many WSN applications such as environmental monitoring, target monitoring and security monitoring， the location information of sensor nodes is very important，many other services are location-based， information is meaningful when it ties together with location. Without increasing the cost of inputs，using WSN's own characteristics to achieve node location function has a broad space for development and important application research value.

This paper uses an emerging short-range, low power, low-cost ZigBee wireless communication technology to form wireless sensor network，and uses the three side location algorithm which is based on the calibration model to realize the positioning of the personnel.

1 ALGORITHM MODEL

The three side ranging centroid localization algorithm is composed of three parts: ranging, positioning and correction. Specific description is as follows：

1) Using RSSI model to obtain the distance between the blind node and beacon node in wireless network;

2) Using the positioning model to obtain the position information of the blind node;

3) To modify the ranging model and the positioning model, reduce the positioning error;

1.1 RSSI Ranging Model

RSSI means Received Signal Strength Indication. Equation (1) shows the relationship between the transmit power and the received power of the signal， PT is the transmitting power of the signal, PR is the received power of the signal，d s the distance from the transceiver chip，n is the propagation path attenuation factor，determined by the current radio propagation environment [3].

$$P_R = P_T / d^n \tag{1}$$

$$P_R(dBm) = P_T(dBm) - 10n\lg r \tag{2}$$

$$P_R(dBm) = P_{R\_1}(dBm) - 10n\lg r \tag{3}$$

PR_1 is the receiving power when the transceiver chip is 1 m apart，From formula (3), it can be seen that

the relationship between the distance of the transceiver chip and the RSSI value is determined by the received power at 1 m and the propagation path attenuation factor. In the process of transmission, the interference of various media to the radio signal is smaller, the distance based on RSSI will be more accurate.

1.2 Three edge ranging centroid positioning model

The three edge location centroid localization algorithm is based on the algorithm of three edge measurement [4],which solves the problem that there is no solution of the system of equations in the triangulation location algorithm and makes the estimated node coordinate value is more accurate.

1.2.1 Three edge measurement

As shown in Figure 1，Let D point coordinate is (x,y)， A, B, C coordinates of the three points, respectively (xa,ya)、(xb,yb)、(xc.yc), Their distance to point D is, respectively da、db和dc.

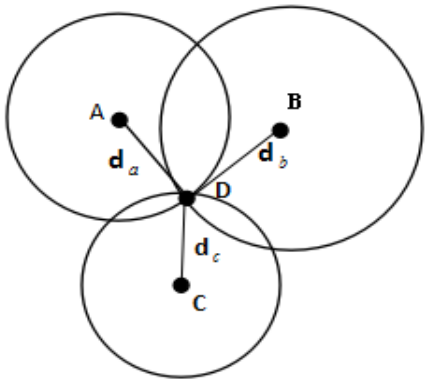

Fig.1 Schematic diagram of three edge measurement mode

Based on the above information, the following equations can be obtained and the coordinates of D can be obtained simultaneously.

$$(x-x_a)^2+(y-y_a)^2=d_a^2 \tag{4}$$

$$(x-x_b)^2+(y-y_b)^2=d_b^2 \tag{5}$$

$$(x-x_c)^2+(y-y_c)^2=d_c^2 \tag{6}$$

1.2.2 Centroid algorithm

Centroid algorithm is an outdoor location algorithm based on WSN connectivity，presented by Bruce et al., University of Southern California： The geometric centroid of all reference nodes in the communication range of the positioning node is used as the estimated position [5]. Assume that the coordinates of the beacon nodes are（x1,y1）、(x2,y2）、(x3,y3)、(x4,y4)、(x5,y5)，the centroid coordinate is:

$$(\frac{x_1+x_2+x_3+x_4+x_5}{5},\frac{y_1+y_2+y_3+y_4+y_5}{5})$$

1.2.3 Three edge ranging centroid localization algorithm

In the actual positioning process due to the error caused by ranging often get the situation shown in Figure 2 [6].

According to equation (4)、(5)、(6), the intersection of circle A and circle C can be obtained separately (xac1,yac1)、(xac2,yac2)，the intersection of circle A and circle B(xab1,yab1)、(xab2,yab2)，the intersection of circle B and circle C (xbc1,ybc1)、(xbc2,ybc2).

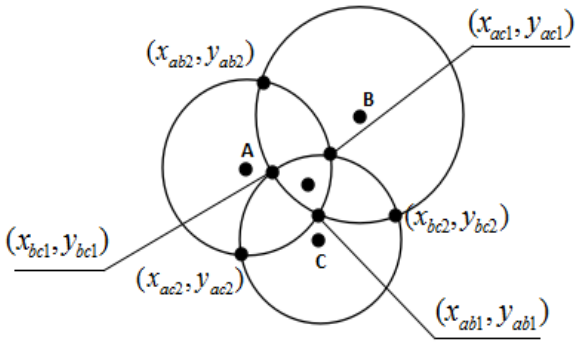

Fig.2 Schematic diagram of centroid location model based on triangulation

Respectively, the intersection of two circles and the third circle center coordinates into the equation（7）and find the value judging distance close to the third circle in two points. As shown in Figure 2，judgment can be obtained that the nearest point from the circle A, circle B and circle C's center respectively (xbc1,ybc1)、(xac1,yac1) and (xab1,yab1).According to the idea of centroid，The centroid of the intersection of three circles is used as the estimated position of the blind node and the coordinate value of the blind node is calculated by formula (8).

$$d=(x-x_0)^2+(y-y_0)^2 \tag{7}$$

$$(x,y)=(\frac{x_{ab1}+x_{ac1}+x_{bc1}}{3},\frac{y_{ab1}+y_{ac1}+y_{bc1}}{3}) \tag{8}$$

1.3 Three side range correction model

In the practical application of the positioning system, due to the interference of environmental factors, the RSSI value will be unstable，under different conditions, the attenuation factor of the electromagnetic wave propagation path will also change. In order to solve these problems, the Gauss correction model and beacon node self calibration model are proposed to improve the positioning accuracy.

1.3.1 Gauss correction model

In the process of transmission, the interference of the event is a small probability event, at this time the RSSI value and the normal value deviation is bigger, and it has a great influence on the distance measurement. Through the Gauss filter selection probability of high RSSI value and then taking the mean [7], can reduce the environmental impacts of disturbance on the value of range, reduce the positioning error. Specific calibration process shown in Figure 3:

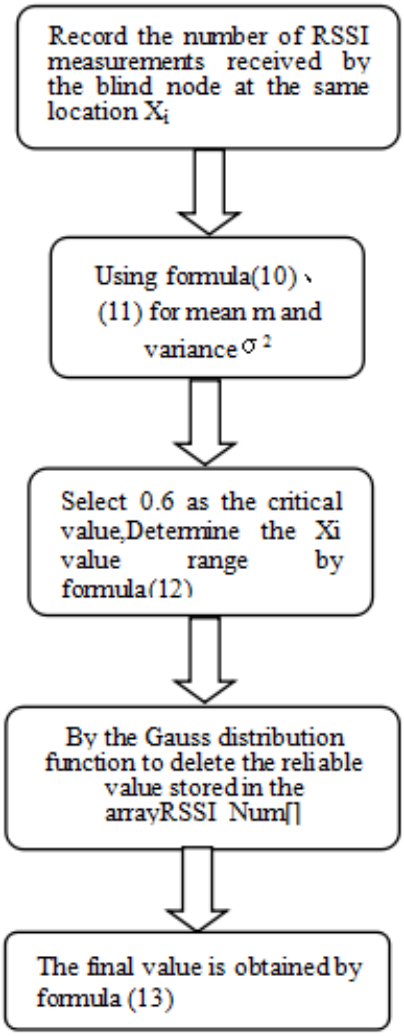

Fig.3 Gaussian correction model flow

$$F(x)=\frac{1}{\sigma\sqrt{2\pi}}e^{-\frac{(x-m)^2}{2\sigma^2}} \tag{9}$$

$$m=\frac{1}{n}\sum_{i=1}^{n}X_i \tag{10}$$

$$\sigma^2=\frac{1}{n-1}\sum_{i=1}^{n}(X_i-m)^2 \tag{11}$$

$$0.6\le F(x)\le 1 \tag{12}$$

$$RSSI=\frac{1}{n}\sum_{i=1}^{n}Rssi\_Num[i] \tag{13}$$

1.3.2 Beacon node self calibration model

The position information of the system is known，By using the beacon nodes to communicate with each other, recording respectively the corresponding transmitting power, the received power and the distance between the transmitting and receiving chips, and the n value of the propagation path attenuation factor can be obtained by formula (1). The measured n value is used as the attenuation factor of the propagation path in the current environment to improve the adaptability of the system. The calibration process is shown in Figure 4:

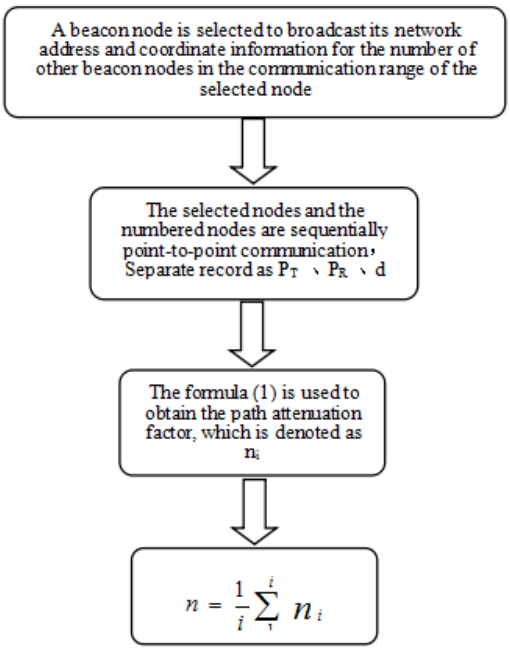

Fig.4 Beacon node self-tuning model flow

2 ALGORITHM IMPLEMENTATION

The implementation of the algorithm is divided into 4 steps: setting up wireless sensor network, ranging, correcting and positioningConsidering the requirement of power consumption and cost, the system uses ZigBee technology to build a wireless sensor network. The specific implementation process of the algorithm is shown in Figure 5:

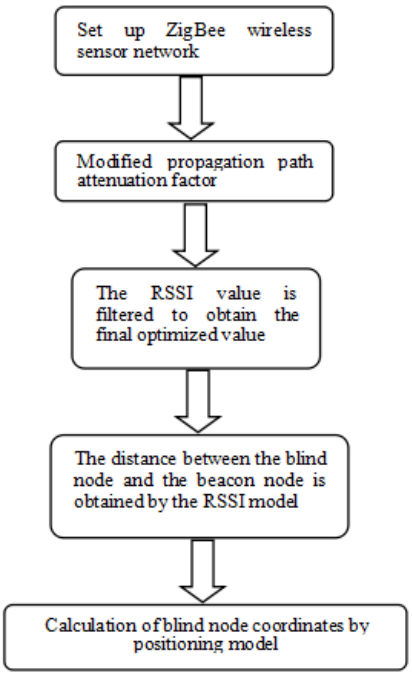

Fig.5 Algorithm implementation process

2.1 The establishment of wireless sensor network

ZigBee wireless sensor network has coordinator, router and terminal three kinds of function nodes. Coordinator responsible for the formation of the network, the router is responsible for routing information within the network frame, the terminal node is responsible for the realization of specific functions [10].

The beacon node in the system acts as a router node with known location information, and its number and density determine the positioning accuracy. Blind nodes act as end nodes and are bound to personnel, and broadcast their own ID information in the network every fixed time.

2.2 Beacon node self-calibration process

All the beacon nodes are added into the same group in the network, and one of the beacon nodes is selected to carry out the correction process in Figure 4, and the propagation path attenuation factor n.

2.3 ranging procedure

① Blind node broadcast identity and network address;

② When the beacon node receives the broadcast information frame, the coordinate information and the network address are returned as the response;

③ The blind node receives the response information and statistics the beacon node which can communicate directly with itself;

④ The blind node communicates point-to-point with the matching beacon node in turn, and records the RSSI value and the coordinates of the corresponding beacon node to the upper computer;

⑤ The upper computer uses the Gaussian filtering model to filter the groups of RSSI values recorded in the above steps and then transforms the ranging model into the distance between the blind node and the many beacon nodes.

2.4 Positioning process

The upper computer collects the distance between the blind node and the beacon node in the communication range, and selects three points with short distance. By using the three - side ranging centroid positioning model, the coordinates of the blind node can be obtained by formula (4) - (8).

3 EXPERIMENTAL TEST

CC2530 radio frequency transceiver chip of TI company is used to build wireless communication platform. The chip is compatible with the IEEE802.15.4 specification, combined with TI's Z-Stack™, the reliable communication distance is above 30 m. One coordinator node, four beacon nodes, one blind node and a simple PC monitoring system were designed in the experiment. The coordinator is responsible for the formation of the network, and the PC is connected in a wired way, and the data in the network is sent to the host computer in real time. After the analysis of the collected data, the computer can calculate the coordinates of the blind node and display. The experiment is divided into the following two parts:

3.1 Verification of the effectiveness of RSSI ranging correction mode:

Two nodes are selected for point-to-point communication, and the error of different calibration models is tested. Select a test point every 0.5m in the range of 0-10 m, using different calibration algorithms:

① No calibration model;

② Use Gaussian correction model;

③ Using the beacon node self-correction model to correct the propagation path attenuation factor, and then using Gaussian correction model.

The range effect of the three models is shown in Fig 6. t can be seen that the Gaussian correction model is better than the other two methods after using the

beacon node self-correction model to modify the propagation path attenuation factor.

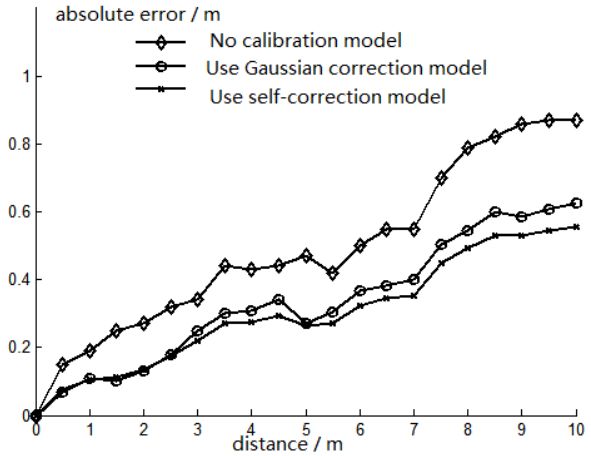

Fig.6 Ranging effect test chart

3.2 Comprehensive detection of positioning effect

Four beacon nodes are placed at the vertices of a diamond with 2.5 m sides，the nodes move within the diamond range. The system positioning accuracy is analyzed using the calibration model，Test results are shown in Table 7, table 1：

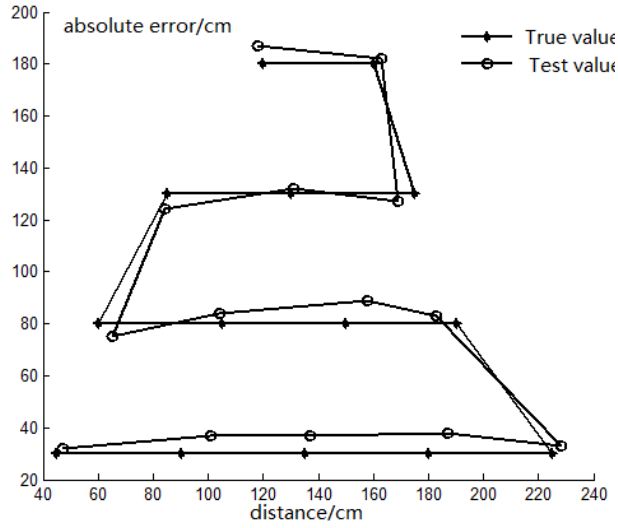

Fig.7 Location effect test

Figure 7 is the comparison of the actual moving curve and the test result of the blind node. Analysis of the data in Table 1 can be obtained in the X direction of the system maximum positioning error is 20 cm which is about 8% of the edge of the positioning range；The maximum positioning error in the Y direction is 9 cm, about 3.6% of the side of the positioning range. From the test results，the system positioning error is small, suitable for most applications of the positioning accuracy requirements.

TABLE I

TEST RESULTS AND THE ACTUAL VALUE OF THE TABLE

(cm)

node number	actual coordinates	test results
1	（45，30）	（47,32）
2	（90,30）	（101,37）
3	（135,30）	（137,37）
4	（180,30）	（200,38）
5	（225，30）	（228,33）
6	（190,80）	（183,83）
7	（150,80）	（158,89）
8	（105,80）	（104,84）
9	（60,80）	（65,75）
10	(80,130)	(84,124)
11	(130,130)	(131,132)
12	(175,130)	(169,127)
13	(160,180)	(163,182)
14	(120,180)	(118,187)

4 CONCLUSION

In this paper, the Gauss correction model and beacon node self calibration model are used to locate the personnel on the basis of the three side ranging centroid localization algorithm. The Gauss filter is used to avoid the interference of small probability events， using beacon node self - tuning model to correct the propagation path attenuation factor so that can reduce the impact of the environment on the positioning accuracy of the system.

After test，The positioning error of the system is less than 10%, which can effectively reduce the position error caused by the environment and improve the positioning accuracy. In the following research, we can combine the CC2591 power amplifier chip to improve the receiving and transmitting sensitivity of the CC2530 chip, further expand the scope of the system, and make the system more practical.

Reference

[1] Chai Shujuan,Zhao Jianping.Research on water qua- lity

monitoring system based on Wireless Sensor Network[J]. Journal of Qufu Normal University, 2008, 34(11): 214-224.

[2] Li Shunhui. Research on data dissemination and time synchronization for wireless sensor network measurement[D]. Hunan University, 2009.

[3] Fang Zhen, Zhao Zhan, Guo Peng, Zhang Yuguo. Analysis of Distance Measurement Based on RSSI[J]. Chinese Journal of Sensors and Actuators,2007,20（11).

[4] Gao Lei, Zheng Xiangquan, Zhang Hong. A node localization for wireless sensor networks based on trilateration and centroid algorithm[J]. Journal of Chongqing Institute of Technology, 2009,23(7):139-141.

[5] Liu Jing, Song Jiayou. Improvement of centroid localization algorithm based on RSSI in Wireless Sensor Networks[J]. Computer CD Software and Applications, 2012（7）：33-34.

[6] Lin Wei, Chen Chuanfeng. RSSI-based Triangle and Centroid Location in Wireless Sensor Network[J]. Modern Electronics Technique,2009（2）:180-182.

[7] Zhu Minghui, Zhang HUiqing. Research on model of indoor distance measurement based on RSSI[J]. Transducer and Microsystem Technologies,2010,29（8）:19-22.

[8] Zhang Jianwu, Zhang Lu, Ying ying, Gao Feng. Research on distance measurement based on RSSI of ZigBee[J]. Chinese Journal of Sensors and Actuators, 2009,22(2):285-288.

[9] Mohebbia M, Barouei J, et al.Modeling and optimization of viscosity in enzyme modified cheese by fuzzy logic and genetic algorithm[J]. Computer and Electronics in Agriculture,2008,62(2):260-265.

[10] Saeid S, Abbas T, Josep S.Spectrum sensing using correlated receiving multiple antennas in cognitive radios[J]. IEEE Trans on Wireless Communications, 2013,12(11):5754-5766.

Design of Electrical Instrument Based on Virtual Instrument Technology

Jirong Dang; Kaihua Jiang; Honhfei Wang

（Jilin university, College of Instrument Science and Electrical Engineering,changchun,130021）

***Abstract*—This design adopts the virtual instrument technology, starting from the perfect virtual electronic test platform developed by Jilin University, in the design of modern intelligent digital multimeter for the purpose, in accordance with the mechanical specification and protocol virtual electronic test platform, developed the virtual digital multimeter. The design adopts the idea of modularization, and designs the virtual digital multimeter as the module board of 3U size, and realizes the communication between the controller and the controller by using the dual port RAM made by FPGA. The main measuring part is composed of a single chip intelligent digital multimeter integrated circuit, which can achieve the purpose of forming a high performance digital multimeter in the most concise way. The instrument driver design in the form of dynamic link library, and the instrument packages the I/O operation into function, function after package is accessed through the USB driver, realize the input and output data. The use of dynamic link library in the form of instrument design, so that the application program does not need to understand the specific implementation details of the device to improve the flexibility of programming and programming efficiency. The application program is developed by LabVIEW8.6, using the CLF node in the way of calling dynamic link library to achieve communication with the USB controller to control the virtual digital multi objective design of the virtual digital multimeter table has a traditional digital universal meter basic measuring function, also has the functions of data storage, analysis, reporting, network communication etc. the advantages, can be applied to electrical and electronic measurement field.**

***Keywords*—Labview digital multimeter virtual number**

ELECTRICAL instrument used as a common tool in personnel inspection of electronic engineering and technical personnel and electronic equipment, more and more people have been used up, with the continuous acceleration of electric power construction, electrical instrument in China has entered a period of rapid development, electrical instrument manufacturing enterprises to keep pace with the times, reached the world advanced level in some technical fields and enterprise concentration continues to increase, expanding the scale of production, the core competitiveness is also growing, already have a considerable advantage. With the development of electric power industry, the further development of electrical instruments is also predictable. The development of electric power industry has become a new challenge to the electrical instrument industry, and it is also an important opportunity and new development space for the electrical instrument industry.

1. INTRODUCTION

1.1. Research Status at Home and Abroad

The electrical instrument has gone through the simulation stage, the digital stage, the three stages of the intelligent multimeter. The analog electrical instrument has the advantages of low cost, low price and complete function, but it has some problems such as low measurement accuracy, large volume, easy damage and so on. Analog electrical instrument by meter, measuring circuit, switching device is composed of three parts, through the mediation of the dial knob, can satisfy the DC and AC resistance, different measurementrequirements.Intelligent multimeter is developed on the basis of digital electrical instrument technology, intelligent multimeter and digital multimeter compared to an increase of microprocessor or microcontroller intelligent control unit. Intelligent multimeter inherits many advantages of digital electrical instrument, and is more accurate, more powerful, with automatic calibration, automatic measurement, automatic data processing and other functions. The intelligent multimeter is also connected with the computer, which can help the technical

personnel to complete the technical measurement and the real-time monitoring and so on. The electrical instrument market, analog instruments have been gradually eliminated by the digital instrument, although intelligent instrument is more powerful, but because of the cost and the cost is high, and therefore there is no digital multimeter and good liquidity. Although the Chinese market is based on digital electric meter instruments, but with the development of China's information technology and micro processing technology, intelligent instrument, the cost will be reduced, and gradually realize the intelligent digital instrument, to make a greater contribution to the progress and development of society.

1.2 . The Significance of The Sesearch

The advantage of virtual instrument technology to make up for the shortage of digital multimeter is a good solution for the design of modern intelligent digital multimeter. The introduction ofvirtualinstrument technology allows developers to customize the functions ofthe instrument,the measurement and error calculation shows the characteristics of integration, easy operation and flexibility. The significance of designing virtual digital multimeter based on virtual electronic test platform:

(1)Toimprove the independent research and development of the virtual electronic test platform of Jilin University, so as to make it better;

(2) Virtual digital multimeter has unlimited display options, flexible, convenient, so that it is not limited by the hardware circuit design;

(3) The results can be displayed in various forms, such as numbers, pointers, and so on, in combination with the visual and graphical images of the figures, and can be directly made into graphs and tables, which are easy to record, edit and form reports;

(4) Not only can carry on the general survey of the digital multimeter, but also can carry on the measurement result to the average value, the extreme value statistical analysis as well as the more complex data analysis and processing;

(5) To make the multimeter intelligent, to realize the automatic switching of the range, automatic zero adjustment, calibration, and has a good man-machine conversation ability, can display the operating state of the instrument, working status and other information;

(6) The observation data can be observed for a long time;

(7) By using the advantages of reconfigurable virtual electronic test platform, it is easy to realize the combined measurement, and can be used in conjunction with the existing modular board of the virtual electronic test platform to accomplish more measurement tasks;

(8) Virtual digital multimeter is a good solution for the network and remote experiment teaching of digital multimeter. As long as the research of the virtual electronic test platform controller with the network interface, it is very easy for the virtual digital multimeter and the test and measurement instrument in the virtual electronic test platform to achieve the network and remote experiment teaching

1.3. Main Research Contents:

a . The measuring range of 1 DC voltage and current is small, the existing range of DC voltage is 0-400V DC current range is 0-100A, we now need to increase the range of DC voltage to about 0-500v, will increase the range of direct current to 0-200A.

b. AC voltage and current measurement can not be normal, we need to make it to the normal measurement, the measuring range of the AC voltage is about 0-500v, the measuring range of AC current is about 0-100A, we can put it on the market and the measurement results of measuring instrument general numerical comparison, to test its correctness.

c. Digital, pointer, graphics and other forms of display measurement results;

d. Analysis and processing of data such as average value and extreme value statistical analysis;

e. Can realize the automatic switch, automatic zero adjustment, calibration;

f. Good man-machine conversation skills, able to display the operation status of the equipment, working conditions, etc.

Interest;

g. Able to observe the data for a long time, the measurement data storage, display playback;

h. To achieve network communication.

2. BASED ON THE VIRTUAL INSTRUMENT TECHNOLOGY OF THE OVERALL DESIGN OF ELECTRICAL

INSTRUMENTS

2.1. Overall Design Ideas:

Thisdesign uses the virtualinstrument technology, starting from the perfect virtual electronic test platform developed by Jilin University, in the design of modern intelligent digital multimeter for the purpose, in accordance with the mechanical specification and protocol virtual electronic test platform, developed the virtual digital multimeter. The design adopts the idea of modularization, and the virtual digital multimeter is designed as a module board of 3U size, which is realized by using FPGA RAMThe communication between the controllers, and. The main measuring part is composed of a single chip intelligent digital multimeterintegrated circuit, which can achieve the purpose of forming a high performance digital multimeter in the most concise way. The instrument driver is designed in the form of a dynamic link library, and the I/O operation related to the instrument is encapsulated into a function. After the function is encapsulated, the input and output of the data are accessed by the USB driver. The use of dynamic link library in the form of instrument design, so that the application program does not need to understand the specific implementation details of the device to improve the flexibility of programming and programming efficiency. The application program is developed by LabVIEW, and it can communicate with the USB controller by calling the dynamic link library with CLF nodes. Design of virtual digital multimeter has a traditional digital universal meter basic measuring function, also has the functions of data storage, analysis, reporting, network communication etc, can be applied to electrical and electronic measurement field. Virtual multimeter board is divided into two parts: software and hardware. The hardware part is composed of three parts: the PC and the virtual multimeter hardware module. The software is composed of the application program, the virtual multimeter, and the USB controller

2.2. Hardware Design Ideas:

The hardware design adopts the idea of modularization, and the virtual digital multimeter is designed as a module board of 3U size. The communication between the controller and the controller is realized by using the dual port RAM made by FPGA. The main measurement consists of a single intelligent digital multimeter IC virtual multimeter device hardware circuit mainly by the front-end and function module, control and interface communication module, measurement module of three parts constitute. The overall structure of the virtual multimeter hardware is shown in Figure 1 below:

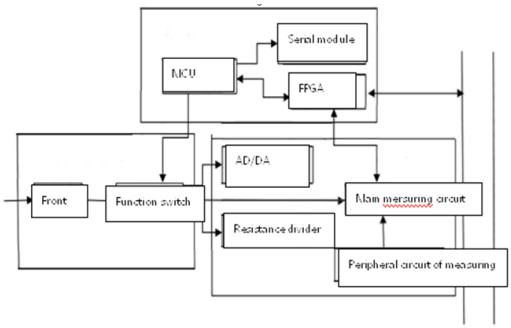

Figure 1 Overall hardware structure

(1). Front end and function conversion module: to complete the input signal attenuation and achieve the main function of the switch.

(2). Measurement module: the main function of the input signal measurement. According to the specific function, the measurement module also includes voltage measurement mode circuit, current measurement mode circuit, AC/DC conversion circuit, diode measurement and resistance measurement circuit. Consisting of MAX134 virtual digital multimeter and some peripheral components, the main resistance voltage divider, integrator and active filter resistor, reference voltage source.

(3). Control and interface communication module: mainly composed of FPGA and MCU, complete system control and bus interface communication function. The microprocessor realizes the communication with the system controller module through the interrupt mechanism and the interface of the system bus through the dual port RAM-IDT7130. Dual port RAM with configuration space and data storage space. The microprocessor is responsible for the initialization of the system (including writing the configuration information to the dual port RAM, setting the initial state of the circuit) and processing the commands sent by the bus, and controlling the corresponding circuit unit.

2.3. Software design ideas as shown in figure 2:

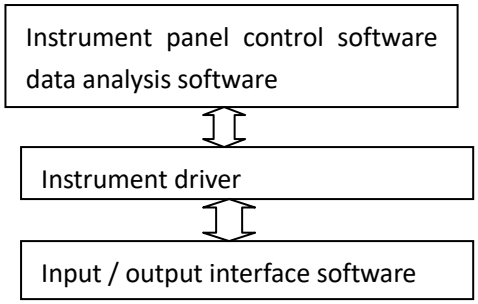

Figure 2 Software framework

The software is the key technology of virtual instrument, by running on a computer software, a virtual instrument graphical interface, which provides a test instrument communication, set the instrument parameters, modify the instrument operation and the realization of the instrument function of man-machine interface to the user; analysis and measurement, on the other hand, the characteristics of computer directly involved in the test signal, complete data input, storage, analysis and output functions.

Virtual instrument software generally uses a hierarchical structure, including the following three parts:

(1). Input / output (I/O) interface software. Between the instrument and the instrument driver, is a complete direct access to data for operation, instrument driver provides information on the transfer of the underlying software instrument internal storage unit, is the foundation and core of the virtual instrument system, the implementation of unified open.

(2). Instrument driver. The essence of the instrument driver is to provide the user with a more abstract set of operating functions for the operation of the instrument. For applications, control the operation of the instrument hardware and communication, it is realized by hardware instrument driver, instrument driver for the operation and management of equipment, and is the basis and unified format provided by calling the I/O software to realize the function of library.

(3). Application software. Application software mainly includes the instrument panel control software and data processing software, complete the tasks are: to achieve the virtual instrument panel using the powerful function of computer graphics, to provide users with the operation of equipment, man-machine interface, data display, data acquisition and processing, display and storage etc..

3. HARDWARE DESIGN OF ELECTRICAL INSTRUMENT BASED ON VIRTUAL INSTRUMENT TECHNOLOGY

3.1. The current measurement circuit of the virtual instrument is shown in Figure 3

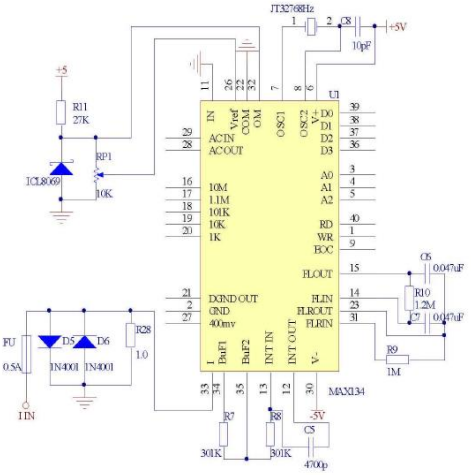

Figure 3 Current measurement circuit

In the figure above the MAX134 33 pin input circuit for the current measurement mode input circuit, 400mA range, R 28 to take the 1 euro, 1W; (for the 4A file, R=0.1 Europe, 10W). The input also increased the 0.5A (for the 4A file, FU take 5A) as the over-current protection fuse, D5, D6 as an overvoltage protection circuit. The reference voltage source ICL8069 provides a reference voltage resistance test time (1.2V), and ICL8069 by a precision potentiometer divider has a reference voltage VR 655mV EF into MAX134 26 feet, to restrain the power frequency interference (50 H Z frequency select VR EF=655mV, 60 H Z frequency VR EF=545mV). In addition the circuit R 7, R 8, C 5 MAX134 internal peripheral integrator integral components; R 9, R 10, C6, C7 for the peripheral circuit of the filter amplifier filter element.

3.2. Voltage measurement mode circuit as shown in figure 4:

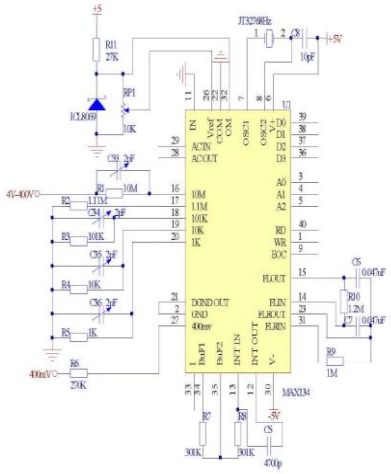

Figure 4 Voltage measurement circuit

Virtual digital universal voltage measurement mode circuit as shown in table DCV, only 400mV range for direct input, 4V-4000V range must pass through the divider network R 1 ~ R 5 (designed by 0.25%, precision resistor 1/4W) input. And R1 ~ R 5 and C4 ~ C7 (used for frequency compensation) constitute a RC wide band lossless attenuator.

3.3. The AC/DC conversion circuit is shown in figure 5:

When the MAX134 in the measurement of AC also need an external AC/DC conversion circuit, the circuit diagram shown in figure C28, C29 D4, D5 capacitor; bidirectional diode limiter; D6, D7 to R24, rectifier protection; R25, C32, C33 two RC filter.

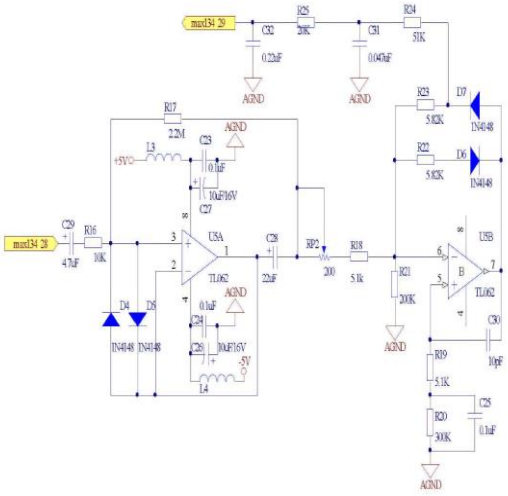

Figure 5 AC/DC conversion circuit

3.4. MCU and serial communication hardware circuit as shown in figure 6:

Join the design of serial communication, a bridge between the measuring module and the virtual electronic test platform bus interface communication module, which not only greatly facilitates the debugging of front-end test circuit, brings the data bus communication module to design experiments, the design for the whole system to play a role in promoting。

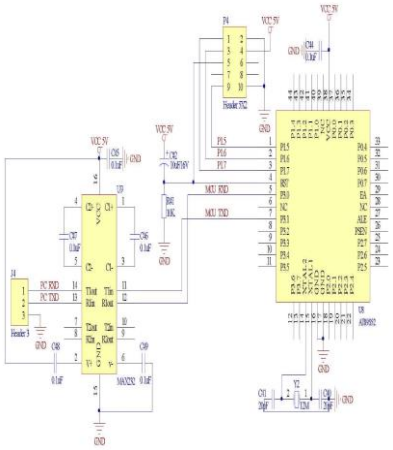

Figure 6 Hardware circuit of serial communication

3.5. Voltage Matching in Circuit Design:

In this system, the virtual electronic test platform can provide the power supply is + 12V and + 5V, the use of the FPGA operating voltage of 3.3V/1.5V, where you need to pay special attention to the problem of voltage conversion. The three most commonly used solutions for voltage conversion

(1). low dropout linear regulator chip. Linear regulator chip is one of the most simple power conversion chip, basically do not require external components. The utility model has the advantages of convenient use, low cost, small ripple and no electromagnetic interference.

(2). Design switching power supply. Switching power supply is also a method to achieve power conversion, and the efficiency is very high, but the design is much more complicated than the use of linear voltage regulator. However, for the design of high current and high power, it is recommended to use switching power supply. Nowswitching power supply inside the synchronous rectification technology can be a good solution to the problem of low voltage, high current.

(3).Resistance voltage divider. The method of resistance divider is simple and low cost. However, the voltage generated by the resistance divider circuit will change with the load, and the output voltage will fluctuate. In addition, the power consumption of this circuit is also relatively large. However, the cost is low and the structure is simple, so it can be used as an

emergency plan. For systems with low power consumption and high power requirements, this scheme is not suitable for use. Comprehensive analysis, the design uses a low dropout linear regulator chip REG1117-3.3 and REG1117-ADJ will provide 5V power supply system for 3.3V and 1.5V for FPGA use, 3.3V and 1.5V power generation.

In the design, in addition to FPGA, MAX134 digital interface is 5V TTL level, AT89S52 operating voltage is also 5V TTL, so pay attention to the different levels of signal driver. EP1C3T144C8 supply voltage of 3.3V, when VCCI NT is connected to 3.3V, the logic level of the input range is -2V~5.75V, the output of the logic level of 0V~ VCC IO, VCC IO can be connected to 3.3V or. Since the 5V TTL and 3.3V conversion standards are the same, and EP1C3T144C8 is able to withstand 5V voltage. Therefore, the level can be directly connected. However, in order to make the design more secure, the design of the FPGA and MAX134, FPGA and AT89S52 between the 150 series of European resistance to pressure, so that the design is more reasonable and safe.

Comprehensive analysis, this design uses low dropout linear regulator chip REG1117-3.3 and REG1117-ADJ will provide 5V power supply system is converted to 3.3V and 1.5V for FPGA, 3.3V and 1.5V power generation circuit diagram of Figure 7 and Figure 8

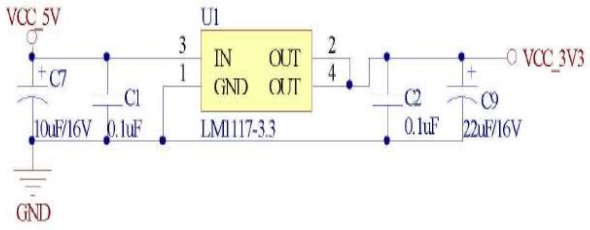

Figure 7 3.3V power supply circuit

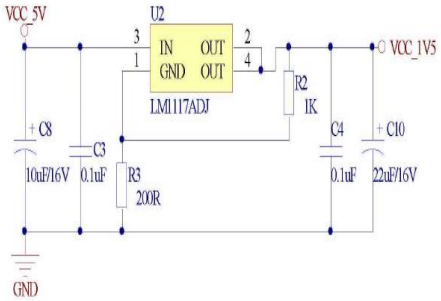

Figure 8 1.5V power supply circuit

3.6. Hardware Circuit PCB Diagram

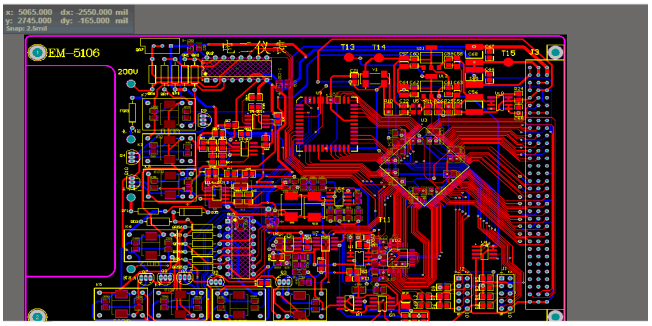

4 SOFTWARE DESIGN OF ELECTRICAL INSTRUMENT BASED ON VIRTUAL INSTRUMENT TECHNOLOGY

The design idea of the virtual digital multimeter is as follows: when the driver is designed, the command related to the hardware operation is encapsulated into a function. Through the operation of graphical user interface, the user calls the dynamic link library through the CLF node, calls the module driver, realizes the communication with the USB controller, and achieves the program control of the hardware module. The driver design includes USB controller driver and DMM driver of two parts, including USB controller driver contains the function of the USB controller module basic read and write operations, the realization of the function of DMM driver contains the hardware control module. The application uses a graphical software Lab VIEW 8.6 development, DMM driver and USB controller driver using VC6.0 development 2.

4.1. Virtual Digital Multimeter Device Driver

Virtual multimeter drive contains the realization of virtual digital multimeter function control module, by calling the USB driver to achieve the control of the digital multimeter card, which is given in the form of dynamic link library. The following describes the main test functions to achieve the call to several major operating functions.

(1). Search equipment

(2).Virtual digital multimeter measurement input setting function

(3). Virtual digital multimeter receiving function

(4). Measurement function

(5) . AD/DA measurement setting function

(6). Voltage range setting function

(7). Resistance range setting function

4.2. Application Design

NI based on the development of the graphical programming language development environment LabVIEW8.6, as the development of digital multimeter application software. Lab VIEW graphical programming is flexible, simple, and with a rich and powerful software package, including numerical function operation, data acquisition, signal processing, input / output control, signal generation, image acquisition, processing and transmission and so on, is the analysis of the development of digital multimeter on the layer of application software are the best choice for functional requirements

According to the design requirements, the digital multimeter application should have the following functions:

(1). The system settings: including the start and end of the collection settings, equipment slot number set, etc.;

(2). Measuring function settings: including voltage, current, resistance, diode, circuit, etc.;

(3). Measuring mode setting: including single, average, continuous;

(4). Sampling rate setting: including 5S/s, 10S/s, 15S/s;

(5). Test g: for each test function set

Different test rrange settinanges;

(6). The results show that the function: digital and graphic display;

(7). The measurement data processing function: can carry on the mean, the extreme value analysis to the data;

(8). Storage and playback functions: to achieve the waveform storage, generate reports, playback.

(9). Network transmission function: to achieve network connectivity

4.3. Software Design of Virtual Multimeter

The software flow of the digital multimeter is shown in Figure 9

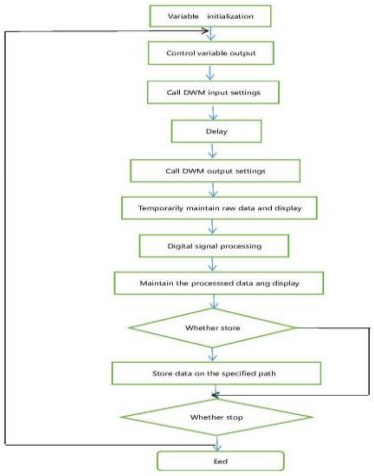

Figure 9 Software flow of digital multimeter

The virtual digital multimeter software panel is shown in Figure 10

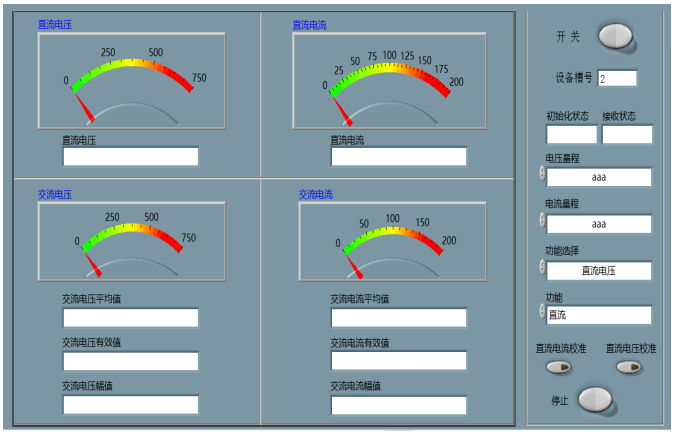

Figure 10 Virtual digital multimeter software panel

4.4. The Interface Mainly Includes The Following Parts:

(1). Data display area

Waveform, pointer, digital display data in three forms, can show the trend of data visualization.

(2) Parameter setting and functional selection area, which includes the basic functions of the virtual digital multimeter, as shown in figure 11:

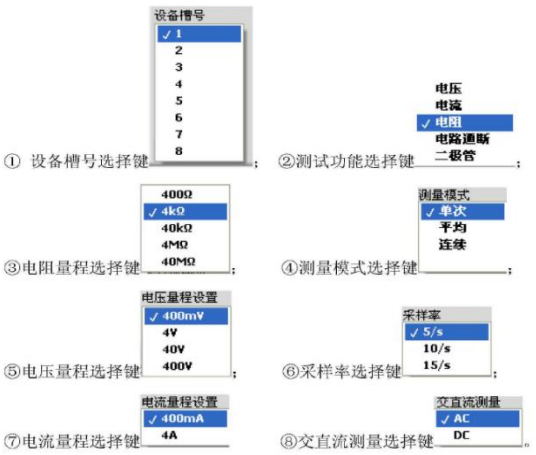

Figure 11 Basic functions of virtual digital multimeter

5 CONCLUSION

This is a virtual instrument technology based on the design of the electrical instrument table, not only can complete the traditional digital universal basic test function table, can also display the measurement results of pointer and other forms of the visual and clear display, and can direct the results of measurements are plotted, for recording, editing and form report. Virtual digital multimeter can also be carried out such as average value, extreme value statistical analysis and more complex data analysis and processing ability of the measurement results with storage and report generation function, and can realize the network communication.

Through the actual test, the results show that the measurement of the resistance, current source, voltage source error, the design of virtual digital multimeter to meet the design requirements. But at the same time, it also reflects some problems, when measuring AC voltage than when the DC error, which may be from AC to DC conversion. The error of the measurement current is larger than that of the measured voltage, which may be caused by the current input switching circuit.

Through a project of the design, proficient in the use of Labview, the hardware circuit design has also been fully understood, in order to achieve the project requirements such as AC voltage, AC current monitoring, provides a strong technical support unit switching range. The project is composed of a software interactive system and a measuring circuit, which facilitates the measurement process and improves the accuracy of the measurement.

Reference

[1] Lin Jun, Xie Xuansong et al. Principle and application of virtual instrument [M]. Science Press.2006. 8, First Edition: 2-6.

[2] Wu Zhongjie, Lin Jun, Wei Jianrong, Xie Xuansong. Virtual testing system of modular instrument key technologies [J]. Chinese Journal of scientific instrument.2005. 8, volume twenty-sixth, eighth: 280-283.

[3] with Xie Xuansong, Yang Yi, Lin Jun. Structure and operation model of graphic language [J].Journal of Jilin University (.2006.), 3, Vol. second, 219-223.

[4] Xie Xuansong, with Yang Yi Lin Jun,.G language hardware virtual model [J]. Chinese Journal of scientific instrument.2006. 3, volume twenty-seventh, Ninth: 1112-1115.

[5] Wu Zhongjie, Lin Jun, Liu Changsheng. Development of Micro Virtual Oscilloscope Based on USB bus [J]. computer engineering and application.2005. 11:109-111.

[6] Wu Zhongjie, Lin Jun,, and [6], the design of micro impedance tester based on Virtual Instrument Technology [J], electrical measurement and instrumentation, 2005 (1): 38-41.

[7] Wei Jianrong. Research and design of reconfigurable measurement and control system [D]. Jilin University.2006. 10: 1-67.

[8] Hu Chuanbo, Zhang Chuanhong,, Ma, Ma. The principle and selection principle of digital multimeter [J]..2003. S1: 320-321.

[9] Lin Zhanjiang. Electronic measurement technology [M]. Electronic Industry Press.2003. 9 133-156.

[10] Li Xueyi. The development status and trend of digital multimeter [J]. foreign electronic measurement technology.1992. 2, 44, 47

[11] Sha Quan, Liu Afang, Wang Ke. Circuit design

optimization of intelligent digital multimeter [J]. power supply technology application.2005. 10, Vol. tenth.

Algorithm of intelligent polygraph system

Qiu Mingjie; Lv Yongqing; Zhu Mingpu
（*College of Instrumentation &Engineering, Jilin University*）

***Abstract*—Based on the widespread application of polygraph and the accuracy requirement of the lie detector, the algorithm design principles of the polygraph system are put forward in this paper on the basis of the established components and processing chip. Respiratory wave, pulse signal and the skin resistance are selected for measurement to establish an algorithm based on MATLAB data processing software. The characteristic value of three sets of parameters can be filtered and extracted by the algorithm. To ensure the accuracy of the test and prediction, discriminant analysis method for mathematical modeling algorithms is applied to the design to achieve the classification of lying and calculate the probability of lying. Finally, the feasibility of the algorithm through the simulation is verified.**

***Key words*—Polygraph system Algorithm Respiratory wave Pulse wave Skin resistance**

0 INTRODUCTION

POLYGRAPH technology in the field of justice has a wide range of applications, with the polygraph device and polygraph technology continues to develop, polygraph integration continues to deepen, and the accuracy requirements are getting higher and higher. There has been several traditional polygraph algorithms[1]: (1) Identification function. In 1952, Ellson proposed for the first time to apply the recognition function of multi-feature quantities to polygraph research. In 1981, Kircher developed the CPS system of which identification function is constructed based on feature building , and the feature quantity are weighed from 5 to 3: skin conduction amplitude, ECG baseline increase and compound respiratory signal.(2) Logical regression. In 1993, Devitt and Honts used a logical regression method, and the difference between the identification function method and ogical regression method is merely on the weighting factor calculation method.(3) Neural network method, which was used by Devitt and Honts in 1993, but the accuracy of polygraph is far less to meet the requirements. (4) Nearest neighbor law. In 2000, Department of Automation of Tsinghua University applied the nearest neighbor law to polygraph. Physiological signals consist of skin conductance, pulsation and respiration.

But the traditional polygraph method cannot judge the lying probability of the tested, but only to a certain degree of accuracy to determine whether the person is lying. To a certain extent, the traditional polygraph method reduces the accuracy of polygraph. In order to improve the polygraph algorithm based on three groups of respiratory signals, pulse signal and skin resistance, this paper presents a new algorithm for extracting and analyzing polygraph data based on discriminant analysis. The algorithm uses wavelet transform, FIR digital filter and other methods to test the physiological signal of the original data .Finally, we can filter and obtain the original value data of the respiratory length, heart rate and skin resistance value, and calculate the coefficient variation of each data group with respect to the baseline. In order to make a judgment on whether the tested person is lying, this paper introduces the "discriminant analysis" commonly used in mathematical modeling into the polygraph algorithm .According to the error rate and the influence of the three sets of parameters described in [2] on the testing results, we can calculate the probability of lying of the person tested to a higher accuracy .So that we can improve the polish of persuasion.

1 ALGORITHM DESIGN

1.1 Design of physiological parameter extraction algorithm

The functions of parameters of the algorithm involved in the design of the extraction algorithm are as follows:

The calculation formula for length of L is

$$L = \sum_{i=1}^{N-1} \left| X_1(i+1) - X_1(i) \right| \quad (1)$$

Where $X(i)$ is the data sequence, L is the length of the parameter.

The calculation formula for amplitude of R is

$$R = MAX - MIN \quad (2)$$

R is the range of data changes, MAX is the maximum value of the data, and MIN is the minimum value.

The coefficient of variation C.V is calculated as

$$C.V = (SD \div MN) \times 100\% \quad (3)$$

Where CV is the coefficient of variation of a set of data, SD is the standard deviation of the data sequence and MN is the average.

1.1.1Design of Eigenvalue Extraction Algorithm for Urine Line Length

The study shows that there is a certain relationship between the length of the respiratory line and the authenticity of the respondent [3]: the shorter the breathing line is at a given time, the higher is the degree of respiratory depression, that is to say the tested person is under more stress and he is more likely to tell a lie. Human emotions are different, the coefficient of variation of the respiratory wave signal sequence and the amplitude of the respiratory data are also different, so it can be used as the eigenvalues of the respiratory data.

Using a set of polygraph problems to test the subject, according to the relevant study [3], the respiratory signal wave of ten seconds after the end of the question has the highest correlation with the problem, so the test interval of each question is selected as 10s.Here, $X(i), i = 1,\ldots,N$ represents the breath wave signal which lasts between the time a question has been put out and another question is to put out. The extraction algorithm of the respiratory wave signal is as follows:

① Use wavelet de-noising analysis on the sequence $X(i)$ and filter out the noise in the signal to get the sequence $X_1(i)$.

②Use the formula (1) to obtain the respiratory line length L_1 of the signal sequence $X_1(i), i = 1,\ldots,N$ after denoising.

③Use the formula (2) to calculate the respiratory signal amplitude R_1 of sequence $X_1(i)$.

④Use the formula (3) to calculate the coefficient of variation of the sequence $X_1(i)$, represented as $C.V_1$.

1.1.2 Pulse signal extraction algorithm design

In the human circulatory system, heart rate, blood volume and blood pressure are due to myocardial contraction and diastolic formation, so the three parameters are closely related, heart rate, pulse strength, blood pressure are corresponded with myocardial pulse intensity and amplitude, and also with changes relating to the psychological state [4].

When people are in the psychological tension, the heart output increases, so do the heart rate and systolic blood pressure, and tension will also increase the peripheral blood circulation resistance, so that the diastolic blood pressure is also increased, causing short Reduced blood volume. So the algorithm select blood pressure parameters, blood volume parameters and heart rate parameters as the pulse signal eigenvalues.

Use a set of polygraph problems to test the subjects, after a large number of scientific experiments, the respiratory signal wave of ten seconds after the end of the question has the highest correlation with the problem, so the test interval of each question is selected as 10s.

The total pulse signal collected of this polygraph problems group is $y(i), i = 1,\ldots,N$, at first use de-noising method on this sequence, the steps are as follows: Wavelet denoising analysis on the sequence $y(i)$, filter out the noise in the signal and get the sequence $y_1(i)$.

1.1.2.1Extraction of blood pressure parameters

When people are in the emotional tension, blood pressure will rise, and the increased degree is proportional to the degree of tension.

In this design, a set of questions are selected to test the subjects. The pulse signal obtained by the test is subjected to low-pass filter to obtain the blood pressure signal. After comparation, we can obtain the minimum value of the blood pressure signal in this group $y_2(i)_{\min}$.Then we subtract the maximum value of the blood pressure signal by $y_2(i)_{\min}$ and the resulting sequence is the blood pressure eigenvalue measure, the blood pressure parameter extraction algorithm step is:

①According to the human body pulse signal frequency, the noise signal is subjected to a low-pass filter with the cut-off frequency of 1 Hz, then we obtain the blood pressure signal $y_2(i)$.

②Find the minimum value $y_2(i)_{\min}$ in the sequence $y_2(i)$.

③In the sequence $y_2(i)$, the blood pressure signal for each problem is recorded as $Y_1(i)$, then find the maximum value $Y_1(i)_{\max}$ of the sequence.

④Calculate the blood pressure parameters for each question according to the formula

$$A = Y_1(i)_{\max} - y_1(i)_{\min} . \quad (4)$$

1.1.2.2Extraction of blood volume parameters

Pulse signal which get through band pass filter with the cut-off frequency from 1 Hz to 3 Hz will be blood volume signal. In the case of stress blood volume will be reduced. We use the blood volume of the signal line length as blood volume parameters measurement. Extraction algorithm of blood volume parameters steps are:

①Let the denoised pulse signal $y_1(i), i = 1,\ldots,N$ get through the band-pass filter with cut-off frequency from 1 Hz to 3 Hz to get blood volume signal $y_3(i)$.

② The blood volume signal of each problem is recorded as $Y_2(i)$ in the sequence $y_3(i)$ and then calculate the blood volume parameter length L_2 of each problem according to the formula.

1.1.2.3Extraction of Heart Rate Parameters

The heart rate of the human body is the number of times the heart beats every minute. The sampling frequency of the pulse sensor used in this design is 25 Hz. In order to improve the frequency resolution, the above-mentioned blood volume signal is extended to 1000 points from 250 sampling points collected at the end of each problem, then carry out the discrete Fourier transform and calculate the amplitude spectrum. Then we can find the frequency point k corresponding to the maximum value between two points (that is, the 40th point to the 120th point) of the amplitude spectrum corresponding to the actual frequency of 1 Hz to 3 Hz. Use the formula

$$f_k = 60 \times \frac{k}{N} f_s \quad (5)$$

to calculate the average heart rate of tested person in this interval. The higher the average heart rate, the more tense the person is on this question. Steps of extraction algorithm of blood pressure parameters are as follows:

①Extent the blood volume signal sequence period of each question to 1024 sample points. And then carry out Fourier transform according to the formula:

$$Y_3(k) = DFT[y_3(n)] = \sum_{n=0}^{N} y_3(n) e^{-j\frac{2\pi}{N}kn} \quad (6)$$

②Use the formula (2) to calculate the magnitude and phase of Y_3 .

③Find the frequency point k corresponding to the maximum value between the two points in the amplitude spectrum corresponding to the actual frequency 1 HZ to 3 HZ, then use the heart rate calculation formula $f_k = 60 \times \frac{k}{N} f_s$ to calculate the average heart rate f_k of the tested person.

1.1.3Design of skin resistance signal extraction algorithm

Studies have shown that[5], when a man's breathing becomes rapid, or is stimulated by emotional stimulation, the sympathetic nervous system will promote skin to contract the muscle, sweat secretion will strengthen the dermal layer and the vertical resistance will reduce .This will result in the decline in human skin resistance, so the average skin resistance can be used as a measure of the parameters of each question. When the human body is stimulated, the peak and the fluctuation degree of the leather signal waveform of the tested person will also change. Therefore, the amplitude sequence of the skin resistance of each question can also be used as the characteristic value of the skin resistance signal. Set a set of questions to test the person, where the collected skin resistance signal during the time from one of the problems begins to 10s after that is $Z(i), i = 1,\ldots,N$. Then the skin resistance of the physiological parameters extraction algorithm steps are: ①Wavelet de-noising analysis of the sequence $Z(i)$, filter out the noise and get the signal $Z_1(i)$.②Let the sequence $Z_1(i)$ get through a low-pass filter with cut-off frequency of 35HZ .filter out the high-frequency noise to get the sequence $Z_2(i)$.③Find the average value of the sequence $Z_2(i)$ which is also the average skin resistance of each question.④Use the formula (2) to calculate the skin resistance amplitude R_2 for this

group of questions. ⑤ Calculate the coefficient of variation $C.V_2$ using equation (3).

1.2Design of Probability Judgment Algorithm

1.2.1A Brief Introduction to the Principle of Discriminant Analysis

In order to evaluate the possibility of lying, this paper proposes an algorithm to calculate the probability of lying. The algorithm is implemented by "discriminant analysis". The principle of discriminant analysis is as follows:

From the perspective of probability theory, the problem can be attributed to the following model. Suppose that there are n members on total:

$$\zeta_1,\ \zeta_2,\ldots,\zeta_n \tag{7}$$

Which ζ_i is a m-dimensional random variable, the distribution function is:

$$F_i(x_{1,\ldots}x_m), i=1,2,\ldots,n \tag{8}$$

$(x_1,..x_m)$ is value of the m random variables that characterize the overall characteristics. In the discriminant analysis, the m variables are called discriminant factors. When there is a new sample point $x=(x_1,..x_m)^T$, you can use the discriminant analysis to determine which overall does the sample point belong to. The discriminant analysis uses Bayesian discriminant method, the basic idea is as follows [6]:

Suppose that there are a total of m members $G_1,G_2,\cdots G_m$, and their prior probabilities are $q_1,q_2,\cdots q_m$, the density function is $f_1(X), f_2(X)\cdots f_m(X)$.In the case where a sample x is observed, the Bayesian formula can be used to calculate the posterior probability from the total g:

$$p(g/x)=\frac{q_g f_g(X)}{\sum_{i=1}^{m} q_g f_g(X)}, g=1,2,\cdots m \tag{9}$$

And when

$$p(h/x)=\max_{1\le g\le m} p(g/x) \tag{10}$$

Judge X comes from the total h.

1.2.2Algorithm design and analysis

The application of discriminant analysis is a set of known characteristics of the sample data, so first this algorithm requires a group of reference experiments to carry out polygraph discrimination according to the known experimental results.

(1)For the extraction data from respiratory wave, select the respiratory length L_1, the coefficient of variation$C.V_1$, and the respiratory signal amplitude R_1 of each question as a discriminant factor.

(2)For the pulse extraction data, select the blood pressure parameters A, blood volume parameters line length L_2 and the average heart rate f_k of each questions as discriminant factor.

(3)For the skin resistance extraction data, select the average value of leather electrical parametersAVG3, skin resistance amplitude sequenceR3 and coefficient of variationC.V3 of each question as a discriminant factor.

(4)Use the discriminant function classify of MATLAB to determine the situation of three groups of unknown parameters of the data. Each parameter is divided into three discriminant factors and each group of discriminant factors are as above. Then record the classification of each question after running the command, that is to classify as lying or not lying a class, and record misjudgment rate of output. Three groups of test results of the false positive rate are recorded as ERR_1, ERR_2, ERR_3.

(5) After scoring the leather, pulse, and breath data, we need to calculate a certain weight before we calculate the probability of lying. Refer to Poly Score (a scoring software) system[2]among them, the leather weight accounted for 71%, pulse for 11, while breathing accounted for only 18%.For the above questions determined that the tested person lied, formula for calculating the probability of lying is

$$P=0.71\times(1-ERR_1)+0.11\times(1-ERR_2)+0.18\times(1-ERR_3) \tag{11}$$

For the question determined that is not lying, the formula for the probability of the person to be lying is calculated as follows

$$P=0.71\times ERR_1+0.11\times ERR_2+0.18\times ERR_3 \tag{12}$$

2 EXPERIMENTAL VERIFICATION

2.1 Experimental results

In order to verify the validity and feasibility of the algorithm of the polygraph system proposed in this paper, a set of simulation cases is designed .Simulation of the case is a digital test, the tested person will randomly select a number from the 1-7 digital cards, after the tested person has exacted the number which is selected, the asker will ask a series of questions. In

order to meet the requirements of the algorithm, first ask five of its control questions, which are set as: ① What is your name? ② Are you a boy or girl? ③Is it sunny today? ④Have you just selected a number? ⑤ Will you go home today? The answers to the five control questions are set as "yes", where the fourth and fifth questions are identified as certain lying questions. The classification of the first five known problems can be set as: (1, 1, 1, 2, 2) in the discriminant analysis, where 1 is the classification of the lie and 2 is the non-lying classification. And then the subjects will be followed by seven digital questions, question mode are: Are you pumping (1-7) in it? We ask the respondent to answer on all questions: No. So the subject must be lying on a question. The parameters of the test are as follows:

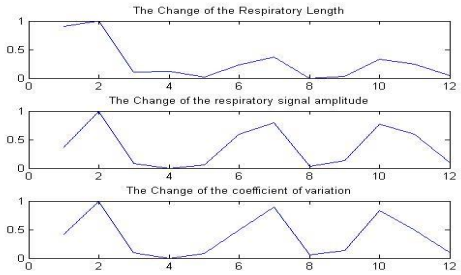

Fig. 1 The Change of the breathing data

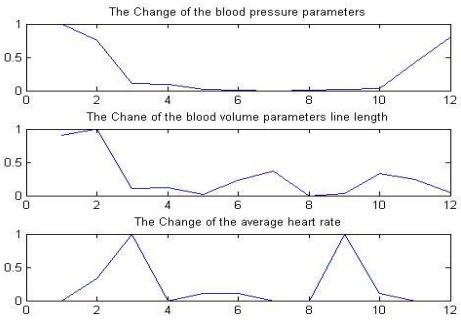

Fig. 2 The Change of the pulse data

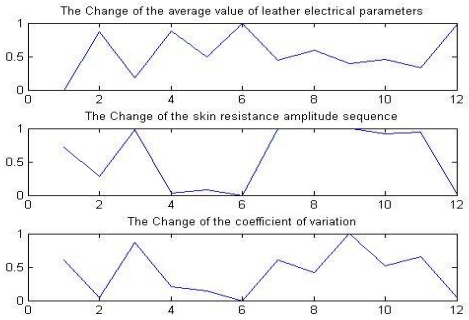

Fig. 3 The Change of the skin resistance data

The number of questions obtained is classified as follows:

(1)For respiratory waves, class=[1;2;1;1;2;2;2],err=0.25.

(2)For pulse parameters, class=[1;1;1;2;2;2;2],err=0.1667.

(3)For skin resistance parameters, class=[2;2;1;2;1;2;2],err=0.15.

According to the formula (9), the probability of lying on the seven tested questions is shown in Table 1:

Table 1 The experimental data

1	2	3	4
33.32%	24.32%	83%	25.99%
5	6	7	
66.69%	16.98%	16.98%	

2.2 Experimental analysis

We have known that the tested person lied on the third question, that is, the 8th data in the figure, on analysis of Fig.1, 2, 3, the three groups of parameters make significant changes on the third question: respiratory rate, amplitude and coefficient of variation decreased; blood pressure, blood volume and heart rate decreased; skin resistance showed a decreasing trend. The classification of the three groups of parameters shows that the subjects are lying on the third question, the calculation of the probability of lying shows that the testees are lying on the third question and the probability is 83%, which is consistent with the experimental situation. So the experiment can verify the feasibility of this polygraph algorithm. But this test shows that the probability of lying on questions 5is also greater. However, the tested person did not actually lie on these questions. So the test accuracy needs further improvement.

The experimental results were shown in Table 2:

Table 2 The experimental results

Group number	The number of the question						
	1	2	3	4	5	6	7
1	14.58%	32.58%	67.41%	14.58%	14.58%	32.58%	14.58%
2	12.78%	23.78%	12.78%	12.78%	76.22%	18%	12.78%
3	27.33%	85.67%	16.33%	16.33%	29%	18%	16.33%

In the first group testee lied on the third question, the probability of lying was 67.4%. In the second group testee lied on the fifth question, the probability of lying was 76.22%. In the third group testee lied on the second question, the probability of lying was 85.67%.From the table, we can conclude that the measured probability values of the other questions were smaller so the polygraph results are consistent with the real situation.

3 CONCLUDING REMARKS

This paper proposes an algorithm based on the study of polygraph system physiological parameters .And through theoretical analysis and experiment, we can verify the effectiveness and accuracy of the algorithm.

The algorithm has the following characteristics: (1) Using wavelet transform and Fourier transform to realize the accurate extraction of the characteristic values of the respiratory wave signal, the pulse wave signal and the skin resistance signal, and filter out the noise in the original signal to the maximum extent; (2) Using the principle of discriminant analysis and through the analysis and processing of the signal eigenvalues measured in the polygraph experiment, the classification of the lying situation and the calculation of the lying probability are realized to a high accuracy, And further through the comparison between the parameters ,we can take out a more accurate determination of the results of polygraph. Experiments show that the results of this algorithm are in accordance with the real situation, so the algorithm is practical and feasible.

Due to the impacts from the subject's psychological quality, test environment, test questions, polygraph skills and other aspects, there exists some deviations on the results of polygraph algorithm analysis, especially in the analysis of skin resistance parameters. Therefore, the next task of this research is to optimize the algorithm, improve the accuracy of polygraph, and eliminate the irrelevant interference in the experiment, so that the reliability of polygraph system can be further guaranteed.

References

[1] ZHI G Y. Comparative study lie detection algorithm and its ASIC implementation [D]. Suzhou: ZHI G Y, 2008; 8 to 14

[2] TONG CH S,AN F Y. Breathing line length (RLL) application in the evaluation chart [J]. Journal of Jilin public security college, 2007; 22 (5): 109-109

[3] ZHANG CH G. Psychological tester for multi-channel physiological parameter extraction algorithm research [D].Yan Shan: Bryan, 2009; 26-37

[4] ZHAO X C, ZUO H F, REN Y J. Areview of Eye Tracker and Eye Tracking Techniques[J]. Computer Engineering And Applications. 2006; (12): 118-121

[5] Li Hao, Liu Jie. Human skin resistance and Breathing Measurements and Analysis of The Relationship, emotional [J]. Science, technology and engineering, 2012, 12 (3) : 662-665

[6] Jhxucn. The basic principle of discriminant analysis [EB/OL].Baidu library

Multi-function controllable intelligent lamp based on embedded system

Ai Yong-heng; Ma Xin; Zhu He

(College of Instrumentation and Electrical Engineering, Jilin University,Changchun 130022,China)

***Abstract*—In order to solve the traditional lamps that is single function and not smart, the embedded system and android APP together applied to the control research of lamps, the android APP or remote device sent control signal to 51 series single chip microcomputer by bluetooth, and single chip microcomputer control of the WS2812B chip, based on RGB code control of lighting, bluetooth control all kinds of scene change, intelligent sensor to turn off the lights, the function of timing closure.**

***Key words*—Embedded system Android bluetooth control Controllable light**

I. INTRODUCTION

IN 21th century,LED room lamp design will be the main stream,it is also energy saving,healthy,artistry and hommization.Intelligent lamp as a multifunctional intelligent lighting device,because of its energy saving,linkage and hommization,it is widely used all over the world among all major areas[1].At present, there are many furniture lamps are not intelligent,it may cause energy wasting,and did not meet environmental protection.At the same time,the development of information technology provides great convenience for people,Intelligent lamp can also live up to it,it can not only complete the simple and convenient remote switch control, but also has the functions of many other ordinary furniture lamps.So,We design a kind of intelligent multifunction lamp controlled by Bluetooth and infrared,WS2812B is used in this design.

II. INTELLIGENT LAMP LIGHT SYSTEM

A. Intelligent lamp light system scheme analysis

At present, there are two main control methods.

The first ,Full-color LED lamps based on SDMX-5124 component cascade control mode, control data of each chip is 12 bits controlling RGB three colors.Each color is 4 bit control data,16 gray level.SDMX5124 is a single chip high integration, low power LED lighting control chip, which uses the original synchronization DMX512 single line LED lighting control mechanism[2], so that the LED lamp cascade control becomes flexible and simple.The SDMX5124 is composed of two parts:communication control module and the three way digital PWM LED dimming control.

The second,Cascade control using WS2812B.WS2-812B is a set of control circuit and light-emitting circuit in one of the intelligent external control LED light source.The appearance of a 5050LED lamp, each element is a pixel.Pixels contained within the intelligent digital interface data latch signal shaping amplifier drive circuit also comprises a high precision internal oscillator and 12V high voltage programmable constant current control part, ensure the effective pixel light color consistency.Data protocol adopts single line to zero code communication,The pixel is reset after the end of DIN, accept the data transmitted from the controller, the 24bit data is first sent over by the first pixel to pixel extraction, internal data latch, the remaining data after the internal plastic processing circuit after shaping amplification through the DOUT port output to start forwarding the next pixel cascade, after each transmission of a pixel signal, reduce 24bit.The pixels are automatically shaped and forwarded, so that the number of pixels is not limited by the signal transmission, only limited signal transmission speed requirements.LED has the advantages of low voltage drive, environmental protection and energy saving, high brightness, large scattering angle, good consistency, low power, long life and so on. The control circuit is integrated on the LED, the circuit is more simple, small size, easy to install.

The control system applies WS2812B control chip, this chip can meet the requirements of intelligent lamp,

relative to the other chip also satisfy the performance demand on the price, but this chip control is easier and convenient.

TABLE 1

LED CHARACTERISTIC PARAMETER

Light Color	dominant wave length （nm）	Luminous intensity （mcd）	Working current （mA）	Working voltage （V）
Red	620-630	550-700	20	1.8-2.2
Greed	515-530	1100-1400	20	3.0-3.2
Blue	465-475	200-400	20	3.2-3.4

B. WS2812B lamp control

For WS2812B control[3], the first is to understand its basic principles.This chip is used for the input signal for 1 and 0 yards of identification, through the high level of time to achieve the difference between the 1 and the 0 yards.Each control signal has 24bit, respectively, GRB three kinds of code, each color code is 8bit, respectively, from high to low into the chip.

If you want to refresh the control data, you need at least 50uS low level can be refreshed[13].

Table 2

Data Transfer Time

TH0	0 yards, high level	0.35us	±150ns
TL0	0 yards, low level	0.8us	±150ns
TH1	q yards, high level	0.7us	±150ns
TL1	1 yards, low level	0.6us	±150ns
Res	frame，low level	Above 50us	

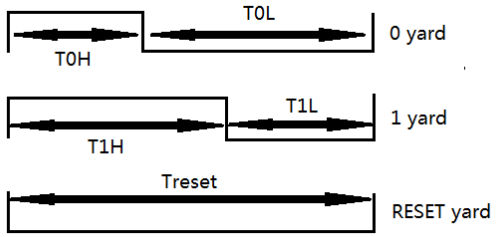

Fig.1 Temporal waveform figure

According to the above chart shows that the chip to achieve the output of 0 yards and 1 yards with the microcontroller control, for 0 yards and 1 yards is us level, through the observation and test of the oscilloscope, found at least should choose the 24M crystal in order to achieve the correct control, the largest crystal however 51 SCM can be used 24M, so choose 24M. Then through the microcontroller input 0-255 RGB code can control the color of the WS2812B transform.

III. INTELLIGENT CONTROL SYSTEM SCHEME

A. System requirements

1. Control system functional requirements

The main controller to realize the functional requirements with a graphical interface, the interface is simple and easy to operate, and with commonly used lamps, lamp has the function of overall layout design, has the function of conventional lamps, lamp with parameter setting function, can control the data transmission function.

2. Technical requirements of intelligent control system

First of all, the intelligent lighting control system needs a man-machine interface, that is, the control panel, LCD screen should be displayed, which requires the system and the operating system to support the display function. Secondly, the data processing system of a large amount of information, and the requirements of real-time data processing module is better, which requires the system to have a high efficiency, high frequency and select the appropriate communication protocol for communication.

B. Infrared induction switch

For intelligent induction off the lights technology, microwave technology and infrared technology. By comparing the two technologies, due to the infrared in the human body and the moving heat source and performance in terms of cost-effective, so the use of infrared sensor[4]. In this regard, the use of HC-SR505 infrared module, this module has three pins, which are positive, inductive output, negative. Therefore, it is possible to control the working state of the infrared module with the high and low level, and then to receive the signal which is induced from the module. If the lamp is set as the induction mode, the lamp will be turned on at the same time[12]. If the signal returns to

a low level, the light will turn off.

C. Bluetooth APP Design

1. Bluetooth communication control to achieve a variety of mode conversion

For remote control, the primary solution is to control the transmission of data, first of all, the mainstream of data transmission methods are ZigBee, Bluetooth, WiFi three ways. By comparing the three methods, combined with China's domestic situation, open WiFi is not very popular, and ZigBee can not be combined with the phone. Therefore, the use of Bluetooth communication,which makes the development of mobile phones on the subsequent convenience of many APP[5]. In the Bluetooth part, the HC-05 module is selected. It has three kinds of working state, the main loop, from three ways. When in command response mode, it can execute all AT instructions, through the AT command can set its working state[11].

Data transfer options, 8 for transmission mode, no parity and start closing character[6~7]. This method is a popular method of transmission, this method is also easy to combine with 51 mcu. For the control, the design of two control methods: Bluetooth controller and Android APP.

2 . Design of Bluetooth remote controller

For remote control design, to meet the various needs of the main controller, which is no longer mentioned. This piece can be divided into three main parts, namely the display part, the keyboard part, the Bluetooth part.

Display part, the display content to have at least 6 modes of control, and each mode, there are other features to display, and there is a display time, showing the location of the RGB24bit code value. Therefore, this part of the comparative screening, in order to display the function and can meet the needs of clear observation of the human eye, select the LCD5110. This liquid crystal display is mostly used in Nokia, is also a classic. This display is 84*48 dot matrix, can display four lines of Chinese characters, the use of low voltage power supply, the normal display of the working current of 200 A, and has power down mode. These features are well suited for battery powered portable communication devices and test equipment. Through the 51 series microcontroller can be very good control LCD5110.

Keyboard part, the application of the 4*4 keyboard, through the continuous scanning with 51 single-chip, data input, thus controlling the display of the contents of the display and Bluetooth data to be sent.

The Bluetooth part, this part and the controlled part is similar, using the AT instruction, and the settings for the lamp which is connected from the machine, remote control part is provided for the host, when power on, two Bluetooth will automatically connect together. At this time when the controller receives the control information of the keyboard, the microcontroller pin will be issued serial control data into the host Bluetooth, and then sent to the slave Bluetooth, the control function[8~9].

3. Android APP design

Through the development of Ecilipse software, the realization of the control system. Its functional modules are as follows:

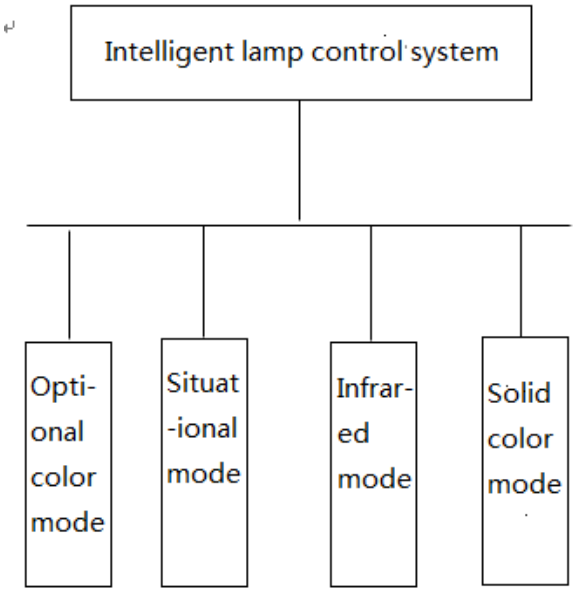

Fig.2 Structure of system function

The main interface is divided into three parts, respectively, the top of the Bluetooth connection, as well as the middle of a variety of functional part of the model, including the final exit and the timing of the exit part. The main interface as shown below:

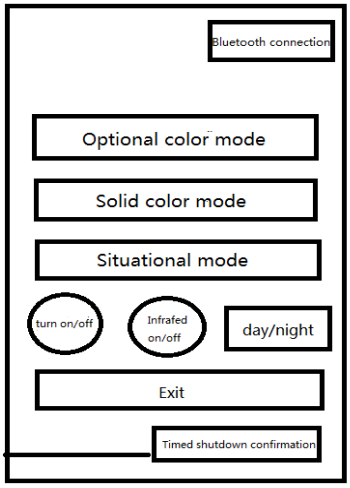

Fig.3 APP main UI

Optional mode interface is as follows:

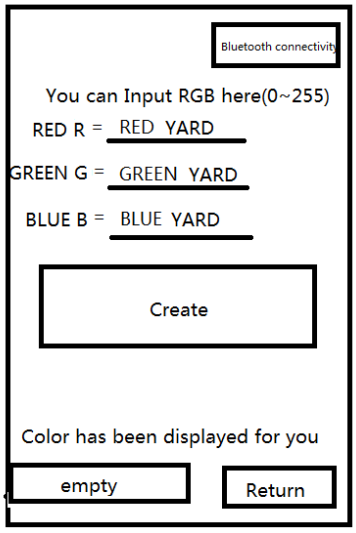

Fig.4 Optional Modle UI

In the free mode, you can enter the RGB code value (0-255), and then click on the middle of the formation of the part, you will be displayed on the color for you on the font to display the color should be displayed on the color. The bottom is the empty RGB value and return to the main interface button. The situational mode and color mode to mention.

The Andriod platform provides API to realize the connection between the Bluetooth devices, connection between Bluetooth devices is mainly divided into four steps: setting the Bluetooth device for LAN may, or data transmission equipment[10] ,connected devices and connected devices. The following basic classes are needed to build the Bluetooth: BluetoothAdapter: represents a local Bluetooth adapter. It is the entry pointforall Bluetooth interactions.Class BluetoothDev -ice: represents a remote Bluetooth device that uses a remote Bluetooth device to connect to or obtain the name, address, type, and binding status of the remote Bluetooth device. Bluetoothsocket class: represents a Bluetooth socket interface, which is the application through the input and output streams and other Bluetooth devices to connect the connection point. Class Blueboothserversocket: represents the opening of a service connection to monitor possible connection requests. In order to connect to two Bluetooth devices, a device must be used as a server to open a service socket. Class Bluetoothclass: describes the general features and capabilities of a Bluetooth device. His read-only attribute set defines the primary and secondary device classes and some related services. However, he did not accurately describe all of the Bluetooth devices and services supported by the device, but as a small hint of the type of device.

IV Emergency power supply

In order to cope with the unexpected situation (power failure), we designed the spare part of this part. In normal operation, the power supply is supplied by the 220V home appliance after a step-down rectifier. When an accident occurs, the relay will be controlled by three 1.5V dry batteries, and then when the call, and then cut back to the original power supply[14]. The relay circuit is as follows:

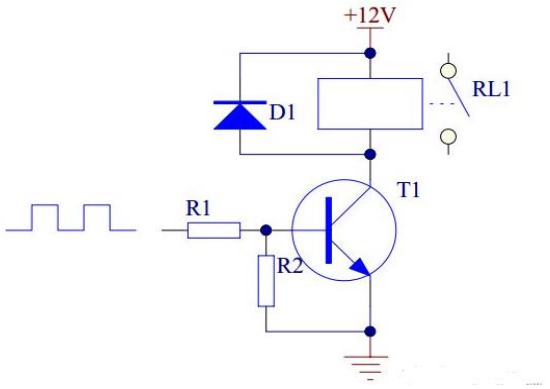

Fig.4 Relay Drive Circuit

V Conclusion

In this paper, a new type of lamp is presented, which combines the lamps and the APP or remote controller of the mobile phone, and turns the ordinary lamp with a single function into a multifunctional controllable

lamp. At the same time, the system uses the infrared technology, when no human body movement, automatically turn off the lights. After verification, this lamp has a certain practicality.

Table 3

Achievements

Function	APP control light switch	APP control scene transformation	APP control color selcetion	Separate remote control	Infrared monitoring automatically turning off
Achieved or not	√	√	√	√	√

According to the final experimental results for analysis, the basic objectives of the target has been achieved, and the original standard is almost the same. But the brightness is not enough because of the light beads chip we selected . Then, we decided to solve the problem of light intensity by using new light beads chip or increasing the nember of light beads chips.

Reference

[1] Chen Yuandeng.LED manufacturing technology and application [J]. Publishing House of electronics industry, 2009 (10):36-42.

[2] Qian Mingguang.DMX512 information format and application of new horizon broadcasting technology [J]. new horizon broadcasting technology, 53-54.

[3] Heng Yang.LED lighting driver design steps [J]. China power press.2010.1 (1): 20-24.

[4] Yang Fan. Sensor technology.[J]. Xi'an Electronic and Science University press.2008. (9): 67-73.

[5] Zhu Xiaorong. Principle and application of wireless network technology.[J]. Publishing House of electronics industry.2008. (7): 112-118.

[6] Sun song. Design and implementation of intelligent lighting system based on Android [D]. Chongqing: Chongqing University, 2014.

[7] Hua Tengfei.The design and implementation of infinite LED color lamp control system based on high performance MCU [D]. Taiyuan: Taiyuan, 2012.

[8] Wang He. Development of intelligent lighting control system [D]. Xi'an: Chang'an University, 2010.

[9] Zhang Shuguang.China intelligent lighting system and its application in engineering construction of electrical construction of electrical [J]. Construction of electrical,2004,5 (1): 122-124.

[10] Li Gang. Crazy Android lecture notes [M]. Beijing: Publishing House of electronics industry, 2015:1-412

[11] Hu Yue, Zhou Tenghe, Liang Dongsheng. The Android platform of intelligent light control system design and implementation technology of.2016. [J]. network based on Bluetooth (5): 14-16.

[12] Dan Chengxiang,Niu Yanwen,Zhang Chun. Design based on sensor[M].Beijing:National Defense Industry Press, 2007

[13] Wang Yihuai.The principle and application of Embedded microcontroller[M].Beijing:Beijing Hope Electronic Press, 2002

[14] Zhang Ji. Research on automatic meteorological information collection technology based on Internet of things [D].Changchun:Changchun University of Science and Technology, 2013

Design of motor experiment teaching management platform based on Java

Hou Xue-zheng; Zhao Ying-da; Wang Yi-ying
（College of instrumentation& Electrical Engineering,Jilin University,Changchun 130012,China)

***Abstract*—The traditional classroom teaching mode is single and inflexible,The cultivation of students is only a simple indoctrination,it has ignored the students' personality differences.Therefore, it can not reflect the thinking abilities, which can stimulate students' potential and good quality cultivation of students.And the course of electrical engineering is an important basic course of electrical engineering and automation.The teaching of this course requires not only the classroom teaching, but also to make the students have more perceptual knowledge, and strengthen the practical teaching.Design of motor experiment teaching management platform based on Java combines classroom teaching with practice teaching,Breaking the single teaching form,it will be the experimental teaching preview, the experimental process, the results of the analysis of coordination, so it can greatly improve the teaching efficiency, facilitate teaching,and benefit to students to know all kinds of professional learning.The design is based on Java language, by ECILIPSE software, which realizes the student / teacher different permissions login, student information query, motor learning, simulation, teacher answering questions, students submit online homework, answer and other functions, is a complete management platform.**

***Key word*—Java program,Design of teaching management platform,Experimental simulation of electrical machine**

0 INTRODUCTION

THE rapid development of computer network has greatly changed the traditional teaching methods and means,and Network teaching in Colleges and universities has become a trend of teaching in the future.Compared with traditional teaching, network teaching has incomparable advantages.The course of electrical engineering is a major basic course of electrical engineering and automation.However, due to limited resources, can not meet each student has an experimental platform, to a certain extent, affect the learning effect of the students.In the course of the experiment, the students were not familiar with the experimental platform, and the misoperation caused the damage of the experiment platform.In practical engineering, how to make students learn to use the integrated knowledge, optimize the control system and meet the requirements of production is the task of the course.Therefore, the teaching needs not only the classroom teaching, but also the students' perceptual knowledge, strengthen the practice teaching, including the experiment and curriculum design.However, due to the limitation of teaching hours, laboratory equipment, laboratory personnel, and experimental conditions, teaching requirements are sometimes difficult to achieve.But the virtual experiment and design are not restricted.We can introduce the MATLAB/Simulink simulation technology and the GUI interface design into the teaching, and develop a visual experimental platform.Through the simulation, the students on the performance of various devices, circuit connection understanding and visualized simulation results, can shoot two hawks with one arrow.The design of the electric motor experiment simulation software, it will put the theory teaching and experiment process together, not only can improve the efficiency of the classroom, but also can make the students learn this course a motor has a learning tool, and improve the learning interest of the students and teachers can understand the students timely preparation and study of this the course.

1 SYSTEM FUNCTION

Design of motor experiment teaching management platform based on Java.Based on the Java language, using ECILIPSE software, realize the student / teacher different permissions login, student information query, motor learning, simulation, teacher answering questions, students submit online homework,

homework answer reference function.Teachers through their own account / password login, it can online Q & A, online to receive the work submitted by students, view student information and other functions;Students through their own student ID password can choose the experiment simulation, online inquiry, online submission and other functions.

The information of teachers and students is stored in the database, and the remote database can be accessed by the management platform. Specific structure shown in figure 1.

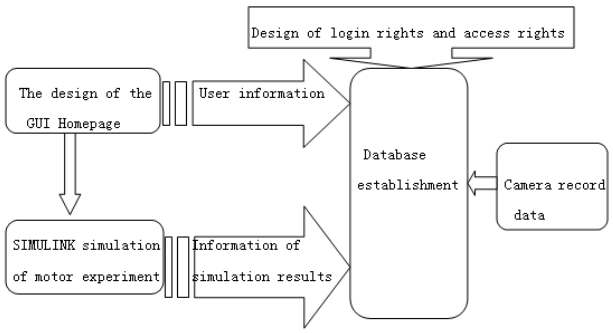

Fig.1 Structure of management system

2 SYSTEM ARCHITECTURE

The teaching management platform uses the C \ S mode, and designs the appropriate database, which is considered as a server-side. In this mode we use the standard network communication protocol -TCP / IP protocol, and the client accesses the server-side database through the IP address.The teaching management platform uses the Eclipse which is an open source, Java-based, extensible development platform for development and the database uses SQL Server 2005 database.For its part, it is a simply framework and a set of services for building a development environment through plug-in components. Eclipse attaches a standard set of plug-ins, including Java development tools (Java Development Kit, JDK).

Key Technologies:

2.1 Man-machine interface uses java-AWT (Abstract Window Toolkit),which provides a set of connections with the local graphical interface and it is basic tools provided by Java to create and set up it's graphical user Interface.

2.2 Remote access using TCP / IP , Transmission Control Protocol / Internet Protocol shorthand, also known as the network communication protocol, is the most basic protocol of the internet ,the basement of international internet,which is composed of The IP layer of the network layer and the TCP protocol of the transport layer. The TCP / IP defines the standard for how electronic devices connect to the Internet and how data is transferred between them.

2.3Java connection with the database, JDBC (Java DataBase Connectivity) is a SQL statement for the implementation of the Java API, for a variety of relational database to provide uniform access, which consists of a group written in the Java language classes and interfaces. JDBC provides a benchmark then you can build more advanced tools and interfaces that enables the database developers to write database applications.

3 TEACHING MANAGEMENT PLATFORM MODULE

This platform includes the following modules:

3.1 Permission Log in module.

Student and teachers have different log -in privileges. Teachers can view students and themselves personal information, and can add/modify/delete them, and can make online q&a, accepting assignments for students;students can choose their own experiments, view the experimental guidance, see the reference answers, open the simulation software Matlab and can ask questions online, submitted to the operation. The log- in interface is shown in Figure 2.

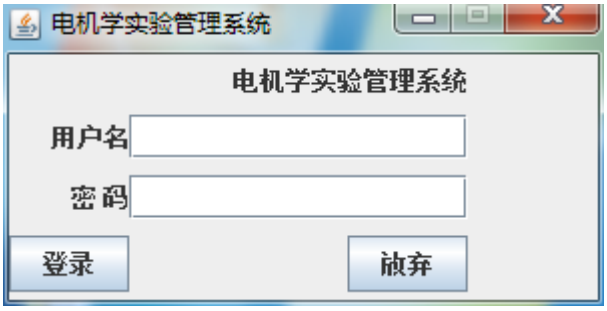

Fig.2 Motor experiment management system login interface

3.2 Online Q & A module.

This module uses TCP / IP protocol,whose server-side creates Socket , selecting the available ports for monitoring and the client has access to the server IP address specified port number for access, connection through the creation of Socket,he connection is successful for information transmission. Answer the module as shown in Fig 3.

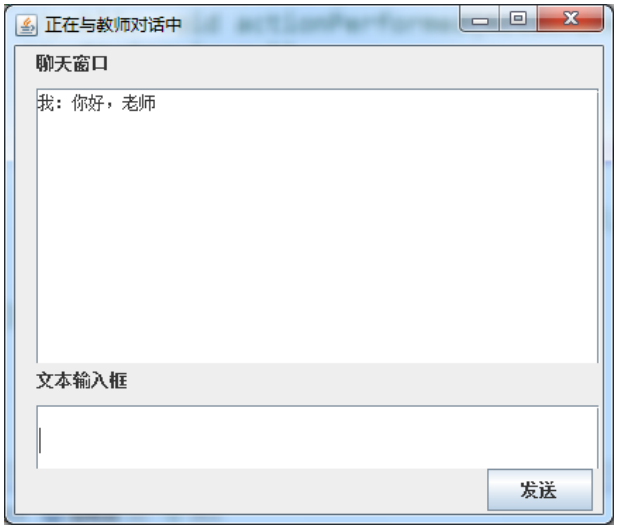

Fig.3 Communication module interface

3.3 Online Submit Job Module.

Similar to the online Q & A module, the server creates a socket, selecting the available port, and the client connects to the server IP address specified port to connect through the socket to the connection is successful, selects the job file and sends them. The server selects the job storage location. File transfer module is shown in Figure 4.

Fig.4 File transfer module interface

3.4 database establishment.

Through the SQL Server 2005 database CV database, it conclus resume student information table, teacher information table and reference answer sheet. Java has an access to the database through JDBC. The database is shown in Figure 5.

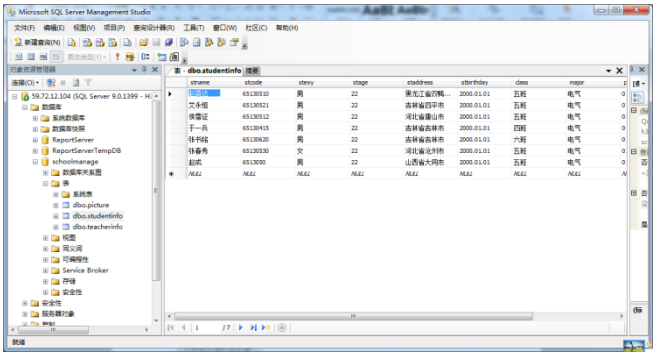

Fig.5 Database software diagram

4 Platform Features

4.1 changed the previous teaching mode.

Traditional classroom teaching model is teacher-centered, teacher-led to guide the whole course, rarely consider the individual situation of students, which is not conducive to the cultivation of individual students. Students of different foundation, different quality, different hobbies, we can not cut down the knowledge of indoctrination.

4.2 changed the previous work mode.

This integrated teaching management platform makes full use of the existing network technology and network resources, integrating curriculum information, student information, teacher information, teaching material information, teaching archives information and other functional modules. Each functional module is independent of each other Sexual and mutual coordination. The coordination of the work between teachers and students can be done easily with this platform.

5 The Significance of This Platform Design

"Based on the JAVA motor experimental teaching management system" for the development of university personnel and more resources in the context of student management has a very positive significance.

5.1To improve the learning quality of part-time students.

This system has solved the problem that under the background of knowledge economy, the life study speed of the student is more and more fast, the number of correspondence education and amateur education students are more and more, and the face-to-face education mode can not satisfy the students' thirst for

knowledge. Of network technology and computer resources, including online learning, access to information, browse information, download information. To facilitate the distance between students and teachers in the teaching of intelligent Q & A requirements to solve the scale of the following grant education by time, space constraints of the problem, keep learning, timely adjustment of learning priorities, better improve their learning.

5.2 Which is conducive to the improvement of students' self-management quality and comprehensive quality evaluation.

This system has found a new and effective management mode in the management of student 's scale, and put forward the mode of student self - restraint and quality integral management system. To the end of the students of the evaluation results, performance management, sorting, control quality scores, identify self-gap, self-management and self-improvement.

5.3 The use of standardized, scientific and improve the level of student information management.

It is helpful for the teachers to grasp the information of the students in time and strengthen the management of the students. It is good for regulating the students' information management and improving the work efficiency.

6 CONCLUDING REMARKS

Based on the JAVA experimental teaching management platform for electrical design, improve the quality of teaching in our hospital will play a role in the process. To complete this design is very grateful to the teachers and the support of the college. But the design in some details need to be further improved, the design will be more perfect, more user-friendly presented in front of the user.

References

[1] TONG Li-jun.Design of motor simulation experiment system based on GUI function in MATLAB [J]. China Electric Power Education. 2010,185 (34): 160-162

[2] Gu Jianrong. And implementation of [D] Comprehensive education platform design JAVA based University of Electronic Science and Technology .2012

[3] Qiu Changli.Design and Implementation of Student Information Management System Based on Network B / S Structure [J]. Modern Information, 2009 (4).

[4] Zhu Lihong. Java-based platform for teaching affairs [D]. University of Electronic Science and Technology, 2007

[5] Yan Hong.Java and Patterns [M] Beijing: Publishing House of Electronics Industry 2002.

[6] Jiang Liqun, Jiang Shujuan, Shen Qi.Java network programming example tutorial [M]. Tsinghua University Press, 2005, first edition.

Soil Temperature and Humidity Monitoring System Based on Wireless Sensor Network

SONG Da-hu; HAN Jia-qi; CHEN Li-kai

(College of Instrumentation and Electrical Engineering,Jilin University,Changchun 130022,China)

***Abstract*—In agricultural production, it is important to grasp the environmental information of crop crops in real time. At present, China's precision agriculture development is still in its infancy, but the mechanization and intelligent development of agriculture must be the main trend of future agricultural development. Most of the existing agricultural information monitoring system uses wired data transmission, such a program for the complex farmland environment has great limitations. Therefore, this paper studies the wireless communication method which is more suitable for agricultural information collection. Based on the simple and low energy consumption of ZigBee technology, the soil moisture monitoring system based on ZigBee technology is studied[1~2].**

***Key words*—Wireless sensor network ZigBee Data acquisition.**

I. INTRODUCTION

THE monitoring and collection of farmland soil information is an important part of agricultural automation and informationization. At present, there are two types of farmland information monitoring system: one is based on distributed control structure, the other is based on field bus technology, they have a fatal problem, that is, through the cable transmission of data. Both structures are transmitted via cable, various sensors and actuators. As the wiring is complex, the farmland light is strong, and the soil has a certain acidity, making the system reliability and anti-jamming performance is reduced, increasing the difficulty of late maintenance, and wireless way can effectively avoid these problems[3~5].

ZigBee (also known as the purple bee protocol) is based on IEEE802.15.4 standard low-power LAN protocol, according to international standards, ZigBee technology is a short-range, low-power wireless communication technology. ZigBee technology has the characteristics of low distance, low complexity, low power consumption, low data rate, low cost and self-organizing network. It is suitable for automatic communication with Bluetooth and WIFI as an emerging wireless communication technology. Control of the field of sensors and actuators and other equipment networking. In the farmland monitoring system, the wireless sensor network based on ZigBee technology is used to realize the automatic detection and control of farmland soil information, which can effectively avoid the cable system problem.

II. THE DESIGN OF THE PROGRAM

According to the needs of soil moisture monitoring system, low complexity, low power consumption and low cost become important consideration for system design. The overall design of the system mainly completes the following work:

- Design a wireless network based on ZigBee technology, the network has three ZigBee equipment, namely, coordinator, router, terminal node. The terminal node in the farmland environment is responsible for passing the soil moisture content data received by the sensor through the router or directly to the coordinator. The coordinator transmits the received data to the host computer through the serial port. ZigBee technical standard transmission distance is 75 meters, and support expansion, can be a good solution to farmland soil information monitoring[6].
- Information monitoring of soil moisture in complex soils is bound to require high reliability of monitoring equipment and low energy consumption. The CC2530 has a different operating mode that can well ensure low energy consumption, and the CC2530 combines Texas

Instruments' industry-leading gold unit ZigBee protocol stack (Z-Stack), which provides a powerful and complete ZigBee solution[5].

- The Z-Stack protocol stack of ZigBee2007 specification is analyzed and researched, and the nodes of network construction, equipment binding, data acquisition, data transmission and data receiving are developed to realize the collection, transmission and reception of soil moisture data. Through the development of host computer software, the soil moisture data packet analysis, display and storage.
- The measured network.

III. SYSTEM HARDWARE DESIGN

A. System Overall Program

The ZigBee wireless sensor network designed in this paper is composed of a PC, a coordinator, a number of routers and a number of terminal nodes. According to the needs of the system, the terminal nodes are generally in different and far-off environment. When the direct communication between the terminal node and the coordinator is not too far away, the router is added as a relay to transmit the data transparently. The overall structure of the system is shown in Fig.1

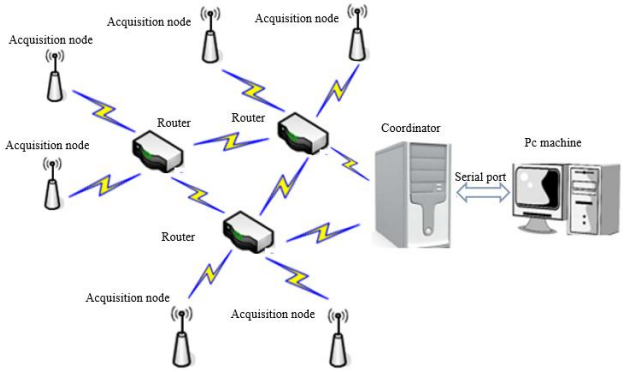

Fig.1 The overall structure of the system

First to the coordinator power, the coordinator to establish a good network, waiting for other nodes to join the network; sensor node after verification to join the network, will be given a 16-bit network address, then the address as the device logo. The sensor node reads the temperature and humidity data collected on the sensor and sends the data packet along with the 16-bit short address to the coordinator through the network. The coordinator transmits the packet to the PC through a fixed format. PC software to analyze the data packet, the temperature and humidity data display and storage. The staff can monitor the whole system through the host computer software, and real-time access to the location of each node temperature and humidity data.

B. System Hardware Selection And Design

- The system uses DHT11 digital temperature and humidity sensor. Choose DHT11, mainly taking into account its response to ultra-fast, anti-interference ability, cost-effective[2]. Compared to analog temperature and humidity sensors based on analog signal measurement, digital temperature and humidity sensor measurement more accurate.
- CC2530 core circuit design in strict accordance with TI's reference circuit, circuit shown in Fig.2.

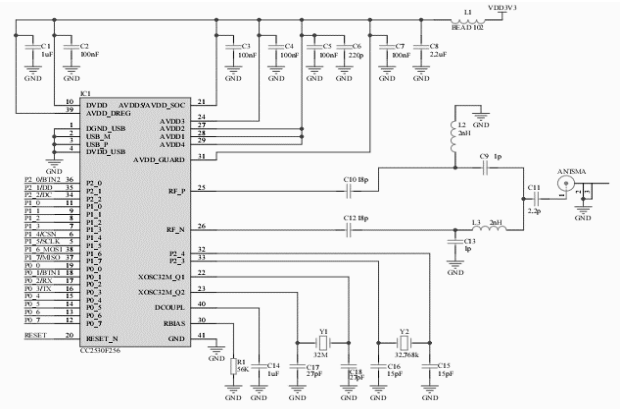

Fig.2 Circuit diagram of the CC2530 core circuit

IV. SYSTEM SOFTWARE DESIGN

This paper designs a ZigBee-based wireless sensor network, mainly by the coordinator, routers, terminal nodes. Coordinator is the center of this network, responsible for receiving data from the terminal node, and through the serial port to the PC, the host computer to complete the data analysis, display and storage. System software design includes: ZigBee protocol stack configuration, network construction program design, data transceiver, temperature and humidity data acquisition and PC software development.

A. System Software Development Platform Overview

First of all, zigBee protocol stack.This paper chooses TI's Z-Stack2007 protocol stack, which supports the coordinator, the router and the terminal node, taking into account the development cost, the difficulty degree and the protocol stack function. ZStack was named the ZigBee Alliance's highest

industry level by ZigBee's National Technical Services, which is widely used by many ZigBee developers around the world[1].

Secondly, zigBee device development software.In this paper, IAR Embedded Workbench for MCS-8051 V8.10 Evaluation (IAR-EW) as a system software development platform, the software set to compile and debug in one, to support the 8051 kernel chip programming. IAR-EW provides CC2530 and other SoC chip related configuration files, can save a considerable part of the workload. Also supports CC2530 development kit USB interface, to facilitate the program to download and debug.

Thirdly, application of Host Computer Development Software.This article uses labview2010 on the host computer display storage interface design. Labview is developed by the National Instruments (NI) company developed the program development tools, with a simple programming, readable characteristics, to facilitate the design and development of programmers[7~8].

B. ZigBee Device Communication

First of all,design.ZigBee protocol stack configuration.ZigBee network in a variety of operations need to use the protocol stack provided by the primitive operation to complete. Users in the specific application development, only by calling API interface to carry out, and no right to know ZigBee protocol stack to achieve the specific details. This article with ZStack-CC2530-2.3.0-1.4.0 protocol stack SampleApp design and development.

Z-Stack is executed by the main () function, the main () function completes the system initialization and starts the polling operating system, as shown in Fig.3.

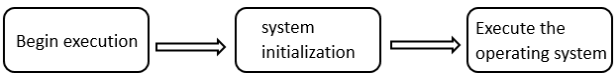

Fig.3 Main () function to perform the process

Secondly, Network construction program design The system uses the topology, which can effectively increase the coverage area of the network and enhance the system stability and reliability. Add the code "afAddrType_t SampleApp_P2P_DstAddr;" in the program SampleApp.c to communicate between devices in the form of on demand. "DemandApp_P2P_DstAddr" to reconfigure, increase the code in Fig.4.

```
SampleApp_P2P_DstAddr.addrMode = (afAddrMode_t)Addr16Bit; //点播
SampleApp_P2P_DstAddr.endPoint = SAMPLEAPP_ENDPOINT;
SampleApp_P2P_DstAddr.addr.shortAddr = 0x0000;            //发给协调器
```

Fig.4 Add the code in SampleApp_P2P_DstAddr

In the above code, the Z-Stack protocol stack specifies that the network address of the coordinator device is 0x0000.

Thirdly, Data transmission and reception. The format of the packets that communicate between the devices in the system is: 64-bit extended IEEE address + temperature and humidity data of the device.

- Gets the 64-bit extended IEEE address of the device.The ZigBee protocol stack has several ways to get the device 64-bit extended IEEE address. The system uses the global variable aExtendedAddress defined by OnBoard.c.
- Data transmission and reception.For data transmission, the point-to-point function "SampleApp_Send_P2P_Message" in the ZigBee protocol stack causes the terminal device to send the collected data to the coordinator.

Data receiving, search SampleApp_ProcessEvent, find the code if (events & SAMPLEAPP_SEND_PERIODIC_MSG_EVT), in which to increase the on-demand send function.

For the receiving side, the search finds SampleApp_MessageMSGCB, as shown in Fig.5.

```
case SAMPLEAPP_P2P_CLUSTERID:
 HalUARTWrite(0, pkt->cmd.Data, pkt->cmd.DataLength);
  break;
```

Fig.5 Add the code in SampleApp_MessageMSGCB

Fourthly, Temperature and humidity data collection The system uses DHT11 digital temperature and humidity sensor. DHT11 uses single bus data communication. A communication time of about 4ms, the data packet from the 5B (40Bit) composition. Data is divided by integer and fractional, high first. Data format: 8bit humidity integer input + 8bit humidity decimal data + 8bit temperature integer data + 8bit temperature decimal data + 8bit checksum data. The check data is equal to the last 8 bits of the first 4 bytes.

According to DHT11 transmission timing preparation of temperature and humidity acquisition program, the program mainly includes: delay function, 8-bit data write, DHT11 sensor start, read function.

C.Using Labview For PC Design

Coordinator will upload the data processing, summary, and then uploaded to the PC through the serial port, the host computer with Labview2010 to

write. Through the front and rear panel design of the host computer temperature and humidity display interface, but also can collect the temperature and humidity data storage. Labview front panel is a number of input and output controls, interface layout, etc .; rear panel is a block diagram, the main serial data read, packet analysis, data storage are in the back panel to operate.

V. SYSTEM TESTING AND ANALYSIS

After the previous work, has been completed based on ZigBee temperature and humidity sensor network design. This chapter will test and analyze the functions of the system networking and data transmission to detect the reliability and stability of the system.

A.Networking Test

The network capacity of the system to test, verify the network reliability and stability. The coordinator is powered on to form a simple network, where a router and two terminal nodes are powered up and authenticated to the access network. The use of the LED lights on the floor to show whether the success of networking: often off the identification of networking failure, flashing that is networking, flashing off that the network is successful. The networking is done as shown in Fig.6.

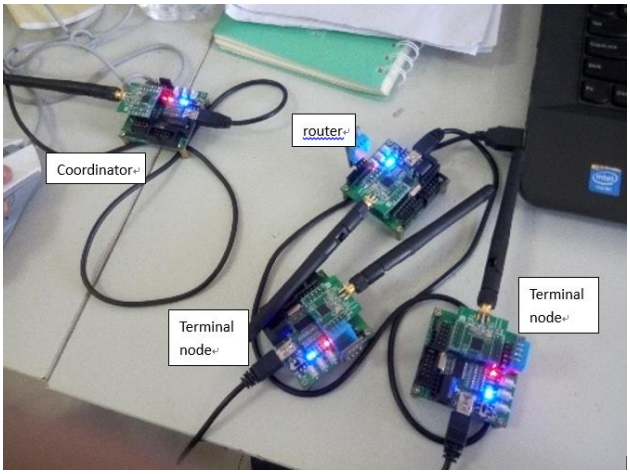

Fig.6 ZigBee network connection complete icon

B.Data Transmission And Display Testing

After the network is completed, the temperature and humidity sensor installed by the router and the two terminal collection node to collect the temperature and humidity information transmitted to the coordinator, the coordinator through the serial port display, the data shown in Fig.7.

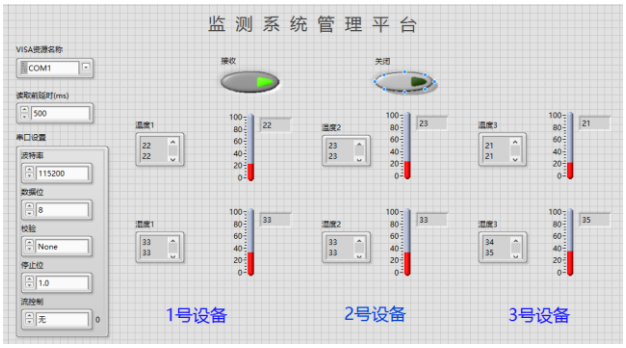

Fig.7 Data receiving display interface

VI. CONCLUSION

This paper designs a soil moisture monitoring system based on ZigBee, which mainly completes the work:

- This paper briefly introduces the development of ZigBee technology and its application at home and abroad in recent years, and puts forward the use of ZigBee technology to build a wireless sensor network to monitor the soil moisture situation.
- According to the case provided by TI, the scheme of wireless sensor network design is given, and the DHT11 digital temperature and humidity sensor is used to transplant the temperature and humidity acquisition function. The program of ZigBee protocol stack, design coordinator, router and terminal node is analyzed. Program, design PC software.
- The system for field testing, the completion of the temperature and humidity data collection and display.

Due to knowledge, ability and other aspects of the restrictions, the system there are some aspects to be improved:

- The system is only completed the monitoring of temperature and humidity data, the function is more single, adding to the environment control and regulation will be an improvement direction.
- The system of the host computer software function to be further strengthened, taking into account the real-time data and data storage, the establishment of computer database will be a good direction.

References

[1] JIA Ke-jin, WANG Wen-zhen, DU Tai-xing, QIAN Chun-yang, LIU Long-fei.Study on Soil Moisture Monitoring System Based on ZigBee Wireless Sensor Network [J]. Water Saving Irrigation, 2014, (03): 69-71 +74.

[2] Yan Lina, Wang Shunzhong, Zhang Tiemin.Design of temperature and humidity measurement and control system based on DHT11 [J]. Journal of Hainan Normal University (Natural Science Edition), 2013, (04): 397-399.

[3] Sun Yuwen.Study and implementation of farmland environmental monitoring system based on wireless sensor network [J]; Journal of Nanjing Agricultural University;

[4] Bu Yongbo, Luo Xiaoling, Chen Y. Temperature and humidity collection system based on DHT11 sensor [J] .Computer & Modern, 2013, (11): 133-135.

[5] Han Dan Ao, Faye Wong. DHT11 digital temperature and humidity sensor application research [J]. Electronic Design Engineering, 2013, (13): 83-85 +88.

[6] Wang Jianxun, Zhou Qingyun. Temperature monitoring system based on DS18B20 and LabVIEW [J]. Laboratory Research and Exploration, 2012, (03): 47-50.

[7] Zhao Qifeng, Min Tao, Yang Qianlong, Tian Yajun.Design of Data Acquisition System Based on LabVIEW Serial Port [J]. Computer Technology and Development, 2011, (11): 224-226 + 230.

[8] Li Junbin, Hu Yongzhong. Application Design of ZigBee Communication Network Based on CC2530 [J]. Electronic Design Engineering, 2011, (16): 108-111.

[9] Zeng Baoguo. Z-STACK protocol stack application development analysis [J]. Internet of things technology, 2011, (03): 71-73.

[10] Lvxiang Feng, GAO Honglin, Ma Liang, Wang Xinhua on LabVIEW serial communication [J]. Foreign Electronic Measurement Technology, 2009, (12): 27-30 + 42.

[11] Zhang Qisong, Yin Hang. Z-Stack analysis and its application in wireless temperature measurement network [J]. Journal of Computer Applications, 2009, (02): 103-105.

[12] Bao Junmin. ZigBee technology in the greenhouse monitoring system application [J]. Agricultural Mechanization Research, 2008, (02): 184-187.

[13] Xu Chao. LabVIEW in real-time measurement and control system application research [D]. Chongqing University, 2005. Application research [D]. Wuhan University of Technology, 2008.

[14] Dai Yuan. Research on farmland information monitoring based on ZigBee wireless sensor network [D]. Northwest A & F University, 2010.

Three - dimensional coordinate motion control system Based on Embedded System

CHEN Wu-nan; YANG Na; LIU Hao

(College of Instrument Science and Electrical Engineering, Jilin University, Changchun 130022, China)

***Abstract*—Motion control is a comprehensive application of mechanical, microelectronics, information, automatic control, sensor measurement, power electronics, interface and programming technology on the basis of scientific and technological development and industrial prosperity, and high performance, high quality and high Precision, high reliability, low energy consumption in the sense of a comprehensive system design and implementation of engineering technology[1-2]. The research and development of the coordinate motion control system is helpful to improve the measurement accuracy and efficiency of the coordinate measuring machine, so as to guarantee the product quality. Therefore, we design a three-dimensional coordinate motion control system based on msp430 single chip microcomputer. The LABVIEW software is used to control the stepping motor of the control system to realize the positioning motion of the three-dimensional coordinates in space.**

***Key words*—Host computer Stepper motor Three-dimensional system Positioning control**

I. INTRODUCTION

THE three-dimensional coordinate motion control system is used for precision control, to achieve in the case of not suitable for manual operation, the object measurement and positioning, it studied the object, including all controlled displacement, speed or acceleration and other electromechanical variables feedback control system[4-5]. The Through the upper computer input instructions, through the serial communication will be sent to the lower computer to the implementation of the instructions. This article uses LABVIEW design PC interface, enter the X, Y, Z three-dimensional coordinates, automatically determine the positive and negative, to reach the specified location.

II. SYSTEM WORKING PRINCIPLE

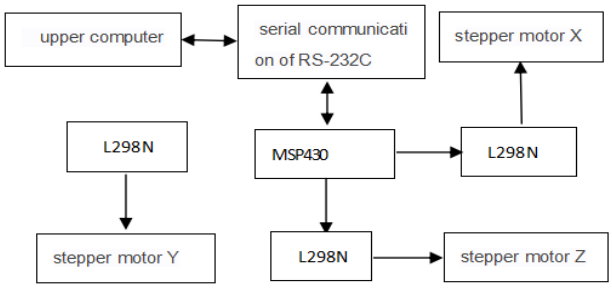

Fig. 1. The overall structure of the system block diagram

As shown in Figure 1: In the PC using labview software design PC control interface through the USB serial port communication, to the MSP430 single-chip microcomputer sends control commands, the microcontroller decodes the control signal sent to the L298N drive module, so as to stepper motor control pulse control three directions Automatic recognition of the motor is reversing and moving distance, that is, to achieve the system's three-dimensional positioning function[7].

III. THE HARDWARE DESIGN OF THE SYSTEM

A. Communication Section

Because the system is mainly controlled by the host computer, so the lower computer and the host computer to communicate between, choose to use RS-232 protocol for communication, PC serial port output RS-232 signal is based on a 3 ~ 7V Voltage, 3 ~ 7V negative voltage pulse chain. This voltage signal needs to be converted to a pulse chain of 0 to 5V for the processor to read and convert the circuit using the MAX232 chip. The MAX232 chip contains a supply voltage converter that converts the + 5V voltage to a voltage of -10 to + 10V required for the RS-232 output level. So only need a +5 V power supply to the system on it.

To achieve the host computer and the next bit of data communication, the host computer and the lower

computer communication format, the baud rate must be consistent, we are using the MSP430 the UART mode, with USB to RS232 serial line to achieve communication with the PC, data format 8,1, N, baud rate 4800, the data transmission to rely on the interrupt to complete. UART is a generic asynchronous serial interface short, its structure is:

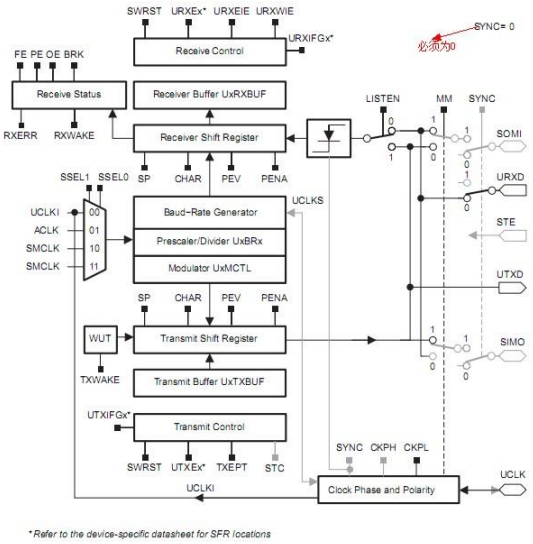

Fig. 2. Schematic diagram of UART

As the experimental requirements to achieve positioning, 16-bit conversion is not easy on the amount of displacement, and can only transfer 8-bit data, it can only transfer hexadecimal number or character that its corresponding ascii code, so the need for input machine string, The lower computer decodes the number.

B. L298 Drive Circuit

L298 drive, L298N is ST's production of a high voltage, high current motor driver chip. The chip is packaged in 15 feet. The main features are: high voltage, the maximum working voltage up to 46V; output current, instantaneous peak current up to 3A, continuous operating current of 2A; rated power 25W. A high-voltage, high-current full-bridge driver with two H-bridges can be used to drive inductive loads such as DC motors and stepper motors, relay coils, and standard logic level signals. With two enable control terminals, Without the impact of the input signal to allow or prohibit the device work has a logic power input, so that the internal logic circuit part of the low voltage operation; can be an external detection resistor, the amount of change back to the control circuit. Using the L298N chip drive motor, the chip can drive a two-phase stepper motor or a four-phase stepper motor, or two DC motors.

In order to avoid the interference of the motor on the microcontroller, the module to join the optocoupler, optical isolation, so that the system can be stable and reliable work. As shown below.

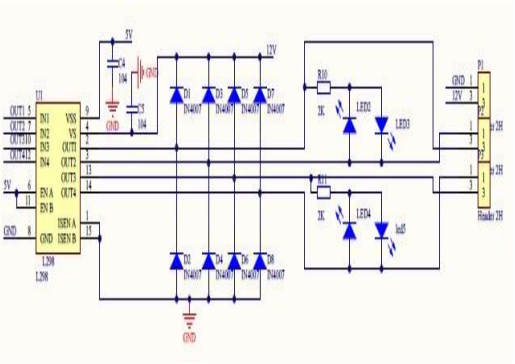

Fig. 3. L298 drive circuit

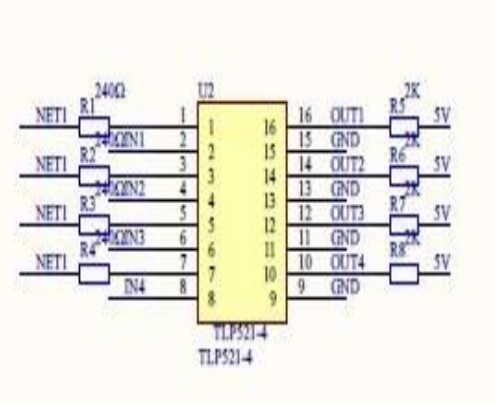

Fig. 4. Optocoupler isolation circuit

IV. HOST COMPUTER DESIGN

After installing the LABVIEW software on the PC, you will need to install the VISA driver and the VISA package. After the installation is successful, the serial port is required for our communication. After the package is installed, we need to design a simple interface, easy to operate, with good human-computer interaction interface.

First set up the communication-related serial communication module, in the front panel control → I / O → VISA resource name set the serial port, and then set the serial port, and its value initialization, set the baud rate, data bits, parity bit, stop Bit and flow control, the corresponding set to communicate with the lower computer, in the back panel diagram to write VISA serial port settings, located in the function panel → instrument I / O → serial port → VISA configuration serial port, VISA configuration serial port function can be connected through the serial port

The VISA write function, the VISA write function, the VISA write function, the VISA write function, and the VISA write function in the function panel → the instrument I / O → serial port. The VISA write function writes the data written to the buffer into the VISA resource name specified device And the interface; the VISA read function reads the specified number of bytes from the serial port specified by the VISA resource name and returns the data to the "read buffer"; the VISA close function closes the session handle or event object of the specified serial port. Add a simple error handler at the end of the program to make a better error. After the entire host computer program is set up with the lower computer after the joint, the positioning coordinates input to the front panel to control the movement of the stepper motor to reach the development location[3][8][9][11][12].

The program front panel and the program block diagram are as follows:

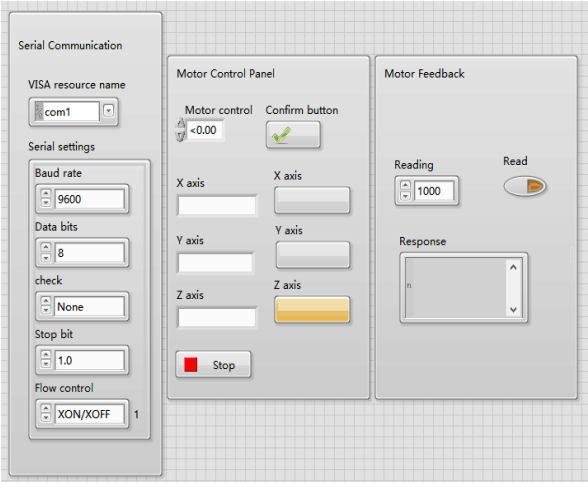

Fig. 5. Host computer control interface

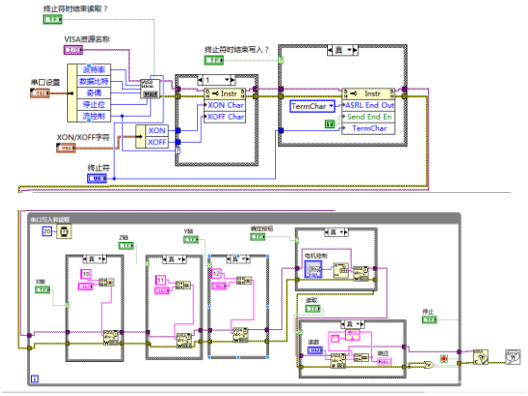

Fig. 6. Host computer rear panel program interface

V. SOFTWARE PART

A. Stepper Motor Control

The stepper motor is an open-loop control element that converts an electrical pulse signal into angular displacement or line displacement. In the case of non-overload, the motor speed, stop the location depends only on the pulse signal frequency and pulse number, without load changes. We use the 57BYG model of hybrid (permanent magnet induction type) stepper motor is a two-phase four-wire stepper motor, it works the way the whole step and half-step way. The whole step can be divided into single four and double four beat, half step is and single, double eight beat. In order to make the system more accurate positioning, so this article uses eight beat work that is: A, AB, B, B / A, / A, / A / B, / B, / BA The Step angle of 0.9 degrees, the motor rotation of a week need 400 pulses, the frequency of the pulse to control the motor speed, through the control of the pulse to control the motor to the steering, by controlling the number of pulses to control the motor stop position, So as to achieve the purpose of positioning.

B. Single Chip Program Flow Chart

Through the host computer interface on the X, Y ,, Z three-axis selection, single-chip select the output port, enter the number of steps of the instructions, through the screw and stepper motor step angle requirements, you can calculate the stepper motor rotation The distance, through the corresponding single-chip stepper motor to a certain number of pulses[6][10].

VI. TEST RESULTS AND ANALYSIS

The host computer control interface design is completed, the next bit machine program is completed, the host computer and the next bit machine through the serial port connection, the hardware drive circuit, stepper motor, the next bit to connect, check the connection line to test, open the host machine LABVIEW control interface input Three-dimensional coordinate command, click the confirmation command stepper motor according to the instructions to move and reach the specified location. After testing, the motor reaches the specified location, although there are certain errors, the basic realization of the design function.

VII. CONCLUDING REMARKS

With the help of instructor teacher Li Zhe, we designed the coordinate motion control system, which has the characteristics of friendly human-computer interaction, simple programming and high efficiency. Through the test, we designed the coordinate motion control system to accurately control the movement of the stepper motor, and achieved the desired results. Thanks for the help of the teacher and the efforts of the team members.

References

[1] Gao Dengbo. Development and Trend of Motion Control Technology [J]. Science and Technology Information, 2007, 32: 72

[2] Ruan Yi, Chen Weijun editor. Motion control system [M]. Beijing: Tsinghua University Press, 2006

[3] Wang Junfeng, Song Wenai, Liu Zhe. Virtual Experiment System for Signal Processing Based on LabVIEW [J]. Foreign Electronic Measurement Technology. 2006 (10)

[4] Xi Zhigang, Zhou Hongfu. Development and status of motion controller [J]. Machine tools, 2005, 4: 5-10

[5] Wu Hong, Jiang Shilong, Gong Xiaoyun, Lv Shu, Li Xiaohui, Yang Zhaohui, Wang Rui, Li Jiulin. Current situation and development of motion controller [C]. CMES (Manufacturing Technology and Machine Tool) 2003 Annual Album, 2004: 24.27

[6] Leng Zengxiang. Overview of motion control system [J]. Jiangsu Mechanical and Electrical Engineering, 1995, (3): 35-44.

[7] Feng Xiubin. Embedded motion controller based on ARM and DSP [J]. Manufacturing Automation, 2009,31 (4): 27-28

[8] Chen Hong, Chen Xin.Study on Single Chip Microcomputer Pulse Generator Based on LabVIEW [J]. Modern Electronics Technique, 2008 (03)

[9] Chen Long, Zhang Xinzheng, Deng Chan.Lab VIEW Control Parallel Communication of Stepping Motor [J]. Electronic Testing. 2007 (10)

[10] Xiong Rong, Shan Yuekang, Zhang Zhi, Zhang Xiancheng.Study on Automatic Zero Cutting System of Steel Tape [J]. Journal of China Institute of Metrology, 2006 (04)

[11] Zhao Dongmei, Zhang Bin.LabVIEW control stepper motor automatic speed [J]. Microcomputer Information. 2006 (28)

[12] Chen Fangquan, Li Jianzhou, Ma Siwen, Fang Yudong. Design and Application of Stepping Motor Based on LabVIEW [J]. Journal of Shanghai University (Natural Science Edition). 2006 (01)

Design of the senor for proton rotation magnetometer based on differential coil mode and test circuit

Mu Huai-zhi; Zhu Kai; Liu Jin-xin; Zhang Chun-xiu

(College of Instrumentation & Electrical Engineering,Jilin University, Changchun 130061,China)

***Abstract*—Proton rotation magnetometer is develop according to the principle of Larmor rotation of proton, used for magnetic exploration in major, which is one of the most widely used magnetometer. Design of the senor for proton rotation magnetometer is the key to the research of proton rotation magnetometer. Currently proton rotation magnetometer which is made in China significantly inferior to import ones. Aiming at the poor anti-interference ability and stability of domestic sensors, the test design a senor for proton rotation magnetometer based on differential coil mode,solidification use POM material. Explore test circuit, including polarization circuit, tuned circuit, pre-amplification circuit, filter circuit and frequency measurement circuit .The experimental results show that the sensor's performance is better than that of domestic senor.**

***Keywords*—differential coil,senor for proton rotation magnetometer,Larmor rotation,anti-interference ability,sta-bility,Signal conditioning**

I.INTRODUCTION

PROTON precession magnetometer is based on Larmor precession principle. Larmor precession principle is that when atomic nucleus with a spin and magnetic moment characteristics is in the external magnetic field, it will be subjected to a moment T which is perpendicular to magnetic permeability and magnetic flux density. The direction of spin angular momentum P is influenced by the moment of the role of T[1-3] . The mode is unchanged while the direction is changed continuously. In China,Proton precession magnetometer is mainly used in electromagnetic exploration and engineering survey.

At present, the technical indicators such as magnetometer sensitivity and measurement accuracy of Canada GSM company were higher than similar products,causing the monopoly of the industry as a whole.As the front end of the instrument,The performance of proton precession magnetometer sensor is the decisive factor.The domestic magnetometer sensor has many problems in the current study, such as process and test level most of the traditional standard,the receiving coil structure and curing material performance is poor due to the late start.The gap of performance between domestic and imported magnetometer is significant,causing that many domestic research still need to rely on imports. Therefore research on a magnetometer proton precession magnetometer sensor take a heavy burden and embark on a long road.

II.MEASURING PRINCIPLE

By the physics,the protons with positive charge have spin characteristics, so the proton will produce closed current and produce spin magnetic moment.Under the influence of external magnetic field,magnetic moment of proton will do the Larmor precession around the external magnetic field as shown in Figure 1.This paper uses the precession of the magnetic moment of the proton which is analyzed in the rectangular coordinate system by using the classical physics theory.

The first order derivative of the moment P of the moment of the magnetic moment M affected by the earth's magnetic field T is equal to the moment.Due to $\vec{M}=\gamma_P \vec{P}$ (γ_p is Proton spin ratio constant)，We can derive formula(1).

$$\frac{d\vec{M}}{dt}=\gamma_P \frac{d\vec{P}}{dt}=\gamma_P[\vec{M}\times\vec{T}]=\begin{vmatrix} \vec{i} & \vec{j} & \vec{k} \\ M_x & M_y & M_z \\ T_x & T_y & T_z \end{vmatrix} \quad (1)$$

In order to facilitate the calculation，we can make

TZ be equal to T（magnetic field of the earth）,TX and TY are equal to zero. When we bring this condition into the (1) solution,we can get three components of the magnetic moment which are respectively shown in(2) (3) (4).

$$\frac{dM_x}{dt} = \gamma_p M_y T \tag{2}$$

$$\frac{dM_y}{dt} = -\gamma_P M_x T \tag{3}$$

$$\frac{dM_z}{dt} = 0 \tag{4}$$

The first derivative of (2) can be solved

$\frac{d^2_{M_x}}{dt^2} + \gamma_p^2 T^2 M_x = 0$,its solution is

$$M_x = A\cos(\gamma_p T_t + \varphi) \tag{5}$$

$$M_y = -A\sin(\gamma_p T_t + \varphi) \tag{6}$$

$$M_z = Const \tag{7}$$

So

$$M = \sqrt{M_x^2 + M_y^2} = Const \tag{8}$$

By the formula (5) - (8), we can see that the magnetic moment M is projected on the X axis according to the cosine law, and is projected on the Y axis according to the sine law. The M of the magnetic moment in the Z axis is fixed. It can be seen from Figure 1 that the magnetic moment M is invariable in the XY plane and the direction changes continuously, that is, in the XY plane.

In summary,Proton magnetic moment M under the action of geomagnetic field T,Precession of the earth's magnetic field,Precession angular frequency ω ,which is called Larmor frequency.

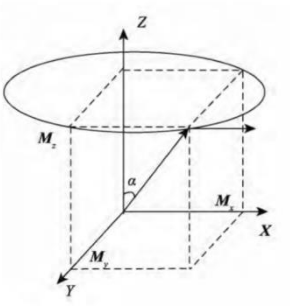

Fig.1 Schematic diagram of precessing of magnetic moment M

According to formula (5) and (6),we can get $\omega = \gamma_p T$;due to $\omega = 2\pi f$,we can get precession frequency is shown in formula(9).

$$f = \frac{\gamma_p}{2\pi} T \tag{9}$$

In formula（9） $\gamma_p = 2.6751 S^{-1} T^{-1}$. Therefore, it is concluded that the relationship between the geomagnetic field intensity T and the precession signal frequency f is shown in formula(10), (11).

$$T = 23.4874 f(nT) \tag{10}$$

$$f = 4257.8 T(Hz) \tag{11}$$

As can be seen from the above, the precession frequency f is proportional to the geomagnetic field intensity T. If we want to get the size of the magnetic field T, we need to indirectly measure the precession frequency f.

In this paper,the magnetic field range which the sensor can measure is 20K-80KnT while the corresponding frequency range is 852.52-3406.08Hz.

III. Sensor Design

A.Coil winding method

Sensors in the actual use of the process, will be subject to a variety of external interference, such as power frequency interference and high frequency interference. The unwinding signal received by the coil at the microvolt level (less than the noise amplitude) is easily submerged by noise[5]. In this paper, in the sensor design to take two reverse coil series differential structure in order to replace the conventional sensor single coil mode, while the use of transceiver one, as shown in Figure 1.Its advantages are as follows:

(1) Reduce the distribution of capacitance:First, there is a non-negligible distributed capacitance between the layers of the coil, and the existence of this phenomenon will cause the subsequent signal processing resonant circuit center frequency point deviation, serious when the immersion signal attenuation, While the noise signal gets a larger gain [6-7].

(2) To suppress external interference[8]: theoretically, two reverse coil parameters are identical. By Lenz's law we can see that due to external

interference in the sensor output generated by the induced electromotive force and the absolute value of the same phase, the opposite direction, that is completely offset. The actual two coils can not guarantee the same parameters, but this differential structure can also inhibit the noise to a certain extent, improve the sensor anti-jamming capability.

(3) The sensor polarization and the intake signal is not synchronized to carry out.If the polarization coil and the receiving coil are respectively made, the increase in the size of the sensor is not conducive to carrying the use. Therefore, in order to reduce the sensor volume, the polarization coil and the receiving coil into one, that is, send and receive one coil.

B. Selection of Hydrogen Proton Solution

According to the proton spin-on magnetometer magnetometer, the polarized material needs to be rich in hydrogen protons. Table 1 lists several hydrogen-rich proton solution and its relaxation time, stability and other parameters[9].

Tab.1 Parameters of solution rich in hydrogen proton

Solu-tion	Chemical formula	T1/s T2/s	Freezing Point/℃	Other
Gly-cerol	$C_3H_8O_3$	0.04 0.03	17	Less Volatile
Kero-sene	C_8H_{18}	0.50 1.00	-47	Volatile
Alco-hol	C_2H_5OH	2.00 3.60	-114	Volatile
Water	H_2O	2.30 3.00	0	Volatile/ Instable

In atomic physics, the process of the nucleus returning from the intensified state to the equilibrium arrangement is called the relaxation process, and the time it takes is called the relaxation time [10]. The relaxation time is divided into spin-lattice or longitudinal relaxation time T1 (the time required for the reaction hydrogen proton to be fully polarized) and the spin-spin or transverse relaxation time T2 (reaction take-in signal decay rate). Observed in Table 1, the parameters of various solutions we can see that glycerol lateral relaxation time is short, and solid at room temperature, is not conducive to the late signal processing and measurement; alcohol and water horizontal relaxation time and longitudinal relaxation time are longer , And volatile. So it is not suitable for being polarized. Kerosene of the parameters are to meet the design requirements, so the choice of kerosene as a polarized material.

C. Sensor Curing Material

Using the POM as a sensor curing material to solve the problem of easy deformation of materials to improve the stability of the field and the use of anti-pressure sensor capacity. At the same time the POM material resistant to aviation kerosene corrosion [11].

IV.SYSTEM HARDWARE CIRCUIT

The hardware circuit designed in this paper is composed of controller, signal conditioning module and frequency measurement module. The controller is composed of STM32 and FPGA. The signal conditioning module is composed of a controller, a polarization circuit, a harmonic circuit, a preamplifier circuit, a filter network and an addition circuit. The frequency measurement module is composed of a controller, a shaping circuit, Screen composition. System hardware block diagram shown in Figure 3.

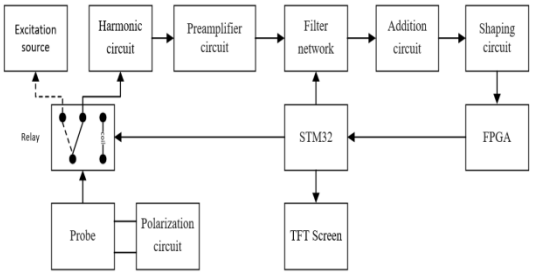

Fig.3 System hardware block diagram

A.Polarization Circuit

Because the geomagnetic field is very weak, it is not feasible to use the coil to sense the weak advancing signal directly, and a new proton macro magnetic moment is usually used to enhance the signal amplitude[4]. The so-called polarization is the coil in the external magnetic field excitation, the solution of the proton magnetic moment will be perpendicular to the direction of the magnetic field deflection process.

The polarization method used in this paper is to control the constant current in the polarization coil is used to control the excitation field to open and turn off. After the end of the polarization need to cut off the

excitation field as soon as possible, and the coil and the switch connection voltage quickly reduced to ensure that the proton around the magnetic field of the normal advance. If the relay switch is used to control the current on and off alone, the voltage across the coil after the end of the polarization will cause a large negative induced electromotive force due to the inductance of the coil, which will damage the relay for a long period of time, and this will result in a large reception of subsequent signals influences. By the design of the polarization circuit as shown in Figure 4 shown in the circuit, in the end of the sensor parallel to the diode and ordinary diode [13].

As can be seen from the beginning of the polarization, due to the one-way conductivity of the diode, the coil will normally generate excitation field. When the polarization is completed, the resulting negative induced electromotive force will break through the zener diode, isolating the voltage at which the coil is in contact with the switch.

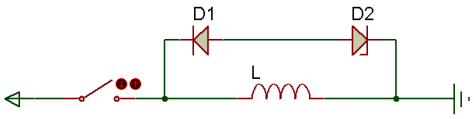

Fig.4 Simple schematic diagram of polarization circuit

B. Harmonic Circuit

When the polarization is complete, the sensor coil will receive the proton spin signal -the Larmor signal. The Larmor signal is a sinusoidal signal attenuated with the e-index, which is usually accompanied by noise interference in the external environment, and the measured Ramos signal spectrum is shown in Figure 5.

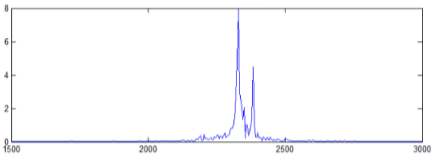

Fig.5 Spectrum of Larmor signal

As can be seen from the spectrum, the signal consists of many frequency components. Where the frequency component corresponding to the maximum value in the spectrum is the frequency to be measured. It is necessary to select the frequency component from the Ramor signal.

In this paper, the LC series resonant method is used to select and amplify the signal. LC series resonant circuit schematic diagram and the amplitude and frequency characteristics of the curve shown in Figure 6-7.

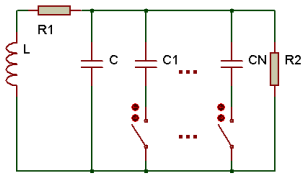

Fig.6 Schematic diagram of LC series resonant circuit

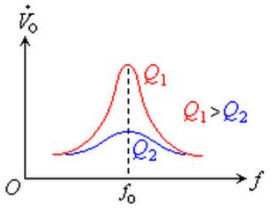

Fig.7 Amplitude frequency characteristic curve of LC series resonant circuit

From the amplitude-frequency characteristic curve, when the circuit resonates, the signal can be amplified at the resonant frequency, at other frequencies outside the bandwidth gain quickly decay. The conditions for resonance are as follows.

$$jwL + \frac{1}{jwC} = 0$$

The resonant frequency is given

$$f = \frac{1}{2\pi\sqrt{LC}}$$

You can see the probe inductance is constant, just control the state of the switch to change the size of the harmonic capacitor, you can change the resonant frequency, to achieve the purpose of frequency selection.

The resonant circuit quality factor is

$$Q' = \frac{R_2 Q}{Q^2 R_1 + R_2}$$

The resonant loop bandwidth is

$$BW = \frac{f}{Q'} = \frac{R_1}{2\pi l} + \frac{2\pi l f^2}{R_2} \text{ [14]}$$

Therefore, if only the signal component at the resonant frequency is amplified, the smaller the bandwidth, the better the quality factor is.

Where the probe inductance L = 34.2mH, the probe resistance R1 = 5.9Ω, the selected frequency resistor R2 = 1K, so the harmonic capacitance C range of

60-1030nF.

C.Preamplifier Circuit

When the signal into the selected frequency, although the amplification, still relatively weak, the need for further amplification, and ultimately the signal can be amplified to measurable range. In the process of signal amplification process, a series of noise is introduced, which needs to be processed by filter network. The design of amplifying and filtering circuit based on the LM258 is shown in Figure 8.After filtering and amplifying the signal, it is necessary to introduce the bias through the addition circuit to obtain the final measurable sinusoidal signal.

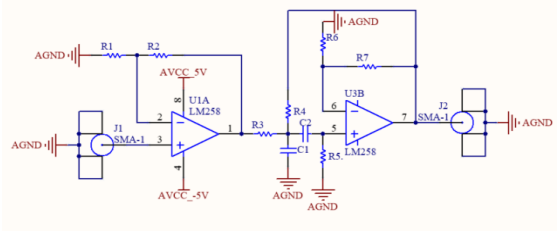

Fig.8 Amplifying and Filtering Circuit

D. Frequency Measurement Module

The design of frequency measurement module to FPGA as the core device, complete the signal frequency parameter measurement. The pre-zero-crossing comparison and hysteresis comparison will be measured signal conditioning to measurable square wave. The design of conditioning circuit based on the ADA4817 and AD8561 is shown in Figure 9. FPGA and STM32 through the SPI protocol to communicate, STM32 by sending different instructions to complete the FPGA measurement. STM32 completes the post- processing of the measurement data and displays the measurement results on the TFT LCD screen.

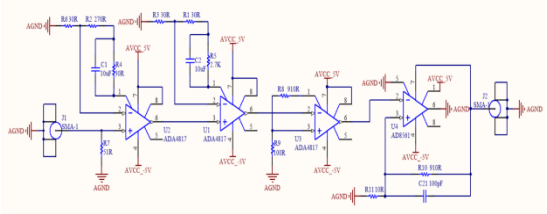

Fig.9 Conditioning Circuit

V.Analysis of Experimental Results

In this paper, some of the modules were tested separately, and then the whole machine test, and the results given a reasonable analysis.

A. harmonic circuit test

The dynamic signal analyzer is used to test the characteristic of the harmonic circuit, and the input signal is Gaussian white noise. The test data is shown in Table 2.

Tab.2 The data of testing of tuned circuit

Center frequency/Hz	BW/Hz
850	10.3
1000	11.2
2000	8.8
3000	12.6
3406	11.0

According to the previous article, the sensor design can measure the magnetic field range of 20000-80000nT, corresponding to the frequency range of the Larmor signal 852.52-3406.08Hz. Harmonic circuit can achieve frequency selection function within the 850-3406Hz according to the data.

B. Frequency Measurement Circuit Test

The input signal is provided by SIGLENT's SDG5162 signal generator, and the test data is shown in Table 3.

It can be seen from the test results that the frequency measurement circuit designed in this paper can accurately measure the frequency in the frequency range of 800 ~ 3500Hz, the relative error of measurement is less than 0.01%.

Tab.3 The data of testing of frequency measurement circuit

Input signal frequency/Hz	Input signal Effective value/V	Measured value/Hz
800	1	800.0039
1500	1	1499.9989
2500	1	2500.0002
2500	1	2500.0017
3500	1	3500.0000

C.Machine Test

Five experiments were carried out on the electromagnetic laboratory, in which the magnetic field was generated by Helmholtz coils.The measured data are shown in Table 4. Analysis of the experimental results, we can see the design of the proton magnetometer sensor, compared to GSM company representative of the imported magnetometer sensor still has a certain gap, but better than similar domestic sensors.

Tab.4 The data of testing of the complete machine

Number	The Sensor/nT	GSM-17T/nT
1	54701.5	54702.2
2	54701.7	54702.1
3	54702.3	54702.2
4	54701.5	54702.2
5	54703.0	54702.3

The test signal is shown in Figure.10

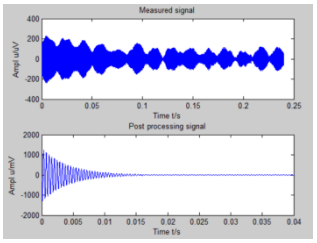

Fig.10 Spectrum of rotation signal

VI..CONCLUSION

In this paper, the magnetism principle of proton spin-on magnetometer is described in detail. Aiming at the problem of anti - jamming ability and poor stability of traditional proton spin - on magnetometer sensor, the differential coil structure is designed and the steel material is used as the sensor skeleton. The difference between the parameters of the polarized solution is analyzed, and the kerosene is used as the sample solution to enhance the initial amplitude of the spinner and improve the signal-to-noise ratio. In this paper, the design of the test circuit, including the polarization circuit, harmonic circuit, preamplifier circuit, filter network, etc., the analysis of the various modules in the test circuit function, and test their performance, respectively, to achieve the desired goal. Machine test, observe the received Larmor signal, and its spectrum. By testing the frequency of the Larmor signal, indirectly obtained magnetic field strength, compared to find better than similar domestic sensor.

References

[1] WU S SH,DAI G X,LIU G CH,et al.An Experimental Study of Proton Free Precession in a Weak Magnetic Field and Its Application to Filed Work[J].Acta Physica Sinica.1965, 21(6): 1175-1187.

[2] GUAN ZH N.Geomagnetic Field and Magnetic Prospecting[M]. Bei Jing: Geological Press,2005.8.

[3] SUN Sh Q, L J, ZHANG Q W, JI Y J,et al.The Investigation of Hydrogen Macroscopic Nuclear Relaxation. Geophysical and Geochemical Exploration, 2005, 29(2): 153-156.

[4] GE J,ZHAO ZH ZH,DONG H N,et al.Design of the Magnetic Field Sensor for Proton Precession Magnetometer Based on DC Pulse polarization[J]. Chinese Journal of Scientific Instrument. 2014, 35(4):850-858.

[5] ZHANG F,HU Y F,et al. Study on Measurement of Super Magnetic Field by Nuclear Magnetic Resonance[D]. Huazhong University of Science and Technology,2009.

[6] SHAO Y Q,WANG Y ZH,CHENG D F,et al．Development of broad frequency band magnetic field sensor based on flux feedback[J].Chinese Journal of Scientific Instrument,2010,31(11):2461-2466.

[7] GUO Y,LU Y K,CHEN B．Research and design of a high performance sensor with alternating low frequency magnetic field[J].Chinese Journal of Sensors and Actuators,2005,18(3):493-495.

[8] WANG Y J,LI W,SUN SH Q,et al.Design for proton rotation magnetometer based onMSP430[J].Journal of Jilin University: Information Science Edition, 2006, 24(3): 336-340.

[9] PAWAR V P,MEHROTRA S C.Dielectric Relaxation Study of Dimethylene Chloride Withethanol Using Time Domain Reflectometry[J].Journal of Molecular Liquids,2003,108(3):95-105.

[10] YI X F,LIN J,DUAN Q M.Research and Development of Portable Nuclear Magnetic Resonance Groundwater Exploration Instrument Based on Double-turn Coils[J].Chinese Journal of Sensors and Actuators,2013,34(1):1-10.

[11] CHENG Y H,LI Y Y,LIU Y.Development and Application of POM Products at Home and Abroad[J].Engineering Plastics Application,2009,37(9):59-64.

[12] ZHAO ZH P，DONG H B．Design of the Low Power Consumption and High Precision Proton Magnetometer[J]. Petroleum Instruments,2007,21(2):13-15.

[13] REN Q CH.The Circuit design of proton precession magnetometer[D]. Jilin University, 2012.

[14] XIAO P.Design and implementation of JPM-1 proton precession magnetometer analog circuit[D].Jilin University,2014.

Teaching System of Virtual Instrument Based on LabVIEW Design and Management System

Wang Shu-hui; Zhang Wen-yang; Xia Shan
(jilin university instrumentation and electrical engineering institute,Changchun 130061)

***Abstract*—Introduces the application of virtual instrument in experiment teaching of nature and necessity, detailed experimental teaching management system of virtual instrument based on LabVIEW implementation. Through the creation of virtual instrument test system, database and network technology, the establishment of databases, development of network virtual laboratory management system, give full play to the advantages of virtual instruments, to maximize hardware resource sharing. Based on a popular virtual instruments development software developed by LabVIEW virtual instrument test system, for example, analyzes the networking of virtual instrument in the experiment teaching of advantage.**

***Keywords*—LabVIEW, virtual instrument, experimental management system**

I. INTRODUCTION

IT is an irresistable trend that using the computer and network technology to change the traditional experimental teaching mode in computer and network era. Virtual instrument system is the product of the combination of computer and network technology and traditional instrument technology.As a hot spot in the field of automation instrumentation,virtual instrument is concerned by people widely with each passing day.Colleges take up the heavy responsibility of cultivating innovative talents for the country.However,most of teaching experimental instruments used in many colleges are still quite backward and traditional in China,which have stiff price， slow update speed and non-customizable function.In order to reform the experimental teaching method,reduce equipment costs and improve equipment utilization,it has become a new trend to introduce virtual instrument into experiment teaching.

II. INTRODUCTION OF VI AND LABVIEW

A. Virtual Instrument

Virtual instrument,taking computer as the core and combining computer with measurement system,is a kind of measuring instrument.It uses computer software to replace some hardware functions of traditional instruments and utilizes computer monitor as a substitute for traditional instrument pane."Virtual" can be understood from two aspects.First,although some of the hardware in the traditional instrument is replaced by software,Its function still exists.Second,it can achieve the function of a variety of traditional instruments with the same set of hardware system as a result of the characteristic that changing the software can change the function of the instrument.Therefore,virtual instrument can meet the needs of all kinds of measurement system maximumly.It can be easy to modify or increase the function of the instrument by modifying the software,and thus truly reflects a new concept which software is the instrument.As with traditional instruments,virtual instrument consists of data acquisition and control, data analysis and processing and result display[1].

B. Virtual Instrument Development software LabVIEW

LabVIEW,which can complete the simulation,data acquisition,instrument control,measurement and data analysis and other tasks,is a graphical development environment with a large number of built-in functions[7].Using LabVIEW,you can also establish a connection with different applications by means of the Internet,ActiveX,DLL, shared libraries,SQL,tcp/ip,XML,OPC,wireless communications or other ways.The program developed using LabVIEW development platform is called virtual instrument program and referred to as vi.The VI consists of 3 parts:the program front panel,block diagram program and icon /connector.Front panel is used to set the input control and output numerical

observation, simulated instrument panel.Each front panel corresponds to a block diagram.The block diagram using LabVIEW graphical programming language,it can be understood as the traditional program source code.Icon/connector is the interface used for calling Sub VI by other VI[2].

III. DESIGN OF EXPERIMENT MANAGEMENT SYSTEM

A. The Scheme of Experiment Management System

The virtual instrument is developed on the LabVIEW platform, using the setting of LabVIEW can set remote release,the background using the access database for data management.In the experimental process,the students can use the virtual instrument developed by LabVIEW for writing the experimental data and waveform in this machine file in real time.The system architecture is shown in Figure 1.

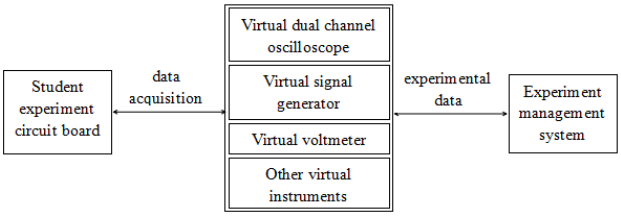

Fig.1. The Structure of Laboratory Management System Based on LabVIEW

As shown in Figure 2, the students entered the client loginfrom the students.Then they write the experimental data and waveform in real time to a local machine file with using the powerful LabVIEW file about reading and writing functions in the course of the experiment. When the experiment was completed in accordance with the requirements of the students fill in the experimental data, upload test report to the application server.

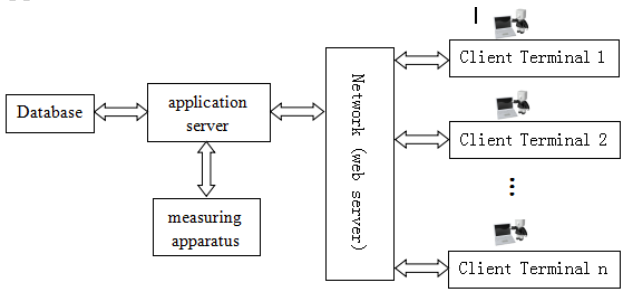

Fig.2. Implementation Mode of Online Virtual Lab

B. Function of Experiment Management System

This laboratory management system function module has the following parts:

1)Electronic Login Module

For a complete system,it is necessary to have a client to verify the top-level program, this program is the login program,which includes landing and registration.Login requires the correct user name and password.And then comparing with the access database in background, it will be successful if match the same results.Registration requires students to create their own user name and password.Laboratory management system users are divided into two categories: administrators and students.Administrator is the highest level.He ensures the normal operation of the system and responsible for the creation of the corresponding database tables.At the time,he can add or delete student accounts, teachers account.The landing interface is shown in Figure 3.

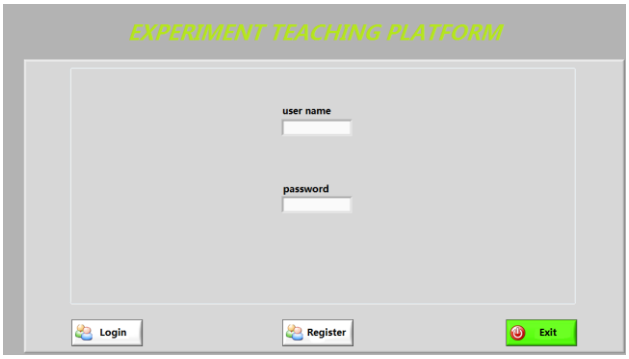

Fig.3. login interface

2)The Scheme of Experiment Management System

When the user verifies the login is successfully,the system will automatically jump to the experimental selection interface,where the user can choose to do according to the corresponding experiments.Each experiment corresponds to a virtual experimental instrument,as shown in Figure 4.Each of these experiments can be selected individually, and each experiment is an independent VI program,which contains the experimental information and data filled in the format are designed for the different experiments.Pointing to open each experiment will be the corresponding experimental purposes,requirements and procedures.In each experiment,virtual instruments are provided to students,such as signal generators,as shown in Figure 5.Students can complete the experiment on their own.after the experiment,fill in the experimental data,and then automatically generate the experimental report [3],there is a local,students can choose to upload to the server for teachers to correct.

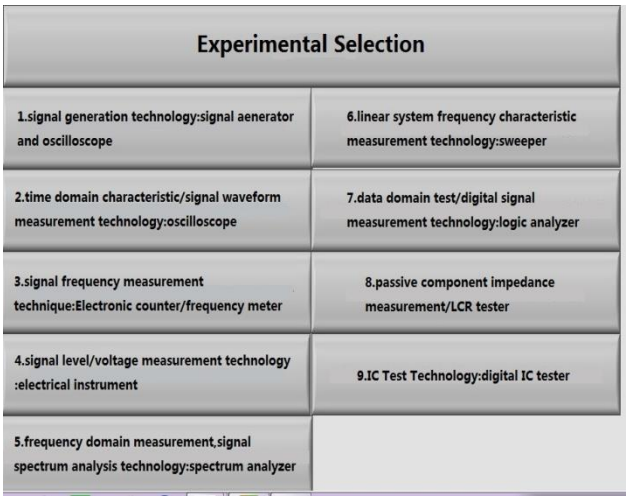

Fig.4. Experiment selection interface diagram

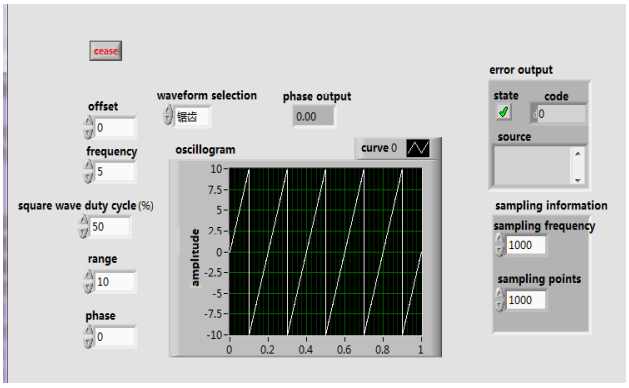

Fig.5. Signal generator

3)Experimental Communication Module

Experimental communication module is mainly composed of TCP communication protocol, UDP communication function, DataSocket communication and shared variables.The TCP function,which provided by LABVIEW,is based on the TCP protocol.Its advantage is to ensure reliable transmission,data is not lost.The process of TCP communication is setting the service name,porting number,connecting the IP address between one and others at the first.Only after the connection,they can communicate.Due to these characteristics of TCP,the program block diagram of students and teachers is designed respectively in the design of the communication part[4,5,8].Teachers use the server name and port number for creating the TCP listener and then wait for the student's connection.The students through the IP and port number to connect to the teacher side, and then ask questions.

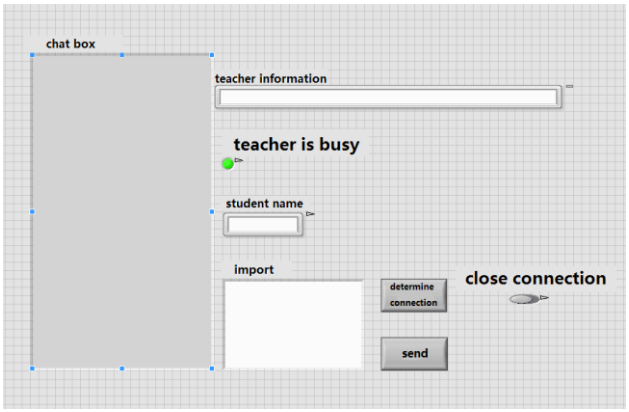

Fig.6. Experimental communication teacher chart

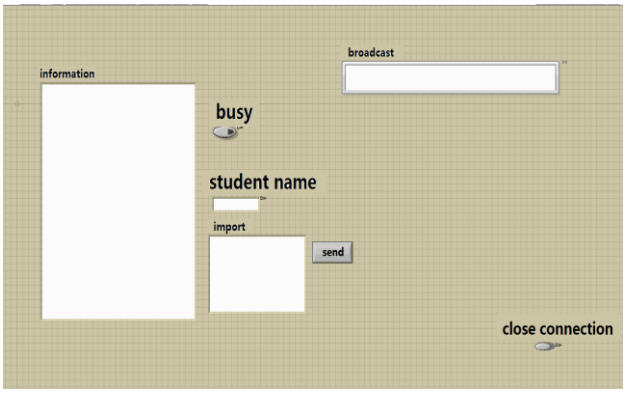

Fig.7. Experimental communication student chart

The broadcasting box of teachers and the teacher information box of students in communication module correspond.The teacher can enter some notification messages on the broadcast.but the students can only receive messages from the teacher information box.The block diagram of the the side of teacher and the student is shown in Figure 8 and figure 9.

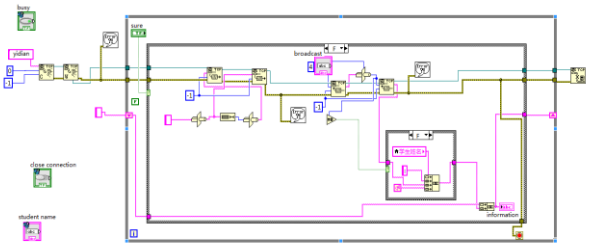

Fig.8. Teacher-side block diagram

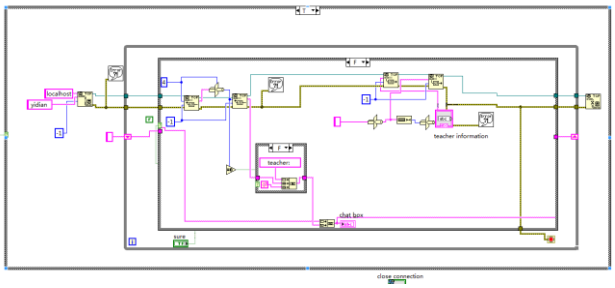

Fig.9. Student side block diagram

4)Report Uploading Module

The technology of report uploading has FTP protocol(text transfer protocol),which is the first to be used for Microsoft Internet file transfer service to achieve the agreement[6].Any computer can become a small FTP server for the client to access the storage and download files by setting up on the Internet.There are two ways to access about FTP server.One is to verify the ID and password through remote login.Only after verification and granted authority by remote server,users can operat file.The other is anonymous login.It means that users do not conduct ID and password authentication, direct access to the remote server.At this time,the remote server will automatically create a ID for the visitors,called anonymous.anyone can use this ID login for accessing.In view of the importance of FTP on the network,LabVIEW FTP services are also carried out a separate development.A series of functions developed specifically for FTP are included in the LabVIEW network communications.

The software module design are as follows:When students click upload test report button, automatically call FTP upload program. After the upload, teachers can input ftp://6513.220idc.cn in any access network browser,.And then after jumping page,teachers need enter the login ID and password to see the upload documents and the experiment report can be downloaded to the local computer for marking.

IV. CONCLUSION

The design of the experiment teaching and management system is based on LabVIEW visual programming platform to develop the host computer virtual instrument system, improve the utilization of experimental equipment. The experiment teaching management system system is designed, which is divided into login module, experiment selection module, experimental information display module, experimental data filling module and experimental report generation module, and it is feasible by experiment. Students through the management system can be in the field or through the campus network to submit experimental reports to achieve a one-click report upload; The experimental communication function allows teachers and students to carry out one-to-one communication in the course of the experiment, provide real-time guidance, timely interaction, effectively prevent a small number of students to report plagiarism and other adverse situation, the teacher is more objective to give experimental results; Achieve a network of management, improve the level of college experimental management, experimental teaching reform in colleges and universities put forward a practical development direction.

References

[1] Yan Hao. Application of network virtual instrument based on LabVIEW in experimental teaching [D]. Wuhan: Huazhong University of Science and Technology, 2007.

[2] Huang Jinwen. New technology of virtual instrument in our country and its development status and prospects of [J]. Technology Innovation Herald, 2008, (31): 8-10.

[3] Huang Fengliang. Xu Ming, Wu Wenting, Xia Chunmei, Feng Li, Wu Fei. Experimental report automatic generation system design of [J]. experimental science and technology, 2011, (9): 48-52.

[4] Wang Qunyan. Research and construction of virtual laboratory based on network [D]. Luoyang: Henan University of Science and Technology, 2007

[5] Ming Fanhua. Research on online experiment system based on virtual instrument [D]. Wuhan: Huazhong University of Science and Technology, 2006

[6] Zhu Wei. Design and implementation of virtual laboratory based on [D]. Chongqing: Chongqing University,, 2007

[7] Yang Leping, Li Haitao, Yang Lei. LabVIEW program design and application [M]. Second ed. Beijing: Publishing House of electronics industry, 2005

[8] Zhang Hongsheng. Remote virtual laboratory based on network [J].modern distance education research, 2005 (2):7678.

Multi-level visualization motor control and test development platform

LI Bo; ZHANG Zhen-feng; WU Qian

(College of instrumentation& Electrical Engineering,Jilin University,Changchun 130012,China)

***Abstract*—In recent years, with the continuous expansion of the scale of running a university, the traditional teaching and experimental equipment has been unable to meet the current pace of development of colleges and universities. Teaching methods to verify the majority, there are experimental mode behind, single content, efficiency is not high, low utilization of resources and other issues. his project is intended to design and develop a set of experimental teaching platform for motor and automatic control courses. The system includes: upper computer (PC), motor (DC brush motor, BLDC, stepper motor), stm32 as the core Machine control system, dynamometer (analog load) and virtual instrument based data acquisition and Labview visualization man-machine control interface. Which can realize the programming control of the motor and realize the function of multi-level visualization teaching research and development combined with the simulation experiment of the host computer and the programming control experiment on the corresponding lower computer. Based on the platform students can carry out independent innovation experiments, teachers can from different angles to apply this teaching platform for experimental teaching.**

***Key words*—Stm32 development board Labview Visualization of human - machine interface motor MATLAB Simulink**

I. PREFACE

"Electromechanical" experimental teaching is necessary to develop a set of common, multi-level set of motor control and testing in one of the experimental teaching platform. First of all, students can directly through the ARM microcontroller provided by the control board, write their own procedures to control the motor to understand the principles of various motor and control methods. At the same time, students can also use the computer to automatically detect, process and plot, quickly complete the drawing of each motor parameter curve, continuous monitoring of the motor test process. We will experiment the motor three-phase current, voltage and speed parameters such as simulation shown. Therefore, the experimental platform can not only be applied to all types of motors, and can be applied to industrial applications. Currently used of the computer automatically detect, process and draw the software, LabVIEW is a powerful virtual instrument design platform software, we use the software to make a visual human-computer interface, with the host computer MATLAB Simulink simulation system made virtual experiment For comparison, real-time display of the parameters click[6]. In the design, taking into account the host computer and the next crew communication and other related issues. The software platform can be applied to his field of motor teaching experiments, but also can be applied and the field of motor design.

II. SYSTEM FUNCTION DESIGN

Multi-level visualization of the motor control and test experimental platform, the hardware from the power module, step-down module, drive module, the next crew module, three motor modules, dynamometer (analog load) module, respectively, DC brushless, three-phase stepper motor drive control; software by Labview visualization man-machine interface, MATLAB Simulink simulation system components, to achieve data control and real-time display[8]. In the experimental platform, students can not only through the dismantling of the various hardware modules, assembly and connection to learn three basic motor performance and work methods, but also through the lower computer stm32 development board programming control, to achieve the design of the motor The three-phase current, three-phase voltage and speed of the motor can be compared with the characteristic curve of MATLAB Simulink simulation,

and the combination of theory and practice can be realized. The concrete structure is shown in Fig. 1.

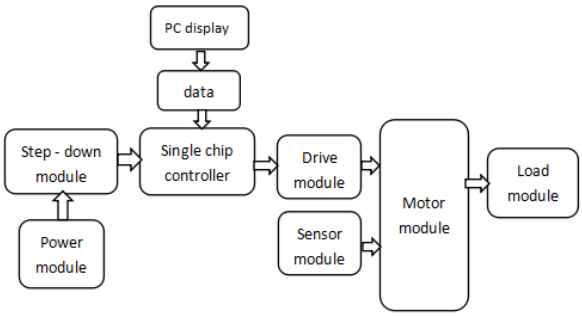

Fig.1 Structure of experiment platform

III. SYSTEM HARDWARE DESIGN

A.system overall program

The main body of the hardware is mainly composed of power module, ascending / descending module, lower computer controller module, driving module, motor module, DC load motor, sensor module and data transmission module. According to the requirements between the different components of the building, constitute a set of modular structures, motor experiments, data display as one of the electrical teaching platform. The actual hardware overall structure, as shown in Figure 1 above.

B. system hardware selection and design

1.Power supply and step-up and down module selection

Power supply part of the use of 24V 150W, allowing the maximum current 2A through the switching power supply, through a 12V ~ 32V step-up and down the module, to meet the three motor voltage requirements.

2. Lower machine control module selection

Using stm32 development board to achieve the control of different kinds of motor drive circuit, JTAG download module and PC to connect, and can be achieved through the USB transmission of real-time transmission of motor parameters.

3.Motor drive module selection

DC brushless motor drive module using MOSFET gate drive IR2110S, the maximum drive motor power 500W, wiring and stm32 control panel MCU to connect[10].

DC brush motor and three-phase stepper motor are used L298N drive circuit control, directly connected with the stm32 development board, using 5V power supply. L298N drive as shown in Figure 2:

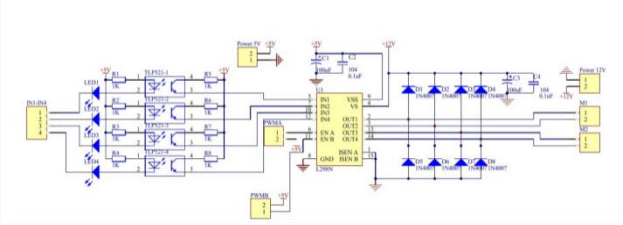

Fig.2 L298N drive circuit diagram

4. Selection of motor modules

BLDC DC brushless motor with 24V 1.5A Hall element of the device, can be directly through the stm32 control board to detect the three-phase voltage, through the current sensor directly detect the three-phase current.

Three-phase stepper motor with 42 stepper motor 42BYGH48-401A torque 0.55N.M, length 48MM + DM422, rated working current 1.5A, driven by L298N motor drive plate.

DC brush motor with 385 standard motor, the motor coil DC resistance 11 ohms, the working voltage from 3V to 30V, 24V rated voltage speed of 8700rpm.

5. Selection of current sensor module

Current sensor with 3A range MAX471 sensor, the internal precision detection resistor. If the detection range exceeds 3A, the current sensor can be connected in parallel to increase the detection range.

IV. SYSTEM SOFTWARE DESIGN

A.system host computer design

System PC is based on Labview visualization of human control interface. LabVIEW is a powerful and flexible tool for the development of virtual instrument technology in the field of instrumentation and analysis software applications[2]. With LABVIEW platform to design the host computer software, through the serial communication control microcontroller speed adjustment, but also to monitor the real-time motor speed, intuitive observation of the motor speed change process. LabVIEW is a standardized data acquisition and virtual instrument control software, which not only provides compliance with GPIB, VXI, RS-232 and RS-485 protocol hardware and data acquisition card, but also built support for TCP / IPActiveX and other software standards The library function. This article selects the software for developing test platform

software. : Host computer interface design as shown in Figure 3:

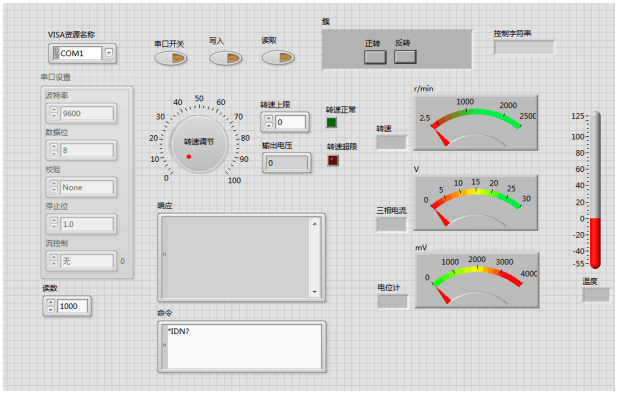

Fig.3 Experimental platform PC display interface map

1.control algorithm

The system of the host computer developed by the LabVIEW platform to achieve the software, because the host computer bear the most important PID control algorithm task, the realization of the way is to use the LabVIEW platform itself contains the PID toolkit to write the program.

2.host computer serial communication

PC software through the serial port to the next bit machine controller to send test commands. After receiving the instruction, the controller starts the motor to test and stores the test data[6]. After the test is completed, the experimental data is returned to the host computer. The host computer receives the data and displays the data in the table, and the fitting curve is presented. LabVIEW graphical display function, the design interface display software, combined with the function selection module, for a variety of characteristics of the test. In LabVIEW, VISA is called the virtual instrument software architecture. As the underlying function module of the communication between the drivers in the LabVIEW program, you can connect different standard I / O devices. It is used in the serial communication equipment, VXI equipment, GPIB Devices, and other communication devices based on computer equipment[10]. We can LabVIEW in the Instrument I / O in the Serial to find the module corresponding to the serial port VI, which is more commonly used VISA Configure Serial Port, VISA Write, VISA Read and other modules, respectively, to achieve serial port, serial write, serial read And other functions. Through the configuration and connection of these functional modules, you can develop the required LabVIEW serial port communication software.

PC graphics display interface shown in Figure 4:

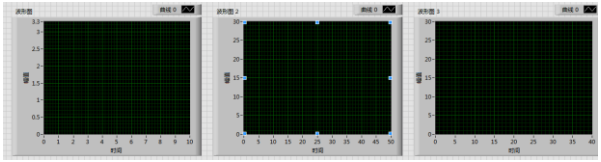

Fig.4 Experimental platform on the host computer waveform display interface map

B. system under the machine design

The design of the lower computer is STM32 as the core of programming control. To achieve serial communication with the host computer, generate and send PWM wave to control the motor speed;

1.Generation of PWM waves

The design uses software to generate PWM signals. Using the timer of the system, the different duty cycle of the PWM is changed by assigning different values to the auto-reload register to change the speed of the motor.

DC brushless brushless motor only two way PWM wave can control its positive and negative and speed control function. Forward all the way to output PWM another two zero, reverse the way to zero two normal output[10].

Two-phase four-wire stepper motor with 8 beat control mode. Ie eight states:

（1） A with A-positive voltage, B and B- are not drained;

（2）A with A-positive voltage, B and B- also to positive voltage;

（4）A and A do not give voltage floating, B and B-positive voltage;

（4）A and A to negative voltage, B and B to positive voltage;

（5）A with A to negative voltage, B and B- not to vacant;

（6）A with A to negative voltage, B and B- to negative voltage;

（7）A and A are not to power vacant, B and B- to negative voltage;

（8）A with A to positive voltage, B and B- to negative voltage;

According to the above eight state power supply, control the pulse width should be on it. The reverse of the stepper motor can change the power supply sequence.

2. Calculation of motor speed

The realization of the motor speed calculation, the system uses a method of timing up counting. Through the microcontroller timer T0 to the timer, and then use the external interrupt INT1 to remember the number of feedback pulses received, by a certain period of time to receive the number of pulses to calculate the speed[7]. The speed will be sent through the send [i] function to connect the serial port to communicate.

```
    u8 send[64];
    //DMA_Cmd(DMA1_Channel1,DISABLE);
     for(k=0;k<6;k++)
{     for(j=0;j<64;j++)
     {  for(i=0;i<64;i++)
     {   send[i]=SendBuff[i+j*64][k]*165/4095;
```

Fig.2 The speed of the sending code

V. PLATFORM FEATURES

A. Programming The motor is controlled

Students can directly through the provision of SCM control board, write their own procedures to control the motor. Through the emulator to complete the preparation of the program programming, more autonomy to learn to master the motor control principle.

B.data collection, real-time display

The experimental platform can have data acquisition function, including real-time display of three-phase voltage motor, real-time display of three-phase motor, real-time display of motor vibration and real-time display of motor operating temperature. And gives the parameter values at each time.

VI. CONCLUDING REMARKS

The experimental platform aims at cultivating students' practical ability, design ability and innovative research ability. Students can train and train the motor drive system, control training, motor control programming, system debugging and new control strategy. Wait. Students can visualize the interface more intuitively in the training, the experimental process to reflect on, re-understanding of the basic principles of the motor and control strategies, the use of playback and other functions of the results of multiple experiments to think more, to cultivate students' innovative thinking ability. The use of standardized and scientific to improve student learning ability, to enhance student learning efficiency.

References

[1] Zhang Dahua. Phase-locked loop integrated circuit CD4046 and its application in the automation instrument [J]. Industrial Mea surement.2003. (6): 30-32.

[2] Lei Zhenshan. LabVIEW 7 Express practical technical tutorial [M]. Beijing: China Railway Publishing House.

[3] Zhao Danqun, Tang Renyuan, Lu Zhanhong. Motor transient torque speed test technology and device. Journal of Shenyang University of Technology. 1990: Vol.12 (No. 4).

[4] Chen Yawen. Practical motor torque test system. Electrical and Mechanical Engineering. 1990: the first phase.

[5] Negenborn R. Robot. Localization and Kalman filters on finding your location in a noisy world [D / OL]. Http: // www. Negenborn.net/ kal - loc / thesis. Pdf.

[6] Zhang Jinmei. Based on the virtual instrument of the motor test system research [D] Jiangsu: Jiangnan University .2008.

[7] Zhu Longji. Control of the motor speed measurement method to achieve [J]. Journal of Anhui University of Science and Technology (Natural Science Edition) .2005 (3): 45-49.

[8] Yang Leping, Li Haitao. LabVIEW design and application. Beijing. Electronic Industry Press .2001.7.

[9] NI Corporation.PID Control Toolset User Manual.2003.11.

[10] Journal of Jinjiang, Yuan Xiaoming, Li Daming.JIN Jiang.YUAN Xiaoming.LI Daming Application of LabVIEW automatic control of DC motor voltage regulator method - Modern electronic technology .2007.30 (18).

[11] Paul I-Hai Lin, Member, IEEE, and Edward E. Messal, Ph.d. Indiana University-Purdue University at Fort Wayne. Design of a Real-Time Rotor inertia Estimation System for DC Motors with a Personal Computer. 1993: 59 ~ 63.

Design of GPS Automatic Control System for Unmanned Aerial Vehicle Imaging Spectrometer

Zhang Pei; Wang Xuheng; Wu Yanqin

(College of Instrument Science and Electrical Engineering, Jilin University, Changchun 130012, China)

***Abstract*—Compared with traditional remote sensing technology, unmanned aerial bearing imaging spectrometer has the advantages of high flexibility, strong emergency capability, low cost, small weather and high resolution, but there are too large data and less effective data The The experiment proves that the result obtained by this method can effectively solve the problem that the data volume is too large and the effective data is small. The external trigger system is designed by using the real-time control of the GPS data.**

***Key words*—UAV remote sensing; GPS data analysis; Automatic control**

I. INTRODUCTION

UAV and remote sensing technology, that is UAV remote sensing, is the use of advanced unmanned aerial vehicle technology, remote sensing sensor technology, telemetry remote control technology, communication technology, GPS differential positioning technology and remote sensing technology, with automation, intelligent , the topic of rapid access to land, resources, the environment of space remote sensing information, remote sensing data processing, modeling and application of analytical application technology. Its application from the initial reconnaissance, early warning and other military fields to the water level monitoring and detection, traffic, disaster assessment, air pollution monitoring, archaeological, oil and gas pipeline monitoring, agriculture, high pressure transmission line inspection, three-dimensional modeling and other non-military areas[1]. UAV remote sensing high efficiency, high resolution and other performance, is the traditional satellite remote sensing can not be compared, more and more researchers and producers of all ages, greatly expanding the scope of application of remote sensing and user base, with a wide range of applications Foreground [2].

The imaging spectrometer is an instrument to acquire the remote sensing data. It can collect the two-dimensional spatial information and one-dimensional spectral information of the target to be measured at the same time, form a three-dimensional data cube, and the imaging spectrometer collects the massive data. Therefore, the validity of the data is especially important, The imaging spectrometer is mounted on the UAV platform. Since the telemetry function of the UAV can only be completed by the UAV flight control and management system. If the imaging spectrometer is set to continuous camera mode, the validity of the data can not be guaranteed.The GPS receiver can output the latitude, longitude, altitude, speed, heading, time and satellite status in continuous or timed way, and can use the above parameters to control the imaging method of the imaging spectrometer in real time. GPS provides two functions for the flight control system. One function is to transfer the parameters such as the three-dimensional positioning of the camera at the time of exposure to the imaging spectrometer for the imaging of the image plus the parameter tag. The other function is to provide the programmable external trigger circuit Trigger the signal source, which can be achieved with GPS signal trigger camera exposure. The programmable external trigger circuit can control the trigger conditions according to the project requirements. The remote sensing data obtained by this method can not only improve the efficiency, but also reduce the overall data volume.

II.SYSTEM STRUCTURE DESIGN

The use of unmanned aerial vehicle GPS data real-time automatic control imaging spectrometer electronic system, that is, through the UAV GPS data

packet (latitude and longitude, height) to extract the imaging spectrometer external trigger signal, according to the actual application requirements to achieve real-time imaging spectrometer External control, the contents of which include three aspects: GPS data filtering and real-time extraction method research, control system, electronic platform design, interface communication protocol and related algorithms. As shown in Figure 1:

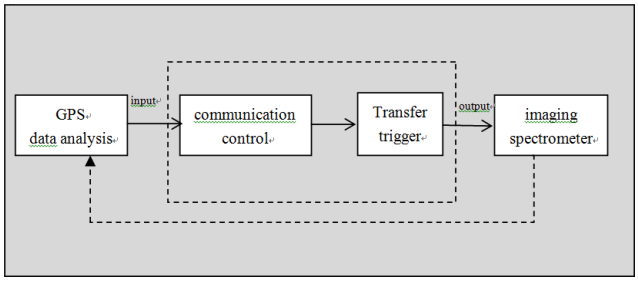

Fig.1. system block diagram

During the operation of the system, the GPS data acquired by the GPS receiver is input to the control system through the serial port according to the specific protocol. The control system will analyze the received GPS data and use the parsed GPS data as the parameter calculation algorithm. Man-machine flight attitude, when the UAV smoothly flight or meet the flight path and other predetermined conditions, the trigger signal output to the imaging spectrometer. In addition, NMEA format GPS data directly into the imaging spectrometer, imaging spectrometer has a dedicated matching interface to receive.

III.SYSTEM HARDWARE

SIMCom8 SIM SIM module is used as the GPS data receiver in the system. SIM908 uses high-performance industrial grade GSM / GPRS quad-band module, integrated GPS function, the working frequency band: GSM850 / EGSM900 / DCS1800 / PCS1900 MHz. Can achieve GPS positioning, GSM communication, GPRS data transmission and other functions. The GPS module has 42 channels to receive, high tracking sensitivity (sensitivity at -160dBm), fast start time (cold start for 30s, hot start for 1s) and accurate positioning (<2.5m CEP) features. Module for the 80-pin package, then the passive antenna, the PWRKEY pin ground to achieve self-starting, but also with the master chip GPIO port connection to achieve autonomous control start.

The master chip uses STM32F103RBT6, which is ARM 32-bit Cortex-M3 core with 72MHz maximum frequency, 128Kb flash memory and 9 communication interfaces. In the system with sufficient speed and communication resources.

Imaging spectrometer selected ADCAir.

Under the control of the STM32F103RBT6 chip, add some auxiliary equipment to form a complete system. as shown in Figure 2:

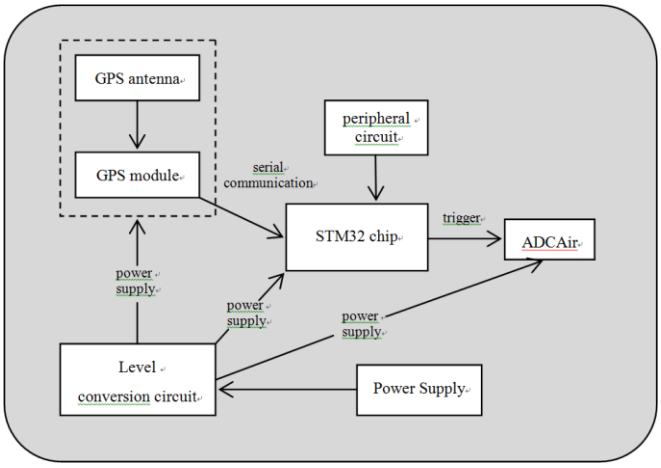

Fig.2. hardware system block diagram

IV.SYSTEM PROGRAM

A.GPS data real-time analysis

The GPS receiver outputs GPS data at a frequency of 1 Hz, and the control system can communicate with the GPS receiver in two ways. First, through the SIM908 module TXD and RXD interface, that is, the module's main serial port (Serial Port), send AT command to query the GPS data; Second, through the SIM908 module GPS / DBG-TXD and GPS / DBG-RXD Interface, that is, the module debug port (Debug Port), the interface output GPS data for the NMEA0183 format. The output order is $ GPZDA, $ GPGGA, $ GPGLL, $ GPVTG, $ GPGSA, $ GPGSV, $ GPRMC. The control system can control the output mode of the serial port through the main serial port, and send AT + CGPSOUT = n (n = 0 ~ 255) to output the data of different modes. Bit4 = 1 output $ GPG; bit4 = 1 output $ GPG; bit4 = 1 output $ GPGS; bit4 = 1 output $ GPGS; bit4 = 1 output $ GPG;

This software system uses $ GPRMC and $ GPGGA two statements.

GPRMC data:

$GPRMC,<1>,<2>,<3>,<4>,<5>,<6>,<7>,<8>,<9>,<

10>,<11>,<12>*hh

<1> UTC time, hhmmss (hours and seconds) format

<2> positioning status, A = active positioning, V = invalid positioning

<3> latitude ddmm.mmmm (degrees) format (the previous 0 will also be transmitted)

<4> Latitude hemisphere N (northern hemisphere) or S (southern hemisphere)

<5> Longitude dddmm.mmmm (degrees) format (the previous 0 will also be transmitted)

<6> Longitude hemisphere E (longitude) or W (west)

<7> Ground rate (000.0 to 999.9, the previous 0 will also be transmitted)

<8> Ground heading (000.0 ~ 359.9 degrees, with true North as the reference, the previous 0 will also be transmitted)

<9> UTC date, ddmmyy (day / month) format

<10> magnetic declination (000.0 ~ 180.0 degrees, the previous 0 will also be transmitted)

<11> Magnetic declination direction, E (east) or W (west)

<12> mode indication (only NMEA0183 3.00 version output, A = autonomous positioning, D = differential, E = estimate, N = data is invalid)

GPGGA data:

$ GPGGA, <1>, <2>, <3>, <4>, <5>, <6>, <7>, <8>, <9> M < , <12> * xx

$ GPGGA: start boot and statement format description (this sentence for GPS positioning data);

<1> UTC time in the format hhmmss.sss;

<2> latitude, the format is ddmm.mmmm (the first bit is also zero);

<3> Latitude hemisphere, N or S (latitude or south latitude)

<4> longitude, format dddmm.mmmm (the first zero will also be transmitted);

<5> longitude hemisphere, E or W (east or west)

<6> positioning quality indication, 0 = positioning is invalid, 1 = positioning is valid;

<7> use the number of satellites, from 00 to 12 (the first zero will also be transmitted)

<8> Level accuracy, 0.5 to 99.9

<9> The height of the antenna from the sea level, -9999.9 to 9999.9 meters M refers to the unit meters

<10> geoid height, -9999.9 to 9999.9 m M refers to the unit meters

<11> Differential GPS data duration (RTCM SC-104), and finally set the number of seconds for RTCM transmission

<12> Differential reference base station label, from 0000 to 1023 (first bit 0 will also be transmitted). <3>, <4>, <5>, <6>, <7>, <8>, <9>, M, <10>, M, <11>

(Jilin University, Laboratory): $ GPGGA, 014015,4352.721987, N, 12518.148164, E, 1,52.737684, -10.920469, M, 12.050686, M, 0000.

The data analysis process is as follows: (a) The serial port receiving format is 8-bit data bits, 1 stop bit, no data check, baud rate is 112500; (b) Find the start character ASCII code '$' ;(c) use the string processing function char * strtok (char * s, const char * delim) to find the start bit of the parameter and return the address; (d) the use of format conversion Function double atof (const char * str) will be converted to a floating-point string; (e) dynamic storage of data to complete the analysis process.

B. Trigger algorithm

The communication interface between THE ADCAIR and the control system is shown in Figure 3, where pin5 is the picture curing line and the low level is triggered. The pin8 is the RS232RX interface, which accesses the GPS data in the NMEA0183 format.

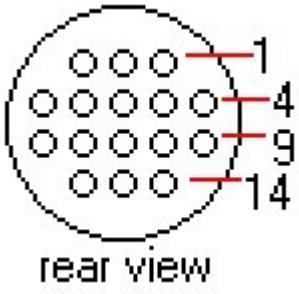

Fig.3. ADCAir communication interface diagram

Read out the GPS data from the memory, the use of latitude and longitude for UAV trajectory tracking, the use of speed ratio (speed and height ratio) on the UAV flight attitude monitoring. Set a free GPIO port of the master chip to push-pull output mode and set it to high level. Control system has been in the monitoring mode, imaging spectrometer mounted on the UAV, UAV into the operating state of the parameters (speed ratio) to meet the trigger conditions, the control system will be low GPIO port, as a trigger source, imaging spectrometer detected Trigger the signal to trigger the completion of the camera. According to different geographical environment, the ratio of speed to speed

is different. Taking Jilin University as an example, the speed ratio is set between 0.05 and 0.13. The results show that the imaging spectrometer can take pictures according to the expected external trigger.

V.CONCLUSION

The design uses the GPS data real-time refresh feature, innovative as a trigger source, the successful realization of the unmanned aerial imaging spectrometer real-time trigger. The results show that the data obtained by the imaging spectrometer is reduced to a certain extent and the effective data rate is increased.

References

[1] Wang Feng, Wu Yudong. UAV remote sensing platform technology research and application [J]. Remote Sensing Information, 2010, (02): 114-118.

[2] Jin Wei, Ge Hongli, Du Huaqiang, Xu Xiaojun. Remote Sensing Development and Application of Unmanned Aerial Vehicle [J]. Remote Sensing Information, 2009, (01): 88-92.

The optimization of parameters and efficiency of Wireless Power Transmission

LI Gang; CHEN Qian; FU Jian; ZHANG Biao

(College of materials Science and Engineering, Jilin University,Changchun 130022,China)

***Abstract*—Based on the principle of Magnetic coupled resonant wireless power transmission ,high frequency sinusoidal signal frequency can be produced by using DDS technique, it can be converted to the PWM wave after the analog circuit. Then let the PWM wave drive the DC inverter full bridge circuit for high frequency AC power to the emissive coil.Power transmission can be realized through the magnetic coupling resonance. The electrical energy through rectification, filtering, boost processing is transported to the LED driver module based on the BUCK circuit to verify the stability and efficiency of wireless power transmission.The Wireless Power Transmission device based on magnetic coupling resonance can optimize the parameters and efficiency of Wireless Power Transmission.**

***Key words*—Magnetic coupling resonance; DDS technology; Full bridge converter; Conversion of electrical energy; Buck circuit**

I.INTRODUCTION

ALONG with the deepening of the electric power industry revolution, the wireless energy transmission technology as a new technology in the transition from theoretical research to practical application. Its application is still expanding: lighting, solar power stations and aerospace systems will become a new field of wireless energy transmission.[1]

This research in wireless power transmission system sets design and parameter optimization and efficiency as guidance, focus on wireless power transmission system and the system parameters and efficiency optimization, including the design of a high frequency signal generator module, the design of transmission coil , transmission distance, etc., and design a LED driver which can transfer to verify the system. Finally meet the project requirements, the completion of the transmission distance and other parameters optimization.

II.BASIC PRINCIPLES

A. Principle of electric Energy Emission

To generate a high and sinusoidal signal frequency can be adjusted by using DDS technique,and then is transformed into a PWM wave can drive the full bridge circuit through the various types of analog circuit, Full bridge circuit serves as high frequency and high power AC-DC inverter, according to the index of reasonable design , high-power AC coil will be loaded into the ring to transmit energy rays.

B. Principle of Electric Energy Transmission

The design of emissive and receiving coil is based on power transmission LC parallel resonant magnetic coupling . The transmitter generates high frequency signals to drive the transmitting coil resonance, magnetic energy will produce the transmitter coil, and then converted into electric energy stored in receiving coil by magnetic field coupling, the receiving coil resonance. Due to the electric energy exchange between the receiving coil capacitance and inductance have the same resonant frequency, the resonance energy transfers between Ever fount in coils. The electric energy obtained needs to be conducted through the bridge rectifier, filter capacitor, DC boost and reduce power loss as far as possible, thereby driving module to transmit enough power for the LED.

C. Principle of LED Driving

LED is a typical nonlinear element,.Only a slightly increase in LED voltage, conduction current will be significantly increased, if the current is not through LED restrictions, LED is easy to burn out. Taking into account of the flow ripple compensation,the formation of a constant current source control and current feedback control circuit should be adopted.[2]

III.SCHEME DESIGN

According to the design requirements of the project, the system is divided into blocks:[3]

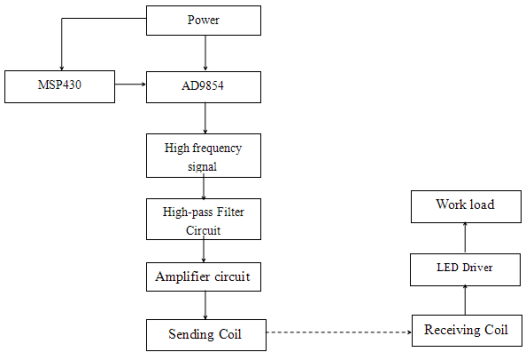

Fig.1 Schematic diagram of system

A. Scheme of High Frequency Signal Transmission Power-supply Module

According to the safety standards and functions of the power supply is divided into: the total power supply, two isolated from each other driver circuit power supply, MSP430f14 circuit board power supply, AD9854 integrated circuit board power supply

High frequency signal generator module

Using MSP430 to control the AD9854 chip to produce a high frequency sine signal with adjustable frequency between 1.2MHz~2MHz, the efficiency of radio transmission is higher in this frequency range.

Amplifier comparison circuit

Because AD9854 only generates one way of precise frequency sine wave, it should be transformed into the frequency range of the voltage equal to the two-way driving PWM wave generated.AD9854 sine wave pulse is 0~0.5V, it can be enlarged, and then can produce different PWM waves, in order to improve the anti-interference ability of the comparator after two different comparators .

Drive amplifying circuit

After four PWM waves are generated, the driving signals of the MOS tube which can drive the whole bridge to be isolated from each other are generated by the same driving circuit.

Full bridge circuit

Two arms of the same bridge can switch the tube complementary, two switches diagonal relative tube conduction through the control of four switches on and off, can produce amplitude is equal to the input voltage of the AC square wave voltage on the output side, the output side LC parallel resonant circuit, can produce effective the value of sinusoidal voltage is equal to the input voltage..[4]

B. Scheme of Transmissive Coils Design

Using LC parallel resonant magnetic coupling to achieve power sending and receiving coil by coil structure of multi wire parallel multi turn to increase the line size, reduce the skin effect, decrease the inductance coil insulation layer to improve the removal of the natural frequency of the 10 wire. Ensure the two LC network should have approximately the same parameters to ensure maximum efficiency of transmission network and achieve energy resonance.

The rectifier circuit adopts the bridge rectifier, the filter circuit is connected with a plurality of small capacitors to obtain stable DC current, and a suitable electrolytic capacitor is connected in parallel to store the energy for the subsequent circuit

The PTN04050CAD boost circuit module will boost 3V voltage up to 12V, then using Boost circuit to enhance the DC voltage of 12V to 24V, this design assures to provide the right LED driving voltage and reduce the power loss at the same time.

C. Scheme of Constant Current Drive Design

Adjust the coil and ensure the receiving voltage op amp parameter greater than 20V, the voltage is used directly for LED driving circuit as a LED driver.

LED selection: 1W, 350mA, the turn-on voltage is 3V, the pressure drop is 3.2-3.4V.

The constant current LED driver circuit based on the buck circuit is adopted, and the MOS tube is used as the main control device, and the PWM wave is generated by the UC3843, combined with the ripple compensation and current feedback control, the output is a constant current source.

IV.SPECIFIC CIRCUIT AND PARAMETER

A. Design of electric energy transmission parameters

AD9854 digital synthesizer is a highly integrated device, on-chip integration of two-way high-speed, high performance digital converter through orthogonal D/A programming can output I,Q signal. In the synthesis of two driving high stability clock, AD9854 will produce a highly stable frequency, phase, amplitude Programmable Sine and cosine

signal.Amplifier circuit and comparator circuit using LM7121 amplifier, LM7121 operational amplifier is a high speed amplifier, power supply voltage of 5V power supply and power supply + 15V, slew rate 1300V/us, bandwidth 235MHz.

Optocoupler using 6N137.6N137 optical coupler for high-speed optical coupler is a single channel, the conversion rate of up to 10MBit/s, the slew rate is as high as 10kV/us, fanout coefficient is 8, the output logic level, open collector output, power supply voltage +5V.Full bridge circuit MOS tube using IRF540, Id maximum value of 33A, Vds maximum 100V, Rds(on):0.04ohm, with superior dU/dt performance.

B．Design of electric energy transmission parameters

Coil parameter design

Current flowing in the coil of this project is not more than 3A, so the 10 models QA-1 155, section 0.44mm diameter copper wire around the outer diameter of the coil is made of organic glass tube 20cm, a total of around 10 turns, measured the winding inductance values were 36.56uH and 36.42uH. according to the signal frequency between 1.2MHz~2MHz. By the formula C=1/ (2πf) ^2*L can choose the high frequency capacitance value between 180pH~500pH. MBR1545 (45V/15A/10ns) rectifier diode selection The filter capacitor is selected 104 (0.1uF), the electrolytic capacitor is selected 35V 100uF.[5]

C．Booster module parameter design

PTN04050CAD Boost module：

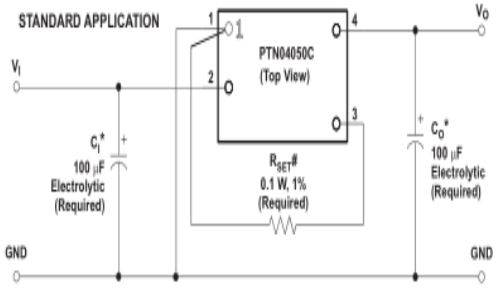

Fig.2 PTN04050CAD Boost module

Input capacitance C1:100uF; output capacitance C0:100uF, to ensure the stability of this capacitor by the combination of ceramic and electrolytic capacitors. Precision resistors (0.1W, 1%): precision resistors as close as possible to the regulator's 1,3 feet.

$$R_{SET} = 15\text{k}\Omega \times \frac{2V}{V_O - 5V} - 2.94\text{k}\Omega$$

BOOST Circuit：

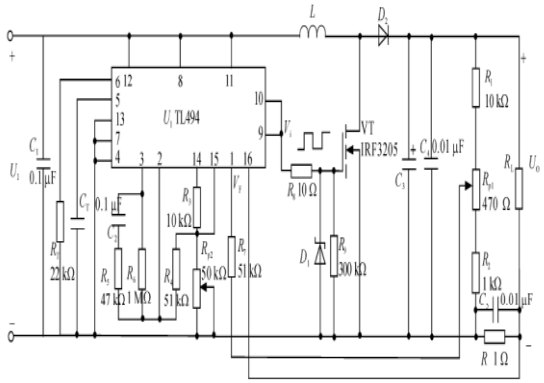

Fig.3 Boost Circuit

Select N channel power field effect transistor IRF3205(55V/110A; select 100uF/50VCapacitance; select 100uH/2A Inductance;The freewheeling diode is MBR10100CT,Schottky diode(100V/10A).D. LED[6] Drive Circuit and Characteristic Parameters

Main Control Loop

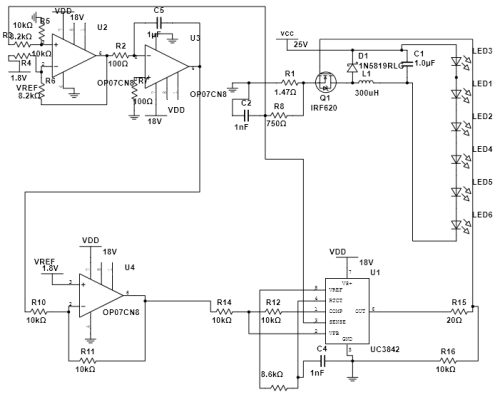

Fig.4 Circuit diagram of LED driver

Chip-supply voltage and reference voltage acquisition

Because the reference voltage stability is directly related to the current constant. The best result and chip power supply voltage requirements higher and 25V are from the input voltage, so two kinds of voltage are obtained through voltage chip LM317 with the external circuit.

Determination of Main Circuit Parameters

Calculation steps:

(1)peripheral circuit operating frequency is calculated according to the corresponding UC3843 related information in the manual and MOS chip peripheral circuit needed drive: capacitor and resistor chip flat rate of 200kHz values obtained by the formula ① C=1uF. type of.R=6.8K.

$$f_s = \frac{1.72}{R_T C_T} \qquad ①$$

(2)Buck circuit inductance value is calculated by the following formula ②into the corresponding data for 300uH;

$$L = \frac{(V_{\text{in}} - V_o)T}{\mathrm{d}I} = \frac{(V_{in} - V_{\text{o}})D}{0.2I_{on}f_s} \qquad ②$$

(3)According to the correlation operation and the pre ssure limiting values are obtained as follows: MOS par ameter selection using IRF630 diode using zener diode 1N5819, capacitor using 50V/1uF.[7]

V.Experimental Results and Conclusions

A. System power waveform results

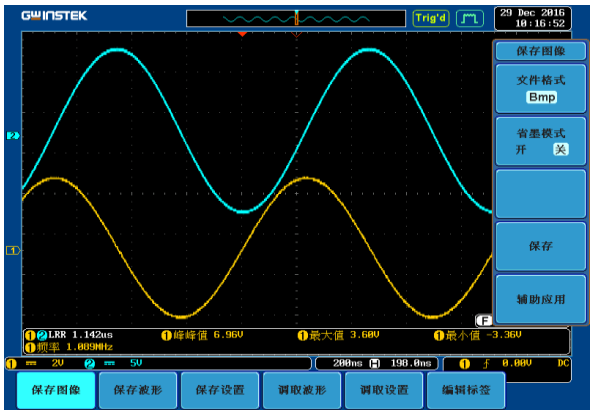

Note: the upper curve as the input waveform, lower as output waveform

Fig.5* System Power waveform

B. System operating parameters

System optimal operating frequency

In this design, the coupling coil L=36.55uH, shunt capacitor C=470pF. set 30cm transmission distance as the goal, under the Vin=10V conditions to determine the best operating frequency:

Table1 Choice of the Best Frequency

f/MHz	1.0	1.03	1.06	1.07	1.08
V_{OUT}/V	1.36	1.92	3.12	3.76	4.40
f/MHz	1.09	1.10	1.11	1.12	1.15
V_{OUT}/V	4.56	4.16	3.52	2.96	1.84

System working distance verification

In f=1.09MHz, Vin=10V conditions, measured at different operating distance of Vout, the data are as follows:

Table2 system working distance verification

d/cm	20	22	24	26
V_{out}/V	7.5	6.4	5.4	5.0
d/cm	28	30	32	34
V_{out}/V	4.8	4.4	3.6	3.1

As can be seen from table 2, the transmission distance can reach 30cm, meet the design requirement. LED Driver circuit results

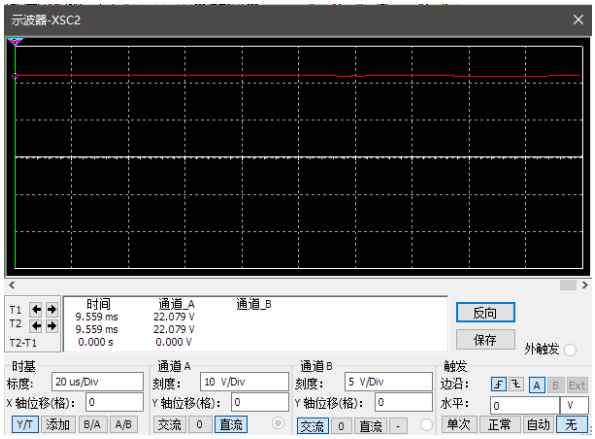

Fig.6 Current Waveform of LED Driver

LED constant current drive results obtained by Figure 6, the brightness of LED can also be changed through the rotation of the sliding rheostat thereby changing the reference voltage,

References

[1] Li Hongchang,Steady state control strategy for magnetic resonance radio energy transmission system: efficiency optimization control [J] Xi'an Jiao Tong University.

[2] Zhang Xiaozhuang,"Magnetic coupled resonant wireless energy transmission distance characteristics and experimental research on the device [D]". Harbin Institute of Technology, 2009.

[3] Zhang Chao. "Magnetically coupled resonant wireless powertransmission system simulation and Experimental Research on the resonator [D]".Tianjin: Hebei University of Technology, 2011.

[4] Yang Minsheng, Wang Yaonan. "A new type of contactless inductive coupled power transfer technology [J]". Journal of Hunan University of Arts and Science: Natural Science Edition, 2010, 22 (): 44-53.

[5] Feng Cizhang, Ma Xikui. "Introduction to engineering electromagnetic field [M]". Beijing: Higher Education Press, 2000.

[6] Singh B, Shrivastava A, Chandra A, et al. A single stage optocoupler-less buck-boost PFC driver for LED lamp at

universal AC mains[C]//IEEE Industry Applications Society Annual Meeting. Lake Buena Vista: IEEE, 2013: 1-6.

[7] SunTianjia,Xie Xiang,Wang Zhihua,Wireless Power Transfer for Medical Microsystem[M].Springer Verlag, 2013

[8] Zhang Yiming, Zhao Zhengming, YuanLiqiang, etc. The comparision of the two basic structures in magnetically coupled resonant wireless power transfer[J].Transactions of China Electrotechnical Society,2013,28(S2):18-22.

[9] Brown W C,The history of power transmission by radio waves[J],IEEE Trans.on Microwave Theory and Techniques, 1984, 32(9): 1230-1242.

[10] Zhang Xian, Yang Qingxin, Chen Haiyan, Li Yang, Cai Yan. “Electromagnetic coupled resonant wireless power transmission system modeling, design and validation of [D]”. Chinese ofthecsee, 2012

[11] Li Yang, Yang Qingxin, Yan Zhuo, Zhang Xian, etc. “Analysis of factors affecting transmission power and efficiency in radio energy transmission system [J]”. new technology of electrical energy, 2012,03:31-34.

Automatic Irrigation System Based On Wireless Sensor Network

XU Mingliang; ZHENG Haiyang; YU Haoran; LI Zhe
(College of Instrument Science and electrical engineering,Jilin University,Changchun 130012)

***Abstract*—Aiming at the shortcomings of current agricultural irrigation system, a system scheme of using wireless sensor networks to control agricultural intelligent irrigation, the system is mainly composed of the host monitoring MCU, ZigBee coordination equipment (gateway node), temperature and humidity sensors, irrigation motor control node and valve control equipment. The temperature and humidity sensor is used to measure the environmental conditions，MCU processing. Then through the ZigBee network, the environmental humidity is transmitted to the host computer through the wireless module. And the host computer command is received to control the actuator. In order to achieve automatic control system of the greenhouse.**

***Key words*—Temperature Humidity ZigBee Network Remote Control**

I. INTRODUCTION

WITH the development of China's economy, the demand for agricultural development in China increased year by year. The lack of water resources in our country, how to conserve water resources has been an urgent problem, and the irrigation water resources there exist the problem of low utilization of a common resource. So realize real-time monitoring of temperature and humidity based on wireless network understand, a series of valuable data of soil, using scientific and effective control of water resources, can greatly save water resources, to achieve efficient water-saving irrigation. However, compared with many developed countries, China has a significant gap in the development of wireless irrigation system. This system for a variety of traditional monitoring system the lack of To optimize the design, a greenhouse remote automatic irrigation system design using ZigBee technology. Through the combination of ZigBee technology and wireless sensor network technology, remote monitoring system can be achieved. The system wiring is very simple, to reduce the planting cost[1].

II. SYSTEM OVERALL DESIGN

According to the main function of automatic irrigation system in wireless sensor network, can be divided into the following 6 parts: environment acquisition module, wireless module, display module, controller module, power amplifier module and actuator module. The overall design block diagram of the system is shown in Figure 1 below.

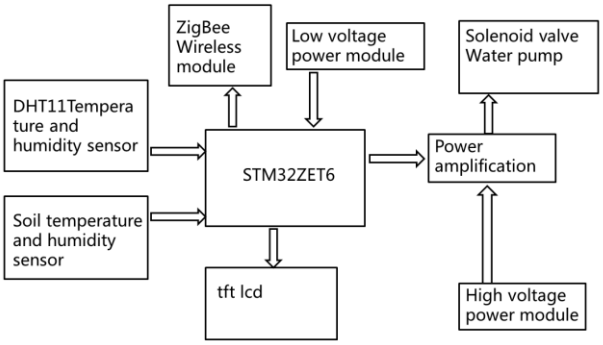

Fig.1 System diagram

The system through the measurement of soil moisture, soil information acquisition, through the controller for processing, and then through the ZigBee network, wireless data transmission to the display on the LCD screen, when the data is not satisfied with the numerical limit set by the STM32 controller, the electromagnetic valve is opened, to irrigate the soil, until the data meet the limit value set close the valve, computer controller[2].

III. SYSTEM HARDWARE DESIGN

Each module of the system is described as follows:

A. The Control Module

The control module is the core of the whole system, which is the control center which connects the various modules of the whole system, and the control module is composed of a controller and a sensor, wherein the controller is adopted by STM32F130ZET6 micro controller, sensor with DHT11 soil temperature and humidity sensor and soil humidity resistance sensor type.STM32F130ZET6 micro controller low price, but also has the advantages of high speed, strong anti-interference, low power consumption, very suitable for use as the main control chip. The micro control with the traditional 8051 Comparing with the micro controller of this type of both in cost and computation speed significantly advantage. Therefore, the microcontroller is used as the main control chip of the system[3]. The soil water temperature sensor DHT11 is a new type of temperature and humidity sensor. DHT11 digital temperature and humidity sensor is a temperature and humidity sensor calibration containing composite digital signal the output, it is used for digital modules acquisition and humidity sensor technology to ensure that the product has high reliability and excellent long-term stability. The sensor includes a resistance type humidity sensitive element and a NTC temperature sensor, and a high performance 8 bit microprocessor. Connection. So the product has excellent quality, fast response, strong anti-interference ability, cost and other advantages. Each DHT11 sensor is calibrated in a very accurate humidity calibration laboratory. The calibration coefficient in the form of a program stored in OTP memory, the sensor to call these calibration factor in the process of signal detection. The single wire serial interface, the system integration becomes easy. Ultra small volume, low power consumption, make it become the best choice for applications in harsh applications. The product is 4 needles single pin package, convenient connection[4].

B. The Remote Monitoring Module

Through the ZigBee node and center node, using the touch screen to realize remote monitoring. The communication host selection of RS232 ZigBee from RS232 to ZigBee., selection of communication distance up to 1600m touch screen selection model for the 3.2 inch TFT touch screen. The touch part of the four wire resistive touch screen. This kind of theory can meet the demand of remote monitoring the system.

C. The Watering Module

Irrigation module: controlled by the control module to pump water. After the experiment, can meet the needs of irrigation

D. The Power Module

Power Module: divided into 220V AC and step-down module. Because the touch screen can not use 220V power supply, so the introduction of the AC-DC module, using 3.3V power supply.

IV. System Software Design

The system uses STM32F103ZET6 microcontroller for data processing, using C language to design and develop the software. The utility model has the advantages of good readability, portability, etc. the design of the whole system is realized by using the modularization idea. Procedures for the reading, transplantation and post - improvement. The figure is shown in Figure 2.

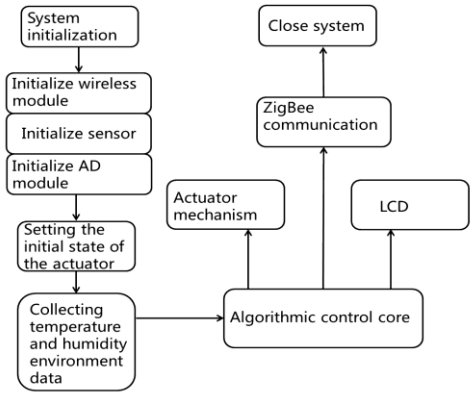

Fig.2 Soft structure chart

A.The temperature and humidity data collected by soil moisture sensor A/D

After the conversion, through the calculation of SCM transmits the data to the host processing after arbitration by wireless module. The communication protocol MODBUS-RTU protocol data transmission, the protocol is a master-slave protocol with a master and a number from a bus station, the communication parameters between each station must be consistent, including data bits, parity check the way, the baud rate and the number of stopbits needed in the program, each site will be set to these parameters. In addition, each station set up from the station address must be different, otherwise it will cause from the conflict between stations[5].

B. The upper computer processing module

Figure 3 is the monitor interface. The interface parameters are divided into two sections, the left side plate can be selected in the planting area, planting varieties, as well as various parameters corresponding to plants, including experts and real time display parameters of temperature, humidity and light. The right side plate for the real-time display of temperature and humidity curve, can be more intuitive understanding of the changes the temperature and humidity.

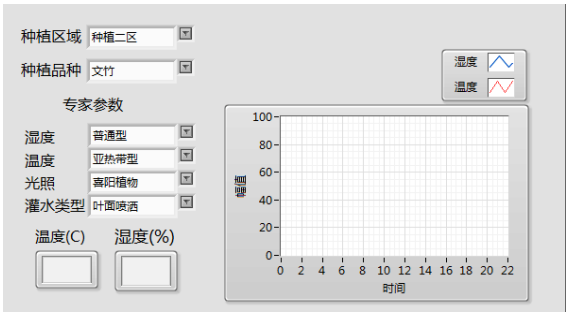

Fig.3 Parameter monitoring chart

V. TEST AND ANALYSIS

The measurement process of soil temperature and humidity: resistive humidity sensor is inserted into the measured soil, open circuit, LCD display the current temperature, humidity, when the soil humidity is lower than the lower limit of the humidity controller, the electromagnetic valve is opened for irrigation on the soil, the LCD display real-time humidity, humidity gradually the humidity rises to the set limit, the controller closes the electromagnetic valve[6].

The results collected in the computer display as follows: after initialization, the controller will soil temperature and humidity sensors to collect data through the ZigBee network transmission to the PC, and the PC, as shown in Figure 4. The humidity is lower than the set threshold, the pump starts to work, the application of water to the soil, reaching the upper threshold, the water pump stops working. The map shows that the system can clearly and intuitively, quickly and accurately reflect the current condition of the soil. After several tests, the system stability is good, can achieve the desired objectives.

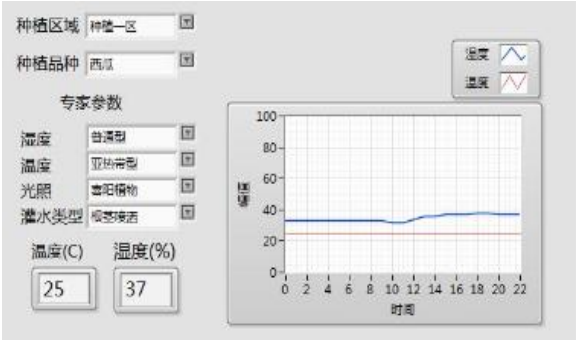

Fig.4 Specific parameter diagram

VI. CONCLUSION

This paper designs an automatic irrigation system of wireless local area network project based on ZigBee, using STM32F103ZET6 as the main control chip, combined with the humidity resistance of soil water temperature sensor to measure the soil temperature and humidity, through the TFT touch screen display measuring different position sensor values, select a motor live solenoid valve, the soil temperature and humidity acquisition the use of ZigBee and network technology, real-time display on the host computer, and complete the relevant arbitration logic in the host computer, the humidity regulated by pump, keep the soil in a certain range of temperature and humidity, increase crop production quality And yield[7].

References

[1] Liu Kui.ZigBee technology and application [J]. science and technology information.2006 (06)

[2] Liu Yaju, Cai Zhenjiang, Zhang Li,,. Design of ZigBee wireless sensor network node based on RF chip [J]Microcomputer information.2007.

[3] Zhuo Yiming. weeks of wireless sensor network monitoring and control system based on greenhouse group Research and implementation of key technologies [D]. Zhejiang University, 2009

[4] Feng Youbing, Zhang Rongbiao, and. Application of wireless network in water saving irrigation [J]. China Rural Water Conservancy and hydropower, 2007

[5] song Lei. Research on greenhouse crop monitoring system

based on wireless sensor network [D]. days Tianjin University of science and technology, 2013

[6] bear. Based on wireless sensor network of farmland soil temperature and humidity monitoring [J]. electronic world, 2014

[7] Wang Meng, Liu Bin, Wang Dan. Computer measurement and control [J].2013,12.

Experimental platform of programmable inverted pendulum control system

Wang Rui-jian; Fang Yu; Wang Jing-xiang
(College of Instrumentation and Electrical Engineering, Jilin University,Changchun 130022,China)

***Abstract*—This paper develops a set of experimental platform for students of the inverted pendulum control system, including the host computer ,slave machine based on DSP, inverted pendulum, DC motor and human-machine interface based on LABVIEW. The platform gives the inverted pendulum control routines, and students can easily carry out independent innovation experiments on the host computer with real-time observation of state parameters. It can also be used to modeling and simulation of the pendulum, andwe can directly compile the host computer to control the invented pendulum motor and practice varieties control methods. Students can also carry out the programming training, system debugging, exploration of new control strategy through the experimental platform.**

***Key words*— Rotary Inverted Pendulum Experiment Platform Control Theory**

I. INTRODUCTION

AS a typical unstable, high-order, strongly coupled, multivariable and nonlinear system, inverted pendulum model is the focus of many experts and scholars in the field of control. The inverted pendulum model can be used to simulate and verify the existing control methods and theories, so as to put forward some new theories and methods [1]. Inverted pendulum is a good experimental platform of the theoretical research, which build a good environment for the automatic control theory teaching and experimental research, in order to examine some control methods and theories. Thus it speeds up the development of new control theory.

Due to the application of control theory is very extensive, the technical methods it brings used in machine control technology, semiconductor processing, precision instruments, artificial intelligence, missile intercept satellite flight control, attitude control of aviation docking control technology and industrial applications and other aspects have great prospects for development.

II. MATHEMATICAL MODEL OF ROTARY INVERTED PENDULUM

Under the condition of ignoring all kinds of resistance and friction, the rotating arm and the swing rod can be abstracted as two homogeneous rods, and the simplified inverted pendulum is shown in Figure 1[2].

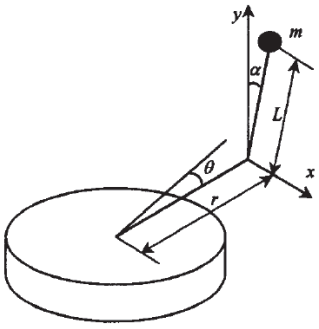

Fig.1 The Model of Rotary Inverted Pendulum

Table I
Relevant Physical Parameter

Symbol	Quantity
r	Length of the rotary arm
θ	Horizontal angular displacement
L	The length of swing rod
α	Vertical angular displacement

In the X and Y directions, the velocity component of the swing rod is:

$$V_x = r\dot{\theta} - Lcos\alpha(\dot{\alpha})$$
$$V_y = -Lsin\alpha(\dot{\alpha}) \quad (1)$$

The dynamic equation of the system is derived by using the Lagrange equation. Set the potential energy surface of the swing arm to zero, and then the potential energy of the system is the gravitational potential

energy of the swing rod.

$$V = mglcos\theta \tag{2}$$

The kinetic energy of the system is composed of 4 parts, including the rotation of the rotating arm in the horizontal plane, the rotation of the swing rod in the vertical plane, the velocity of the center of gravity of the swing rod along the $x$axis and the speed along the y axis. The corresponding kinetic components are represented by T_1, T_2, T_3, T_4 respectively.

$$\begin{aligned} T_1 &= J_1\frac{\theta^2}{2} \\ T_2 &= J_1\frac{\alpha^2}{2} \\ T_3 &= \frac{m(r\theta - Lcos\alpha(\alpha))^2}{2} \\ T_4 &= \frac{m(-Lsin\alpha(\alpha))^2}{2} \end{aligned} \tag{3}$$

According to the thin rod inertia formula (rotating shaft at one end of the rod)

$$J = \frac{mR^2}{12} \tag{4}$$

Where $R = 2L$, R for the pendulum rod length.

As ***Lagrange equation*** shows

$$L(q,q) = T(q,q) - V(q,q) \tag{5}$$

L is a Lagrange operator, q is a generalized coordinate, T is the kinetic energy of the system, V is the potential energy of the system. Then substitution the Lagrange formula for these variables above, finishing state equation

$$\begin{bmatrix} \dot{\theta} \\ \ddot{\theta} \\ \dot{\alpha} \\ \ddot{\alpha} \end{bmatrix} = \begin{bmatrix} 0 & 1 & 0 & 0 \\ 0 & \frac{-4G}{4J_1+mr^2} & \frac{3rg}{4J_1+mr^2} & 0 \\ 0 & 0 & 0 & 1 \\ 0 & \frac{-3rG}{(4J_1+mr^2)L} & \frac{3(J_1+mr^2)}{(4J_1+mr^2)L} & 0 \end{bmatrix} \begin{bmatrix} \theta \\ \dot{\theta} \\ \alpha \\ \dot{\alpha} \end{bmatrix} + \begin{bmatrix} 0 \\ \frac{4\eta_m\eta_g K_i K_g}{(4J_1+mr^2)R_m} \\ 0 \\ \frac{3r\eta_m\eta_g K_i K_g}{(4J_1+mr^2)LR_m} \end{bmatrix} V_m \tag{6}$$

Where

$$G = \frac{\eta_m\eta_g K_i K_m K_g^2 + B_{eq}R_m}{R_m} \tag{7}$$

Table II

Meaning Of The Parameter

Symbol	quantity
B_{eq}	Viscous damping coefficient
η_m	Motor efficiency
η_g	Retarder efficiency
K_i	Proportion coefficient of Motor torque
K_g	Proportion coefficient of retarder
V_m	Armature voltage
K_m	Back EMF codfficient

By the state equation, controlled variable is the motor input voltage, measurement variables are the rotating arm angle and the swing rod angle, and get the conclusion: the rotary inverted pendulum control system is a double input and single output closed-loop control system.

III. PID CONTROLLER DESIGN

PID control is one of the control strategies that developed earlier among the various controllers and its algorithm is simple and has good robustness and adaptability. It is widely used in industrial control process. In the last century until 30s, except in the simplest environment where controllers were consisted by the switch, PID control is the only way to be applied. After that, with the rapid development of modern technology, more and more control methods came into being, such as fuzzy PID [3], neural network control technology, etc.

From the analysis above, the stability control of rotary inverted pendulum includes two aspects, one is balance control, and the other is rotating arm position control. It is necessary to design two control loops to respectively control the position and balance by double closed loop PID controller whose inner loop controls the balance and the outer loop controls the position, as shown in figure 2:

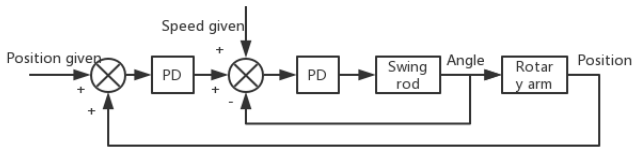

Fig.2 System control loop

The inner loop is a swing rod angle control loop, which is a negative feedback loop. The outer loop is the rotary arm position control loop, which is a positive feedback loop. The control frequency of the inner ring is 1-5 times higher than that of the outer ring. In the contradiction of position control and balance control, the "position" and "balance" are two aspects of contradiction, and the "balance" is the main aspect of the contradiction, the position control is the secondary contradictions. Although the formation of local positive feedback, thanks to the negative control of the inner loop and the characteristics of the inverted pendulum, the contradiction of the balance control and the position control has been resolved [4]. The simulation results of the system by MATLAB are shown in figure 3.

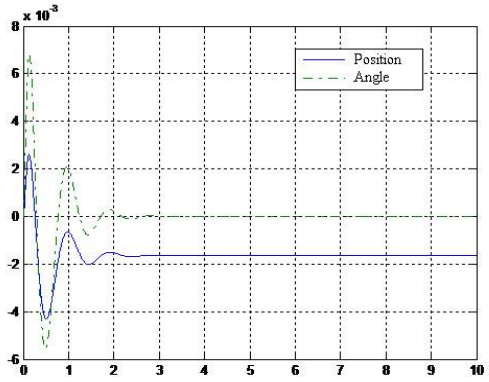

Fig.3 Step response of the system

IV. Experimental Platform Designs

The inverted pendulum is shown in figure 4. The inverted pendulum has two equilibrium states, one is the static balance state as the swing rod falls down, and the other is the dynamic balance state as the swing rod stands up. Therefore, it is necessary to break the original natural state of static balance, and make it run to the dynamic balance state.

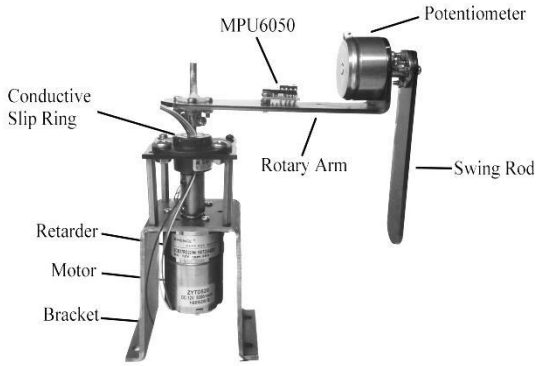

Fig.4 Actual object of reverted pendulum

The input of the inverted pendulum system is the expected value of the rotary arm angle (position) and the angle of the swing rod. Sensors (conductive plastic potentiometer and MPU6050) collected the position data of the rotary arm and the swing rod in every sampling period, and then the real-time controller (TMS320F2812) generates the PWM signal according to the PID control algorithm. The TB6612 motor driver amplifies the PWM signal and then drives the motor to rotate, and thus realize the closed-loop pendulum angle and rotating arm position control.

TMS320 F2812 is one of the TI Company's C2000 series higher cost device. The device integrates rich and advanced peripherals, such as Flash memory and 128kB 4kB boot ROM, mathematical operation table, motor control peripherals, serial communication peripherals, 2kB OTP and ROM 16 channel high performance 12 bit ADC module, provides two sample and hold circuit which can realize dual channel signal synchronous sampling at the same time. It also has the very high precision (32 bits) and the processing capacity (up to 150MIPS), which can be widely used in electric power automation, motor control and frequency conversion household appliances and other fields [5].

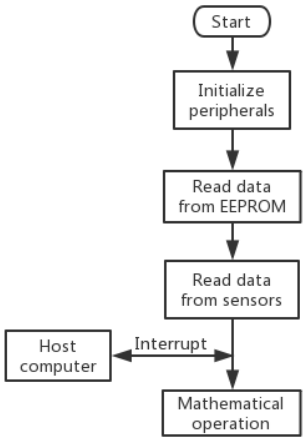

Fig.5 Flow chart of the slave software

The key executing mechanism of the system is the motor, the motor drives the rotary arm to rotate, and then the swing rod can swing and stand upside down. In this experiment, the DC motor with excellent performance is selected as the driving motor, which can meet the requirements of torque and simple control circuit.

The swing rod is connected with the rotary arm by a conductive plastic angular displacement sensor [6]. The swing of the swing rod drives the potentiometer to rotate, the output voltage and the pendulum angle corresponding to the voltage, through the filter into the controller, the AD conversion unit of the controller can converts the voltage signal into the digital signal, so as to detect the angle of the swing rod for further processing.

In order to meet the requirements of the rotating arm can rotate freely and ensure the reliable electrical connection with the base, avoid winding phenomenon during rotate, the conductive slip ring is used to solve this problem. The conductive ring has 6 wires, isolated from each other. By the internal six brushes and slip ring, the angle sensor, MPU6050 and controller located on the base were reliably connected, and resolve the contradiction.

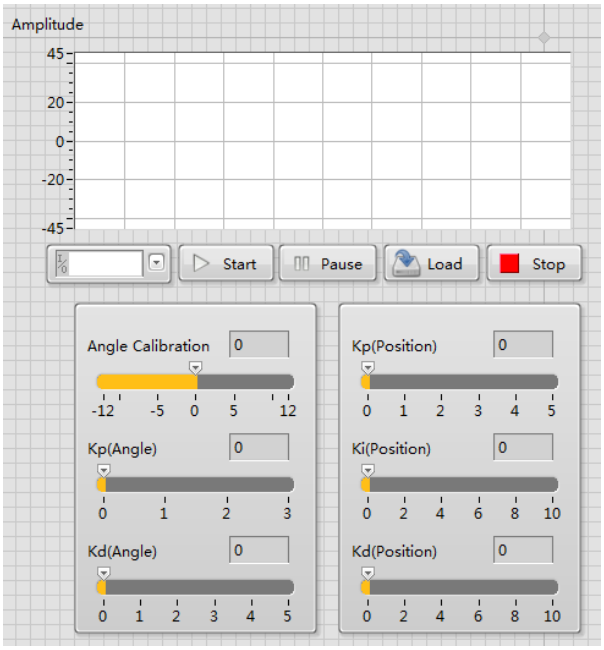

Fig.6 Host GUI of LabView

The host computer is designed by LABVIEW, communicates with the controller by serial port [7]. Under the control of the host computer, the controller feds back the data of the position of the rotary arm and the angle of the swing rod in order to display the state of the inverted pendulum controller. Controller generates different duty cycle of the PWM signal and the steering logic signal, and then motor driver TB6612 drive the motor according to these signals, realize the rotation of the rotating arm.

V. PLATFORM TEST

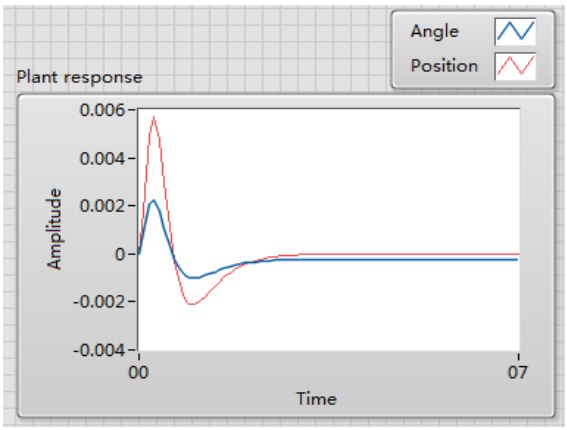

Fig.7 Data measured

After the test, the swing rod of the experimental platform can quickly stands up, and can automatically track the given position. Figure above is the actual measured data which means that the pendulum has been stable and affected by external noise. It can be

seen in the disturbance, the swing rod (blue curve shown) angle increases positively, and the rotary arm rotated at a faster speed, a greater amplitude, trying to hold up the tilt swing arm back upright. When the angle speed of the swing rod decreases to 0 the rotary arm rotated backwards, trying to move back to the original given position, and generates an overshoot. After a round of adjustment, the swing rod eventually returned to the stable inverted state and the rotary arm returned to the given position.

VI. CONCLUSIONS

The inverted pendulum is recognized as typical experimental equipment in the automatic control theory. It is also the object of control theory teaching and scientific research. Through the research on inverted pendulum system, the theory can not only solve the control problem, but also will involve three basic theories: mechanics, mathematics and electrical (including computers). The research and application of various control theories and methods, especially in engineering practice, inverted pendulum builds a bridge from control theory to practice. Experimental platform of programmable inverted pendulum control system consists of PC as host and inverted pendulum control system as slave. Students can write control algorithm in computer and simulate, then control the inverted pendulum, observe the experimental parameters. It's a convenient, high precision, accuracy experimental platform, and it can lower the threshold of development, accelerated experiment process.

References

[1] SONG Guojie. Research on Double Inverted Pendulum Control Using Adaptive Fuzzy PID[J]. Journal of Huaqiao University (Natural Science),2016,37(1):74-75

[2] Wu Aiguo, Zhang Xiaoming, Zhang Zhao. A Control System Based on the Lagrange Modeling Method for a Single Link Rotary Inverted Pendulum[J]. ENGINEERING SCIENCE,2005,7(10):11-15

[3] Bryson, A. E., Luenberger， D. G. The Synthesis of Regulator Logic Using State-Variable Control[J]. Proceeding of the IEEE, 1970, 58(11):1803-1811.

[4] Ruan Xiaogang. Research and design of the two-wheeled self-balancing robot[M].2012.2

[5] GAO Cui-yun, JIANG Zhao-hui, SUN Bing. The Design of DSP Minimum System based on TMS320 F2812[J].JOURNAL OF ELECTRICAL & ELECTRONIC EDUCATION,2009:83-85.

[6] Li Jie. Application of conductive plastic potentiometer[J]. Automation and instrumentation,1990:47-49.

[7] Ma Yinping, Wang Changkun,Ye Zhibin. Design and Realization of Data Communication Based on LabVIEW[J]. Industrial Control Computer,2015,28:61-62

Study on the service life of the electric cables in EMU

Changyingng Liu; Shuiyi Kuang; Kefei Dong; Xin Zhou
(College of materials Science and Engineering, Jilin University,Changchun 130012,China)

***Abstract*—According to The Arrhenius Thermal Aging Equatin,the project achieves the aim of assessing the service life of electrical cable on EMUs.Based on Matlab,the project uses the least square method to fit the experimental data and takes sample,then uses particle swarm method to optimize the data.Finally we set a systematic assessing model which can be displayed on the interface programmed by Matlab.**

***Key words*—EMUs Electrical cable The least square method Particle swarm method Service life assessing**

I.INTRODUCTION

SINCE the twenty-first century, rail transit has become one of the important modes of transportation for people to travel. Therefore, the safe operation of rail transit has a direct impact on the travel safety of the masses, and the power cable is the key factor affecting the safe operation of rail transit , So the evaluation of the life of the power cable is critical. At present, the evaluation of the service life of the cable is mainly based on the statistical method and the accelerated test method. The acceleration test method is mainly based on the Arrhenius thermal aging equation. When calculating the aging life of the cable, the calculation is large and the work is cumbersome, which is not conducive to the technical staff[1]. This paper mainly based on Arrhenius thermal aging equation, using Matlab software for data fitting, editing optimization algorithm program, and through the interface to the evaluation results show, simplifying the cumbersome workload, so that technical staff easy to master and operate.

II.BASIC PRINCIPLES

According to the thermal aging mechanism and the Arrhenius model, the performance degradation rate caused by the thermal reaction of the cable insulation material is inversely proportional to the exponential of the activation energy, inversely proportional to the reciprocal of the reciprocal of temperature, as follows:

$$\partial m / \partial t = A_0 \exp[-E_a /(kT)]$$

In the formula: m is a product of a characteristic worthy of degradation (we use the cable insulation material elongation at break for the cable insulation material caused by the thermal degradation of the performance),k is the Boltzmann number, T is the absolute temperature, constant, t is the reaction time, is the reaction activation energy.

Assuming that the initial degradation rate of the reaction material is m_0, the corresponding time is t_0, the material reacts to the time t_1, the degradation rate is m_1: when the temperature T is fixed,there is:

$$m_1 - m_0 = \int_{t_0}^{t_1} A_0 \exp[-E_a /(kT)]dt$$

Then:

$$m_1 - m_0 = A_0 \exp[-E_a /(kT)]^{(t_1 - t_0)}$$

Assuming that t=t1-t0,then:

$$t = [(m_0 - m_1) / A_0] * \exp(E_a / kT)$$

When the degradation rate of the material becomes a certain degradation rate M, it can be considered that the material completely doesn't work, and reach the service life,.If we take the two sides of the formula for the logarithm,we can get[2-4]:

$$Lnt = Ln[(m_1 - m_0) / A_0] + E_a /(kT)$$

Assuming that $A=Ln[(m_1 - m_0)/A_0]$, $B=Ea/k$, then we can get that:

$$Lnt=A+B/T$$

Among them A and B are unknown parameters. The

above equation shows the relationship between the thermal aging life of the cable insulation material and the heat aging temperature, that is, the logarithm of the thermal aging life is linear with the reciprocal of the heat aging temperature,called the derivative equation of the Arrhenius equation[5].

The parameter A indicates the change in the degradation rate of the cable insulation material in the high temperature thermal aging test, that is, the ratio of the change in elongation at break to the constant A0. The parameter B represents the ratio of the activation energy of the reaction to the Boltzmann's constant K in the thermal aging test.

III.THERMAL AGING TEST

In the process of cable aging, the molecular chain of the insulating material is continuously degraded and the elongation at break is also reduced. Therefore, the elongation at break reflects the thermal aging reaction of the insulating material objectively.

Select the power cable insulation material for the thermal aging test material, calculated by the following formula power cable insulation elongation at break.

$$k = k_1 / k_0$$

$$k_1 = \delta l_1 / l_0 * 100\%$$

$$k_0 = \delta l / l_0 * 100\%$$

In the formula,K is the breaking elongation,k1 is the breaking elongation for the aging of the experimental material, and k0 is the average elongation at break for the initial experimental material. L0 is the pattern line spacing, δl1 is the aging pattern after the mark before the line spacing change value,δl is the pattern of broken before the line spacing changes[6-7].

In order to achieve a short time to achieve the process of cable insulation aging, the laboratory uses high temperature accelerated insulation material thermal aging, the experimental material selected nine kinds of EMU commonly used cable which are 204025/A，152083/B，152082/A，264080/C，152002/C，-LL/DI，101025/A，162001/A，352080/A , following is experimental data:

Table1. 135 ℃ hot air aging elongation retention rate after aging /%

model time	0h	216h	456h	648h	984h	1104h
204025/A	100	97.11	89.64	78.12	45.93	25.17
152083/B	100	98.93	91.78	85.42	58.12	36.18
152082/A	100	96.19	88.04	76.47	42.15	28.49
264080/C	100	91.24	90.68	69.94	35.69	17.12
152002/C	100	98.92	92.46	87.52	60.43	38.14
-LL/DI	100	96.59	89.72	80.43	55.96	34.29
101025/A	100	99.24	94.27	89.26	70.43	51.28
162001/A	100	96.48	89.11	74.29	40.96	30.24
352080/A	100	95.19	87.64	75.29	41.18	20.64

Table1. 150 ℃ hot air aging elongation retention rate after aging /%

model time	0h	144h	192h	264h	337h	408h
204025/A	100	90.02	78.14	60.93	47.15	28.17
152083/B	100	91.59	80.57	62.84	49.26	30.92
152082/A	100	88.43	71.84	58.26	40.18	25.43
264080/C	100	85.19	66.43	49.15	35.29	19.96
152002/C	100	92.43	80.96	64.19	52.76	39.18
-LL/DI	100	91.59	78.63	59.17	46.64	29.54
101025/A	100	95.28	87.14	75.64	55.84	46.74
162001/A	100	90.96	80.15	64.19	50.64	31.72
352080/A	100	89.64	76.19	60.47	47.26	29.54

Table1. 165 ℃ hot air aging elongation retention rate after aging /%

model time	0h	24h	48h	72h	96h	120h
204025/A	100	93.77	82.46	70.18	47.82	30.47
152083/B	100	94.82	85.96	75.46	60.72	41.83
152082/A	100	91.46	78.49	68.17	45.62	28.59
264080/C	100	89.18	77.42	64.92	44.13	26.59
152002/C	100	95.78	87.14	80.29	71.23	54.82
-LL/DI	100	94.77	86.24	74.18	61.05	40.29
101025/A	100	97.14	92.18	88.65	79.24	67.28
162001/A	100	92.57	83.14	71.29	49.28	31.84
352080/A	100	90.48	80.22	65.41	41.29	30.85

Table1. 180 ℃ hot air aging elongation retention rate after aging /%

model time	0h	12h	24h	36h	48h	60h
204025/A	100	91.78	66.85	38.17	20.43	18.69
152083/B	100	92.06	67.14	39.85	21.99	20.43
152082/A	100	90.47	65.72	36.82	19.74	16.43
264080/C	100	87.64	60.41	35.29	18.14	15.42
152002/C	100	92.78	69.14	41.25	25.41	20.79
-LL/DI	100	91.92	67.44	39.02	20.79	19.14
101025/A	100	94.77	70.28	45.29	31.46	25.94
162001/A	100	91.11	67.42	39.46	22.18	19.06
352080/A	100	89.47	61.26	37.26	19.17	18.02

Experimental data processing takes the 101025 / A model cable for example, the rest of the data processing process is the same.

Use matlab to simulate the thermal aging data of 101025 / A model cable with the aging time as the abscissa and the breaking elongation as the vertical axis. The fitting results are shown in Fig.1. According to the requirement of breaking elongation retention, the corresponding failure time, ie, aging time, of the cable at different experimental temperatures is taken. Assuming that the cable elongation retention rate is 70%, the cable reaches the corresponding failure time and is intercepted by Matlab software The corresponding failure time of the cable at different experimental temperatures is shown in Table 5.

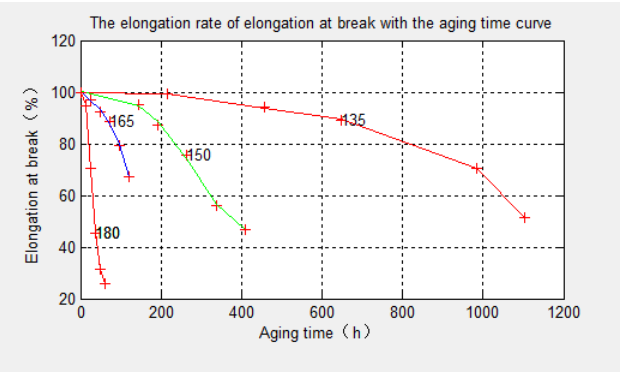

Fig.1 Curve of elongation at break of 101025 / A cable at different experimental temperatures with aging time

Table 5 Erosion elongation retention rate of 70% 101025 / A cable at different experimental temperatures aging time

temp/℃	135	150	165	180
time/h	986.163	281.352	115.386	23.9938

IV.Optimization Algorithm and Optimization

Error Analysis

A. Particle swarm optimization

The aging time t at four different experimental temperatures T and 70% elongation at different experimental temperatures is known, according to the derivative equation of the Arrhenius equation:

$$Lnt=A+B/T$$

We can optimize the unknown parameters A and B, the optimization method using particle swarm optimization algorithm.

Particle swarm algorithm is to think of the individual in the group as a particle moving at a certain speed in the D-dimensional space. All particles have an appropriate value determined by the optimized function. The velocity of the particle determines the direction and position of the particle, and Towards the best position of their own history and the best place for group history. Particle swarm algorithm initialization is a group of random particles, through continuous iteration to find the optimal solution.

Main steps of algorithm as follow:

(1)Initialize, set the learning factors c1, c2, the maximum evolutionary algebra maxDT (the maximum number of iterations), the number of initialized population N, the spatial dimension D (unknown number).

(2)Calculate the fitness value for each particle $F(x_i)$.

(3)Comparing the current fitness value $F(x_i)$ with the individual historical best position Pbest, if $F(x_i)$ is better than Pbest, then consider Pbest as present $F(x_i)$ and define Pbest as the position of the current particle.

(4)Comparing the current fitness value $F(x_i)$ with the universal historical best position Pbest, if $F(x_i)$ is better than Pbest, then consider Pbest as present $F(x_i)$.

(5)Update the speed and position of the particle, the particle velocity updated formula and the location updated formula are as follow:

$$V_{id} = w \times V_{id} + c_1 \times r_1 \times (P_{id} - X_{id}) + c_2 \times r_2 \times (P_{gd} - X_{id})$$

$$Xid = Xid + V_{id}$$

In the formula,w is the inertia weight, c1, c2 is the learning factor, r1, r2 is the random number in the

fixed interval, Pid is the best position of the individual of the d particle, Pgd is the best position of the group, Xid is the current position of the d particle.

(6)If the end condition is satisfied or the maximum number of iterations is reached, the operation is ended, otherwise the iteration from (2)[8-11].

B．Parameter setting and running result

Algorithm initialization parameter setting:

C1=C2=2.8，D=2，maxDT=300，N=400

Fitness function:

sum=sum+abs[A1(j)*x(2)+x(1)-B1(j)];

In the formula,Sum is the return value of the function, initialized as sum = 0, x (1), x (2) is the optimization parameter, A is the array of different experimental temperatures A = [180 165 150 135], defined as the fracture at different test temperatures (B = [27.37 91.74 300.87 907.35] when the elongation retention rate is 70%, then A1 = l ./ (A + 273.15) (l is the unit array) in the fitness function, B1 = log (B).

Algorithm Run Results:

x(1)=28.490764，x(2)=14442.220376.

Then we can get 101025 / A cable life evaluation equation is:

Lnt=28.490764+14442.230376*（1/T）.

Assuming that the actual operating temperature of the 101025 / A cable is 75 ℃, the retention rate of the elongation at break is 70% as the end of the cable life, and the service life of the 101025 / A cable is evaluated.

T = 446801h = 18616.7 days = 51007 years.

C．Error Analysis

When the experimental temperature is 135 ℃ and the elongation at break is 70%, the experimental data of 101025 / A are brought into the program. The results are shown in Fig.2.

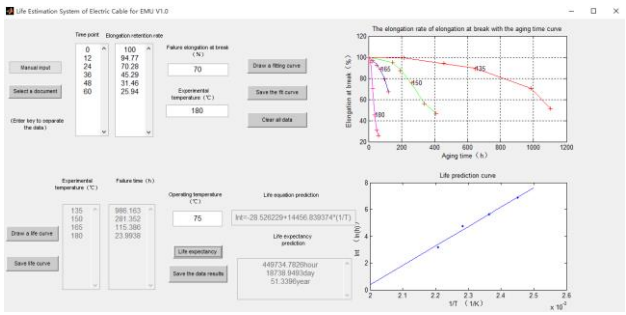

Fig.2 . 101025 / A cable at 135 ℃ elongation retention rate of 70% of the operating results

The results show that the service life of the 101025 / A cable is 986.163 hours when the elongation at break of 70 ℃ is 70%, and the service life of the 101025 / A cable is 988.7901 after the particle swarm optimization algorithm Hours, we can see that there is an error between the optimization result and the actual result. After multiple runs of multiple sets of data, the error is about 1%, and the lower the temperature the smaller the error.

Main reasons for the existence of errors are as follows:

(1)data fitting using the Matlab software to test the data obtained by fitting the curve, and then in the fitting curve to intercept the elongation at break corresponding to the life of the data, the process inevitably there will be errors.

(2)The optimization algorithm uses the particle swarm optimization algorithm, the optimization algorithm itself has a certain degree of uncertainty, and therefore will lead to some error.

(3)The thermal aging test of the cable is only carried out at 135 ℃, 150 ℃, 165 ℃, 180 ℃ four groups, the data obtained is relatively small, the optimization algorithm can only be optimized according to four points, relatively speaking, there is a certain Of the uncertainty, resulting in the existence of errors.

V.SYSTEM INTERFACE AND FUNCTIONAL DESCRIPTION

In order to avoid complicated operation, reduce the operation over, easy to use, design software interface as shown in Figure.3.

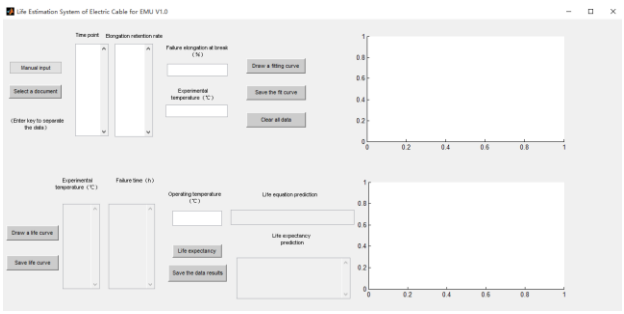

Fig.3 software operation interface map

A．Experimental data processing function

The input of the experimental data is manual input and file input (txt and excel). When the data is entered manually, the data points are separated by carriage

return. The data file also requires txt text data to be divided into two columns, namely time data points And breakage elongation retention data points.

The experimental data curve fitting can fit the curve of cable elongation retention and the corresponding experimental time at different experimental temperatures. The fitting curve under different temperature experiments is plotted in the same coordinate system, and it can be clearly seen that different temperature The elongation retention rate of the cable under the test time varies with the experimental time, as shown in Fig.1

Through the experimental data, the curve of the elongation retention rate of the fracture with time is fitted. According to the requirement of breaking elongation retention rate, the corresponding failure time, that is, the aging time and the interception time data of the cable at different experimental temperatures are taken in the corresponding data display area display..

B．Cable life prediction and equation fitting function

Through the processing of the data, we can get the fitting curve of the cable life and the corresponding fitting equation. By fitting the equation, we can predict the cable life at different working temperatures and input the expected operating temperature of the cable to obtain the corresponding cable life time.

C．Data save and clear function

The software design process, a total of two fitting curve coordinate system, fitting the curve as an intermediate result and the final result, the requirements can be selected according to the actual needs of storage, storage format default JPG picture format. The final result of the software is the cable fitting equation and the life of the cable at a certain temperature. According to the actual needs, the intermediate data points and the final fitting equation and the result of the cable life can be saved. The default is txt text format. The result is the carriage return line Open, the data text is saved as shown in Figure.4.

Experimental temperature	135℃	150℃	165℃	180℃
Failure time	986.163小时	281.352小时	115.386小时	23.9938小时
Fit the equation	lnt=-28.526229+14456.839374*(1/T)			
Operating temperature	75℃			
Predicted life expectancy	449735小时=18738.9天=51.3396年			

Fig.4 . Data TXT format to save the results

The software data clear function is used for a certain type of cable prediction is completed, the next model cable prediction, or the middle of the input operation errors, etc., can be cleared to facilitate the cable again to predict the life of the cable.

References

[1] Zhang Daopeng et al.The Fast Calculation Method of Cable Life [J] The 17th China Association for Science and Technology Annual Meeting - Sub - 7 Integrated Rail Transit System Academic Salon Proceedings 2015 U269 P5.

[2] ChenDong et al. Research on Evaluation Model of Insulation Aging Life of Power Cable [J] Fiber and Cable and Its Application Technology 2015 No. 5 P37-38,46.

[3] Zhang Tieyan et al. A life evaluation method of power cable based on improved Weibull distribution model [J] Journal of Engineering Science (China University of Science and Technology).

[4] Zhao Cong. Evaluation and Prospect of High Performance XLPE Cable Life [J] Electrical Technology, 2014, No.4 P60-65.

[5] Yu Zhongqii. Evaluation Method of Working Life of Cable [J] Journal of Tianjin University of Commerce 2002 Vol 22 No.3 P32-34.

[6] Yu Jinhua et al. Study on the Extraction Technology of XLPE Cable Insulation Aging Based on the Significance Test Method [J]. East China Electric Power, 2013, (06): 1279 (in Chinese) [J]. -1282.

[7] Zhou Yunjie et al.Effect of Accelerated Thermal Aging on Insulation Mechanical Properties and Dielectric Properties of XLPE Cable [J]. East China Electric Power, 2014, (08): 1606-1610.

[8] Tian ye.Particle swarm optimization algorithm and its application [J] .Journal of Jilin University, 2010.

[9] Xu Qinghe.Improved Particle Swarm Optimization Algorithm and Its Application [D]. Hangzhou Dianzi University, 2009.

[10] Fang Jun.Particle Swarm Optimization and Its Application [D]. University of Electronic Science and Technology of China, 2006.

[11] Huang Wanping.Adaptive particle swarm optimization algorithm and its application research [D]. Zhejiang University, 2006.

The service life of the emu air switch simulation and evaluation research

LIU Chang-ying; LIU Zhen-bo; LI Yu-xiang; LI de

(College of materials Science and Engineering, Jilin University,Changchun 130022,China)

***Abstract*—Both family circuit of residential and industrial production lines, even trains, ships and aircraft and other kinds of even the circuit on the transportation system, cannot leave the air switch, so the control and the protection of the quality safety and the service life of the air switch must be attached great importance to.In this topic,the mechanical operating life test and the electrical life test of the Air switch is performed.In the aspect of hardware,according to the open source, impedance load test are the requirements of the test of main circuit is designed,Design for PLC control of operating mechanism to realize the drive circuit of empty close break-brake operations.Based on condition monitoring circuit of data acquisition card,detect voltage and current in the process of open electrical life test In real time.In the aspect of software,Based on the LAVIEW,Life test control software is designed.It has a test parameter Settings, as well as the device debugging and life test automatically, and other functions.The test device can realize open automatic fault detection, do the operating life test of air switch and improve the test efficiency.It is reliability online prediction of open research provides an effective means of test.**

***Key words*—Air switch Operating life test Condition monitoring Fault detection**

I.INTRODUCTION

WITH the rapid development of urban rail transit, especially the speed of up to a great development, and urban rail line extending unceasingly, the coverage is more and more widely, the impact of regional population will be more and more.How to ensure the safe, accurate, quick and comfortable service standard in the comfortable, improve the quality of service, so how to urban rail operations generated by the electric loss prevention and control, it is very important to improve people's quality of life.At present,the rapid development of rail transportation technology in the world,and Rapid changes have taken place in people's life and work.also Air switch application in rail transit vehicles is more and more widely.Air switch[1], also known as air circuit breaker[2], it is a kind of circuit breaker[3], in the low-voltage distribution network and the electric drive system is very important of a kind of electrical appliances,It combines control and multiple protection functions in one[4].It can finish the contact and segmented circuit, and can for the short circuit, circuit and electric equipment such as serious overload and under voltage protection, or for not frequent start motor.Both family circuit of residential and industrial production lines, trains, ships and aircraft and other kinds of even the circuit on the transportation system[5], cannot leave the air switch control and protection.Air switch in the control and protection circuit system directly[6], or indirectly, to protect the safety of the production and living, protecting the people's life safety.So the air quality safety and service life of the switch must be considerable attention and strict protection.Is integrated from various aspects[7], therefore, how to accurately evaluate the service life of rail transit air switch is the the main topics of the research and design.

II.THE SYSTEM OVERALL DESIGN

Air switch life test device structure is shown in figure 1,Overall mainly includes PC, drive circuit, detection circuit and main circuit of four modules.

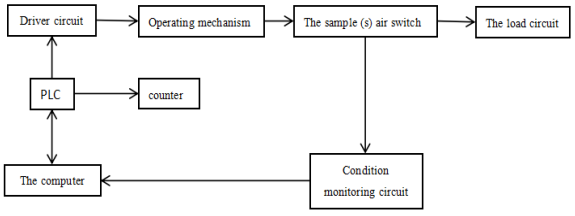

Fig.1 Air switch life test device structure

Using PLC control drive circuit,then Drive circuit in the control switch operating mechanism to achieve air switch try close break-brake operations, operating

mechanism simulating manual operation as far as possible,make no impact on the switch operation. Monitoring air switch try product information related to electrical parameters of current voltage monitoring circuit in contact state,Collection, analysis and processing, feedback to the computer,Computer according to the feedback information indicates a control on the PLC to make the sample open.This cycle until the monitoring circuit detecting circuit fault, records its cycle counter.According to the information on the computer drawing curve of service life of air switch.

III.THE SYSTEM HARDWARE DESIGN

A. The main circuit design

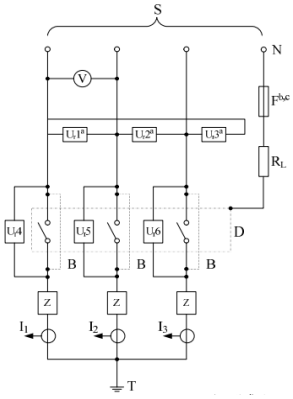

Fig.2 Main circuit

S—The power supply；V—Voltage meter；

Ur1~Ur6Voltage apparatus

N—Power supply neutral；R L Fault current limiting resistor;

Z—The load impedance；D—The sample (s) switch；

I1~I3—Current sensor；

B—Setting with temporary connections； T—Take place：

1, Ur connections between neutral point within 1 ~ Ur3 can instead.

2, such as the sample (s) as long as a test, can be directly down to a branch circuit.

3, dc, F should take extreme power connection.

Air switch test article through to in the process of test condition and breaking the same.The electrical life test on the main circuit and its validation and circuit breaking capacity test is the same.

Test time and space to open try work in normal situation, so they can simulate the load impedance Z after try,Contacts between the arc in the process of test case, try the interelectrode voltage will be close to the rated voltage of the circuit,making alternate with arcing conditions close to the actual situation.Before the sample (s) on the other hand, if put Z, then try each of the voltage during the experiments are much more than the low rated voltage, thus reducing the feasibility of producing electric arcing, reduces the examination conditions.

Stipulated in accordance with the electric life testing voltage value, current value and the power factor of load resistance R and inductance L:

$$R=\frac{u}{\sqrt{3}I}\cos\varphi(\Omega) \qquad (1)$$

$$L=\frac{1}{314}\frac{u}{\sqrt{3}I}\sqrt{1-\cos^{\wedge}2\varphi}\,(H) \qquad (2)$$

U for the electrical life test conditions specified in the connect or breaking voltage; I for the electrical life test conditions specified in the connected or breaking current;cosφfor the electrical life test conditions specified in the power factor of the circuit connected or breaking.

B. Condition monitoring design

The test device can collect real-time test of air switch voltage current value, and can according to the change of the voltage current worth quickly determine whether the sample (s) open to malfunction，so this requires the rate of data acquisition,to deliver the data to PC, PC according to the received information, PLC issue instructions, PLC sends control signals to drive circuit, implement open try switching.This test is A simple data acquisition card, at the same time, including A/D conversion, digital input, digital output and other commonly used detection and control function.The data acquisition card used as shown in figure 3.

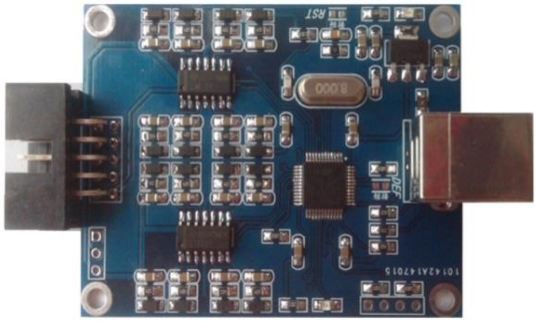

Fig.3 Data acquisition card physical figure

Using the data acquisition card to the work of air switch current voltage of the real-time acquisition,of voltage and current data collected will be transmitted to the PC, able to draw up the current voltage variation at the time of the open work, provide data support for the PC sends out control instructions.

c．Drive circuit design

Drive circuit receives the instruction from the upper machine, and converts instruction to corresponding electrical signal, and thus drive the corresponding devices to make mechanical action.In air switch life test, the driver circuit is mainly to realize the open close break-brake operations,using PLC of Siemens 2000, control of steering gear, to realize the air switch points brake.PLC of Siemens S7-200 as shown in figure 4.

Fig.4 S7-200 Real figure

Based on the collected air switch current voltage data changes at work,PC issue instructions, to 2000, Siemens PLC will receive the instruction into corresponding electrical signals, control steering gear rotating Angle, make empty gate opening and closing points from the operating structure makes the corresponding mechanical action.Realizing the air switch close break-brake.Air switch failure, immediately stop working.

IV.THE SYSTEM SOFTWARE DESIGN

A．The system software

Air switch life test device of the system software running under the Windows operating system.Based on the LAVIEW, friendly man-machine interface is designed.The user can carry on the operation of style device, only need to input the corresponding test according to requirements of the test parameters, test software using method and reference.System software simple operation, easy to users are familiar with and master.Open the life test system main interface as shown in figure 5.

Fig.5 Air switch device life test system software main interface

B．Parameters set

System software includes parameter setting, life test and version information,parameter is set mainly for testing mechanical life test and electric life testing request parameter data set.Mechanical life test parameter design interface is shown in figure 6.

Fig.6 Mechanical life parameter Settings interface

Electrical life test parameter Settings interface as shown in figure 7.parameters set much current voltage,Compared with the mechanical life.

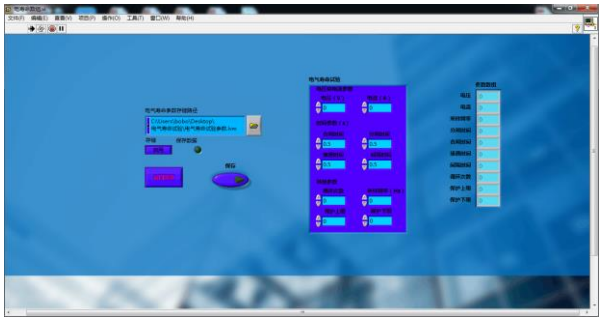

Fig.7 Long-life electrical parameter Settings interface

Parameter Settings including break-brake frequency, protection on the lower limit and the corresponding current voltage Settings,and It is able to set up test data store address.

C. The test interface

The corresponding mechanical life test and electric life testing interface as shown in figure 8 and figure 9.

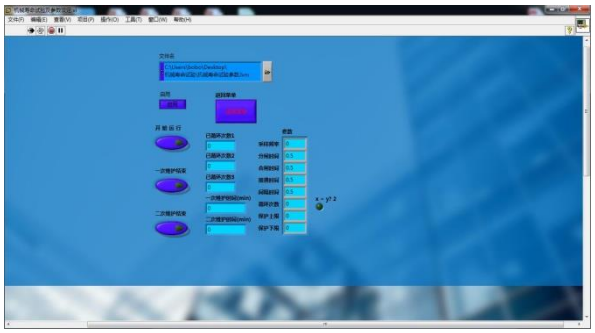

Fig.8 Mechanical life test interface

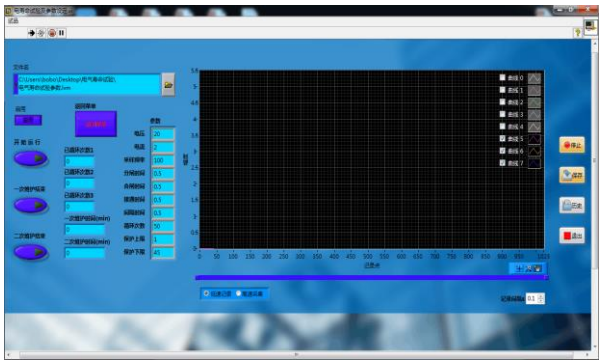

Fig.9 Electrical life test interface

Before test interface displays parameter Settings interface by setting the corresponding parameters, and maintain the button with the sample (s) for air switch test maintenance requirements,Also it has a data store button. Able to change the data memory address.Electrical life test and mechanical life test interface, compared to the current voltage real-time monitoring of the coordinate chart.Real time recording air switch current voltage changes at work, and can be deposited into the corresponding data file.

V.THE SYSTEM SOFTWARE DESIGN

Completing the prototype air switch life testing device，According to the above scheme design.Using LABVIEW programming design the user interface, realize the PC and data acquisition card and the real-time communication of PLC,and Data storage and human-computer interaction.this System display intuitive, simple to use convenient.To life test, the sample (s) open air switch working current voltage change as shown in figure 10 and figure 11.

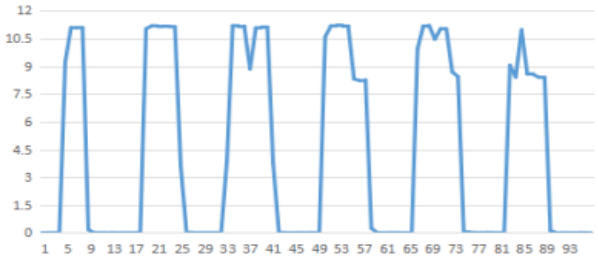

Fig.10 Voltage variation

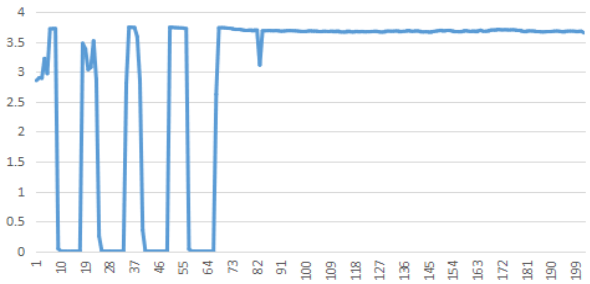

Fig.11 Current variation

Software real-time record current voltage change during the air switch operation.In figure 10 and figure 11, the abscissa is the number of data acquisition, ordinate is corresponding to the current value and voltage value, it can distinguish whether the air switch failureAccording to the current voltage change.In figure 10, 1 to 60 times data acquisition display air switch work normally,64 times of data collected after the open fault,it Can judge fault current value and voltage value.

VI.CONCLUSION

Air switch[8] is to protect the kind of electrical appliances, is responsible for the connected, bearing and breaking the current conditions of normal or abnormal conditions.Air switch life test is to validate test items of air switch operating performance ability,

and is the important method for testing the quality[9].It can make try close break-brake fault self-diagnosis, test data is automatically saved,through the open work current voltage monitoring.The air switch life test device design is reasonable, basic meet life test requirements, improve the test efficiency.It can be the life test of air switch,having a certain practicality.But the experiment is relatively rough, remains to be perfect.Test environment (humidity, temperature, the sample (s) open fixed, etc.) the impact on the air switch life without careful consideration,for future research, these factors should be a detailed analysis to make the experiment more rigorous.

References

[1] Liu Jianguo. Low-voltage electrical reliability work and development. Electrotechnical journal, 2004.1:5-8.

[2] Liu Jianguo, Li Wenhua. The reliability of the low-voltage electrical test and type test technology. Journal of hebei university of technology, 2004, Vol. 33, no. 2:1-8.

[3] Liu Jianguo, Zhang Naikuan. Overseas research and application of low voltage apparatus reliability. Low-voltage electrical appliances, 1996, No. 1:7-10.

[4] Li Liqiao. Low-voltage electrical reliability test data statistical analysis: master degree theses of master of []. Hebei university of technology, 2007.

[5] Du taihang, Zhu Junqiao,Wang Jinwei, etc. LabSQL application in the electric life testing equipment. Low-voltage electrical appliances, 2010, No. 12:57-6.

[6] Wu Wenminh, Shen Jianwei, Wang Jiayang. An intelligent circuit breaker life test equipment development. Electrician electrical, 2009, No. 5:54-56.

[7] Wang Peng. A new type of circuit breaker on-line monitoring system for electric life. Automation of electric power systems, 2009, Vol. 33, no. 9 have closed - 111.

[8] Xu Hui. Circuit breaker electrical life monitoring system based on Rogowski coil study: master degree theses of master of []. North China electric power university, 2009

[9] Meng Fanzhong. Vacuum circuit breaker and practical technology. Beijing: China water conservancy and hydropower press, 2009.

Research on positioning system based on ultrasonic distance measurement

Long Tao; Liu Tan; Wu Yuheng
（*jilin university instrument science and engineering institute,changchun,130021*）

***Abstract*—This paper mainly introduces a kind of ultrasonic positioning system based on ultrasonic ranging technology. Using the wireless communication module Si4432 and STM32F103 microcontroller to control the hardware part of the control circuit, and using processing to carry out the development of the host computer software, an ultrasonic positioning system is constructed. In order to improve the accuracy of ultrasonic positioning system, the positioning system becomes more intelligent and accurate with the use of multi-point positioning mutual compensation.**

***keywords*—Ultrasonic Location Telecommunications**

I. INTRODUCTION

ULTRASONIC technology is widely used because of its low cost, simple structure and easy to implement. At present, the market of ultrasonic transceiver technology is mature and inexpensive, so the application is more extensive. At present, the wireless positioning system is widely used, its basic principle is to receive several fixed locations of the radio point of the radio, so as to get the location of the main body. The principle of ultrasonic positioning is similar to that of a radio positioning system, except that the attenuation of the ultrasonic wave in the air is large and only applies to a smaller range. Ultrasound in the air in the transmission distance is generally only a few tens of meters. Short distance ultrasonic ranging system has been widely used in practice. Based on the ultrasonic ranging technology, a system can be designed for small-scale moving object positioning.

II . PRINCIPLE AND STRUCTURE OF ULTRASONIC POSITIONING SYSTEM

A. System Principle

Now there are many ways to measure ultrasonic distance, for example, TOF (time of flight), amplitude phase joint detection, phase detection, and acoustic amplitude detection.

In this design, the TOF (time of flight) is selected to realize the measurement of the distance between the ultrasonic wave and the final target body. The method comprises the following steps: the ultrasonic transmitting device is fixedly mounted on the positioning target body, and a transmitting device of the ultrasonic transmitting end first transmits a synchronizing signal through the wireless communication module, the time delay of each receiving device of the wireless receiving end to the ultrasonic receiving end can be neglected After the synchronization signal, and then start the launch of ultrasonic signals. When the receiver of the ultrasonic receiver receives the synchronization signal, the microcontroller of the ultrasonic receiver immediately starts its timer as the timing initial value. When the receiving device of the ultrasonic receiver receives the ultrasonic signal, the microcontroller of the ultrasonic receiver immediately closes its timer , As the final value of the time. The time it elapses is the time that the ultrasonic wave emitting device emits an ultrasonic wave to the ultrasonic wave receiving apparatus to receive the ultrasonic wave, i.e., the transit time. The distance traveled by the transit time and the velocity of the ultrasonic wave in the air medium is calculated. The calculated value is the distance between the ultrasonic source and the receiver, so the distance can be measured by measuring the transit time.

In the ultrasonic positioning system based on ultrasonic ranging technology discussed and designed in this paper, the ultrasonic transmitter has an ultrasonic transmitter, and the ultrasonic receiver has four ultrasonic receivers. The position information of

any three ultrasonic receiving devices at the ultrasonic receiving end can determine the position information of the primary ultrasonic transmitting device. In the design of the ultrasonic transmitter has an ultrasonic transmitter, ultrasonic receiver has three ultrasonic receiver device ultrasonic positioning system, for example, ultrasonic positioning diagram shown in Fig 1.

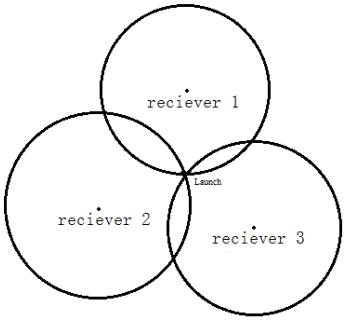

Fig.1 Ultrasonic positioning schematic

In the process of sensor node positioning, the unknown node uses the trilateral measurement method to calculate its own position after obtaining the distance to the nearby beacon node. It is known that the coordinates of the three nodes of A, B, and C are $(x_a,y_a,z_a),(x_b,y_b,z_b),(x_c,y_c,z_c)$, as well as their distance to the unknown node D are d_a,d_b,d_c, respectively, assuming that the coordinates of node D are. Then, the following formula exists

$$(x-x_a)^2+(y-y_a)^2+(z-z_a)^2=d_a^2$$
$$(x-x_b)^2+(y-y_b)^2+(z-z_b)^2=d_b^2$$
$$(x-x_c)^2+(y-y_c)^2+(z-z_c)^2=d_c^2$$

The coordinates of the emission point can be obtained by solving the ternary quadratic equations.

B. System Structure

The positioning system is composed of a receiving module, a receiving control module, a transmitting module, a transmitting control module and a wireless transmission module. The structure of the system is shown in Fig 2.

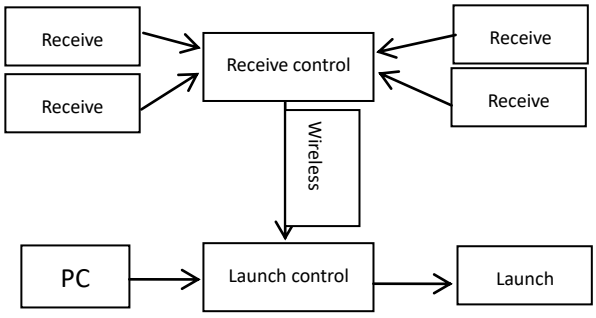

Fig.2 Ultrasonic positioning structure

According to the above figure, the design of the positioning method: PC as the core, by its control to complete the positioning process, in turn:

1, the PC sends a start measurement command to the transmitter, the delay is waiting;

2, the transmitter sends ultrasonic waves, and notify the receiver to start timing;

3, PC machine delay after the end, from the receiver to read the distance data, according to the receiving point layout to calculate the coordinates, and according to the need to release coordinates and display.

III. THE DESIGN OF SYSTEM HARDWARE

The system comprises three modules: an ultrasonic transmitting module, an ultrasonic receiving module and an ultrasonic control module. The ultrasonic control module is a single chip system, including signal transmission function, signal judgment and analysis function. The Si4432 wireless communication module is also integrated on the ultrasonic control module to compensate the measurement error of the ultrasonic positioning system. The operation of each module of the system is as follows:

A. Ultrasonic Transmitter Module

In this design, the launch of the ultrasonic transmitter device selection of piezoelectric ceramic transducer, it is voltage-driven, its power and drive voltage is proportional. Based on the above principle, the use of step-up transformer with a boost ratio of 1:20 to raise the voltage, and ultimately can output about 50V peak voltage.

In addition, most of the classic 51 series microcontroller generates square wave pulse drive signal, but the ultrasonic transmitter requires a sine wave type signal, so the square wave drive signal should be converted into a sine wave drive signal. Using the principle of resonance, through the ultrasonic transmitter and the transmitter and the step-up transformer matching, and thus to achieve the square wave drive signal is converted into a sine wave drive signal purposes. The circuit design is shown in Fig 3.

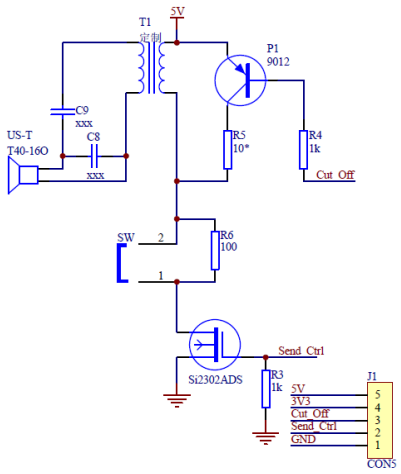

Fig.3 Transmission module circuit

B. Ultrasonic Receiving Module

The ultrasonic receiving circuit in the ultrasonic positioning system is designed as a resonant circuit, and when the ultrasonic receiving device receives an ultrasonic pulse signal of 40 kHz, a weak voltage signal of the same frequency as the ultrasonic transmitter is generated. The ultrasonic receiving device detects the received microwave signal and amplifies the signal through the amplifier circuit. The generated pulse signal is sent to the interrupt terminal of the receiver of the ultrasonic receiver. Once the microcontroller receives the interrupt signal, the ultrasonic receiver The microcontroller stops its internal timer, indicating that the timer stops. The circuit is shown in Fig 4.

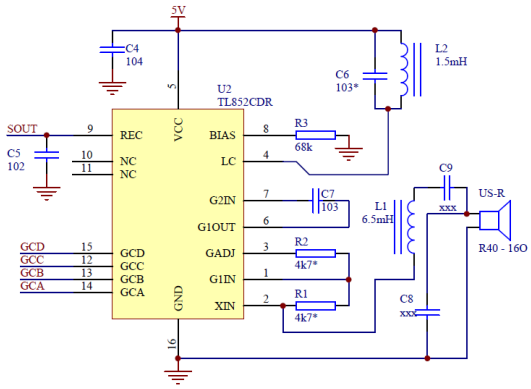

Fig.4 Receive module circuit

C. Ultrasonic Control Module

In this system, the ultrasonic transmitter module and the ultrasonic receiver module are designed separately by function. In the design of the two are not added to control the ultrasonic to achieve the launch, transmission and reception of the part, for the design of the ultrasonic positioning system control module. The module consists of an enhanced 51 series microcontroller STC12F103, which is used to control the ultrasonic transmitter at the end of an ultrasonic transmitter and ultrasonic receiver of the four ultrasonic receivers. Since the control portion of the ultrasonic transmission module and the control portion of the ultrasonic receiver module are substantially the same in function realization, the control signal socket is different, so that for the sake of simplicity of design, the control section of the ultrasonic transmission module and the ultrasonic receiver module Both functions require the same two control modules. The Si4432 wireless communication module is also integrated on the control module to compensate for the measurement error of the ultrasonic positioning system.

IV. The Design of System Software

When the PC host computer receives the data ultrasonic transmitter to send out the, the first need to determine the ultrasonic sensor ranging data obtained by all the effective, if the data is too large or too small, does not meet the requirements, the need to remove invalid data. For example, when the measured distance value is the maximum value, it is possible that any ultrasonic receiving apparatus at the ultrasonic receiving side can not receive the ultrasonic pulse signal for a long time because the software program design is processed to a maximum value. In addition, the relationship between the triangles can be used to determine the validity of the data. When you have determined all the valid data, it uses the working principle and positioning algorithm of ultrasonic positioning to calculate the specific position coordinates of the positioning target, and then carries on the drawing in the PC host computer display interface, displays the target moving trajectory graph, realizes the real time The location of the display. Finally, the resulting position data is returned to the ultrasonic transmitter side of the microcontroller to facilitate the need for positioning devices used.

V. Error Analysis

There are many factors that cause the response time of the ultrasonic distance measurement system at different distances. Generally, it can be attributed to

the following three main errors:

A. The Attenuation of the New Ultrasonic Signal in the Propagation Process

Ultrasonic signal in the propagation process, with the detection of the increase in distance weakened, resulting in more difficult to detect acoustic signal, ranging accuracy is reduced.

B. Received Ultrasonic Waves to the Detected Hysteresis

The error comes from the detection of the circuit sensitivity, determine the deviation from the actual sound waves to the circuit to confirm and output the corresponding signal is certainly lag. This is related to the strength of the acoustic signal, the principle of the detection circuit and the sensitivity of the circuit, and the core of the ultrasonic distance measurement. If the ultrasonic sensor sensitivity is too low, greatly limits the detection distance. Sound attenuation is the square relationship of distance. As the judgment hysteresis changes with the strength of the sound waves, this part of the error is the main source of data instability.

C. Start Timing and Start the Deviation between the Ultrasonic Emissions

From the system principle, from the start of the ultrasonic module to the ultrasonic launch is actually completed, there is a small time difference.

VI. IN CONCLUSION

In this paper, the system based on ultrasonic ranging is introduced, and the real-time follow-up of positioning target is realized by using ultrasonic sensor and radio device. As the PC development environment and computing power are better than the single-chip, coordinate calculation easier to achieve, and can easily achieve the positioning of the object trajectory display, which is required by many positioning systems, positioning system more intelligent.

References

[1] GU Juanjuan. Study on Ultrasonic Location Technology of Wireless Sensor Networks [D]. Southeast University, 2008.

[2] Zhang Ting, Design of Ultrasonic Positioning System [D]. Chang'an University, 2014.

[3] Hua Rui, Hao Yongping, Yang Fang. Design of Ultrasonic Positioning System [J]. Foreign Electronic Measurement Technology, 2009, (06): 65-67.

[4] Cai Lei, Zhou Ting-ting, Guo Yun-peng, Chen Su-fang, Wu Han-gang. Intelligent Follower Car Based on Ultrasonic Location [J]. Electronic Measurement Technology, 2013, (11): 76-79.

Measurement of transistor output characteristics based on Virtual Instrument System

Zhang BingRen; Jiang mengjie; Li yuwu; Kou deli

(College of of Instrument Science and electrical engineering, Jilin University,Changchun 130012,China)

***Abstract*—Virtual instrument technology is the use of high-performance modular hardware, combined with flexible and efficient software to complete a variety of testing, measurement and application, the realization of the instrument into the computer, with the development of science and technology more and more widely used.In this paper, we introduce a VII-EM based autonomous system of Jilin University to design a measuring instrument for measuring transistor output characteristics.Realization of communication between computer and data acquisition card through the DLL mode USB driver, to achieve data acquisition and processing requirements at the same time, based on the design of LabVIEW virtual instrument application, finally completed the test transistor output characteristics.**

Key words—virtual instrument data acquisition LabVIEW Graphic instrument transistor

I. INTRODUCTION

IN electronic products, and resistors, capacitors, inductors, generally used forsignalamplification, conversion and other functions of the transistor is one of the components of the circuit. With the rapid development of modern technology, transistors gradually large-scale integration, complexity, its form and use more widely, the transistor as an important part of semiconductor devices, their precise use of scientific research personnel attention to the problem, the face of a wide range, Different functions of the transistor, scientific research personnel in order to meet the needs of the need to use special equipment to detect its characteristic parameters, according to the test results used to filter. The original transistor characteristics of the measurement instrument, with a good dynamic, real-time tracking, transistor characteristics, such as intuitive design, but it is cumbersome, inconvenient to operate, reading error, can not be stored on the measurement data and deep processing. In order to overcome the shortcomings of the analog transistor diagram instrument, combined with the test technology, micro-controller technology and virtual instrument technology to design a digital transistor diagram instrument. The graphic instrument has the advantages of intuitive data, accurate test results, powerful analysis and so on[1].

II. PROCEDURE FOR PAPER SUBMISSION

A.Overall design

Based on the virtual electronic instrument integrated system of Jilin University, nine kinds of modular electronic measuring instruments, such as signal generator, oscilloscope, LCR tester, logic analyzer and so on, are the same as the above-mentioned instrumental scheme and technical route. The As shown in the figure, the virtual instrument measurement subsystem mainly includes the measured object (crystal transistor), the virtual signal generator, the peripheral circuit, the data acquisition card and the PC host platform.

Virtual electronic measuring instruments, such as analog signal generator[2], virtual oscilloscope, virtual spectrum analyzer, virtual circuit tester, etc. This paper focuses on the virtual oscilloscope, virtual icon and the corresponding USB data acquisition card for the A virtual instrument measurement subsystem that measures the output characteristics of active electronic devices. In this paper, the entire measurement subsystem is based on the PC host for the hardware to build a platform, compatible with the virtual electronic measurement system under the conditions of the new measurement module.

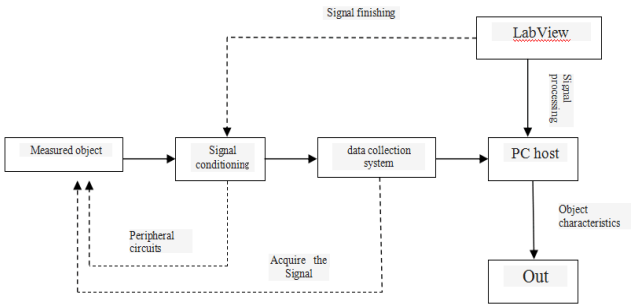

Figure1 The overall block diagram

(1).object to be measured: that is, the research objectives in this paper, active electronic devices, including transistors, as the main research object[3].

(2).signal conditioning: In order to meet the measurement of active electronic device output characteristics (in the case of transistors) requirements, the need for a specific step waveform. The generation of the step waveform requires amplification, isolation, filtering, excitation, linearization, and conversion of the time domain and frequency domain to the original signal.

(3).data acquisition system hardware: based on compatible with the data acquisition system before the new device for the collection of active device output signal characteristics of the USB data acquisition card.

(4).virtual instrument construction: virtual instrument software development platform Lab View as a tool to build active device output signal characteristics of the virtual instrument, the icon through the intuitive graphics show the measured output characteristics of the object, but also with Digital high-precision features.

B.Hardware part of the design

According to the system block diagram, based on the platform of Jilin University virtual instrument, using data acquisition card to form data acquisition module, taking C9018 transistor as an example, using typical test circuit to form transistor peripheral circuit as shown in Figure 2

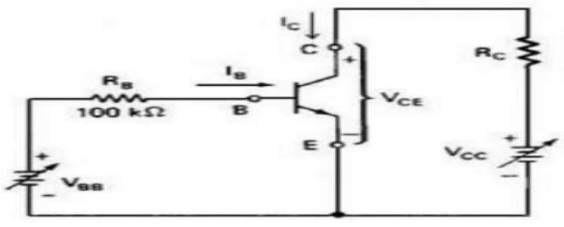

Figure 2 Typical circuit

According to the above hardware circuit, it is necessary to measure the output characteristic curve of the transistor with two input signals: the fixed current value base current and the smooth change of the collector scan voltage; in order to complete the output characteristics of the transistor need to be measured in different fixed Voltage value Ib value of the collector current Ic with the collector scan voltage changes in the value, that is, then need to change the value of the base current value of the value of Ib, that is, a fixed cycle of the step jump signal[4].

C.Software part of the design

According to the system principle and the hardware design request, based on Jilin University virtual instrument platform may carry on the system software:

(1), base step waveform and sine half wave design;

(2), the collector sine half wave scan voltage waveform design;

(3), virtual instrument diagram of the experimental panel and the design of the block diagram;

II .SPECIFIC IMPLEMENTATION PLAN

(1) .signal conditioning: Lab VIEW virtual platform provides the basic source of sine wave, square wave, sawtooth and triangular wave. From the basic signal to the target signal needs to go through a series of algorithms. Where the algorithm handles the digital logic operations of the Express Numeric submodule and the time domain analysis of the Time Domain Math module. And finally get the target signal ladder waveform and sine half wave waveform[5].

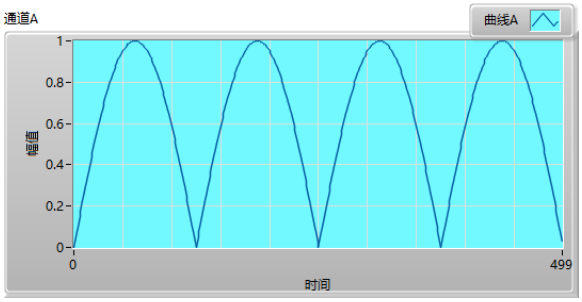

Figure 3 sinusoidal half-wave signal

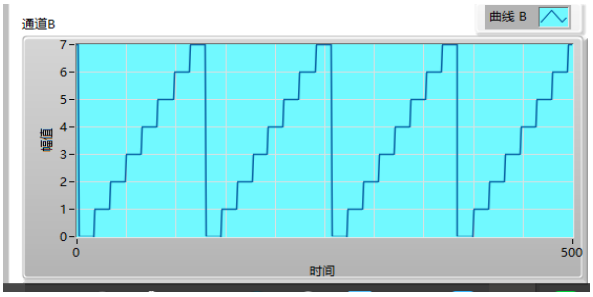

Figure 4 ladder signal

(2) .signal synchronization:

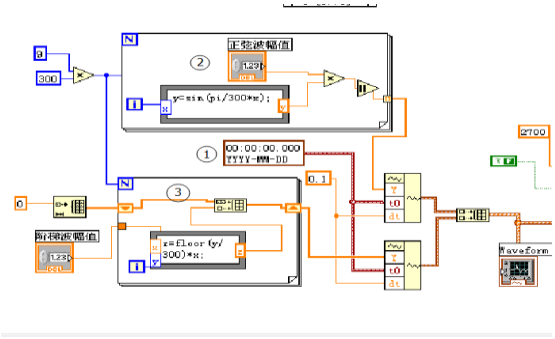

Figure 5 Block diagram of signal synchronization

As shown above, where: (1).on behalf of the output signal to maintain the sine half-wave voltage and ladder signal to keep pace, (2). said sine half-wave signal (3). that ladder signal.

(3) . the working principle and role of the instrument

Based on the experimental platform of virtual instrument measurement system of Jilin University, the existing virtual oscilloscope module is improved. Virtual oscilloscope is the analog input signal through the conditioning circuit into the AD input voltage range, and then through the high-speed AD converter analog signal front-end fast sampling, through the FIFO cache, and use its digital signal processing technology to store the data in real time Fast processing, get the signal waveform parameters, and by the oscilloscope display.

The oscilloscope displays the time-varying waveforms that show time-domain information. Therefore, when improving the oscilloscope, you need to modify the parameters of the X and Y coordinates of the front panel of the experiment. That is, the X axis represents the sine half-wave sweep voltage emitted by the signal generator. The Y axis represents the drain current flowing through the field effect transistor The To this end on the basis of the original need to modify the block diagram is as follows.

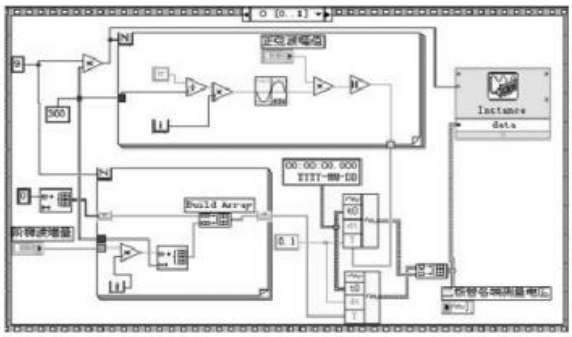

Figure 6 Modify one of the block diagrams

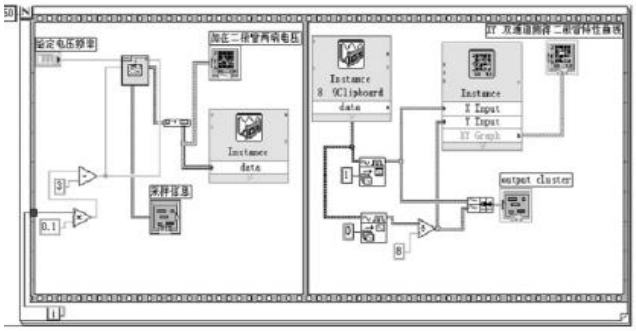

Figure 7 Modify the program block diagram of the two

Through the bundling of the two sets of data collected as the waveform of the X, Y, axis data in the form of a curve displayed on the panel, so the image of the transistor to observe the characteristics of the output characteristics of the curve[6].

(4) . the final picture shows the image display: through the host computer to receive the lower computer icon hardware module collected data for data processing in the Labview front panel shows a cluster of characterization of the transistor curve.

III.CALCULATION RESULTS AND COMPARISON

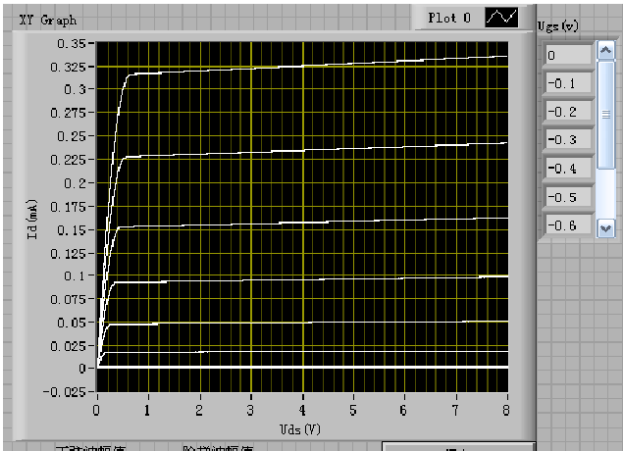

Figure 8 Experimental results

Figure 7 shows the output characteristic of the C9018 transistor. It shows that the measurement result of the transistor is measured with a virtual plotter. The scanning voltage range is 8V, the step current increment is 20μA, the Y-axis scale is milliamperes, the step number is Level 7. It takes about 10 seconds to complete the entire picture. Curve from the discrete point of the composition, because the LCD screen resolution is limited, the adjacent point of no change from a straight line. It can be seen from the figure that the whole instrument is working properly. And the device's product specifications are basically consistent.

IV. CONCLUSION

Virtual instrument technology is more and more widely used, from the actual needs of teaching experimental equipment, the design of the use of USB interface, cheap, portable, easy to use virtual transistor characteristics of the instrument, through the entire study design process, the basic control of the transistor characteristics The principle of data acquisition technology and virtual instrument technology and further deepen the ability of software programming, hardware and software coordination for the work and system development has a profound understanding of the post-scientific research work has laid a good foundation[7].

Test results show that: the development of the LabVIEW and USB interface based on the characteristics of the virtual transistor diagram can be normal operation. The overall system error is within the allowable range. The entire system is scalable, in the future can continue on this basis to improve the instrument testing capabilities.

References

[1] ZHAO Zhong-yi. Principle, Maintenance, Verification and Application of Semiconductor Tube Characteristic Graphs. Beijing: Electronic Industry Press, 1994, 1-3

[2] LIU Jun-hua.Design of Virtual Instrument Based on Lab VIEW. Beijing: Electronic Industry Press, 2003, 1-5

[3] Shou Jiyong.Virtual test instrument based on USB: [Master's thesis], Chengdu: University of Electronic Science and Technology, 200

[4] Design and Implementation of Simple Transistor Diagram Based on LABVIEW Environment, Shanxi, Taiyuan University of Technology, 2013

[5] Cypress Semiconductor Corporation. The EZ-USB Technical Reference Manual. 2000

[6] Anchor Chip Inc. Anchor EZ-USB Frameworks. Anchor Chip Inc. 1998

[7] HUO Guo-ping, WANG Shen, YE Qi-xin. Lab VIEW7.1 Programming and Virtual Instrument Design. Beijing: Tsinghua University Press, 2005, 1-2

[8] Analog Device, Inc. AD420 Datasheet. 1999

[9] Li Zhongming. A high-precision simple backward control channel solution. Electric Drive Automation, 2004, 26 (4): 36-38

[10] Yan Rongjiang. EZ-USB2100 series of single-chipprinciple, programming and application. Beijing: Beijing University of Aeronautics and Astronautics Press, 2002, 2-8

[11] Chen Xihui, Zhang Yinhong. Based on Lab VIEW8.20 programming from entry to master [M]. Beijing: Tsinghua University Press, 2008

[12] Chen Shuxue, Liu Xuan. Lab VIEW [M]. Beijing: Electronic Publishing House, 2011

[13] Qi Xingming, Tian Jingjing. Getting Started and Actual Combing in Lab Game [M]. Beijing: Electronic Industry Press, 2011.

Noise Suppression Of Wavelet Transform In PM2.5 Gas Detection

Li Kaiyan; Li Liangbing; Liu Kewei

(College of materials Science and Engineering, Jilin University,Changchun 130012,China)

***Abstract*—In the field of gas concentration detection, noise interference is an important factor affecting the accuracy of detection. Especially for the low concentration of the signal peak to a smaller sample, the real signal masked by noise, resulting in reduced noise detection accuracy. At the hardware level of the suppression effect is not ideal, and will add to the cost. But the software simple noise the algorithm can only unilateral processing in time domain or frequency domain, can not achieve the role of both. The wavelet algorithm is widely used in data processing, in both time domain and frequency domain processing. The noise using wavelet algorithm to PM2.5 gas detection process Suppression, mainly by determining the appropriate wavelet, the optimal decomposition level and threshold of the signal decomposition and reconstruction. Based on the characteristics of wavelet transform, using Mallet decomposition algorithm to decompose the signal into different frequency bands, setting a threshold, the useful signal's frequency band retained zero vector. The other treatment the method can effectively preserve the effective peak gas detection process, the interference peak filtering noise generated by the increase in the variance and the signal noise based on ordinary low-pass filter on more than 12 percentage points.**

***Key words*—Wavelet transform The decomposition and reconstruction The threshold The wavelet to mania.**

0 FOREWORD

IN recent years, a substantial increase in particle concentration in air in China, especially in the fine particulate matter (PM2.5) increased most significantly, has brought great distress to people's health class life. So detection of the concentration of pollutants in the atmosphere caused by the professionals concerned, how to strengthen the detection effect of detector the optimization of detection method has been called hot research attention in the field of [1].

From the middle of last century, researchers have begun to detect the concentration of pollutants in the atmosphere were studied. Until today, the dust concentration detection method of the typical weight method, beta ray absorption method, piezoelectric crystal oscillation method, light attenuation [2]. and light scattering method for early representative products include EPA-5000 the dust concentration tester of SCK company in the United States, sampling the beta ray absorption method to detect [3].TE DR-400 of particle concentration, TSI, MOLD8520, are sampling optical attenuation method, the structure of the online membrane sensor and data acquisition circuit The improvement of the sampling sensitivity reached 0.001. the major domestic Binta green technology limited production of LD-5C., but these instruments are improved, the hardware design and instrument structure of the high cost, not suitable for the widespread use of [4]. with the development of software and algorithms, slowly appeared through the filter. The main instrument software should CEL Microdust, sampling Fourier transform analysis and filtering of sampling signal, the Jiangsu SANHENG GC100 using Calman filtering method. But these algorithms can only be respectively of the data in the time domain or frequency domain Can not be a comprehensive analysis of noise and filtering, filtering effect is not obvious, the accuracy is not high [5].

With the development of wavelet theory, in recent years, has been widely used in the field of data processing. In 1984 Grossmann J. and French geologist A. Morlet for the first time the idea of wavelet transform is applied to seismic data processing, then Y. Meyer and S. Mallat proposed the principle of multiresolution analysis, wavelet theory development today, gradually improve image processing, wavelet algorithm in seismic data processing, mechanical testing, and many other aspects have been applied to [6]

In the process of measurement and monitoring

technology of signal processing, often use the idea of wavelet transform, in order to improve the detection accuracy and sensitivity. The method to improve the detection accuracy and sensitivity through the software can not only reduce the corresponding expenses, but also can effectively improve the accuracy of monitoring data, the application of [7]. wavelet transform algorithm the right to collect the interference signal filtering, denoising and baseline correction, if we choose proper wavelet function and threshold processing method, it can effectively remove the influence of impurities on a signal to signal acquisition, thereby improving the monitoring accuracy.

The PM2.5 signal was low, small amplitude data changes slowly, the useful signal is easily disturbed by external noise, causing a great impact on the signal acquisition analysis. This design uses the wavelet transform algorithm, combined with the hardware optimization above, in order to filter out noise, improve the detection accuracy.

1 WAVELET TRANSFORM ALGORITHM

Assume $\varphi(t)$ is a square integrable function, if the Fourier transform of $\varphi(t)$ to meet the conditions that:

$$\int_{-\infty}^{+\infty}\frac{|\Psi(\omega)|^2}{\omega}d\omega<\infty$$

Then $\varphi(t)$ is called a basic wavelet or mother wavelet functions,by Scaling and translation,there will be $\psi_{a,b}(t)=a^{-\frac{1}{2}}\psi\left(\frac{t-b}{a}\right)$, $a>0, b\in R$

a is the scaling factor, b is the translation factor.By adjusting the size of a and b to conform to the signal analysis. the window size is fixed, but its shape can be changed of wavelet analysis method.wavelet analysis has multi-resolution characteristics , which has high frequency resolution and low time resolutionIn in the low frequency part, with high temporal resolution and low frequency resolutionthe in the high frequency part[8].

F(t) can be completely reconstructed by wavelet $W_\psi f(a,b)$ transform, the reco-nstruction formula is

$$f(t)=\frac{1}{c\psi}\int_{-\infty}^{+\infty}W_\psi f(a,b)\psi_{a,b}(t)db$$

In the gas detection system, using wavelet transform for signal processing mainly has two kinds of method is the use of Mallat decomposition algorithm to decompose the signal into different frequency bands. Set a detection information information so that the frequency band within this band is separated, and other space vectors were set to zero, can achieve the useful frequency band signal detection other frequency signal removal. Another is the use of wavelet analysis to the noise on the traverse the band (such as Gauss white noise) for signal denoising, using wavelet decomposition threshold denoising to mesh [9].

2 NOISE ANALYSIS

The first step is to filter the noise of the collected signal analysis to determine the type of noise in order to be targeted for processing.

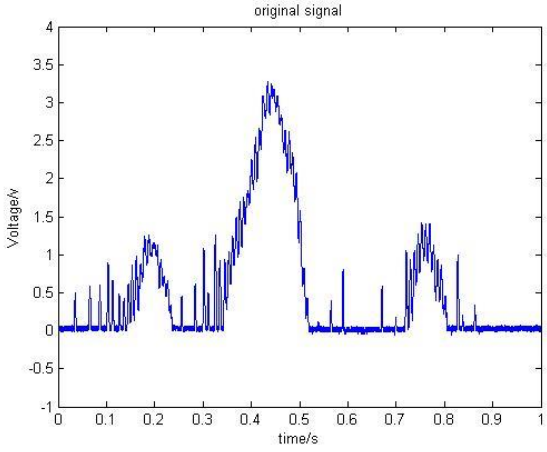

Fig1: Dust sensors signal

Figure 1 is a noisy PM2.5 signal collected. The larger signal is a useful signal to be retained, on both sides of the magnitude of 1.2V signal is due to the floating signal caused by the gas flow. The useful signal amplitude reached 3.4V, but due to the presence of noise, the signal amplitude of the real peak and not so high. The burr is the noise signal, the noise of high frequency harmonics in the time domain and frequency domain and the effective signals are superimposed on each other, reduce the detection accuracy of the effective signal.3. Wavelet parameter selection.

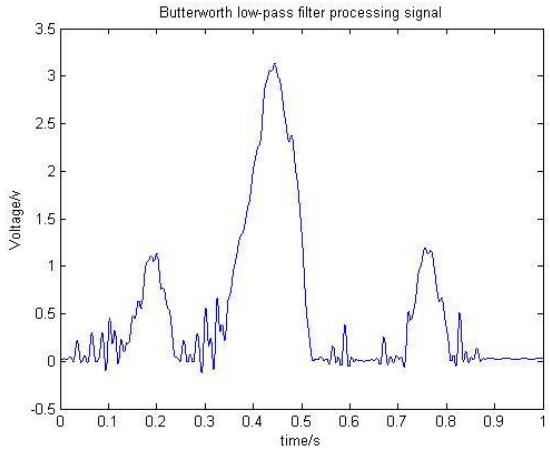

Fig2 Butterworth low-pass filter

After the filtering effect of Butterworth low-pass filter graph is shown in Figure 2. The cut-off frequency of the filter is 80Hz and 190hz, the filtering effect only filter noise interference than 190hz, noise below 190hz inclusion can't remove the effective signal, by further decreasing the low-pass cutoff frequency will cause distortion of effective signal. Thus, by using the method of time domain or frequency domain with time domain or frequency domain can only filter out part of the interference wave alone, it is difficult to translate these noise and harmonic signal filter clean. Using wavelet algorithm by noise decomposition, can in the time domain and frequency domain simultaneously for this processing. Signal noise characteristics, wavelet algorithm is suitable for the signal noise filtering.

3 WAVELET PARAMETER SELECTION

3.1 Signal decomposition

Wavelet transform is mainly for the signal decomposition of noise, when the selection of db8 wavelet basis, the decomposition layer selected 8 layers, the decomposition effect diagram as shown in figure:

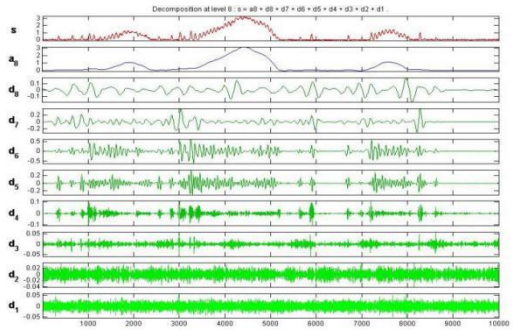

Fig3 Wavelet decomposition effect

After decomposition, high frequency and low frequency signals are separated, the useful signal is mainly reflected in the eighth layer, first layer to the seventh layer mainly contains noise information. These noises are superimposed on each other, at the level of different signal with different degree. The low frequency A8 coefficients effectively reflect the characteristics of signal. The parameters of wavelet transform are selected a comparison of the selected.

3.2 Selection of wavelet bases

The different wavelet functions, the denoising effect is also different. Whether the orthogonal basis function and the effect of denoising and wavelet functions. Using wavelet symmetry symmetry good no phase distortion, good orthogonality of wavelet redundancy is smaller, denoising can get better denoising effect [10]. symmetry and selection good wavelet regularity.

The comparison of several common wavelet bases is shown in table 1:

Table 1

Several common wavelet properties

wavelet base	Haar	Db	Bior	Coif	Sym
orthogonality	Y	Y	N	Y	Y
Double orthogonality	Y	Y	Y	Y	Y
Tight branch	Y	Y	Y	Y	Y
symmetry	symmetry	approximate	asymmetric	asymmetric	asymmetric

Notes:Y is exist;N is deny.

The signal to noise ratio (SNR) and the mean square error of these wavelet bases are shown in table two:

Table 2

The signal to noise ratio and mean square error of different wavelet base after processing

wavelet base	SNR	MSE	wavelet base	SNR	MSE
Db2	28.999	0.177	Sym2	28.999	0.177
Db3	29.573	0.171	Sym3	29.573	0.171
Db4	30.078	0.166	Sym4	29.904	0.168
wavelet base	SNR	MSE	wavelet base	SNR	MSE
Coif2	29.750	0.169	Bior2.2	29.454	0.172
Coif3	29.857	0.168	Bior2.4	29.626	0.170
Coif4	29.921	0.168	Bior2.6	29.658	0.170

Note: SNR is the signal to noise ratio, MSE is the mean square error

The signal-to-noise ratio (SNR) and minimum mean square error (MSE) is to determine the denoising effect. On the basis of higher signal to noise ratio, mean square deviation is smaller, the better filtering effect. Different wavelet for signal processing after the signal-to-noise ratio of Db4>Coif4>Sym4>Bior2.6, variance comparison results after Db4<Coif4<Sym4<Bior2.6.Db4 treatment, the maximum signal-to-noise ratio, mean variance the smallest, the signal will not be submerged in noise, and eliminate noise effectively, thus selecting the wavelet in signal processing.

3.3 Determination of decomposition level

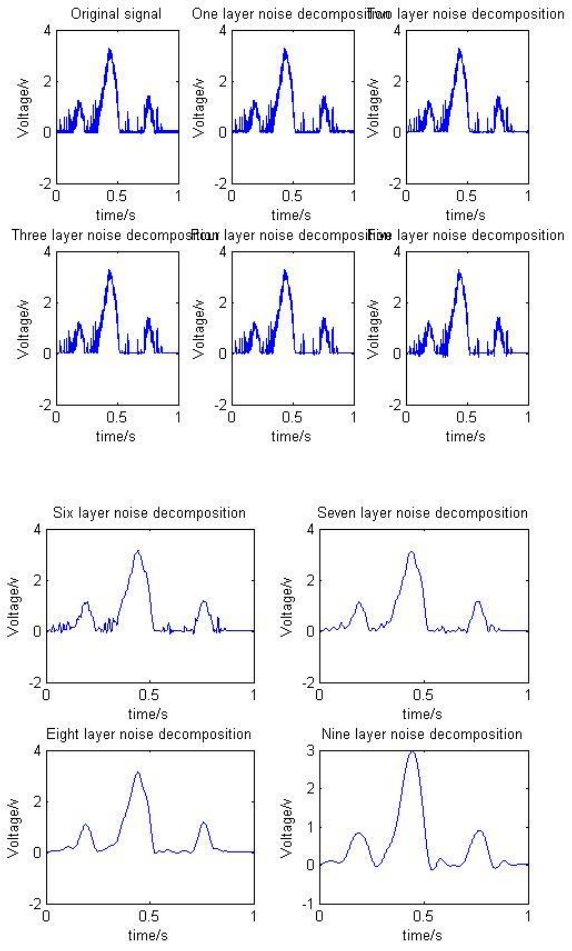

Fig4 Different decomposition layer rendering

By comparing with the different decomposition level of signal de manic effect after the map, 1 layer to the 5 layer decomposition, the decomposition level is less, after the decomposition of the results with the original signal difference, peak and burrs are still outstanding. Up to 6 layers and 7 layers of decomposition, noise suppression is better, most high frequency noise was removed, and the peak burr no longer exists. But some of the useful signal frequency is very close to the noise signal in the time domain graph still exists, is reflected in some small fluctuations and disturbances. Up to 8 layers, small fluctuations and disturbances have been filtered, but continued to increase to 9 the number of decomposition. After the original signal was decomposed. The destruction, the amplitude is reduced, so it can be concluded that the greater the number of wavelet decomposition, the better the filtering effect, but the decomposition level is too large will damage the useful signal, and the amount of calculation will be increased. Therefore, the 8 layer decomposition effect is the best.

3.4 threshold selection

In the signal denoising analysis using wavelet transform, threshold denoising effect is an important choice of the hard threshold and soft threshold.

Hard threshold:

$$w_{a,j}s(n) = \begin{cases} w_{a,j}s(n) & |w_{a,j}s(n)| > \lambda \\ 0 & |w_{a,j}s(n)| \le \lambda \end{cases}$$

Soft threshold:

$$w_{a,j}s(n) = \begin{cases} \sin(w_{a,j}s(n)) & |w_{a,j}s(n)| > \lambda \\ 0 & |w_{a,j}s(n)| \le \lambda \end{cases}$$

The use of Matlab function library for signal denoising methods are mainly the following three:

(1) the default threshold denoising function (ddencmp): mainly through the default threshold signal, and then use the function wdencmp () on signal denoising;

(2) a given threshold denoising processing, mainly through the function appcoef () to get the wavelet coefficients of each level, through the function thselect () function to be given threshold, finally using wthresh () to signal to eliminate manic;

(3) forced noise elimination: this method can effectively filter the high frequency noise by the high frequency coefficients after wavelet decomposition, but this method is easy to lose the useful components of the signal.

Different ways to eliminate the effect of the following:

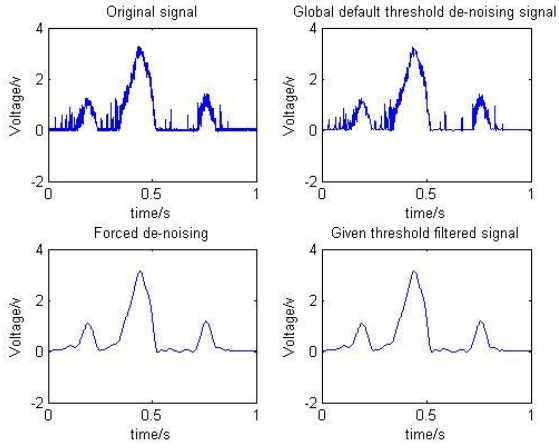

Fig5 Different ways od de-noising filter graph

When the global default threshold denoising, filtering effect and little difference after the original signal, most of the high frequency signal remains, spikes and prominent. With the mandatory elimination of burr noise and given threshold filtering, the filtering effect is obvious. The high frequency interference signal is filtered out effectively. Prominent compulsory denoising and given threshold denoising can remove noise very well, it takes the given threshold denoising. The filtering effect of different threshold are also different, the following is a given threshold under four different threshold selection rule filtering effect.

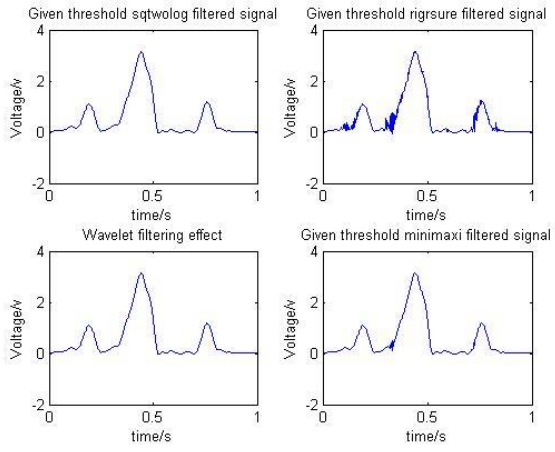

Fig6 Different default threshold processing effect

Different threshold selection rules of the filtering effect is different, although most of the given threshold rigrsure filter the high frequency noise, but there are still residual interference and the effective signal is superimposed, signal still exists. The given threshold burr although minimaxi has better effect than rigrsure, will filter out the noise superimposed part, but still have an impact on the effective signal, burr still exists, the amplitude of useful signal low. Given the threshold sqtwolog and heursure anti manic effect is obvious. The good filter noise. But the stubborn sqtwolog filter Compared with heursure, the effect is not smooth, and the given threshold heursure filter is the best.

Final filtering effect:

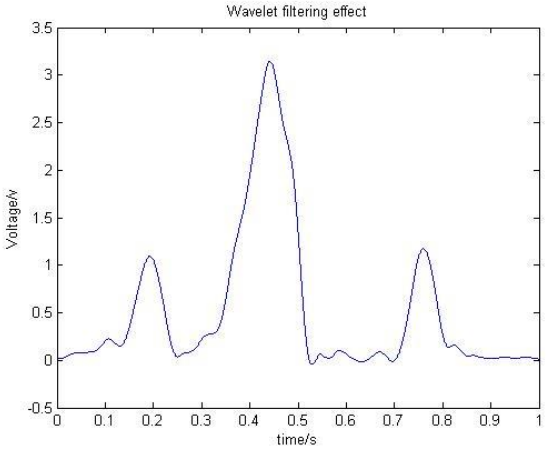

Fig7 The signal after wavelet transform processing

Compared with the Butterworth low-pass filter, the wavelet transform signal to noise ratio 30.078, low pass filter 26.681, the signal to noise ratio improved 12%. mean square error reduction (wavelet transform 0.166, low-pass filter, 0.189), the filtering effect is better.

4. CONCLUSION

①. By comparing Db, Coif, Sym, Bior four different wavelet bases which are different from the sampled signal, the SNR and the minimum mean square error (MSE) are compared, and Db4 is chosen as the wavelet basis function.

②.The analysis of the different layers, the 8 layer decomposition is the most appropriate. Below the 8 layer can not completely filter the noise interference, higher than the 8 layer will damage the effective signal peak.

③.Given the way the heursure threshold denoising compared to the default threshold denoising method and forced denoising method, can retain the effective signal peaks effectively, filter out the interference signal. And achieve the smooth filtering effect, the most close to the real signal.

The wavelet function and Butterworth low-pass filter, through signal processing after wavelet transform is good enough to retain the useful signal in the original signal, the success of the filtering of the

noise signal, improve signal-to-noise ratio, reduce the variance, so that the useful signal to be collected more prominent. And achieve the smooth filtering effect. Very good performance characteristics of real signals.

Reference

[1] Xie Dong, Zhang Xing, Cao Renxian. Islanding detection based on wavelet transform and neural network [J]. proceedings of the Chinese society of Electrical Engineering,2014,34(4): 537-544

[2] Ma Min, Zhang Caixia, Lu Chengchao,. ECT image processing based on wavelet transform [J]. Journal of Central South University (NATURAL SCIENCE EDITION), 2016,47 (6): 1947-1952[3]. WeiLiJiang, signal denoising based on wavelet transform.

[3] Tanaka, Li Shujiang, Wang Yanhong, Gao Hsien Wen. Short term combined wind speed wind farm wavelet transform [J]. to forecast the short term wind speed forecasting of wind farm based on combination of wavelet transform based on 2015,30 (9): 112-120

[4] Wu Qiuling, Wu Meng. A new method for speech information hiding based on wavelet transform [J]. Journal of electronics and information technology, 2016, (): 834-860

[5] Chen Huan. Harmonic detection and analysis based on wavelet transform [D]. HeFei University of Technology: HeFei University of Technology, 2016 20-50

[6] Feng, Shaolong1, Gao, Dan1,Liao, Fen1,Zhou, Furong1,Wang,Xinming2.The health effects of ambient PM2.5 and potential mechanisms.[J]. Ecotoxicol Environ Saf.2016,128(6513):67-74

[7] Chen Li, Qin pan, Zhang Jingwen, et al. PM2.5 prediction based on spatio temporal data model [J]. Chinese Journal of scientific instrument, 2016,36 (21): 1-10

[8] Yin Xiangfei. Efficiency of urban PM2.5 in China [J]. Journal of Beijing Institute of Technology (SOCIAL SCIENCE EDITION), 2016,0 (4): 49-57

[9] Du Shiyong, Bai Zhipeng, Hou Yong, et al. PM2.5 monitoring method and application [M]. Beijing: Science Press, 2016.1-143

[10] Hu Miao, Xie Jialiang, Wu Duanfa, Ceng Rong, Li Qiliang, Zhou Xuefang, Qian Zhengfeng, Wei Yizhen, Xiang Zhen, Cai Ju. Based on the CCD to PM2.5 measurement of scattering laser signal [J]. (J) 2015, 35 (2): 16-22

Development of Micro Motion Signal Simulation Software Based on GPU and Cloud Storage Technology

Zhang Xin[1]; Han Yu[2]; Wang Meng[1]

(1.College of Instrument Science and Electrical Engineering, Jilin University, Changchun 130022, China;
2.College of Computer Science and Technolog , Jilin University, Changchun 130022, China)

***Abstract*—The project aims to develop a software that can be used to simulate the movement of micro-motion signals in the geological structure and to be intuitively observed according to the relevant algorithm. Combined with the GPU acceleration method and the idea of the cloud to help more perfect to carry out the corresponding algorithm practice. Mainly using C + + and MATLAB mixed programming method to complete the program backbone, the use of Python language fast to complete the network programming, and use Qt interface and internal core interface to complete the compiler. In a sense is a multi-programming language programming a bold exploration, but also a new programming technology in the optimization of other disciplines to solve the problem of mathematics in an experiment.**

***Key words*—simulated jogging signal C ++ network programming GPU acceleration**

I. PREFACE

AT the moment when people live on the ground, there are tiny vibrations that do not feel for people. This kind of ground motion, the application of highly sensitive instruments can be observed and recorded. This type of vibration is divided into two categories. People generally referred to short-period fretting as a regular micro-motion, the long-term micro-action called the ground pulse[1].

In May 1983, the magnitude of the earthquake in the middle of the Sea of Japan was 7.7, which caused great damage to Japan's Akita Prefecture and Aomori Prefecture.Among them, the damage caused by liquefaction of foundation was more prominent. In this paper, the relationship between liquefaction damage and regular fretting behavior is studied in detail. The relationship between liquefaction damage and regular micro-motion is studied in detail. After summarizing and summarizing, it is proved that the observation of regular motion may become an important method for seismic liquefaction prediction.

With the advancement of modern technology, it is becoming more and more convenient for frequent micro-motion detection, but it is necessary to browse and analyze the seismic data in the research process. Dealing with such a large-scale data is a very difficult problem.

Data collection software bundled with the acquisition instrument, on the one hand the function is often too simple, can not meet the complex data analysis. Rely on the traditional practice, engineering and technical personnel have to master a certain degree of computer programming knowledge and a certain computer algorithm, which has brought some difficulties. And it is often difficult to satisfy the hypothesis of a stationary stochastic process for the collected field. M a t l a b provides a number of powerful library functions, easy to debug, do not need advanced programming skills and mathematical knowledge, so as to effectively solve the problem[2].

So summed up the relevant knowledge, the preparation of procedures used to deal with large-scale computer data. The formation of software automatically on the fretting signal recording data anomaly picking, recording, analysis, and the formation of image, intuitive image information. It is necessary to develop an analysis software that is user-friendly, efficient, real-time, easy to operate and easy to develop and develop in the future[3]. So that the real-time processing of the micro-exploration field experiment data.

II. SYSTEM FUNCTION DESIGN

The project aims to develop a software that can be used to simulate the movement of micro-motion signals in the geological structure and to be intuitively observed according to the relevant algorithm. Combined with the GPU acceleration method and the idea of the cloud to help more perfect to carry out the corresponding algorithm practice. Mainly using C + + and MATLAB mixed programming method to complete the program backbone, the use of Python language fast to complete the network programming, and use Qt interface and internal core interface to complete the compiler. In a sense is a multi-programming language programming a bold exploration, but also a new programming technology in the optimization of other disciplines to solve the problem of mathematics in an experiment.

III. MICRO MOTION SIGNAL SIMULATION ALGORITHM

At present, the wave equation commonly used in numerical simulation can be divided into two groups: second order elastic wave wave equation and first order displacement stress elastic wave equation group. The software uses the first order displacement stress elastic wave equation staggered grid difference algorithm[4]. The numerical simulation of the wave equation is based on the given subsurface structure model and the corresponding parameters, and the geological model is discretized. In the method of theoretical calculation, all the grid points in the calculation area can be obtained at each time Elastic wave wavelength value, and then simulate the seismic wave propagation in the underground media.

According to the given initial condition and boundary condition, the stress component value is obtained by using the formula, and then the wavelength component of any grid node is obtained by using the stress component value of this moment. The detector in this paper is received on the ground, and the Rayleigh wave field value observed on the ground is the target of our final solution. That is, the displacement of each point at different times along the horizontal and vertical components and the normal stress and shear stress at each point at different times are the values of our signal simulation. Can use a fixed time wave field value, get wave field snapshot, simulate the wave propagation in the medium[5]. This is because we recursively calculated by a data body, according to different observations, processing requirements, extract the required part of the data, the formation of different profiles, to facilitate research. The simulated wavefield snapshot is shown in Figure 1[6].

IV.GPU ACCELERATION TECHNOLOGY

In view of the portability of the program, the program parallel algorithm part of the use of a higher degree of compatibility OpenCL standard library. OpenCL is a framework for writing programs for heterogeneous platforms that can be made up of CPUs, GPUs, or other types of processors. OpenCL consists of a language (based on C99) for writing kernels (functions that run on OpenCL devices) and a set of APIs for defining and controlling the platform. OpenCL provides a parallel computing mechanism based on task segmentation and data segmentation. The core idea of the algorithm is to automatically identify and generate thecorresponding computing environment based on the number and type of available devices on the local computer. Separate the computing device from the host. Build an independent computing space. The grid granularity thickness is calculated based on the number of split points of the synchronization points to be performed. Combined with the current number of available computing devices, the design of the model by the man-made, and then automatically set the command from the host to the computing device to be calculated after the completion of computing equipment to read data. The whole process is like a batch processor, its essence lies in the preparation of the appropriate kernels. OpenCL divides the computing resources into different levels of the grid, mapping the actual problem cores to the logical model from the workgroup to the work item. For example, for the formation of the structure, due to the calculation of the current moment of the speed of the need for the two time corresponding data. OpenCl can share memory, the speed of a certain moment, with the previous moment of stress data is divided into two grids, the formation of staggered grid. Since the calculation of each point is only related to the corresponding points of the first two moments, the points are calculated independently at the same time.

Can be prepared for the corresponding kernel program, each point will be divided into a computing core, while the calculation. In the case of a small amount of data, parallel computing is not necessarily more time-saving and computational resources than traditional serials due to the write-in memory and the time-consuming consumption of the environment and memory. But with the further increase in the size of the algorithm will increase the complexity of the algorithm and memory leak problems, the need for timely control of the release of memory and application.The specific model is to create two containers, if the calculation of the shorter time and smaller scale can not be released and then can access the results of any time. Taking into account the storage costs, the program is only for the choice of time to calculate the data, through the OpenCl calculation of data, the calculation is completed after the experimental data through the MATLAB engine into MATLAB. Use the corresponding drawing function to draw the wave field snapshot to observe the spread of the waveform. And automatically stored into the corresponding folder to ensure that later read. In the innovation on the use of OpenCl for parallel computing, with MATLAB engine graphics rendering, give full play

Two different language advantages. But in the data transmission convergence due to the level of restrictions, can not be completed in the same compiler environment compiler. Using Xcode's clang and g ++, respectively, compiled parallel computing part and MATLAB engine part. There are similar problems.

V.LAN SET UP

The LAN section is written in Python. In view of the convenience of the Python language and the limited operating environment. Using Python2.7 version. Use HTML to write web interface, Python prepared background. Use HTTP protocol to coordinate communication. Use the terminal or SHELL to run the corresponding interpreter Python program. Open the computer's 8001 port, the Python file where the folder is mapped to a list of data. The operation of this file will also be displayed on the prepared web page. As long as the device in the same WiFi environment, whether it is mobile phone or computer, tablet. Access this folder via the browser's visit to the suggested URL. You can also send data to this folder via a web page. And updated in real time. For the calculation process that takes a long time. You can not wait for the results, through this feature can use the phone at any time to monitor the results generated. At the same time due to the use of HTTP protocol can send any format files. In essence, is through the establishment of a program to the machine outside the machine, the use of streaming data transmission. Simple structure, stable operation. Run as shown:

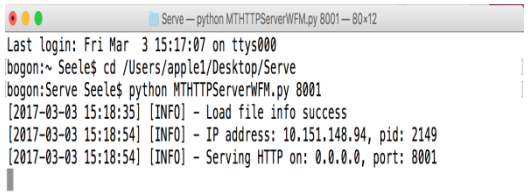

Figure 1 :LAN operation diagram

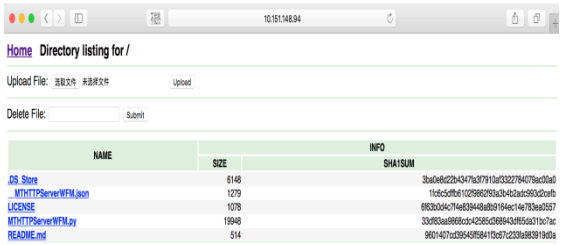

Figure 2 :LAN display

VI.INTERFACE DESIGN

Interface part, using Qt5 for packaging. The kernel program package compilation completed, the use of Qt's console command by clicking the button to stimulate the pre-set slot mechanism. Generate the corresponding process using non-blocking. Interface generation using the latest Qt-Designer manually drag the window with the setup slot, the code is automatically generated. In addition to the background of the code, the front desk interface can be automatically generated. Even beginners who have just learned can easily use the powerful Qt library to create a favorite interface. Because Qt is written in C ++ language. There is no need to install an additional virtual machine with a runtime environment that can be done easily across platforms.

The interface consists of the main screen and

function buttons. At the top, you can modify the time to be calculated. Choose whether to display a wavefield snapshot or a wave field view. Due to the existence of Vx and Vy two kinds of speed. Refresh the contents of the main screen according to the selection. Open the local and cloud storage folder. As well as a key to upload the local folder to the cloud function

Figure 3 interface design

VII.MATLAB MAPPING

After opening the software, according to the different views on the micro wave signal propagation process in different time to display the dialog box, in the moment of input specific time specific micro signal propagation.When you click to call the MATLAB generation micro signal each time the forward modeling, divided into x y two directions.In 0.6s, 0.8s, 1.0s, 1.8s for example, to generate the wave field as shown below.

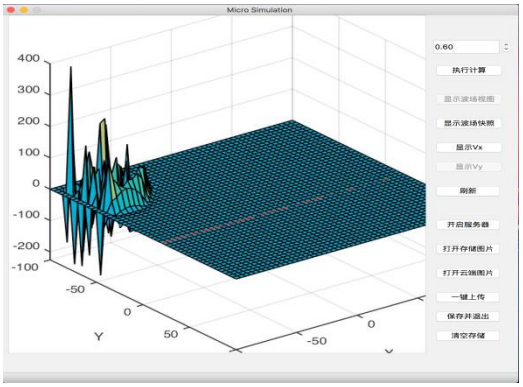

Figure 4 0.6s moment wave field of view

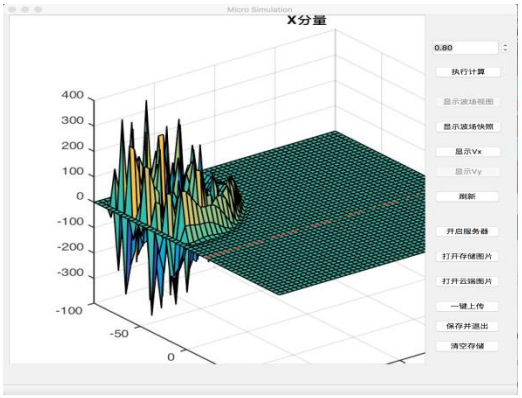

Figure 5 0.8s moment wave field of view

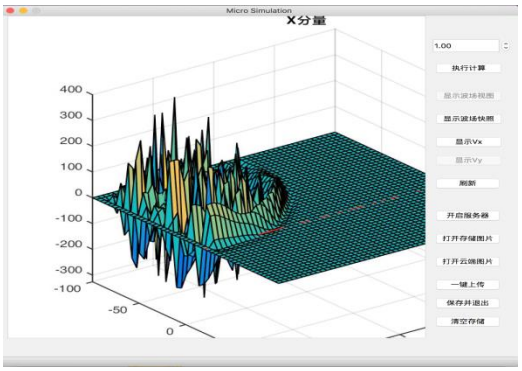

Figure 6 1.0s moment wave field of view

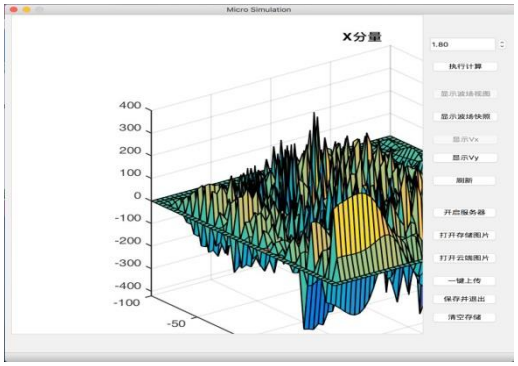

Figure 7 1.8s moment wave field of view

VIII.CONCLUDING REMARKS

The analog signal method using staggered grid finite difference software, can be obtained at any time in the observation period. The wavelength snapshots in the simulation process, the data needed for calculation is too large, calculated by GPU to assist the operation.To build a part of LAN, which can even share, in the same wireless devices to upload and download data. But for the influence of various equipments and the logic of the upper design is also lack of knowledge. In the development of this project in the very obvious.

References

[1] Peng Yuanqian, Li Xueying, high Dengping. Differences of the data processing method of field pulsation observation [J]. Shanxi earthquake, 2000, (2).

[2] Sun Yongjun, Xu Peifen, Su Qun Ling, Li Chuanjin. Progress, progress of investigation and study of the [J]. method of micro Earth Physics 2009, 24 (1).

[3] Yang Boxiong, Chen Zhigao, Liu Haibo and Hu Xin, Lu J, ou tonggeng,. Data processing and spectral characteristics of rock and soil micro signal analysis [J]. rock and soil mechanics, 2008, 29 (3).

[4] Wu Yingting. High order staggered grid finite difference elastic wave field numerical simulation [D]. Xi'an: Xi'an University of technology, 2010

[5] Zhou Xiaohua, Chen Zubin, Zeng Xiaoxian, Jiao Jian. The staggered grid finite difference method to simulate the fretting signal [J]. Journal of Jilin University (Earth Science Edition), 2012, 42 (3).

[6] Li Yangsen, Meng Fanshun. Elastic Rayleigh wave staggered grid finite difference numerical simulation [J]. Journal of Chongqing University of Science and Technology (NATURAL SCIENCE EDITION), 2012, 14 (5).

Basic experimental research on positioning for GPS systems and BeiDou systems

Qiang Wang; Li Gong; Qing-long Meng

(College of Instrumentation&Electrical Engineering Jilin University,chang chun,130022,China）

***Abstract*—The Beidou system is developed in our country and global satellite positioning and navigation system, in the global range for all types of users to provide high accuracy, high reliable positioning, navigation and timing services, and has a short message communication skills. Current domestic various navigation and positioning equipment mainly by the Beidou system and GPS system, with the country to develop the cause of the Big Dipper, the popularity of the Beidou system continues to improve. This research mainly through the simulation of different application environment (dynamic / static, sunny / rainy day, open / forest,), the domestic UM220-III n type dual-mode positioning navigation chip, measurement system was built up, measuring and recording the compass and GPS positioning data of the latitude and longitude of, elevation, precision factor and so on), and by and Google Earth map data standard comparison and analysis calculated two system positioning performance of the qualitative and quantitative results, and the measurement basis can be provided for the follow-up product development.**

***Key words*—Beidou system; GPS system; UM220 - III N; Simulation environment; The positioning performance; qualitative ;quantitative**

1. INTRODUCTION

CHINA'S Beidou satellite navigation system is China's own development of the global satellite navigation system[1],It has high precision, high reliability positioning, navigation, timing services and short message communication capabilities[2].China's current civil navigation and positioning equipment on the market more use of GPS systems, less Beidou equipment, but the Beidou industry is developing rapidly. In order to study the performance difference between the two systems, this paper uses the data processing capability of the host computer software and MATLAB software by measuring the positioning data, including latitude and longitude, elevation, precision attenuation factor and response speed, in the Beiqi system and GPS system under different environments , The direct qualitative evaluation and quantitative evaluation of the two systems are analyzed and calculated.

2.RESEARCH FOUNDATION

2.1 UM220-III N-type dual-mode positioning navigation module

The UM220-III N dual-system high-performance GNSS module, based on the company's fully independent intellectual property rights dual system multi-frequency high-performance SoC chip, can simultaneously support BD2 B1, GPS L1 two frequency points, especially for low cost , Low power consumption. Its typical power consumption value is only 120mW, can receive the RF input 1559 ~ 1577MHz, can -40 ℃ ~ +85 ℃ in the normal work. Positioning accuracy of 2.5m, the first positioning time only 32s. Chip has a UART programmable serial port 1 and universal serial port 2, can be easily connected with the peripheral and data transmission[3].

Fig. 1 UM220 - III N figure shape

2.2 Positioning system accuracy factor

PDOP three-dimensional position accuracy factor: latitude, longitude and elevation and other square error of the square root. HDOP Horizontal Component Accuracy Factor: An open root value for the sum of squares of errors such as latitude and longitude. VDOP

vertical component accuracy factor. The three meet the following relationship

$$HDOP^2+VDOP^2=PDOP^2 \quad (1)$$

The size of the DOP value is proportional to the error of the GPS positioning, the greater the DOP value, the greater the positioning error, and the lower the positioning accuracy. PDOP is a direct reflection of the distribution of GPS satellites, when the PDOP is large, indicating that the air four GPS satellites geometric distribution is not too ideal, they constitute the graphics circumference is too short, positioning accuracy is low, and vice versa[4].

2.3 Data filtering

Any measurement is always inevitable in the error, in order to improve the measurement accuracy, it is necessary to eliminate or reduce the error as much as possible[5].In the field measurement process, we follow the user manual on the requirements of the standard operation, each measurement to control a single variable changes to ensure the correctness of the measured data. In the process of screening data, in order to prevent the data has obvious floating that is rough error, we judge according to the three criteria (each experiment has a lot of data we can assume that obey the normal distribution). After a screening, the second screening was performed by the precision factor. Finally, we recorded 10 of the more stable data.

2.4 Error Analysis

The earth ellipsoid model is $\frac{x^2+y^2}{a^2}+\frac{z^2}{b^2}=1$

Where a is the equatorial radius (radius of the earth) and b is the radius of the polar axis (the short radius of the earth). As countries use different data to calculate and therefore a, b two values of different sizes. In this paper, we use WGS - 84 ellipsoid, that is, a = 6 378 137. 000 m, b = 6 356 752. 314 m. Calculate the arc length of each latitude, as follows:

S_a=[cosB1×（ 6378137-237.6111×B1 ）+cosB2×(6378137-237.6111×B2）]

B1, B2 is the latitude of two points (take degree). The average arc length of the latitude is approximately equal to about 111,000 m[6].

3. RESEARCH PROGRAM

3.1 Experiment system

As the UM220-III N has two high-speed serial port, with 232 to serial mode, to communicate with the computer, the use of the core and independent research and development of the host computer Unicore Software can quickly read latitude and longitude, elevation, timing information, accuracy factor and other key information.

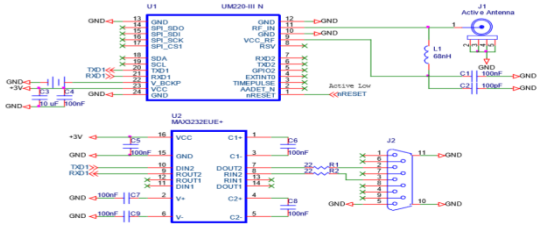

Fig. 2 experimental system circuit diagram

3.2 Exceptional environmental testing

The purpose of this experiment is to test the Beidou / GPS system in a variety of abnormal environment positioning effect. Reference standard for Google Earth standard latitude and longitude data. The latitude and longitude, altitude error and so on are used to quantitatively analyze the positioning quality of the two systems under different conditions.

(1)Open conditions: Changchun City Cultural Center at the center of the measurement. This square area is large, no trees interfere with, and there is no large building interference around.

(2)Simulated forest conditions: Changchun Nanhu Park trees are lush, can play a very good occlusion effect, so meet the conditions of the simulated woods.

(3)thunderstorms and sunny conditions: in thunderstorms and sunny days under these two different conditions, choose the Jilin University geological palace measurement, the antenna external, reduce interference.

3.3 Dynamic testing

The purpose of this experiment is to study the positioning effect of the two positioning modes of Beidou / GPS in the state of motion of the receiver or antenna (including the corresponding noise ratio, the accuracy factor in the high speed state, the standard deviation of latitude and longitude in the slow state, , Tracking speed (high-speed state from tracking to a track to a certain number of the required time) and so on.

Slow state:As the GPS is used in the distance around

the Earth orbit, so the distance led to the inevitable existence of the error. Even if more than three satellite data superposition, the best positioning error or about 10 meters, and the Beidou positioning error is also above the value. So within 1m of operating radius, the receiver can be considered the same position.

To achieve the purpose we use the remote control car to measure, manually control its diameter in the range of 2m back and forth movement, due to the actual conditions, the car running speed can reach about 15cm / s, in the car to install the fixed frame, fixed receiver , And support the high antenna, so as to stay away from the ground, reduce the magnetic field interference.

High speed state:

Taking into account the representative, the speed to be able to 32.18km / h above, and can run for some time. We choose in the ring road, traffic less places with a small car equipped with a receiver and measurement, speed control, you can choose to 32.18 ~ 80.45km / h sub-file measurement.

4 EXPERIMENTAL RESULTS AND ANALYSIS

4.1 Abnormal environment analysis

4.1.1 Sunny weather,Openly

Cultural Square Google Maps data for 125.301315329 °E,43.877616194 °N.altitude227.9m. Horizontal comparison, the two systems in the sunny weather can get more accurate data. Its accuracy factor is below 7, are reliable positioning of the data. But in numerical values, the Big Dipper is higher than the GPS values, which indicates that the absolute accuracy is not high for GPS. The reason for this is as follows:

（1）The current Beidou satellite only 22, and GPS has 24, indicating that at the same time to observe the number of Beidou satellite and no GPS, the actual measurement found in the north to track to 7 to 8, and GPS can track to 8 to 10 stars. Tracking the more satellites, the receiver in the analysis of three-dimensional coordinates of the more accurate, more accurate measurement results.

（2）Beidou civilian board itself is not high precision, technology is not yet mature, the chip internal algorithm needs to be improved.

Beidou system: $\delta_3 = 0.000000271°$

The error caused by the change in longitude is about

s_3 =0.02171m

δ_4 =0.00008669 °

The error caused by latitude changes is about

s_4 =9.622m

and so

S_{BD2}=9.622m.

Similarly available

S_{GPS2} =1.661m

Contrast can be found in both the linear error is less than 10m, but the GPS error is smaller than the Big Dipper. In the open underground, if the accuracy of about 10m, you can use the Big Dipper or GPS system. If the required accuracy of 2m or less, you can only use GPS system.

4.1.2 Forest environment

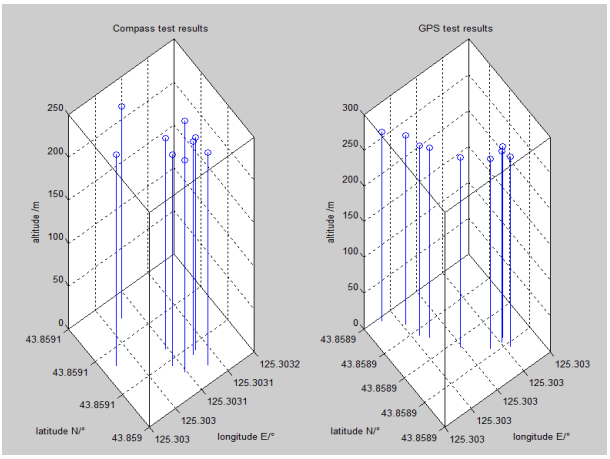

Fig. 3 Effect of deep forest environment test

By the Google Earth to get the exact point of the measurement data for the coordinates 125.302310611 °E，43.858591700 °N.

In the deep forest environment, the accuracy of the positioning of the two systems have had an impact, compared to the open conditions HDOP, VDOP, PDOP values have increased. But the impact on the Beidou system is relatively large. The corresponding values are 4.24,6.56,7.81, indicating that the total position and elevation of the total error has been more than 7, the accuracy is poor.

Beidou mode, the measured latitude and longitude average125.3030496 °，43.85906268 °E。

$\delta_5 = 0.000738989°$

The error caused by the change in longitude is about

s_5=59.22m

The same can be latitude impact

δ_6=0.00047098°

s_6=52.28m

S_{BD3}=78.99m.

So in the jungle, the Beidou system obtained by the positioning of the largest linear error of about 78.99m.

Repeat the above steps, available in GPS mode:

l_3=52.86m

l_4=32.10m

S_{GPS3}=61.84m

Can be obtained in the jungle GPS maximum linear error of about 61.84m, compared to the Beidou straight line error, can be found, GPS measurement results more accurate, which in the accuracy factor values of the two can also be verified. In summary, in the jungle, if the positioning accuracy of 70m or less, should use the GPS system, 80 m or more, you can consider the choice of the Beidou system.

4.1.3 Indoor environment

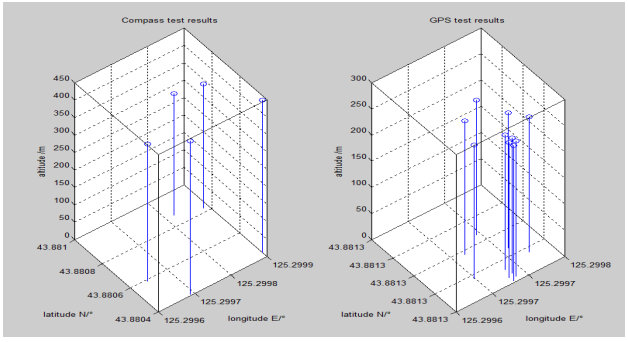

Fig. 4 indoor, sunny weather test results

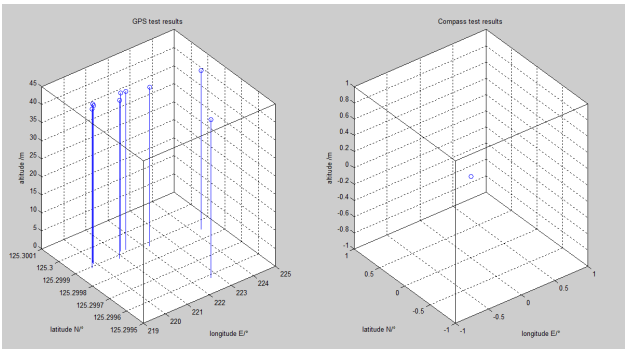

Fig. 5 indoor, thunderstorm weather test results

The above two experiments for the indoor conditions: thunderstorms, sunny weather comparison experiments.

Under the indoor conditions, due to the modern housing structure of the frame structure, sometimes the formation of electromagnetic shielding, electromagnetic interference caused by the transmission. In the satellite positioning system, because the receiver receives the satellite transmission of high-frequency electromagnetic waves (1561 ~ 1575.42MHz), so the indoor will be on the positioning timing will have an impact.

Beidou system In the clear room, you can clearly find the accuracy of the Beidou system factors are significantly increased vertical component accuracy factors have reached more than 10, indicating that the measurement results are poor stability, prone to error data. Its linear error will rise to more than 100 meters.

In the case of thunderstorms, by using the fixed bracket to the antenna outside the house, to reduce the electromagnetic frequency of the house to simulate the outdoor environment. Measure found that in the 5 minutes of waiting time, the Beidou system can not track more than three satellites, that is, can not resolve the space three-dimensional coordinates, can not be normal positioning. This indicates that the thunderstorm weather Beidou satellite signal is unstable and can not be measured normally.

GPS system In the sunny room, GPS can accurately locate the location, the corresponding precision factor is low, the error is small. In the three-dimensional map can be found in the GPS measurement points are basically concentrated in a small area, the positioning effect is good.

In the thunderstorms, the accuracy factor is slightly increased, indicating that the positioning error has

increased. But the total PDOP of 2.38, cf. sunny weather 2.256, the impact is not large.

Horizontal comparison point of view, measured in indoor conditions, if the higher accuracy requirements, should use the GPS system.

4.2 Dynamic analysis

4.2.1 Low speed analysis

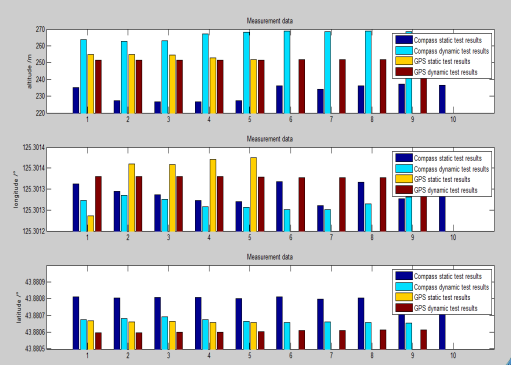

Fig. 6 test results of low speed remote control car

Beidou system: at low speed, if the receiver is in motion state, the Big Dipper system has a greater impact on the positioning effect. There was a significant change in altitude, with an average relative change of 14.8% and a change in longitude δ 1=0.000023202 °,To static data as a benchmark, can be calculated by the longitude of the impact of change is about

s_7 =1.8680458m

The same token can be obtained by the latitude change of δ 2= 0.000136409 °, bringing about the effect of about

s_8 =9.7001956m

GPS system: low-speed state of the GPS positioning effect of the impact of small, the average change in the amount of K = 2.103m, compared to the Big Dipper system is much better. As the movement brought about by the longitude change

Δ_3 =0.000011371 °,

l_5 =0.9155073m

Due to the latitude of the ovement Δ_4 =0.000056361 °,

Can get its impact is about

l_6 =4.0078933m

Longitudinal contrast, the Beidou system in the state of motion is usually the conditions of its stability and stability of the GPS is not good, due to the movement of the measurement results range is relatively large changes. Its altitude changes more than 10m, the longitude impact of 1.8680458m, latitude impact of 9.7001956m, compared to the GPS system can be seen that the stability of poor, greater error. In the case of a vertical comparison, it is necessary to use a GPS system in a situation where the elevation accuracy is high (30 m or less) in a case where the elevation accuracy is not high (about 30 m in accuracy).

4.2.2 High speed analysis

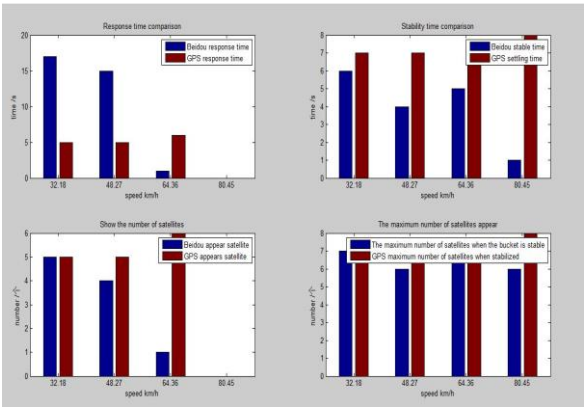

Fig. 7 test results of high speed performance

Through the observation of the Beidou system data, the speed of 32.18km / h, the first track to the satellite when the 17s, you can observe the five stars. Accuracy factor only HDOP lower, VDOP and PDOP are greater than 7, are not credible interval. Although the positioning data can be observed, but at this time the positioning data error. In the stability of its value is also larger.

When the speed rises to a speed of 48.27km / h, through the same place, the first observation of the satellite about 15s, but only observed 4 stars. And at this time HDOP, VDOP, PDOP has exceeded the measurement range, reflecting the data received under such conditions are all dummy data, there is no practical value. Stable to 5, the need for 29s, which indicates that the tracking speed has been significantly reduced at this time. And the three precision factors have a corresponding increase, indicating that the positioning effect of the trend is getting worse.

When the speed rose to 80.45km / h, due to the speed too fast to receive any satellite signals HDOP, VDOP, PDOP three values are infinite, indicating that this section Beidou system in the speed of 80.45km / h has lost normal The positioning ability.

The data of GPS system in four different speeds are analyzed, and the first time is tracked to 7 satellites in 6s time at 32.18km / h. At 48.27km / h, 6 satellites are tracked for the first time in 4s; 64.36km / h, the first time within 5s to track seven satellites, 80.45km / h in 1s track to 6 satellites, taking into account the residual effect of the receiver, that in the 0 ~ 80.45km / h speed, There is little impact on GPS positioning performance. The three kinds of precision factor values increase with the increase of velocity, indicating that the faster the dynamic condition, the worse the positioning effect, which is common to the GPS system and the Beidou system.

Horizontal comparison point of view, in the high-speed state, to be able to complete the positioning function, should use GPS system. Its positioning accuracy and tracking speed (less than 80.45km / h) can meet the usual requirements. While the Beidou system in the dynamic conditions of positioning is poor, higher than 32.18km / h speed has been a big error.

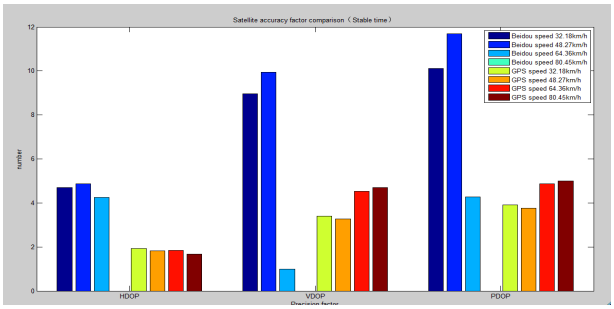

Fig. 8 test results of high speed precision factor

The graph above shows the comparison of the precision factor after running for a long period of time (ie, the two systems tend to be stable). It is found that the accuracy of GPS system is not significant in steady state, and there is no significant difference with the accuracy of tracking system. This shows that the stability of GPS system is good at high speed and there is no obvious deviation.

For the Beidou system, the data can be measured at 64.36km / h in steady state, but the abnormally low measurement value occurs at 64.36km / h. The reason is as follows:

(1): by traffic lights, traffic restrictions, the car can not be a long time to maintain a constant 64.36km / h speed, during which there is a decline in speed. Resulting in a decrease in the measurement accuracy factor.

(2): The receiver and the antenna are not normally reset, resulting in the reproduction of the last speed gear measurement data with uncontrollable vehicle speed reduction, resulting in unusually low measured values.

Overall, the stability of the state, the Big Dipper system error is large, the measurement results vary greatly, the stability is poor, not suitable for high-speed state.

5 CONCLUDING REMARKS

Through this experiment, we compared the performance of the Beidou system and the GPS system to get the following conclusions: latitude and longitude and other information display, the static measurement of the GPS system to get the data than the Beidou system is more reliable, in the dynamic measurement GPS system data More stable than the Beidou system; response time on the static when the Big Dipper system faster, and in the case of high-speed chip can not keep up with the GPS system will lead to faster response, indicating that the Beidou positioning system there is still much room for development.

In the course of the experiment, our judgment of the response time is based on the time when the satellite appears rather than according to the receiver chip light when the light as a judge standard, which may have an impact on the measurement results. Moreover, we did not verify the Beidou system SMS notification function, a single comparison of some information, may have a certain impact on the conclusions.

References

[1] Wang Quan.The design and application of Beidou satellite communication satellite system[D].Northwestern University,2009,in Chinese.

[2] Chen Chao. Wireless automatic control system of Beidou satellite timing schedule of the research and design of [D]. based on Wuhan Polytechnic University,2012,in Chinese.

[3] UM220-III N User manual,in Chinese.

[4] Zhang Miaoyan, Zhang Jun, Zhu Yanbo.Research on HDOP and VDOP of satellite navigation

system[J].Telemetry and remote control,2009,02:6-12,in Chinese.

[5] Fei Jie Tai, Error Theory and Data Processing (M), Beijing: Mechanical Industry Press, 2011,04: 10-11,in Chinese

[6] Li Zhenxi,Li Jiaxun.Based on latitude and longitude to calculate the distance between two points and the measurement error[J].Mapping and spatial geographic information,2013,11:235-237,in Chinese

The Design of the Elderly Tumble Monitoring System Based on Wearable Platform

Cai Jing; Fan Yiyao; Dong Zijian; Xue Qi

(College of Instrumentation&Electrical Engineering,JiLin University， Changchun 130026,China)

***Abstract*—Aiming at the problems of the elderly tumble and harm, we designed a wearable platform based on human area network which detects physiological status when the elderly fell down .It mainly includes fall state detection module, the human physiological state detection module, GPS positioning module and the remote monitoring module. When the elderly falls, the fall state detection module confirmed by the triaxial acceleration data immediately ,the system communicates with the remote monitoring platform, transmit a message about the elderly physiological state information and GPS location information to the guardian by the wireless communication. The guardian can succor the elderly in time. The Experimental results show the system is effective for the elderly fall status detection and relief, It can shorten hours, has well social significance.**

***Key words*—wearable; fall detection; fall state detection detection; GPS positioning; remote monitoring**

I.INTRODUCTION

ALONG with the aggravation of Global aging and the increase of the aged,the supervision of health of the aged is becoming an important social problem[1].During to the decrease of body function,the probability of the tumble on the aged is extremely high.Researches show that,it is general that the aged can easily get injured or even death in the fall .The portion of the fall of the aged who over 65 reaches to 30%,especially.The mortality in the fall is approaching 0.051% which is bad to life[2].

The fall is a kind of change in posture, which is occurred burst,no intension and no autonomous,people fall in the same plane or different.Today the effective technology of monitoring are mainly classified into 3 class-es: (1)The analysis based on video image; (2)The analysis based on audio signals; (3)The detection mode which is wearable and portable[3].Video image analysis can not ensure the safety of the users privacy .As for the audio,it is complex to install an audio signal device and the capital input is very high.Wearable detection is easy to use and costs less,and it can guarantee more accuracy. Comprehensive consideration,the wearable detection of the aged has become the main method[4].

This paper designs the monitoring system based on the detection of the fall of the aged and increases the function of the real-time detection of physical,the remote alarm , GPS positioning and improves the algorithm of fall,increases the normal gesture of people's movement and the gesture of dynamic threshold settings which makes more accuracy.

II.SYSTEM COMPOSITION

The system is mainly composed of four sections which are the acceleration detection、measurement of heart rate 、GPS location 、platform of remote monitoring.The framework is shown in the figure 1:

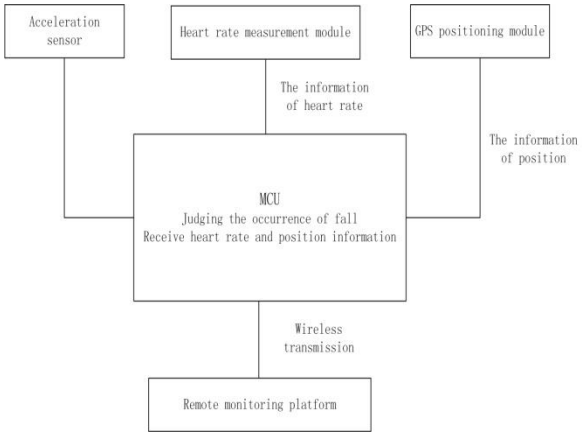

Fig.1 System composition block diagram

When the fall happens,the micro controller determines the messages of the acceleration and collects the ECG signal by heart rate measuring module,besides,calculates the heart rate.In addition, the microcontroller will transfer the falling state results、

the value of heart rate and messages of location from GPS to the remote monitoring platform then sends the messages to alarm[5].

III.MODULE OF HEART-RATE MONITORING

The module of heart-rate monitoring adopts electrocardio signal amplifying with single lead. This module combines advantages of power efficiency、high accuracy and facility in design.The heart-rate signals via the snubber circuit、the preamplifier circuit and the filtering circuit then we can receive the heart-rate signal wave form in the figure 2[6].

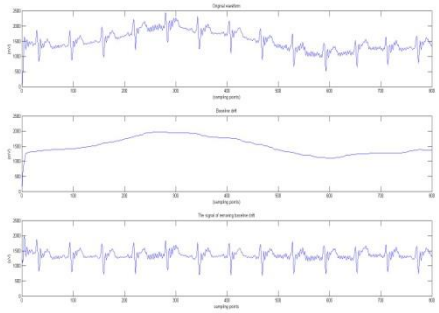

Fig.2 ECG signal wave

Regard 60% of the average peak value as the based threshold to locate the R wave[7].Suppose the time interval of the adjoining R wave is T0（unit s）then the heart-rate f0（unit number of times/min）

$$f_0 = \frac{60}{T_0}$$

To assign heart-rate by measuring how many RR intervals in one minute[8].

IV.GPS POSITIONING MODULE

GPS location realizes its function by communication between positioning module and remote monitoring platform,and the measurement of location messages can be called by Baidu maps built-in mobile phone's remote monitoring platform.

V. DESIGN OF THE ALGORITHM OF TUMBLE

There are basic static postures in daily life,including supine、prone、side、sit straight、sit forward、sit leaning back、straight、stand forward、stand leaning back、squat and so on.Regard left-leaning and right-leaning when sit or stand as the static postures.These basic static postures are combined to form the basic active postures of the human body,including lay down、down、rise、stoop、sit down、stand up walk、jogging、jete、go upstairs、go downstairs and fall.It can be divided into 4 situations by different directions when fall[9].The acceleration and the angle will change when people do some activities，and these factors can judge whether people fall or not[10].

The traditional falling monitoring algorithm is based on the same plane that people accomplish these movements.However,it is definitely possible that taking a jete or big leap may happen between two planes. The judgment that in the single plane is easy to cause erroneous judgement.

To measure the amplitude of acceleration and the angle of gesture, figure 3 shows that the space coordinate system established by sensors.Firstly,the direction of Z axis is defined vertical direction,the direction of X axis and Y axis are defined horizontal direction .There are two quantities that should be measured to detect the fall which are SVM(the amplitude of acceleration) and Φ(the angle of gesture)[11,13].

The sensor of triaxial accelerometer can detect the acceleration of vertical direction a_z and horizontal direction a_x and a_y directly,which:

$$SVM = \sqrt{a_x^2 + a_y^2 + a_z^2}$$

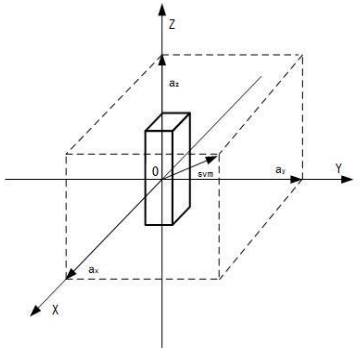

Fig.3 Space coordinates system

The angle of gesture is defined as the angle between body and vertical direction.On account of the obvious changing middle area that normal activity and fall ,the sensor of acceleration is setted in the side[12].

Supposing the body is in the straight state at first,the gyroscope inside the sensor of acceleration is perpendicular to the surface, meanwhile,the body gesture angle is defined as 0 °.During the procedure of movement , single chip computer takes the data returned from gyroscope every t ms.We set that the gyroscope costs N ms to move from Z axis to Z1 axis,at this time ,the single chip computer reads m times of the speed value of angle successively[13].

As is shown in the figure 4: the dashed lines point out the original position of the gyroscope,this moment,the included angle between the Z axis and the Z1 axis is the gesture angle.

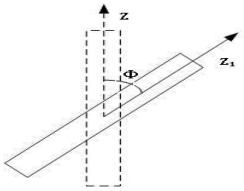

Fig.4 Definition graph of posture angle

Supposing the speed of angle velocity read in N ms from microcontroller are ω1，ω2，…… ω_m ,that is:

$$\Phi = \frac{\left(\omega_1 \times t + \omega_2 \times t \ldots\ldots + \omega_m \times t\right)}{1000}$$

$$Fall = \{(SVM > T_{SVM}) \cap (\Phi > T_{\phi})\}$$

T_{SVM}, T_{ϕ} are amplitude of acceleration vector and the threshold of gesture angle. When fall is equal to 1,we can make the judgement that fall happened.

VI. TEXT AND RESULTS

（1）The collection of original data in normal activity

The figure 5 is the curve changing along with SVM measured in normal activity.

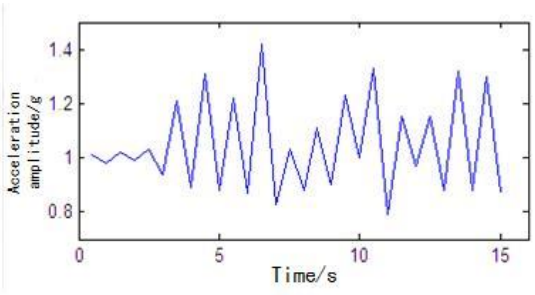

Fig.5.(a) Curve of SVM during walking

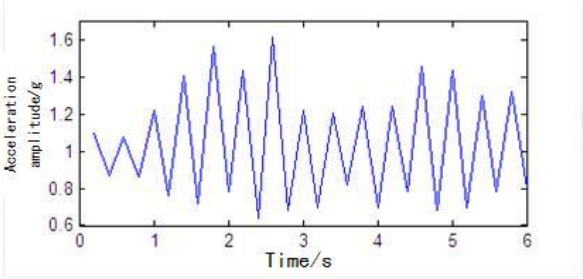

Fig.5(b) Curve of SVM during jogging

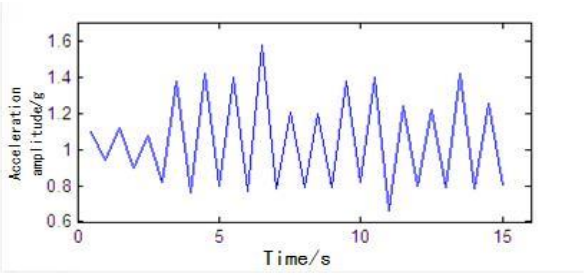

Fig.5(c) Curve of SVM during going upstairs

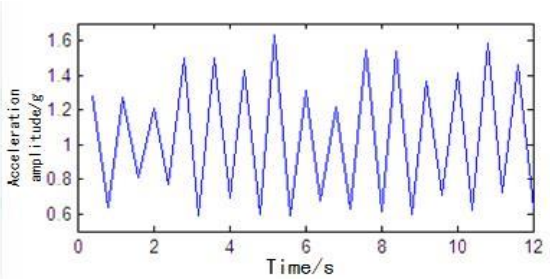

Fig.5(d) Curve of SVM during going downstairs

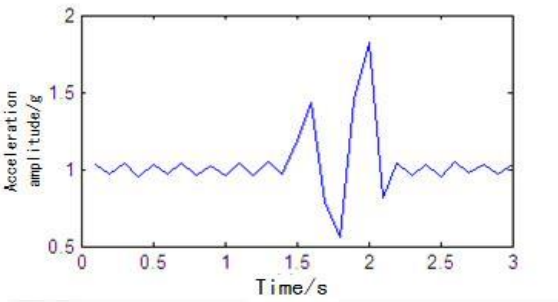

Fig.5(e) Curve of SVM during skipping in same plane

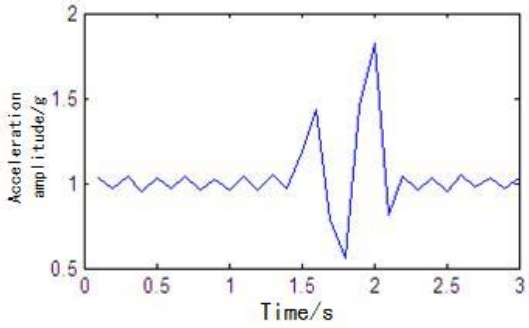

Fig.5(f) Curve of SVM during skipping from different plane

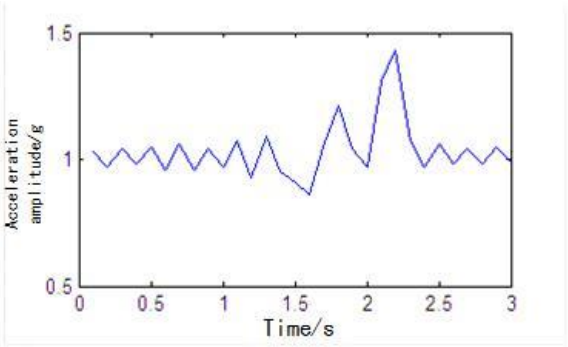

Fig.5(g) Curve of SVM during sitting down and standing up again

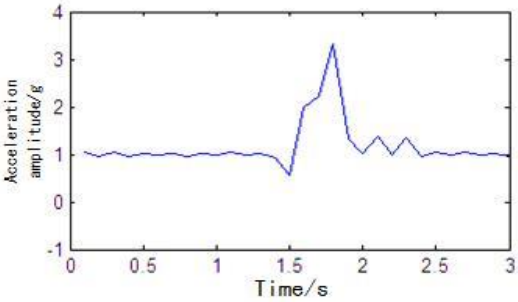

Fig.5(h) Curve of SVM during laying down(prostrating) and standing up again

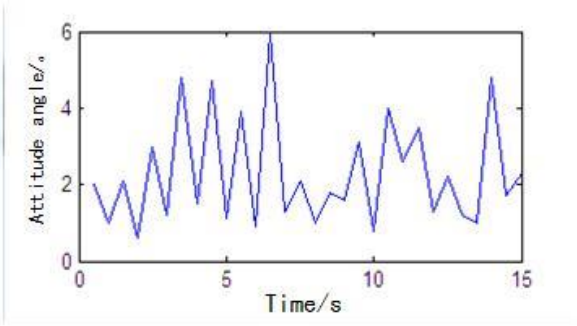

Fig.6(a) Curve of Φ during walking

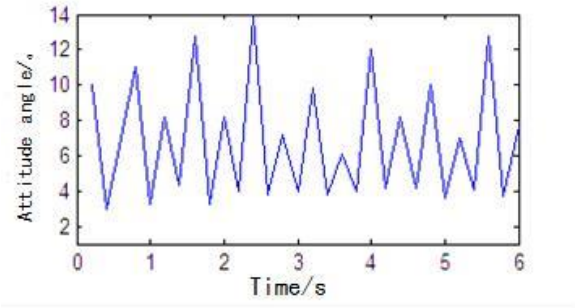

Fig.6(b) Curve of Φ during jogging

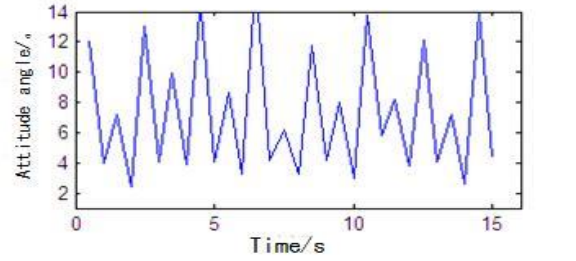

Fig.6(c) Curve of Φ during going upstairs

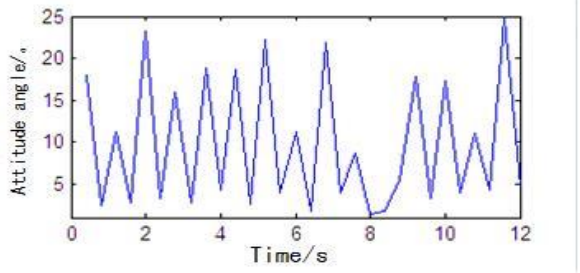

Fig.6(d) Curve of Φ during going downstairs

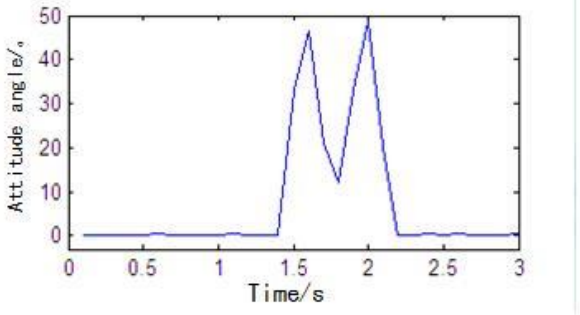

Fig.6(e) Curve of Φ during skipping in same plane

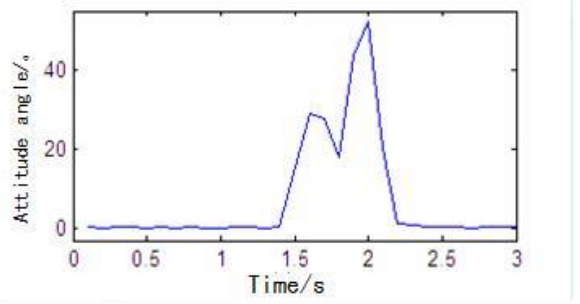

Fig.6(f) Curve of Φ during skipping from different plane

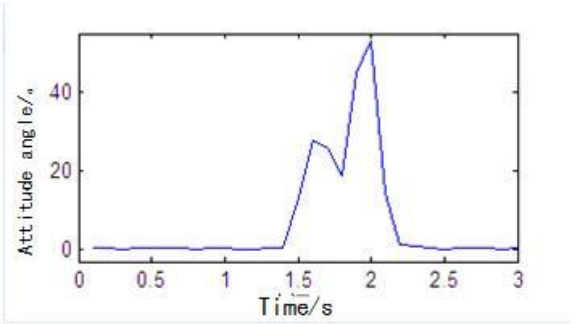

Fig.6(g) Curve of Φ during sitting down and standing up again

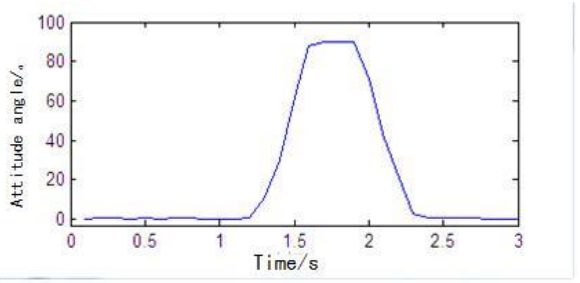

Fig.6(h) Curve of Φ during laying down(prostrating) and standing up again

(2)The collection of original data in the procedure of tumble

The procedure of fall is a procedure that happened from up-right or sit to lean even lay down.The severe actions result in significant change in the angle of body gesture and acceleration in every directions[14]. The procedure of falling is divided into three stages.

① Human torso stay straight before falling,this time,the acceleration of the X axis and the Y axis are 0,the acceleration of the Z axis is -g[15].

②Human torso lean in a short time and the gesture is changing severely.There are accelerations of three directions undergo changes and the acceleration change in the Z axis is the most obvious.The angle of body gesture is growing bigger and bigger[16].

③ The acceleration of the Z axis is 0 after falling,because the body torso is laying down on the plane.The acceleration of the X axis and the Y axis are bigger,the angle of body gesture is 90^{o} [17].

We commissioned a study into 4 kinds of falling which are forward 、backward、towards the left and toward the right.The figure 7 is the SVM measured from different directions vary in time.

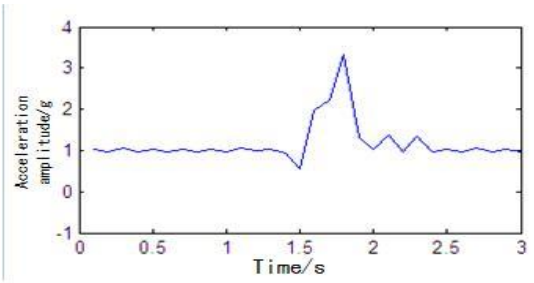

Fig.7(a) Curve of SVM during falling Forward

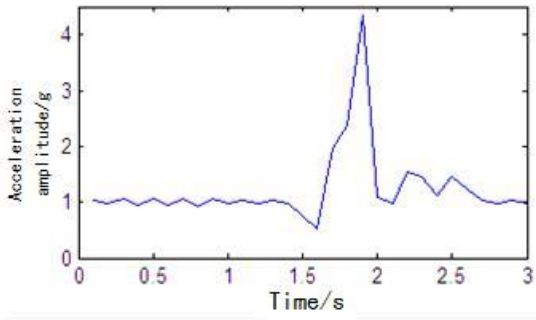

Fig.7(b) Curve of SVM during falling backward

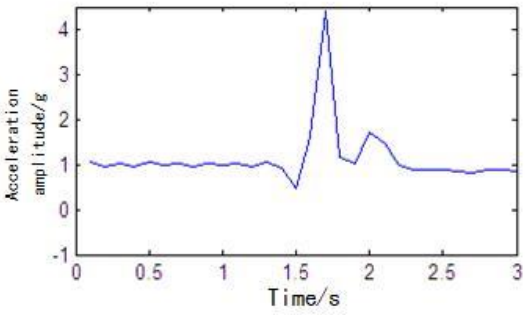

Fig.7.(c)Curve of SVM during falling towards the left

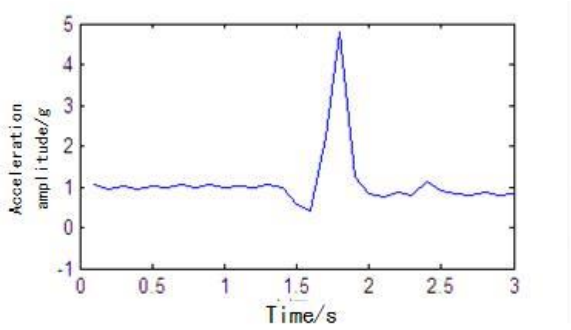

Fig.7.(d) Curve of a and SVM during falling towards the right

The figure 8 are the curves that Φ(the angle of gesture) changing with time.

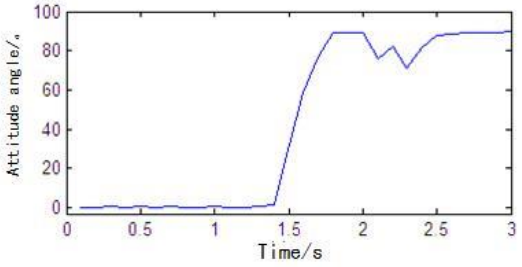

Fig.8(a) Curve of Φ during falling forward

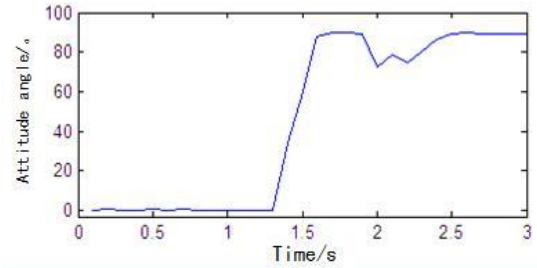

Fig.8(b) Curve of Φ during falling backward

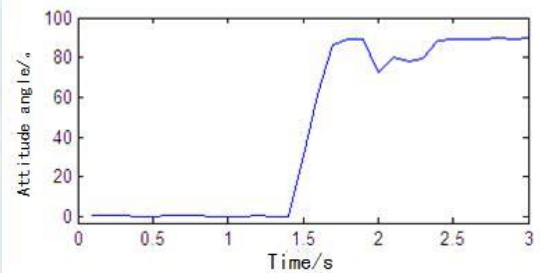

Fig.8(c) Curve of Φ during falling towards the left

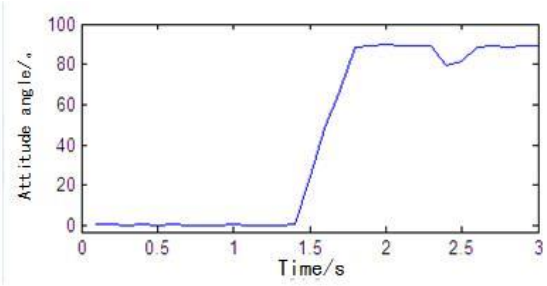

Fig.8(d) Curve of Φ during falling towards the right

(3)Result analysis

As the data of normal activity shown in the chart 1: N1 is the number of normal action ,from 1 to 8 ,there are the procedures of walk、jogging、go upstairs、go downstairs、jete in the same plane、jete from one plane to another、straight to sit down and straight、straight to lie prostrate and stand up. Chart 2 shows the data of falling,N2 is the number of different directions.

From 1 to 4 there are the directions of forward、backward、left-side and right-side,in the meantime, $SVM_{\max}$ is the biggest amplitude of the acceleration, $\phi_{\max}$ is the biggest angle of the gesture.

Table.1 Test results during normal activity

N1	(1)	(2)	(3)	(4)
SVM_{max}	3.33	4.34	4.48	4.88
Φmax	89.9	89.8	89.8	89.9
	(5)	(6)	(7)	(8)
SVM_{max}	3.33	4.34	4.48	4.88
Φmax	89.9	89.8	89.8	89.9

Table.2 Test results during falling

N2	(1)	(2)	(3)	(4)
SVM_{max}	3.33	4.34	4.48	4.88
Φmax	89.9	89.8	89.8	89.9

When the data in chart 1 is compared with that in chart 2:set the reasonable angle of gesture threshold is T_ϕ and set the amplitude of acceleration threshold is TSVM[18].When these amplitudes are beyond threshold,people can make judgement that whether falling happened.

VII.CONCLUSION

This descriptive study of design that detects the aged falling and based on wearable technology.By contrasting the gravitational acceleration a_g SVM and Φ in different conditions which are in normal state and in falling state,we can gain a convenient and practical method that can judge the falling which will help the aged in time.This allocation have the value of economic and society.

References

[1] YAO M,MA Y N,GAO X,JIN Z Z.A Wearable Pre-impact Fall Early Warning and Protection System Based on Inertial Sensor[J].Journal of Integration Technology,2015,04(5):69-77.

[2] CHEN J,WANG Y W. ZigBee - based Localization and human fall detection system[J]. Electronic and Applied Technology, 2012, 38(12):29-35.

[3] LIU P,LU T C,LV Y Y,et al.MEMS Tri-Axial Accelerometer Based Fall Detection[J]. Chinese Journal of Sensors and Actuators 2014,27(4):570-574

[4] CAI J,TIAN R Y,LIU L,et al.Design and implementation of movement monitoring system based on the human body sensor and Android technology[J].Electronic and Applied Technology, 2015,41(9):63-66.

[5] WEN J,MA Z L,XUE Z B.Human fall detector based on wireless communication and GPS positioning[J]. Applied Science and Technology, 2014,41(4):22-28.

[6] DONG W C,MENG L J,ZHANG H X.Design of Portable and Low Noise ECG Monitor[J]. Modern Electronics Technique,2009,32(5):127-130.

[7] YANG B,DONG Y G. Capacitive coupled non-contact electrodes and ECG signal acquisition[J]. Chinese Journal of Scientific Instrument,2016, 36(5): 1072-1078

[8] CAO Y T,CHEN J L.Improved threshold extraction of R peak[J].Electronic Measurement Technology,

2015,38(12): 107-110

[9] SHI T,HE Z N,JIANG N,WANG X M,.Design of Fall Detection System for the Old on Android Platform[J].Electronic Sci,2014,27(9):82-84.

[10] CUI Y H,ZHAN L.Fall detection system based on three-axis acceleration sensor for the elderly[J].Modern Electronics Technique, 2013, 36(3):130-132

[11] XU J P,LI J T,PENG S,et al.Fall detection system based on three-axis acceleration sensor for the elderly[J] . Computer Simulation , 2014 , 31(12):434-450

[12] ZHUO C B,YANG L P.ZHOU L,LUO D.Design of Fall Detection System Based on MPU6050 Acceleration Transducer[J].Chinese Journal of Electron Devices,2015,08:821-825.

[13] HAN Y D,LI Z.Data Acquisition and Pre-processing Based on MEMAccelerometer [J].Instrument Technique and Sensor, 2015,(2):16-19.

[14] WANG X M,ZHANG L,LI T T.Design and Implementation of Multiple Tilt Sensor Driver on Android Platform[J],Instrument Technique and Sensor,2013,09:18-20.

[15] CHENG T,YANG S S,FENG R,et al.Algorithm for falling dowm detection of solitary elderly person based on binocular vision calibration[J]. Transducer and Microsystem Technologies, 2014,33(10):100-103

[16] JIN C,YIN Y Y.Old man fall detection algorithm research based on discriminant analysis of statistical[J]. Application Research of Computers,2014,31(1):89-91.

[17] WU Z Q,CAO L,WANG K,LV Q W.Design of human fall detection system based on smart phone[J].Computer Engineering and Design, 2014,35(4):1465-1470.

Sparse Inversion Method of T2 Spectrum Based on the L1 norm for Low-field Nuclear Magnetic Resonance

Chang Xing; Sun Jia; Li Tian-Wei

（jilin university instrument science and engineering institute,changchun,130021）

***Abstract*—The technology of low-field nuclear magnetic resonance (LF-NMR) in its non-destructive, non-invasive, in situ, green and other advantages is widely used in food, agriculture, energy and chemical sectors. Recently, this technology has played an increasingly large role in the field of food-safety supervision. Conventional T_2 spectrum inversion methods such as the non-negative singular value decomposition (SVD) algorithm can only reflect T_2 spectrum in a smooth model. However, for a sparse model, the inversion result of non-negative SVD algorithm is quite smooth, leading to low resolution of T_2 spectrum and inaccuracy analysis.To solve this issue, we propose a sparse T_2 spectrum inversion algorithm based on the L1 norm minimization constraint. In this paper, we establish the sparse model expression of NMR echo curve, and obtain the T_2 sparse spectrum inversion result based on the inner truncated Newton-point method. Furthermore, the effectiveness of L1 sparse inversion algorithm is examined by the synthetic data of the smooth and the spare model with different peak numbers and signal to noise ratios (SNRs). The synthetic results show that compared with the non-negative SVD algorithm, the L1 sparse algorithm is suitable for both the smooth model and the sparse model with higher inversion accuracy. When the number of T_2 peaks in a sparse model changes from a single peak to a quad peak, the L1 sparse algorithm can still obtain accurate inversion results, while the SVD algorithm results in a gradual deterioration, and cannot even determine the peak number. Under the sparse model, when the SNR of the measured NMR curve is gradually changed from 5 dB to 50 dB, the L1 sparse algorithm at 20 dB or more can obtain accurate inversion results of the peak error of less than 10%, the peak position error and the average error of amplitude of less than 5%. However, the non-negative SVD algorithm cannot get accurate results at each SNR. Finally, L1 sparse inversion algorithm is applicable to multiple sets of frying oil samples to prove the accuracy and robustness. The inversion results of seven sets of frying oil samples showed that the L1 sparse algorithm is better than non-negative SVD algorithm. The obtained T_2 spectrum shows three peaks obviously, and the T_{21} peak area ratio S_{21} and the single component relaxation time T_{2w} are higher linearly with frying time. Then according to the relationship between S_{21} or T_{2w} and the parameters of the frying oil such as acid value, viscosity and absorbance, we can detect effectively the quality change of frying oil over time. The inversion results of the T_2 spectrum at different SNRs are consisted with the synthetic results, i.e., when the signal-to-noise ratio is reduced, the T_2 spectral inversion results of the L1 sparse algorithm are better than the non-negative SVD algorithm when SNR is greater than 20 dB.**

***keywords*—Low-Field Nuclear Magnetic Resonance, T_2 spectrum inversion, sparse representation, L1-norm minimization constraint.**

I. INTRODUCTION

FOOD safety is not only closely related to the health and life safety of the broad masses of the people,but also to social stability and economic development. Since 2010,drainage oil, clenbuterol, plasticizer exceed, cadmium rice and other events frequently,we can see the food quality and food safety issues have become a strong social hot issues.The face of illegal food rampant,the urgent need for effective and reliable detection method to monitor food health, food safety.Since the discovery of Nuclear Magnetic Resonance (NMR) in 1946, NMR has evolved into an important analytic and detection technique for a wide range of industries such as agricultural food,energy exploration,polymer materials and life sciences [1-3] .The NMR phenomena are classified into High Field NMR (HF-NMR) and Low Field NMR (LF-NMR),the former is mainly used to analyze the chemical properties of the substance, and the latter is used to detect the physical properties of the material

characteristic.Compared to HF-NMR,the advantage of LF-NMR is that the instrument is low in cost, small in size, capable of in-situ, real-time and rapid measurement[4],At the same time on the detection of samples with non-destructive, non-invasive and non-polluting and other characteristics, in the field of food safety supervision plays an increasingly important role for poor quality grease detection, water injection testing, milk adulteration, pathogens and heavy metals Ion detection and so has a significant application potential[5].However, due to the LF-NMR magnetic field strength, the detection resolution is not high. Therefore, it can improve the detection resolution and accuracy of harmful food components by improving the inversion algorithm, and whether the LF-NMR method can be effectively used for food safety testing vital.

At present at home and abroad for LF-NMR technology for frying oil quality determination, mainly based on T_2 spectrum analysis method.The [6] in the laboratory after 60h fried soybean oil samples, LF-NMR detection of the relaxation map(the T_2 spectrum) peak and soybean oil acid value, viscosity, absorbent and the content of polar compounds have good correlation, the oil quality evaluation of soybean oil.The oil samples of frying oil were tested in [7] and [8].The characteristic peaks of frying oil were found from the T_2 spectrum of LF-NMR,and the peak amplitude increased linearly with the increase of the incorporation ratio. However,due to the low magnetic field strength of LF-NMR, when the content of frying oil in the sample is small or affected by noise, the T_2 spectrum obtained by inversion is limited, and the linearity of the frying oil content is poor, Characteristic peaks of oil.Therefore,in LF-NMR technology, it is urgent to solve the problem of how to improve the resolution of T_2 spectrum inversion under low magnetic field strength.

In recent 20 years, the research on NMR inversion algorithm has made important progress, including non-negative least squares[9]、penalty function method [10]and Singular Value Decomposition （ SVD ） [11].Many scholars have carried on the optimization of these algorithms,the[12] proposed a regularization algorithm based on L2 norm constraints, improve the continuity of spectrum distribution, but because of the smooth parameter will cause the spectrum distortion. The literature [13],by adding the damping term to the coefficient matrix to optimize the non-negative SVD decomposition method, it can be accepted within a certain range of error tolerance, and can not get ideal results when mixed with noise.Literature[14],by establishing the relationship between SNR and singular value of the best number of reservations to improve the non-negative SVD truncation,but need to calculate Signal to Noise Ratio(SNR). It can be seen that the non-negative SVD algorithm is a commonly used inversion algorithm,but the T_2 spectrum obtained by this algorithm is generally continuous distribution. For a single homogeneous sample or a sample containing only a few discrete values, the non-negative SVD inversion result too smooth, can not reflect the discrete or sparse T_2 spectrum.In the literature [15],the multiexponential inversion is combined with the non-negative least squares method and the nonlinear fitting method to improve the resolution of the T_2 spectrum. However, the method also uses the value as an inversion parameter to increase the uncertainty of the inversion result.In [16], according to the above, proposed a linear regression least squares method to improve the nonlinear optimization algorithm and accelerate the convergence rate.However, these algorithms need to know the number of T_2 lines, the result depends on the initial value and SNR, when the SNR is low, the inversion results there is a large error. Therefore, how to obtain robust sparse results in the case of unknown number of lines and low signal-to-noise ratio is one of the difficulties that the T_2 spectrum inversion algorithm is urgently needed to solve.

Sparse representation is a hot topic in the field of signal processing, image restoration and wireless communication. It has the advantages of complex signal thinning, obvious difference of feature and small

influence of noise in information extraction and parameter analysis[17]. By establishing the sparse representation model of the NMR echo signal on the T_2 spectrum,the L0 norm minimization constraint problem is obtained to obtain the sparse coefficient, that is, the amplitude of the T_2 spectrum.owever, the minimization of the L0 norm is a NP-hard problem, which is then transformed into a convex optimization problem of L1 norm because there is a unique global optimal solution for L1 norm minimization. Therefore, with the continuous development of signal sparse representation, the algorithm of L1 norm minimization problem is of great concern, such as greedy algorithm[18] and iterative contraction algorithm[19] can solve this optimization problem well, but usually Subject to the amount of data and model dimensions;The Homotopy Algorithm[20] and the Interior Point Method[21] can be used to deal with large-scale high-dimensional data, but requires a lot of computation time and iteration times. Truncated Newton Interior Point Method[22] is based on the interior point method, using the Pretreatment Conjugate Gradient (PCG) algorithm to calculate the search step size, reducing the calculation time, which can quickly deal with large data, often used in optical molecular imaging, radio communication,facial expression recognition and so on.

In this paper, we propose a T_2 spectrum sparse inversion algorithm based on L1 norm reduction constraint (hereinafter referred to as L1 sparse algorithm), aiming at improving the low-field NMR T_2 spectrum resolution and introducing sparse theory into T_2 spectral inversion method. The inversion results of the non-negative SVD algorithm and the L1 sparse algorithm in the smooth and sparse T_2 spectrum models are compared by simulating the NMR echo data. Finally, the low-field NMR experiments and spectral inversion of the frying oil samples are carried out. Accuracy and Superiority of Spectral Sparse Inversion Algorithm with L1 Norm Minimization Constraints.

II.LF-NMR PRINCIPLE

The low-field NMR technique resonates the hydrogen proton ^{1}H in the sample by applying a radio frequency pulse. The magnetization vector M is continuously attenuated after the pulse is stopped. The attenuation process of the transverse magnetization vector M_{xy} is called lateral relaxation and the attenuation of M_{xy} to 37% of the time for the transverse relaxation time T_2 , T_2 and its corresponding amplitude constitute the T_2 spectrum, through the analysis of the T_2 information related to the sample spectrum, the quality of the sample to be tested.

A.LF-NMR Measurement Sequence

LF-NMR experiments typically emit two measurement sequences: spin echo (SE) sequence and CPMG sequence. The SE sequence is the first 90 ºpulse, at time τ to impose a 180 ºpulse, and at the time 2τ to obtain the peak of the spin echo signal, by changing the value of τ , respectively, 90 ºand 180 ° pulse, you can get a number of spin echo signal The The CPMG sequence is subjected to 180 ° pulses on the basis of the SE sequence, resulting in multiple attenuated spin echo signals. CPMG sequence and spin echo signal as shown in Figure 1, at time to apply a 90 ° pulse, after the time t=2τ after the first 180 ° pulse, you can get the first echo signal; At time t=3τ a second 180 ° pulse is applied and a second echo signal is obtained at time t=4τ . And so on, every 180 ºpulse at time $t=(2n-1)\tau$, at time $t=n\tau$ to get an echo signal, the peak of these echo signals is an exponentially decay curve, the NMR echo curve.

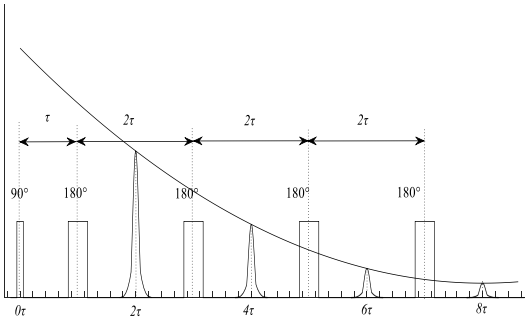

Fig.1.Principle diagram of CPMG sequence measurement and NMR echo signal in LF-NMR.

The function expression of the NMR echo curve is shown in equation (1).

$$y(t)=\sum_{i=1}^{m}x_i\cdot e^{-\frac{t}{T_{2i}}},t=2n\tau(n=1,2,3,\cdots) \tag{1}$$

τ is the half-echo time; n is the number of echoes; $y(t)$ is the peak amplitude of the echo signal corresponding to time t; m is the number of relaxation components; x_i is the amplitude of each relaxation component ($i=1,2,\cdots,m$) ; T_{2i} for the relaxation of the relaxation time; T_{2i} and x_i one by one correspondence, constitute a T_2 spectrum.

B.T_2 Spectral Inversion Method

The T_2 spectral inversion is based on the NMR echo curve, and the coefficient matrix $\mathbf{A}=(a_{\{i,j\}})_{\{n\times m\}}$ $a_{\{i,j\}}=e^{-\frac{2j\tau}{T_{2i}}}$ is calculated by setting the decay time T_{2i} of the appropriate relaxation component to establish a $\boldsymbol{y}=\mathbf{A}\boldsymbol{x}$ order linear system of equations. Through the inversion algorithm to solve the equations, you can get the decay time T_{2i} corresponding to the relaxation component.

At present, the commonly used method of T_2 spectral inversion is non-negative SVD[11] . The T_2 spectra obtained by inversion by non-negative SVD algorithm are continuously distributed, as shown in Figure 2. Figure 2 simulates a smooth model of the spectrum, the number of points is 36, according to the index distribution in the interval 1~10^4 ms. Set the echo interval 2τ = 1.2 ms, the number of echo $n=1500$. The coefficient matrix $\mathbf{A}$ and the echo signal y are calculated according to the formula (1), as shown in Fig. 2 (a). The results are shown in Fig. 2 (b), where the black line is the simulated spectral model and the blue line is the spectrum obtained by inversion of the non-negative SVD algorithm. The two are in good agreement only. There is a certain error when T_2 is little. Therefore, the non-negative SVD algorithm has better spectral inversion effect for this smooth model. However, for a single homogeneous sample or a sample containing only a few discrete values, the non-negative SVD inversion results are too smooth.

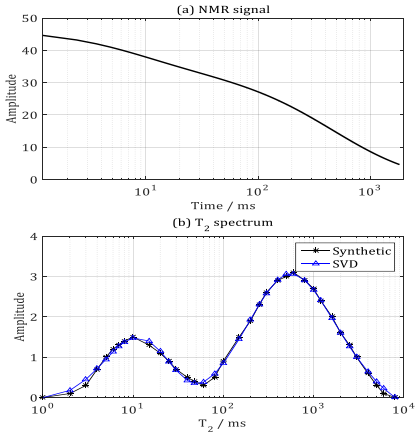

Fig. 2. Non-negative SVD inversion result of a smooth model: (a) NMR echo signal of the smooth model; (b) T_2 spectrum of the smooth model.

III.L1-NORM SPARSE INVERSION ALGORITHM

L1-norm minimization of T_2 spectrum sparse inversion algorithm to L1 norm relaxation component T_2 to minimize the amplitude constraints based on, which can be transformed into a convex optimization problem, and is solved by truncated Newton interior point method, the T_2 spectrum obtained the optimal

sparse mode solution.

A.L1-norm minimization constraint for sparse model

In the practical application of LF-NMR, it is often necessary to deal with some sparse spectrum. Therefore, the sparse model is established in the analysis and processing of NMR echo signal:

$$\min \ \|\boldsymbol{x}\|_0 \quad \text{s.t.} \quad \boldsymbol{y}=\mathbf{A}\boldsymbol{x} \tag{2}$$

Where $\|\boldsymbol{x}\|_0$ is the L0-norm of $\boldsymbol{x}$, the number of nonzero elements in the $\boldsymbol{x}$ vector ; $\boldsymbol{x}=[x_1,x_2,\cdots,x_m]^{\mathrm{T}}$ represents the unknown relaxation component amplitude, which is the sparse coefficient of dictionary $\mathbf{A}$,The L0-norm minimization constraint guarantees that only a small number of elements in $\boldsymbol{x}$ are not zero;

$\boldsymbol{y}=[y_1,y_2,\cdots,y_n]^{\mathrm{T}}$ represents NMR echo signal; $\mathbf{A}$ matrix is a sparse model of the dictionary;The formula (2) is a set of n linear equations with m unknowns $x_1,x_2,\cdots,x_m$.

Since the L0 norm minimization problem in expression (2) is a NP-hard problem, and L1 norm is the optimal convex approximation of L0 norm, and it is easier to optimize the solution, taking into account the fact that there is bound to the noise in the actual observation signal , So according to the expression (2) based on the L1 norm minimization constraints of the noise-containing sparse model:

$$\min \ \|\boldsymbol{x}\|_1 \quad \text{s.t.} \quad \|\mathbf{A}\boldsymbol{x}-\boldsymbol{y}_{\text{obs}}\|_2 \le \varepsilon \tag{3}$$

Where $\|\boldsymbol{x}\|_1=\sum_{i=1}^{n}|\boldsymbol{x}_i|$ is the L1-norm of $\boldsymbol{x}$, $\|\cdot\|_2$ is the L2-norm, and the parameter $\varepsilon>0$ represents the allowable error, which is calculated from the noise estimate of the noisy echo signal $\boldsymbol{y}_{\text{obs}}$.

B.T_2 Spectral Inversion Method

On the basis of the internal point method[23], the new logarithmic barrier function and the central path are established, and the approximate solution of the Newtonian system is calculated by a Pretreatment Conjugate Gradient (PCG) algorithm[24], Thereby reducing the computation time.

The L1-norm minimization problem in expression (3) is a linear programming problem (LP) with inequality constraints.According to the thought of regularization, set variable $\boldsymbol{w}=\mathbf{A}\boldsymbol{x}-\boldsymbol{y}_{\text{obs}}$, the formula (3) can be transformed into quadratic programming problem, as the original problem of interior point method (P):

$$\text{P}: \ \min\left\{f_p(\boldsymbol{x})=\|\boldsymbol{w}\|_2^2+\lambda\|\boldsymbol{x}\|_1\right\} \quad \text{s.t.} \quad \boldsymbol{w}=\mathbf{A}\boldsymbol{x}-\boldsymbol{y}_{\text{obs}} \tag{4}$$

Where $f_p(\boldsymbol{x})$ is the original objective function.

According to the Lagrangian multiplier method, we obtain the corresponding Lagrangian function and the dual problem (D), as shown in expressions (5) and (6):

$$L(\boldsymbol{x},\boldsymbol{w},\boldsymbol{v})=\|\boldsymbol{w}\|_2^2+\lambda\|\boldsymbol{x}\|_1+\boldsymbol{v}^{\mathrm{T}}(\mathbf{A}\boldsymbol{x}-\boldsymbol{y}_{\text{obs}}-\boldsymbol{w}) \tag{5}$$

$$\text{D}: \ \max\left\{f_d(\boldsymbol{v})=\inf(L(\boldsymbol{x},\boldsymbol{w},\boldsymbol{v}))\right\} \quad \text{s.t.} \quad \lambda\ge\left|\mathbf{A}^T\boldsymbol{v}\right| \tag{6}$$

Where $f_d(\boldsymbol{v})$ is the dual function of $f_p(\boldsymbol{x})$,The dual feasible point of construction is $\boldsymbol{v}=2\tau(\mathbf{A}\bar{\boldsymbol{x}}-\boldsymbol{y}_{\text{obs}})$, τ is a proportional constant.The difference between the original objective function and the dual function is the dual gap $gap=f_p(\boldsymbol{x})-f_d(\boldsymbol{v})$ .By maximizing the dual function $f_d(\boldsymbol{v})$, the corresponding optimal solution $\boldsymbol{v}^*$ and the smallest dual gap can be obtained.

According to the truncated Newton method, the original problem P(4) is transformed into an equivalent convex optimization problem (7):

$$\min \|\boldsymbol{w}\|_2^2+\lambda\sum_{i=1}^{m}u_i \quad \text{s.t.} \quad -u_i\le x_i\le u_i \tag{7}$$

The logarithmic barrier function $\varphi(\boldsymbol{x},\boldsymbol{u})$ of the inequality constraint $-u_i\le x_i\le u_i$ can be expressed as:

$$\phi(\boldsymbol{x},\boldsymbol{u}) = -\sum_{i=1}^{m}\lg(u_i + x_i) - \sum_{i=1}^{m}\lg(u_i - x_i) \tag{8}$$

Therefore, the unconstrained form of the original problem P (4) is:

$$\min \left\{ \psi_t(\boldsymbol{x},\boldsymbol{u}) = t\|\boldsymbol{w}\|_2^2 + t\sum_{i=1}^{m}\lambda u_i + \phi(\boldsymbol{x},\boldsymbol{u}) \right\} \tag{9}$$

The function $\psi_t(\boldsymbol{x},\boldsymbol{u})$ is a smooth, lower-bound convex function with a unique minimum value. In the process of calculating its minimum value, a function is affected by the parameter t, which is called the central path. The parameter t is defined as:

$$t := \begin{cases} \max\{\min\{2nr/gap, rt\}, t\} & s \ge s_{\min} \\ t & s < s_{\min} \end{cases} \tag{10}$$

Where $r > 1$ and $s_{\min} \in (0,1]$ are preset parameters,

$s = \beta^k$ is the step size for backtracking search, k is the minimum number of retries to satisfy the backtracking search condition (11), and α, β is the preset parameter.

$$\psi_t(\boldsymbol{x} + \beta^k\Delta\boldsymbol{x}, \boldsymbol{u} + \beta^k\Delta\boldsymbol{u}) \le \psi_t(\boldsymbol{x},\boldsymbol{u}) + \alpha\beta^k\nabla\psi_t(\boldsymbol{x},\boldsymbol{u})^T\begin{bmatrix}\Delta\boldsymbol{x}\\ \Delta\boldsymbol{u}\end{bmatrix} \tag{11}$$

Using the PCG algorithm to solve the following Newton system (12), we can get the search direction:

$$\nabla^2\psi_t(\boldsymbol{x},\boldsymbol{u})\begin{bmatrix}\Delta\boldsymbol{x}\\ \Delta\boldsymbol{u}\end{bmatrix} = -\nabla\psi_t(\boldsymbol{x},\boldsymbol{u}) \tag{12}$$

According to the cut-off Newton interior point method, the algorithm steps to solve the L1 norm minimization constraint problem (3) are as follows:

$\alpha = 0.01, \beta = 0.5, r = 2, s = 1$
$\lambda = 1, \varepsilon = 0.01, \boldsymbol{x} = \boldsymbol{0}, \boldsymbol{u} = \boldsymbol{1}$
$t = 1/\lambda$
while $(gap/f_d) > \varepsilon$ *do*
  $\nabla^2\psi_t(\boldsymbol{x},\boldsymbol{u})[\Delta\boldsymbol{x};\Delta\boldsymbol{u}] = -\nabla\psi_t(\boldsymbol{x},\boldsymbol{u})$
  $s = \beta^k$
  $\boldsymbol{x} = \boldsymbol{x} + s\Delta\boldsymbol{x}$
  $\boldsymbol{u} = \boldsymbol{u} + s\Delta\boldsymbol{u}$
  $f_p = \|\mathbf{A}\boldsymbol{x} - \boldsymbol{y}_{\text{obs}}\|_2^2 + \lambda\|\boldsymbol{x}\|_1$
  $\boldsymbol{v} = 2\tau(\mathbf{A}\bar{\boldsymbol{x}} - \boldsymbol{y}_{\text{obs}})$
  $f_d = -(0.25\boldsymbol{v}^T\boldsymbol{v} - \boldsymbol{v}^T\boldsymbol{y}_{\text{obs}})$
  $gap = f_p - f_d$
  $t = \max\{\min(2nr/gap, rt), t\}$
end while

C.Inversion Results

Construct a sparse model of T_2 spectrum, the number of points is 36, the index is distributed in 1~10^4ms, as shown in Figure 3. Echo interval 2τ = 1.2ms, the number of echo n=1500, by calculating the NMR echo curve, as shown in Figure 3 (a) below. In Fig. 3 (b), the black star is the simulation model, and the red line is the T_2 spectrum obtained by inversion using the L1 sparse algorithm.It can be seen from the comparison that the T_2 spectrum obtained by L1 sparse algorithm is basically the same as the sparse model of structure, and the errors of each point are small. Therefore, the L1 sparse algorithm is better for the T_2 spectrum in sparse model.

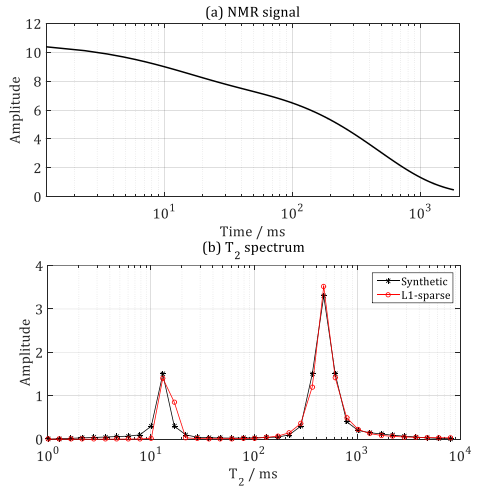

Fig.3.L1 sparse inversion result of a sparse model:

(a) NMR echo signal of the sparse model;

(b) T_2 spectrum of the sparse model.

IV.Inversion Analysis Of Simulation Model

In order to verify the effect of L1 sparse algorithm and traditional non-negative SVD method on smooth model and sparse model, we can compare the accuracy of the two methods in dealing with the sparse model with different T_2 peak numbers, and verify the sparse Inversion results, this paper establishes a number of simulation models for inversion experiments.

In the course of the experiment, there are four parameters related to SNR, peak error, peak position error and amplitude mean error. The formulas are as follows (13) to (16).

Signal-to-noise ratio (SNR) is defined as:

$$\mathrm{SNR}=10\times\lg\frac{\|y\|_2^2}{\|y_{obs}-y\|_2^2} \qquad (13)$$

Where y is the simulated ideal echo signal obtained according to equation (1), and y_{obs} is the noisy echo signal after adding a certain proportion of noise.

The number of peaks structure of T_2 spectrum of T_2 peak model is k, the peak value of h_{0k}, the corresponding relaxation time is $T_{2k}^{'}$, the number of points (the number of relaxation component) is m, the amplitude of the relaxation component used for x_{0i}. algorithm to invert the signal y_{obs} peak T_2 spectrum is h_k, corresponding to the peak the relaxation time is T_{2k}^{*}, the amplitude corresponding to the relaxation time for the x_i, the peak peak amplitude error, position error and average error definition respectively:

The peak error is calculated as:

$$\Delta h=\frac{1}{k}\sum_{i=1}^{k}\left|\frac{h_{0i}-h_i}{h_{0i}}\right|\times100\% \qquad (14)$$

The peak position error is calculated as:

$$\Delta T_2=\frac{1}{k}\sum_{i=1}^{k}\left|\frac{T_{2k}^{'}-T_{2k}^{*}}{T_{2k}^{'}}\right|\times100\% \qquad (15)$$

The mean value of the error is calculated as:

$$\Delta x=\frac{1}{m}\sum_{i=1}^{m}\left|\frac{x_{0i}-x_i}{x_{0i}}\right|\times100\% \qquad (16)$$

A.Inversion Comparison of Smooth Model and Sparse Model

Firstly, the T_2 spectra of the smooth model and the sparse model are constructed respectively. The number of points is 36, the distribution is in the range of 1 ~ 10^4 ms, the echo interval 2τ = 1.2 ms, and the number of echoes n=1500.The NMR echo curves are obtained by adding the signal to noise ratio 20 dB of Gaussian white noise,as shown in Figure 4(a)and(b).The T_2 spectral inversion is performed using the non-negative SVD algorithm and the L1 sparse algorithm, respectively. The results are shown in Fig. 4 (c) and (d). By comparison you can see:For the smooth model, the non-negative SVD algorithm and the L1 sparse algorithm inversion result are in agreement with the simulated T_2 spectrum. Only at the

smaller T_2, the inversion results of the two methods are biased due to the large value of τ.For the sparse model, the T_2 spectrum obtained by the L1 sparse algorithm is closer to the simulation model than the non-negative SVD algorithm.This is because the non-negative SVD algorithm assumes that the T_2 spectrum is continuously distributed and that the inversion result for the sparse model is too smooth.Therefore,the L1 sparse algorithm is suitable for both the smooth model and the sparse model.

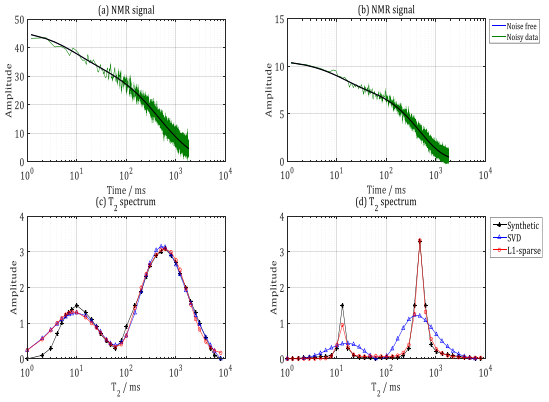

Fig.4.Comparison of the inversion results between non-negative SVD algorithm and L1 sparse algorithm in the smooth model and the sparse model: (a) NMR echo signal of the smooth model; (b) NMR echo signal of the sparse model; (c) smooth model inversion result; (d) sparse model inversion result

B.Inversion of T_2 peak number variation

In order to verify the effect of the two methods on the inversion of different T_2 peaks, four sparse models of the T_2 peak number from four to four peak are simulated, as shown by the black star in Figure 5, and the non-negative SVD Algorithm and L1 sparse algorithm inversion, the inversion results shown in Figure 5, blue and red lines shown.

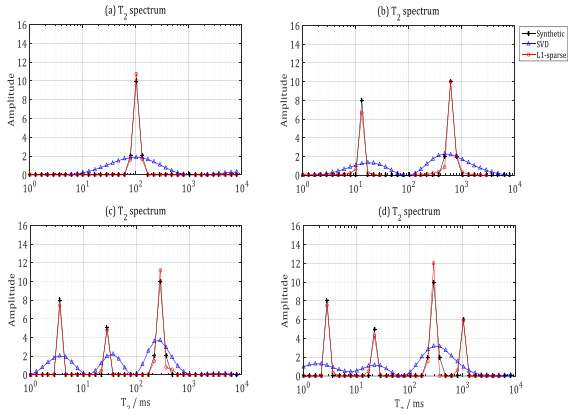

Fig.5.Comparison of inversion results of the multimodal model with different T_2 peaks:

(a) single peak T_2 spectrum; (b) two peak T_2 spectrum; (c) three peak T_2 spectrum;(d) four peak T_2 spectrum..

It can be seen from Figure 5, L1 sparse algorithm in dealing with different T_2 peak number of sparse model, the inversion of the T_2 spectrum are closer to the simulation model,there is a small error between the peak of the T_2 spectrum and the simulation model, and the corresponding T_2 value is basically equal to the simulation model.In Figure 5(d), the amplitude average error Δx of the four peaks of the T_2 spectrum obtained by the L1 sparse algorithm is only 8.6%, and the T_2 position is equal to the simulation model. And the T_2 spectra of the non-negative SVD algorithm are smooth and the peak error Δh and the peak position error ΔT_2 of the T_2 spectrum are larger.Especially the four-peak T_2 spectrum, the amplitude average error Δx and the peak position error ΔT_2 of the T_2 spectrum obtained by the non-negative SVD algorithm are 65.7% and 19.93 ms respectively, which can not reflect the peak size and position of each peak, and the fourth T_2 peak Is not

obvious.Therefore, it can be concluded that the T_2 peak and amplitude of L1 sparse algorithm are better than non-negative SVD.

C.Inversion Results Of Different SNR

In order to verify the inversion effect of L1 sparse algorithm under different signal-to-noise ratio (SNR), the signal-to-noise ratio is 50 dB, 30 dB, 20 dB, 15 dB in the NMR curve of sparse model, 10 dB and 5 dB Gaussian white noise, followed by the SNR curve with different signal to noise ratio using L1 sparse algorithm for inversion. In order to verify the statistical results of different noise data, 100 groups of noise data are randomly generated under different SNRs. The inversion results of non-negative SVD and L1 sparse algorithms are depicted in Figure 6,The darker regions represent the probability that the inversion results are greater, and the lighter regions represent less chance of occurrence,and the black curve represents the constructed T_2 spectrum. The average error of the T_2 spectrum of the 100 inversion results is shown in Table 1.

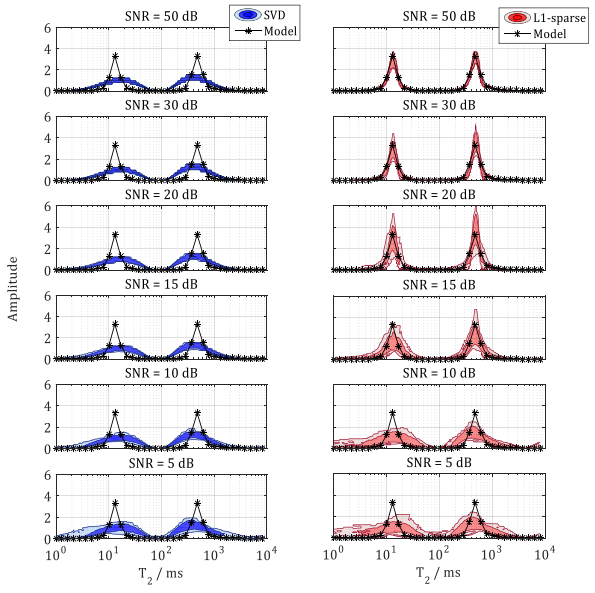

Fig.6.Comparison of the inversion results with different SNRs.

TABLE I

ERROR ANALYSIS OF THE INVERSION RESULTS OF T_2 SPECTRUM WITH DIFFERENT SNRS

SNR	Δh /%		ΔT_2 /%		Δx /%	
	SVD	L1	SVD	L1	SVD	L1
50dB	40.10	3.37	23.18	0.00	26.60	0.62
30dB	40.02	6.13	23.36	0.00	26.72	1.74
20dB	40.16	10.45	23.44	2.38	26.98	4.28
15dB	40.59	17.52	23.19	8.82	27.63	7.69
10dB	41.82	31.05	24.23	12.50	30.45	19.42

V.INVERSION EXAMPLES OF EXPERIMENTS

In order to verify the inversion effect of the L1 norm sparse inversion method in practical application, the frying oil samples were prepared by frying sweet potatoes. The NMR echo curves of each group of frying oil samples were obtained by low field nuclear magnetic resonance analysis instrument And the NMR echo curves were retrieved by two inversion methods.

A.Frying Oil LF-NMR Experiment

Low-field nuclear magnetic resonance (NMR) techniques can be used to detect the quality of frying oil. The principle is to obtain the NMR echo curve $y_{\text{obs}}(t)$ of the frying oil sample by low-field nuclear magnetic resonance spectrometry and to invert the T_2 spectrum of the frying oil. If the frying oil sample is treated as a whole, the relaxation time is T_{2w} and the corresponding amplitude is x^*, then $y_{\text{obs}}(t)$ can be expressed as:

$$y_{\text{obs}}(t) = x^* e^{-\frac{t}{T_{2w}}} \quad (17)$$

By inversion, the one-component relaxation time of the sample can be obtained T_{2w}(ms).

The resulting T_2 spectra have three peaks, called T_{21} peak, T_{22} peak and T_{22} peak [6], where the

peak area of the T_{21} peak is proportional to the total area and the single component relaxation time of the S_{21} and T_2 spectra T_{2w},and soybean oil acid value, viscosity, absorbance and polar component content and other indicators there is a good correlation between the use of low-field nuclear magnetic resonance detection of S_{21} and T_{2w}, can effectively reflect the quality of frying oil [21].

First make frying oil.Fry the fresh sweet potato chips with Arowana oil and pour 3L soybean oil into the frying pan and keep the oil temperature in the range of 190 to 200℃. Place 100g of fresh sweet potato chips in the frying oven,5 minutes after the fried sweet potato chips will be removed, and re-placed fresh sweet potato chips.Samples of soybean oil were sampled every 4 hours, fried for 24 hours, sampled 7 times, and 10 ml of frying oil was taken from each sample. The frying time was divided into 7 groups according to the frying time.(0 h、4 h、8 h、12 h、16 h、20 h、24 h).

Through NMI20 desktop nuclear magnetic resonance imaging analyzer(Magnetic field strength of 0.5±0.08T, the instrument main frequency of 21.3 MHz),The hard pulse CPMG sequence was applied to the seven experimental samples. The 90°pulse width was 19μs, the sampling wait time TR was 1500 ms, the half echo time τ was 300 μs, and the number of echoes was set according to the length of the relaxation process 1000-4000.By circulating 180 °pulse, generate multiple echo signals, measured to obtain the NMR echo curve shown in Figure 7.It can be seen from Figure 7 that the longer the time of soybean oil frying, the faster the NMR echo curve is attenuated.

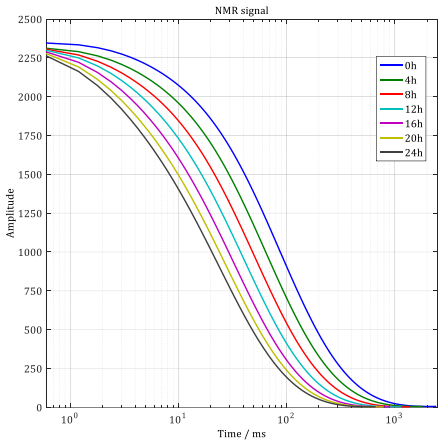

Fig.7.NMR echo signals from LF-NMR measurements of frying oil samples.

B.Frying oil T_2 spectrum inversion comparison

The NMR spectra of seven groups of samples were obtained from the low nuclear magnetic resonance experiment of frying oil. The non-negative SVD algorithm and L1 sparse algorithm were used to invert, and the T_2 spectrum obtained by inversion was shown in Fig.8. Compared with the two groups of inversion results in Figure 8, it is found that there are three peaks in the T_2 spectrum retrieved by L1 sparse algorithm, which correspond to T_{21} peak, T_{22} peak and T_{23} peak of frying oil respectively.The T_2 spectra obtained by the non-negative SVD algorithm have only two peaks, which indicates that the inversion result is too smooth and can not distinguish the three peaks of the frying oil effectively.

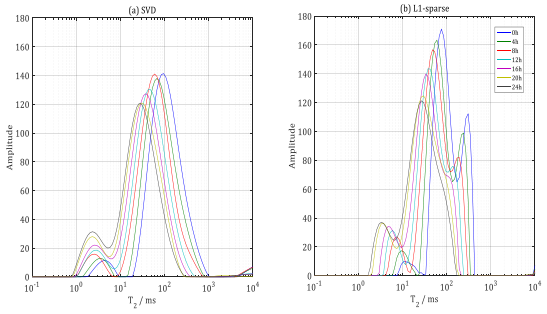

Fig.8.Comparison of T_2 spectrum inversion results based on the two methods for frying oil samples: (a) non-negative SVD algorithm; (b) L1-sparse algorithm

At the same time,The ratio S_{21} of the peak area of the T_{21} peak to the total area is linearly increasing with the frying time, and the one-component relaxation time T_{2w} decreases linearly with the frying time, as shown in Figure 9.L1 sparse algorithm results are linearly fitted: $y_{S_{21}} = 0.49x + 3.11$ and $y_{T_{2w}} = -1.23x + 107.76$.

The fitting coefficients R^2 are 0.994 and 0.995, respectively, which represent the degree of fitting of the model to the data.Therefore, according to S_{21} and T_{2w} and soybean oil acid value, viscosity, absorbance and polarity components such as the correlation between the indicators, can effectively detect the quality of frying oil changes [6].In the spectrum obtained by the non-negative SVD algorithm, the linear relationship between the frying time and S_{21} and T_{2w} is $y_{S_{21}} = 0.42x + 3.65$ and $y_{T_{2w}} = -6.01x + 176.81$ .The fitting coefficient R_2 is 0.971 and 0.965 respectively, which shows that the non - negative SVD algorithm is inferior to the L1 sparse algorithm for the NMR electromagnetic echo curve.

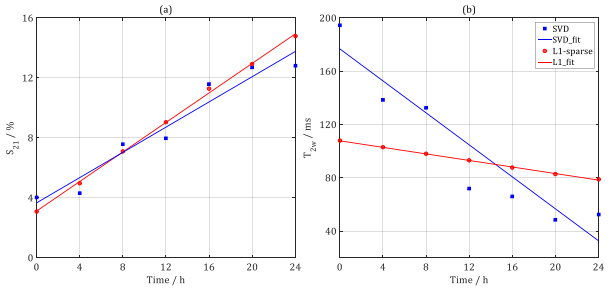

Fig.9.The correlation between the frying time and (a) the peak area ratio S_{21}, (b) as well as the single relaxation time T_{2w}

VI.CONCLUSION

Aiming at the problem that the conventional nonnegative Singular Value Decomposition (SVD) algorithm can not accurately invert the T_2 spectrum of the sparse model, this paper proposes a sparse inversion algorithm based on the L1 norm minimization constraint, and establishes the sparse model expression of the NMR echo curve The problem of minimization of L1 norm is solved by using the cut off Newton interior point method, and the high resolution exact inversion of T_2 spectrum in sparse model is realized.

Through the model simulation and low field NMR data inversion, the following conclusions are obtained:

1)The simulation results of the smooth model and the sparse model show that the L1 sparse algorithm is suitable for both the smooth model and the sparse model, and has higher inversion accuracy compared with the SVD algorithm.

2)When the peak number of the sparse model changes from a single peak to a four-peak value, the L1 sparse algorithm can still get an accurate inversion result, and the SVD algorithm results in a gradual deterioration and can not even determine the number of peaks.

3)In the sparse model, when the SNR of the measured NMR curve changes gradually from 5 dB to 50 dB, the L1 sparse algorithm can obtain accurate inversion results at 20 dB or more, the peak error Δh is within the range of 10%, the peak position error ΔT_2 And the amplitude average error Δx is within the range of 5%, and the inversion result of the SVD algorithm can not get accurate results at all signal-to-noise ratios.

4)The measured data inversion results of 7 groups of frying oil samples showed that the L1 algorithm outperforms the SVD algorithm in sparse results, obtained T_2 spectra clearly showing three peaks, and a higher degree of T_{21} peak area ratio S_{21} and single relaxation time T_{2w} changes linearly with time, then according to the relationship between S_{21} and T_{2w} and acid value, the viscosity of frying oil the absorbance and the parameters such as the quality of frying oil can detect the changes with time.

The research of this paper can not only be used in the field of rapid detection of food quality, fresh milk

moisture and waste oil identification, but also can be applied to nuclear magnetic logging interpretation, core analysis of oil reservoir, geophysical exploration of complex oil and gas reservoir fluid identification and petrochemical and other aspects.

References

[1] Marcone M F, Wang S, Albabish W, Nie S, Somnarain D, Hill A 2013 Food Res.Int.51-729.

[2] Li X, Xiao L Z, Liu H B, Zhang Z F, Guo B X, Yu H J, Zong F R 2013 Acta Phys. Sin.62-147602 (in Chinese).

[3] Wang S, Munro R A, Shi L, Kawamura I, Okitsu T, Wada A, Kim S Y, Jung K H, Brown L S, Ladizhansky V 2013 Nat.Methods10-1007.

[4] DalitzF, Cudaj M, Maiwald M, Guthausen G 2012 Prog Nucl.Mag.Res.Sp.60-52.

[5] Shen Y G, Xiao Z Q, Chen S S, Zhang Y L, Jiang, W, Lai K Q 2013 J Food Sci.Technol.31-37 (in Chinese).

[6] Wang Y W, Wang X, Liu B L, Shi R, Yang P Q 2012 Food Sci.33-171 (in Chinese).

[7] Zhang Q, Saleh A M, Shen Q 2012 Food Bioprocess Technol. 6-2562.

[8] Zhu W, Wang X, Chen, L. 2017 Food Chem.216-268.

[9] Bro R, De Jong S 1997 J. Chemom.11-393.

[10] Butler J P, Dawson S V 1981 Siam J. Numer. Anal.18-381.

[11] Wang W M, Li P, Ye C H 2001 Sci. China A 31-730 (in Chinese).

[12] Chen S, Wang H, Yang P, Zhang X 2014 J. Biomed. Eng.31-682 (in Chinese).

[13] Li P J, Ge C, Sun G P, Chen X, Wang Y K 2010 Well Logging Technol.34-215 (in Chinese) .

[14] Lin F, Wang Z W, Liu Q H, Ding Y, Li C C 2009 J.Jilin Univ.(Earth Sci. Ed.)39-1150 (in Chinese).

[15] Wang H, Li G Y 2005 Acta Phys.Sin.54-1431 (in Chinese).

[16] Wu L, Chen F, Huang C Y, Ding G H, Ding Y M 2016 Acta Phys.Sin.65-107601 (in Chinese) .

[17] Chen W C, Wang W, Gao J H, Jiang C F, Lei J L 2013 Chinese J. Geophys.56-2771 (in Chinese) .

[18] Mallat S G, Zhang Z 1993 IEEE T.Signal Proces.41-3397

[19] Zhou W 2013 M.S. Thesis (Guangzhou: South China University of Technology) (in Chinese) .

[20] Zhang L Q, Wang J Y 2008 Chinese J. Eng. Geophys.5-509 (in Chinese) .

[21] Wei H, Sasaki H, Kubokawa J, Yokoyama R 1998 IEEE T. Power Syst.13-870.

[22] Koh K, Kim S J, Boyd S 2007 J.Mach.Learn.Res.8-1519.

[23] Stern A S, Donoho D L, Hoch J C 2007 J. Mag. Res.188-295.

[24] Berman P, Levi O, Parmet Y, Saunders M, Wiesman Z 2013 Concept Mag. Res. A 42-72.

[25] Karmarkar N.A new polynomial-time algorithm for linear programming 1984 Combinatorica 4-373.

Study on Noise suppression of Airborne Electromagnetic Profiles Data Based on Adaptive width Filtering

Gao Dianyao; Liu Xueying

(The College of Instrumentation and Electrical Engineering, Jilin University, Changchun 130022,China)

***Abstract*—Using the traditional filtering technology, the airborne time-domain electromagnetic data can be filtered, but owing to the fixed window width, it can remove the surface of the noise signal, but weaken anomaly amplitude. Proposed in this paper, the main adaptive filtering denoising method, according to the characteristics of local signal, judges the abnormal signal area based on adaptive window width smooth algorithm, for non anomalous local signals filtering based on larger window wide, for anomalous local signal filtering based on smaller window wide, this method not only removes the noise, but also maintains the abnormal amplitude of the original signal. This paper compares the filtering denoising results using FIR filter, IIR filter and adaptive filter, and verifies the validity of the adaptive filtering denoising method by the imaging results of measured data.**

***Keywords*—Airborne Time-domain Electromagnetic Data, Adaptive Filtering Algorithm, FIR Filter, IIR Filter**

I. INTRODUCTION

TIME domain electromagnetic method is a favorable tool for mining. With the improvement of the transient electromagnetic system and the maturity of the technology,more and more information can be obtained from the airborne electromagnetic data. Therefore, the development of airborne electromagnetic data processing method is also very important. Because of its machine Flight load detection mode, transmitting coil will swing in the detection process; at the same time, the flight speed and flight attitude change will cause the detection system of device parameter instability and detect changes in pressure and temperature during the flight can also introduce the system noise, affecting the quality of data and imaging precision serious restriction airborne electromagnetic detection system of inversion and interpretation of underground abnormal body, reduce the depth of exploration[1-4].

With the development of the research on the electromagnetic detection technology and instrument, the research of the background field removal,data filtering,stack and extraction methods of airborne electromagnetic noise[5-6]. Although the original data in time domain airborne electromagnetic exploration, after multiple processing and filtering section, the signal-to-noise ratio of the data has been greatly improved, but still contains advanced residual noise, the detection ability of the deep influence of the underground.

Trace in the superposition of airborne electromagnetic data, the commonly used time domain airborne electromagnetic detection system is also put some new extraction technology of Macnae stack(1984) of cutting(pruning) method for removing atmospheric interference; Buselli(1992) and Cameron proposed Strack(median filtering method) proposed pruning averaging method;Sutarno and Vozoff(1989) inhibited the static nonlinear filtering technique is adopted.Accoding to Macnae(1984), Lane(1998) using the technology of controlling the frequency of lower than the transmission signal, Fugro company using the

method of notch; THEM system using polynomial fitting method to remove the movement noise[7].

Due to the shallow geophysical exploration project objectives, in recent years, Chinese scholars havecarried out the principal component denoising, Dr Zhu[8][9] will wish success into the root of time domain airborne electromagnetic inversion,the amount of success to encounter the noise characteristics in principal component inversion of noisy data because the inversion results have been achieved in the other methods. This paper puts forward the technology of airborne electromagnetic noise profile data processing based on adaptive filter,analyzes the characteristics of the noise space,the study of adaptive bandwidth smoothing algorithm,designs the adaptive low-pass filter,and compared with FIR filter and IIR filter wave,the denoising by comparing the simulated data and the measured data,verify the effective denoising algorithm in this paper.

II.ADAPTIVE FILTERING METHOD

A.Denoising principle of adaptive filtering

According to the adaptive window width smoothing algorithm[10], a low pass filter bank is designed to take the number of the first section as an example,the specific algorithm is as follows:

The window width value W_L、W_U is the minimum and the maximum window adjustment range . First,use the maximum window width to filter the profile data smoothing $\hat{x}_k$, get $\hat{x}_{fk}$, and calculate the second order difference $\Delta_k(j)$ (type(1))

$$\Delta_k(j)=\left(\frac{2}{W_U-1}\right)\sum_{i=1}^{[(W_U-1)/2]}2\hat{x}_{fk}(j)-\hat{x}_{fk}(j+i)-\hat{x}_{fk}(j-i) \quad (1)$$

In the type j=1,2…n ,[.]indicates the rounding down.Calculated by $\hat{x}_k$ calculate the second-order difference $\Delta_k(j)$ reflect the local gradient change rate of the smoothing filtered profile data $\hat{x}_{fk}$. Absolute value at the profile $\hat{x}_{fk}$ exception is larger,and approaching zero in the flat part.

Use type(2) to transform the second order difference $\Delta_k(j)$ from the adaptive window width $W_k(j)$ of the smoothing filter of each measurement point.Between the minimum window widths and the maximum window width：

$$W_k(j)=[W_U-(W_U-W_L)(\frac{|\Delta_k(j)|}{\Delta_T}-\frac{1}{2})] \quad (2)$$

Among them$\Delta_T$is the two order difference threshold,if Δ_T is too small, the window width $W_k(j)$ is too small, it will have influence on the flat section. If $W_k(j)$ is too large, not can cause anomalies along the profile, but reduce the abnormal amplitude.The conventional fixed bandwidth low pass filter,according to the profile data adaptive bandwidth smoothing algorithm designed of low pass filter, not only can effectively remove the high frequency noise on the spatial profile data,but also can ensure the profile data of the amplitude.

B. Design of adaptive Filter

Adaptive filtering technology is based on the characteristics of the local signals with different window width filtering compared with the traditional filtering method, the adaptive filtering technique according to the characteristics of the local signals with different window width to determine the area of filtering, abnormal signal, non local signal abnormalities with larger bandwidth filter, local abnormal signal by small the width of the window filtering, so as to remove the noise, but also to maintain the original signal amplitude anomaly. In this paper, the maximum window width of the adaptive filter is 51, and the minimum bandwidth is 3.

III.DENOISING INSTANCE OF SIMULATION DATA

In order to observe the three degree of filter effect, this paper designs a homogeneous half space earth model, conductivity was 0.01S/m, a total of 1000

measured points, system of helicopter borne time domain airborne electromagnetic detection, the measurement of central loop, the transmitting coil radius is 7.5m, the emission current of 25Hz for positive and negative square wave. Flight height is 30m, the normalized emission current of the earth model is one-dimensional forward calculation and Simulation for the field data, the forward adding 10% data in the Gauss white noise, can be obtained after the extraction of the measuring point 16 off-time electromagnetic response profile data, as shown in Figure 1.

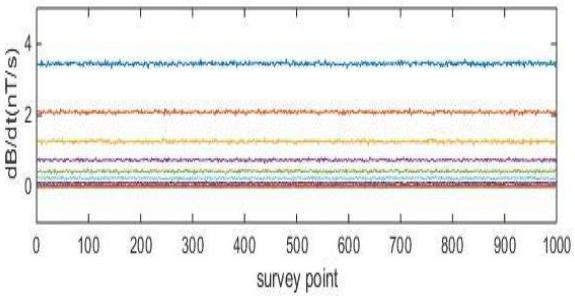

Fig.1 16channels of homogeneous half space earth model

It can be seen that the data of the model contains high frequency spatial noise, which is used to compare the denoising effect. In this paper, FIR, IIR, adaptive window width filter is used to filter the noise. Design of the IIR, FIR filters are low pass filter, the cut-off frequency between 0-1 adjustable, thenumber of arbitrary value, the design of adaptive window width filter,the maximum window width of 51, the minimum window width of 3. Three figures shows the four methods for the post profile curves of the electromagnetic profiledata.

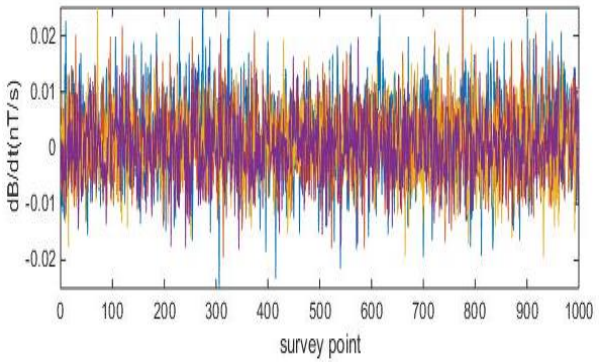

Fig.2 Homogeneous half space the earth model four channels curve after denoising result

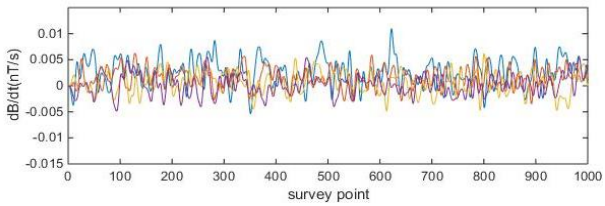

(a) Result of FIR filtering

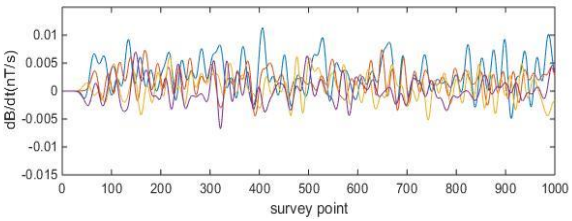

(b) Result of IIR filtering

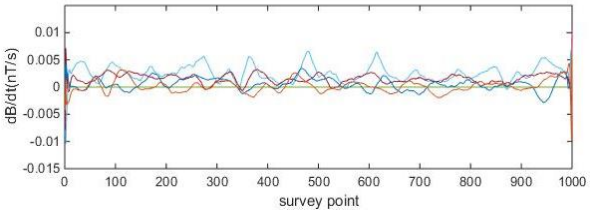

(c) Result of adaptive filtering

Fig.3 Result of filtering

Contrast to Figure3(a), Figure3(b), Figure3(c) can be seen by FIR, IIR filtered profile curve (Figure3(a), Figure3(b)) of the advanced data showed no abnormalities, and the adaptive algorithm filtered profile curve (Figure3(c)) of advanced data not only ensures the abnormal amplitude, and decreases the noisedata.

IV.DENOISING EXAMPLES OF MEASURED DATA

In the major project of the national high technology research and development program of support, Aero Geophysical Survey and remote sensing center and Jilin University developed China's first set of system of helicopter airborne time domain airborne electromagnetic detection (CHTEMindex simulation system.). January 2012, the system in Henan province for the first time in a successful test, and the area of the field survey, found that the region of the earth showed

a high resistance characteristics, resistivity of 3000~8000/ m. In this case, taking a survey line of Henan field flight survey as an example, the 17 section data of the length of about 8.5 km measured line is selected. As shown in Figure3, in the vicinity of the measuring point 3000 with an amplitude of about 1500 nT/s of the anomaly.

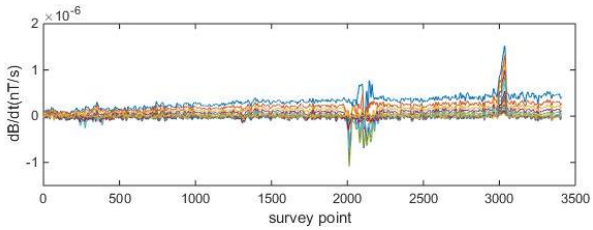

Fig.4 17 channels profile of field data from airborne time domain electromagnetic survey in Henan Province, China

Firstly, the profile data of the measured line are FIR, IIR and adaptive window width algorithm, and the results are shown in Figure 5(a), Figure 5(b) and Figure5(c). After comparing the three denoising data profiles, we can see that the adaptive window width filtering algorithm has achieved the best denoising results as shown in Figure5(c), the removal of the measured line of high frequency noise.

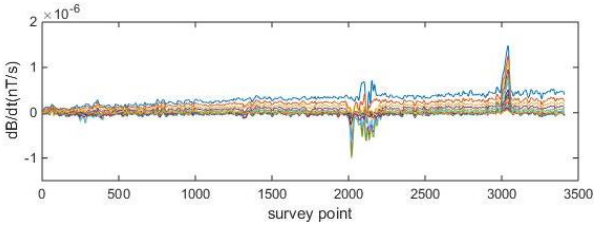

(a) Result of FIR filtering

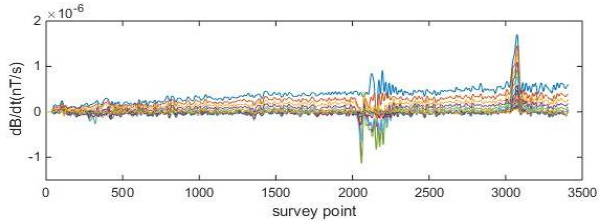

(b) Result of IIR filtering

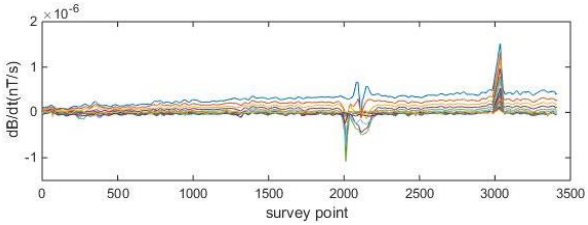

(c) Result of adaptive filtering

Fig.5 Result of filtering

From Figure5(a), Figure5(b) can be seen, the two conventional filter FIR, IIR filter denoising effect is not obvious, the noise level is almost no decline. The data of the measured line is filtered by the adaptive window width algorithm. The maximum bandwidth of the filter is 51, the minimum bandwidth is 3, and the filtering result is shown in Figure5(c). It can be seen from Figure5(c), after the adaptive algorithm, the noise reduction than the FIR and IIR filter noise decreased significantly.

The last four data of the late channel data is the last 17 data, and the filter can be more effective to filter the filter. Figure5 is the original data of the image of thelate Tao, Figure7(a), Figure7(b), Figure7(c), respectively, three kinds of filters on the original data channel filter results.

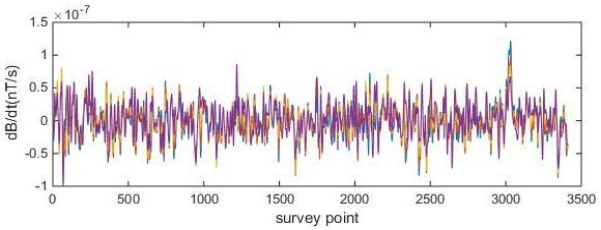

Fig.6 The original data terminal image

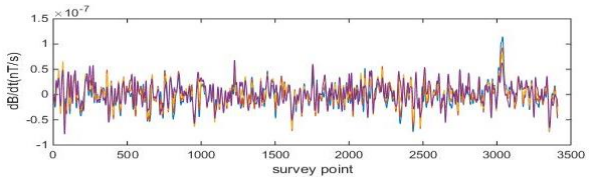

(a) Result of FIR filtering

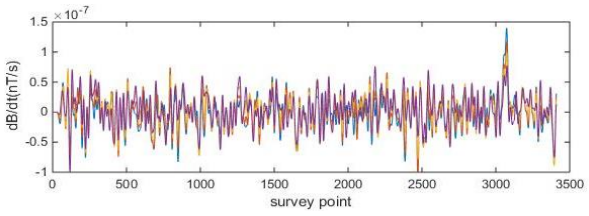

(b) Result of IIR filtering

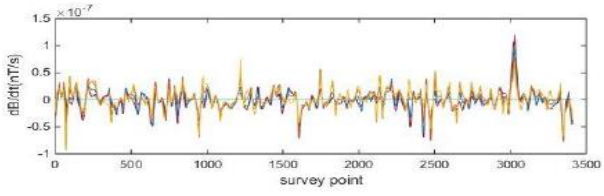

(c) Result of adaptive filtering

Fig7.Result of filtering

In Figure7(a), Figure7(b), Figure7(c), the contrast can be seen, the regular FIR filter, IIR filter profile after treatment (Figure7(a) , Figure7(b)) of advanced data had no obvious abnormalities, can not reflect the deep earth body the model, and there is still more noise with high frequency, and adaptive bandwidth filtering (Figure7(c)) after the data of late ensure abnormal amplitude, and the amplitude of noise is obviously reduced, the high frequency noise significantly reduced.

V.CONCLUSION

1.The airborne electromagnetic data processing transform is applied to the GUI interface, after the original profile data processing of three kinds of filtering algorithm, not only can filter the high frequency noise in spatial profile data, also remove uncorrelated noise profile data, adaptive filtering algorithm can improve the SNR of advanced data, provides a new ideas for geophysical data processing such as noise.

2.This paper adopts adaptive filtering algorithm, low pass filter design can be based on the local characteristics of airborne electromagnetic data transform section, adaptively changing the bandwidth of the filter can not only remove high frequency spatial noise effectively, but also effectively maintain the abnormal amplitude, is better than that of FIR, the filtering performance of IIR filter, the filter can also be for effectively measuring line electromagnetic data filtering.

Reference

[1] Lane R, Green A, Golding C, et, al. An example of 3Dconductivity mapping using the TEMPEST airborne electromagnetic system [J]. Exploration Geophysics, 2000, 31(2):162-172.

[2] Macnae, J C,Ltagne Y, West G F. Noise processing techniques for time-domain EM system [J].Geophysics,1984, 49(7):934-948.

[3] Riddsdill-Smiath T A, Dentith M C. The wavalet transform in aeromagnetic processing [J].Geophysics, 1999,64(4):1003-1013.

[4] Buselli G, Hwang H S. AEM noise reduction with remote referencing[J]. Exploration Geophysics, 1998,29(2):71-76.

[5] Li Nan.Time domain electromagnetic data preprocessing technology research [D]. Changchun:Jilin University,2009.

[6] Lv Dongwei. Pod time domain helicopter electromagnetic data processing method [D].Chengdu: ChengduUniversity of Technology, 2011.

[7] Auken,E.,Westergaard,J.A.,Christiansen,A.V.,andSorensen, K.L. Processing and inversion of SkyTEM data for high resolution hydrogeophysical surveys[C].Australian Society of Exploration Geophysicists, Extended Abstracts. l9th Geophysical Conference and Exhibition..

[8] Zhu Kaiguang, Wang Lingqun, Xie bin et al. A method for noise removal from airborne electromagnetic data based on principal component analysis [J]. China Journal of nonferrous metals, 2013, 23 (9): 2430-2435.

[9] Wang Lingqun, Li Bingbing, Lin Jun et al. The noise removal method for the reconstruction of the main components of airborne electromagnetic data [J]. Journal of Geophysics, 2015 (8): 2803-2811.

[10] Li Xiuwen, Xu Jinwu, Yang et al. Application of the gradient adaptive window width in the analysis of variable speed mechanical order ratio [J].Instrument technology and Sensor, 2013 (1): 68-76.

A soft fetching manipulator research based on the piezoelectric thin film sensor

QIAN Cheng-hui; JIANG Yao; LI Shu-hao; LIU Hong-li; XIN Yi

(Jilin University College of Instrument Science and electrical engineering, Jilin Changchun 130026,China)

***Abstract*—Design a soft fetching manipulator by using the new film sensor PVDF which based on the piezoelectric effect and the thermoelectric effect,judge the grasping state through the change of charge quantity in the process of grasping and releasing,using the fuzzy control theory to achieve the soft fetching by regulating the steering gear rotate.Its grasping quality is less than 1 kg and the volume is less than $10^{-3}m^3$,at the same time it can grab objects move steady 0.6 meters to the specified location that the error is less than 3 cm;It add hot sense perception function,when the temperature is higher than 60 degrees Celsius the manipulator can bounce off automatically.The soft fetching manipulator which based on the piezoelectric thin film sensor overcomes the disadvantages of the traditional manipulator can't judge the clamping force independently,which improve the bionic function.**

***Key words*—PVDF;manipulator;fuzzy control ;piezoelectric effect ;thermoelectric effect**

I. INTRODUCTION

WITH the development of society, the manipulator has been applied to many fields, instead of people to complete a variety of actions, improve our quality of life. There is a bone prosthesis implanted medical science research, an intelligent knee joint with the pace and has improved damping sensing function of prosthetic hand [1,2].

The current design of the prosthetic hand by visual judgment whether hold objects, but the health of people through the hand skin tactile sensor to determine whether hold objects, vision is mainly used for holding the object position and holding position feedback judgement. The design of the PVDF piezoelectric film sensor to determine the tactile and thermal sensation signal, can make the mechanical hand on their own judgment object, and can grasp fragile objects and keep the egg intact, good soft grasping function. In addition into the thermal perception function, encountered high temperature objects, the robot will automatically open, so as not to damage the manipulator [3-9].

II. BASIC PRINCIPLE

A. Principle of Tactile Sense

The sensitive material of the tactile sensor is PVDF, which can be extracted from the PVDF signal by[10 ,11], which is different from the contact and sliding response. The touch signal is continuous voltage obtained by charge amplifier charge generating object exerts a force on the sensor when the value of the slip signal from; and the object on the sensor surface of a transverse cut relative sliding force generated by the sensor to the charge amplifier after the formation of the. The test shows that the peak value of the signal wave generated by the tactile sense is larger than that of the series of wave peaks, and the thermal sense signal is a step signal. Therefore, the sensor signal input to the main controller for the characteristic value of treatment, the results, and the results obtained by the preset program variance, show sensory threshold, and finally set the tactile slip threshold were compared, it can distinguish between tactile and thermal sensation.

B. Charge Amplifier Principle

In fact, the charge amplifier is a negative feedback amplifier, but considering the actual factors, the equivalent circuit diagram of the charge amplifier is shown in the figure 1.

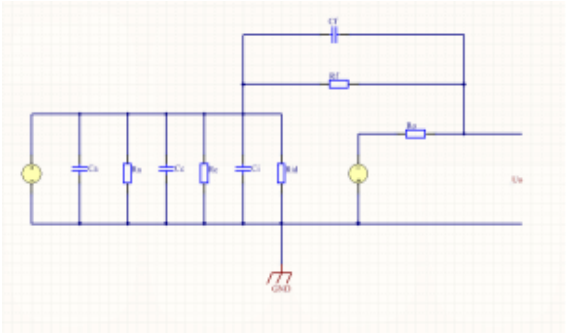

Fig.1. Equivalent circuit of charge amplifier

Let C_c, R_C distribution cable insulation resistance and capacitance, Ci input capacitance amplifier, rid and RO respectively for the op amp differential input and output resistances, equivalent input resistance and capacitance amplifier for:

$$(R_a//R_c//r_{id})>>R_f/(1+A);$$

$$C=C_a+C_c+C_i+(1+A)C_f;$$

The resistance is converted into admittance to calculate the power supply angle frequency of the piezoelectric sensor, and the output voltage of the actual charge amplifier is ignored by R_O.

$$U_o=-A*U_i;$$

If the following conditions are met

$$(R_a//R_c//r_{id})>>R_f/(1+A);$$

$$(1+A)C_f>>C_a+C_c+C_i;$$

Then

R = Rf / (1+A) G = (1+A) Gf and C (1+A) = Cf, to approximately

$$U_O \approx -AQ\frac{1}{1+j\omega(1+A)G_f+(1+A)C_f};$$

So the charge amplifier and the output of the piezoelectric element self capacitance and the size of cable length is independent of the output voltage depends only on the input charge Q and feedback circuit parameters of C_f and R_f. When the working frequency is high enough, G_f<<. C_f, the Gf can also be omitted, so

$$U_O=-AQ\frac{1}{(1+A)C_f}.$$

III. Overall Design

A. System Design Block Diagram

The system consists of signal acquisition, signal processing, processor feedback control, actuator actuator and human-computer interaction interface, as is shown in the figure 2.

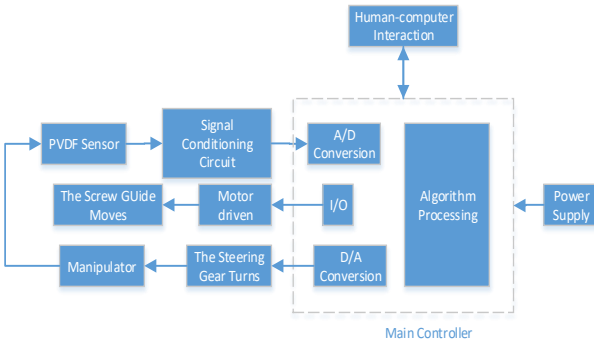

Fig.2. System block diagram

The block diagram of the system, PVDF will capture the signal processed by the signal conditioning circuit, sent to the processor algorithm analysis through A/D conversion, through the regulation of servo manipulator realize grasping function, and then use the stepping motor to move smoothly capture objects.

B. Manipulator Design

All bracket parts mechanical hand with aluminum 3mm thickness, has good stability, a hand through the steering control, equipped with MG996 metal gear, the output is more stable, the working voltage of 3.0V-7.2V, the steering joints are imported bearing cup type, not only can turn to a more flexible, but also can make the steering gear steering in the same circle. The manipulator is fixed on a two-dimensional guide screw, the stepper motor control can make the manipulator move up and down, which can capture the moving objects from one place to another smoothly. Among them, the screw guide rail length can be changed according to the actual situation, to meet the requirements of different occasions.

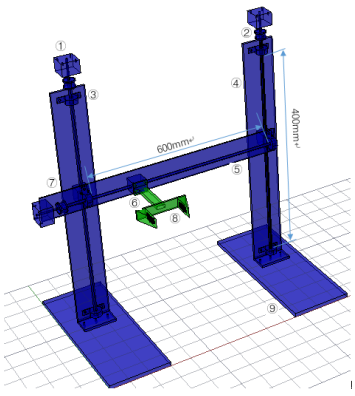

Fig.3. The structure of two dimensional screw guide rail

C. Signal Conditioning Circuit

Because of the PVDF piezoelectric film sensor charge release signal, so the signal processing of the

first by a charge amplifier as preamplifier circuit, PVDF has the characteristics of high output impedance, according to impedance matching principle, the charge amplifier circuit level 10M ohm high resistance measurement, in order to improve the accuracy of the signal. In addition, the first stage inverter amplifier is used to amplify the signal, so that the MCU can capture and then feedback the signal system. Because the human body movement frequency is generally lower than 100Hz, so the design of 100Hz low-pass Butterworth filter, remove the interference signal. Finally, connect the 50Hz power frequency trap circuit, the use of dual T band stop filter, remove power interference, signal conditioning circuit diagram is shown in figure 4.

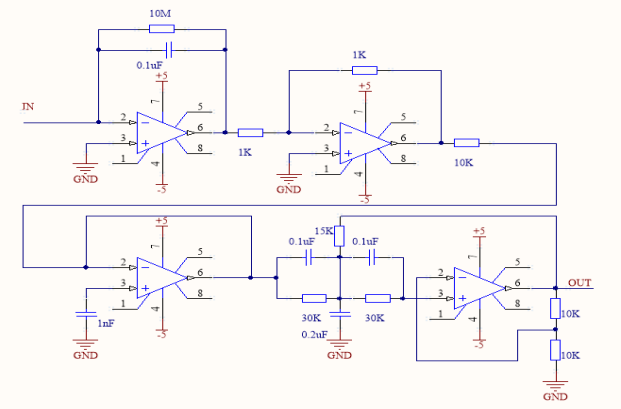

Fig.4. Schematic diagram of signal conditioning circuit

IV. Software Design

The output voltage value of the sensor can not accurately judge the relative sliding of the object, and the design of the control model is very difficult because of the randomness of the object. Therefore, the simulation of the human brain thinking design fuzzy control soft grasp strategy.The overall process works according to the following flowchart.

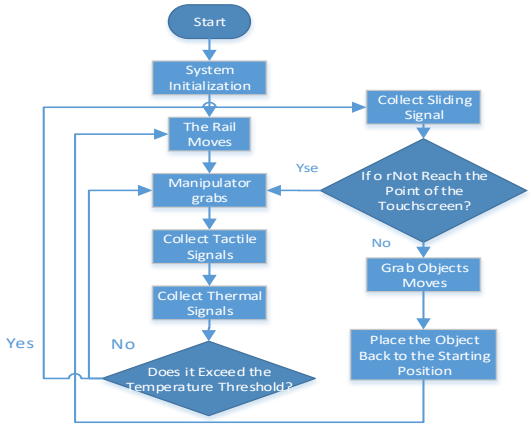

Fig.5. Software flow chart

V. Test Results and Analysis

At room temperature, will be filled with water quality is about the cup and the quality of 50g is about 60g of the egg as the object of measurement, testing the mechanical characteristics of soft grasp. After the experiment concluded that the manipulator can smoothly grabbed the cup and the egg, and egg cups has no deformation, not broken.

Fig.6. Grab eggs physical map

Fig.7. Cups capture physical map

Through the analysis of the data collected by the piezoelectric film sensor, the clamping force of the manipulator is judged, and the minimum pressure can not be reached. From the above two picture can be seen, the manipulator can grasp safety hardness

smaller objects and not damaged, realize the soft grasping function.

Will burn to 40 degrees Celsius to 70 degrees Celsius temperature ranging from hot water into the cup, start the mechanical hand to close the cup, measurement of thermal perception function. After the experiment, when the temperature is close to or above 60 degrees Celsius at a distance of about 5mm cup manipulator when will quickly bounce, realizes the heat perception function.

VI. CONCLUSION

The use of PVDF piezoelectric film sensor will charge piezoelectric effect and thermoelectric effect generated by the charge amplifier signal conditioning circuit into a voltage signal, using 32 ARM Cortex-M3 kernel microcontroller (STM32F103 Series) controller. 12 bit A/D converter is used to convert the analog signal generated by the signal conditioning circuit into digital signal, and then form a closed loop negative feedback control system by fuzzy control theory. The soft manipulator piezoelectric film sensor to capture low egg brittle objects do not fall off and not to make it broken based on the grasp quality can reach 1kg, move smoothly to the designated location offset error can be less than 3cm, is close to the temperature higher than 60 DEG C when the object manipulator can quickly bounce, achieve soft grasp the function, can be widely used in medical, information service, many areas of scientific research, bring more convenience to people.

References

[1] JIN Dewen, WANG RenCheng. Artificial intelligent prosthesis[J]. Chinese Journal of Clincal Rehabilitation, 2002,5(20):2994-2995.

[2] LI TianBo, CHEN Ling, CHEN KunHua.et al. Design of myoelectric controled prostheic hand system basedon MSP430[J]. Transducer and Microsystem Tcchnologies, 2012,31(4):75-78.

[3] JIANG MingWen, WANG RenCheng, LUO ZhiZeng.et al. Myoelectric prosthetic hand with tactile and slip feedback fuctions[J].Journal of Tsinghua University(Sci&Tech), 2004, 44(8):1051-1053.

[4] LIU Xu, WU Peng, LU YanJun.Preparation Solutions of Flexible PVDF Piezoelectric Film Sensor[J]. Instrument Technique and Sensor, 2016,(1):4-6.

[5] HAN YaLi, QI Bing, YU JianMing. et al. Development and Experimental Study of Elastic Actuator for a Power-Assisted Knee Exoskeleton[J]. Robot, 2014,36(6):668-675.

[6] CHEN WeiDong, DONG YanRu, CHEN Ying. Experiment and Research of a New Tactile and Slip Sensor[J]. PIEZOELECT RICS&ACOU STOOPTICS, 2010,32(4):571-574.

[7] LUO ZhiZeng, WANG RenCheng. Study of Tactile Sensor In Bionical Artificial Hand[J]. Journal of Sensor Technology, 2003,(3):233-237.

[8] WEI Cheng. ZHAO Yang, WANG HongLiu. et al. Space Robot Soft-hard Grasping Based on Sliding Mode Control[J]. JOURNAL OF MACHINICAL ENGINEERING, 2011, 47(1):43-54.

[9] XIANG Ting, CHEN JinJun. Soft grabbing manipulator research based on a new piezoresistive sensor[J]. Manufacturing Automation, 2013,35(6):69-71.

[10] XIN Yi, TIAN HongYing, QI XiaoHui. et al. Tactile-slip Sense Recognition System Made of PVDF Film Based on LabVIEW[j]. PIEZOELECT RICS&ACOU STOOPTICS, 2015,37(5):793-801.

[11] XIN Yi, YANG QingYu, ZHENG HaoTian. Study of Tactile&Slip Sensor on Structure and Signal Conditioning Circuit Design Based on PVDF Pizzoelectric Film[J]. PIEZOELECT RICS & ACOU STOOPTICS, 2014,36(1):76-84.

[12] DENG WeiLi, QIN Lan, LIU Jun. ea al. Simulation analysis of a quasi-static charge amplifier based on multisim[J]. Foreign Electronic Measurement Technology, 2009,28(4):25-35.